



## TABLE OF CONTENTS

|  |           |
|--|-----------|
| <b>TABLE OF CONTENTS</b> .....   | <b>1</b>  |
| <b>DOCUMENT CHANGE RECORD</b> .....                                      | <b>12</b> |
| <b>1. INTRODUCTION</b> .....   | <b>15</b> |
| 1.1 PURPOSE OF DOCUMENT .....  | 15        |
| 1.2 SCOPE .....  | 15        |
| 1.3 DEFINITIONS, ACRONYMS AND ABBREVIATIONS .....                        | 15        |
| 1.3.1 <i>Scientific identifiers and units</i> .....                      | 16        |
| 1.3.2 <i>Documents identifiers</i> .....                                 | 17        |
| 1.4 LIST OF SYMBOLS .....  | 17        |
| 1.5 REFERENCES .....   | 20        |
| 1.5.1 <i>Applicable documents</i> .....                                  | 20        |
| 1.5.2 <i>Reference documents</i> .....                                   | 21        |
| 1.6 DEFINITION .....   | 23        |
| 1.7 CODING / SIZING .....  | 24        |
| <b>2. OVERVIEW OF SPECIFICATION</b> .....                                | <b>25</b> |
| 2.1 APPROACH OF AUXILIARY DATA PRODUCT SPECIFICATION .....               | 25        |
| 2.2 SUMMARY OF TOOLS / MODULES REQUIRED .....                            | 26        |
| 2.3 SUMMARY OF COMPUTER RESOURCE REQUIREMENTS .....                      | 26        |
| <b>3. SPECIFICATION OF MERISAT INTERNAL AUXILIARY DATA PRODUCT</b> ..... | <b>29</b> |
| 3.1 C.P. MERIS WAVELENGTH FOR BAND <i>B</i> .....                        | 29        |
| 3.2 C.P. FRESNEL REFLECTION COEFFICIENTS FOR OCEAN CASE-I & II .....     | 30        |
| <b>4. MERIS PRODUCTS OVERVIEW</b> .....                                  | <b>32</b> |
| <b>5. SPECIFICATION OF L1B/L2 DATA PRODUCT</b> .....                     | <b>33</b> |
| <b>6. SPECIFICATION OF L1B/L2 AUXILIARY DATA PRODUCT</b> .....           | <b>34</b> |
| 6.1 MERIS INSTRUMENT .....   | 34        |
| 6.2 LEVEL-1B CONTROL PARAMETERS .....                                    | 34        |
| 6.2.1 <i>C.P.</i> .....  | 34        |
| 6.2.2 <i>MPH</i> .....   | 34        |
| 6.2.3 <i>SPH</i> .....   | 34        |
| 6.2.4 <i>GADS General</i> .....  | 34        |
| 6.2.4.1 Julian day to milliseconds conversion factor .....               | 34        |
| 6.2.4.2 Maximum number of missing packets allowed .....                  | 35        |
| 6.2.5 <i>(Deleted)</i> .....   | 36        |
| 6.2.6 <i>GADS Solar Parameters</i> .....                                 | 36        |
| 6.2.6.1 Solar flux reference values .....                                | 36        |
| 6.2.6.2 Square of Sun-Earth distance at reference date .....             | 37        |
| 6.2.7 <i>(Deleted)</i> .....   | 38        |
| 6.2.8 <i>GADS Exception Handling</i> .....                               | 38        |
| 6.2.8.1 Default radiance values for saturated samples.....               | 38        |
| 6.2.8.2 Default radiance values for above range samples.....             | 39        |
| 6.2.9 <i>GADS Level-0 Extraction</i> .....                               | 40        |
| 6.2.9.1 Blank sample thresholds.....                                     | 40        |

|   |           |
|---|-----------|
| 6.2.9.2 Blank sample difference thresholds.....   | 41        |
| 6.2.9.3 Scaling factor for floating point values coding.....                                    | 42        |
| <b>6.2.10 GADS Geolocation.....</b>   | <b>43</b> |
| 6.2.10.1 Mean Earth radius.....   | 43        |
| 6.2.10.2 Number of tie points per frame for full swath.....                                     | 43        |
| 6.2.10.3 AC distance between tie points.....  | 44        |
| 6.2.10.4 FR product AC pixel size.....  | 45        |
| 6.2.10.5 RR product AC pixel size.....  | 46        |
| <b>6.2.11 GADS Flagging.....</b>  | <b>47</b> |
| 6.2.11.1 Width of blooming contamination for FR.....  | 47        |
| 6.2.11.2 Width of blooming contamination for RR.....  | 48        |
| 6.2.11.3 Saturation recovery width for FR.....  | 49        |
| 6.2.11.4 Saturation recovery width for RR.....  | 49        |
| 6.2.11.5 Azimuth angle range for sun glint risk.....  | 50        |
| 6.2.11.6 Zenith angle range for sun glint risk.....   | 51        |
| 6.2.11.7 Band saturation levels for FR samples.....   | 52        |
| 6.2.11.8 Maximum valid radiances.....   | 53        |
| 6.2.11.9 Threshold value for percentage of out of range image samples.....                      | 54        |
| 6.2.11.10 Threshold value for percentage of out of range blank samples.....                     | 55        |
| 6.2.11.11 Land processing bands.....  | 56        |
| 6.2.11.12 Threshold for setting transmission error flag (mean number of errors per packet)..... | 57        |
| 6.2.11.13 Threshold for setting format error flag (mean number of errors per packet).....       | 58        |
| <b>6.2.12 GADS Radiometric.....</b>   | <b>58</b> |
| 6.2.12.1 Switch enabling FR non-linearity corrections.....                                      | 58        |
| 6.2.12.2 Switch enabling RR non-linearity corrections.....                                      | 59        |
| 6.2.12.3 Switch enabling AC straylight correction.....  | 60        |
| 6.2.12.4 (Spare).....   | 61        |
| <b>6.2.13 GADS Classification.....</b>  | <b>61</b> |
| 6.2.13.1 View zenith angles for GADS radiometric thresholds.....                                | 61        |
| 6.2.13.2 Sun zenith angles for GADS radiometric thresholds.....                                 | 62        |
| 6.2.13.3 Relative azimuth angles for GADS radiometric thresholds.....                           | 63        |
| 6.2.13.4 (Spare).....   | 64        |
| 6.2.13.5 (Spare).....   | 64        |
| 6.2.13.6 (Spare).....   | 65        |
| 6.2.13.7 (Spare).....   | 65        |
| 6.2.13.8 Index of band for GADS radiometric thresholds.....                                     | 65        |
| 6.2.13.9 (Spare).....   | 66        |
| <b>6.2.14 GADS Resampling.....</b>  | <b>66</b> |
| 6.2.14.1 Resampling switch.....   | 66        |
| 6.2.14.2 Number of AC samples used in product FR imagette.....                                  | 67        |
| 6.2.14.3 Number of AC samples used in product FR scene.....                                     | 68        |
| 6.2.14.4 Number of AC samples used in product RR.....   | 68        |
| 6.2.14.5 FR across track pixel to tie point sub-sampling factor (number of samples).....        | 69        |
| 6.2.14.6 RR across track pixel to tie point sub-sampling factor (number of samples).....        | 70        |
| 6.2.14.7 FR frame to tie frame sub-sampling factor (number of samples).....                     | 71        |
| 6.2.14.8 RR frame to tie frame sub-sampling factor (number of samples).....                     | 72        |
| 6.2.14.9 Tie frame to summary quality ADS frame sub-sampling factor.....                        | 73        |
| 6.2.14.10 Maximum across track angular distance allowing pixel selection in FR.....             | 74        |
| 6.2.14.11 Maximum across track angular distance allowing pixel selection in RR.....             | 74        |
| <b>6.2.15 GADS Scaling Factor.....</b>  | <b>75</b> |
| 6.2.15.1 Scaling factor - altitude.....   | 75        |
| 6.2.15.2 Scaling factor - roughness.....  | 76        |
| 6.2.15.3 Scaling factor - zonal wind.....   | 77        |
| 6.2.15.4 Scaling factor - meridional wind.....  | 78        |
| 6.2.15.5 Scaling factor - atmospheric pressure.....   | 79        |
| 6.2.15.6 Scaling factor - ozone.....  | 80        |
| 6.2.15.7 Scaling factor - relative humidity.....  | 80        |
| 6.2.15.8 Scaling factor - radiances.....  | 81        |
| <b>6.2.16 GADS Straylight Evaluation Parameters.....</b>  | <b>82</b> |
| 6.2.16.1 Number of spectral regions.....  | 82        |

|  |    |
|--|----|
| 6.2.16.2 Band index of default radiance for pixels with all bands saturated.....                         | 83 |
| 6.2.16.3 Default radiance for pixels with all bands saturated.....                                       | 84 |
| 6.2.16.4 (Spare).....  | 85 |
| 6.2.16.5 (Spare).....  | 85 |
| 6.2.16.6 Interpolation coefficients for spectral region flux estimation.....                             | 85 |
| 6.2.16.7 Flag register showing bands which can be used for radiance estimation of saturated samples..... | 86 |
| 6.2.16.8 FR threshold on saturated samples counts to flag for straylight risk.....                       | 87 |
| 6.2.16.9 RR threshold on saturated samples counts to flag for straylight risk.....                       | 88 |
| 6.2.17 (Deleted).....  | 89 |
| 6.2.18 (Deleted).....  | 89 |
| 6.2.19 (Deleted).....  | 89 |
| 6.2.20 GADS Radiometric Thresholds LUT.....  | 89 |
| 6.2.20.1 Radiometric thresholds, $L_{TOA_2}(\theta_s, \theta_v, \Delta\phi)$ .....                       | 89 |
| 6.2.21 GADS Browse Configuration Parameters.....   | 92 |
| 6.3 RADIOMETRIC CALIBRATION.....   | 93 |
| 6.4 DIGITAL ELEVATION & ROUGHNESS MODEL.....   | 93 |
| 6.5 LAND/SEA MASK.....   | 93 |
| 6.6 ECMWF.....   | 93 |
| 6.7 AEROSOL CLIMATOLOGY.....   | 93 |
| 6.8 ENVISAT-1 ORBIT STATE VECTORS.....   | 93 |
| 6.9 ENVISAT-1 PLATFORM ATTITUDE.....   | 93 |
| 6.10 LEVEL-2 CONTROL PARAMETERS.....   | 93 |
| 6.10.1 C.P.....  | 93 |
| 6.10.2 MPH.....  | 94 |
| 6.10.3 SPH.....  | 94 |
| 6.10.4 GADS General.....   | 94 |
| 6.10.4.1 Number of iterations for ChI1 calculation.....  | 94 |
| 6.10.4.2 Flag indicating the presence of stratospheric aerosols.....                                     | 95 |
| 6.10.4.3 Default radiances for saturated pixels.....   | 96 |
| 6.10.4.4 Maximum optical thickness for land aerosols.....  | 97 |
| 6.10.4.5 Scaling factor - reflectances.....  | 97 |
| 6.10.4.6 Scaling factor - algal pigment index.....   | 98 |
| 6.10.4.7 Scaling factor - yellow substance.....  | 99 |
| 6.10.4.8 Scaling factor - suspended sediments.....   | 99 |
| 6.10.4.9 Scaling factor - aerosol Angstroem exponent.....  | 99 |
| 6.10.4.10 Scaling factor - aerosol optical thickness.....  | 99 |
| 6.10.4.11 Scaling factor - cloud optical thickness.....  | 99 |
| 6.10.4.12 Scaling factor - surface pressure.....   | 99 |
| 6.10.4.13 Scaling factor - water vapour.....   | 99 |
| 6.10.4.14 Scaling factor - photosynthetically active radiation.....                                      | 99 |
| 6.10.4.15 Scaling factor - TOA vegetation index.....   | 99 |
| 6.10.4.16 Scaling factor - BOA vegetation index.....   | 99 |
| 6.10.4.17 Scaling factor - cloud albedo.....   | 99 |
| 6.10.4.18 Scaling factor - cloud top pressure.....   | 99 |
| 6.10.4.19 Offset - reflectances.....   | 99 |
| 6.10.4.20 Offset - algal pigment index.....  | 99 |
| 6.10.4.21 Offset - yellow substance.....   | 99 |
| 6.10.4.22 Offset - suspended sediments.....  | 99 |
| 6.10.4.23 Offset - aerosol Angstroem exponent.....   | 99 |
| 6.10.4.24 Offset - aerosol optical thickness.....  | 99 |
| 6.10.4.25 Offset - cloud optical thickness.....  | 99 |
| 6.10.4.26 Offset - surface pressure.....   | 99 |
| 6.10.4.27 Offset - water vapour.....   | 99 |
| 6.10.4.28 Offset - photosynthetically active radiation.....  | 99 |
| 6.10.4.29 Offset - TOA vegetation index.....   | 99 |
| 6.10.4.30 Offset - BOA vegetation index.....   | 99 |
| 6.10.4.31 Offset - cloud albedo.....   | 99 |
| 6.10.4.32 Offset - cloud top pressure.....   | 99 |

|           |   |    |
|-----------|---|----|
| 6.10.4.33 | Scaling factor - rectified near-infrared reflectance .....  | 99 |
| 6.10.4.34 | Offset - rectified near-infrared reflectance.....   | 99 |
| 6.10.4.35 | Scaling factor - rectified red reflectance.....   | 99 |
| 6.10.4.36 | Offset - rectified red reflectance .....  | 99 |
| 6.10.5    | <i>GADS Smile Effect Correction</i> .....   | 99 |
| 6.10.5.1  | Square of Sun-Earth distance at reference date .....  | 99 |
| 6.10.5.2  | Array of per band switches enabling smile effect correction for land pixels reflectance.....  | 99 |
| 6.10.5.3  | Array of per band switches enabling smile effect correction for water pixels reflectance.....   | 99 |
| 6.10.5.4  | Array of pairs of band indices for estimating reflectance spectral derivative (land pixels) .....   | 99 |
| 6.10.5.5  | Array of pairs of band indices for estimating reflectance spectral derivative (water pixels) .....  | 99 |
| 6.10.5.6  | Theoretical central wavelengths of MERIS spectral bands .....   | 99 |
| 6.10.5.7  | Reference solar fluxes at theoretical central wavelengths and bandwidths.....   | 99 |
| 6.10.5.8  | MERIS RR pixels characterized wavelengths.....  | 99 |
| 6.10.5.9  | Reference solar fluxes for MERIS RR pixels.....   | 99 |
| 6.10.5.10 | MERIS FR pixels characterized wavelengths.....  | 99 |
| 6.10.5.11 | Reference solar fluxes for MERIS FR pixels.....   | 99 |
| 6.10.6    | <i>GADS Atmospheric Corrections for Case-I Waters</i> .....   | 99 |
| 6.10.6.1  | Reflectance thresholds to set the negative reflectance flag.....  | 99 |
| 6.10.6.2  | Threshold for absorbing aerosol test at 510 nm.....   | 99 |
| 6.10.6.3  | Threshold for blue aerosol test at 510 nm.....  | 99 |
| 6.10.6.4  | List of indices of aerosol assemblages.....   | 99 |
| 6.10.6.5  | Total number of ocean-aerosol assemblages .....   | 99 |
| 6.10.6.6  | Number of passes within the algorithm .....   | 99 |
| 6.10.6.7  | Number of polynomial coefficients relating ( $\rho_{\text{path}} / \rho_{\text{R}}$ ) to the aerosol optical thickness ( $\tau^{\text{a}}$ )..... | 99 |
| 6.10.6.8  | Indices of models that shall trigger the AERO_BLUE flag.....  | 99 |
| 6.10.6.9  | (Spare).....  | 99 |
| 6.10.6.10 | (Spare).....  | 99 |
| 6.10.6.11 | Maximum allowed value for aerosol optical thickness at 865 nm.....  | 99 |
| 6.10.6.12 | Threshold on depth for flagging shallow water .....   | 99 |
| 6.10.6.13 | (Spare).....  | 99 |
| 6.10.6.14 | (Spare).....  | 99 |
| 6.10.6.15 | Threshold for flagging aerosol optical thickness .....  | 99 |
| 6.10.6.16 | Switch to test for absorbing aerosols.....  | 99 |
| 6.10.6.17 | Ceiling value of solar zenith angle for modifying annotation flag.....  | 99 |
| 6.10.6.18 | (Spare).....  | 99 |
| 6.10.6.19 | Threshold for pressure correction.....  | 99 |
| 6.10.6.20 | Number of wavelengths used in the LUTs .....  | 99 |
| 6.10.6.21 | Number of aerosol models used at each pass.....   | 99 |
| 6.10.6.22 | Switch to use an aerosol climatology .....  | 99 |
| 6.10.7    | <i>GADS Classification Parameters</i> .....   | 99 |
| 6.10.7.1  | Threshold on MERIS differential snow index (MDSI).....  | 99 |
| 6.10.7.2  | Numerator band index for spectral ratio 1 .....   | 99 |
| 6.10.7.3  | Denominator band index for spectral ratio 1 .....   | 99 |
| 6.10.7.4  | Lower threshold for spectral ratio 1.....   | 99 |
| 6.10.7.5  | Upper threshold for spectral ratio 1 .....  | 99 |
| 6.10.7.6  | Numerator band index for spectral ratio 2 .....   | 99 |
| 6.10.7.7  | Denominator band index for spectral ratio 2 .....   | 99 |
| 6.10.7.8  | Lower threshold for spectral ratio 2.....   | 99 |
| 6.10.7.9  | Upper threshold for spectral ratio 2 .....  | 99 |
| 6.10.7.10 | Index of band for test on TOA reflectance (with band numbering starting at 1) .....   | 99 |
| 6.10.7.11 | Thresholds on TOA reflectance at band b_bright2.....  | 99 |
| 6.10.7.12 | Index of band for GADS threshold on Rayleigh corrected reflectance.....   | 99 |
| 6.10.7.13 | Zenith angles for GADS threshold on Rayleigh corrected reflectance .....  | 99 |
| 6.10.7.14 | Stored indices for ( $\theta_s \times \theta_v$ ) combinations for GADS threshold on Rayleigh corrected reflectance .....                         | 99 |
| 6.10.7.15 | Relative azimuth angles for GADS threshold on Rayleigh corrected reflectance.....   | 99 |
| 6.10.7.16 | Apparent pressure thresholds over land (off/close to the coastline).....  | 99 |
| 6.10.7.17 | Apparent pressure threshold over water .....  | 99 |
| 6.10.7.18 | Minimum reflectance value at 753.75 nm to consider apparent pressure over land .....  | 99 |
| 6.10.7.19 | Minimum spectral slope between 753.75 nm and 778.75 nm to consider apparent pressure over water.....  | 99 |
| 6.10.7.20 | Band indices for MDSI computation.....  | 99 |

|   |    |
|---|----|
| 6.10.8 GADS Reflectance Thresholds.....   | 99 |
| 6.10.8.1 Thresholds on Rayleigh-corrected TOA reflectance above land, $\rho_{RC\_2}(\theta_s \times \theta_v, \Delta\phi)$ .....  | 99 |
| 6.10.8.2 Thresholds on Rayleigh-corrected TOA reflectance above ocean, $\rho_{RC\_2}(\theta_s \times \theta_v, \Delta\phi)$ ..... | 99 |
| 6.11 ATMOSPHERE PARAMETERS.....   | 99 |
| 6.11.1 C.P.....   | 99 |
| 6.11.1.1 C.P. Rayleigh optical thickness, $\tau^R(\lambda, P_s)$ .....  | 99 |
| 6.11.2 MPH.....   | 99 |
| 6.11.3 SPH.....   | 99 |
| 6.11.4 GADS General.....  | 99 |
| 6.11.4.1 Rayleigh transmittance coefficients.....   | 99 |
| 6.11.4.2 Rayleigh optical thicknesses.....  | 99 |
| 6.11.4.3 Nominal wavelengths of MERIS spectral bands.....   | 99 |
| 6.11.4.4 Solar zenith angles for GADS Rayleigh reflectance over ocean.....  | 99 |
| 6.11.4.5 View zenith angles for GADS Rayleigh reflectance over ocean.....   | 99 |
| 6.11.4.6 Relative azimuth angles for GADS Rayleigh reflectances over ocean (tabulated values).....                                | 99 |
| 6.11.4.7 Zenith angles for GADS Rayleigh scattering function.....   | 99 |
| 6.11.4.8 Stored indices for $(\theta_s \times \theta_v)$ combinations for GADS Rayleigh scattering function.....                  | 99 |
| 6.11.4.9 Constants used for Rayleigh phase function (A,B).....  | 99 |
| 6.11.4.10 Air masses (downward and upward atmospheric paths).....   | 99 |
| 6.11.4.11 Reference wavelengths for GADS O2 transmittances around 778.75 nm.....  | 99 |
| 6.11.4.12 TOA normalized radiances at 778.75 nm for GADS O2 transmittances around 778.75 nm.....                                  | 99 |
| 6.11.4.13 Solar zenith angles for GADS O2 transmittances around 778.75 nm.....  | 99 |
| 6.11.4.14 View zenith angles for GADS O2 transmittances around 778.75 nm.....   | 99 |
| 6.11.4.15 Relative azimuth angles for GADS O2 transmittances around 778.75 nm.....  | 99 |
| 6.11.4.16 Threshold for flagging low pressure water.....  | 99 |
| 6.11.4.17 Standard water vapour content.....  | 99 |
| 6.11.4.18 Standard ozone content.....   | 99 |
| 6.11.4.19 Standard surface pressure.....  | 99 |
| 6.11.4.20 Wind-speeds for GADS Rayleigh reflectance over ocean.....   | 99 |
| 6.11.4.21 Maximum valid pressure.....   | 99 |
| 6.11.4.22 Angstrom exponents for ADS photosynthetically active radiation (PAR).....   | 99 |
| 6.11.4.23 Ozone contents for ADS photosynthetically active radiation (PAR).....   | 99 |
| 6.11.4.24 Aerosol optical thicknesses at 865 nm for ADS photosynthetically active radiation (PAR).....                            | 99 |
| 6.11.4.25 Water vapour contents for photosynthetically active radiation (PAR).....  | 99 |
| 6.11.4.26 Reference wavelengths for GADS apparent pressure parameters.....  | 99 |
| 6.11.4.27 Reference wavelengths for GADS polynomial coefficients for H2O transmittance retrieval at 708.75 nm.....                | 99 |
| 6.11.4.28 Pressure scale height to account for altitude.....  | 99 |
| 6.11.4.29 Zenith angles for GADS apparent pressure parameters.....  | 99 |
| 6.11.4.30 Reference pressure levels for GADS apparent pressure parameters.....  | 99 |
| 6.11.4.31 Aerosol scattering phase function.....  | 99 |
| 6.11.4.32 Fresnel reflection coefficients, FR( $\theta$ ).....  | 99 |
| 6.11.5 GADS Optical Thicknesses.....  | 99 |
| 6.11.5.1 (Spare).....   | 99 |
| 6.11.5.2 (Spare).....   | 99 |
| 6.11.5.3 (Spare).....   | 99 |
| 6.11.5.4 Rayleigh optical thicknesses for standard pressure, $\tau^R(\lambda, P_s)$ .....   | 99 |
| 6.11.5.5 Ozone optical thicknesses for 1 cm-atm, $\tau^{O_3}(\lambda)$ .....  | 99 |
| 6.11.6 GADS H2O Transmission.....   | 99 |
| 6.11.6.1 (Spare).....   | 99 |
| 6.11.6.2 Polynomial coefficients for H2O transmittance retrieval around 708.75 nm (21 shifted filters).....                       | 99 |
| 6.11.6.3 Polynomial coefficients for H2O transmittance retrieval at the 15 MERIS wavelengths.....                                 | 99 |
| 6.11.7 GADS Rayleigh Scattering Function.....   | 99 |
| 6.11.7.1 Fourier series terms of polynomial coefficients for multiplicative Rayleigh scattering function retrieval.....           | 99 |
| 6.11.8 GADS Rayleigh Spherical Albedo.....  | 99 |
| 6.11.8.1 Rayleigh spherical albedo, $S_R(\tau^R)$ .....   | 99 |
| 6.11.9 ADS O2 Transmission around 778.75 nm.....  | 99 |
| 6.11.9.1 O2 transmittances around 778.75 nm (21 shifted filters).....   | 99 |
| 6.11.10 ADS Apparent Pressure Parameters.....   | 99 |

|  |    |
|--|----|
| 6.11.10.1 O2 Rayleigh transmittances around 778.75 nm (21 shifted filters).....  | 99 |
| 6.11.10.2 O2 aerosol transmittances around 778.75 nm (21 shifted filters; Ha=2 km) .....                                     | 99 |
| 6.11.10.3 O2 aerosol Fresnel transmittances around 778.75 nm (21 shifted filters; Ha=2 km).....                              | 99 |
| 6.11.10.4 O2 atmospheric transmittances around 778.75 nm (21 shifted filters; 21 layers; Ha=2 km) .....                      | 99 |
| 6.11.11 (Spare).....   | 99 |
| 6.11.12 ADS Rayleigh Reflectance Over Ocean.....   | 99 |
| 6.11.12.1 Rayleigh reflectance over ocean.....   | 99 |
| 6.11.13 ADS Photosynthetically Active Radiation.....   | 99 |
| 6.11.13.1 Photosynthetically active radiation, PAR( $\alpha, U_{H_2O}, U_{O_3}, \tau^a$ ).....                               | 99 |
| 6.12 WATER-VAPOUR PARAMETERS .....   | 99 |
| 6.12.1 C.P.....  | 99 |
| 6.12.2 MPH.....  | 99 |
| 6.12.3 SPH.....  | 99 |
| 6.12.4 GADS General.....   | 99 |
| 6.12.4.1 Solar zenith angles.....  | 99 |
| 6.12.4.2 View zenith angles.....   | 99 |
| 6.12.4.3 Relative azimuth angles.....  | 99 |
| 6.12.4.4 Threshold value on radiance at 885 nm for marking pixel as invalid for water vapour processing.....                 | 99 |
| 6.12.4.5 Minimum threshold for out of range output value of water vapour content .....                                       | 99 |
| 6.12.4.6 Maximum threshold for out of range output value of water vapour content.....  | 99 |
| 6.12.4.7 Sun irradiances at 778.75 nm, 865 nm, 885nm and 900 nm (consistent with cloud LUTs).....                            | 99 |
| 6.12.4.8 Aerosol optical thicknesses at 885 nm.....  | 99 |
| 6.12.4.9 Surface albedos.....  | 99 |
| 6.12.4.10 Cloud optical thicknesses at 550nm.....  | 99 |
| 6.12.4.11 Wind-speeds for GADS polynomial coefficients for water vapour retrieval over ocean.....                            | 99 |
| 6.12.4.12 Latitudes for ADS surface albedo slope between 900 nm & 885 nm and ADS surface albedo at 885 nm.....               | 99 |
| 6.12.4.13 Longitudes for ADS surface albedo slope between 900 nm & 885 nm and ADS surface albedo at 885 nm.....              | 99 |
| 6.12.4.14 Offset and scaling factor for surface albedo ratio between 900 nm & 885 nm.....                                    | 99 |
| 6.12.4.15 Scaling factor for surface albedo at 885 nm.....   | 99 |
| 6.12.4.16 Bad data value for surface albedo ratio between 900 nm & 885 nm .....  | 99 |
| 6.12.4.17 Minimum valid values for neural network inputs.....  | 99 |
| 6.12.4.18 Maximum valid values for neural network inputs.....  | 99 |
| 6.12.4.19 Minimum valid value for neural network output.....   | 99 |
| 6.12.4.20 Maximum valid value for neural network output.....   | 99 |
| 6.12.5 GADS Neural Network for Water-Vapour Retrieval over Land.....   | 99 |
| 6.12.5.1 Neural network (NN) parameters for water vapour retrieval over land.....  | 99 |
| 6.12.6 ADS Polynomial Coefficients for Water-Vapour Retrieval over Ocean (without Sun Glint).....                            | 99 |
| 6.12.6.1 Polynomial coefficients for water vapour retrieval over ocean (no glint).....                                       | 99 |
| 6.12.7 (Deleted).....  | 99 |
| 6.12.8 ADS Polynomial Coefficients for Water-Vapour Retrieval over Clouds.....   | 99 |
| 6.12.8.1 Polynomial coefficients for water vapour retrieval over clouds.....   | 99 |
| 6.12.9 ADS Surface Albedo Slope between 900 nm and 885 nm.....   | 99 |
| 6.12.9.1 Surface albedo slope between 900 nm and 885 nm.....   | 99 |
| 6.12.10 ADS Aerosol Corrections.....   | 99 |
| 6.12.10.1 Polynomial coefficients for aerosol corrections at 885 nm.....   | 99 |
| 6.12.11 ADS Surface Albedo at 885 nm.....  | 99 |
| 6.12.11.1 Surface albedo map at 885 nm.....  | 99 |
| 6.13 OCEAN-AEROSOL PARAMETERS .....  | 99 |
| 6.13.1 C.P.....  | 99 |
| 6.13.1.1 C.P. AOT at 550 nm (boundary layer) for all ocean-aerosol assemblages, $\tau_{\square}^{a1}(iaer, itau)$ .....      | 99 |
| 6.13.1.2 C.P. AOT at 550 nm (dust layer) for all ocean-aerosol assemblages, $\tau_{\square}^{a2}(iaer, itau)$ .....          | 99 |
| 6.13.1.3 C.P. AOT at 550 nm (troposphere layer) for all ocean-aerosol assemblages, $\tau_{\square}^{a3}(iaer, itau)$ .....   | 99 |
| 6.13.1.4 C.P. FUB-scattering phase matrices and IOPs for all the aerosol models.....   | 99 |
| 6.13.1.5 C.P. UdL-scattering phase matrices and IOPs for all the aerosol models.....   | 99 |
| 6.13.1.6 C.P. TOA normalized radiances, $L_{TOA}(\lambda, \theta_s, \theta_v, \Delta\phi)$ .....                             | 99 |
| 6.13.1.7 C.P. FUB total and Rayleigh optical thicknesses, $\tau(iaer, type, itau, iband)$ .....                              | 99 |
| 6.13.1.8 C.P. Spectral dependence of the AOT (without normalization at reference wavelength), $f(iaer, \lambda, itau)$ ..... | 99 |
| 6.13.2 MPH.....  | 99 |

|   |    |
|---|----|
| 6.13.3 SPH.....   | 99 |
| 6.13.4 GADS General.....  | 99 |
| 6.13.4.1 Nominal wavelengths of the 15 MERIS spectral bands.....  | 99 |
| 6.13.4.2 (Spare).....   | 99 |
| 6.13.4.3 Solar zenith angles.....   | 99 |
| 6.13.4.4 View zenith angles.....  | 99 |
| 6.13.4.5 Relative azimuth angles.....   | 99 |
| 6.13.4.6 Wind-speeds.....   | 99 |
| 6.13.4.7 Vicarious adjustment gains.....  | 99 |
| 6.13.4.8 (spare).....   | 99 |
| 6.13.5 GADS Spectral Optical Thickness.....   | 99 |
| 6.13.5.1 Spectral dependence factor of the total AOT (with normalization at reference wavelength).....                                | 99 |
| 6.13.6 GADS Aerosol Optical Thickness at 865 nm.....  | 99 |
| 6.13.6.1 Aerosol optical thickness at 865 nm, $\tau_{865}^a(\text{iaer}, \tau^a)$ .....   | 99 |
| 6.13.7 GADS Aerosol Single Scattering Albedo.....   | 99 |
| 6.13.7.1 Aerosol single scattering albedo, $\omega_o^a(\text{iaer}, \lambda)$ .....   | 99 |
| 6.13.8 GADS Aerosol Forward Scattering Proportion.....  | 99 |
| 6.13.8.1 Aerosol forward scattering proportion, $fp^a(\text{iaer}, \lambda)$ .....  | 99 |
| 6.13.9 GADS Blue TOA Reflectance Threshold - ROGC.....  | 99 |
| 6.13.9.1 Threshold on the glint corrected blue TOA reflectance $\rho_{GC}(412.5)$ .....   | 99 |
| 6.13.10 ADS Coefficients of $\rho_T/\rho_R$ to $\tau_a$ Relation.....   | 99 |
| 6.13.10.1 Polynomial coefficients for $(\rho_T / \rho_R)$ to total AOT relationship.....  | 99 |
| 6.13.11 ADS Transmittances.....   | 99 |
| 6.13.11.1 Total downward transmittance (direct+diffuse).....  | 99 |
| 6.13.11.2 Total upward transmittance (direct+diffuse).....  | 99 |
| 6.14 LAND-AEROSOL PARAMETERS.....   | 99 |
| 6.14.1 C.P.....   | 99 |
| 6.14.1.1 C.P. Imaginary parts of refractive indices for land-aerosol models.....  | 99 |
| 6.14.2 MPH.....   | 99 |
| 6.14.3 SPH.....   | 99 |
| 6.14.4 GADS General.....  | 99 |
| 6.14.4.1 Zenith angles.....   | 99 |
| 6.14.4.2 Stored indices for $(\theta_s, \theta_v)$ combinations.....  | 99 |
| 6.14.4.3 Relative azimuth angles.....   | 99 |
| 6.14.4.4 Cosine of scattering angles.....   | 99 |
| 6.14.4.5 Indices of band numbers (starting from 1) for in-land waters and islands screening.....                                      | 99 |
| 6.14.4.6 Threshold for in-land waters screening spectral slope test.....  | 99 |
| 6.14.4.7 Threshold for islands screening spectral slope test.....   | 99 |
| 6.14.4.8 Aerosol optical properties (real part of refractive index, Angstrom exponent) for land-aerosol models.....                   | 99 |
| 6.14.4.9 Aerosol optical thicknesses at 550 nm.....   | 99 |
| 6.14.4.10 Gamma coefficient for ARVI computation.....   | 99 |
| 6.14.4.11 Aerosol optical thickness increment for iterative procedure.....  | 99 |
| 6.14.4.12 Dense dark vegetation, DDV(biome,month).....  | 99 |
| 6.14.4.13 Latitudes for DDV climatology.....  | 99 |
| 6.14.4.14 Longitudes for DDV climatology.....   | 99 |
| 6.14.4.15 Effective radius values.....  | 99 |
| 6.14.4.16 Record numbers of GADS multiplicative function to account for volcanic aerosol multiple scattering effects.....             | 99 |
| 6.14.4.17 Volcanic aerosol optical thicknesses, $\tau^{va}(\text{iaer})$ .....  | 99 |
| 6.14.4.18 Reflectance threshold at 865 nm for DDV screening.....  | 99 |
| 6.14.4.19 Ground reflectance threshold at 665 nm for iterative aerosol identification.....  | 99 |
| 6.14.4.20 List of band indices (starting from 1) to be used for land aerosols remote sensing.....                                     | 99 |
| 6.14.5 GADS Reflectance Thresholds for Inland Waters and Islands Screening.....   | 99 |
| 6.14.5.1 $\alpha$ - Constant applied to threshold for inland waters screening.....  | 99 |
| 6.14.5.2 TOA reflectance thresholds at 665 nm for inland waters screening, $\rho_{T,665}(\theta_s \times \theta_v, \Delta\phi)$ ..... | 99 |
| 6.14.5.3 $\alpha$ - Constant applied to threshold for islands screening.....  | 99 |
| 6.14.5.4 TOA reflectance thresholds at 865 nm for islands screening, $\rho_{T,865}(\theta_s \times \theta_v, \Delta\phi)$ .....       | 99 |
| 6.14.5.5 Altitude threshold above which in-land waters screening is disabled.....   | 99 |
| 6.14.6 ADS ARVI Thresholds for DDV models.....  | 99 |



|  |    |
|--|----|
| 6.14.6.1 ARVI thresholds used for DDV models, $ARVI\_thresh(iddv, \theta_s \times \theta_v, \Delta\phi)$ .....                                   | 99 |
| 6.14.7 ADS Standard Surface Reflectance Ranges for DDV Models .....  | 99 |
| 6.14.7.1 Mean DDV reflectances for 412.5 nm, 442.5 nm, 490 nm and 665 nm, $\rho_{DDV\_mean}(iaer, \lambda)$ .....                                | 99 |
| 6.14.8 ADS Aerosol Spherical Albedo .....  | 99 |
| 6.14.8.1 Aerosol spherical albedo, $S_a(iaer, \tau^a)$ .....   | 99 |
| 6.14.9 ADS Aerosol Transmittance .....   | 99 |
| 6.14.9.1 Aerosol transmittance, $T_a(iaer, \theta_s, \tau^a)$ .....  | 99 |
| 6.14.10 ADS Multiplicative Function to account for Aerosol Multiple Scattering Effects .....   | 99 |
| 6.14.10.1 Fourier series terms of polynomial coefficients for multiplicative aerosol scattering function retrieval .....                         | 99 |
| 6.14.11 ADS Aerosol Phase Function times Single Scattering Albedo .....  | 99 |
| 6.14.11.1 Aerosol phase function times single scattering albedo, $\omega_o^a(iaer).P_a(iaer, \cos\Theta)$ .....                                  | 99 |
| 6.14.12 ADS Volcanic Aerosol Spherical Albedo .....  | 99 |
| 6.14.12.1 Volcanic aerosol spherical albedo, $S_{va}(iaer, \lambda)$ .....   | 99 |
| 6.14.13 ADS Volcanic Aerosol Transmittance .....   | 99 |
| 6.14.13.1 Volcanic aerosol transmittance, $T_{va}(iaer, \lambda, \theta_s)$ .....  | 99 |
| 6.14.14 ADS Volcanic Aerosol Reflectance .....   | 99 |
| 6.14.14.1 Volcanic aerosol phase function times single scattering albedo, $\omega_o^{va}(iaer, \lambda).P_{va}(iaer, \lambda, \cos\Theta)$ ..... | 99 |
| 6.14.14.2 Spectral dependence of the volcanic aerosol optical thickness (with normalization at reference wavelength) .....                       | 99 |
| 6.14.15 GADS Dense Dark Vegetation Climatology .....   | 99 |
| 6.14.15.1 Biome index, $DDV\_clim(lat, long)$ .....  | 99 |
| 6.14.16 ADS DDV Parameters for Bidirectionality Correction .....   | 99 |
| 6.14.16.1 Rayleigh-ground DDV coupling bidirectionality term, $\bar{\rho}_{RG}(iddv, \lambda, \theta_v)$ .....                                   | 99 |
| 6.14.16.2 Aerosol-ground DDV coupling bidirectionality term, $\bar{\rho}_{aG}(iddv, \lambda, iaer, \theta_s \times \theta_v, s)$ .....           | 99 |
| 6.14.16.3 Ground DDV albedo, $\rho_{DDV}(iddv, \lambda)$ .....   | 99 |
| 6.14.17 ADS Aerosol Parameters for Bi-Directionality Correction .....  | 99 |
| 6.14.17.1 Polynomial coefficients for aerosol-molecule coupling bidirectionality term retrieval .....  | 99 |
| 6.14.17.2 (Spare) .....  | 99 |
| 6.14.18 ADS DDV Reflectance Correction Parameters .....  | 99 |
| 6.14.18.1 Monthly adjustment for bands at 412.5 nm, 442.5 nm, 490 nm & 665 nm, $C(month, lat, long, band)$ .....                                 | 99 |
| 6.14.18.2 Linear corrections for bands at 412.5 nm, 442.5 nm, 490 nm & 665 nm, $LC(month, lat, long, band)$ .....                                | 99 |
| 6.14.18.3 Minimum and maximum seasonal variation of ARVI, $[\Delta ARVI_{min}, \Delta ARVI_{max}](month, DDV model)$ .....                       | 99 |
| 6.15 OCEAN CASE-I PARAMETERS .....   | 99 |
| 6.15.1 C.P. .....  | 99 |
| 6.15.1.1 C.P. Extinction coefficient and single scattering albedo for chlorophyll .....  | 99 |
| 6.15.2 MPH .....   | 99 |
| 6.15.3 SPH .....   | 99 |
| 6.15.4 GADS General .....  | 99 |
| 6.15.4.1 Wind-speeds for GADS geometrical factor $R_{goth}$ .....  | 99 |
| 6.15.4.2 Wavelengths for ADS $f_1/Q$ .....   | 99 |
| 6.15.4.3 Solar zenith angles for ADS $f_1/Q$ .....   | 99 |
| 6.15.4.4 Solar zenith angles for GADS thresholds and ADS glint reflectance .....   | 99 |
| 6.15.4.5 Zenith angles in water for ADS $f_1/Q$ .....  | 99 |
| 6.15.4.6 Zenith angles in water for GADS geometrical factor $R_{goth}$ .....   | 99 |
| 6.15.4.7 View zenith angles for GADS thresholds and ADS glint reflectance .....  | 99 |
| 6.15.4.8 Relative azimuth angles for ADS $f_1/Q$ .....   | 99 |
| 6.15.4.9 Relative azimuth angles for GADS thresholds and ADS glint reflectance .....   | 99 |
| 6.15.4.10 Chlorophyll contents for ADS $f_1/Q$ .....   | 99 |
| 6.15.4.11 Aerosol optical thicknesses for ADS $f_1/Q$ .....  | 99 |
| 6.15.4.12 Wind-speeds for ADS $f_1/Q$ .....  | 99 |
| 6.15.4.13 Initial algal pigment index value for ADS $f_1/Q$ .....  | 99 |
| 6.15.4.14 $C_i$ constants for downward atmospheric transmittance .....   | 99 |
| 6.15.4.15 $C_7$ constant for scattering detection .....  | 99 |
| 6.15.4.16 Factor relating $b_p/a$ to reflectance just below water surface for a sun at zenith .....  | 99 |
| 6.15.4.17 Wind-speeds for GADS glint reflectance .....   | 99 |
| 6.15.4.18 Wind azimuth orientations for GADS glint reflectance .....   | 99 |
| 6.15.4.19 (Spare) .....  | 99 |

|           |  |    |
|-----------|--|----|
| 6.15.4.20 | Value of $f/Q$ factor for a nadir viewing angle at 510 nm                                      | 99 |
| 6.15.4.21 | Mean value of chlorophyll content  | 99 |
| 6.15.4.22 | Water refractive index   | 99 |
| 6.15.4.23 | Value of $\Delta\rho_{510}$ to set the annotation flag   | 99 |
| 6.15.4.24 | Value of the scattering angle $\Theta_p$ for a nadir viewing                                   | 99 |
| 6.15.4.25 | Scaling factor for decoding mean value of water-leaving reflectance at 510 nm                  | 99 |
| 6.15.4.26 | Offset for decoding mean value of water-leaving reflectance at 510nm                           | 99 |
| 6.15.4.27 | Scaling factor for decoding variability value of water-leaving reflectance at 510nm            | 99 |
| 6.15.4.28 | Offset for decoding variability value of water-leaving reflectance at 510nm                    | 99 |
| 6.15.4.29 | Latitudes for mean values of water-leaving reflectance at 510nm                                | 99 |
| 6.15.4.30 | Longitudes for water-leaving reflectance mean values at 510nm (tabulated values)               | 99 |
| 6.15.4.31 | Chlorophyll contents for ADS $f_0$ factor  | 99 |
| 6.15.5    | <i>GADS Geometrical factor <math>R_{goth}</math></i>   | 99 |
| 6.15.5.1  | Geometrical factor $R_{goth}(\theta', w_s)$  | 99 |
| 6.15.6    | <i>GADS Thresholds</i>   | 99 |
| 6.15.6.1  | Threshold on water reflectance at 560 nm for input validity                                    | 99 |
| 6.15.6.2  | Chlorophyll content range (thresholds) for output validity                                     | 99 |
| 6.15.6.3  | (Spare)  | 99 |
| 6.15.6.4  | (Spare)  | 99 |
| 6.15.6.5  | Low glint threshold  | 99 |
| 6.15.6.6  | Medium glint threshold   | 99 |
| 6.15.6.7  | Wind-speed threshold for whitecaps flagging  | 99 |
| 6.15.6.8  | Reflectance thresholds at 708.75 nm for turbid water identification                            | 99 |
| 6.15.6.9  | Water vapour high glint threshold  | 99 |
| 6.15.6.10 | Shallow water depth threshold  | 99 |
| 6.15.7    | <i>GADS Log10 polynomial coefficients</i>  | 99 |
| 6.15.7.1  | Log10 polynomial coefficients for 443, 490 and 510 nm  | 99 |
| 6.15.7.2  | Convergence criterium for iterative chlorophyll retrieval                                      | 99 |
| 6.15.7.3  | Irradiance reflectance ratio validity range for algal1 computation using log10 polynomials     | 99 |
| 6.15.7.4  | Highest order of log10 polynomial coefficients used in the Case-1 waters algorithm             | 99 |
| 6.15.7.5  | Bands selected for computation of chlorophyll content (Chl1) (band number starting at 1)       | 99 |
| 6.15.8    | <i>ADS <math>f/Q</math> Factor</i>   | 99 |
| 6.15.8.1  | $f/Q$ factor   | 99 |
| 6.15.9    | <i>ADS Glint reflectance</i>   | 99 |
| 6.15.9.1  | Glint reflectance  | 99 |
| 6.15.10   | <i>ADS Mean water-leaving reflectance at 510nm</i>   | 99 |
| 6.15.10.1 | Mean value of water-leaving reflectance at 510 nm, $\rho_{510\_mean}(\text{month, lat, long})$ | 99 |
| 6.15.10.2 | Variability of water-leaving reflectance at 510 nm, $\rho_{510\_var}(\text{month, lat, long})$ | 99 |
| 6.15.11   | <i>GADS <math>f_0</math> factor</i>  | 99 |
| 6.15.11.1 | Factor $f_0$   | 99 |
| 6.16      | <i>OCEAN CASE-II PARAMETERS</i>  | 99 |
| 6.16.1    | <i>C.P.</i>  | 99 |
| 6.16.2    | <i>MPH</i>   | 99 |
| 6.16.3    | <i>SPH</i>   | 99 |
| 6.16.4    | <i>GADS General</i>  | 99 |
| 6.16.4.1  | Wavelengths (tabulated values)   | 99 |
| 6.16.4.2  | Number of polynomial coefficients in $F_p$ computation   | 99 |
| 6.16.4.3  | Wind-speeds for ADS $F_p$ factor   | 99 |
| 6.16.4.4  | View zenith angles for ADS $F_p$ factor  | 99 |
| 6.16.4.5  | Solar zenith angles for ADS $F_p$ factor   | 99 |
| 6.16.4.6  | Relative azimuth angles for ADS $F_p$ factor   | 99 |
| 6.16.4.7  | View zenith angles for GADS anomalous scattering detection                                     | 99 |
| 6.16.4.8  | Solar zenith angles for GADS anomalous scattering detection                                    | 99 |
| 6.16.4.9  | Relative azimuth angles for GADS anomalous scattering detection                                | 99 |
| 6.16.4.10 | Conversion factors for Chl2  | 99 |
| 6.16.4.11 | Conversion factors for SPM   | 99 |
| 6.16.4.12 | Absorption coefficients of pure water  | 99 |
| 6.16.4.13 | Backscattering coefficients of pure water  | 99 |
| 6.16.4.14 | Specific backscattering coefficients of coccoliths   | 99 |

|           |  |    |
|-----------|--|----|
| 6.16.4.15 | Specific backscattering coefficients of SPM .....  | 99 |
| 6.16.4.16 | Number of iterations in bright pixel atmospheric correction for band set LOW and band set HIGH .....   | 99 |
| 6.16.4.17 | Threshold value on total suspended particulate matters to raise CASE2_S flag .....   | 99 |
| 6.16.4.18 | Convergence criteria on bbp in the BPAC iterations .....   | 99 |
| 6.16.4.19 | Convergence criteria on bb in the rhow_to_bb routine .....   | 99 |
| 6.16.4.20 | Number of iterations in the rhow_to_bb routine .....   | 99 |
| 6.16.4.21 | Specific absorption coefficients of coccoliths .....   | 99 |
| 6.16.4.22 | Specific absorption coefficients of SPM .....  | 99 |
| 6.16.4.23 | Initial estimate of backscatters at 778.75 nm for the LOW and HIGH band estimates .....  | 99 |
| 6.16.4.24 | Initial estimate of the Angstrom exponent .....  | 99 |
| 6.16.4.25 | Threshold on water-leaving reflectance at 778.75 nm to activate the HIGH band set .....  | 99 |
| 6.16.4.26 | Threshold on water-leaving reflectance at 778.75 nm to deactivate the LOW band set .....   | 99 |
| 6.16.4.27 | Minimum TOA normalized radiance measurable at 708.75 nm .....  | 99 |
| 6.16.4.28 | bbp value to initialize the rhow_to_bb routine .....   | 99 |
| 6.16.4.29 | Threshold for flagging yellow substance dominated waters .....   | 99 |
| 6.16.4.30 | Chl values for GADS anomalous scattering detection .....   | 99 |
| 6.16.4.31 | Floor values for NN inputs [reflectance threshold, floor NN input] .....   | 99 |
| 6.16.4.32 | Threshold for white scatterers detection .....   | 99 |
| 6.16.5    | <i>GADS Case II Yellow Substance Detection Coefficients</i> .....  | 99 |
| 6.16.5.1  | B <sub>i</sub> constants .....   | 99 |
| 6.16.5.2  | A <sub>i</sub> constants for H(443 nm, 560 nm) estimation .....  | 99 |
| 6.16.5.3  | A <sub>i</sub> constants for H(490 nm, 560 nm) estimation .....  | 99 |
| 6.16.5.4  | A <sub>i</sub> constants for H(510 nm, 560 nm) estimation .....  | 99 |
| 6.16.5.5  | Ni exponents .....   | 99 |
| 6.16.6    | <i>GADS Anomalous Scattering Detection</i> .....   | 99 |
| 6.16.6.1  | Threshold on reflectance at 560nm .....  | 99 |
| 6.16.7    | <i>GADS Coefficient of F' Factor to IOPs Relation</i> .....  | 99 |
| 6.16.7.1  | Coefficients of F <sub>p</sub> factor to IOPs relation for 4 wind-speeds .....   | 99 |
| 6.16.8    | <i>GADS CASE-II Water Neural Network Parameters</i> .....  | 99 |
| 6.16.8.1  | Case-2 waters neural network parameters .....  | 99 |
| 6.16.8.2  | Switch for reflectance log-scaling .....   | 99 |
| 6.17      | CLOUD PARAMETERS .....   | 99 |
| 6.17.1    | <i>C.P.</i> .....  | 99 |
| 6.17.1.1  | C.P. Normalized TOA radiances, L <sub>TOA</sub> (λ, θ <sub>s</sub> , θ <sub>v</sub> , Δφ) .....  | 99 |
| 6.17.1.2  | C.P. Cloud spherical albedos, Calb(θ <sub>s</sub> ) .....  | 99 |
| 6.17.2    | <i>MPH</i> .....   | 99 |
| 6.17.3    | <i>SPH</i> .....   | 99 |
| 6.17.4    | <i>GADS General</i> .....  | 99 |
| 6.17.4.1  | Latitudes for ADS surface albedo at 761.875 nm .....   | 99 |
| 6.17.4.2  | Longitudes for ADS surface albedo at 761.875 nm .....  | 99 |
| 6.17.4.3  | Solar zenith angles for ADS polynomial coefficients for cloud albedo retrieval & for ADS polynomial coefficients for cloud optical thickness retrieval .....     | 99 |
| 6.17.4.4  | View zenith angles for ADS polynomial coefficients for cloud albedo retrieval & for ADS polynomial coefficients for cloud optical thickness retrieval .....      | 99 |
| 6.17.4.5  | Relative azimuth angles for ADS polynomial coefficients for cloud albedo retrieval & for ADS polynomial coefficients for cloud optical thickness retrieval ..... | 99 |
| 6.17.4.6  | Surface albedos for ADS polynomial coefficients for cloud albedo retrieval & for ADS polynomial coefficients for cloud optical thickness retrieval .....         | 99 |
| 6.17.4.7  | Surface albedo scaling factor .....  | 99 |
| 6.17.4.8  | Cloud top pressure neural network solar flux at 753.75 nm & for the 761.875 nm / 753.75 nm ratio .....   | 99 |
| 6.17.4.9  | Minimum acceptable radiance value for TOA reflectance at 753.75 nm .....   | 99 |
| 6.17.4.10 | Maximum acceptable radiance value for TOA reflectance at 753.75 nm .....   | 99 |
| 6.17.4.11 | Minimum acceptable radiance value for TOA reflectance at 761.875 nm .....  | 99 |
| 6.17.4.12 | Maximum acceptable radiance value for TOA reflectance at 761.875 nm .....  | 99 |
| 6.17.4.13 | Switch to use spectral shift index .....   | 99 |
| 6.17.4.14 | FR-band#11 wavelengths for surface pressure neural network .....   | 99 |
| 6.17.4.15 | RR-band#11 wavelengths for surface pressure neural network .....   | 99 |
| 6.17.4.16 | FR residual stray-light correction factor .....  | 99 |
| 6.17.4.17 | RR residual stray-light correction factor .....  | 99 |

|           |  |    |
|-----------|--|----|
| 6.17.4.18 | Minimum acceptable value for surface albedo .....  | 99 |
| 6.17.4.19 | Maximum acceptable value for surface albedo.....   | 99 |
| 6.17.4.20 | Cloud top pressures (CTP) for ADS cloud type index.....  | 99 |
| 6.17.4.21 | Cloud optical thicknesses (CTP) for ADS cloud type index.....  | 99 |
| 6.17.4.22 | Number of cloud top pressures .....  | 99 |
| 6.17.4.23 | Number of cloud optical thicknesses.....   | 99 |
| 6.17.4.24 | Solar flux at 753.75 nm for cloud LUTs.....  | 99 |
| 6.17.4.25 | Minimum valid values for surface pressure neural network inputs .....  | 99 |
| 6.17.4.26 | Maximum valid values for surface pressure neural network inputs.....   | 99 |
| 6.17.4.27 | Minimum valid value for surface pressure neural network output.....  | 99 |
| 6.17.4.28 | Maximum valid value for surface pressure neural network output.....  | 99 |
| 6.17.4.29 | Default AOT value for surface pressure neural network .....  | 99 |
| 6.17.4.30 | Maximum allowed surface pressure difference .....  | 99 |
| 6.17.5    | <i>GADS Surface Albedo</i> .....   | 99 |
| 6.17.5.1  | Surface albedo at 761.875 nm, $S_{alb}(month,latitude,longitude)$ .....  | 99 |
| 6.17.6    | <i>ADS Polynomial Coefficients for Cloud Albedo Retrieval</i> .....  | 99 |
| 6.17.6.1  | Polynomial coefficients for cloud albedo retrieval.....  | 99 |
| 6.17.7    | <i>ADS Polynomial Coefficients for Cloud Optical Thickness Retrieval</i> .....   | 99 |
| 6.17.7.1  | Polynomial coefficients for cloud optical thickness retrieval.....   | 99 |
| 6.17.8    | <i>GADS Cloud Top Pressure Neural Network for not null Surface Albedo</i> .....  | 99 |
| 6.17.8.1  | Cloud top pressure neural network for not null surface albedo .....  | 99 |
| 6.17.9    | <i>GADS Cloud Top Pressure Neural Network for null Surface Albedo</i> .....  | 99 |
| 6.17.9.1  | Cloud top pressure neural network for null surface albedo .....  | 99 |
| 6.17.10   | <i>GADS Cloud type index</i> .....   | 99 |
| 6.17.10.1 | Cloud type index.....  | 99 |
| 6.17.11   | <i>GADS Surface Pressure Neural Network Parameters</i> .....   | 99 |
| 6.17.11.1 | Surface pressure neural network.....   | 99 |
| 6.18      | LAND VEGETATION INDEX PARAMETERS .....   | 99 |
| 6.18.1    | <i>C.P.</i> .....  | 99 |
| 6.18.2    | <i>MPH</i> .....   | 99 |
| 6.18.3    | <i>SPH</i> .....   | 99 |
| 6.18.4    | <i>GADS General</i> .....  | 99 |
| 6.18.4.1  | Blue wavelength band number for TOA-VI computation .....   | 99 |
| 6.18.4.2  | Red wavelength band number for TOA-VI computation.....   | 99 |
| 6.18.4.3  | Near-infrared wavelength band number for TOA-VI computation .....  | 99 |
| 6.18.4.4  | $K_i$ normalization parameters for blue, red & NIR bands and for vegetated & bright soils .....                        | 99 |
| 6.18.4.5  | $\Theta_i$ normalization parameters for blue, red & NIR bands and for vegetated & bright soils.....                    | 99 |
| 6.18.4.6  | $\rho_i$ normalization parameters for blue, red & NIR bands and for vegetated & bright soils .....                     | 99 |
| 6.18.4.7  | Maximum reflectances for blue, red and NIR bands used in TOA-VI computation.....                                       | 99 |
| 6.18.4.8  | Polynomial coefficients for blue, red and NIR bands for TOA-VI computation .....                                       | 99 |
| 6.18.4.9  | Infrared to NIR reflectance ratio threshold for TOA-VI computation .....   | 99 |
| 6.18.4.10 | Red wavelength band number for BOA-VI computation .....  | 99 |
| 6.18.4.11 | Near-infrared wavelength band #1 for BOA-VI computation .....  | 99 |
| 6.18.4.12 | Near-infrared wavelength band #2 for BOA-VI computation .....  | 99 |
| 6.18.4.13 | Near-infrared wavelength band #3 for BOA-VI computation .....  | 99 |
| 6.18.4.14 | BOA-VI acceptable range .....  | 99 |
| 6.18.4.15 | Maximum value of top of aerosol reflectance in red band to allow the MTCI computation.....                             | 99 |
| 6.18.4.16 | Minimum value of top of aerosol reflectance in NIR band#2 for MTCI.....  | 99 |
| 6.18.4.17 | Minimum value of top of aerosol reflectance difference between NIR#1 and red bands to allow the MTCI computation ..... | 99 |
| 6.18.4.18 | Minimum value of top of aerosol reflectance difference between NIR#3 and red bands to allow the MTCI computation.....  | 99 |

## DOCUMENT CHANGE RECORD

| <i>Issue</i> | <i>Rev.</i> | <i>Date</i>   | <i>Chapter/Paragraph Number, Change Description (and Reasons)</i>   |
|--------------|-------------|---------------|---|
| Draft        | -           | Nov. 14, 1997 | - Draft release of the document.  |
| 1            | -           | Feb. 20, 1998 | - Release of the first issue of the document.   |
| 1            | A           | Apr. 29, 1998 | - Updated revision following the discussions and comments from the FUB and LISE institutes. Most of modifications were made inside the sections keeping the same structure.   |
| 1            | B           | Feb. 10, 2000 | - Updated revision for MERISAT v1.0 draft.  |
| 2            | -           | Feb. 02, 2001 | - Changes are related to the requests in the documents:<br>. TOS-EMS/00-45/jcd (23/05/2000), 1 <sup>st</sup> list of comments in Issue 1b,<br>. TOS-EMS/00-49/jcd (25/05/2000), 2 <sup>nd</sup> list of comments in Issue 1b.                           |
| 2            | A           | June 08, 2001 | - Implemented changes from:<br>. Ludovic Bourg's mail (12/03/01)<br>. Ludovic Bourg's mail (22/05/01)<br>. Fax EMS/01-36/jcd (08/06/01)<br>- Sections have been changed to match as much as possible with IODD  |
| 2            | B           | Dec. 15, 2002 | - Implemented changes from:<br>. Ludovic Bourg's mail (24/08/01)<br>. Error in LUT Polynomial coefficients for O2 correction (Section 6.11.6, field#1)<br>. Comments from Jean-Claude Debruyne's mail (26/11/02)<br>⇒ Version in-line with MERISAT v1.2 |
| 2            | C           | July 18, 2003 | - Some change implemented with IODD v6.1.   |
| 2            | D           | Oct. 31, 2003 | - Complete revision of the document<br>- All changes implemented with IODD v6.1<br>⇒ Version in-line with MERISAT v1.3  |
| 2            | E           | May 14, 2004  | - Changes implemented with IODD v7.2<br>⇒ Version in-line with MERISAT v1.4   |
| 2            | F           | Nov 30, 2005  | - Version in-line with IODD v7.2 and MERISAT v1.5<br>- LUT-122 is now provided by ACRI.   |

| <i>Issue</i> | <i>Rev.</i> | <i>Date</i>   | <i>Chapter/Paragraph Number, Change Description (and Reasons)</i>  |
|--------------|-------------|---------------|--|
| 3            | -           | July 16, 2009 | <ul style="list-style-type: none"> <li>- Upgrade MERISAT v1.5 into v2.0 by including updated and optimized RTCs. New tool is in line with IODD v7.3a.</li> <li>- Main changes in the LUT recipes:               <ul style="list-style-type: none"> <li>• LUT303: Use of MAR90 assemblage (<i>iaer#3</i>) and a wind-speed of 5m/s to generate the TOA normalized radiances over a wind-roughened reflective sea surface.</li> <li>• LUTs for Ocean-Aerosol parameters: New definition of aerosol assemblages over ocean and set of aerosol optical thickness at 550nm in the 3 aerosol layers (<i>i.e.</i>, boundary, tropospheric, stratospheric layers).</li> <li>• LUTs for Cloud parameters (LUT220 &amp; 223): Polynomial fits for retrieving the cloud albedo and the cloud optical thickness are estimated on TOA normalized radiances computed for a spectral extraterrestrial solar irradiance (<math>E_o</math>) of <math>1 W.m^{-2}.\mu m^{-1}</math>.</li> <li>• LUTs for Water-Vapor parameters (LUT121, 122, 123, 124, 125): All these LUTs, which are for now generated by the FUB (Freie Universität of Berlin, Germany) institute, are provided by ACRI.</li> </ul> </li> </ul> |
| 3            | A           | July 21, 2009 | <ul style="list-style-type: none"> <li>- Additional wind-speed in atmospheric LUTs over ocean: Use of a new set of 3 wind-speeds (1.5, 5.0 &amp; 10 m/s):               <ul style="list-style-type: none"> <li>• LUT110: <i>Rayleigh</i> reflectance over ocean.</li> <li>• LUT143: Polynomial coefficients for (rhoT/rhoR) to AOT relation.</li> </ul> </li> <li>- New complementary recipes for generating atmospheric LUTs over ocean with RTC/UPRAD (SO), by including polarization processes:               <ul style="list-style-type: none"> <li>• LUT110: <i>Rayleigh</i> reflectance over ocean.</li> <li>• LUT138: Spectral dependence of the AOT.</li> <li>• LUT139: Aerosol optical thickness at 865 nm.</li> <li>• LUT140: Aerosol single scattering albedo.</li> <li>• LUT141: Aerosol forward scattering proportion.</li> <li>• LUT143: Polynomial coefficients for (rhoT/rhoR) to AOT relation.</li> </ul> </li> <li>- MERISAT tool in line with IODD v8.0.</li> </ul>   |

| <i>Issue</i> | <i>Rev.</i> | <i>Date</i>   | <i>Chapter/Paragraph Number, Change Description (and Reasons)</i>   |
|--------------|-------------|---------------|---|
| 3            | B           | Jan. 19, 2011 | <ul style="list-style-type: none"> <li>- Main changes in the LUT recipes:               <ul style="list-style-type: none"> <li>• LUTs for Atmosphere parameters:                   <ul style="list-style-type: none"> <li>- remove previous LUT103 &amp; LUT104 (Thresholds on absolute difference in pressure for Cloud/Bright surfaces discrimination over land &amp; over ocean).</li> <li>- replace previous LUT099 and (21 sets of polynomial coefficients for O2 transmittance retrieval at 778.75 nm) and previous LUT105 (21 set of polynomial coefficients for surface pressure retrieval) by 5 new LUTs generated at FUB, and provided by ACRI :                       <ul style="list-style-type: none"> <li>LUT099: O2 transmittances around 778.75 nm (21 shifted filters)</li> <li>LUT103: O2 Rayleigh transmittances around 778.75 nm</li> <li>LUT104: O2 aerosol transmittances around 778.75 nm, with <math>H_a=2</math> km</li> <li>LUT105: O2 aero. <i>Fresnel</i> transmittances around 778.75 nm, with <math>H_a=2</math> km</li> <li>LUT107: O2 atmospheric transmittances around 778.75 nm, with <math>H_a=2</math> km</li> </ul> </li> </ul> </li> <li>• LUTs for Water-Vapour parameters: Introduction of a surface albedo map at 865 nm (LUT126) in the ADF.</li> <li>• LUTs for Ocean-Aerosol parameters: Introduction of the atmospheric transmittances (up/down).                   <ul style="list-style-type: none"> <li>LUT485: Total downward transmittance (direct+diffuse)</li> <li>LUT486: Total upward transmittance (direct+diffuse)</li> </ul> </li> <li>• LUTs for Ocean-Case2 parameters:                   <ul style="list-style-type: none"> <li>- replace previous LUT371 (reflectance versus IOPs) by a new LUT generated at BioOptika (Plymouth, UK), and provided by ACRI :                       <ul style="list-style-type: none"> <li>LUT371: Coefficients of F' to IOPs relation</li> </ul> </li> <li>- introduction of case2 waters neural network parameters (LUT372)</li> </ul> </li> <li>• LUTs for Cloud parameters:                   <ul style="list-style-type: none"> <li>- introduction of cloud top pressure neural network for not null surface albedo and for null surface albedo (LUT384 &amp; LUT385), generated at FUB, and provided by ACRI</li> <li>- introduction of surface pressure neural network (LUT503), generated at FUB, and provided by ACRI</li> </ul> </li> </ul> </li> </ul> <p>MERISAT tool in line with IODD v8.0a (delivered by ACRI on Sept., 15<sup>th</sup> - 2009)</p> |
| 3            | C           | Feb. 27, 2011 | <p>MERISAT tool in line with IODD v8.0a (delivered by ACRI on Feb., 15<sup>th</sup> - 2011)</p>   |

## 1. INTRODUCTION

### 1.1 PURPOSE OF DOCUMENT

The ground processing of the MERIS instrument data requires the use of a vast amount of geophysical models. For processing speed, configuration control, evolution capacity, these models are used primarily in the form of tabulated parameters, limiting on-line computations to interpolation and/or model fitting. The management of these parameter tables implies the availability of adequate production, quality control methods, and sufficient storage.

This document defines the scientific content of all MERIS level-1b and 2 auxiliary data products, which allows their generation. For each data product field, the latter comprise:

- a description of the procedure used for generation
- a description of the tool module used for generation
- the accuracy required and the level of scientific content needed for generation
- an evaluation of computer resources required for generation
- a description of the procedure used for the acceptance of data generation

### 1.2 SCOPE

This work concerns the Level 2 processing at the ENVISAT-1 Ground Segment of the MERIS instrument data.

### 1.3 DEFINITIONS, ACRONYMS AND ABBREVIATIONS

|        |   |
|--------|---|
| ADF    | Auxiliary Data File (or Product)  |
| ADS    | Annotation Data Set   |
| ADSR   | ADS Record  |
| AOT    | Aerosol Optical Thickness   |
| BDS    | Boundary Dust-Soot-like particles   |
| BDW    | Boundary Dust-Water soluble particles                                     |
| BPAC   | Bright Pixel Atmospheric Correction                                       |
| BRDF   | Bidirectional Reflectance Distribution Function                           |
| CESBIO | Centre d'Etudes Spatiales de la Biosphère, (Toulouse - France)            |
| C.P.   | MERISAT internal Configuration Parameters section                         |
| DDV    | Dark Dense Vegetation   |
| ECMWF  | European Centre for Medium-term Weather Forecast                          |
| ESFT   | Exponential Sum Fitting Technique (for computing gaseous transmittivity)  |
| FR     | Full Resolution   |
| FUB    | Freie Universität Berlin, Institute for Space Science, (Berlin - Germany) |



|          |   |
|----------|---|
| GADS     | Global/General ADS  |
| GAME     | Global Absorbtion ModEl   |
| IOP      | Inherent Optical Properties   |
| IPF      | Instrument Processor Facilities (MERIS processor)   |
| LBL      | Line-By-Line computation  |
| LISE/UdL | Laboratoire Interdisciplinaire en Sciences de l'Environnement, Université du Littoral, (Wimereux - France)  |
| LOV      | Laboratoire d'Océanographie de Villefranche/Mer (Villefranche/Mer - France)   |
| LUT      | Look-Up Table   |
| MERIS    | MEdium Resolution Imaging Spectrometer  |
| MERISAT  | MERIS Auxiliary data Tool software  |
| MOMO     | Matrix-Operator MethOd (see [RD-1] <i>Fell, F., and J. Fischer, 2001. "Numerical simulation of the light field in the atmosphere-ocean system using the matrix-operator method", <i>Journal of Quantitative Spectroscopy &amp; Radiative Transfer</i>: 69 (3), 351-388.</i> |
|          | [RD-2] for more details)  |
| MPH      | Main Product Header   |
| MTCI     | MERIS Terrestrial Chlorophyll Index   |
| N/A      | Not Applicable  |
| NIR      | Near InfraRed (spectral region)   |
| NN       | Neural Network (tool)   |
| ODOC     | Optical Dissolved Organic Carbon  |
| OTC      | Optical Thickness Code  |
| RH       | Relative Humidity   |
| RR       | Reduced Resolution  |
| RTC      | Radiative Transfer Code   |
| SAM      | Standard Aerosol Model (standard assemblage)  |
| SO       | Successive Orders method for the <i>atmosphere</i> (see [RD-3] & [RD-4] for more details)   |
| SPH      | Specific Product Header   |
| SPM      | Suspended Particulate Matter  |
| TBD      | To Be Defined   |
| TOA      | Top of Atmosphere   |
| WV       | Water Vapor   |
| WCRP     | World Climate Research Program  |

### 1.3.1 Scientific identifiers and units

|            |  |
|------------|--|
| <i>cot</i> | cloud optical thickness  |
| <i>ctp</i> | cloud top pressure   |
| <i>deg</i> | degree (angle unit)  |
| <i>dl</i>  | dimensionless  |
| <i>DU</i>  | Dobson Unit [ $10^{-3} \text{ atm-cm}$ ]   |
| <i>hPa</i> | hecto Pascal [ $10^2 \text{ Pa}$ ] ( <i>pressure unit</i> )<br>( <i>Nb: 1 atm = 760.31 torr = 1013.25 hPa ; 1 torr = 1 mmHg = 1.333 mbar</i> ) |
| <i>kB</i>  | Kilo-bytes (1024 bytes)  |

|               |                                       |
|---------------|---------------------------------------|
| <i>MB</i>     | Mega-bytes (1024 <i>kB</i> )          |
| $\mu\text{m}$ | micrometer ( <i>wavelength unit</i> ) |
| <i>n.u.</i>   | non unit ( <i>unitless</i> )          |
| <i>sr</i>     | steradian ( <i>solid angle unit</i> ) |
| <i>W</i>      | watt ( <i>power unit</i> )            |

### 1.3.2 Documents identifiers

|      |                                      |
|------|--------------------------------------|
| ATBD | Algorithm Theoretical Basis Document |
| DDD  | Detailed Design Document             |
| DPM  | Detailed Processing Model document   |
| IODD | Input/Output Data Definition         |
| SRD  | Software Requirement Document        |

## 1.4 LIST OF SYMBOLS

|             |  |
|-------------|--|
| <i>a, b</i> | parameters of the particle size distribution ( <i>n.u.</i> )   |
| $a_v$       | weights associated with monochromatic absorption coefficients used in ESFT ( <i>n.u.</i> )                           |
| $dN(r)$     | number of particle per volume unit with a radius between <i>r</i> and <i>r + dr</i> ( $\text{cm}^{-3}$ )             |
| <i>E</i>    | spectral irradiance ( $\text{W m}^{-2} \mu\text{m}^{-1}$ )   |
| $E_0$       | spectral solar irradiance at TOA ( $\text{W m}^{-2} \mu\text{m}^{-1}$ )  |
| $F_0$       | spectral solar radiance ( $\text{W m}^{-2} \text{sr}^{-1} \mu\text{m}^{-1}$ )  |
| <i>g</i>    | assymetry factor of phase function (2 <sup>nd</sup> <i>Hapke's</i> parameter) ( <i>n.u.</i> )                        |
| <i>h</i>    | width of the hot-spot (4 <sup>th</sup> <i>Hapke's</i> parameter) ( <i>n.u.</i> )                                     |
| <i>ind</i>  | index for selecting the type of particle size distribution ( <i>n.u.</i> )   |
| $I_s$       | maximum order of the <i>Legendre</i> polynomial decomposition of the phase function and the radiance ( <i>n.u.</i> ) |
| <i>k</i>    | either imaginary part of the refractive index ( <i>n.u.</i> )<br>or wavenumber ( $\text{cm}^{-1}$ )                  |
| $k_a$       | absorption efficiency ( <i>n.u.</i> )  |
| $k_e$       | extinction efficiency ( <i>n.u.</i> )  |
| $k_s$       | scattering efficiency ( <i>n.u.</i> )  |
| $k_v$       | monochromatic absorption coefficients ( $\text{cm}^2 \text{g}^{-1}$ )  |
| <i>L</i>    | spectral radiance ( $\text{W m}^{-2} \text{sr}^{-1} \mu\text{m}^{-1}$ )  |
| <i>m</i>    | real part of the refractive index ( <i>n.u.</i> )  |

|                          |  |
|--------------------------|--|
| $M$                      | either the number of <i>Fourier</i> terms ( <i>n.u.</i> )<br>or the airmass (defined as $[1/\cos \vartheta_s + 1/\cos \vartheta_v]$ or $[1/\mu_s + 1/\mu_v]$ ) ( <i>n.u.</i> ) |
| $n$                      | index for selecting a MERIS spectral band ( <i>n.u.</i> )<br>or complex refractive index ( <i>n.u.</i> )   |
| $n_a$                    | refractive index of air ( <i>n.u.</i> )  |
| $n_w$                    | refractive index of pure water ( <i>n.u.</i> )   |
| $n(r)$                   | particle size distribution ( $cm^{-3} \mu m^{-1}$ )  |
| $N$                      | either number of size distributions used in the <i>Mie's</i> computation ( <i>n.u.</i> )<br>or number of discrete atmospheric zenithal angles ( <i>n.u.</i> )                  |
| $N^*$                    | number of discrete oceanic zenithal angles ( <i>n.u.</i> )   |
| $n_2$                    | number of scattering angles in the <i>Mie's</i> computation ( <i>n.u.</i> )  |
| $n_i / n$                | component mixing ratio ( <i>i.e.</i> , volume percentage of particles characterized by the $i^{th}$ size distribution) ( <i>n.u.</i> )   |
| $p$                      | normalized scattering phase function ( $sr^{-1}$ )   |
| $P_s$                    | surface pressure ( <i>mbar or hPa</i> )  |
| $Q_a$                    | absorption cross section ( $m^{-2}$ )  |
| $Q_e$                    | extinction cross section ( $m^{-2}$ )  |
| $Q_s$                    | scattering cross section ( $m^{-2}$ )  |
| $r$                      | geometrical radius of a scatterer ( $\mu m$ )  |
| $r_{//}, r_{\perp}$      | <i>Fresnel</i> reflection coefficients in the // and $\perp$ direction to the incidence plane ( <i>n.u.</i> )  |
| $t_{//}, t_{\perp}$      | <i>Fresnel</i> transmission coefficients in the // and $\perp$ direction to the incidence plane ( <i>n.u.</i> )  |
| $r_{\min}, r_{\max}, dr$ | minimum and maximum radius ( $\mu m$ ), and radius increment ( $\mu m$ ) of the particles in a given size distribution   |
| $S$                      | amplitude of the hot-spot ( $3^{rd}$ <i>Hapke's</i> parameter) ( <i>n.u.</i> )   |
| $T(u)$                   | spectrally integrated transmission function for an absorber amount $u$ ( <i>n.u.</i> )   |
| $U_{H_2O}$               | total water vapor content ( $g cm^{-2}$ )  |
| $U_{O_2}$                | total oxygen vapor content ( $g cm^{-2}$ )   |
| $U_{O_3}$                | total ozone content ( $cm - atm$ )   |
| $w_i$                    | <i>Gaussian</i> weights ( <i>n.u.</i> )  |
| $w_s$                    | wind-speed above sea level ( $m s^{-1}$ )  |
| $\delta_{i,j}$           | <i>Dirac's</i> delta function ( <i>n.u.</i> )  |

|                  |   |
|------------------|---|
| $\Delta\phi$     | relative azimuthal angle ( <i>deg</i> )   |
| $\Delta\nu$      | spectral interval ( $s^{-1}$ or <i>hertz</i> )  |
| $\varphi_0$      | illumination azimuthal angle ( <i>deg</i> )   |
| $\varphi_s$      | solar azimuthal angle ( <i>deg</i> )  |
| $\varphi_v$      | viewing azimuthal angle ( <i>deg</i> )  |
| $\lambda$        | wavelength ( $\mu m$ or <i>nm</i> )   |
| $\mu$            | cosine of zenithal angle ( <i>n.u.</i> )  |
| $\mu_i$          | <i>Gaussian</i> angles ( <i>n.u.</i> )  |
| $\sigma_a$       | absorption coefficient (aerosols / molecules) ( $m^{-1}$ )                                    |
| $\sigma_a^P$     | absorption coefficient for phytoplankton ( $m^{-1}$ )   |
| $\sigma_a^{spm}$ | absorption coefficient for SPM ( $m^{-1}$ )   |
| $\sigma_a^{ys}$  | absorption coefficient for yellow substance ( $m^{-1}$ )                                      |
| $\sigma_a^w$     | absorption coefficient for pure sea water ( $m^{-1}$ )  |
| $\sigma_e$       | extinction coefficient (aerosols / molecules) ( $m^{-1}$ )                                    |
| $\sigma_e^P$     | extinction coefficient for phytoplankton ( $m^{-1}$ )   |
| $\sigma_e^{spm}$ | extinction coefficient for SPM ( $m^{-1}$ )   |
| $\sigma_e^{ys}$  | extinction coefficient for yellow substance ( $\sigma_e^{ys} = \sigma_a^{ys}$ ) ( $m^{-1}$ )  |
| $\sigma_e^w$     | extinction coefficient for pure sea water ( $m^{-1}$ )  |
| $\sigma_s$       | scattering coefficient (aerosols / molecules) ( $m^{-1}$ )                                    |
| $\sigma_s^P$     | scattering coefficient for phytoplankton ( $m^{-1}$ )   |
| $\sigma_s^{spm}$ | scattering coefficient for SPM ( $m^{-1}$ )   |
| $\sigma_s^w$     | scattering coefficient for pure sea water ( $m^{-1}$ )  |
| $\theta$         | scattering angle ( <i>deg</i> )   |
| $\theta_p$       | phase function truncation angle ( <i>deg</i> )  |
| $\vartheta_c$    | critical zenithal angle for total internal reflection ( <i>deg</i> )                          |
| $\vartheta_0$    | illumination zenithal angle ( <i>deg</i> )  |
| $\vartheta_s$    | solar zenithal angle ( <i>deg</i> )   |
| $\vartheta_v$    | viewing zenithal angle ( <i>deg</i> )   |
| $\rho_s$         | reflectance of ground surface or ocean bottom assumed to be <i>Lambertian</i> ( <i>n.u.</i> ) |

|                   |  |
|-------------------|--|
| $\rho_G$          | specular reflection of sunlight over ocean waves ( <i>n.u.</i> )             |
| $\rho_F$          | Fresnel reflectance at the air-sea interface ( <i>n.u.</i> )                 |
| $\rho_{DDV}$      | Ground DDV albedo ( <i>n.u.</i> )  |
| $\bar{\rho}_{aG}$ | Aerosol-ground DDV coupling bidirectionality term ( <i>n.u.</i> )            |
| $\bar{\rho}_{aR}$ | Aerosol-molecule coupling bidirectionality term ( <i>n.u.</i> )              |
| $\bar{\rho}_{RG}$ | Rayleigh-ground DDV coupling bidirectionality term ( <i>n.u.</i> )           |
| $\tau$            | optical thickness ( <i>n.u.</i> )  |
| $\tau^a$          | aerosol optical thickness ( <i>n.u.</i> )                                    |
| $\tau^c$          | cloud optical thickness ( <i>n.u.</i> )                                      |
| $\tau^R$          | Rayleigh (molecular) optical thickness ( <i>n.u.</i> )                       |
| $\tau^{O_3}$      | ozone optical thickness ( <i>n.u.</i> )                                      |
| $\omega$          | single scattering albedo (1 <sup>st</sup> Hapke's parameter) ( <i>n.u.</i> ) |
| $\omega_o$        | single scattering albedo ( <i>n.u.</i> )                                     |
| $\omega_o^p$      | single scattering albedo for phytoplankton ( <i>n.u.</i> )                   |
| $\omega_o^{spm}$  | single scattering albedo for SPM ( <i>n.u.</i> )                             |
| $\omega_o^w$      | single scattering albedo for pure sea water ( <i>n.u.</i> )                  |
| $\Omega$          | solid angle ( <i>sr</i> )  |

## 1.5 REFERENCES

This section contains a list of applicable and reference documents for the Product Specifications document. The reader must refer to the STD document [\[AD-1\]](#) PO-MA-BOM-GS-0003 "Software Transfer Document for MERIS Level-2 Auxiliary Data Tool S/W" ] to obtain the issue number of each document pertaining to the current MERISAT software release [\[AD-2\]](#).

### 1.5.1 Applicable documents

| No     | Document               | Title   |
|--------|------------------------|---|
| [AD-1] | PO-MA-BOM-GS-0003      | "Software Transfer Document for MERIS Level-2 Auxiliary Data Tool S/W"  |
| [AD-2] | PO-MA-BOM-GS-0008      | "Software User's Manual for MERIS level-2 Auxiliary data Tool software" |
| [AD-3] | PO-TN-MEL-GS-0002-i7r2 | "MERIS Level-2 Detailed Processing Model & Parameter Data List"         |
| [AD-4] | PO-TN-MEL-GS-0002-i7r0 | "MERIS Level-1b Detailed Processing Model & Parameter Data List"        |

|        |                            |  |
|--------|----------------------------|--|
| [AD-5] | <i>PO-TN-MEL-GS-0005</i>   | "MERIS Level-2 ATBD: Algorithm Theoretical Basis Document"   |
| [AD-6] | <i>PO-TN-MEL-GS-0026</i>   | "Reference Model for MERIS Level-2 Processing – 3rd MERIS Reprocessing"  |
| [AD-7] | <i>PO-RS-PAR-GS-0003</i>   | "Specification of the Contents of the MERIS Radiative Transfer Tools used to Generate the Level-2 Auxiliary Data Products" |
| [AD-8] | <i>PO-TN-MEL-GS-0003</i>   | "MERIS Input/Output Data Definition"   |
| [AD-9] | <i>Presentation slides</i> | "MERIS Water Vapor retrieval"  |

## 1.5.2 Reference documents

| No      | Reference (authors, title, journal)  |
|---------|--|
| [RD-1]  | <b>Fell, F., and J. Fischer, 2001.</b> "Numerical simulation of the light field in the atmosphere-ocean system using the matrix-operator method", <i>Journal of Quantitative Spectroscopy &amp; Radiative Transfer</i> : 69 (3), 351-388.  |
| [RD-2]  | <b>Fell, F., and J. Fischer, 2001.</b> "Numerical simulation of the light field in the atmosphere-ocean system using the matrix-operator method", <i>Journal of Quantitative Spectroscopy &amp; Radiative Transfer</i> : 69 (3), 351-388.  |
| [RD-3]  | <b>Deuzé, J.L., M. Herman, and R. Santer, 1989.</b> "Fourier series expansion of the transfer equation in the atmosphere-ocean system", <i>Journal of Quantitative Spectroscopy &amp; Radiative Transfer</i> : 41 (6), 483-494.  |
| [RD-4]  | <b>Lenoble, J., M. Herman, J.L. Deuzé, B. Lafrance, R. Santer and D. Tanré, 2007.</b> "A successive order of scattering code for solving the vector equation of transfer in the Earth's atmosphere with aerosols", <i>Journal of Quantitative Spectroscopy &amp; Radiative Transfer</i> , 107, pp. 479-507 ( <a href="https://doi.org/10.1016/j.jqsrt.2007.03.010">doi: 10.1016/j.jqsrt.2007.03.010</a> ). |
| [RD-5]  | <b>Vermote, E., D. Tanré, J.L. Deuzé, M. Herman, and J.J. Morcrette, 1997.</b> "Second simulation of the satellite signal in the solar spectrum, 6S: An overview", <i>I.E.E.E. Transactions on Geoscience &amp; Remote Sensing</i> : 35 (3), 675-687.  |
| [RD-6]  | <b>Hansen, J.E., and L. Travis, 1974.</b> "Light scattering in planetary atmospheres", <i>Space Science Reviews</i> : 16, 527-610.   |
| [RD-7]  | <b>Cox, C., and W. Munk, 1954.</b> "Measurements of roughness of the sea surface from photographs of the sun glitter", <i>Journal of the Optical Society of America</i> : 44 (11), 838-888.  |
| [RD-8]  | <b>Shettle, E.P., and R.W. Fenn, 1979.</b> "Models for the aerosols of the lower atmosphere and the effects of humidity variations on their optical properties", <i>Environmental Research Papers, AFGL-TR-79-0214</i> , Hanscom (Mass.).  |
| [RD-9]  | <b>Kaufman, Y.J., and D. Tanré, 1992.</b> "Atmospherically resistant vegetation index (ARVI) for EOS-MODIS", <i>I.E.E.E. Transactions on Geoscience &amp; Remote Sensing</i> : 30, 261-270.  |
| [RD-10] | <b>Morel, A., and B. Gentili, 1996.</b> "Diffuse reflectance of oceanic waters. III- Implications of bidirectionality for the remote-sensing problem", <i>Applied Optics</i> : 35, 261-270.  |
| [RD-11] | <b>Prieur, L., and S. Sathyendranath, 1981.</b> " An optical classification of coastal and oceanic waters based on the specific spectral absorption curves of phytoplankton pigments, dissolved organic matter, and other particulate materials", <i>American Society of Limnology &amp; Oceanography</i> : 26, 671-689.   |
| [RD-12] | <b>Morel, A., and M. André, 1991.</b> " Pigment distribution and primary production in the western Mediterranean as derived and modeled from Coastal Zone Color Scanner observations", <i>Journal of Geophysical Research</i> : 96, 12685-12698.   |
| [RD-13] | <b>Pope, R.M., and E.S. Fry, 1997.</b> "Absorption spectrum (380-700nm) of pure water: II. Integrating cavity measurements", <i>Applied Optics</i> : 36, 8710-8723.  |

- [RD-14] **Hale, G.M., and M.R. Querry, 1973.** "Optical constants of water in the 200nm to 200µm wavelength region", *Applied Optics*: **12**, 555-563.
- [RD-15] **Santer, R., and F. Zagolski, 2010.** "Inherent optical properties of the aerosols – IOPA", in reponse to RFQ/3-11641/06/I-OL, Intended Rider 1 to ESRIN Contract 18109/04/I-OL for Atmospheric Correction for MERIS Over Coastal Waters: Towards a New Aerosol Climatology: 40 p.

## 1.6 DEFINITION

The 15 MERIS bands are described in table below:

| <i>Band #</i> | <i><math>\lambda</math> (nm)</i> | <i><math>\Delta\lambda</math> (nm)</i> | <i>Description</i>                       |
|---------------|----------------------------------|--|--|
| 1             | 412.50                           | 10                                     | <i>Aerosol and ocean color retrieval</i> |
| 2             | 442.50                           | 10                                     | <i>Aerosol and ocean color retrieval</i> |
| 3             | 490.00                           | 10                                     | <i>Aerosol and ocean color retrieval</i> |
| 4             | 510.00                           | 10                                     | <i>Aerosol and ocean color retrieval</i> |
| 5             | 560.00                           | 10                                     | <i>Aerosol and ocean color retrieval</i> |
| 6             | 620.00                           | 10                                     | <i>Aerosol and ocean color retrieval</i> |
| 7             | 665.00                           | 10                                     | <i>Aerosol and ocean color retrieval</i> |
| 8             | 681.25                           | 7.5                                    | <i>Aerosol and ocean color retrieval</i> |
| 9             | 708.75                           | 10                                     | <i>Aerosol and ocean color retrieval</i> |
| 10            | 753.75                           | 7.5                                    | <i>Clouds</i>                            |
| 11            | 761.875                          | 3.75                                   | <i>Clouds</i>                            |
| 12            | 778.75                           | 15                                     | <i>Aerosol and ocean color retrieval</i> |
| 13            | 865.00                           | 20                                     | <i>Aerosol and ocean color retrieval</i> |
| 14            | 885.00                           | 10                                     | <i>Water vapor</i>                       |
| 15            | 900.00                           | 10                                     | <i>Water vapor</i>                       |



## 1.7 CODING / SIZING

The following data types are used to code the MERIS level-1b & 2 auxiliary data products:

| <i>Variable Type</i>            | <i>Type</i> | <i>Size</i> | <i>Description</i>   |
|---------------------------------|-------------|-------------|--|
| Character                       | char        | 1 byte      | <i>sc</i> : signed char<br><i>uc</i> : unsigned char                           |
| 2-byte Integer                  | short       | 2 bytes     | <i>ss</i> : signed short integer<br><i>us</i> : unsigned short integer         |
| 4-byte Integer                  | long        | 4 bytes     | <i>sl</i> : signed long integer<br><i>ul</i> : unsigned long integer           |
| 8-byte Integer                  | long long   | 8 bytes     | <i>sd</i> : signed long long integer<br><i>ud</i> : unsigned long long integer |
| Single precision floating point | float       | 4 bytes     | <i>fl</i> : single precision floating point                                    |
| Double precision floating point | double      | 8 bytes     | <i>db</i> : double precision floating point                                    |

Conventions used for byte and bit numbering in bit fields are:

- bytes and bits numbering always starts at 0
- byte 0 is always the most significant

## 2. OVERVIEW OF SPECIFICATION

### 2.1 APPROACH OF AUXILIARY DATA PRODUCT SPECIFICATION

For each auxiliary data product field described, the information is presented following a standardized template. The specification is provided for the following categories: reference, dependencies, tool, procedure, scientific content, resources and acceptance. In this section, each category is defined and the descriptors used are presented.

#### Reference:

References to applicable documents are given. The variable name given corresponds to the output variable used in [AD-3] & [AD-4], and provides the means of tracing where the LUT is being used. When "no variable used" is specified, the field is used only for the generation of the LUT described under "Dependencies".

#### Dependencies:

In this section, all the LUTs that depend on the given auxiliary data product field are listed.

#### Tool:

A description of the tool modules which will be used for the generation of the field is given.

#### Procedure:

A description of the procedure that will be used for the generation of the field is given. It specifies mainly the inputs/outputs and the processing steps in the sequence of modules. In the outputs, the variable name is given, as well the units and the dimensions of the variable. Under unit description, [dl] means that the variable is dimensionless.

#### Scientific content:

The level of scientific content or a relevant physical description is given to help understanding the purpose of the LUT. For more details on the algorithms used, refer to [AD-5] or [AD-6].

#### Resources:

An evaluation of the computer resources required to generate the data for the specified accuracy is given. It includes the Output disk space and the CPU time for a typical case.

#### Acceptance:

A description of the procedure which will be used in the acceptance for the data generated.

## 2.2 SUMMARY OF TOOLS / MODULES REQUIRED

These tools / modules are summarized in table hereafter, and a full description (*i.e.*, theory and data dictionary) for each of them is given in [\[AD-7\]](#).

| <i>Tools/Modules required</i>  | <i>Status</i> |
|--|---------------|
| <b>LISE/UdL Modules</b>  |               |
| OTC/SCAMAT   | Available     |
| OTC/COMPUTE_FSP  | Available     |
| RTC/UPRAD (GAME, SO)   | Available     |
| RTC/GAUSS  | Available     |
| RTC/MOS (lut_rhob_aR, lut_rhob_agddv,<br>lut_rhob_Rgddv, lut_alb_gddv) | Available     |
| OTC/OZONE  | Available     |
| OTC/RAYLEIGH   | Available     |
| <b>FUB Modules</b>   |               |
| OTC/MIE  | Available     |
| OTC/SCFP_2   | Available     |
| RTC/MOMO   | Available     |
| <b>MERISAT Modules</b>   |               |
| Integration  | Available     |
| Interpolation  | Available     |
| Simplex  | Available     |
| Polynomial fit   | Available     |

## 2.3 SUMMARY OF COMPUTER RESOURCE REQUIREMENTS

This summary is limited to the LUTs generated on a single computer equipped with a linux operating system. The CPU time was obtained using the MERISAT-S/W v2.0 on a single computer.

| <i>Reference to <a href="#">[AD-8]</a></i> | <i>LUT #</i> | <i>CPU time [s]</i>              | <i>Disk space [bytes]</i> |
|--|--------------|----------------------------------|---------------------------|
| <b>L1b CONTROL PARAMETERS</b>              |              |                                  |                           |
| ✓ Section 6.2.20, ADS field 1              | 017          | 26                               | 10944                     |
| <b>L2 CONTROL PARAMETERS</b>               |              |                                  |                           |
| ✓ Section 6.10.8, ADS record 1 field 1     | 303          | 3243243243<br>2432432432<br>4324 | 5928                      |
| ✓ Section 6.10.8, ADS record 2 field 1     | 303          | 685                              | 5928                      |

| Reference to [AD-8]                      | LUT # | CPU time [s]                | Disk space [bytes] |
|--|-------|-----------------------------|--------------------|
| <b>ATMOSPHERE PARAMETERS</b>             |       |                             |                    |
| ✓ Section 6.11.4, GADS field 1           | 074   | 21                          | 12                 |
| ✓ Section 6.11.5, GADS field 4           | 097   | 1                           | 60                 |
| ✓ Section 6.11.5, GADS field 5           | 098   | 1                           | 60                 |
| ✓ Section 6.11.6, GADS field 2           | 106   | 55674                       | 336                |
| ✓ Section 6.11.6, GADS field 3           | 100   | 39767                       | 240                |
| ✓ Section 6.11.7, GADS field 1, 2 & 3    | 101   | 691                         | 3744               |
| ✓ Section 6.11.8, GADS field 1           | 102   | 17                          | 68                 |
| ✓ Section 6.11.12, GADS fields 1, 2 & 3  | 110   | [FUB] 1024<br>[UdL] 259     | 1345500            |
| <b>OCEAN-AEROSOL PARAMETERS</b>          |       |                             |                    |
| ✓ Section 6.13.5, GADS field 1           | 138   | [FUB] 3<br>[UdL] 3          | 14280              |
| ✓ Section 6.13.6, GADS field 1           | 139   | [FUB] 1<br>[UdL] 1          | 952                |
| ✓ Section 6.13.7, GADS field 1           | 140   | [FUB] 1<br>[UdL] 1          | 2040               |
| ✓ Section 6.13.8, GADS field 1           | 141   | [FUB] 2<br>[UdL] 2          | 2040               |
| ✓ Section 6.13.9, ADSR field 1           | 142   | 31                          | 29900              |
| ✓ Section 6.13.10, ADSR field 1, 2 & 3   | 143   | [FUB] 101663<br>[UdL] 47841 | 137241000          |
| ✓ Section 6.13.11, ADSR field 1, 2 & 3   | 485   | 21600                       | 985320             |
| ✓ Section 6.13.12, ADSR field 1          | 486   | 7200                        | 185640             |
| <b>LAND-AEROSOL PARAMETERS</b>           |       |                             |                    |
| ✓ Section 6.14.5, ADSR field 2           | 159   | 7078                        | 5928               |
| ✓ Section 6.14.5, ADSR field 4           | 438   | 7078                        | 5928               |
| ✓ Section 6.14.6, ADSR field 1           | 160   | 94428                       | 118560             |
| ✓ Section 6.14.8, ADSR field 1           | 167   | 2044                        | 4992               |
| ✓ Section 6.14.9, ADSR field 1           | 168   | 1022                        | 59904              |
| ✓ Section 6.14.10, ADSR field 1          | 169   | 177329                      | 606528             |
| ✓ Section 6.14.11, ADSR field 1          | 170   | 2458                        | 25896              |
| ✓ Section 6.14.12, ADSR field 1          | 315   | 363                         | 1080               |
| ✓ Section 6.14.13, ADSR field 1          | 316   | 183                         | 12960              |
| ✓ Section 6.14.14, ADSR field 1          | 317   | 40                          | 14940              |
| ✓ Section 6.14.16, ADSR field 1          | 320   | 5                           | 3840               |
| ✓ Section 6.14.16, ADSR field 2          | 321   | 6                           | 9734400            |
| ✓ Section 6.14.16, ADSR field 3          | 322   | 7                           | 320                |
| ✓ Section 6.14.17, ADSR field 1          | 324   | 54                          | 14976              |
| <b>Other Parameters</b>                  |       |                             |                    |
| ✓ Section 6.15.6, GADS field 8           | 197   | 24                          | 51300              |
| ✓ Section 6.15.8, GADS field 1, 2, 3 & 4 | 203   | 4356                        | 786240             |
| <b>Final Summary</b>                     |       |                             |                    |
| ✓ Section 6.17.6, GADS field 1, 2 & 3    | 220   | 1312200                     | 1312200            |
| ✓ Section 6.17.7, GADS field 1, 2, 3 & 4 | 223   | 19016                       | 1749600            |
| <b>Total</b>                             |       | <b>1904530</b>              | <b>154343584</b>   |

| <i>C.P. Sections</i>            | <i>Number of LUTs</i> | <i>Disk space per LUT [bytes]</i> | <i>Total disk space [bytes]</i> |
|---------------------------------|-----------------------|-----------------------------------|---------------------------------|
| <i>L1b CONTROL PARAMETERS</i>   |                       |                                   |                                 |
| ✓3.1                            | 1                     | 60                                | 60                              |
| ✓3.2                            | 1                     | 1820                              | 1820                            |
| <i>ATMOSPHERE PARAMETERS</i>    |                       |                                   |                                 |
| ✓6.11.1.1                       | 1                     | 60                                | 60                              |
| <i>OCEAN-AEROSOL PARAMETERS</i> |                       |                                   |                                 |
| ✓6.13.1.1                       | 1                     | 952                               | 952                             |
| ✓6.13.1.2                       | 1                     | 952                               | 952                             |
| ✓6.13.1.3                       | 1                     | 952                               | 952                             |
| ✓6.13.1.4                       | 1                     | 4140                              | 4140                            |
| ✓6.13.1.5                       | 1                     | 3060                              | 3060                            |
| ✓6.13.1.6                       | 9180<br>4320          | 29900<br>29900                    | 274482000<br>129168000          |
| ✓6.13.1.7                       | 1                     | 24480                             | 24480                           |
| ✓6.13.1.8                       | 1                     | 14280                             | 14280                           |
| <i>LAND-AEROSOL PARAMETERS</i>  |                       |                                   |                                 |
| ✓6.14.1.1                       | 1                     | 312                               | 312                             |
| <i>OCEAN CASE-I PARAMETERS</i>  |                       |                                   |                                 |
| ✓6.15.1.1                       | 1                     | 216                               | 216                             |
| <i>CLOUD PARAMETERS</i>         |                       |                                   |                                 |
| ✓6.17.1.1                       | 1754                  | 48600                             | 85244400                        |
| ✓6.17.1.2                       | 1754                  | 108                               | 189432                          |
| <b>Total</b>                    |                       |                                   | <b>489135116</b>                |

### 3. SPECIFICATION OF MERISAT INTERNAL AUXILIARY DATA PRODUCT

#### 3.1 C.P. MERIS WAVELENGTH FOR BAND B

Reference: Wvl[b] LUT400

[AD-8] Section 5.3.1.4, SPH field 31

PARBLEU provided

Dependencies:

None

Tool:

None

Procedure:

Input: *b* MERIS spectral band# (15 values) *see* [Section 3.1](#), (LUT400)

Output: *Wvl[b]* Nominal MERIS wavelengths for the 15 spectral bands  
units: [*nm*]

Step: User specified.

Scientific content:

Nominal wavelengths of the 15 MERIS spectral bands

Current baseline: {412.5, 442.5, 490.0, 510.0, 560.0, 620.0, 665.0, 681.25, 708.75, 753.75, 761.875, 778.75, 865.0, 885.0, 900.0} *nm*

Resources:

Estimated CPU time: -

Output disk space:  $15 \times 4$  bytes/fl = 60 bytes

Acceptance:

Correspond to the latest definition.

### 3.2 C.P. FRESNEL REFLECTION COEFFICIENTS FOR OCEAN CASE-I & II

Reference: FR[ $w_s, \theta'$ ] LUT417

Configuration file

ACRI provided

Dependencies:

None

Tool:

None

Procedure:

Input:  $w_s$  Wind-speed above sea level (5 values: {0; 0.0001;4;8;16} m/s)  
 $\theta'$  Zenith angles in water (91 values: [0;90] deg. with step of 1 deg.)

Output: FR[ $w_s, \theta'$ ] Fresnel reflection coefficients  $\mathcal{R}(w_s, \theta')$   
units: [dl]

Step: User specified.

Scientific content:

Fresnel reflection coefficients  $\mathcal{R}(w_s, \theta')$  tabulated for 5 wind-speeds ( $w_s$ ) and for 91 zenith angles in water ( $\theta'$ )

Current baseline: 5 × 91 values (see table below)

Resources:

Estimated CPU time: -  
Output disk space: 5 × 91 x 4 bytes/fl = 1820 bytes

Acceptance:

Correspond to the latest definition.

| $\theta$<br>(deg) | $\mathcal{R}(\theta, w_s)$<br>$w_s=0$ | $\mathcal{R}(\theta, w_s)$<br>$w_s=0.0001$ | $\mathcal{R}(\theta, w_s)$<br>$w_s=4$ | $\mathcal{R}(\theta, w_s)$<br>$w_s=8$ | $\mathcal{R}(\theta, w_s)$<br>$w_s=16$ |
|-------------------|---------------------------------------|--|---------------------------------------|---------------------------------------|--|
| 0                 | 0.02125                               | 0.02094                                    | 0.02097                               | 0.02105                               | 0.02150                                |
| 1                 | 0.02125                               | 0.02091                                    | 0.02099                               | 0.02110                               | 0.02147                                |
| 2                 | 0.02125                               | 0.02092                                    | 0.02094                               | 0.02114                               | 0.02144                                |
| 3                 | 0.02125                               | 0.02095                                    | 0.02102                               | 0.02104                               | 0.02144                                |
| 4                 | 0.02125                               | 0.02097                                    | 0.02094                               | 0.02101                               | 0.02148                                |
| 5                 | 0.02126                               | 0.02096                                    | 0.02090                               | 0.02105                               | 0.02147                                |
| 6                 | 0.02126                               | 0.02095                                    | 0.02100                               | 0.02104                               | 0.02154                                |
| 7                 | 0.02126                               | 0.02099                                    | 0.02099                               | 0.02105                               | 0.02183                                |
| 8                 | 0.02126                               | 0.02100                                    | 0.02097                               | 0.02098                               | 0.02191                                |
| 9                 | 0.02127                               | 0.02099                                    | 0.02095                               | 0.02115                               | 0.02206                                |
| 10                | 0.02127                               | 0.02099                                    | 0.02094                               | 0.02116                               | 0.02241                                |
| 11                | 0.02127                               | 0.02091                                    | 0.02090                               | 0.02133                               | 0.02306                                |
| 12                | 0.02128                               | 0.02093                                    | 0.02109                               | 0.02145                               | 0.02327                                |
| 13                | 0.02133                               | 0.02094                                    | 0.02114                               | 0.02159                               | 0.02370                                |
| 14                | 0.02137                               | 0.02100                                    | 0.02128                               | 0.02167                               | 0.02463                                |
| 15                | 0.02143                               | 0.02107                                    | 0.02145                               | 0.02199                               | 0.02545                                |
| 16                | 0.02146                               | 0.02122                                    | 0.02155                               | 0.02241                               | 0.02638                                |
| 17                | 0.02155                               | 0.02123                                    | 0.02175                               | 0.02256                               | 0.02804                                |
| 18                | 0.02170                               | 0.02138                                    | 0.02187                               | 0.02286                               | 0.03022                                |
| 19                | 0.02178                               | 0.02144                                    | 0.02202                               | 0.02350                               | 0.03208                                |
| 20                | 0.02190                               | 0.02156                                    | 0.02242                               | 0.02391                               | 0.03372                                |
| 21                | 0.02210                               | 0.02171                                    | 0.02276                               | 0.02443                               | 0.03703                                |
| 22                | 0.02237                               | 0.02190                                    | 0.02317                               | 0.02601                               | 0.04076                                |
| 23                | 0.02261                               | 0.02213                                    | 0.02374                               | 0.02730                               | 0.04486                                |
| 24                | 0.02294                               | 0.02255                                    | 0.02447                               | 0.02884                               | 0.05001                                |
| 25                | 0.02335                               | 0.02285                                    | 0.02474                               | 0.03106                               | 0.05483                                |
| 26                | 0.02386                               | 0.02329                                    | 0.02618                               | 0.03357                               | 0.06144                                |
| 27                | 0.02438                               | 0.02376                                    | 0.02703                               | 0.03644                               | 0.06865                                |
| 28                | 0.02508                               | 0.02446                                    | 0.02831                               | 0.04031                               | 0.07668                                |
| 29                | 0.02593                               | 0.02540                                    | 0.03089                               | 0.04533                               | 0.08664                                |
| 30                | 0.02681                               | 0.02624                                    | 0.03378                               | 0.05231                               | 0.09773                                |
| 31                | 0.02794                               | 0.02756                                    | 0.03732                               | 0.05971                               | 0.10897                                |
| 32                | 0.02909                               | 0.02897                                    | 0.04139                               | 0.06869                               | 0.12166                                |
| 33                | 0.03091                               | 0.03072                                    | 0.04670                               | 0.07954                               | 0.13646                                |
| 34                | 0.03338                               | 0.03311                                    | 0.05447                               | 0.09248                               | 0.15212                                |
| 35                | 0.03570                               | 0.03572                                    | 0.06500                               | 0.10751                               | 0.16927                                |
| 36                | 0.03878                               | 0.03907                                    | 0.07689                               | 0.12445                               | 0.18823                                |
| 37                | 0.04205                               | 0.04314                                    | 0.09238                               | 0.14488                               | 0.20682                                |
| 38                | 0.04649                               | 0.04886                                    | 0.11208                               | 0.16743                               | 0.22797                                |
| 39                | 0.05268                               | 0.05539                                    | 0.13472                               | 0.19266                               | 0.25123                                |
| 40                | 0.05972                               | 0.06439                                    | 0.16347                               | 0.21976                               | 0.27463                                |
| 41                | 0.06838                               | 0.07594                                    | 0.19647                               | 0.24938                               | 0.29938                                |
| 42                | 0.07985                               | 0.09529                                    | 0.23428                               | 0.28338                               | 0.32753                                |
| 43                | 0.09589                               | 0.12213                                    | 0.27621                               | 0.31770                               | 0.35511                                |
| 44                | 0.11899                               | 0.16774                                    | 0.32387                               | 0.35947                               | 0.38285                                |
| 45                | 0.15238                               | 0.23620                                    | 0.37676                               | 0.39986                               | 0.41170                                |

| $\theta$<br>(deg) | $\mathcal{R}(\theta, w_s)$<br>$w_s=0$ | $\mathcal{R}(\theta, w_s)$<br>$w_s=0.0001$ | $\mathcal{R}(\theta, w_s)$<br>$w_s=4$ | $\mathcal{R}(\theta, w_s)$<br>$w_s=8$ | $\mathcal{R}(\theta, w_s)$<br>$w_s=16$ |
|-------------------|---------------------------------------|--|---------------------------------------|---------------------------------------|--|
| 46                | 0.20426                               | 0.33440                                    | 0.43319                               | 0.44050                               | 0.43934                                |
| 47                | 0.30306                               | 0.46703                                    | 0.49054                               | 0.48138                               | 0.46729                                |
| 48                | 0.57047                               | 0.61171                                    | 0.54910                               | 0.52514                               | 0.50016                                |
| 49                | 0.99998                               | 0.74817                                    | 0.60431                               | 0.56677                               | 0.52962                                |
| 50                | 0.99998                               | 0.86008                                    | 0.65845                               | 0.60953                               | 0.56041                                |
| 51                | 0.99998                               | 0.93299                                    | 0.71357                               | 0.64918                               | 0.58925                                |
| 52                | 0.99998                               | 0.97398                                    | 0.76274                               | 0.68827                               | 0.61775                                |
| 53                | 0.99998                               | 0.99172                                    | 0.80779                               | 0.72825                               | 0.64609                                |
| 54                | 0.99998                               | 0.99793                                    | 0.84699                               | 0.76455                               | 0.67473                                |
| 55                | 0.99998                               | 0.99958                                    | 0.88388                               | 0.79884                               | 0.70134                                |
| 56                | 0.99998                               | 0.99994                                    | 0.91470                               | 0.83069                               | 0.73117                                |
| 57                | 0.99998                               | 0.99998                                    | 0.93960                               | 0.86141                               | 0.75837                                |
| 58                | 0.99998                               | 0.99998                                    | 0.95909                               | 0.88965                               | 0.78525                                |
| 59                | 0.99998                               | 0.99998                                    | 0.97386                               | 0.91423                               | 0.81158                                |
| 60                | 0.99998                               | 0.99998                                    | 0.98385                               | 0.93457                               | 0.83643                                |
| 61                | 0.99998                               | 0.99997                                    | 0.99101                               | 0.95198                               | 0.86142                                |
| 62                | 0.99998                               | 0.99997                                    | 0.99533                               | 0.96662                               | 0.88457                                |
| 63                | 0.99998                               | 0.99997                                    | 0.99773                               | 0.97731                               | 0.90681                                |
| 64                | 0.99998                               | 0.99996                                    | 0.99907                               | 0.98569                               | 0.92587                                |
| 65                | 0.99998                               | 0.99996                                    | 0.99963                               | 0.99151                               | 0.94327                                |
| 66                | 0.99998                               | 0.99996                                    | 0.99982                               | 0.99508                               | 0.95829                                |
| 67                | 0.99998                               | 0.99997                                    | 0.99995                               | 0.99764                               | 0.97085                                |
| 68                | 0.99998                               | 0.99997                                    | 0.99995                               | 0.99880                               | 0.98037                                |
| 69                | 0.99998                               | 0.99997                                    | 0.99997                               | 0.99941                               | 0.98752                                |
| 70                | 0.99998                               | 0.99997                                    | 0.99997                               | 0.99979                               | 0.99265                                |
| 71                | 0.99998                               | 0.99997                                    | 0.99999                               | 0.99997                               | 0.99625                                |
| 72                | 0.99998                               | 0.99997                                    | 0.99999                               | 0.99998                               | 0.99814                                |
| 73                | 0.99998                               | 0.99997                                    | 0.99999                               | 0.99999                               | 0.99921                                |
| 74                | 0.99998                               | 0.99997                                    | 1.00000                               | 0.99999                               | 0.99970                                |
| 75                | 0.99998                               | 0.99997                                    | 0.99998                               | 1.00000                               | 0.99995                                |
| 76                | 0.99998                               | 0.99996                                    | 0.99999                               | 1.00000                               | 0.99999                                |
| 77                | 0.99998                               | 0.99997                                    | 1.00000                               | 1.00000                               | 0.99998                                |
| 78                | 0.99998                               | 0.99995                                    | 1.00000                               | 0.99998                               | 1.00000                                |
| 79                | 0.99998                               | 0.99995                                    | 0.99999                               | 1.00000                               | 0.99999                                |
| 80                | 0.99998                               | 0.99994                                    | 0.99999                               | 1.00000                               | 0.99999                                |
| 81                | 0.99998                               | 0.99995                                    | 0.99998                               | 0.99998                               | 0.99997                                |
| 82                | 0.99998                               | 0.99993                                    | 0.99996                               | 0.99998                               | 0.99997                                |
| 83                | 0.99998                               | 0.99995                                    | 0.99996                               | 0.99995                               | 0.99996                                |
| 84                | 0.99998                               | 0.99996                                    | 0.99994                               | 0.99995                               | 0.99995                                |
| 85                | 0.99998                               | 0.99996                                    | 0.99995                               | 0.99994                               | 0.99994                                |
| 86                | 0.99998                               | 0.99996                                    | 0.99993                               | 0.99992                               | 0.99994                                |
| 87                | 0.99998                               | 0.99991                                    | 0.99992                               | 0.99992                               | 0.99993                                |
| 88                | 0.99997                               | 0.99992                                    | 0.99993                               | 0.99994                               | 0.99994                                |
| 89                | 0.99991                               | 0.99990                                    | 0.99991                               | 0.99991                               | 0.99991                                |
| 90                | 1.00000                               | 1.00000                                    | 1.00000                               | 1.00000                               | 1.00000                                |



#### **4. MERIS PRODUCTS OVERVIEW**

Not covered in this document

## 5. SPECIFICATION OF L1B/L2 DATA PRODUCT

Not covered in this document

## 6. SPECIFICATION OF L1B/L2 AUXILIARY DATA PRODUCT

### 6.1 MERIS INSTRUMENT

Not covered in this document

### 6.2 LEVEL-1B CONTROL PARAMETERS

#### 6.2.1 C.P.

None

#### 6.2.2 MPH

Not covered in this document (*see* [\[AD-8\]](#) for a detailed description)

#### 6.2.3 SPH

Not covered in this document (*see* [\[AD-8\]](#) for a detailed description)

#### 6.2.4 GADS General

##### 6.2.4.1 Julian day to milliseconds conversion factor

Reference: MS\_to\_JD, LUT001

[\[AD-8\]](#) Section 6.2.4, GADS field 1

ACRI provided

Dependencies:

None

Tool:

None

Procedure:

Input: none

Output: *MS\_to\_JD* *Julian* day to milliseconds conversion factor  
units: [ms/day]  
Step: User specified.

Scientific content:

Conversion factor used to convert variables expressed as *Julian* day into milliseconds

Current baseline: 86400000 ms

Resources:

Estimated CPU time: -  
Output disk space: 1 × 4 bytes/sl = 4 bytes

Acceptance:

Corresponds to the latest definition.

6.2.4.2 *Maximum number of missing packets allowed*

Reference: Max\_gap\_P, LUT002

[AD-8] Section 6.2.4, GADS field 2

ACRI provided

Dependencies:

None

Tool:

None

Procedure:

Input: none  
Output: *Max\_gap\_P* Maximum number of missing packets allowed  
units: [dl]  
Step: User specified.

Scientific content:

Maximum number of packets that can be missed

Current baseline: 16

Resources:

Estimated CPU time: -  
Output disk space: 1 × 1 byte/uc = 1 byte

Acceptance:

Corresponds to the latest definition.

**6.2.5 (Deleted)**

Reference:

[AD-8] Section 6.2.5

**6.2.6 GADS Solar Parameters**

*6.2.6.1 Solar flux reference values*

Reference:  $F_0[b]$ , LUT224

[AD-8] Section 6.2.6, GADS field 1

ACRI provided

Dependencies:

None

Tool:

None

Procedure:

Input:  $b$  MERIS spectral band# (15 values), *see* [Section 3.1](#) for the nominal wavelengths (LUT400)

Output:  $F_0[b]$  Solar flux reference values in the 15 MERIS bands (15 values)

units:  $[W.m^{-2}.\mu m^{-1}]$

Step: User specified.

Scientific content:

Extraterrestrial spectral solar irradiance in the 15 MERIS bands

Current baseline: {1714.7673340, 1878.8929443, 1928.3371582, 1928.9362793, 1803.0762939,  
1650.7738037, 1531.6264648, 1472.1680908, 1407.9426270, 1266.0428467,  
1254.5811768, 1177.2595215, 958.38519287, 929.83801270, 895.45959473}  
 $W.m^{-2}.\mu m^{-1}$

Resources:

Estimated CPU time: -  
Output disk space: 15 × 4 bytes/fl = 60 bytes

Acceptance:

Corresponds to the latest definition.

**6.2.6.2 Square of Sun-Earth distance at reference date**

Reference:  $Dsun0^2$ , LUT225

[AD-8] Section 6.2.6, GADS field 2

ACRI provided

Dependencies:

None

Tool:

None

Procedure:

Input: none  
Output:  $Dsun0^2$  Square of *Sun-Earth* distance at reference date  
units:  $[m^2]$   
Step: User specified.

Scientific content:

*Sun-Earth* distance given a reference date used to compute the corrective factor ( $1/Dsun0^2$ ) to apply to the extraterrestrial solar irradiance

Current baseline:  $2.2402379 \cdot 10^{22} m^2$

Resources:

Estimated CPU time: -  
Output disk space:  $1 \times 4 \text{ bytes/fl} = 4 \text{ bytes}$

Acceptance:

Correspond to the latest definition.

**6.2.7 (Deleted)**

Reference:

[AD-8] Section 6.2.7

**6.2.8 GADS Exception Handling**

*6.2.8.1 Default radiance values for saturated samples*

Reference: Def\_rad[b], LUT226

[AD-8] Section 6.2.8, GADS field 1

ACRI provided

Dependencies:

None

Tool:

None

Procedure:

Input:  $b$  MERIS spectral band# (15 values), see [Section 3.1](#) for the nominal wavelengths (LUT400)

Output:  $Def\_rad[b]$  Default radiance values for saturated samples in the 15 MERIS bands  
units:  $[W.m^{-2}.\mu m^{-1}.sr^{-1}]$

Step: User specified.

Scientific content:

Default radiance values in the 15 MERIS spectral bands used for the saturated samples

Current baseline: {619.98608398, 693.83856201, 758.02069092, 700.52618408, 610.46539307,  
535.78985596, 448.10375977, 453.98617554, 412.82760620, 566.97033691,  
580.60144043, 237.70004272, 232.57832336, 399.39666748, 355.34863281}  
 $W.m^{-2}.\mu m^{-1}.sr^{-1}$

Resources:

Estimated CPU time: -  
Output disk space:  $15 \times 4$  bytes/fl = 60 bytes

Acceptance:

Corresponds to the latest definition.

**6.2.8.2 Default radiance values for above range samples**

Reference: Def\_rad0[b], LUT227

[AD-8] Section 6.2.8, GADS field 2

ACRI provided

Dependencies:

None

Tool:

None

Procedure:

Input: *b* MERIS spectral band# (15 values), see [Section 3.1](#) for the nominal wavelengths (LUT400)

Output: *Def\_rad0[b]* Default radiance values for above range samples in the 15 MERIS bands  
units:  $[W.m^{-2}.\mu m^{-1}.sr^{-1}]$

Step: User specified.

Scientific content:



Default radiance values in the 15 MERIS spectral bands used for above range samples

Current baseline: {620.93359375, 694.89892578, 759.17913818, 701.59674072, 611.39831543,  
536.60864258, 448.78857422, 454.67996216, 413.45849609, 567.83679199,  
581.48876953, 238.06330872, 232.93376160, 400.00704956, 355.89169312}  
 $W.m^{-2}.\mu m^{-1}.sr^{-1}$

Resources:

Estimated CPU time: -  
Output disk space: 15 × 4 bytes/fl = 60 bytes

Acceptance:

Corresponds to the latest definition.

**6.2.9 GADS Level-0 Extraction**

6.2.9.1 *Blank sample thresholds*

Reference: Blank\_thr[b], LUT228

[AD-8] Section 6.2.9, GADS field 1

ACRI provided

Dependencies:

None

Tool:

None

Procedure:

Input: *b* MERIS spectral band# (15 values), see [Section 3.1](#) for the nominal wavelengths (LUT400)

Output: *Blank\_thr[b]* Blank sample thresholds in the 15 MERIS bands (15 values)  
units: [dl]

Step: User specified.

Scientific content:

Blank sample thresholds used for the 15 MERIS spectral bands

Current baseline: {52, 52, 52, 52, 52, 52, 52, 52, 52, 26, 52, 52, 26, 26, 26}

Resources:

Estimated CPU time: -  
Output disk space: 16 × 2 bytes/us = 32 bytes

Acceptance:

Corresponds to the latest definition.

**6.2.9.2 Blank sample difference thresholds**

Reference: Blank\_dif\_thr[b], LUT229

[AD-8] Section 6.2.9, GADS field 2

ACRI provided

Dependencies:

None

Tool:

None

Procedure:

Input: *b* MERIS spectral band# (15 values), see Section 3.1, (LUT400)

Output: *Blank\_dif\_thr[b]*  
Blank sample difference thresholds in the 15 MERIS bands (15 values)

units: [*dl*]

Step: User specified.

Scientific content:

Blank sample difference thresholds used for the 15 MERIS spectral bands

Current baseline: {4, 4, 4, 4, 4, 4, 4, 4, 4, 2, 4, 4, 2, 2, 2} [*dl*]

Resources:

Estimated CPU time: -  
Output disk space: 16 × 2 bytes/us = 32 bytes

Acceptance:

Corresponds to the latest definition.

6.2.9.3 *Scaling factor for floating point values coding*

Reference: PK\_scale, LUT230

[AD-8] Section 6.2.9, GADS field 3

ACRI provided

Dependencies:

None

Tool:

None

Procedure:

Input: none

Output: PK\_scale Scaling factor for floating point values coding  
units: [dl]

Step: User specified.

Scientific content:

Scaling factor used for coding the floating point values

Current baseline: -32768

Resources:

Estimated CPU time: -

Output disk space: 1 × 2 bytes/us = 2 bytes

Acceptance:

Corresponds to the latest definition.

## 6.2.10 GADS Geolocation

### 6.2.10.1 Mean Earth radius

Reference: Re, LUT231

[AD-8] Section 6.2.10, GADS field 1

ACRI provided

Dependencies:

None

Tool:

None

Procedure:

Input: none

Output: Re Mean Earth radius  
units: [m]

Step: User specified.

Scientific content:

Mean value used for the Earth radius

Current baseline: 6363885 m

Resources:

Estimated CPU time: -  
Output disk space: 1 × 4 bytes/ul = 4 bytes

Acceptance:

Corresponds to the latest definition.

### 6.2.10.2 Number of tie points per frame for full swath

Reference: NJ, LUT232

[AD-8] Section 6.2.10, GADS field 2

ACRI provided

Dependencies:

None

Tool:

None

Procedure:

Input: none

Output: *NJ* Number of tie points per frame for full swath  
units: [*dl*]

Step: User specified.

Scientific content:

Number of tie points per frame used for the full swath

Current baseline: 71

Resources:

Estimated CPU time: -

Output disk space:  $1 \times 2 \text{ bytes/us} = 2 \text{ bytes}$

Acceptance:

Corresponds to the latest definition.

*6.2.10.3 AC distance between tie points*

Reference: Dx\_t, LUT233

[AD-8] Section 6.2.10, GADS field 3

ACRI provided

Dependencies:

None

Tool:

None

Procedure:

Input: none

Output:  $Dx_t$  AC distance between tie points

units: [m]

Step: User specified.

Scientific content:

Distance between tie points used in the atmospheric correction procedure

Current baseline: 16640 m

Resources:

Estimated CPU time: -

Output disk space:  $1 \times 2$  bytes/us = 2 bytes

Acceptance:

Corresponds to the latest definition.

6.2.10.4 FR product AC pixel size

Reference:  $Pix^{FR}$ , LUT234

[AD-8] Section 6.2.10, GADS field 4

ACRI provided

Dependencies:

None

Tool:

None

Procedure:

Input: none

Output:  $Pix^{FR}$  FR product AC pixel size

units: [m]

Step: User specified.

Scientific content:

Pixel size of the atmospherically corrected product in the full resolution mode

Current baseline: 260 m

Resources:

Estimated CPU time: -

Output disk space: 1 × 4 bytes/fl = 4 bytes

Acceptance:

Corresponds to the latest definition.

*6.2.10.5 RR product AC pixel size*

Reference: Pix<sup>RR</sup>, LUT235

[AD-8] Section 6.2.10, GADS field 5

ACRI provided

Dependencies:

None

Tool:

None

Procedure:

Input: none

Output: Pix<sup>RR</sup> RR product AC pixel size

units: [m]

Step: User specified.

Scientific content:

Pixel size of the atmospherically corrected product in the reduced resolution mode

Current baseline: 1040 *m*

Resources:

Estimated CPU time: -  
Output disk space: 1 × 4 bytes/fl = 4 bytes

Acceptance:

Corresponds to the latest definition.

## 6.2.11 GADS Flagging

### 6.2.11.1 Width of blooming contamination for FR

Reference: Glint\_bloom\_K<sup>FR</sup>, LUT236

[AD-8] Section 6.2.11, GADS field 1

ACRI provided

Dependencies:

None

Tool:

None

Procedure:

Input: none

Output: *Glint\_bloom\_K<sup>FR</sup>*  
Width of blooming contamination for FR

units: [dl]

Step: User specified.

Scientific content:

Width (in pixels) of blooming contamination in the full resolution mode

Current baseline: 5

Resources:



Estimated CPU time: -  
Output disk space: 1 × 2 bytes/us = 2 bytes

Acceptance:

Corresponds to the latest definition.

6.2.11.2 *Width of blooming contamination for RR*

Reference: Glint\_bloom\_K<sup>RR</sup>, LUT237

[AD-8] Section 6.2.11, GADS field 2

ACRI provided

Dependencies:

None

Tool:

None

Procedure:

Input: none

Output: *Glint\_bloom\_K<sup>RR</sup>*  
Width of blooming contamination for RR

units: [dl]

Step: User specified.

Scientific content:

Width (in pixels) of blooming contamination in the reduced resolution mode

Current baseline: 1

Resources:

Estimated CPU time: -  
Output disk space: 1 × 2 bytes/us = 2 bytes

Acceptance:

Corresponds to the latest definition.

### 6.2.11.3 Saturation recovery width for FR

Reference: Sat\_Rec\_K<sup>FR</sup>, LUT238

[AD-8] Section 6.2.11, GADS field 3

ACRI provided

#### Dependencies:

None

#### Tool:

None

#### Procedure:

Input: none

Output: Sat\_Rec\_K<sup>FR</sup>  
Saturation recovery width for FR

units: [dl]

Step: User specified.

#### Scientific content:

Width (in pixels) of saturation recovery in the full resolution mode

Current baseline: 0

#### Resources:

Estimated CPU time: -

Output disk space: 1 × 2 bytes/us = 2 bytes

#### Acceptance:

Corresponds to the latest definition.

### 6.2.11.4 Saturation recovery width for RR

Reference: Sat\_Rec\_K<sup>RR</sup>, LUT239

[AD-8] Section 6.2.11, GADS field 4

ACRI provided

Dependencies:

None

Tool:

None

Procedure:

Input: none

Output:  $Sat\_Rec\_K^{RR}$   
Saturation recovery width for RR

units: [dl]

Step: User specified.

Scientific content:

Width (in pixels) of saturation recovery in the reduced resolution mode

Current baseline: 0

Resources:

Estimated CPU time: -

Output disk space:  $1 \times 2 \text{ bytes/us} = 2 \text{ bytes}$

Acceptance:

Corresponds to the latest definition.

6.2.11.5 Azimuth angle range for sun glint risk

Reference: Glint\_thr\_azi, LUT240

[AD-8] Section 6.2.11, GADS field 5

ACRI provided

Dependencies:

None

Tool:

None

Procedure:

Input: none

Output: *Glnt\_thr\_azi*  
Azimuth angle range for sun glint risk

units:  $[10^{-6} \text{ deg.}]$

Step: User specified.

Scientific content:

Threshold in azimuth angle to avoid the risk of sun glint contamination

Current baseline: 1.064 *deg.*

Resources:

Estimated CPU time: -

Output disk space:  $1 \times 4 \text{ bytes/ul} = 4 \text{ bytes}$

Acceptance:

Corresponds to the latest definition.

6.2.11.6 *Zenith angle range for sun glint risk*

Reference: *Glnt\_thr\_zen*, LUT241

[AD-8] Section 6.2.11, GADS field 6

ACRI provided

Dependencies:

None

Tool:

None

Procedure:

Input: none

Output: *Glnt\_thr\_zen*  
Zenith angle range for sun glint risk

units: [10<sup>-6</sup> deg.]

Step: User specified.

Scientific content:

Threshold in zenith angle to avoid the risk of sun glint contamination

Current baseline: 1.064 deg

Resources:

Estimated CPU time: -

Output disk space: 1 × 4 bytes/ul = 4 bytes

Acceptance:

Corresponds to the latest definition.

6.2.11.7 *Band saturation levels for FR samples*

Reference: Sat\_sample<sup>FR</sup>[b], LUT242

[AD-8] Section 6.2.11, GADS field 7

ACRI provided

Dependencies:

None

Tool:

None

Procedure:

Input: *b* MERIS spectral band# (15 values), see [Section 3.1](#) for the nominal wavelengths (LUT400)

Output: *Sat\_sampleFR[b]*

Band saturation levels for FR samples in band #0 and 15 MERIS bands  
(16 values)

units: [nc]

Step: User specified.

Scientific content:

16 values of band saturation levels for the full resolution mode. 16 bands are considered: band#0 + 15 MERIS spectral bands

Current baseline: {8190, 8190, 8190, 8190, 8190, 8190, 8190, 8190, 8190, 8190, 8190, 4095, 8190, 8190, 4095, 4095} nc

Resources:

Estimated CPU time: -  
Output disk space: 16 × 2 bytes/us = 32 bytes

Acceptance:

Corresponds to the latest definition.

**6.2.11.8 Maximum valid radiances**

Reference: Sat\_rad[b], LUT243

[AD-8] Section 6.2.11, GADS field 8

ACRI provided

Dependencies:

None

Tool:

None

Procedure:

Input: *b* MERIS spectral band# (15 values), see [Section 3.1](#) for the nominal wavelengths (LUT400)

Output: *Sat\_rad[b]* Maximum valid radiances in the 15 MERIS bands (15 values)

units: [ $W.m^{-2}.\mu m^{-1}.sr^{-1}$ ]

Step: User specified.

Scientific content:

Maximum valid radiances in the 15 MERIS spectral bands

Current baseline: {615.86456299, 689.22607422, 752.98150635, 695.86920166, 606.40710449,  
532.22802734, 445.12484741, 450.96813965, 410.08322144, 563.20117188,  
576.74169922, 236.11985779, 231.03218079, 396.74154663, 352.98632812}  
 $W.m^{-2}.\mu m^{-1}.sr^{-1}$

Resources:

Estimated CPU time: -  
Output disk space: 15 × 4 bytes/fl = 60 bytes

Acceptance:

Corresponds to the latest definition.

6.2.11.9 *Threshold value for percentage of out of range image samples*

Reference: Pc\_thresh\_image, LUT244

[AD-8] Section 6.2.11, GADS field 9

ACRI provided

Dependencies:

None

Tool:

None

Procedure:

Input: none  
Output: Pc\_thresh\_image  
Threshold value for percentage of out of range image samples  
units: [%]  
Step: User specified.

Scientific content:

Threshold value for the percentage of acceptable out of range image samples

Current baseline: 25 %

Resources:

Estimated CPU time: -  
Output disk space: 1 × 2 bytes/us = 2 bytes

Acceptance:

Corresponds to the latest definition.

*6.2.11.10 Threshold value for percentage of out of range blank samples*

Reference: Pc\_thresh\_blank, LUT245

[AD-8] Section 6.2.11, GADS field 10

ACRI provided

Dependencies:

None

Tool:

None

Procedure:

Input: none  
Output: Pc\_thresh\_image  
Threshold value for percentage of out of range image samples  
units: [%]  
Step: User specified.

Scientific content:

Threshold value for the percentage of acceptable out of range blank samples

Current baseline: 25 [%]

Resources:



Estimated CPU time: -  
Output disk space: 1 × 2 bytes/us = 2 bytes

Acceptance:

Corresponds to the latest definition.

6.2.11.11 *Land processing bands*

Reference: land\_proc[b], LUT246

[AD-8] Section 6.2.11, GADS field 11

ACRI provided

Dependencies:

None

Tool:

None

Procedure:

Input: *b* MERIS spectral band# (15 values), see [Section 3.1](#) for the nominal wavelengths (LUT400)

Output: *land\_proc[b]* Flag to activate the land processing in the 15 MERIS bands (15 values)  
units: [*dl*]

Step: User specified.

Scientific content:

Flag for activating [1] or not [0] the processing over land for each of the 15 MERIS spectral bands

Current baseline: {1, 1, 1, 0, 0, 0, 1, 1, 0, 1, 1, 0, 1, 1, 1}

Resources:

Current baseline:

Resources:

Estimated CPU time: -

Output disk space:  $15 \times 1 \text{ byte/uc} = 15 \text{ bytes}$

Acceptance:

Corresponds to the latest definition.

6.2.11.12 *Threshold for setting transmission error flag (mean number of errors per packet)*

Reference: Trans\_thresh, LUT247

[AD-8] Section 6.2.11, GADS field 12

ACRI provided

Dependencies:

None

Tool:

None

Procedure:

Input: none

Output: *Trans\_thresh* Threshold for setting transmission error flag (mean number of errors per packet)

units: [dl]

Step: User specified.

Scientific content:

Threshold to set the data transmission error flag

Current baseline: 0

Resources:

Estimated CPU time: -

Output disk space:  $1 \times 4 \text{ bytes/fl} = 4 \text{ bytes}$

Acceptance:

Corresponds to the latest definition.

6.2.11.13 *Threshold for setting format error flag (mean number of errors per packet)*

Reference: Format\_thresh, LUT248

[AD-8] Section 6.2.11, GADS field 13

ACRI provided

Dependencies:

None

Tool:

None

Procedure:

Input: none

Output: *Format\_thresh* Threshold for setting format error flag (mean number of errors per packet)

units: [dl]

Step: User specified.

Scientific content:

Threshold to set the data format error flag

Current baseline: 0

Resources:

Estimated CPU time: -

Output disk space: 1 × 4 bytes/fl = 4 bytes

Acceptance:

Corresponds to the latest definition.

**6.2.12 GADS Radiometric**

6.2.12.1 *Switch enabling FR non-linearity corrections*

Reference: FR\_NonLin\_F, LUT249

[AD-8] Section 6.2.12, GADS field 1

ACRI provided

Dependencies:

None

Tool:

None

Procedure:

Input: none

Output: *FR\_NonLin\_F* Switch enabling FR non-linearity corrections

units: [dl]

Step: User specified.

Scientific content:

Switch used to launch the non-linearity corrections in the full resolution mode

Current baseline: 1

Resources:

Estimated CPU time: -

Output disk space: 1 × 1 byte/uc = 1 byte

Acceptance:

Corresponds to the latest definition.

6.2.12.2 *Switch enabling RR non-linearity corrections*

Reference: RR\_NonLin\_F, LUT250

[AD-8] Section 6.2.12, GADS field 2

ACRI provided

Dependencies:

None

Tool:

None

Procedure:

Input: none

Output: *RR\_NonLin\_F* Switch enabling RR non-linearity corrections

units: [*dl*]

Step: User specified.

Scientific content:

Switch used to launch the non-linearity corrections in the reduced resolution mode

Current baseline: 1

Resources:

Estimated CPU time: -

Output disk space: 1 × 1 byte/uc = 1 byte

Acceptance:

Corresponds to the latest definition.

*6.2.12.3 Switch enabling AC straylight correction*

Reference: Stray\_corr\_AC\_s, LUT251

[AD-8] Section 6.2.12, GADS field 3

ACRI provided

Dependencies:

None

Tool:

None

Procedure:

Input: none  
Output: *Stray\_corr\_AC\_s*  
Switch enabling AC straylight correction  
units: [dl]  
Step: User specified.

Scientific content:

Switch used to launch the non-linearity corrections in the reduced resolution mode  
Current baseline: 1

Resources:

Estimated CPU time: -  
Output disk space: 1 × 1 byte/uc = 1 byte

Acceptance:

Corresponds to the latest definition.

6.2.12.4 (Spare)

Reference:

[AD-8] Section 6.2.12, GADS field 4

**6.2.13 GADS Classification**

6.2.13.1 View zenith angles for GADS radiometric thresholds

Reference: VZA, LUT253

[AD-8] Section 6.2.13, GADS field 1.

ACRI provided

Dependencies:

None

Tool:

None

Procedure:

Input: none  
Output: *VZA* View zenith angles (12 values)  
units:  $[10^{-6} \text{ deg}]$   
Step: User specified.

Scientific content:

Set of 12 view zenith angles ( $\theta_v$ ) selected from a *Gauss* quadrature generated for 24 discrete directions with the RTC/Gauss tool (UdL)

Current baseline: 12 *Gaussian* angles

| <i>i</i> | $\theta_v$ [deg.] | <i>i</i> | $\theta_v$ [deg.] |
|----------|-------------------|----------|-------------------|
| 0        | 2.840906          | 6        | 58.455477         |
| 1        | 17.638419         | 7        | 65.877652         |
| 2        | 28.768427         | 8        | 69.588762         |
| 3        | 36.189726         | 9        | 73.299882         |
| 4        | 43.611442         | 10       | 77.011011         |
| 5        | 51.033390         | 11       | 80.722147         |

Resources:

Estimated CPU time: -  
Output disk space:  $12 \times 4 \text{ bytes/ul} = 48 \text{ bytes}$

Acceptance:

Corresponds to the latest definition

6.2.13.2 Sun zenith angles for GADS radiometric thresholds

Reference: SZA, LUT254

[AD-8] Section 6.2.13, GADS field 2.

ACRI provided

Dependencies:

None

Tool:

None

Procedure:

Input: none

Output: *SZA* Solar zenith angles (12 values)

units:  $[10^{-6} \text{ deg}]$

Step: User specified.

Scientific content:

Set of 12 solar zenith angles ( $\theta_s$ ) selected from a *Gauss* quadrature generated for 24 discrete directions with the RTC/Gauss tool (UdL)

Current baseline: 12 *Gaussian* angles

| $i$ | $\theta_s$ [deg.] | $i$ | $\theta_s$ [deg.] |
|-----|-------------------|-----|-------------------|
| 0   | 2.840906          | 6   | 58.455477         |
| 1   | 17.638419         | 7   | 65.877652         |
| 2   | 28.768427         | 8   | 69.588762         |
| 3   | 36.189726         | 9   | 73.299882         |
| 4   | 43.611442         | 10  | 77.011011         |
| 5   | 51.033390         | 11  | 80.722147         |

Resources:

Estimated CPU time: -

Output disk space:  $12 \times 4 \text{ bytes/ul} = 48 \text{ bytes}$

Acceptance:

Corresponds to the latest definition

**6.2.13.3 Relative azimuth angles for GADS radiometric thresholds**

Reference: RAA, LUT255

[AD-8] Section 6.2.13, GADS field 3.

ACRI provided



Dependencies:

None

Tool:

None

Procedure:

Input: none

Output: *RAA* Relative azimuth angles (19 values)  
units:  $[10^{-6} \text{ deg}]$

Step: User specified.

Scientific content:

Set of 19 relative azimuth angles ( $\Delta\phi$ ) regularly spaced

Current baseline: 19 angles in  $[0;180] \text{ deg.}$  by step of  $10 \text{ deg.}$

Resources:

Estimated CPU time: -

Output disk space:  $19 \times 4 \text{ bytes/ul} = 76 \text{ bytes}$

Acceptance:

Corresponds to the latest definition

6.2.13.4 (*Spare*)

Reference:

[AD-8] Section 6.2.13, GADS field 4.

6.2.13.5 (*Spare*)

Reference:

[AD-8] Section 6.2.13, GADS field 5.

6.2.13.6 (Spare)

Reference:

[AD-8] Section 6.2.13, GADS field 6.

6.2.13.7 (Spare)

Reference:

[AD-8] Section 6.2.13, GADS field 7.

6.2.13.8 Index of band for GADS radiometric thresholds

Reference:  $b_{test}$  LUT256

[AD-8] Section 6.2.13, GADS field 8.

ACRI provided

Dependencies:

None

Tool:

None

Procedure:

Input: none

Output:  $b_{test}$  Index of band for GADS radiometric thresholds

units: [dl]

Step: User specified.

Scientific content:

MERIS spectral band selected for computing the radiometric thresholds (LUT017)

Current baseline: 2

Resources:

Estimated CPU time: -

Output disk space:  $1 \times 1$  byte/uc = 1 byte

Acceptance:

Corresponds to the latest definition.

6.2.13.9 (*Spare*)

Reference:

[AD-8] Section 6.2.13, GADS field 9.

**6.2.14 GADS Resampling**

6.2.14.1 *Resampling switch*

Reference: Resampling\_switch, LUT257

[AD-8] Section 6.2.14, GADS field 1

ACRI provided

Dependencies:

None

Tool:

None

Procedure:

Input: none

Output: *Resampling\_switch* Resampling switch

units: [dl]

Step: User specified.

Scientific content:

Swith used for the resampling

Current baseline: 1

Resources:

Estimated CPU time: -

Output disk space:  $1 \times 1 \text{ byte/uc} = 1 \text{ byte}$

Acceptance:

Corresponds to the latest definition.

*6.2.14.2 Number of AC samples used in product FR imagette*

Reference:  $NC^{IM}$ , LUT258

[AD-8] Section 6.2.14, GADS field 2

ACRI provided

Dependencies:

None

Tool:

None

Procedure:

Input: none

Output:  $NC^{IM}$  Number of AC samples used in product FR imagette  
units: [dl]

Step: User specified.

Scientific content:

Number of AC samples used in the product imagette for the full resolution mode

Current baseline: 1153

Resources:

Estimated CPU time: -

Output disk space:  $1 \times 2 \text{ bytes/us} = 2 \text{ bytes}$

Acceptance:

Corresponds to the latest definition.

6.2.14.3 Number of AC samples used in product FR scene

Reference: NC<sup>FR</sup>, LUT259

[AD-8] Section 6.2.14, GADS field 3

ACRI provided

Dependencies:

None

Tool:

None

Procedure:

Input: none

Output: NC<sup>FR</sup> Number of AC samples used in product FR scene  
units: [dl]

Step: User specified.

Scientific content:

Number of AC samples used in the product scene for the full resolution mode

Current baseline: 2241

Resources:

Estimated CPU time: -

Output disk space: 1 × 2 bytes/us = 2 bytes

Acceptance:

Corresponds to the latest definition.

6.2.14.4 Number of AC samples used in product RR

Reference: NC<sup>RR</sup>, LUT260

[AD-8] Section 6.2.14, GADS field 4

ACRI provided

Dependencies:

None

Tool:

None

Procedure:

Input: none

Output:  $NC^{RR}$  Number of AC samples used in product RR

units: [dl]

Step: User specified.

Scientific content:

Number of AC samples used in the product for the reduced resolution mode

Current baseline: 1121

Resources:

Estimated CPU time: -

Output disk space:  $1 \times 2 \text{ bytes/us} = 2 \text{ bytes}$

Acceptance:

Corresponds to the latest definition.

*6.2.14.5 FR across track pixel to tie point sub-sampling factor (number of samples)*

Reference: DJ<sup>FR</sup>, LUT261

[AD-8] Section 6.2.14, GADS field 5

ACRI provided

Dependencies:

None

Tool:

None

Procedure:

Input: none

Output:  $DJ^{FR}$  FR across track pixel to tie point sub-sampling factor (number of samples)

units: [dl]

Step: User specified.

Scientific content:

Number of samples (in full resolution mode) used to tie point sub-sampling factor

Current baseline: 64

Resources:

Estimated CPU time: -

Output disk space:  $1 \times 1$  byte/uc = 1 byte

Acceptance:

Corresponds to the latest definition.

**6.2.14.6 RR across track pixel to tie point sub-sampling factor (number of samples)**

Reference:  $DJ^{RR}$ , LUT262

[AD-8] Section 6.2.14, GADS field 6

ACRI provided

Dependencies:

None

Tool:

None

Procedure:

Input: none

Output:  $DJ^{RR}$  RR across track pixel to tie point sub-sampling factor (number of samples)  
units:  $[dl]$   
Step: User specified.

Scientific content:

Number of samples (in reduced resolution mode) used to tie point sub-sampling factor  
Current baseline: 16

Resources:

Estimated CPU time: -  
Output disk space:  $1 \times 1 \text{ byte/uc} = 1 \text{ byte}$

Acceptance:

Corresponds to the latest definition.

*6.2.14.7 FR frame to tie frame sub-sampling factor (number of samples)*

Reference:  $DF^{FR}$ , LUT263

[\[AD-8\]](#) Section 6.2.14, GADS field 7

ACRI provided

Dependencies:

None

Tool:

None

Procedure:

Input: none  
Output:  $DF^{FR}$  FR frame to tie frame sub-sampling factor (number of samples)  
units:  $[dl]$   
Step: User specified.

Scientific content:



Number of samples (in full resolution mode) used to tie frame sub-sampling factor

Current baseline: 64

Resources:

Estimated CPU time: -  
Output disk space: 1 × 1 byte/uc = 1 byte

Acceptance:

Corresponds to the latest definition.

6.2.14.8 RR frame to tie frame sub-sampling factor (number of samples)

Reference:  $DF^{RR}$ , LUT264

[AD-8] Section 6.2.14, GADS field 8

ACRI provided

Dependencies:

None

Tool:

None

Procedure:

Input: none  
Output:  $DF^{RR}$  RR frame to tie frame sub-sampling factor (number of samples)  
units: [dl]  
Step: User specified.

Scientific content:

Number of samples (in reduced resolution mode) used to tie frame sub-sampling factor

Current baseline: 16

Resources:

Estimated CPU time: -  
Output disk space: 1 × 1 byte/uc = 1 byte

Acceptance:

Corresponds to the latest definition.

**6.2.14.9 Tie frame to summary quality ADS frame sub-sampling factor**

Reference: DFSQ, LUT265

[AD-8] Section 6.2.14, GADS field 9

ACRI provided

Dependencies:

None

Tool:

None

Procedure:

Input: none

Output: *DFSQ* Tie frame to summary quality ADS frame sub-sampling factor  
units: [*dl*]

Step: User specified.

Scientific content:

Tie frame used for quality of frame sub-sampling factor

Current baseline: 8

Resources:

Estimated CPU time: -  
Output disk space: 1 × 1 byte/uc = 1 byte

Acceptance:

Corresponds to the latest definition.

6.2.14.10 Maximum across track angular distance allowing pixel selection in FR

Reference: Max\_ $d\psi^{FR}$ , LUT266

[AD-8] Section 6.2.14, GADS field 10

ACRI provided

Dependencies:

None

Tool:

None

Procedure:

Input: none

Output: Max\_ $d\psi^{FR}$  Maximum across track angular distance allowing pixel selection in FR  
units: [10<sup>-6</sup>deg.]

Step: User specified.

Scientific content:

Maximum across track angular distance used for the pixel selection in the full resolution mode

Current baseline: 0.038311 deg.

Resources:

Estimated CPU time: -

Output disk space: 1 × 4 bytes/ul = 4 bytes

Acceptance:

Corresponds to the latest definition.

6.2.14.11 Maximum across track angular distance allowing pixel selection in RR

Reference: Max\_ $d\psi^{RR}$ , LUT267

[AD-8] Section 6.2.14, GADS field 11

ACRI provided

Dependencies:

None

Tool:

None

Procedure:

Input: none

Output:  $Max\_d\psi^{RR}$  Maximum across track angular distance allowing pixel selection in RR  
units:  $[10^{-6}deg.]$

Step: User specified.

Scientific content:

Maximum across track angular distance used for the pixel selection in the full resolution mode

Current baseline: 0.153243 *deg.*

Resources:

Estimated CPU time: -

Output disk space:  $1 \times 4 \text{ bytes/ul} = 4 \text{ bytes}$

Acceptance:

Corresponds to the latest definition.

## 6.2.15 GADS Scaling Factor

### 6.2.15.1 Scaling factor - altitude

Reference: Alt\_scale, LUT268

[AD-8] Section 6.2.15, GADS field 1

ACRI provided

Dependencies:

None

Tool:

None

Procedure:

Input: none

Output: *Alt\_scale*      Scaling factor for altitude  
units:      [*dl*]

Step:      User specified.

Scientific content:

Scaling factor used for altitude level

Current baseline: 1

Resources:

Estimated CPU time: -

Output disk space: 1 × 4 bytes/fl = 4 bytes

Acceptance:

Corresponds to the latest definition.

6.2.15.2 *Scaling factor - roughness*

Reference:      *Rough\_scale*,      LUT269

[AD-8]      Section 6.2.15, GADS field 2

ACRI provided

Dependencies:

None

Tool:

None

Procedure:

Input: none

Output: *Rough\_scale* Scaling factor for roughness  
units: [dl]

Step: User specified.

Scientific content:

Scaling factor used for roughness level

Current baseline: 1

Resources:

Estimated CPU time: -  
Output disk space: 1 × 4 bytes/fl = 4 bytes

Acceptance:

Corresponds to the latest definition.

*6.2.15.3 Scaling factor - zonal wind*

Reference: *Zwind\_scale*, LUT270

[AD-8] Section 6.2.15, GADS field 3

ACRI provided

Dependencies:

None

Tool:

None

Procedure:

Input: none

Output: *Zwind\_scale* Scaling factor for zonal wind  
units: [dl]

Step: User specified.

Scientific content:

Scaling factor used for zonal wind

Current baseline: 0.1

Resources:

Estimated CPU time: -  
Output disk space: 1 × 4 bytes/fl = 4 bytes

Acceptance:

Corresponds to the latest definition.

6.2.15.4 *Scaling factor - meridional wind*

Reference: Mwind\_scale, LUT271

[AD-8] Section 6.2.15, GADS field 4

ACRI provided

Dependencies:

None

Tool:

None

Procedure:

Input: none  
Output: *Mwind\_scale* Scaling factor for meridional wind  
units: [*dl*]  
Step: User specified.

Scientific content:

Scaling factor used for meridional wind

Current baseline: 0.1

Resources:

Estimated CPU time: -  
Output disk space: 1 × 4 bytes/fl = 4 bytes

Acceptance:

Corresponds to the latest definition.

*6.2.15.5 Scaling factor - atmospheric pressure*

Reference: Patm\_scale, LUT272

[AD-8] Section 6.2.15, GADS field 5

ACRI provided

Dependencies:

None

Tool:

None

Procedure:

Input: none

Output: Patm\_scale Scaling factor for atmospheric pressure  
units: [dl]

Step: User specified.

Scientific content:

Scaling factor used for atmospheric pressure

Current baseline: 0.1

Resources:

Estimated CPU time: -  
Output disk space: 1 × 4 bytes/fl = 4 bytes

Acceptance:

Corresponds to the latest definition.



#### 6.2.15.6 Scaling factor - ozone

Reference: O3\_scale, LUT273

[AD-8] Section 6.2.15, GADS field 6

ACRI provided

#### Dependencies:

None

#### Tool:

None

#### Procedure:

Input: none

Output: O3\_scale      Scaling factor for ozone content  
units: [dl]

Step: User specified.

#### Scientific content:

Scaling factor used for ozone content

Current baseline: 0.01

#### Resources:

Estimated CPU time: -

Output disk space:  $1 \times 4 \text{ bytes/fl} = 4 \text{ bytes}$

#### Acceptance:

Corresponds to the latest definition.

#### 6.2.15.7 Scaling factor - relative humidity

Reference: RH\_scale, LUT274

[AD-8] Section 6.2.15, GADS field 7

ACRI provided

Dependencies:

None

Tool:

None

Procedure:

Input: none

Output: *RH\_scale*      Scaling factor for relative humidity  
units:      [*dl*]

Step:      User specified.

Scientific content:

Scaling factor used for relative humidity

Current baseline: 0.1

Resources:

Estimated CPU time: -

Output disk space: 1 × 4 bytes/fl = 4 bytes

Acceptance:

Corresponds to the latest definition.

**6.2.15.8 Scaling factor - radiances**

Reference: Rad\_scale[b],      LUT275

[AD-8]      Section 6.2.15, GADS field 8

ACRI provided

Dependencies:

None

Tool:

None

Procedure:

**Input:** *b* MERIS spectral band# (15 values), see [Section 3.1](#) for the nominal wavelengths (LUT400)

**Output:** *Rad\_scale* Scaling factor for radiances (15 values)  
**units:** [*dl*]

**Step:** User specified.

Scientific content:

Scaling factors (15 MERIS spectral bands) used for radiances

Current baseline: {0.0094748391, 0.0106034772, 0.0115843304, 0.0107056797, 0.0093293404, 0.0081881238, 0.0068480745, 0.0069379713, 0.0063089724, 0.0086646341, 0.0088729495, 0.0036326132, 0.0035543414, 0.0061037163, 0.0054305592}

Resources:

Estimated CPU time: -  
Output disk space: 15 × 4 bytes/fl = 60 bytes

Acceptance:

Corresponds to the latest definition.

**6.2.16 GADS Straylight Evaluation Parameters**

*6.2.16.1 Number of spectral regions*

Reference: SR, LUT276

[AD-8] Section 6.2.16, GADS field 1

ACRI provided

Dependencies:

None

Tool:

None

Procedure:

Input: none  
Output: *SR* Number of spectral regions (5 values)  
units: [*dl*]  
Step: User specified.

Scientific content:

Number of spectral regions used for straylight evaluation parameters  
Current baseline: 5

Resources:

Estimated CPU time: -  
Output disk space:  $1 \times 2 \text{ bytes/us} = 2 \text{ bytes}$

Acceptance:

Corresponds to the latest definition.

*6.2.16.2 Band index of default radiance for pixels with all bands saturated*

Reference: *b\_satpix*, LUT277

[AD-8] Section 6.2.16, GADS field 2

ACRI provided

Dependencies:

None

Tool:

None

Procedure:

Input: none  
Output: *b\_satpix* Band index of default radiance for pixels with all bands saturated  
units: [*dl*]

Step: User specified.

Scientific content:

MERIS band # to be used for setting default radiance for pixels having all the spectral band saturated.

Current baseline: 10

Resources:

Estimated CPU time: -  
Output disk space:  $1 \times 2$  bytes/us = 2 bytes

Acceptance:

Corresponds to the latest definition.

*6.2.16.3 Default radiance for pixels with all bands saturated*

Reference: rad\_satpix, LUT278

[AD-8] Section 6.2.16, GADS field 3

ACRI provided

Dependencies:

None

Tool:

None

Procedure:

Input: none  
Output: rad\_satpix Default radiance for pixels with all bands saturated  
units:  $[W.m^{-2}.\mu m^{-1}.sr^{-1}]$   
Step: User specified.

Scientific content:

Default radiance to be used for pixels having all the spectral band saturated.

Current baseline: 844.80181885  $W.m^{-2}.\mu m^{-1}.sr^{-1}$

Resources:

Estimated CPU time: -  
Output disk space: 1 × 4 bytes/fl = 4 bytes

Acceptance:

Corresponds to the latest definition.

6.2.16.4 (*Spare*)

Reference:

[AD-8] Section 6.2.16, GADS field 4

6.2.16.5 (*Spare*)

Reference:

[AD-8] Section 6.2.16, GADS field 5

6.2.16.6 *Interpolation coefficients for spectral region flux estimation*

Reference: P[b,SR], LUT281

[AD-8] Section 6.2.16, GADS field 6

ACRI provided

Dependencies:

None

Tool:

LUT276

Procedure:

Inputs: *b* MERIS spectral band# (15 values), see [Section 3.1](#) for the nominal wavelengths (LUT400)  
*SR* Spectral region # (5 values), see [Section 6.2.16.1](#), (LUT276)

Output: *P[b,SR]* Interpolation coefficients for spectral region flux estimation given in each of the 15 MERIS bands

units: [*dI*]

Step: User specified.

Scientific content:

Default radiance to be used for pixels having all the spectral band saturated.

Current baseline: 15 x 5 values (see table below)

| $\lambda$ [nm] | SR-1       | SR-2       | SR-3       | SR-4       | SR-5       |
|----------------|------------|------------|------------|------------|------------|
| 412.500        | 0.20192300 | 0.00000000 | 0.00000000 | 0.00000000 | 0.00000000 |
| 442.500        | 0.29807699 | 0.00000000 | 0.00000000 | 0.00000000 | 0.00000000 |
| 490.000        | 0.25961500 | 0.00000000 | 0.00000000 | 0.00000000 | 0.00000000 |
| 510.000        | 0.14615400 | 0.12307700 | 0.00000000 | 0.00000000 | 0.00000000 |
| 560.000        | 0.00769231 | 0.41538501 | 0.00000000 | 0.00000000 | 0.00000000 |
| 620.000        | 0.00000000 | 0.38461500 | 0.01923080 | 0.00000000 | 0.00000000 |
| 665.000        | 0.00000000 | 0.07692310 | 0.15865400 | 0.00000000 | 0.00000000 |
| 681.250        | 0.00000000 | 0.00000000 | 0.16826899 | 0.00000000 | 0.00000000 |
| 708.750        | 0.00000000 | 0.00000000 | 0.27884600 | 0.00000000 | 0.00000000 |
| 753.750        | 0.00000000 | 0.00000000 | 0.19951899 | 0.00000000 | 0.00000000 |
| 761.875        | 0.00000000 | 0.00000000 | 0.09615380 | 0.00000000 | 0.00000000 |
| 778.750        | 0.00000000 | 0.00000000 | 0.07925720 | 0.32218501 | 0.00000000 |
| 865.000        | 0.00000000 | 0.00000000 | 0.00006968 | 0.40858400 | 0.00000000 |
| 885.000        | 0.00000000 | 0.00000000 | 0.00000000 | 0.13461500 | 0.00000000 |
| 900.000        | 0.00000000 | 0.00000000 | 0.00000000 | 0.13186800 | 0.46428600 |

Resources:

Estimated CPU time: -  
Output disk space: 15 x 5 x 4 bytes/fl = 300 bytes

Acceptance:

Corresponds to the latest definition.

*6.2.16.7 Flag register showing bands which can be used for radiance estimation of saturated samples*

Reference: Bs, LUT282

[AD-8] Section 6.2.16, GADS field 7

ACRI provided

Dependencies:

None

Tool:

None

Procedure:

Input: none

Output: *Bs* Flag register showing bands which can be used for radiance estimation of saturated samples

units: [*dl*]

Step: User specified.

Scientific content:

Flag register indicating bands which can be used to estimate the radiance for saturated samples

Current baseline: 15871

Resources:

Estimated CPU time: -

Output disk space:  $1 \times 2 \text{ bytes/us} = 2 \text{ bytes}$

Acceptance:

Corresponds to the latest definition.

*6.2.16.8 FR threshold on saturated samples counts to flag for straylight risk*

Reference: Sat\_Stray\_Thr<sup>FR</sup>, LUT283

[AD-8] Section 6.2.16, GADS field 8

ACRI provided

Dependencies:

None

Tool:

None

Procedure:



Input: none

Output:  $Sat\_Stray\_Thr^{FR}$  FR threshold on saturated samples counts to flag for straylight risk

units: [dl]

Step: User specified.

Scientific content:

Threshold on saturated samples counts used in the full resolution mode to flag the risk of straylight

Current baseline: 2775

Resources:

Estimated CPU time: -

Output disk space:  $1 \times 2 \text{ bytes/us} = 2 \text{ bytes}$

Acceptance:

Corresponds to the latest definition.

*6.2.16.9 RR threshold on saturated samples counts to flag for straylight risk*

Reference:  $Sat\_Stray\_Thr^{RR}$ , LUT284

[AD-8] Section 6.2.16, GADS field 9

ACRI provided

Dependencies:

None

Tool:

None

Procedure:

Input: none

Output:  $Sat\_Stray\_Thr^{RR}$  RR threshold on saturated samples counts to flag for straylight risk

units: [dl]

Step: User specified.

Scientific content:

Threshold on saturated samples counts used in the reduced resolution mode to flag the risk of straylight

Current baseline: 693

Resources:

Estimated CPU time: -

Output disk space:  $1 \times 2 \text{ bytes/us} = 2 \text{ bytes}$

Acceptance:

Corresponds to the latest definition.

**6.2.17 (Deleted)**

Reference:

[AD-8] Section 6.2.17

**6.2.18 (Deleted)**

Reference:

[AD-8] Section 6.2.18

**6.2.19 (Deleted)**

Reference:

[AD-8] Section 6.2.19

**6.2.20 GADS Radiometric Thresholds LUT**

*6.2.20.1 Radiometric thresholds,  $L_{TOA_2}(\theta_s, \theta_v, \Delta\varphi)$*

Reference: Class\_thr\_t[ $\theta_s, \theta_v, \Delta\varphi$ ], LUT017

[AD-8] Section 6.2.20, ADS field 1.

Dependencies:

LUT253, LUT254, LUT255, LUT256

Tools:

OTC/RAYLEIGH  
RTC/UPRAD (SO)

Procedure:

Inputs:  $\theta_v$  View zenith angle [*deg.*], see [Section 6.2.13.1](#), (LUT253)  
 $\theta_s$  Sun zenith angle [*deg.*], see [Section 6.2.13.2](#), (LUT254)  
 $\Delta\phi$  Relative azimuth angle [*deg.*], see [Section 6.2.13.3](#), (LUT255)  
 $n(\lambda)$  MERIS band index [*dl*], see [Section 6.2.13.8](#), (LUT256)

Output:  $class\_thr\_t[\theta_s, \theta_v, \Delta\phi]$   
Radiometric thresholds on TOA reflectance at  $\lambda$  nm as a function of the sun zenith angle, view zenith angle and relative azimuth angle between the illumination and viewing directions.

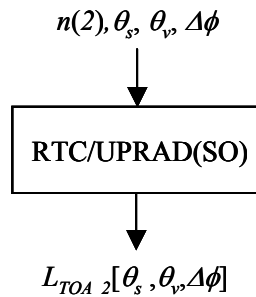
units: [*dl*]

Step-1: Generate TOA normalized radiance  $L_{TOA,2}[\theta_s, \theta_v, \Delta\phi]$  with the RTC/UPRAD (SO) over a slightly reflective surface under a continental atmosphere. The selected aerosol model is the Junge model#27 ( $m=1.44, \alpha=0$ ).

**RTC/UPRAD (SO) Inputs (LAND)**

| Variable        | Value                  | Comments   |
|-----------------|------------------------|--|
| <i>out_file</i> | "/OUTPUT/uprad_out"    |  |
| <i>i_branch</i> | 1                      |  |
| $n(\lambda)$    | 2                      | 442.5 nm (see <a href="#">Section 6.2.13.8</a> ) |
| $U_{H2O}$       | 0                      |  |
| $U_{O2}$        | 0                      |  |
| <i>ESFT</i>     | -                      | N/A  |
| $P_s$           | 1013.25                |  |
| $t^R(\lambda)$  | tauR                   | Computed with OTC/RAYLEIGH                       |
| <i>aerosol1</i> | "/INPUT/sc_land27_b05" | Junge model #27 ( $m=1.44, \alpha=0$ )           |
| $t^{a1}(550)$   | 1.2                    |  |
| <i>aerosol2</i> | -                      |  |
| $t^{a2}(550)$   | 0                      |  |
| <i>aerosol3</i> | -                      |  |
| $t^{a3}(550)$   | 0                      |  |
| <i>cloud1</i>   | -                      | N/A  |
| <i>cloud2</i>   | -                      | N/A  |
| <i>cloud3</i>   | -                      | N/A  |
| <i>phyto</i>    | -                      | N/A  |

| Variable                   | Value                           | Comments  |
|----------------------------|---------------------------------|---|
| $\sigma_{e,\lambda}^p$     | -                               | N/A   |
| $\omega_{o,\lambda}^p$     | -                               | N/A   |
| <i>spm</i>                 | -                               | N/A   |
| $\sigma_{e,\lambda}^{spm}$ | -                               | N/A   |
| $\omega_{o,\lambda}^{spm}$ | -                               | N/A   |
| $\sigma_{e,\lambda}^{ys}$  | -                               | N/A   |
| <i>vertical</i>            | "/INPUT/vertical_out"           | Not used, vertical distribution determined in RTC/SO ( $H_a=2\text{ km}; H_R=8\text{ km}$ ) |
| $I_s$                      | 79                              |   |
| $\rho_s$                   | 0.08                            |   |
| $E_o$                      | 1                               |   |
| $\sigma_{e,\lambda}^w$     | -                               | N/A   |
| $\omega_{o,\lambda}^w$     | -                               | N/A   |
| $w_s$                      | 0                               |   |
| $n_s, n_v, n_{\Delta\phi}$ | 12, 12, 18                      |   |
| $\theta_s$                 | values stored in $\theta_s[]$   | see Section 6.2.13.2  |
| $\theta_v$                 | values stored in $\theta_v[]$   | see Section 6.2.13.1  |
| $\Delta\phi$               | values stored in $\Delta\phi[]$ | see Section 6.2.13.3  |
| <i>pol</i>                 | 1                               |   |



Step-2: Build  $class\_thr\_t[\theta_s, \theta_v, \Delta\phi]$  as follows,

$$class\_thr\_t[\theta_s, \theta_v, \Delta\phi] = \frac{\pi \cdot L_{TOA\_2}[\theta_s, \theta_v, \Delta\phi]}{\cos \theta_s}$$

If  $class\_thr\_t[\theta_s, \theta_v, \Delta\phi] > 1$  then  $class\_thr\_t[\theta_s, \theta_v, \Delta\phi] = 1$

Scientific content:

In the pixels classification algorithm, the MERIS reflectances at 442.5nm are respectively compared with these radiometric thresholds  $class\_thr\_t[\theta_s, \theta_v, \Delta\phi]$ . If the reflectance is lower than the corresponding threshold value then the pixel is not considered as a bright pixel. The thresholds are computed with inputs which generate the high boundary of a mean range of reflectance.

Resources:

Estimated CPU time: 26 sec  
Output disk space:  $12 \times 12 \times 19 \times 4$  bytes/fl = 10944 bytes

Acceptance:

Comparison with another RTC.

**6.2.21 GADS Browse Configuration Parameters**

Reference: CP, LUT285

[AD-8] Section 6.2.21

ACRI provided

Dependencies:

None

Tool:

None

Procedure:

None

Scientific content:

Configuration parameters

Current baseline: 816 values [dl]

Resources:

Estimated CPU time: -  
Output disk space:  $816 \times 1$  bytes/uc = 816 bytes

Acceptance:

Corresponds to the latest definition.

### **6.3 RADIOMETRIC CALIBRATION**

Not covered in this document

### **6.4 DIGITAL ELEVATION & ROUGHNESS MODEL**

Not covered in this document

### **6.5 LAND/SEA MASK**

Not covered in this document

### **6.6 ECMWF**

Not covered in this document

### **6.7 AEROSOL CLIMATOLOGY**

Not covered in this document

### **6.8 ENVISAT-1 ORBIT STATE VECTORS**

Not covered in this document

### **6.9 ENVISAT-1 PLATFORM ATTITUDE**

Not covered in this document

### **6.10 LEVEL-2 CONTROL PARAMETERS**

#### **6.10.1 C.P.**

Not covered in this document (*see* [\[AD-8\]](#) for a detailed description)

### 6.10.2 MPH

Not covered in this document (see [AD-8] for a detailed description)

### 6.10.3 SPH

Not covered in this document (see [AD-8] for a detailed description)

### 6.10.4 GADS General

#### 6.10.4.1 Number of iterations for Chl1 calculation

Reference: Niter, LUT018

[AD-8] Section 6.10.4, GADS field 1

ACRI provided

Dependencies:

None

Tool:

None

Procedure:

Input: none

Output: *Niter* Number of iterations for Chl1 calculation  
units: [dl]

Step: User specified.

Scientific content:

Number of iterations used for chlorophyll calculation (see Morel's algorithm)

Current baseline: 3

Resources:

Estimated CPU time: -

Output disk space:  $1 \times 2 \text{ bytes/us} = 2 \text{ bytes}$

Acceptance:

If convergence is not achieved within the specified number of iterations (3), some other problems could be present.

6.10.4.2 *Flag indicating the presence of stratospheric aerosols*

Reference: Strat\_Corr, LUT019

[AD-8] Section 6.10.4, GADS field 2

ACRI provided

Dependencies:

None

Tool:

None

Procedure:

Input: none

Output: *Strat\_Corr* Flag indicating the presence of stratospheric aerosols  
units: [dl]

Step: User specified.

Scientific content:

Flag used to indicate the presence of stratospheric aerosols

Current baseline: 0

Resources:

Estimated CPU time: -

Output disk space: 1 × 1 byte/uc = 1 byte

Acceptance:

Corresponds to the latest definition.



#### 6.10.4.3 Default radiances for saturated pixels

Reference: rad\_satpix2[b], LUT020

[AD-8] Section 6.10.4, GADS field 3

ACRI provided

#### Dependencies:

None

#### Tool:

None

#### Procedure:

Input: *b* MERIS spectral band# (15 values), see [Section 3.1](#) for the nominal wavelengths (LUT400)

Output: *rad\_satpix2[b]* Default radiances for saturated pixels in the 15 MERIS bands (15 values)

units: [ $W.m^{-2}.\mu m^{-1}.sr^{-1}$ ]

Step: User specified.

#### Scientific content:

Default radiances in the 15 MERIS spectral bands used for the saturated pixels

Current baseline: {619.98608398, 693.83856201, 758.02069092, 700.52618408, 610.46539307, 535.78985596, 448.10375977, 453.98617554, 412.82760620, 566.97033691, 580.60144043, 237.70004272, 232.57832336, 399.39666748, 355.34863281}  
 $W.m^{-2}.\mu m^{-1}.sr^{-1}$

#### Resources:

Estimated CPU time: -

Output disk space:  $15 \times 4 \text{ bytes/fl} = 60 \text{ bytes}$

#### Acceptance:

Corresponds to the latest definition.

#### 6.10.4.4 Maximum optical thickness for land aerosols

Reference: AOT\_max, LUT021

[AD-8] Section 6.10.4, GADS field 4

ACRI provided

Dependencies:

None

Tool:

None

Procedure:

Input: none

Output: AOT\_max Maximum optical thickness for land aerosols

units: [dl]

Step: User specified.

Scientific content:

Maximum aerosol optical thickness used in the land aerosol algorithm

Current baseline: 2.0

Resources:

Estimated CPU time: -

Output disk space: 1 × 4 bytes/fl = 4 bytes

Acceptance:

Corresponds to the latest definition.

#### 6.10.4.5 Scaling factor - reflectances

Reference: Refl\_scale[b], LUT022

[AD-8] Section 6.10.4, GADS field 5

ACRI provided

Dependencies:

None

Tool:

None

Procedure:

Input: *b* MERIS spectral band# (15 values), *see Section 3.1* for the nominal wavelengths (LUT400)

Output: *Refl\_scale[b]* Scaling factor for reflectance in each of the 15 MERIS bands(15 values)  
units: [*dl*]

Step: User specified.

Scientific content:

Scaling factors to be applied to reflectances in the 15 MERIS spectral bands

Current baseline: {1.8311106 10<sup>-5</sup>, 1.8311106 10<sup>-5</sup>, 1.8311106 10<sup>-5</sup>, 1.8311106 10<sup>-5</sup>, 1.8311106 10<sup>-5</sup>,  
1.8311106 10<sup>-5</sup>, 1.8311106 10<sup>-5</sup>, 1.8311106 10<sup>-5</sup>, 1.8311106 10<sup>-5</sup>, 1.8311106 10<sup>-5</sup>,  
1.8311106 10<sup>-5</sup>, 1.8311106 10<sup>-5</sup>, 1.8311106 10<sup>-5</sup>, 1.8311106 10<sup>-5</sup>, 1.8311106 10<sup>-5</sup>}

Resources:

Estimated CPU time: -  
Output disk space: 15 × 4 bytes/fl = 60 bytes

Acceptance:

Corresponds to the latest definition.

**6.10.4.6 Scaling factor - algal pigment index**

Reference: Chl\_scale, LUT023

[AD-8] Section 6.10.4, GADS field 6

ACRI provided

Dependencies:

None

Tool:

None

Procedure:

Input: none

Output: *Chl\_scale*      Scaling factor for algal pigment index  
units:      [*dl*]

Step:      User specified.

Scientific content:

Scaling factor to be applied to algal pigment index

Current baseline: 0.0157480314

Resources:

Estimated CPU time: -

Output disk space: 1 × 4 bytes/fl = 4 bytes

Acceptance:

Corresponds to the latest definition.

*6.10.4.7 Scaling factor - yellow substance*

Reference:      ODOC\_scale,      LUT024

[AD-8]      Section 6.10.4, GADS field 7

ACRI provided

Dependencies:

None

Tool:

None

Procedure:

Input:      none

Output: *ODOC\_scale* Scaling factor for yellow substance  
units: [dl]  
Step: User specified.

Scientific content:

Scaling factor to be applied to yellow substance  
Current baseline: 0.0137898242

Resources:

Estimated CPU time: -  
Output disk space: 1 × 4 bytes/fl = 4 bytes

Acceptance:

Corresponds to the latest definition.

*6.10.4.8 Scaling factor - suspended sediments*

Reference: SPM\_scale, LUT025

[AD-8] Section 6.10.4, GADS field 8

ACRI provided

Dependencies:

None

Tool:

None

Procedure:

Input: none  
Output: *SPM\_scale* Scaling factor for suspended sediments  
units: [dl]  
Step: User specified.

Scientific content:

Scaling factor to be applied to suspended sediments

Current baseline: 0.0157480314

Resources:

Estimated CPU time: -  
Output disk space: 1 × 4 bytes/fl = 4 bytes

Acceptance:

Corresponds to the latest definition.

6.10.4.9 *Scaling factor - aerosol Angstroem exponent*

Reference: alpha\_scale, LUT412

[AD-8] Section 6.10.4, GADS field 9

ACRI provided

Dependencies:

None

Tool:

None

Procedure:

Input: none

Output: alpha\_scale Scaling factor for the Angstroem exponent of the aerosols (spectral dependence)

units: [dl]

Step: User specified.

Scientific content:

Scaling factor to be applied to the aerosol spectral dependence (*Angstroem exponent -  $\alpha$* ) computed between 778.75 and 865 nm as follows:

$$\alpha = - \frac{\text{Log}[\tau_{865}^{\alpha} / \tau_{778.75}^{\alpha}]}{\text{Log}[865 / 778.75]}$$

Current baseline: 0.0110236220

Resources:

Estimated CPU time: -  
Output disk space: 1 × 4 bytes/fl = 4 bytes

Acceptance:

Corresponds to the latest definition.

*6.10.4.10 Scaling factor - aerosol optical thickness*

Reference: AOT\_scale, LUT026

[AD-8] Section 6.10.4, GADS field 10

ACRI provided

Dependencies:

None

Tool:

None

Procedure:

Input: none  
Output: AOT\_scale Scaling factor for aerosol optical thickness  
units: [dl]  
Step: User specified.

Scientific content:

Scaling factor to be applied to the aerosol optical thickness

Current baseline: 0.0062992126

Resources:

Estimated CPU time: -  
Output disk space: 1 × 4 bytes/fl = 4 bytes

Acceptance:

Corresponds to the latest definition.

6.10.4.11 *Scaling factor - cloud optical thickness*

Reference: COT\_scale, LUT027

[AD-8] Section 6.10.4, GADS field 11

ACRI provided

Dependencies:

None

Tool:

None

Procedure:

Input: none

Output: COT\_scale Scaling factor for cloud optical thickness  
units: [dl]

Step: User specified.

Scientific content:

Scaling factor to be applied to the cloud optical thickness

Current baseline: 1.0

Resources:

Estimated CPU time: -

Output disk space: 1 × 4 bytes/fl = 4 bytes

Acceptance:

Corresponds to the latest definition.

6.10.4.12 *Scaling factor - surface pressure*

Reference: Press\_scale, LUT028



[AD-8] Section 6.10.4, GADS field 12

ACRI provided

Dependencies:

None

Tool:

None

Procedure:

Input: none

Output: *Press\_scale* Scaling factor for surface pressure  
units: [dl]

Step: User specified.

Scientific content:

Scaling factor to be applied to the surface pressure

Current baseline: 2.5590550900

Resources:

Estimated CPU time: -

Output disk space: 1 × 4 bytes/fl = 4 bytes

Acceptance:

Corresponds to the latest definition.

6.10.4.13 *Scaling factor - water vapour*

Reference: WV\_scale, LUT029

[AD-8] Section 6.10.4, GADS field 13

ACRI provided

Dependencies:

None

Tool:

None

Procedure:

Input: none

Output: *WV\_scale*      Scaling factor for water vapour content  
units:      [*dl*]

Step:      User specified.

Scientific content:

Scaling factor to be applied to the water-vapour content

Current baseline: 0.0299999993

Resources:

Estimated CPU time: -

Output disk space: 1 × 4 bytes/fl = 4 bytes

Acceptance:

Corresponds to the latest definition.

**6.10.4.14 Scaling factor - photosynthetically active radiation**

Reference:    PAR\_scale,                    LUT030

[AD-8]    Section 6.10.4, GADS field 14

ACRI provided

Dependencies:

None

Tool:

None

Procedure:

Input: none  
Output: *PAR\_scale* Scaling factor for photosynthetically active radiation  
units: [*dl*]  
Step: User specified.

Scientific content:

Scaling factor to be applied to the photosynthetically active radiation (PAR)  
Current baseline: 6.6399998665

Resources:

Estimated CPU time: -  
Output disk space: 1 × 4 bytes/fl = 4 bytes

Acceptance:

Corresponds to the latest definition.

*6.10.4.15 Scaling factor - TOA vegetation index*

Reference: TOAVI\_scale, LUT031

[AD-8] Section 6.10.4, GADS field 15

ACRI provided

Dependencies:

None

Tool:

None

Procedure:

Input: none  
Output: *TOAVI\_scale* Scaling factor for TOA vegetation index  
units: [*dl*]  
Step: User specified.

Scientific content:

Scaling factor to be applied to the vegetation index computed at TOA

Current baseline: 0.0039370079

Resources:

Estimated CPU time: -

Output disk space: 1 × 4 bytes/fl = 4 bytes

Acceptance:

Corresponds to the latest definition.

*6.10.4.16 Scaling factor - BOA vegetation index*

Reference: BOAVI\_scale, LUT032

[AD-8] Section 6.10.4, GADS field 16

ACRI provided

Dependencies:

None

Tool:

None

Procedure:

Input: none

Output: *BOAVI\_scale* Scaling factor for BOA vegetation index

units: [*dl*]

Step: User specified.

Scientific content:

Scaling factor to be applied to the vegetation index computed at BOA

Current baseline: 0.0216535442

Resources:

Estimated CPU time: -  
Output disk space: 1 × 4 bytes/fl = 4 bytes

Acceptance:

Corresponds to the latest definition.

*6.10.4.17 Scaling factor - cloud albedo*

Reference: CA\_scale, LUT033

[AD-8] Section 6.10.4, GADS field 17

ACRI provided

Dependencies:

None

Tool:

None

Procedure:

Input: none

Output: CA\_scale Scaling factor for cloud albedo  
units: [dl]

Step: User specified.

Scientific content:

Scaling factor to be applied to the cloud albedo

Current baseline: 0.0039370079

Resources:

Estimated CPU time: -  
Output disk space: 1 × 4 bytes/fl = 4 bytes

Acceptance:

Corresponds to the latest definition.

#### 6.10.4.18 Scaling factor - cloud top pressure

Reference: CTP\_scale, LUT034

[AD-8] Section 6.10.4, GADS field 18

ACRI provided

#### Dependencies:

None

#### Tool:

None

#### Procedure:

Input: none

Output: CTP\_scale Scaling factor for cloud top pressure  
units: [dl]

Step: User specified.

#### Scientific content:

Scaling factor to be applied to the cloud albedo

Current baseline: 4.0275592804

#### Resources:

Estimated CPU time: -

Output disk space: 1 × 4 bytes/fl = 4 bytes

#### Acceptance:

Corresponds to the latest definition.

#### 6.10.4.19 Offset - reflectances

Reference: Refl\_offset[b], LUT035

[AD-8] Section 6.10.4, GADS field 19

ACRI provided

Dependencies:

None

Tool:

None

Procedure:

Input: *b* MERIS spectral band# (15 values), see [Section 3.1](#) for the nominal wavelengths (LUT400)

Output: *Refl\_offset[b]* Offset factor for reflectance in each of the 15 MERIS bands(15 values)  
units: [*dl*]

Step: User specified.

Scientific content:

Offset factors to be applied to the reflectances in the 15 MERIS spectral bands

Current baseline: {-0.200018317, -0.200018317, -0.200018317, -0.200018317, -0.200018317,  
-0.200018317, -0.200018317, -0.200018317, -0.200018317, -0.200018317,  
-0.200018317, -0.200018317, -0.200018317, -0.200018317, -0.200018317}

Resources:

Estimated CPU time: -  
Output disk space: 15 × 4 bytes/fl = 60 bytes

Acceptance:

Corresponds to the latest definition.

**6.10.4.20 Offset - algal pigment index**

Reference: Chl\_offset, LUT036

[AD-8] Section 6.10.4, GADS field 20

ACRI provided

Dependencies:

None

Tool:

None

Procedure:

Input: none

Output: *Chl\_offset* Offset factor for algal pigment index  
units:  $[Log_{10}(mg.m^{-3})]$

Step: User specified.

Scientific content:

Offset factor to be applied to algal pigment index

Current baseline:  $-2.0157480240 Log_{10}(mg.m^{-3})$

Resources:

Estimated CPU time: -

Output disk space:  $1 \times 4 \text{ bytes/fl} = 4 \text{ bytes}$

Acceptance:

Corresponds to the latest definition.

**6.10.4.21 Offset - yellow substance**

Reference: ODOC\_offset, LUT037

[AD-8] Section 6.10.4, GADS field 21

ACRI provided

Dependencies:

None

Tool:

None

Procedure:



Input: none  
Output: *ODOC\_offset* Offset factor for yellow substance  
units:  $[Log_{10}(m^{-1})]$   
Step: User specified.

Scientific content:

Offset factor to be applied to yellow substance  
Current baseline:  $-2.5513918400 Log_{10}(m^{-1})$

Resources:

Estimated CPU time: -  
Output disk space:  $1 \times 4 \text{ bytes/fl} = 4 \text{ bytes}$

Acceptance:

Corresponds to the latest definition.

**6.10.4.22 Offset - suspended sediments**

Reference: SPM\_offset, LUT038

[AD-8] Section 6.10.4, GADS field 22

ACRI provided

Dependencies:

None

Tool:

None

Procedure:

Input: none  
Output: *SPM\_offset* Offset factor for suspended sediments  
units:  $[Log_{10}(g.m^{-3})]$   
Step: User specified.

Scientific content:

Offset factor to be applied to suspended sediments

Current baseline:  $-2.0157480240 \text{ Log}_{10}(g.m^{-3})$

Resources:

Estimated CPU time: -

Output disk space:  $1 \times 4 \text{ bytes/fl} = 4 \text{ bytes}$

Acceptance:

Corresponds to the latest definition.

6.10.4.23 *Offset - aerosol Angstroem exponent*

Reference:  $\alpha\_offset$ , LUT413

[AD-8] Section 6.10.4, GADS field 23

ACRI provided

Dependencies:

None

Tool:

None

Procedure:

Input: none

Output:  $\alpha\_offset$  Offset factor for the Angstroem exponent of the aerosols (spectral dependence)

units:  $[dl]$

Step: User specified.

Scientific content:

Offset factor to be applied to the aerosol spectral dependence (*Angstroem exponent -  $\alpha$* ) computed between 778.75 and 865 nm.

Current baseline: -0.3110236230

Resources:

Estimated CPU time: -  
Output disk space: 1 × 4 bytes/fl = 4 bytes

Acceptance:

Corresponds to the latest definition.

**6.10.4.24 Offset - aerosol optical thickness**

Reference: AOT\_offset, LUT039

[AD-8] Section 6.10.4, GADS field 24

ACRI provided

Dependencies:

None

Tool:

None

Procedure:

Input: none  
Output: AOT\_offset Offset factor for aerosol optical thickness  
units: [dl]  
Step: User specified.

Scientific content:

Offset factor to be applied to the aerosol optical thickness

Current baseline: -0.0062992130

Resources:

Estimated CPU time: -  
Output disk space: 1 × 4 bytes/fl = 4 bytes

Acceptance:

Corresponds to the latest definition.

#### 6.10.4.25 Offset - cloud optical thickness

Reference: COT\_offset, LUT040

[AD-8] Section 6.10.4, GADS field 25

ACRI provided

#### Dependencies:

None

#### Tool:

None

#### Procedure:

Input: none

Output: COT\_offset Offset factor for cloud optical thickness  
units: [dl]

Step: User specified.

#### Scientific content:

Offset factor to be applied to the cloud optical thickness

Current baseline: -1.0

#### Resources:

Estimated CPU time: -

Output disk space: 1 × 4 bytes/fl = 4 bytes

#### Acceptance:

Corresponds to the latest definition.

#### 6.10.4.26 Offset - surface pressure

Reference: Press\_offset, LUT041

[AD-8] Section 6.10.4, GADS field 26

ACRI provided

Dependencies:

None

Tool:

None

Procedure:

Input: none

Output: *Press\_offset* Offset factor for surface pressure  
units: [hPa]

Step: User specified.

Scientific content:

Offset factor to be applied to the surface pressure

Current baseline: 447.4409484900 hPa

Resources:

Estimated CPU time: -

Output disk space: 1 × 4 bytes/fl = 4 bytes

Acceptance:

Corresponds to the latest definition.

6.10.4.27 *Offset - water vapour*

Reference: WV\_offset, LUT042

[AD-8] Section 6.10.4, GADS field 27

ACRI provided

Dependencies:

None

Tool:

None

Procedure:

Input: none

Output: *WV\_offset* Offset factor for water vapour content  
units:  $[g.cm^{-2}]$

Step: User specified.

Scientific content:

Offset factor to be applied to the water-vapour content

Current baseline:  $-0.0299999993 g.cm^{-2}$

Resources:

Estimated CPU time: -

Output disk space:  $1 \times 4 \text{ bytes/fl} = 4 \text{ bytes}$

Acceptance:

Corresponds to the latest definition.

**6.10.4.28 Offset - photosynthetically active radiation**

Reference: PAR\_offset, LUT043

[AD-8] Section 6.10.4, GADS field 28

ACRI provided

Dependencies:

None

Tool:

None

Procedure:

Input: none

Output: *PAR\_offset* Offset factor for photosynthetically active radiation  
units: [ $\mu\text{Einstein.m}^{-2}$ ]  
Step: User specified.

Scientific content:

Offset factor to be applied to the photosynthetically active radiation (PAR)

Current baseline: 513.0302124  $\mu\text{Einstein.m}^{-2}$

Resources:

Estimated CPU time: -  
Output disk space: 1 × 4 bytes/fl = 4 bytes

Acceptance:

Corresponds to the latest definition.

6.10.4.29 *Offset - TOA vegetation index*

Reference: TOAVI\_offset, LUT044

[AD-8] Section 6.10.4, GADS field 29

ACRI provided

Dependencies:

None

Tool:

None

Procedure:

Input: none  
Output: *TOAVI\_offset* Offset factor for TOA vegetation index  
units: [*dl*]  
Step: User specified.

Scientific content:

Offset factor to be applied to the vegetation index computed at TOA

Current baseline: -0.0039370079

Resources:

Estimated CPU time: -  
Output disk space: 1 × 4 bytes/fl = 4 bytes

Acceptance:

Corresponds to the latest definition.

6.10.4.30 *Offset - BOA vegetation index*

Reference: BOAVI\_offset, LUT045

[AD-8] Section 6.10.4, GADS field 30

ACRI provided

Dependencies:

None

Tool:

None

Procedure:

Input: none  
Output: *BOAVI\_offset* Offset factor for BOA vegetation index  
units: [dl]  
Step: User specified.

Scientific content:

Offset factor to be applied to the vegetation index computed at BOA

Current baseline: -0.0216535442

Resources:

Estimated CPU time: -



Output disk space: 1 × 4 bytes/fl = 4 bytes

Acceptance:

Corresponds to the latest definition.

*6.10.4.31 Offset - cloud albedo*

Reference: CA\_offset, LUT046

[AD-8] Section 6.10.4, GADS field 31

ACRI provided

Dependencies:

None

Tool:

None

Procedure:

Input: none

Output: CA\_offset Offset factor for cloud albedo  
units: [dl]

Step: User specified.

Scientific content:

Offset factor to be applied to the cloud albedo

Current baseline: -0.0039370079

Resources:

Estimated CPU time: -

Output disk space: 1 × 4 bytes/fl = 4 bytes

Acceptance:

Corresponds to the latest definition.

6.10.4.32 *Offset - cloud top pressure*

Reference: CTP\_offset, LUT047

[AD-8] Section 6.10.4, GADS field 32

ACRI provided

Dependencies:

None

Tool:

None

Procedure:

Input: none

Output: CTP\_offset Offset factor for cloud top pressure  
units: [hPa]

Step: User specified.

Scientific content:

Offset factor to be applied to the cloud albedo

Current baseline: -4.0275592804 hPa

Resources:

Estimated CPU time: -

Output disk space: 1 × 4 bytes/fl = 4 bytes

Acceptance:

Corresponds to the latest definition.

6.10.4.33 *Scaling factor - rectified near-infrared reflectance*

Reference: NIR\_refl\_scale, LUT048

[AD-8] Section 6.10.4, GADS field 33

ACRI provided

Dependencies:

None

Tool:

None

Procedure:

Input: none

Output: *NIR\_refl\_scale*  
Scaling factor for rectified near-infrared reflectance

units: [dl]

Step: User specified.

Scientific content:

Scaling factor to be applied to the rectified near-infrared reflectance

Current baseline: 0.0039370079

Resources:

Estimated CPU time: -

Output disk space: 1 × 4 bytes/fl = 4 bytes

Acceptance:

Corresponds to the latest definition.

**6.10.4.34 Offset - rectified near-infrared reflectance**

Reference: NIR\_refl\_offset, LUT049

[AD-8] Section 6.10.4, GADS field 34

ACRI provided

Dependencies:

None

Tool:

Input: none

Output: *NIR\_refl\_offset*

Offset factor for rectified near-infrared reflectance

units: [*dl*]

Step: User specified.

Procedure:

None

Scientific content:

Offset factor to be applied to the rectified near-infrared reflectance

Current baseline: -0.0039370079

Resources:

Estimated CPU time: -

Output disk space: 1 × 4 bytes/fl = 4 bytes

Acceptance:

Corresponds to the latest definition.

**6.10.4.35 Scaling factor - rectified red reflectance**

Reference: Red\_refl\_scale, LUT050

[AD-8] Section 6.10.4, GADS field 35

ACRI provided

Dependencies:

None

Tool:

None

Procedure:

Input: none

Output: *Red\_refl\_scale*

Scaling factor for rectified red reflectance

units: [dl]

Step: User specified.

Scientific content:

Scaling factor to be applied to the rectified red reflectance

Current baseline: 0.0039370079

Resources:

Estimated CPU time: -

Output disk space:  $1 \times 4 \text{ bytes/fl} = 4 \text{ bytes}$

Acceptance:

Corresponds to the latest definition.

6.10.4.36 *Offset - rectified red reflectance*

Reference: Red\_refl\_offset, LUT051

[AD-8] Section 6.10.4, GADS field 36

ACRI provided

Dependencies:

None

Tool:

None

Procedure:

Input: none

Output: *Red\_refl\_offset*  
Offset factor for rectified red reflectance

units: [dl]

Step: User specified.

Scientific content:

Offset factor to be applied to the rectified red reflectance

Current baseline: -0.0039370079

Resources:

Estimated CPU time: -

Output disk space: 1 × 4 bytes/fl = 4 bytes

Acceptance:

Corresponds to the latest definition.

### 6.10.5 GADS Smile Effect Correction

#### 6.10.5.1 Square of Sun-Earth distance at reference date

Reference:  $D_{sun0}^2$ , LUT420

[AD-8] Section 6.10.5.1

ACRI provided

Dependencies:

None

Tool:

None

Procedure:

Input: none

Output:  $D_{sun0}^2$  Square of *Sun-Earth* distance at reference date

units:  $[m^2]$

Step: User specified.

Scientific content:

Square of *Sun-Earth* distance at a reference date used for the corrective factor ( $1/D_{sun0}^2$ ) to be applied to the extraterrestrial solar irradiance.

Current baseline:  $2.2402379 \cdot 10^{22} m^2$

Resources:

Estimated CPU time: -  
Output disk space: 1 × 4 bytes/fl = 4 bytes

Acceptance:

Corresponds to the latest definition.

6.10.5.2 Array of per band switches enabling smile effect correction for land pixels reflectance

Reference: (No variable used), LUT421

[AD-8] Section 6.10.5.2

ACRI provided

Dependencies:

None

Tool:

None

Procedure:

Input: none

Output: *(no variable)* Array of per band switches enabling smile effect correction for land pixels reflectance (15 values)

units: [dl]

Step: User specified.

Scientific content:

Array of per band switches allowing to correct for the smile effect the land pixels reflectance

Current baseline: {1, 1, 1, 1, 1, 1, 1, 1, 1, 1, 0, 1, 1, 1, 0}

Resources:

Estimated CPU time: -  
Output disk space: 15 × 1 byte/uc = 15 bytes

Acceptance:

Corresponds to the latest definition.

6.10.5.3 Array of per band switches enabling smile effect correction for water pixels reflectance

Reference: (No variable used), LUT422

[AD-8] Section 6.10.5.3

ACRI provided

Dependencies:

None

Tool:

None

Procedure:

Input: none

Output: *(no variable)* Array of per band switches enabling smile effect correction for water pixels reflectance (15 values)

units: [dl]

Step: User specified.

Scientific content:

Array of per band switches allowing to correct for the smile effect the water pixels reflectance

Current baseline: {1, 1, 1, 1, 1, 1, 1, 0, 1, 1, 0, 1, 1, 1, 0}

Resources:

Estimated CPU time: -

Output disk space: 15 × 1 byte/uc = 15 bytes

Acceptance:

Corresponds to the latest definition.



6.10.5.4 Array of pairs of band indices for estimating reflectance spectral derivative (land pixels)

Reference: (No variable used), LUT423

[AD-8] Section 6.10.5.4

ACRI provided

Dependencies:

None

Tool:

None

Procedure:

Input: none

Output: *(no variable)* Array of pairs of band indices for estimating reflectance spectral derivative (land pixels) (15 values)

units: [dl]

Step: User specified.

Scientific content:

Array of per band indices to estimate the reflectance spectral derivative over land pixels

Current baseline: {1, 1, 1, 1, 1, 1, 1, 1, 1, 1, 1, 1, 1, 1, 1}

Resources:

Estimated CPU time: -

Output disk space:  $15 \times 2 \times 1$  byte/uc = 30 bytes

Acceptance:

Corresponds to the latest definition.

6.10.5.5 Array of pairs of band indices for estimating reflectance spectral derivative (water pixels)

Reference: (No variable used), LUT424

[AD-8] Section 6.10.5.5

ACRI provided

Dependencies:

None

Tool:

None

Procedure:

Input: none

Output: *(no variable)* Array of pairs of band indices for estimating reflectance spectral derivative (water pixels) (15 values)

units: [dl]

Step: User specified.

Scientific content:

Array of per band indices to estimate the reflectance spectral derivative over water pixels

Current baseline: {1, 1, 1, 1, 1, 1, 1, 1, 1, 1, 1, 1, 1, 1, 1}

Resources:

Estimated CPU time: -

Output disk space:  $15 \times 2 \times 1$  byte/uc = 30 bytes

Acceptance:

Corresponds to the latest definition.

6.10.5.6 *Theoretical central wavelengths of MERIS spectral bands*

Reference: Wvl[b], LUT425

[AD-8] Section 6.10.5.6

ACRI provided

Dependencies:

None

Tool:

None

Procedure:

Input:  $b$  MERIS spectral band# (15 values), *see* [Section 3.1](#) for the nominal wavelengths (LUT400)

Output:  $Wvl[b]$  Theoretical central wavelengths of MERIS spectral bands (15 values)  
units:  $[nm]$

Step: User specified.

Scientific content:

Nominal wavelengths of the 15 MERIS spectral bands

Current baseline: {412.5, 442.5, 490.0, 510.0, 560.0, 620.0, 665.0, 681.25, 708.75, 753.75, 761.875, 778.75, 865.0, 885.0, 900.0} *nm*

Resources:

Estimated CPU time: -  
Output disk space:  $15 \times 4$  bytes/fl = 60 bytes

Acceptance:

Corresponds to the latest definition.

**6.10.5.7 Reference solar fluxes at theoretical central wavelengths and bandwidths**

Reference:  $F_0[b]$ , LUT426

[\[AD-8\]](#) Section 6.10.5.7

ACRI provided

Dependencies:

None

Tool:

None

Procedure:

Input:  $b$  MERIS spectral band# (15 values), *see* [Section 3.1](#) for the nominal wavelengths (LUT400)

Output:  $F_o[b]$  Reference solar fluxes at theoretical central wavelengths and bandwidths (15 values)

units:  $[W.m^{-2}.\mu m^{-1}]$

Step: User specified.

Scientific content:

Reference extraterrestrial solar fluxes in the 15 MERIS spectral filters

Current baseline: {1713.6920166, 1877.5660400, 1929.2629395, 1926.8909912, 1800.4580078, 1649.7049561, 1530.9270020, 1470.2290039, 1405.4739990, 1266.1999512, 1253.0040283, 1175.7370605, 958.76300049, 929.78601074, 895.46002197}  
 $W.m^{-2}.\mu m^{-1}$

Resources:

Estimated CPU time: -  
Output disk space:  $15 \times 4$  bytes/fl = 60 bytes

Acceptance:

Corresponds to the latest definition.

**6.10.5.8 MERIS RR pixels characterized wavelengths**

Reference: Wvl\_RR[b,p], LUT427

[\[AD-8\]](#) Section 6.10.5.8

ACRI provided

Dependencies:

None

Tool:

None

Procedure:

Inputs:  $b$  MERIS spectral band# (15 values), *see* [Section3.1](#) for the nominal wavelengths (LUT400)

$p$  MERIS RR pixel# (925 values)  
Output:  $Wvl\_RR[b,p]$  MERIS RR pixels characterized wavelengths (15 x 925 values)  
units:  $[nm]$   
Step: User specified.

Scientific content:

15 wavelengths given for each of the 925 MERIS-RR pixels  
Current baseline: 15 x 925 values

Resources:

Estimated CPU time: -  
Output disk space:  $15 \times 925 \times 4 \text{ bytes/fl} = 55500 \text{ bytes}$

Acceptance:

Corresponds to the latest definition.

**6.10.5.9 Reference solar fluxes for MERIS RR pixels**

Reference:  $F_0\_RR[b,p]$ , LUT428

[AD-8] Section 6.10.5.9

ACRI provided

Dependencies:

None

Tool:

Inputs:  $b$  MERIS spectral band# (15 values), see [Section3.1](#) for the nominal wavelengths (LUT400)  
 $p$  MERIS RR pixel# (925 values)  
Output:  $F_0\_RR[b,p]$  Reference solar fluxes for MERIS RR pixels (15 x 925 values)  
units:  $[nm]$   
Step: User specified.

Procedure:

None

Scientific content:

15 reference values of extraterrestrial solar flux given for each of the 925 MERIS-RR pixels

Current baseline: 15 x 925 values [ $W.m^{-2}.\mu m^{-1}$ ]

Resources:

Estimated CPU time: -

Output disk space: 15 x 925 x 4 bytes/fl = 55500 bytes

Acceptance:

Corresponds to the latest definition.

**6.10.5.10 MERIS FR pixels characterized wavelengths**

Reference: Wvl\_FR[b,p], LUT429

[AD-8] Section 6.10.5.10

ACRI provided

Dependencies:

None

Tool:

None

Procedure:

Inputs: *b* MERIS spectral band# (15 values), see Section3.1,(LUT400)  
*p* MERIS FR pixel# (3700 values)

Output: Wvl\_FR[b,p] MERIS FR pixels characterized wavelengths (15 x 3700 values)  
units: [nm]

Step: User specified.

Scientific content:

15 wavelengths given for each of the 3700 MERIS-FR pixels

Current baseline: 15 x 3700 values [nm]

Resources:

Estimated CPU time: -  
Output disk space:  $15 \times 3700 \times 4$  bytes/fl = 222000 bytes

Acceptance:

Corresponds to the latest definition.

6.10.5.11 Reference solar fluxes for MERIS FR pixels

Reference:  $F_0\_FR[b,p]$ , LUT430

[AD-8] Section 6.10.5.11

ACRI provided

Dependencies:

None

Tool:

None

Procedure:

Inputs:  $b$  MERIS spectral band# (15 values), see Section 3.1, (LUT400)  
 $p$  MERIS FR pixel# (3700 values)

Output:  $F_0\_FR[b,p]$  Reference solar fluxes for MERIS FR pixels (15 x 3700 values)  
units:  $[nm]$

Step: User specified.

Scientific content:

15 reference values of extraterrestrial solar flux given for each of the 3700 MERIS-FR pixels

Current baseline:  $15 \times 3700$  values  $[W.m^{-2}.\mu m^{-1}]$

Resources:

Estimated CPU time: -  
Output disk space:  $15 \times 3700 \times 4$  bytes/fl = 222000 bytes

Acceptance:

Corresponds to the latest definition.

**6.10.6 GADS Atmospheric Corrections for Case-I Waters**

*6.10.6.1 Reflectance thresholds to set the negative reflectance flag*

Reference: DRO\_thresh[b], LUT054

[AD-8] Section 6.10.6, GADS field 1

ACRI provided

Dependencies:

None

Tool:

None

Procedure:

Input: *b* MERIS spectral band# (15 values), see [Section 3.1](#) for the nominal wavelengths (LUT400)

Output: *DRO\_thresh[b]*  
Reflectance thresholds to set the negative reflectance flag (15 values)

units: [*dl*]

Step: User specified.

Scientific content:

Thresholds on reflectance for the 15 MERIS spectral bands to set negative reflectance flag

Current baseline: {-0.005799998, -0.004600000, -0.002900000, -0.002400000, -0.001700000,  
-0.001200000, -8.300004 10<sup>-4</sup>, -7.100002 10<sup>-4</sup>, -6.500001 10<sup>-4</sup>, 0., 0., 0., 0., 0., 0.}

Resources:

Estimated CPU time: -

Output disk space: 15 × 4 bytes/fl = 60 bytes

Acceptance:



Corresponds to the latest definition.

#### 6.10.6.2 Threshold for absorbing aerosol test at 510 nm

Reference: DRO510\_thresh1, LUT055

[AD-8] Section 6.10.6, GADS field 2

ACRI provided

#### Dependencies:

None

#### Tool:

None

#### Procedure:

Input: none

Output: *DRO510\_thresh1*  
Threshold for absorbing aerosol test at 510nm

units: [dl]

Step: User specified.

#### Scientific content:

*DRO510\_thresh1* is a threshold defined in the atmospheric correction algorithm above case-1 waters useful to break the loop of convergence. A change could be expected if MERIS sensitivity is better than the expected value and the algorithm can handle this enhancement. This parameter is also related to the selected absorbing aerosol model.

Current baseline: 0.003

#### Resources:

Estimated CPU time: -

Output disk space: 1 × 4 bytes/fl = 4 bytes

#### Acceptance:

According to the instrument specification.

### 6.10.6.3 Threshold for blue aerosol test at 510 nm

Reference: DRO510\_thresh2, LUT056

[AD-8] Section 6.10.6, GADS field 3

ACRI provided

#### Dependencies:

None

#### Tool:

None

#### Procedure:

Input: none

Output: *DRO510\_thresh2*  
Threshold for blue aerosol test at 510nm

units: [dl]

Step: User specified.

#### Scientific content:

*DRO510\_thresh2* is a threshold defined in the atmospheric correction algorithm above case-1 waters useful to break the loop of convergence. A change could be expected if MERIS sensitivity is better than the expected value and the algorithm can handle this enhancement. This parameter is also related to the selected blue aerosol model.

Current baseline: 1000

#### Resources:

Estimated CPU time: -

Output disk space: 1 × 4 bytes/fl = 4 bytes

#### Acceptance:

According to the instrument specification.

### 6.10.6.4 List of indices of aerosol assemblages

Reference: list\_of\_iaer, LUT057

[AD-8] Section 6.10.6, GADS field 4

ACRI provided

Dependencies:

None

Tool:

None

Procedure:

Input: none

Output: *list\_of\_aer* List of indices of aerosol assemblages  
units: [dl]

Step: User specified.

Scientific content:

The list of indices of aerosol assemblages is tabulated as an array of 10 by 20 values. Indices of aerosol assemblages, between 1 and 34, refer to these assemblages described in the 'Ocean aerosols' file (see [AD-8] Section 6.13 and [AD-6]). Each 5-element sub-array correspond to one pass of the atmospheric correction algorithm. The total number of passes is specified in Section 6.10.6.6, which does not mean that the remaining sub-arrays of the list are void. Within each sub-array, the algorithm employs a fixed number of models, specified in Section 6.10.6.21.

Current baseline: 10 x 20 values (reference numbers defined according to [AD-8])

Resources:

Estimated CPU time: -

Output disk space: 10 x 20 x 1 byte/uc = 200 bytes

Acceptance:

According to the current accepted definition for the list of aerosol models.

**6.10.6.5 Total number of ocean-aerosol assemblages**

Reference: N\_aer, LUT058

[AD-8] Section 6.10.6, GADS field 5

ACRI provided

Dependencies:

None

Tool:

None

Procedure:

Input: none

Output:  $N_{aer}$  Total number of ocean-aerosol assemblages  
units: [dl]

Step: User specified.

Scientific content:

$N_{aer}$  specifies the total number of aerosol assemblages used in the atmospheric corrections algorithm over case-1 waters. This parameter depends on the selected aerosol models. For more details, refer to [AD-6].

Current baseline: 34

Resources:

Estimated CPU time: -

Output disk space:  $1 \times 1$  byte/uc = 1 byte

Acceptance:

Corresponds to the latest definition.

6.10.6.6 *Number of passes within the algorithm*

Reference:  $N_{pass}$ , LUT059

[AD-8] Section 6.10.6, GADS field 6

ACRI provided

Dependencies:

None

Tool:

None

Procedure:

Input: none

Output:  $N_{pass}$  Number of passes within the algorithm  
units: [dl]

Step: User specified.

Scientific content:

$N_{pass}$  specifies the maximum number of aerosol assemblages, which are passed through the aerosol database used in the atmospheric corrections algorithm.

Current baseline: 4

Resources:

Estimated CPU time: -

Output disk space:  $1 \times 1$  byte/uc = 1 byte

Acceptance:

Corresponds to the latest definition.

**6.10.6.7 Number of polynomial coefficients relating ( $\rho_{path}/\rho_R$ ) to the aerosol optical thickness ( $\tau^a$ )**

Reference:  $N_{coef}$ , LUT060

[AD-8] Section 6.10.6, GADS field 7

ACRI provided

Dependencies:

None

Tool:

None

Procedure:

Input: none

Output:  $N\_coef$  Number of polynomial coefficients relating  $(\rho_{path}/\rho_R)$  to the aerosol optical thickness  $(\tau^a)$

units:  $[dl]$

Step: User specified.

Scientific content:

$N\_co$  defines the number of polynomial coefficients fit used for determining the aerosol optical thickness from the path to *Rayleigh* reflectances ratio  $(\rho^*/\rho_R)$ . This relation is defined as follows ([AD-9], slide 7/41):

$$\frac{\rho^*(\lambda, w_s, \tau^a, \mathcal{G}_s, \mathcal{G}_v, \Delta\phi)}{\rho_R(\lambda, w_s, \tau^a, \mathcal{G}_s, \mathcal{G}_v, \Delta\phi)} = \sum_{i=0}^2 k_i(\lambda, w_s, \mathcal{G}_s, \mathcal{G}_v, \Delta\phi) \cdot (\tau^a)^i$$

Current baseline: 3

Resources:

Estimated CPU time: -

Output disk space:  $1 \times 1$  byte/uc = 1 byte

Acceptance:

An error analysis should be performed within the process to extract the  $k_i$  coefficients. The acceptable error has to be specified by the user.

6.10.6.8 Indices of models that shall trigger the AERO\_BLUE flag

Reference: iaer\_blue, LUT0465

[AD-8] Section 6.10.6, GADS field 8

ACRI provided

Dependencies:

None

Tool:

None

Procedure:

Input: none

Output: *iaer\_blue* Indices of models that trigger the AERO\_BLUE flag (50 values)  
units: [dl]  
Step: User specified.

Scientific content:

*iaer\_blue* is an index used to trigger the blue aerosol models

Current baseline: {32, 33, 34, 0}

Resources:

Estimated CPU time: -  
Output disk space:  $50 \times 1 \text{ byte/uc} = 50 \text{ bytes}$

Acceptance:

Corresponds to the latest definition.

6.10.6.9 (Spare)

Reference:

[AD-8] Section 6.10.6, GADS field 9

6.10.6.10 (Spare)

Reference:

[AD-8] Section 6.10.6, GADS field 10

6.10.6.11 Maximum allowed value for aerosol optical thickness at 865 nm

Reference: AOT\_max, LUT064

[AD-8] Section 6.10.6, GADS field 11

ACRI provided

Dependencies:

None

Tool:

None

Procedure:

Input: none

Output: *AOT\_max* Maximum allowed value for aerosol optical thickness at 865nm  
units: [dl]

Step: User specified.

Scientific content:

Maximum allowed value for aerosol optical thickness at 865nm

Current baseline: 0.8

Resources:

Estimated CPU time: -  
Output disk space: 1 × 4 bytes/fl = 4 bytes

Acceptance:

Corresponds to the latest definition.

*6.10.6.12 Threshold on depth for flagging shallow water*

Reference: Depth\_limit, LUT065

[AD-8] Section 6.10.6, GADS field 12

ACRI provided

Dependencies:

None

Tool:

None

Procedure:

Input: none



Output: *Depth\_limit* Threshold on depth for flagging shallow water  
units: [m]  
Step: User specified.

Scientific content:

Threshold on the depth used to flag shallow water  
Current baseline: 40

Resources:

Estimated CPU time: -  
Output disk space:  $1 \times 4 \text{ bytes/fl} = 4 \text{ bytes}$

Acceptance:

Corresponds to the latest definition.

6.10.6.13 (*Spare*)

Reference:

[AD-8] Section 6.10.6, GADS field 13

6.10.6.14 (*Spare*)

Reference:

[AD-8] Section 6.10.6, GADS field 14

6.10.6.15 *Threshold for flagging aerosol optical thickness*

Reference: AOT865\_thresh, LUT068

[AD-8] Section 6.10.6, GADS field 15

ACRI provided

Dependencies:

None

Tool:

None

Procedure:

Input: none

Output: *AOT865\_thresh*  
Threshold for flagging aerosol optical thickness

units: [dl]

Step: User specified.

Scientific content:

If the derived aerosol optical thickness is larger than the threshold value, *AOT865\_thresh*, an annotation flag will be raised. This threshold value cannot be freely changed due to the fact that the tables for the atmospheric corrections would need to be then modified accordingly.

Current baseline: 0.6

Resources:

Estimated CPU time: -

Output disk space: 1 × 4 bytes/fl = 4 bytes

Acceptance:

Corresponds to the latest definition.

6.10.6.16 *Switch to test for absorbing aerosols*

Reference: Test\_abs\_aer, LUT069

[AD-8] Section 6.10.6, GADS field 16

ACRI provided

Dependencies:

None

Tool:

None

Procedure:

Input: none

Output: *Test\_abs\_aer* Switch to test for absorbing aerosols  
units: [dl]  
Step: User specified.

Scientific content:

Switch used for testing the absorbing aerosols: ([0]/[1]: off / on)  
Current baseline: 1

Resources:

Estimated CPU time: -  
Output disk space: 1 × 1 byte/uc = 1 byte

Acceptance:

Corresponds to the latest definition.

*6.10.6.17 Ceiling value of solar zenith angle for modifying annotation flag*

Reference: SZA\_limit, LUT070

[AD-8] Section 6.10.6, GADS field 17

ACRI provided

Dependencies:

None

Tool:

None

Procedure:

Input: none  
Output: *SZA\_limit* Ceiling value of solar zenith angle for modifying annotation flag  
units: [10<sup>-6</sup>deg.]  
Step: User specified.

Scientific content:

This *SZA\_limit* threshold defines an angular limit beyond which an annotation flag will be raised, indicating that the solar zenith angle  $\theta_s$  is out of range. This value can be changed in the case where the data far from the zenith appear not to be reliable.

Current baseline: 70 deg.

Resources:

Estimated CPU time: -  
Output disk space: 1 × 4 bytes/ul = 4 bytes

Acceptance:

Corresponds to the latest definition.

6.10.6.18 (*Spare*)

Reference:

[AD-8] Section 6.10.6, GADS field 18

6.10.6.19 *Threshold for pressure correction*

Reference: Press\_tolerance, LUT072

[AD-8] Section 6.10.6, GADS field 19

ACRI provided

Dependencies:

None

Tool:

None

Procedure:

Input: none

Output: *Press\_tolerance*  
Threshold for pressure correction

units: [hPa]

Step: User specified.

Scientific content:

This threshold is used to activate a pressure correction.

Current baseline: 5 hPa

Resources:

Estimated CPU time: -

Output disk space: 1 × 4 bytes/fl = 4 bytes

Acceptance:

Corresponds to the latest definition.

6.10.6.20 Number of wavelengths used in the LUTs

Reference: N\_wvl, LUT073

[AD-8] Section 6.10.6, GADS field 20

ACRI provided

Dependencies:

None

Tool:

None

Procedure:

Input: none

Output: N\_wvl Number of wavelengths used in the LUTs  
units: [dl]

Step: User specified.

Scientific content:

N\_wvl corresponds to the number of selected wavelengths according to their relevance to the physical problem study.

Current baseline: 15

Resources:

Estimated CPU time: -  
Output disk space: 1 × 1 byte/uc = 1 byte

Acceptance:

Corresponds to the latest definition.

6.10.6.21 Number of aerosol models used at each pass

Reference: N\_basic\_aer, LUT286

[AD-8] Section 6.10.6, GADS field 21

ACRI provided

Dependencies:

None

Tool:

None

Procedure:

Input: none

Output: N\_basic\_aer Number of aerosol models used at each pass  
units: [dl]

Step: User specified.

Scientific content:

N\_basic\_aer corresponds to the number of standard aerosol models (SAMs) in list (Section 6.10.6.4) selected according to the relevance of their inherent optical properties.

Current baseline: 16

Resources:

Estimated CPU time: -  
Output disk space: 1 × 1 byte/uc = 1 byte

Acceptance:

Corresponds to the latest definition.

6.10.6.22 *Switch to use an aerosol climatology*

Reference: Climato\_aux, LUT287

[AD-8] Section 6.10.6, GADS field 22

ACRI provided

Dependencies:

None

Tool:

None

Procedure:

Input: none

Output: *Climato\_aux* Switch to use an aerosol climatology  
units: [dl]

Step: User specified.

Scientific content:

Switch to activate the use of an aerosol climatology: ([0]/[1]: off / on).

Current baseline: 1

Resources:

Estimated CPU time: -

Output disk space: 1 × 1 byte/uc = 1 byte

Acceptance:

Corresponds to the latest definition.

## 6.10.7 GADS Classification Parameters

### 6.10.7.1 Threshold on MERIS differential snow index (MDSI)

Reference: MDSI\_thresh, LUT288

[AD-8] Section 6.10.7, GADS field 1

ACRI provided

#### Dependencies:

None

#### Tool:

None

#### Procedure:

Input: none

Output: *MDSI\_thresh* Threshold on MERIS differential snow index  
units: [dl]

Step: User specified.

#### Scientific content:

Threshold on MERIS differential snow index.

Current baseline: 0.014

#### Resources:

Estimated CPU time: -

Output disk space: 1 × 4 bytes/fl = 4 bytes

#### Acceptance:

Corresponds to the latest definition.

### 6.10.7.2 Numerator band index for spectral ratio 1

Reference: b\_slope1\_n, LUT289

[AD-8] Section 6.10.7, GADS field 2



ACRI provided

Dependencies:

None

Tool:

None

Procedure:

Input: none

Output: *b\_slope1\_n* Numerator band index for spectral ratio 1  
units: [dl]

Step: User specified.

Scientific content:

Numerator band index used in the spectral ratio 1

Current baseline: 2

Resources:

Estimated CPU time: -

Output disk space: 1 × 1 byte/uc = 1 byte

Acceptance:

Corresponds to the latest definition.

**6.10.7.3 Denominator band index for spectral ratio 1**

Reference: b\_slope1\_d, LUT290

[AD-8] Section 6.10.7, GADS field 3

ACRI provided

Dependencies:

None

Tool:

None

Procedure:

Input: none

Output: *b\_slope1\_d* Denominator band index for spectral ratio 1  
units: [dl]

Step: User specified.

Scientific content:

Denominator band index used in the spectral ratio 1

Current baseline: 10

Resources:

Estimated CPU time: -

Output disk space: 1 × 1 byte/uc = 1 byte

Acceptance:

Corresponds to the latest definition.

*6.10.7.4 Lower threshold for spectral ratio 1*

Reference: Slope\_1\_low, LUT291

[AD-8] Section 6.10.7, GADS field 4

ACRI provided

Dependencies:

None

Tool:

None

Procedure:

Input: none

Output: *Slope\_1\_low* Lower threshold for spectral ratio 1  
units: [dl]

Step: User specified.

Scientific content:

Lower threshold for the spectral ratio 1

Current baseline: 0.

Resources:

Estimated CPU time: -  
Output disk space: 1 × 4 bytes/fl = 4 bytes

Acceptance:

Corresponds to the latest definition.

*6.10.7.5 Upper threshold for spectral ratio 1*

Reference: Slope\_1\_high, LUT292

[AD-8] Section 6.10.7, GADS field 5

ACRI provided

Dependencies:

None

Tool:

None

Procedure:

Input: none

Output: *Slope\_1\_high* Upper threshold for spectral ratio 1  
units: [dl]

Step: User specified.

Scientific content:

Upper threshold for the spectral ratio 1

Current baseline:  $10^6$

Resources:

Estimated CPU time: -

Output disk space:  $1 \times 4 \text{ bytes/fl} = 4 \text{ bytes}$

Acceptance:

Corresponds to the latest definition.

*6.10.7.6 Numerator band index for spectral ratio 2*

Reference:  $b\_slope2\_n$ , LUT293

[AD-8] Section 6.10.7, GADS field 6

ACRI provided

Dependencies:

None

Tool:

None

Procedure:

Input: none

Output:  $b\_slope2\_n$  Numerator band index for spectral ratio 2  
units:  $[dl]$

Step: User specified.

Scientific content:

Numerator band index used in the spectral ratio 2

Current baseline: 9

Resources:

Estimated CPU time: -

Output disk space: 1 × 1 byte/uc = 1 byte

Acceptance:

Corresponds to the latest definition.

6.10.7.7 Denominator band index for spectral ratio 2

Reference: b\_slope2\_d, LUT294

[AD-8] Section 6.10.7, GADS field 7

ACRI provided

Dependencies:

None

Tool:

None

Procedure:

Input: none

Output: *b\_slope2\_d* Denominator band index for spectral ratio 2  
units: [dl]

Step: User specified.

Scientific content:

Denominator band index used in the spectral ratio 2

Current baseline: 14

Resources:

Estimated CPU time: -

Output disk space: 1 × 1 byte/uc = 1 byte

Acceptance:

Corresponds to the latest definition.

6.10.7.8 Lower threshold for spectral ratio 2

Reference: Slope\_2\_low, LUT295

[AD-8] Section 6.10.7, GADS field 8

ACRI provided

Dependencies:

None

Tool:

None

Procedure:

Input: none

Output: *Slope\_2\_low* Lower threshold for spectral ratio 2  
units: [dl]

Step: User specified.

Scientific content:

Lower threshold for the spectral ratio 2

Current baseline: 0

Resources:

Estimated CPU time: -

Output disk space: 1 × 4 bytes/fl = 4 bytes

Acceptance:

Corresponds to the latest definition.

6.10.7.9 Upper threshold for spectral ratio 2

Reference: Slope\_2\_high, LUT296

[AD-8] Section 6.10.7, GADS field 9

ACRI provided

Dependencies:

None

Tool:

None

Procedure:

Input: none

Output: *Slope\_2\_high* Upper threshold for spectral ratio 2  
units: [dl]

Step: User specified.

Scientific content:

Upper threshold for the spectral ratio 2

Current baseline:  $10^6$

Resources:

Estimated CPU time: -

Output disk space:  $1 \times 4$  bytes/fl = 4 bytes

Acceptance:

Corresponds to the latest definition.

*6.10.7.10 Index of band for test on TOA reflectance (with band numbering starting at 1)*

Reference: b\_bright2, LUT297

[AD-8] Section 6.10.7, GADS field 10

ACRI provided

Dependencies:

None

Tool:

None

Procedure:

Input: none

Output: *b\_bright2* Index of band for test on TOA reflectance (with band numbering starting at 1)

units: [*dl*]

Step: User specified.

Scientific content:

Band index (*b\_bright2*) used to test the TOA reflectance

Current baseline: 2

Resources:

Estimated CPU time: -

Output disk space: 1 × 1 byte/uc = 1 bytes

Acceptance:

Corresponds to the latest definition.

**6.10.7.11 Thresholds on TOA reflectance at band *b\_bright2***

Reference: rho\_thresh1, rho\_thresh2, LUT298

[AD-8] Section 6.10.7, GADS field 11

ACRI provided

Dependencies:

None

Tool:

None

Procedure:

Input: none

Output: *rho\_thresh1, rho\_thresh2*  
Thresholds (min, max) on TOA reflectance at band *b\_bright2* (2 values)



units: [dl]

Step: User specified.

Scientific content:

Range of thresholds on TOA reflectance at band *b\_bright2*

Current baseline: {0.185, 0.03}

Resources:

Estimated CPU time: -

Output disk space: 2 × 4 bytes/fl = 8 bytes

Acceptance:

Corresponds to the latest definition.

**6.10.7.12 Index of band for GADS threshold on Rayleigh corrected reflectance**

Reference: b\_bright, LUT299

[AD-8] Section 6.10.7, GADS field 12

ACRI provided

Dependencies:

None

Tool:

None

Procedure:

Input: none

Output: *b\_bright* Index of band for GADS threshold on *Rayleigh* corrected reflectance

units: [dl]

Step: User specified.

Scientific content:

Band index (*b\_bright*) used for testing threshold on the *Rayleigh* corrected reflectance

Current baseline: 2

Resources:

Estimated CPU time: -  
Output disk space: 1 × 1 byte/uc = 1 byte

Acceptance:

Corresponds to the latest definition.

6.10.7.13 Zenith angles for GADS threshold on Rayleigh corrected reflectance

Reference: ZA, LUT300

[AD-8] Section 6.10.7, GADS field 13

ACRI provided

Dependencies:

None

Tool:

None

Procedure:

Input: none  
Output: ZA Zenith angles (12 values)  
units: [10<sup>-6</sup> deg]  
Step: User specified.

Scientific content:

Set of 12 zenith angles ( $\theta$ ) selected from the *Gauss* quadrature generated for 24 discrete directions with the RTC/Gauss tool (UdL)

Current baseline: 12 *Gaussian* angles (see [Section 6.2.13.1](#))

Resources:

Estimated CPU time: -  
Output disk space: 12 × 4 bytes/ul = 48 bytes

Acceptance:

Corresponds to the latest definition.

**6.10.7.14 Stored indices for  $(\theta_s \times \theta_v)$  combinations for GADS threshold on Rayleigh corrected reflectance**

Reference: SVZA\_index, LUT301

[AD-8] Section 6.10.7, GADS field 14

ACRI provided

Dependencies:

None

Tool:

None

Procedure:

Input: none

Output: SVZA\_index Stored indices for  $(\theta_s \times \theta_v)$  combinations (78 values)  
units: [dl]

Step: User specified.

Scientific content:

Current baseline: 78 angular combinations (SZA x VZA)

Note: Due to the fact that the matrix is symmetrical in the  $(\theta_s \times \theta_v)$  directions, we can then store only a half triangular matrix, *i.e.*,  $N(N+1)/2$  instead of  $N^2$  elements (78 instead of 144).

*Table of indices associated with each of the 78  $(\theta_s \times \theta_v)$  combinations*

| $i \setminus j$ | $\theta[0]$ | $\theta[1]$ | $\theta[2]$ | $\theta[3]$ | $\theta[4]$ | $\theta[5]$ | $\theta[6]$ | $\theta[7]$ | $\theta[8]$ | $\theta[9]$ | $\theta[10]$ | $\theta[11]$ |
|-----------------|-------------|-------------|-------------|-------------|-------------|-------------|-------------|-------------|-------------|-------------|--------------|--------------|
| $\theta[0]$     | 1           |             |             |             |             |             |             |             |             |             |              |              |
| $\theta[1]$     | 2           | 13          |             |             |             |             |             |             |             |             |              |              |
| $\theta[2]$     | 3           | 14          | 24          |             |             |             |             |             |             |             |              |              |
| $\theta[3]$     | 4           | 15          | 25          | 34          |             |             |             |             |             |             |              |              |
| $\theta[4]$     | 5           | 16          | 26          | 35          | 43          |             |             |             |             |             |              |              |

|              |    |    |    |    |    |    |    |    |    |    |    |    |
|--------------|----|----|----|----|----|----|----|----|----|----|----|----|
| $\theta[5]$  | 6  | 17 | 27 | 36 | 44 | 51 |    |    |    |    |    |    |
| $\theta[6]$  | 7  | 18 | 28 | 37 | 45 | 52 | 58 |    |    |    |    |    |
| $\theta[7]$  | 8  | 19 | 29 | 38 | 46 | 53 | 59 | 64 |    |    |    |    |
| $\theta[8]$  | 9  | 20 | 30 | 39 | 47 | 54 | 60 | 65 | 69 |    |    |    |
| $\theta[9]$  | 10 | 21 | 31 | 40 | 48 | 55 | 61 | 66 | 70 | 73 |    |    |
| $\theta[10]$ | 11 | 22 | 32 | 41 | 49 | 56 | 62 | 67 | 71 | 74 | 76 |    |
| $\theta[11]$ | 12 | 23 | 33 | 42 | 50 | 57 | 63 | 68 | 72 | 75 | 77 | 78 |

$\theta[i]$  see [Section 6.10.7.13](#)

Resources:

Estimated CPU time: -  
Output disk space:  $78 \times 2 \times 1 \text{ byte/uc} = 156 \text{ bytes}$

Acceptance:

Corresponds to the latest definition.

**6.10.7.15 Relative azimuth angles for GADS threshold on Rayleigh corrected reflectance**

Reference: RAA, LUT302

[AD-8] Section 6.10.7, GADS field 15

ACRI provided

Dependencies:

None

Tool:

None

Procedure:

Input: none

Output: RAA Relative azimuth angles (19 values)  
units:  $[10^{-6} \text{ deg}]$

Step: User specified.

Scientific content:

Set of 19 relative azimuth angles ( $\Delta\phi$ ) regularly spaced

Current baseline: 19 values in  $[0;180]deg.$  by step of  $10deg.$

Resources:

Estimated CPU time: -  
Output disk space:  $19 \times 4$  bytes/ul = 76 bytes

Acceptance:

Corresponds to the latest definition.

*6.10.7.16 Apparent pressure thresholds over land (off/close to the coastline)*

Reference: Ps\_thresh\_L1, LUT466  
Ps\_thresh\_L2,

[AD-8] Section 6.10.7, GADS field 16

ACRI provided

Dependencies:

None

Tool:

None

Procedure:

Input: none

Output: *Ps\_thresh\_L1, Ps\_thresh\_L2*  
Apparent surface pressure thresholds over land, off the coastline and close to the coastline respectively.

units: [hPa]

Step: User specified.

Scientific content:

Threshold on the apparent surface pressure over land

Current baseline: 200 hPa

Resources:

Estimated CPU time: -  
Output disk space:  $2 \times 4$  bytes/fl = 8 bytes

Acceptance:

Corresponds to the latest definition.

*6.10.7.17 Apparent pressure threshold over water*

Reference:  $Ps\_thresh\_W$ , LUT467

[AD-8] Section 6.10.7, GADS field 17

ACRI provided

Dependencies:

None

Tool:

None

Procedure:

Input: none  
Output:  $Ps\_thresh\_W$  Apparent surface pressure threshold over water  
units: [hPa]  
Step: User specified.

Scientific content:

Threshold on the apparent surface pressure over water  
Current baseline: 500 hPa

Resources:

Estimated CPU time: -  
Output disk space:  $1 \times 4$  bytes/fl = 4 bytes

Acceptance:

Corresponds to the latest definition.

6.10.7.18 *Minimum reflectance value at 753.75 nm to consider apparent pressure over land*

Reference: rho754\_min, LUT468

[AD-8] Section 6.10.7, GADS field 18

ACRI provided

Dependencies:

None

Tool:

None

Procedure:

Input: none

Output: rho754\_min Minimum reflectance value at 753.75nm to consider apparent pressure over land

units: [dl]

Step: User specified.

Scientific content:

Minimum reflectance at 753.75 nm to consider apparent surface pressure over land

Current baseline: 500

Resources:

Estimated CPU time: -

Output disk space: 1 × 4 bytes/fl = 4 bytes

Acceptance:

Corresponds to the latest definition.

6.10.7.19 *Minimum spectral slope between 753.75 nm and 778.75 nm to consider apparent pressure over water*

Reference: slope754\_779\_min, LUT469

[AD-8] Section 6.10.7, GADS field 19

ACRI provided

Dependencies:

None

Tool:

None

Procedure:

Input: none

Output: *slope754\_779\_min*

Minimum spectral slope between 753.75nm and 778.75nm to consider apparent pressure over water

units: [dl]

Step: User specified.

Scientific content:

Minimum spectral slope between 753.75nm and 778.75nm to consider apparent surface pressure over water

Current baseline: 0.0799999982

Resources:

Estimated CPU time: -

Output disk space: 1 × 4 bytes/fl = 4 bytes

Acceptance:

Corresponds to the latest definition.

*6.10.7.20 Band indices for MDSI computation*

Reference: MDSI\_b1, MDSI\_b2 LUT470

[AD-8] Section 6.10.7, GADS field 20

ACRI provided

Dependencies:



None

Tool:

None

Procedure:

Input: none

Output: *MDSI\_b1, MDSI\_b2*  
Band indices (*b1,b2*) for MDSI computation (2 values)

units: [*dl*]

Step: User specified.

Scientific content:

Band indices selected to compute the MERIS differential snow index

Current baseline: {62, 25}

Resources:

Estimated CPU time: -

Output disk space:  $2 \times 1 \text{ byte/uc} = 2 \text{ bytes}$

Acceptance:

Corresponds to the latest definition.

## 6.10.8 GADS Reflectance Thresholds

### 6.10.8.1 Thresholds on Rayleigh-corrected TOA reflectance above land, $\rho_{RC\_2}(\theta_s \times \theta_v, \Delta\varphi)$

Reference: Rho\_rc\_LUT, LUT303

[AD-8] Section 6.10.8, ADS record 1 field 1

Dependencies:

LUT299, LUT300, LUT301, LUT302

Tools:

OTC/RAYLEIGH

RTC/UPRAD (SO)

Procedure:

Inputs:  $n(\lambda)$  MERIS band index [ $dl$ ], see Section 6.10.7.12, (LUT299).  
 $\theta_s \times \theta_v$  Stored indices for angular combinations [ $dl$ ] (78 values), see Section 6.10.7.14, (LUT301).  
 $\theta$  Zenith angle [ $deg$ ], see Section 6.10.7.13, (LUT300).  
 $\Delta\phi$  Relative azimuth angle [ $deg$ ], see Section 6.10.7.15, (LUT302).

Output:  $Rho\_rc\_LUT[\theta_s \times \theta_v, \Delta\phi]$   
Radiometric thresholds on *Rayleigh* corrected TOA reflectance at  $\lambda$  nm as a function of the solar zenith angle, view zenith angle and relative azimuth angle between sun and viewing directions.

units: [ $dl$ ]

Step-1: Generate TOA normalized radiance  $L_{TOA\_2}[\theta_s, \theta_v, \Delta\phi]$  with the RTC/UPRAD (SO) over a reflective land surface under a continental atmosphere. The selected aerosol model is the *Junge* model #37 ( $m=1.44, \alpha=-1$ ).

**RTC/UPRAD (SO) Inputs (LAND)**

| Variable               | Value                   | Comments                                       |
|------------------------|-------------------------|--|
| <i>out_file</i>        | "./OUTPUT/uprad_out"    |  |
| <i>i_branch</i>        | 1                       |  |
| $n(\lambda)$           | 2                       | 442.5 nm (see Section 6.10.7.12)               |
| $U_{H2O}$              | 0                       |  |
| $U_{O2}$               | 0                       |  |
| <i>ESFT</i>            | -                       | N/A  |
| $P_s$                  | 1013.25                 |  |
| $\tau^R(\lambda)$      | tauR                    | Computed with OTC/RAYLEIGH                     |
| <i>aerosol1</i>        | "./INPUT/sc_land37_b02" | <i>Junge</i> model #37 ( $m=1.44, \alpha=-1$ ) |
| $\tau^{a1}(550)$       | 2.0                     |  |
| <i>aerosol2</i>        | -                       |  |
| $\tau^{a2}(550)$       | 0                       |  |
| <i>aerosol3</i>        | -                       |  |
| $\tau^{a3}(550)$       | 0                       |  |
| <i>cloud1</i>          | -                       | N/A  |
| <i>cloud2</i>          | -                       | N/A  |
| <i>cloud3</i>          | -                       | N/A  |
| <i>phyto</i>           | -                       | N/A  |
| $\sigma_{e,\lambda}^p$ | -                       | N/A  |
| $\omega_{o,\lambda}^p$ | -                       | N/A  |
| <i>spm</i>             | -                       | N/A  |

| Variable                   | Value                             | Comments  |
|----------------------------|-----------------------------------|---|
| $\sigma_{e,\lambda}^{spm}$ | -                                 | N/A   |
| $\omega_{o,\lambda}^{spm}$ | -                                 | N/A   |
| $\sigma_{e,\lambda}^{ys}$  | -                                 | N/A   |
| vertical                   | "/INPUT/vertical_out"             | Not used, vertical distribution determined in RTC/SO ( $H_a=2\text{ km}; H_R=8\text{ km}$ )               |
| $I_s$                      | 79                                |   |
| $\rho_s$                   | 0.1                               |   |
| $E_o$                      | 1                                 |   |
| $\sigma_{e,\lambda}^w$     | -                                 | N/A   |
| $\omega_{o,\lambda}^w$     | -                                 | N/A   |
| $w_s$                      | 0                                 |   |
| $n_s, n_v, n_{\Delta\phi}$ | 12, 12, 19                        |   |
| $\theta_s$                 | values stored in $\theta_s$ [ ]   | For all angular combinations, see <a href="#">Section 6.10.7.14</a> and <a href="#">Section 6.10.7.13</a> |
| $\theta_v$                 | values stored in $\theta_v$ [ ]   | For all angular combinations, see <a href="#">Section 6.10.7.14</a> and <a href="#">Section 6.10.7.13</a> |
| $\Delta\phi$               | values stored in $\Delta\phi$ [ ] | see <a href="#">Section 6.10.7.15</a>   |
| pol                        | 1                                 |   |

Step-2: Generate TOA *Rayleigh* normalized radiance  $L_{R,2}[\theta_s, \theta_v, \Delta\phi]$  with the RTC/UPRAD (SO) over a black land surface (*i.e.*, without specular reflection).

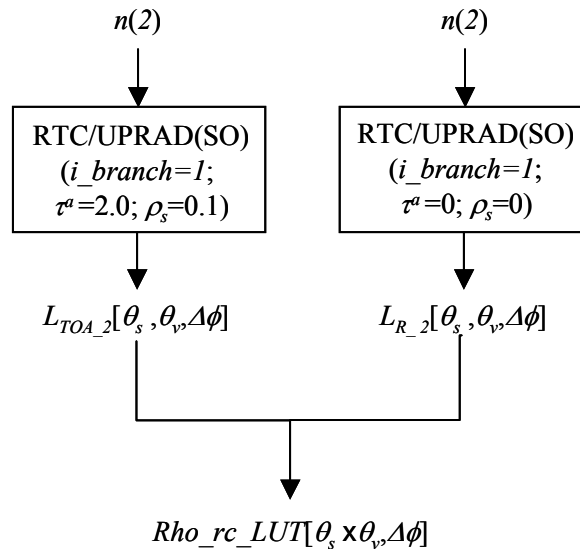
**RTC/UPRAD (SO) Inputs (LAND)**

| Variable          | Value               | Comments  |
|-------------------|---------------------|---|
| out_file          | "/OUTPUT/uprad_out" |   |
| i_branch          | 1                   |   |
| $n(\lambda)$      | 2                   | 442.5 nm (see <a href="#">Section 6.10.7.12</a> ) |
| $U_{H2O}$         | 0                   |   |
| $U_{O2}$          | 0                   |   |
| ESFT              | -                   | N/A   |
| $P_s$             | 1013.25             |   |
| $\tau^R(\lambda)$ | tauR                | Computed with OTC/RAYLEIGH                        |
| aerosol1          | -                   |   |
| $\tau^{a1}(550)$  | 0                   |   |
| aerosol2          | -                   |   |
| $\tau^{a2}(550)$  | 0                   |   |
| aerosol3          | -                   |   |
| $\tau^{a3}(550)$  | 0                   |   |

| Variable                   | Value                             | Comments  |
|----------------------------|-----------------------------------|---|
| <i>cloud1</i>              | -                                 | N/A   |
| <i>cloud2</i>              | -                                 | N/A   |
| <i>cloud3</i>              | -                                 | N/A   |
| <i>phyto</i>               | -                                 | N/A   |
| $\sigma_{e,\lambda}^p$     | -                                 | N/A   |
| $\omega_{o,\lambda}^p$     | -                                 | N/A   |
| <i>spm</i>                 | -                                 | N/A   |
| $\sigma_{e,\lambda}^{spm}$ | -                                 | N/A   |
| $\omega_{o,\lambda}^{spm}$ | -                                 | N/A   |
| $\sigma_{e,\lambda}^{ys}$  | -                                 | N/A   |
| <i>vertical</i>            | "/INPUT/vertical_out"             | Not used, vertical distribution determined in RTC/SO ( $H_R=8$ km)  |
| $I_s$                      | 79                                |   |
| $\rho_s$                   | 0                                 |   |
| $E_o$                      | 1                                 |   |
| $\sigma_{e,\lambda}^w$     | -                                 | N/A   |
| $\omega_{o,\lambda}^w$     | -                                 | N/A   |
| $w_s$                      | 0                                 |   |
| $n_s, n_v, n_{\Delta\phi}$ | 12, 12, 19                        |   |
| $\theta_s$                 | values stored in $\theta_s$ [ ]   | For all angular combinations, see <a href="#">Section 6.10.7.14</a> and <a href="#">Section 6.10.7.13</a> |
| $\theta_v$                 | values stored in $\theta_v$ [ ]   | For all angular combinations, see <a href="#">Section 6.10.7.14</a> and <a href="#">Section 6.10.7.13</a> |
| $\Delta\phi$               | values stored in $\Delta\phi$ [ ] | see <a href="#">Section 6.10.7.15</a>   |
| <i>pol</i>                 | 1                                 |   |

Step-3: Build  $Rho\_rc\_LUT[\theta_s \times \theta_v, \Delta\phi]$  such as,

$$Rho\_rc\_LUT[\theta_s \times \theta_v, \Delta\phi] = \pi \frac{L_{TOA\_2}[\theta_s, \theta_v, \Delta\phi] - L_{R\_2}[\theta_s, \theta_v, \Delta\phi]}{\cos \theta_s}$$



Scientific content:

In the pixels classification algorithm over land, the *Rayleigh*-corrected MERIS reflectances at 442.5 nm are respectively compared with these radiometric thresholds  $Rho\_rc\_LUT[\theta_s \times \theta_v, \Delta\phi]$ . If the *Rayleigh*-corrected reflectance is lower than the threshold then the pixel is not considered as a bright pixel. The thresholds are computed with inputs which generate the high boundary of a mean range of *Rayleigh*-corrected reflectance.

Resources:

Estimated CPU time: 324 sec  
Output disk space:  $78 \times 19 \times 4$  bytes/fl = 5928 bytes

Acceptance:

Comparison with another RTC.

6.10.8.2 Thresholds on *Rayleigh*-corrected TOA reflectance above ocean,  $\rho_{RC\_2}(\theta_s \times \theta_v, \Delta\phi)$

Reference: Rho\_rc\_LUT, LUT303

[AD-8] Section 6.10.8, ADS record 2 field 1

Dependencies:

LUT299, LUT300, LUT301, LUT302

Tools:

OTC/RAYLEIGH  
RTC/UPRAD (SO)

Procedure:

- Inputs:  $n(\lambda)$  MERIS band index [ $dl$ ], see Section 6.10.7.12, (LUT299).  
 $\theta_s \times \theta_v$  Stored indices for angular combinations [ $dl$ ] (78 values), see Section 6.10.7.14, (LUT301).  
 $\theta$  Zenith angle [ $deg$ ], see Section 6.10.7.13, (LUT300).  
 $\Delta\phi$  Relative azimuth angle [ $deg$ ], see Section 6.10.7.15, (LUT302).

Output:  $Rho\_rc\_LUT[\theta_s \times \theta_v, \Delta\phi]$   
Radiometric thresholds on *Rayleigh* corrected TOA reflectance at  $\lambda$  nm as a function of the solar zenith angle, view zenith angle and relative azimuth angle between sun and viewing directions.

units: [ $dl$ ]

Step-1: Generate TOA normalized radiance  $L_{TOA,2}[\theta_s, \theta_v, \Delta\phi]$  with the RTC/UPRAD (SO) over a wind-roughened reflective sea surface (*i.e.*, including the glitter contribution or the multiple specular reflections) under a maritime atmosphere. The ocean aerosol assemblage #3 is selected (see Table in Section 6.13.5.1).

**RTC/UPRAD (SO) Inputs (OCEAN)**

| Variable               | Value                 | Comments                           |
|------------------------|-----------------------|------------------------------------|
| <i>out_file</i>        | "/OUTPUT/uprad_out"   |                                    |
| <i>i_branch</i>        | 2                     |                                    |
| $n(\lambda)$           | 2 (442.5 nm)          | 442.5 nm (see Section 6.10.7.12)   |
| $U_{H2O}$              | 0                     |                                    |
| $U_{O2}$               | 0                     |                                    |
| <i>ESFT</i>            | -                     | N/A                                |
| $P_s$                  | 1013.25               |                                    |
| $t^R(\lambda)$         | tauR                  | Computed with OTC/RAYLEIGHh        |
| <i>aerosol1</i>        | "/INPUT/sc_mar90_b02" | Ocean aerosol assemblage#3 (MAR90) |
| $t^{a1}(550)$          | 2.0                   |                                    |
| <i>aerosol2</i>        | "/INPUT/sc_conti_b02" | Ocean aerosol assemblage#3 (CONTI) |
| $t^{a2}(550)$          | 0.025                 |                                    |
| <i>aerosol3</i>        | "/INPUT/sc_H2SO4_b02" | Ocean aerosol assemblage#3 (H2SO4) |
| $t^{a3}(550)$          | 0.005                 |                                    |
| <i>cloud1</i>          | -                     | N/A                                |
| <i>cloud2</i>          | -                     | N/A                                |
| <i>cloud3</i>          | -                     | N/A                                |
| <i>phyto</i>           | -                     | N/A                                |
| $\sigma_{e,\lambda}^p$ | -                     | N/A                                |
| $\omega_{o,\lambda}^p$ | -                     | N/A                                |

| Variable                   | Value                            | Comments  |
|----------------------------|----------------------------------|---|
| $spm$                      | -                                | N/A   |
| $\sigma_{e,\lambda}^{spm}$ | -                                | N/A   |
| $\omega_{o,\lambda}^{spm}$ | -                                | N/A   |
| $\sigma_{e,\lambda}^{ys}$  | -                                | N/A   |
| <i>vertical</i>            | "/INPUT/vertical_out"            | Not used, vertical distribution determined in RTC/SO (optically homogeneous layers)                       |
| $I_s$                      | 79                               |   |
| $\rho_s$                   | 0.036                            |   |
| $E_o$                      | 1                                |   |
| $\sigma_{e,\lambda}^w$     | -                                | N/A   |
| $\omega_{o,\lambda}^w$     | -                                | N/A   |
| $w_s$                      | 5.0                              |   |
| $n_s, n_v, n_{\Delta\phi}$ | 12, 12, 19                       |   |
| $\theta_s$                 | values stored in $\theta_s[ ]$   | For all angular combinations, see <a href="#">Section 6.10.7.14</a> and <a href="#">Section 6.10.7.13</a> |
| $\theta_v$                 | values stored in $\theta_v[ ]$   | For all angular combinations, see <a href="#">Section 6.10.7.14</a> and <a href="#">Section 6.10.7.13</a> |
| $\Delta\phi$               | values stored in $\Delta\phi[ ]$ | see <a href="#">Section 6.10.7.15</a>   |
| <i>pol</i>                 | 1                                |   |

Step-2: Generate TOA *Rayleigh* normalized radiance  $L_{R_2}[\theta_s, \theta_v, \Delta\phi]$  with the RTC/UPRAD (SO) over a wind-roughened black sea surface (*i.e.*, including the glitter contribution or the multiple specular reflections).

**RTC/UPRAD (SO) Inputs (LAND)**

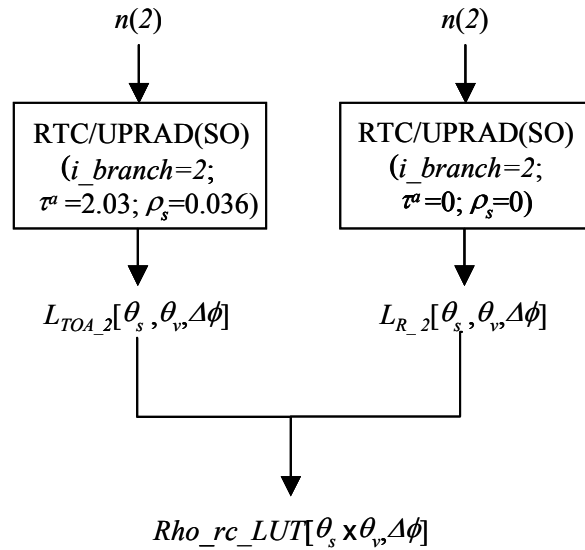
| Variable          | Value               | Comments                                       |
|-------------------|---------------------|--|
| <i>out_file</i>   | "/OUTPUT/uprad_out" |  |
| <i>i_branch</i>   | 2                   |  |
| $n(\lambda)$      | 2 (442.5 nm)        | 442.5 nm ( <a href="#">Section 6.10.7.12</a> ) |
| $U_{H2O}$         | 0                   |  |
| $U_{O2}$          | 0                   |  |
| <i>ESFT</i>       | -                   | N/A  |
| $P_s$             | 1013.25             |  |
| $\tau^R(\lambda)$ | tauR                | Computed with OTC/RAYLEIGH                     |
| <i>aerosol1</i>   | -                   |  |
| $\tau^{a1}(550)$  | 0                   |  |
| <i>aerosol2</i>   | -                   |  |
| $\tau^{a2}(550)$  | 0                   |  |

| Variable                   | Value                            | Comments  |
|----------------------------|----------------------------------|---|
| <i>aerosol3</i>            | -                                |   |
| $\tau^{a3}(550)$           | 0                                |   |
| <i>cloud1</i>              | -                                | N/A   |
| <i>cloud2</i>              | -                                | N/A   |
| <i>cloud3</i>              | -                                | N/A   |
| <i>phyto</i>               | -                                | N/A   |
| $\sigma_{e,\lambda}^p$     | -                                | N/A   |
| $\omega_{o,\lambda}^p$     | -                                | N/A   |
| <i>spm</i>                 | -                                | N/A   |
| $\sigma_{e,\lambda}^{spm}$ | -                                | N/A   |
| $\omega_{o,\lambda}^{spm}$ | -                                | N/A   |
| $\sigma_{e,\lambda}^{ys}$  | -                                | N/A   |
| <i>vertical</i>            | "/INPUT/vertical_out"            | Not used, vertical distribution determined in RTC/SO ( $H_R=8$ km)  |
| $I_s$                      | 79                               |   |
| $\rho_s$                   | 0                                |   |
| $E_o$                      | 1                                |   |
| $\sigma_{e,\lambda}^w$     | -                                | N/A   |
| $\omega_{o,\lambda}^w$     | -                                | N/A   |
| $w_s$                      | 5.0                              |   |
| $n_s, n_v, n_{\Delta\phi}$ | 12, 12, 19                       |   |
| $\theta_s$                 | values stored in $\theta_s$ []   | For all angular combinations, see <a href="#">Section 6.10.7.14</a> and <a href="#">Section 6.10.7.13</a> |
| $\theta_v$                 | values stored in $\theta_v$ []   | For all angular combinations, see <a href="#">Section 6.10.7.14</a> and <a href="#">Section 6.10.7.13</a> |
| $\Delta\phi$               | values stored in $\Delta\phi$ [] | see <a href="#">Section 6.10.7.15</a>   |
| <i>pol</i>                 | 1                                |   |

Step-3: Build  $Rho\_rc\_LUT[\theta_s \times \theta_v, \Delta\phi]$  such as,

$$Rho\_rc\_LUT[\theta_s \times \theta_v, \Delta\phi] = \pi \frac{L_{TOA\_2}[\theta_s, \theta_v, \Delta\phi] - L_{R\_2}[\theta_s, \theta_v, \Delta\phi]}{\cos \theta_s}$$





Scientific content:

In the pixels classification algorithm over ocean, the *Rayleigh*-corrected MERIS reflectances at  $442.5\text{nm}$  are respectively compared with these radiometric thresholds  $Rho\_rc\_LUT[\theta_s \times \theta_v, \Delta\phi]$ . If the *Rayleigh*-corrected reflectance is lower than the corresponding threshold value then the pixel is not considered as a bright pixel. The thresholds are computed with inputs which generate the high boundary of a mean range of *Rayleigh*-corrected reflectance.

Resources:

Estimated CPU time: 685 sec  
Output disk space:  $78 \times 19 \times 4$  bytes/fl = 5928 bytes

Acceptance:

Comparison with another RTC.

## 6.11 ATMOSPHERE PARAMETERS

### 6.11.1 C.P.

#### 6.11.1.1 C.P. Rayleigh optical thickness, $\tau^R(\lambda, P_s)$

Reference: tauR LUT410

Configuration file

PARBLEU provided

Dependencies:

LUT076, LUT092

Tool:

OTC/RAYLEIGH

Procedure:

Inputs:  $\lambda$  MERIS wavelength [nm], see [Section 6.11.4.3](#), (LUT076)  
 $P_s$  Standard surface pressure [hPa], see [Section 6.11.4.19](#), (LUT092)

Output:  $\tau^R$  Rayleigh optical thickness (tauR)

units: [dl]

Step: User specified.

Scientific content:

Rayleigh optical thicknesses in the 15 MERIS spectral bands computed with Travis/Hansen formulation.

Current baseline: {0.3152799904, 0.2359099984, 0.1551550031, 0.1317140013, 0.0899119973,  
0.0594329983, 0.0447300002, 0.0405620001, 0.0345579982, 0.0269440003,  
0.0258019995, 0.0236169994, 0.0154590001, 0.0140990000, 0.0131759997}

Resources:

Estimated CPU time: -

Output disk space: 15 × 4 bytes/fl = 60 bytes

Acceptance:

Corresponds to the latest definition.

### 6.11.2 MPH

Not covered in this document (see [AD-8] for a detailed description)

### 6.11.3 SPH

Not covered in this document (see [AD-8] for a detailed description)

### 6.11.4 GADS General

#### 6.11.4.1 Rayleigh transmittance coefficients

Reference:  $t_0, t_1, t_2$ , LUT074

[AD-8] Section 6.11.4, GADS field 1.

Dependencies:

LUT075, LUT080

Tools:

RTC/UPRAD (SO)  
Polynomial fit

Procedure:

Inputs:  $\theta_s$  Solar zenith angle [deg], see Section 6.11.4.4, (LUT080)  
 $\tau^R$  Rayleigh optical thickness [dl], see Section 6.11.4.2, (LUT075)

Output:  $t_0, t_1, t_2$  Rayleigh transmittance coefficients (second order polynomial)  
units: [dl]

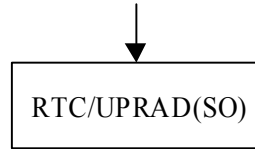
Step-1: Calculate the Rayleigh transmittance  $T_{R\_RTC}[\tau^R, \theta_s]$  corresponding to the first order of Legendre decomposition ( $I_s=0$ ) of phase function with the RTC/UPRAD (SO). For extracting the total atmospheric transmittance, we need to set  $I_s=0$  and  $\theta_v=-1$ .

**RTC/UPRAD (SO) Inputs (LAND)**

| Variable       | Value               | Comments                                     |
|----------------|---------------------|--|
| out_file       | "/OUTPUT/uprad_out" |  |
| i_branch       | 1                   |  |
| n( $\lambda$ ) | 1                   | Not used. Rayleigh transmittance is computed |

| Variable                   | Value                 | Comments   |
|----------------------------|-----------------------|--|
|                            |                       | as function of $\tau^R$ (tabulated values).                        |
| $U_{H2O}$                  | 0                     |  |
| $U_{O2}$                   | 0                     |  |
| $ESFT$                     | -                     | N/A  |
| $P_s$                      | 1013.25               |  |
| $\tau^R(\lambda)$          | see inputs            | see Section 6.11.4.2   |
| <i>aerosol1</i>            | -                     |  |
| $\tau^{a1}(550)$           | 0                     |  |
| <i>aerosol2</i>            | -                     |  |
| $\tau^{a2}(550)$           | 0                     |  |
| <i>aerosol3</i>            | -                     |  |
| $\tau^{a3}(550)$           | 0                     |  |
| <i>cloud1</i>              | -                     | N/A  |
| <i>cloud2</i>              | -                     | N/A  |
| <i>cloud3</i>              | -                     | N/A  |
| <i>phyto</i>               | -                     | N/A  |
| $\sigma_{e,\lambda}^p$     | -                     | N/A  |
| $\omega_{o,\lambda}^p$     | -                     | N/A  |
| <i>spm</i>                 | -                     | N/A  |
| $\sigma_{e,\lambda}^{spm}$ | -                     | N/A  |
| $\omega_{o,\lambda}^{spm}$ | -                     | N/A  |
| $\sigma_{e,\lambda}^{ys}$  | -                     | N/A  |
| <i>vertical</i>            | "/INPUT/vertical_out" | Not used, vertical distribution determined in RTC/SO ( $H_R=8$ km) |
| $I_s$                      | 0                     |  |
| $\rho_s$                   | 0                     |  |
| $E_o$                      | 1                     |  |
| $\sigma_{e,\lambda}^w$     | -                     | N/A  |
| $\omega_{o,\lambda}^w$     | -                     | N/A  |
| $w_s$                      | 0                     |  |
| $n_s, n_v, n_{\Delta\phi}$ | 12, 1, 1              | Use a loop for 12 $\theta_s$                                       |
| $\theta_s$                 | see inputs            | see Section 6.11.4.4   |
| $\theta_v$                 | -1                    | To get the total atmospheric transmittance                         |
| $\Delta\phi$               | 0                     |  |
| <i>pol</i>                 | 1                     |  |

Input table



$T_{R\_RTC}[\tau^R, \theta_s]$

Step-2: Calculate the corresponding value of  $T_{R\_ANA}[\tau^R, \theta_s]$  with the analytical expression used in the 6S code [RD-5].

$$T_{R\_ANA}(\tau^R, \theta_s) = [(2/3 + \cos \theta_s) + (2/3 - \cos \theta_s) \exp(-\tau^R / \cos \theta_s)] / [4/3 + \tau^R]$$

Step-3: Calculate  $t_0$ ,  $t_1$  and  $t_2$  coefficients with the polynomial fit as follows,

$$T_{R\_RTC}(\tau^R, \theta_s) = t_0 + t_1 \cdot T_{R\_ANA}(\tau^R, \theta_s) + t_2 \cdot [T_{R\_ANA}(\tau^R, \theta_s)]^2$$

Scientific content:

Compute the *Rayleigh* transmittance for removing the *Rayleigh* scattering effects in MERIS data. The *Rayleigh* optical thicknesses ( $\tau^R$ ) and the solar zenith angles ( $\theta_s$ ) have to cover the MERIS range.

Resources:

Estimated CPU time: 21 sec  
Output disk space: 3 × 4 bytes/fl = 12 bytes

Acceptance:

Comparison with another RTC.

6.11.4.2 *Rayleigh optical thicknesses*

Reference: tauR, LUT075

[AD-8] Section 6.11.4, GADS field 2.

ACRI provided

Dependencies:

None

Tool:

Input: none

Output: tauR *Rayleigh* optical thickness (17 values)  
units: [dl]  
Step: User specified.

Procedure:

None

Scientific content:

Set of 17 values of *Rayleigh* optical thicknesses.

Current baseline: tauR values in [0.02;0.34] by step of 0.02

Resources:

Estimated CPU time: -  
Output disk space:  $17 \times 4$  bytes/fl = 68 bytes

Acceptance:

Corresponds to the latest definition.

**6.11.4.3 Nominal wavelengths of MERIS spectral bands**

Reference: Wvl, LUT076

[AD-8] Section 6.11.4, GADS field 3.

ACRI provided

Dependencies:

None

Tool:

None

Procedure:

Input: none  
Output: Wvl *Nominal wavelengths of MERIS spectral bands* (15 values)  
units: [nm]

Step: User specified.

Scientific content:

Nominal wavelengths for the 15 MERIS spectral bands

Current baseline: {412.5, 442.5, 490.0, 510.0, 560.0, 620.0, 665.0, 681.25, 708.75, 753.75, 761.875, 778.75, 865.0, 885.0, 900.0} *nm*

Resources:

Estimated CPU time: -  
Output disk space: 15 × 4 bytes/fl = 60 bytes

Acceptance:

Corresponds to the latest definition.

*6.11.4.4 Solar zenith angles for GADS Rayleigh reflectance over ocean*

Reference: SZA, LUT077

[AD-8] Section 6.11.4, GADS field 4.

ACRI provided

Dependencies:

None

Tool:

None

Procedure:

Input: none  
Output: SZA Solar zenith angle (23 values)  
units: [10<sup>-6</sup> deg]  
Step: User specified.

Scientific content:

Set of 23 solar zenith angles ( $\theta_s$ ) selected from the *Gauss* quadrature generated for 25 discrete directions (including zenith) with the RTC/Gauss tool (UdL).

Current baseline: 23 values corresponding to the first 23 angles from the *Gauss* quadrature

| $\theta_s$ [deg.] | $\theta_s$ [deg.] | $\theta_s$ [deg.] | $\theta_s$ [deg.] |
|-------------------|-------------------|-------------------|-------------------|
| 0.000000          | 21.347983         | 43.611442         | 65.877652         |
| 2.840906          | 25.058051         | 47.322394         | 69.588762         |
| 6.521063          | 28.768427         | 51.033390         | 73.299882         |
| 10.222955         | 32.479006         | 54.744420         | 77.011011         |
| 13.929756         | 36.189726         | 58.455477         | 80.722147         |
| 17.638419         | 39.900547         | 62.166556         |                   |

Resources:

Estimated CPU time: -  
Output disk space: 23 × 4 bytes/ul = 92 bytes

Acceptance:

Corresponds to the latest definition.

6.11.4.5 View zenith angles for GADS Rayleigh reflectance over ocean

Reference: VZA, LUT078

[AD-8] Section 6.11.4, GADS field 5.

ACRI provided

Dependencies:

None

Tool:

None

Procedure:

Input: none  
Output: VZA View zenith angle (13 values)  
units: [10<sup>-6</sup> deg]  
Step: User specified.



Scientific content:

Set of 13 view zenith angles ( $\theta_v$ ) selected from the *Gauss* quadrature generated for 25 discrete directions (including nadir) with the RTC/Gauss tool (UdL).

Current baseline: 13 values corresponding to the first 13 angles from the *Gauss* quadrature

| $\theta_v$ [deg.] | $\theta_v$ [deg.] |
|-------------------|-------------------|
| 0.000000          | 25.058051         |
| 2.840906          | 28.768427         |
| 6.521063          | 32.479006         |
| 10.222955         | 36.189726         |
| 13.929756         | 39.900547         |
| 17.638419         | 43.611442         |
| 21.347983         |                   |

Resources:

Estimated CPU time: -  
Output disk space: 13 × 4 bytes/ul = 52 bytes

Acceptance:

Corresponds to the latest definition.

**6.11.4.6 Relative azimuth angles for GADS Rayleigh reflectances over ocean (tabulated values)**

Reference: RAA, LUT079

[AD-8] Section 6.11.4, GADS field 6.

ACRI provided

Dependencies:

None

Tool:

None

Procedure:

Input: none

Output: *RAA* Relative azimuth angle (25 values)  
units:  $[10^{-6} \text{ deg}]$   
Step: User specified.

Scientific content:

Set of 25 relative azimuth angles ( $\Delta\phi$ ) between illumination and viewing directions regularly spaced

Current baseline: 25 values within  $[0;180] \text{ deg.}$ , with a step of  $7.5 \text{ deg.}$

| $\Delta\phi[\text{deg.}]$ | $\Delta\phi[\text{deg.}]$ | $\Delta\phi[\text{deg.}]$ | $\Delta\phi[\text{deg.}]$ | $\Delta\phi[\text{deg.}]$ |
|---------------------------|---------------------------|---------------------------|---------------------------|---------------------------|
| 0.00                      | 37.50                     | 75.00                     | 112.50                    | 150.00                    |
| 7.50                      | 45.00                     | 82.50                     | 120.00                    | 157.50                    |
| 15.00                     | 52.50                     | 90.00                     | 127.50                    | 165.00                    |
| 22.50                     | 60.00                     | 97.50                     | 135.00                    | 172.50                    |
| 30.00                     | 67.50                     | 105.00                    | 142.50                    | 180.00                    |

Resources:

Estimated CPU time: -  
Output disk space:  $25 \times 4 \text{ bytes/ul} = 100 \text{ bytes}$

Acceptance:

Corresponds to the latest definition.

**6.11.4.7 Zenith angles for GADS Rayleigh scattering function**

Reference: ZA, LUT080

[AD-8] Section 6.11.4, GADS field 7.

ACRI provided

Dependencies:

None

Tool:

None

Procedure:

Input: none

Output:     ZA             Zenith angle (12 values)  
          units:     [10<sup>-6</sup> deg]  
  
Step:         User specified.

Scientific content:

Set of 12 angles ( $\theta$ ) selected from the *Gauss* quadrature generated for 24 discrete directions with the RTC/Gauss tool (UdL)

Current baseline: 12 *Gaussian* angles (see [Section 6.10.7.13](#))

Resources:

Estimated CPU time:     -  
Output disk space:     12 × 4 bytes/ul = 48 bytes

Acceptance:

Corresponds to the latest definition.

**6.11.4.8 Stored indices for ( $\theta_s \times \theta_v$ ) combinations for GADS Rayleigh scattering function**

Reference:     SVZA\_index,             LUT081

[\[AD-8\]](#)     Section 6.11.4, GADS field 8.

ACRI provided

Dependencies:

None

Tool:

Input:         none  
  
Output:        SVZA\_index     Stored indices for ( $\theta_s \times \theta_v$ ) combinations (78 values)  
          units:     [dl]  
  
Step:         User specified.

Procedure:

None

Scientific content:

Current baseline: 78 angular combinations (SZA x VZA) (*see* [Section 6.10.7.14](#))

Note: Due to the fact that the matrix is symmetrical in the  $(\theta_s \times \theta_v)$  directions, we can then store only a half triangular matrix, *i.e.*,  $N(N+1)/2$  instead of  $N^2$  elements (78 instead of 144).

Resources:

Estimated CPU time: -  
Output disk space:  $78 \times 2 \times 1$  byte/uc = 156 bytes

Acceptance:

Corresponds to the latest definition.

6.11.4.9 Constants used for Rayleigh phase function (A,B)

Reference: {A,B}, LUT082

[\[AD-8\]](#) Section 6.11.4, GADS field 9.

ACRI provided

Dependencies:

None

Tool:

None

Procedure:

Input: none

Output:  $A, B$  Constants used for the anisotropy of Rayleigh phase function (2 values)

units:  $[dl]$

Step: User specified.

Scientific content:

These 2 constants (A,B) are used to correct the Rayleigh phase function for the molecular anisotropy. The letters which derive from the 6S code [\[RD-5\]](#) are determined empirically.

Current baseline:  $A = 0.9587256$ ;  $B = 0.0412744$

Resources:

Estimated CPU time: -  
Output disk space:  $2 \times 4$  bytes/fl = 8 bytes

Acceptance:

Corresponds to the latest definition.

6.11.4.10 Air masses (downward and upward atmospheric paths)

Reference: AM, LUT083

[AD-8] Section 6.11.4, GADS field 10.

ACRI provided

Dependencies:

None

Tool:

None

Procedure:

Input: none

Output: *AM* Air mass for the 2 atmospheric paths (up/down) (6 values)  
units: [*dI*]

Step: User specified.

Scientific content:

The air mass (*M*) is defined as,

$$M = \frac{1}{\cos \theta_s} + \frac{1}{\cos \theta_v}$$

This requires a set of  $\theta_s$  and  $\theta_v$  values which falls in a given range of MERIS air mass values.

Current baseline:  $M = \{2.0; 2.3; 2.6; 2.9; 3.2; 3.5\}$

Resources:

Estimated CPU time: -  
Output disk space:  $6 \times 4$  bytes/fl = 24 bytes

Acceptance:

Corresponds to the latest definition.

6.11.4.11 Reference wavelengths for GADS O2 transmittances around 778.75 nm

Reference: Wvl\_FiltO2, LUT095

[AD-8] Section 6.11.4, GADS field 11.

FUB/ACRI provided

Dependencies:

None

Tool:

None

Procedure:

Input: none

Output: *Wvl\_FiltO2* Nominal wavelengths for the 21 MERIS O2 filters around 778.75 nm (21 values)

units: [nm]

Step: User specified.

Scientific content:

Set of 21 MERIS O2 filters (around 778.5 nm) used for computation of residual O2 absorption around 778.75 nm.

Current baseline: {777.5, 777.6, 777.7, 777.8, 777.9, 778.0, 778.1, 778.2, 778.3, 778.4, 778.5, 778.6, 778.7, 778.8, 778.9, 779.0, 779.1, 779.2, 779.3, 779.4, 779.5} nm

Resources:

Estimated CPU time: -

Output disk space: 21 × 4 bytes/fl = 84 bytes

Acceptance:

Corresponds to the latest definition.

6.11.4.12 TOA normalized radiances at 778.75 nm for GADS O2 transmittances around 778.75 nm

Reference: LN\_779, LUT085

[AD-8] Section 6.11.4, GADS field 12.

FUB/ACRI provided

Dependencies:

None

Tool:

None

Procedure:

Input: none

Output: LN\_779 TOA normalized radiance at 778.75 nm (25 values)

units: [ $sr^{-1}$ ]

Step: User specified.

Scientific content:

$L_{TOA\_779}$  [ ] is a vector which contains 25 typical values of TOA normalized radiances at 778.75 nm.

Current baseline:  $L_{TOA\_779} = \{0.002, 0.012, 0.022, 0.032, 0.042, 0.052, 0.062, 0.072, 0.082, 0.092, 0.102, 0.112, 0.122, 0.132, 0.142, 0.152, 0.162, 0.172, 0.182, 0.192, 0.202, 0.212, 0.222, 0.232, 0.242\} sr^{-1}$

Resources:

Estimated CPU time: -

Output disk space:  $25 \times 4$  bytes/fl = 100 bytes

Acceptance:

Corresponds to the latest definition.

6.11.4.13 Solar zenith angles for GADS O2 transmittances around 778.75 nm

Reference: SZA\_TO2, LUT086

[AD-8] Section 6.11.4, GADS field 13.

FUB/ACRI provided

Dependencies:

None

Tool:

None

Procedure:

Input: none

Output: *SZA\_TO2* Solar zenith angle ( $\theta_{s, TO2}$ ) (15 values)  
units: [ $10^{-6}$  deg]

Step: User specified.

Scientific content:

Set of 15 solar zenith angles ( $\theta_{s, TO2}$ ) regularly spaced.

Current baseline: 15 values within [10;80] deg., with a step of 5 deg.

Resources:

Estimated CPU time: -

Output disk space:  $15 \times 4$  bytes/ul = 60 bytes

Acceptance:

Corresponds to the latest definition.

**6.11.4.14 View zenith angles for GADS O2 transmittances around 778.75 nm**

Reference: VZA\_TO2, LUT087

[AD-8] Section 6.11.4, GADS field 14.

FUB/ACRI provided

Dependencies:

None

Tool:



None

Procedure:

Input: none

Output: *VZA\_TO2* View zenith angle ( $\theta_{v, TO2}$ ) (10 values)

units:  $[10^{-6} \text{ deg}]$

Step: User specified.

Scientific content:

Set of 10 view zenith angles ( $\theta_{v, TO2}$ ) regularly spaced.

Current baseline: 10 values within  $[0;45] \text{ deg.}$ , with a step of 5 *deg*

Resources:

Estimated CPU time: -

Output disk space:  $10 \times 4 \text{ bytes/ul} = 40 \text{ bytes}$

Acceptance:

Corresponds to the latest definition.

**6.11.4.15 Relative azimuth angles for GADS O2 transmittances around 778.75 nm**

Reference: RAA\_TO2, LUT088

[AD-8] Section 6.11.4, GADS field 15.

FUB/ACRI provided

Dependencies:

None

Tool:

None

Procedure:

Input: none

Output: *RAA\_TO2* Relative azimuth angle ( $\Delta\phi_{TO2}$ ) (19 values)  
units:  $[10^{-6} deg]$   
Step: User specified.

Scientific content:

Set of 19 relative azimuth angles ( $\Delta\phi_{TO2}$ ) between illumination and viewing directions regularly spaced  
Current baseline: 19 values within  $[0;180] deg.$ , with a step of 10 *deg.*

Resources:

Estimated CPU time: -  
Output disk space:  $19 \times 4 \text{ bytes/ul} = 76 \text{ bytes}$

Acceptance:

Corresponds to the latest definition.

**6.11.4.16 Threshold for flagging low pressure water**

Reference:  $P_{\text{thresh}}$ , LUT089

[AD-8] Section 6.11.4, GADS field 16.

ACRI provided

Dependencies:

None

Tool:

None

Procedure:

Input: none  
Output:  $P_{\text{thresh}}$  Threshold for flagging low pressure water  
units:  $[hPa]$   
Step: User specified.

Scientific content:

This threshold is applied on pressure to discriminate high elevation inland waters. The value is determined empirically.

Current baseline:  $P_{thresh} = 900 \text{ hPa}$

Resources:

Estimated CPU time: -  
Output disk space:  $1 \times 4 \text{ bytes/fl} = 4 \text{ bytes}$

Acceptance:

Corresponds to the latest definition.

6.11.4.17 *Standard water vapour content*

Reference: uH2O\_std, LUT090

[AD-8] Section 6.11.4, GADS field 17

ACRI provided

Dependencies:

None

Tool:

None

Procedure:

Input: none  
Output: *uH2O\_std* Standard water vapour content  
units:  $[\text{g.cm}^{-2}]$   
Step: User specified.

Scientific content:

$u_{H2Ostd}$  defines the standard total water vapor content in the atmosphere (Mid-Latitude Summer) to be considered in the computations. It represents a weight of the total atmospheric column. The LUT will be produced based on this value; the atmospheric transmission will be influenced by how much water vapor is considered by the radiative transfer model.

Current baseline:  $1.42 \text{ g.cm}^{-2}$

This value defines also the standard water vapor content for field 1 from Section 6.11.4 [AD-8].

Resources:

Estimated CPU time: -  
Output disk space: 1 × 4 bytes/fl = 4 bytes

Acceptance:

Corresponds to the latest definition.

6.11.4.18 Standard ozone content

Reference: uO3\_std, LUT091

[AD-8] Section 6.11.4, GADS field 18.

ACRI provided

Dependencies:

None

Tool:

None

Procedure:

Input: none  
Output: uO3\_std Standard ozone content  
units: [cm-atm]  
Step: User specified.

Scientific content:

The clear-sky atmospheric correction algorithm requires a standard value of the total ozone amount. This value is used to generated the LUT of the ozone optical thickness (see Section 6.11.5.5) and is set up to the value corresponding to the Mid-Latitude Summer profile (WRCP) which is 350 DU (or 0.35 cm-atm).

Current baseline: 0.35 cm-atm

Resources:

Estimated CPU time: -

Output disk space: 1 × 4 bytes/fl = 4 bytes

Acceptance:

Corresponds to the latest definition.

6.11.4.19 Standard surface pressure

Reference: Ps\_std, LUT092

[AD-8] Section 6.11.4, GADS field 19.

ACRI provided

Dependencies:

None

Tool:

None

Procedure:

Input: none

Output: Ps\_std Standard surface pressure  
units: [hPa]

Step: User specified.

Scientific content:

The clear sky atmospheric correction algorithm requires a standard value of the surface pressure. This value is used to generate the LUT of the *Rayleigh* optical thickness (see Section 6.11.5.5) and is set up to the surface pressure from the Mid-Latitude Summer profile (WRCP) which is 1013.25 hPa.

Current baseline: 1013.25 hPa

This value defines also the standard surface pressure for field 2 from Section 6.11.4 [AD-8].

Resources:

Estimated CPU time: -

Output disk space: 1 × 4 bytes/fl = 4 bytes

Acceptance:

Corresponds to the latest definition.

**6.11.4.20 Wind-speeds for GADS Rayleigh reflectance over ocean**

Reference:  $W_s$ , LUT093

[AD-8] Section 6.11.4, GADS field 20.

ACRI provided

Dependencies:

None

Tool:

None

Procedure:

Input: none

Output:  $W_s$  Wind-speed just above sea level (3 values)  
units:  $[m.s^{-1}]$

Step: User specified.

Scientific content:

For the atmospheric corrections over ocean, the wind-speed values will be set to 1.5, 5.0 and  $10m.s^{-1}$ .

Current baseline:  $\{1.5, 5.0, 10.0\} m.s^{-1}$

Resources:

Estimated CPU time: -  
Output disk space:  $3 \times 4$  bytes/fl = 12 bytes

Acceptance:

Corresponds to the latest definition.

**6.11.4.21 Maximum valid pressure**

Reference: Max\_Press, LUT304

[AD-8] Section 6.11.4, GADS field 21.

ACRI provided

Dependencies:

None

Tool:

None

Procedure:

Input: none

Output: *Max\_Press* Maximum valid surface pressure  
units: [*hPa*]

Step: User specified.

Scientific content:

Maximum valid value of surface pressure

Current baseline: 1050 *hPa*

Resources:

Estimated CPU time: -

Output disk space: 1 × 4 bytes/fl = 4 bytes

Acceptance:

Corresponds to the latest definition.

6.11.4.22 *Angstrom exponents for ADS photosynthetically active radiation (PAR)*

Reference: alpha\_PAR, LUT305

[AD-8] Section 6.11.4, GADS field 22.

ACRI provided

Dependencies:

None

Tool:

None

Procedure:

Input: none

Output: *alpha\_PAR* *Angstroem* exponent used for PAR (20 values)  
units: [dl]

Step: User specified.

Scientific content:

Current baseline: {-0.8, -0.653, -0.505, -0.358, -0.210, -0.063, 0.084, 0.232, 0.379, 0.526, 0.674,  
0.821, 0.969, 1.116, 1.263, 1.411, 1.558, 1.706, 1.853, 2.000}

Resources:

Estimated CPU time: -

Output disk space: 20 × 4 bytes/fl = 80 bytes

Acceptance:

Corresponds to the latest definition.

6.11.4.23 Ozone contents for ADS photosynthetically active radiation (PAR)

Reference: uO3\_PAR, LUT306

[AD-8] Section 6.11.4, GADS field 23.

ACRI provided

Dependencies:

None

Tool:

None

Procedure:

Input: none



Output: *uO3\_PAR* Ozone content used for PAR (20 values)  
units:  $[10^{-3} \text{ cm-atm}]$  or  $[DU]$

Step: User specified.

Scientific content:

Set of 20 ozone contents used for the PAR computation

Current baseline: {200.000, 210.526, 221.052, 231.578, 242.104, 252.630, 263.156, 273.682, 284.208, 294.734, 305.260, 315.786, 326.312, 336.838, 347.364, 357.890, 368.416, 378.942, 389.468, 399.994}  $10^{-3} \text{ cm-atm}$

Resources:

Estimated CPU time: -  
Output disk space:  $20 \times 4 \text{ bytes/fl} = 80 \text{ bytes}$

Acceptance:

Corresponds to the latest definition.

**6.11.4.24 Aerosol optical thicknesses at 865 nm for ADS photosynthetically active radiation (PAR)**

Reference: AOT865\_PAR, LUT307

[AD-8] Section 6.11.4, GADS field 24.

ACRI provided

Dependencies:

None

Tool:

None

Procedure:

Input: none  
Output: *AOT865\_PAR* Aerosol optical thickness at 865 nm used for PAR (20 values)  
units:  $[dl]$   
Step: User specified.

Scientific content:

Set of 20 AOT-865 values used for the PAR computation

Current baseline: {0.15, 0.30, 0.45, 0.60, 0.75, 0.90, 1.05, 1.20, 1.35, 1.50, 1.65, 1.80, 1.95, 2.10, 2.25, 2.40, 2.55, 2.70, 2.85, 3.00}

Resources:

Estimated CPU time: -  
Output disk space: 20 × 4 bytes/fl = 80 bytes

Acceptance:

Corresponds to the latest definition.

**6.11.4.25 Water vapour contents for photosynthetically active radiation (PAR)**

Reference: uH2O\_PAR, LUT094

[AD-8] Section 6.11.4, GADS field 25.

ACRI provided

Dependencies:

None

Tool:

None

Procedure:

Input: none  
Output: uH2O\_PAR Water vapour content for PAR (20 values)  
units: [g.cm<sup>-2</sup>]  
Step: User specified.

Scientific content:

Set of 20 water vapour contents used for the PAR computation

Current baseline: {0.0, 0.3, 0.6, 0.9, 1.2, 1.5, 1.8, 2.1, 2.4, 2.7, 3.0, 3.3, 3.6, 3.9, 4.2, 4.5, 4.8, 5.1, 5.4, 5.7} g.cm<sup>-2</sup>

Resources:

Estimated CPU time: -  
Output disk space: 20 × 4 bytes/fl = 80 bytes

Acceptance:

Corresponds to the latest definition.

6.11.4.26 Reference wavelengths for GADS apparent pressure parameters

Reference: Wvl\_FiltPs, LUT471

[AD-8] Section 6.11.4, GADS field 26.

FUB/ACRI provided

Dependencies:

None

Tool:

None

Procedure:

Input: none

Output: Wvl\_FiltPs Nominal wavelengths for the 21 MERIS O2 filters around 761.7nm (21 values)

units: [nm]

Step: User specified.

Scientific content:

Set of 21 MERIS O2 filters (around 761.7nm) used for computation of apparent pressure parameters

Current baseline: {760.7, 760.8, 760.9, 761.0, 761.1, 761.2, 761.3, 761.4, 761.5, 761.6, 761.7, 761.8, 761.9, 762.0, 762.1, 762.2, 762.3, 762.4, 762.5, 762.6, 762.7} nm

Resources:

Estimated CPU time: -  
Output disk space: 21 × 4 bytes/fl = 84 bytes

Acceptance:

Corresponds to the latest definition.

**6.11.4.27 Reference wavelengths for GADS polynomial coefficients for H2O transmittance retrieval at 708.75 nm**

Reference: Wvl\_FiltH2O, LUT096

[AD-8] Section 6.11.4, GADS field 27.

ACRI provided

Dependencies:

None

Tool:

None

Procedure:

Input: none

Output: *Wvl\_FiltH2O* Nominal wavelengths for the 21 MERIS O2 filters around 708.75 nm (21 values)

units: [nm]

Step: User specified.

Scientific content:

Set of 21 MERIS H2O filters (around 708.75 nm) used for computation of polynomials of H2O retrieval at 708.75 nm.

Current baseline: {707.75, 707.85, 707.95, 708.05, 708.15, 708.25, 708.35, 708.45, 708.55, 708.65, 708.75, 708.85, 708.95, 709.05, 709.15, 709.25, 709.35, 709.45, 709.55, 709.65, 709.75} nm

Dependencies:

None

Resources:

Estimated CPU time: -

Output disk space:  $21 \times 4 \text{ bytes/fl} = 84 \text{ bytes}$

Acceptance:

Corresponds to the latest definition.

6.11.4.28 *Pressure scale height to account for altitude*

Reference:  $H_p$ , LUT414

[AD-8] Section 6.11.4, GADS field 28.

ACRI provided

Dependencies:

None

Tool:

None

Procedure:

Input: none

Output:  $H_p$  Pressure scale height  
units: [m]

Step: User specified.

Scientific content:

$H_p$  corresponds to the standard *Rayleigh* scale height useful to define the vertical distribution of the molecules in the atmosphere. A typical value is around 8 km.

Current baseline: 8430 m

Resources:

Estimated CPU time: -

Output disk space:  $1 \times 4 \text{ bytes/fl} = 4 \text{ bytes}$

Acceptance:

Corresponds to the latest definition.

6.11.4.29 Zenith angles for GADS apparent pressure parameters

Reference: ZA\_Ps, LUT472

[AD-8] Section 6.11.4, GADS field 29.

FUB/ACRI provided

Dependencies:

None

Tool:

None

Procedure:

Input: none

Output: ZA\_Ps Zenith angle (24 values)

units: [10<sup>-6</sup> deg]

Step: User specified.

Scientific content:

Set of 24 zenith angles ( $\theta_{Ps}$ ) selected from the *Gauss* quadrature generated for 24 discrete directions with the RTC/Gauss tool (UdL)

Current baseline: 24 *Gaussian* angles

{2.840906, 6.521063, 10.222955, 13.929756, 17.638419, 21.347983, 25.058051, 28.768427, 32.479006, 36.189726, 39.900547, 43.611442, 47.322394, 51.033390, 54.744420, 58.455477, 62.166556, 65.877652, 69.588762, 73.299882, 77.011011, 80.722147, 84.433286, 88.144429} deg.

Current baseline: 24 *Gaussian* angles

| $i$ | $\theta_{Ps}$ [deg.] |
|-----|----------------------|
| 1   | 2.840906             |
| 2   | 17.638419            |
| 3   | 28.768427            |
| 4   | 36.189726            |
| 5   | 43.611442            |
| 6   | 51.033390            |

| $i$ | $\theta_{Ps}$ [deg.] |
|-----|----------------------|
| 7   | 58.455477            |
| 8   | 65.877652            |
| 9   | 69.588762            |
| 10  | 73.299882            |
| 11  | 77.011011            |
| 12  | 80.722147            |

| $i$ | $\theta_{Ps}$ [deg.] |
|-----|----------------------|
| 13  | 58.455477            |
| 14  | 65.877652            |
| 15  | 69.588762            |
| 16  | 73.299882            |
| 17  | 77.011011            |
| 18  | 80.722147            |

| $i$ | $\theta_{Ps}$ [deg.] |
|-----|----------------------|
| 18  | 58.455477            |
| 19  | 65.877652            |
| 20  | 69.588762            |
| 21  | 73.299882            |
| 22  | 77.011011            |
| 124 | 80.722147            |

Resources:

Estimated CPU time: -  
Output disk space: 24 × 4 bytes/ul = 96 bytes

Acceptance:

Corresponds to the latest definition.

6.11.4.30 Reference pressure levels for GADS apparent pressure parameters

Reference: Ps\_level, LUT473

[AD-8] Section 6.11.4, GADS field 30.

FUB/ACRI provided

Dependencies:

None

Tool:

None

Procedure:

Input: none  
Output: Ps\_level Pressure level (21 values)  
units: [hPa]  
Step: User specified.

Scientific content:

Ps\_level corresponds to a reference level of pressure within the atmosphere. A set of 21 reference pressure levels has been defined to compute the O2 transmittance in the atmospheric layers.

Current baseline: {3.963, 64.35, 124.10, 177.00, 228.30, 279.10, 329.70, 380.50, 430.50, 480.00, 529.60, 579.70, 629.80, 679.70, 729.40, 778.30, 827.60, 877.00, 926.40, 975.50, 1007.00} hPa

Resources:

Estimated CPU time: -  
Output disk space: 21 × 4 bytes/fl = 84 bytes

Acceptance:

Corresponds to the latest definition.

6.11.4.31 Aerosol scattering phase function

Reference: P[Theta], LUT474

[AD-8] Section 6.11.4, GADS field 31.

FUB/ACRI provided

Dependencies:

None

Tool:

None

Procedure:

Input: none

Output: P[Theta] Aerosol scattering phase function (181 values)

units: [dl]

Step: User specified.

Scientific content:

P[Theta] corresponds to a reference aerosol scattering phase function used to estimate the aerosol reflectance in the algorithm of the apparent surface pressure retrieval over ocean.

Current baseline: 181 values (see table below)

| $\Theta$ | $P(\Theta)$  | $\Theta$ | $P(\Theta)$ | $\Theta$ | $P(\Theta)$ | $\Theta$ | $P(\Theta)$ | $\Theta$ | $P(\Theta)$ |
|----------|--------------|----------|-------------|----------|-------------|----------|-------------|----------|-------------|
| 0.00     | 162.99707031 | 36.00    | 2.18402076  | 72.00    | 0.35232785  | 108.00   | 0.11797373  | 144.00   | 0.15353890  |
| 1.00     | 146.77873230 | 37.00    | 2.07215595  | 73.00    | 0.34090927  | 109.00   | 0.11851433  | 145.00   | 0.16376551  |
| 2.00     | 107.48479462 | 38.00    | 1.98779583  | 74.00    | 0.33279648  | 110.00   | 0.11922964  | 146.00   | 0.17394768  |
| 3.00     | 65.62915039  | 39.00    | 1.88332319  | 75.00    | 0.31797865  | 111.00   | 0.11565626  | 147.00   | 0.18173359  |
| 4.00     | 37.43303299  | 40.00    | 1.75853372  | 76.00    | 0.29913065  | 112.00   | 0.11080770  | 148.00   | 0.19141671  |
| 5.00     | 25.55327416  | 41.00    | 1.65484393  | 77.00    | 0.28656775  | 113.00   | 0.11004089  | 149.00   | 0.20750234  |
| 6.00     | 22.46920776  | 42.00    | 1.58498788  | 78.00    | 0.28102630  | 114.00   | 0.11214274  | 150.00   | 0.22815083  |
| 7.00     | 20.33006477  | 43.00    | 1.51557219  | 79.00    | 0.27285829  | 115.00   | 0.11143742  | 151.00   | 0.24914345  |
| 8.00     | 16.86425018  | 44.00    | 1.42409563  | 80.00    | 0.25816941  | 116.00   | 0.10724268  | 152.00   | 0.27072391  |



| $\Theta$ | $P(\Theta)$ | $\Theta$ | $P(\Theta)$ | $\Theta$ | $P(\Theta)$ | $\Theta$ | $P(\Theta)$ | $\Theta$ | $P(\Theta)$ |
|----------|-------------|----------|-------------|----------|-------------|----------|-------------|----------|-------------|
| 9.00     | 13.76597023 | 45.00    | 1.33284354  | 81.00    | 0.24484374  | 117.00   | 0.10491300  | 153.00   | 0.29469413  |
| 10.00    | 12.28894234 | 46.00    | 1.26866007  | 82.00    | 0.23910907  | 118.00   | 0.10687347  | 154.00   | 0.31666332  |
| 11.00    | 11.66075325 | 47.00    | 1.21956766  | 83.00    | 0.23540635  | 119.00   | 0.10863673  | 155.00   | 0.32848474  |
| 12.00    | 10.71770287 | 48.00    | 1.15709174  | 84.00    | 0.22592986  | 120.00   | 0.10633057  | 156.00   | 0.32964382  |
| 13.00    | 9.43953133  | 49.00    | 1.08264983  | 85.00    | 0.21342674  | 121.00   | 0.10311270  | 157.00   | 0.32967153  |
| 14.00    | 8.49027920  | 50.00    | 1.02221227  | 86.00    | 0.20622739  | 122.00   | 0.10385237  | 158.00   | 0.33588240  |
| 15.00    | 8.04110909  | 51.00    | 0.98243231  | 87.00    | 0.20435572  | 123.00   | 0.10703281  | 159.00   | 0.34421989  |
| 16.00    | 7.65051746  | 52.00    | 0.94140410  | 88.00    | 0.19978008  | 124.00   | 0.10733543  | 160.00   | 0.34724367  |
| 17.00    | 7.03037500  | 53.00    | 0.88575059  | 89.00    | 0.18984088  | 125.00   | 0.10450944  | 161.00   | 0.34656248  |
| 18.00    | 6.38895464  | 54.00    | 0.83101839  | 90.00    | 0.18137538  | 126.00   | 0.10374737  | 162.00   | 0.34989890  |
| 19.00    | 5.98838997  | 55.00    | 0.79422116  | 91.00    | 0.17912635  | 127.00   | 0.10701992  | 163.00   | 0.35779950  |
| 20.00    | 5.74152136  | 56.00    | 0.76624566  | 92.00    | 0.17798997  | 128.00   | 0.10983634  | 164.00   | 0.36203635  |
| 21.00    | 5.41101217  | 57.00    | 0.72823948  | 93.00    | 0.17169216  | 129.00   | 0.10876875  | 165.00   | 0.35879293  |
| 22.00    | 4.98262072  | 58.00    | 0.68236607  | 94.00    | 0.16311909  | 130.00   | 0.10715967  | 166.00   | 0.35511181  |
| 23.00    | 4.63211727  | 59.00    | 0.64657664  | 95.00    | 0.15929438  | 131.00   | 0.10953519  | 167.00   | 0.35756677  |
| 24.00    | 4.42061949  | 60.00    | 0.62444222  | 96.00    | 0.15970851  | 132.00   | 0.11408349  | 168.00   | 0.36152691  |
| 25.00    | 4.22177887  | 61.00    | 0.60025442  | 97.00    | 0.15733890  | 133.00   | 0.11572338  | 169.00   | 0.35930768  |
| 26.00    | 3.94303012  | 62.00    | 0.56547582  | 98.00    | 0.15029354  | 134.00   | 0.11460783  | 170.00   | 0.35453612  |
| 27.00    | 3.65591860  | 63.00    | 0.53184748  | 99.00    | 0.14465398  | 135.00   | 0.11588175  | 171.00   | 0.35852292  |
| 28.00    | 3.45675206  | 64.00    | 0.51096666  | 100.00   | 0.14413634  | 136.00   | 0.12112684  | 172.00   | 0.37301677  |
| 29.00    | 3.31405163  | 65.00    | 0.49544522  | 101.00   | 0.14396863  | 137.00   | 0.12577237  | 173.00   | 0.38728613  |
| 30.00    | 3.13546038  | 66.00    | 0.47191370  | 102.00   | 0.13895395  | 138.00   | 0.12677671  | 174.00   | 0.39612490  |
| 31.00    | 2.91700602  | 67.00    | 0.44287798  | 103.00   | 0.13207152  | 139.00   | 0.12775595  | 175.00   | 0.41098920  |
| 32.00    | 2.73442030  | 68.00    | 0.42159078  | 104.00   | 0.12942442  | 140.00   | 0.13301189  | 176.00   | 0.44470310  |
| 33.00    | 2.61357641  | 69.00    | 0.40985852  | 105.00   | 0.13017468  | 141.00   | 0.14043850  | 177.00   | 0.49079248  |
| 34.00    | 2.49636769  | 70.00    | 0.39567378  | 106.00   | 0.12814954  | 142.00   | 0.14515032  | 178.00   | 0.52844256  |
| 35.00    | 2.34108186  | 71.00    | 0.37335825  | 107.00   | 0.12218850  | 143.00   | 0.14777000  | 179.00   | 0.54623860  |
|          |             |          |             |          |             |          |             | 180.00   | 0.55010635  |

Resources:

Estimated CPU time: -  
Output disk space: 181 × 4 bytes/fl = 724 bytes

Acceptance:

Corresponds to the latest definition.

6.11.4.32 Fresnel reflection coefficients,  $FR(\theta)$

Reference: FR[ $\theta$ ], LUT475

[AD-8] Section 6.11.4, GADS field 32.

ACRI provided

Dependencies:

None

Tool:

None

Procedure:

Input: none

Output:  $FR[\theta]$  Fresnel reflection coefficients (91 values)

units: [dl]

Step: User specified.

Scientific content:

Fresnel reflection coefficients  $\mathcal{R}(\theta')$  are tabulated for 91 zenith angles in water ( $\theta'$ )

Current baseline: 91 values (see table below)

| $\theta'$ | $\mathcal{R}(\theta')$ | $\theta'$ | $\mathcal{R}(\theta')$ | $\theta'$ | $\mathcal{R}(\theta')$ | $\theta'$ | $\mathcal{R}(\theta')$ | $\theta'$ | $\mathcal{R}(\theta')$ |
|-----------|------------------------|-----------|------------------------|-----------|------------------------|-----------|------------------------|-----------|------------------------|
| 0.00      | 0.02111184             | 18.00     | 0.02123160             | 36.00     | 0.02363891             | 54.00     | 0.04210184             | 72.00     | 0.16209671             |
| 1.00      | 0.02111184             | 19.00     | 0.02126205             | 37.00     | 0.02399266             | 55.00     | 0.04449888             | 73.00     | 0.17775223             |
| 2.00      | 0.02111186             | 20.00     | 0.02129826             | 38.00     | 0.02438855             | 56.00     | 0.04715630             | 74.00     | 0.19517079             |
| 3.00      | 0.02111193             | 21.00     | 0.02134103             | 39.00     | 0.02483108             | 57.00     | 0.05010236             | 75.00     | 0.21455821             |
| 4.00      | 0.02111211             | 22.00     | 0.02139124             | 40.00     | 0.02532520             | 58.00     | 0.05336849             | 76.00     | 0.23614559             |
| 5.00      | 0.02111250             | 23.00     | 0.02144984             | 41.00     | 0.02587637             | 59.00     | 0.05698968             | 77.00     | 0.26019257             |
| 6.00      | 0.02111321             | 24.00     | 0.02151788             | 42.00     | 0.02649064             | 60.00     | 0.06100485             | 78.00     | 0.28699115             |
| 7.00      | 0.02111438             | 25.00     | 0.02159653             | 43.00     | 0.02717467             | 61.00     | 0.06545739             | 79.00     | 0.31687006             |
| 8.00      | 0.02111619             | 26.00     | 0.02168708             | 44.00     | 0.02793583             | 62.00     | 0.07039560             | 80.00     | 0.35019988             |
| 9.00      | 0.02111884             | 27.00     | 0.02179092             | 45.00     | 0.02878228             | 63.00     | 0.07587335             | 81.00     | 0.38739878             |
| 10.00     | 0.02112257             | 28.00     | 0.02190961             | 46.00     | 0.02972304             | 64.00     | 0.08195070             | 82.00     | 0.42893934             |
| 11.00     | 0.02112764             | 29.00     | 0.02204485             | 47.00     | 0.03076811             | 65.00     | 0.08869468             | 83.00     | 0.47535643             |
| 12.00     | 0.02113435             | 30.00     | 0.02219852             | 48.00     | 0.03192854             | 66.00     | 0.09618008             | 84.00     | 0.52725661             |
| 13.00     | 0.02114306             | 31.00     | 0.02237268             | 49.00     | 0.03321659             | 67.00     | 0.10449042             | 85.00     | 0.58532888             |
| 14.00     | 0.02115415             | 32.00     | 0.02256960             | 50.00     | 0.03464583             | 68.00     | 0.11371904             | 86.00     | 0.65035748             |
| 15.00     | 0.02116804             | 33.00     | 0.02279179             | 51.00     | 0.03623134             | 69.00     | 0.12397022             | 87.00     | 0.72323740             |
| 16.00     | 0.02118522             | 34.00     | 0.02304200             | 52.00     | 0.03798980             | 70.00     | 0.13536061             | 88.00     | 0.80499220             |
| 17.00     | 0.02120621             | 35.00     | 0.02332325             | 53.00     | 0.03993977             | 71.00     | 0.14802073             | 89.00     | 0.89679611             |
|           |                        |           |                        |           |                        |           |                        | 90.00     | 1.00000000             |

Resources:

Estimated CPU time: -  
Output disk space: 91 × 4 bytes/fl = 364 bytes

Acceptance:

Corresponds to the latest definition.

### 6.11.5 GADS Optical Thicknesses

#### 6.11.5.1 (Spare)

Reference:

[AD-8] Section 6.11.5, GADS field 1.

#### 6.11.5.2 (Spare)

Reference:

[AD-8] Section 6.11.5, GADS field 2.

#### 6.11.5.3 (Spare)

Reference:

[AD-8] Section 6.11.5, GADS field 3.

#### 6.11.5.4 Rayleigh optical thicknesses for standard pressure, $t^R(\lambda, P_s)$

Reference: tauR, LUT097

[AD-8] Section 6.11.5, GADS field 4.

Dependencies:

LUT076, LUT092

Tool:

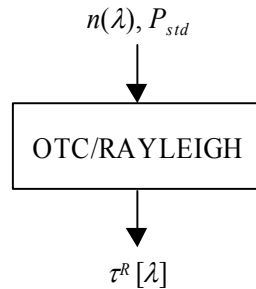
OTC/RAYLEIGH

Procedure:

Inputs:  $\lambda$  Wavelength [nm], see Section 6.11.4.3, (LUT076)  
 $P_{std}$  Surface pressure [hPa], see Section 6.11.4.19, (LUT092)

Output:  $\tau^R[\lambda]$  *Rayleigh* optical thickness for each band  $\lambda$   
units: [dl]

Step: Compute the *Rayleigh* optical thickness  $\tau^R[\lambda]$  using the OTC/RAYLEIGH.



Scientific content:

The *Rayleigh* optical thicknesses  $\tau^R[\lambda]$  are computed with formula from *Hansen and Travis* [RD-6] using a standard surface pressure (1013.25 hPa). The latter are essential in the atmospheric correction algorithm for removing the *Rayleigh* scattering effects from TOA reflectances.

Resources:

Estimated CPU time: 1 sec  
Output disk space: 15 × 4 bytes/fl = 60 bytes

Acceptance:

Comparison with other OTC.

6.11.5.5 Ozone optical thicknesses for 1 cm-atm,  $\tau^{O_3}(\lambda)$

Reference: tauO3\_norm, LUT098

[AD-8] Section 6.11.5, GADS field 5.

Dependencies:

LUT076

Tool:

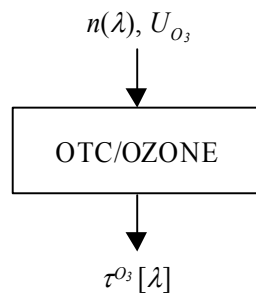
OTC/OZONE

Procedure:

Inputs:  $\lambda$  Wavelength [*nm*], see Section 6.11.4.3, (LUT076)  
 $U_{O_3}$  Total ozone amount [*cm-atm*], value fixed to 1 *cm-atm*

Output:  $\tau^{O_3}[\lambda]$  Ozone optical thickness for each band  $\lambda$   
units: [*dl*]

Step: Compute the ozone optical thickness  $\tau^{O_3}[\lambda]$  using OTC/OZONE.



Scientific content:

The ozone optical thicknesses  $\tau^{O_3}[\lambda]$  are computed with a LBL code using a total ozone amount of 1 *cm-atm*. The latter are essential in the atmospheric correction algorithm for computing the total O<sub>3</sub> transmittivity.

Resources:

Estimated CPU time: 1 *sec*  
Output disk space: 15 × 4 bytes/fl = 60 bytes

Acceptance:

Comparison with  $\tau^{O_3}[\lambda]$  derived from a LBL code.

**6.11.6 GADS H2O Transmission**

6.11.6.1 (*Spare*)

Reference:

[AD-8] Section 6.11.6, GADS field 1.

6.11.6.2 Polynomial coefficients for H2O transmittance retrieval around 708.75 nm (21 shifted filters)

**NOTE:** The recipe of this LUT is presently not included in the MERISAT tool. This LUT is currently generated with an input user specified file.

Reference: H2OCorr\_Poly\_LUT[ $\lambda'$ ,  $k$ ], LUT106

[AD-8] Section 6.11.6, GADS field 2

Dependencies:

LUT096

Tools:

RTC/UPRAD (GAME)  
RTC/GAUSS  
Polynomial fit

Procedure:

Inputs:  $\lambda'$  21 reference wavelengths [nm] corresponding to the 21 spectral shifts ( $\Delta\lambda$ ) of  $\pm 0.1$  nm applied on the MERIS H<sub>2</sub>O filter centred at 708.75 nm, see Section 6.11.4.26, (LUT096)  
 $k$  Polynomial coefficient orders [dl],  $k = [0;3]$

Output: H2OCorr\_Poly\_LUT[ $\lambda'$ ,  $k$ ]  
H<sub>2</sub>O transmittance polynomial coefficients

units: [dl]

**Warning:** The process for generating this table is time-consuming. To avoid loosing data in case of a power failure, several temporary binary files are created after few hours of processing:  $X_{xx}.LUT100$  and  $TH2O_{xx}.LUT100$  ( $xx$  stands for the 21 reference wavelengths). This allows one to resume the processing after a power failure. If we want fully restart the generation procedure, then the temporary binary files should be first deleted before relaunching the process.

Step-1: Compute Gaussian angles ( $n=6$ ) for a total of 21 [ $n.(n+1)/2$ ] indices of ( $\theta_s \times \theta_v$ ) combinations with the RTC/GAUSS. Due to the large time of processing, use only a subset of 21 indices of ( $\theta_s \times \theta_v$ ) combinations to generate this table.

Step-2: Generate TOA normalized radiances  $L_{TOA\_14}[\theta_s \times \theta_v, U_{H_2O}, \rho_s, \tau^{a1}]$  and  $L_{TOA\_15}[\theta_s \times \theta_v, U_{H_2O}, \rho_s, \tau^{a1}]$  for a non-absorbing/absorbing H<sub>2</sub>O atmosphere over a black/reflective surface with the RTC/UPRAD (GAME).

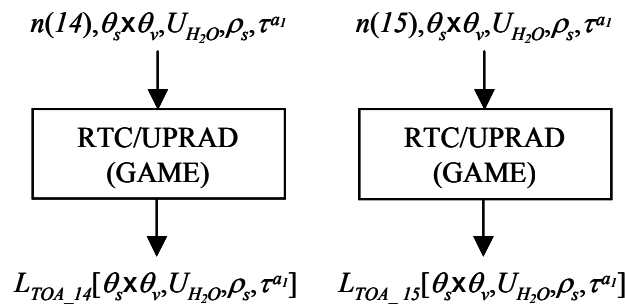
**RTC/UPRAD (GAME) Inputs (LAND)**

| Variable | Value | Comments |
|----------|-------|----------|
|----------|-------|----------|

| Variable  | Value   | Comments   |
|---|---|--|
| <i>out_file</i>                                     | "/OUTPUT/uprad_out"                             |  |
| <i>i_branch</i>                                     | 1   |  |
| <i>n(λ)</i>   | 14 and 15                                       | 885 nm & 900 nm  |
| <i>U<sub>H2O</sub></i>                              | 1<br>1.5, 3.0, 4.5, 6.0, 7.5, 9.0, 12.0         | For GAME computations without H <sub>2</sub> O<br>For GAME computations with H <sub>2</sub> O                              |
| <i>U<sub>O2</sub></i>                               | 0   |  |
| <i>ESFT</i>   | "/INPUT/RKLM_NO",<br>"/INPUT/RKLM_AL"           | For case $u_{H2O}=1$ (without H <sub>2</sub> O absorption)<br>For case $u_{H2O} \neq 1$ (with H <sub>2</sub> O absorption) |
| <i>P<sub>s</sub></i>                                | 1013.25   |  |
| <i>τ<sup>R</sup>(λ)</i>                             | 0   |  |
| <i>aerosol1</i>                                     | "/INPUT/sc_conti_b14",<br>"/INPUT/sc_conti_b15" | Continental aerosols   |
| <i>τ<sup>a1</sup>(550)</i>                          | 0.1, 0.3 and 0.6                                |  |
| <i>aerosol2</i>                                     | -   |  |
| <i>τ<sup>a2</sup>(550)</i>                          | 0   |  |
| <i>aerosol3</i>                                     | -   |  |
| <i>τ<sup>a3</sup>(550)</i>                          | 0   |  |
| <i>cloud1</i>                                       | -   | N/A  |
| <i>cloud2</i>                                       | -   | N/A  |
| <i>cloud3</i>                                       | -   | N/A  |
| <i>phyto</i>  | -   | N/A  |
| <i>σ<sub>e,λ</sub><sup>p</sup></i>                  | -   | N/A  |
| <i>ω<sub>o,λ</sub><sup>p</sup></i>                  | -   | N/A  |
| <i>spm</i>  | -   | N/A  |
| <i>σ<sub>e,λ</sub><sup>spm</sup></i>                | -   | N/A  |
| <i>ω<sub>o,λ</sub><sup>spm</sup></i>                | -   | N/A  |
| <i>σ<sub>e,λ</sub><sup>ys</sup></i>                 | -   | N/A  |
| <i>vertical</i>                                     | "/INPUT/vertical_out"                           | Vertical distribution of the aerosols as a decreasing exponential ( $H_a=2 km$ )   |
| <i>I<sub>s</sub></i>                                | 60  |  |
| <i>ρ<sub>s</sub></i>                                | 0, 0.2, 0.4 and 0.6                             | Only the first value is considered for reducing the computation time   |
| <i>E<sub>o</sub></i>                                | 1   |  |
| <i>σ<sub>e,λ</sub><sup>w</sup></i>                  | -   | N/A  |
| <i>ω<sub>o,λ</sub><sup>w</sup></i>                  | -   | N/A  |
| <i>w<sub>s</sub></i>                                | 0   |  |
| <i>n<sub>s</sub>, n<sub>v</sub>, n<sub>Δφ</sub></i> | 6, 6, 1   | Loop for 21 $\theta_s \times \theta_v$ combinations  |
| <i>θ<sub>s</sub></i>                                | Gaussian angles                                 | Computed with RTC/GAUSS  |
| <i>θ<sub>v</sub></i>                                | Gaussian angles                                 | Computed with RTC/GAUSS  |

| Variable     | Value | Comments |
|--------------|-------|----------|
| $\Delta\phi$ | 0     |          |
| pol          | 0     |          |

Note: In order to reduce the computation times, the upwelling TOA radiances will be simulated over a black surface only (which allows to include the oceanic surface cases) and with a subset of 21 indices of  $(\theta_s, x, \theta_v)$  combinations.



Step-3: Compute the ratio  $x[\theta_s, x, \theta_v, U_{H_2O}, \rho_s, \tau^{a1}]$  as follows,

$$x[\theta_s, x, \theta_v, U_{H_2O}, \rho_s, \tau^{a1}] = L_{TOA\_15}[\theta_s, x, \theta_v, U_{H_2O}, \rho_s, \tau^{a1}] / L_{TOA\_14}[\theta_s, x, \theta_v, U_{H_2O}, \rho_s, \tau^{a1}]$$

Step-4: Select a shifted MERIS H<sub>2</sub>O filter ( $\lambda'$ ) and generate TOA normalized radiances  $L_{TOA\_g\_H2O}[\lambda', \theta_s, x, \theta_v, U_{H_2O}, \rho_s, \tau^{a1}]$  for an absorbing H<sub>2</sub>O atmosphere and  $L_{TOA\_g\_noH2O}[\lambda', \theta_s, x, \theta_v, \rho_s, \tau^{a1}]$  for a non-absorbing H<sub>2</sub>O atmosphere, over a black/reflective surface with the RTC/UPRAD (GAME).

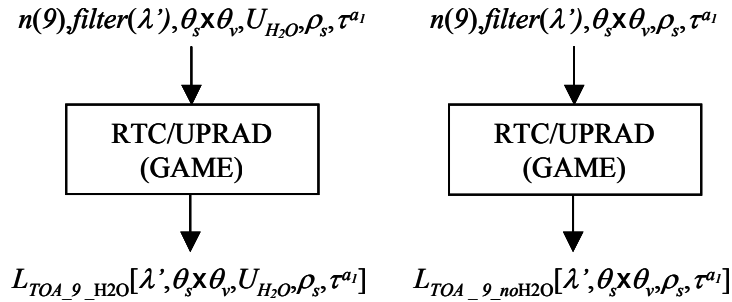
**RTC/UPRAD (GAME) Inputs (LAND)**

| Variable          | Value                                     | Comments   |
|-------------------|---|--|
| out_file          | "/OUTPUT/uprad_out"                       |  |
| i_branch          | 1   |  |
| n( $\lambda$ )    | 9   | 708.75 nm  |
| $U_{H_2O}$        | 1<br>1.5, 3.0, 4.5, 6.0, 7.5, 9.0, 12.0   | For GAME computations without H <sub>2</sub> O<br>For GAME computations with H <sub>2</sub> O  |
| $U_{O_2}$         | 0   |  |
| ESFT              | "/INPUT/RKLM_NO",<br>"/INPUT/RKLM_H2O_xx" | For case $u_{H_2O}=1$ (without H <sub>2</sub> O absorption)<br>For case $u_{H_2O} \neq 1$ (with H <sub>2</sub> O absorption), xx varies from 0 to (NbFiltH2O-1), see Section 6.11.4.26 |
| $P_s$             | 1013.25                                   |  |
| $\tau^R(\lambda)$ | 0   |  |
| aerosol1          | "/INPUT/sc_conti_b09"                     |  |
| $\tau^{a1}(550)$  | 0.1, 0.3 and 0.6                          |  |
| aerosol2          | -   |  |



| <i>Variable</i>            | <i>Value</i>           | <i>Comments</i>   |
|----------------------------|------------------------|---|
| $t^{a2}(550)$              | 0                      |   |
| <i>aerosol3</i>            | -                      |   |
| $t^{a3}(550)$              | 0                      |   |
| <i>cloud1</i>              | -                      | N/A   |
| <i>cloud2</i>              | -                      | N/A   |
| <i>cloud3</i>              | -                      | N/A   |
| <i>phyto</i>               | -                      | N/A   |
| $\sigma_{e,\lambda}^p$     | -                      | N/A   |
| $\omega_{o,\lambda}^p$     | -                      | N/A   |
| <i>spm</i>                 | -                      | N/A   |
| $\sigma_{e,\lambda}^{spm}$ | -                      | N/A   |
| $\omega_{o,\lambda}^{spm}$ | -                      | N/A   |
| $\sigma_{e,\lambda}^{ys}$  | -                      | N/A   |
| <i>vertical</i>            | "/INPUT/vertical_out"  | Vertical distribution of the aerosols as a decreasing exponential ( $H_a=2$ km) |
| $I_s$                      | 60                     |   |
| $\rho_s$                   | 0, 0.2, 0.4 and 0.6    | Only the first value is considered for reducing the computation time            |
| $E_o$                      | 1                      |   |
| $\sigma_{e,\lambda}^w$     | -                      | N/A   |
| $\omega_{o,\lambda}^w$     | -                      | N/A   |
| $w_s$                      | 0                      |   |
| $n_s, n_v, n_{\Delta\phi}$ | 6, 6, 1                | Loop for 21 $\theta_s \times \theta_v$ combinations                             |
| $\theta_s$                 | <i>Gaussian angles</i> | Computed with RTC/GAUSS   |
| $\theta_v$                 | <i>Gaussian angles</i> | Computed with RTC/GAUSS   |
| $\Delta\phi$               | 0                      |   |
| <i>pol</i>                 | 0                      |   |

Note: In order to reduce the computation times, the upwelling TOA radiances will be simulated over a black surface only (which allows to include the oceanic surface cases) and with a subset of 21 indices of ( $\theta_s \times \theta_v$ ) combinations. Moreover, each of the 'RKLM\_H2O\_xx' files ( $xx=[0..20]$ ) contains the ESFT coefficients for computing H2O and O2 transmittances, both for all the 15 MERIS bands. Only the H2O ESFT coefficients for the MERIS band#9 differ between these 21 files.



Step-5: Compute the H<sub>2</sub>O transmittance in the selected shifted MERIS H<sub>2</sub>O filter  $\lambda'$  as follows,

$$T_{H2O\_9}[\lambda', \theta_s \times \theta_v, U_{H2O}, \rho_s, \tau^{a1}] = L_{TOA\_9\_H2O}[\lambda', \theta_s \times \theta_v, U_{H2O}, \rho_s, \tau^{a1}] / L_{TOA\_9\_noH2O}[\lambda', \theta_s \times \theta_v, \rho_s, \tau^{a1}]$$

Step-6: Repeat steps 4 and 5 for each shifted MERIS H<sub>2</sub>O filter  $\lambda'$ .

Step-7: For each shifted MERIS H<sub>2</sub>O filter  $\lambda'$ , apply a polynomial fit on the ratio  $x[\theta_s \times \theta_v, U_{H2O}, \rho_s, \tau^{a1}]$  as function of the H<sub>2</sub>O transmittance in the selected shifted MERIS H<sub>2</sub>O filter  $\lambda'$ ,  $T_{H2O\_9}[\lambda', \theta_s \times \theta_v, U_{H2O}, \rho_s, \tau^{a1}]$ , for retrieving polynomial coefficients  $a_h[\lambda']$ ,  $b_h[\lambda']$ ,  $c_h[\lambda']$  and  $d_h[\lambda']$ ,

$$\begin{aligned} T_{H2O\_9}[\lambda', \theta_s \times \theta_v, U_{H2O}, \rho_s, \tau^{a1}] = & a_h[\lambda'] \\ & + b_h[\lambda'] \cdot x[\theta_s \times \theta_v, U_{H2O}, \rho_s, \tau^{a1}] \\ & + c_h[\lambda'] \cdot x[\theta_s \times \theta_v, U_{H2O}, \rho_s, \tau^{a1}]^2 \\ & + d_h[\lambda'] \cdot x[\theta_s \times \theta_v, U_{H2O}, \rho_s, \tau^{a1}]^3 \end{aligned}$$

### Scientific content:

These sets of polynomial coefficients are useful to compute the residual H<sub>2</sub>O absorption within the 21 shifted MERIS band #9 (708.75 nm) (*i.e.*, by taking the smile effect into account) whatever the illumination ( $\theta_s$ ) and viewing ( $\theta_v$ ) configuration, whatever the absorber amount, whatever the surface reflectance ( $\rho_s$ ), and whatever the aerosol optical thickness ( $\tau^{a1}$ ), by using the H<sub>2</sub>O transmittance in the MERIS band #15 (900 nm).

Note that up today the recipe for generating this LUT is not yet included in the MERISAT tool v1.4. This LUT should have to be completed for a MLS profile with several water vapor amounts ( $U_{H2O}$ ), using a continental aerosol model with several aerosol optical thicknesses ( $\tau^{a1}$ ), and over a black surface ( $\rho_s=0$ ) for reducing the computation times.

### Resources:

Estimated CPU time: 55674 sec  
Output disk space: 21 × 4 × 4 bytes/fl = 336 bytes

### Acceptance:

These polynomial coefficients can be tested by applying them to the ratio  $x[\theta_s \times \theta_v, U_{H_2O}, \rho_s, \tau^{at}]$  computed with another RTC, and by comparing the H<sub>2</sub>O transmittances (within the 21 shifted MERIS band #9) derived from these polynomial fits with those generated using the same other RTC.

### 6.11.6.3 Polynomial coefficients for H<sub>2</sub>O transmittance retrieval at the 15 MERIS wavelengths

Reference:  $a_h(b), b_h(b), c_h(b), d_h(b),$  LUT100

[AD-8] Section 6.11.6, GADS field 3.

Dependencies:

LUT076

Tools:

RTC/UPRAD (GAME)  
RTC/GAUSS

Procedure:

Inputs:  $\lambda$  15 MERIS wavelengths [nm], see Section 6.11.4.3, (LUT076)  
 $k$  Polynomial coefficient orders [dl],  $k = [0;3]$

Output:  $a_h[\lambda], b_h[\lambda], c_h[\lambda], d_h[\lambda]$   
H<sub>2</sub>O transmittance polynomial coefficients for 10 MERIS wavelengths  $\lambda$  [nm], {510, 560, 620, 665, 681.25, 708.75, 753.75, 778.75, 865, 885}.

units: [dl]

**Warning:** The process for generating this table is time-consuming. To avoid loosing data in case of a power failure, several temporary binary files are created after few hours of processing: *X.LUT100* and *TH2O.LUT100*. This allows one to resume the processing after a power failure. If we want fully restart the generation procedure, then the temporary binary files should be first deleted before relaunching the process.

Step-1: Compute *Gaussian* angles ( $n=12$ ) for a total of 78  $[n.(n+1)/2]$  indices of  $(\theta_s \times \theta_v)$  combinations with the RTC/GAUSS. Due to the large time of processing, use only a subset of 21 indices of  $(\theta_s \times \theta_v)$  combinations to generate this table.

Step-2: Generate TOA normalized radiances  $L_{TOA\_14}[\theta_s \times \theta_v, U_{H_2O}, \rho_s, \tau^{at}]$  and  $L_{TOA\_15}[\theta_s \times \theta_v, U_{H_2O}, \rho_s, \tau^{at}]$  for a non-absorbing/absorbing H<sub>2</sub>O atmosphere over a black/reflective surface with the RTC/UPRAD (GAME).

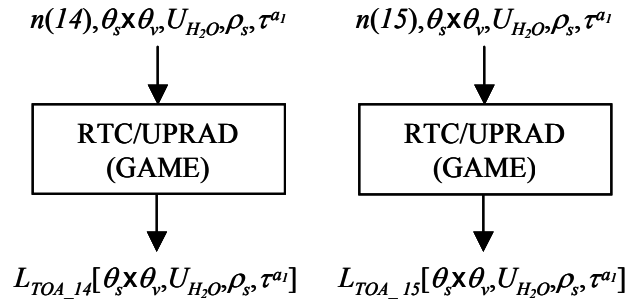
**RTC/UPRAD (GAME) Inputs (LAND)**

| Variable | Value | Comments |
|----------|-------|----------|
|----------|-------|----------|

| Variable  | Value   | Comments   |
|---|---|--|
| <i>out_file</i>                                     | "/OUTPUT/uprad_out"                             |  |
| <i>i_branch</i>                                     | 1   |  |
| <i>n(λ)</i>   | 14 and 15                                       | 885 nm & 900 nm  |
| <i>U<sub>H2O</sub></i>                              | 1<br>1.5, 3.0, 4.5, 6.0, 7.5, 9.0, 12.0         | For GAME computations without H <sub>2</sub> O<br>For GAME computations with H <sub>2</sub> O                              |
| <i>U<sub>O2</sub></i>                               | 0   |  |
| <i>ESFT</i>   | "/INPUT/RKLM_NO",<br>"/INPUT/RKLM_AL"           | For case $u_{H2O}=1$ (without H <sub>2</sub> O absorption)<br>For case $u_{H2O} \neq 1$ (with H <sub>2</sub> O absorption) |
| <i>P<sub>s</sub></i>                                | 1013.25   |  |
| <i>τ<sup>R</sup>(λ)</i>                             | 0   |  |
| <i>aerosol1</i>                                     | "/INPUT/sc_conti_b14",<br>"/INPUT/sc_conti_b15" | Continental aerosols   |
| <i>τ<sup>a1</sup>(550)</i>                          | 0.1, 0.3 and 0.6                                |  |
| <i>aerosol2</i>                                     | -   |  |
| <i>τ<sup>a2</sup>(550)</i>                          | 0   |  |
| <i>aerosol3</i>                                     | -   |  |
| <i>τ<sup>a3</sup>(550)</i>                          | 0   |  |
| <i>cloud1</i>                                       | -   | N/A  |
| <i>cloud2</i>                                       | -   | N/A  |
| <i>cloud3</i>                                       | -   | N/A  |
| <i>phyto</i>  | -   | N/A  |
| <i>σ<sub>e,λ</sub><sup>p</sup></i>                  | -   | N/A  |
| <i>ω<sub>o,λ</sub><sup>p</sup></i>                  | -   | N/A  |
| <i>spm</i>  | -   | N/A  |
| <i>σ<sub>e,λ</sub><sup>spm</sup></i>                | -   | N/A  |
| <i>ω<sub>o,λ</sub><sup>spm</sup></i>                | -   | N/A  |
| <i>σ<sub>e,λ</sub><sup>ys</sup></i>                 | -   | N/A  |
| <i>vertical</i>                                     | "/INPUT/vertical_out"                           | Vertical distribution of the aerosols as a decreasing exponential ( $H_a=2$ km)  |
| <i>I<sub>s</sub></i>                                | 60  |  |
| <i>ρ<sub>s</sub></i>                                | 0, 0.2, 0.4 and 0.6                             | Only the first value is considered for reducing the computation time   |
| <i>E<sub>o</sub></i>                                | 1   |  |
| <i>σ<sub>e,λ</sub><sup>w</sup></i>                  | -   | N/A  |
| <i>ω<sub>o,λ</sub><sup>w</sup></i>                  | -   | N/A  |
| <i>w<sub>s</sub></i>                                | 0   |  |
| <i>n<sub>s</sub>, n<sub>v</sub>, n<sub>Δφ</sub></i> | 12, 12, 1                                       | Use a loop for 78 $\theta_s \times \theta_v$ combinations only for minimizing the computation time.                        |
| <i>θ<sub>s</sub></i>                                | Gaussian angles                                 | Computed with RTC/GAUSS  |

| Variable     | Value           | Comments                |
|--------------|-----------------|-------------------------|
| $\theta_v$   | Gaussian angles | Computed with RTC/GAUSS |
| $\Delta\phi$ | 0               |                         |
| pol          | 0               |                         |

Note: In order to reduce the computation times, the upwelling TOA radiances will be simulated over a black surface only (which allows to include the oceanic surface cases) and with a subset of 21 indices of  $(\theta_s, \theta_v)$  combinations.



Step-3: Compute the ratio  $x[\theta_s \times \theta_v, U_{H_2O}, \rho_s, \tau^{a1}]$  as follows,

$$x[\theta_s \times \theta_v, U_{H_2O}, \rho_s, \tau^{a1}] = L_{TOA\_15}[\theta_s \times \theta_v, U_{H_2O}, \rho_s, \tau^{a1}] / L_{TOA\_14}[\theta_s \times \theta_v, U_{H_2O}, \rho_s, \tau^{a1}]$$

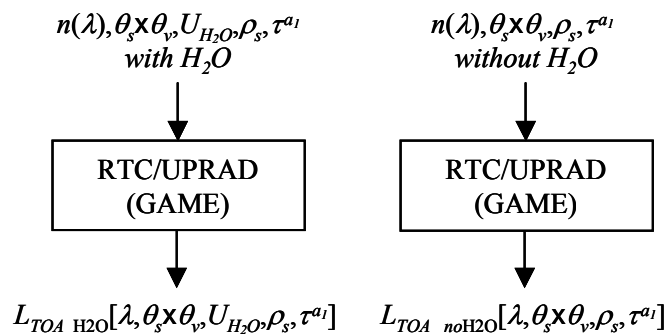
Step-4: Generate TOA normalized radiances with H<sub>2</sub>O absorption  $L_{TOA\_H2O}[\lambda, \theta_s \times \theta_v, U_{H_2O}, \rho_s, \tau^{a1}]$  and without H<sub>2</sub>O absorption  $L_{TOA\_noH2O}[\lambda, \theta_s \times \theta_v, U_{H_2O}, \rho_s, \tau^{a1}]$ , over a black surface with the RTC/UPRAD (GAME) for each of the 10 specified MERIS spectral bands  $n(\lambda)$ .

**RTC/UPRAD (GAME) Inputs (LAND)**

| Variable          | Value                                   | Comments   |
|-------------------|---|--|
| out_file          | "/INPUT/uprad_out"                      |  |
| i_branch          | 1                                       |  |
| $n(\lambda)$      | 4, 5, 6, 7, 8, 9, 10, 12, 13 and 14     | 510, 560, 620, 665, 681.25, 708.75, 753.75, 778.75, 865 & 885 nm   |
| $U_{H2O}$         | 1<br>1.5, 3.0, 4.5, 6.0, 7.5, 9.0, 12.0 | For GAME computations without H <sub>2</sub> O<br>For GAME computations with H <sub>2</sub> O                              |
| $U_{O2}$          | 0                                       |  |
| ESFT              | "/INPUT/RKLM_NO",<br>"/INPUT/RKLM_AL"   | For case $u_{H2O}=1$ (without H <sub>2</sub> O absorption)<br>For case $u_{H2O} \neq 1$ (with H <sub>2</sub> O absorption) |
| $P_s$             | 1013.25                                 |  |
| $\tau^R(\lambda)$ | 0                                       |  |
| aerosoll          | "/INPUT/sc_conti_bxx"                   | Continental aerosols, xx depends on $n(\lambda)$   |
| $\tau^{a1}(550)$  | 0.1, 0.3 and 0.6                        |  |
| aerosol2          | -                                       |  |
| $\tau^{a2}(550)$  | 0                                       |  |

| Variable                   | Value                 | Comments  |
|----------------------------|-----------------------|---|
| <i>aerosol3</i>            | -                     |   |
| $\tau^{a3}(550)$           | 0                     |   |
| <i>cloud1</i>              | -                     | N/A   |
| <i>cloud2</i>              | -                     | N/A   |
| <i>cloud3</i>              | -                     | N/A   |
| <i>phyto</i>               | -                     | N/A   |
| $\sigma_{e,\lambda}^p$     | -                     | N/A   |
| $\omega_{o,\lambda}^p$     | -                     | N/A   |
| <i>spm</i>                 | -                     | N/A   |
| $\sigma_{e,\lambda}^{spm}$ | -                     | N/A   |
| $\omega_{o,\lambda}^{spm}$ | -                     | N/A   |
| $\sigma_{e,\lambda}^{ys}$  | -                     | N/A   |
| <i>vertical</i>            | "/INPUT/vertical_out" | Vertical distribution of the aerosols as a decreasing exponential ( $H_a=2\text{ km}$ )             |
| $I_s$                      | 60                    |   |
| $\rho_s$                   | 0, 0.2, 0.4 and 0.6   | Only the first value is considered for reducing the computation time                                |
| $E_o$                      | 1                     |   |
| $\sigma_{e,\lambda}^w$     | -                     | N/A   |
| $\omega_{o,\lambda}^w$     | -                     | N/A   |
| $w_s$                      | 0                     |   |
| $n_s, n_v, n_{\Delta\phi}$ | 12, 12, 1             | Use a loop for 78 $\theta_s \times \theta_v$ combinations only for minimizing the computation time. |
| $\theta_s$                 | Gaussian angles       | Computed with RTC/GAUSS   |
| $\theta_v$                 | Gaussian angles       | Computed with RTC/GAUSS   |
| $\Delta\phi$               | 0                     |   |
| <i>pol</i>                 | 0                     |   |

Note: In order to reduce the computation times, the upwelling TOA radiances will be simulated over a black surface only (which allows to include the oceanic surface cases) and with a subset of 21 indices of ( $\theta_s, \theta_v$ ) combinations.



Step-5: Compute the H<sub>2</sub>O transmittance in the 10 MERIS bands as follows,

$$T_{H_2O}[\lambda, \theta_s \times \theta_v, U_{H_2O}, \rho_s, \tau^{a1}] = L_{TOA\_H_2O}[\lambda, \theta_s \times \theta_v, U_{H_2O}, \rho_s, \tau^{a1}] / L_{TOA\_noH_2O}[\lambda, \theta_s \times \theta_v, \rho_s, \tau^{a1}]$$

Step-6: Apply a polynomial fit on the ratio  $x[\theta_s \times \theta_v, U_{H_2O}, \rho_s, \tau^{a1}]$  as function of the H<sub>2</sub>O transmittance in each  $\lambda$  of 10 selected MERIS bands  $T_{H_2O}[\lambda, \theta_s \times \theta_v, U_{H_2O}, \rho_s, \tau^{a1}]$ , for retrieving polynomial coefficients  $a_h[\lambda]$ ,  $b_h[\lambda]$ ,  $c_h[\lambda]$  and  $d_h[\lambda]$ ,

$$\begin{aligned} T_{H_2O}[\lambda, \theta_s \times \theta_v, U_{H_2O}, \rho_s, \tau^{a1}] = & a_h[\lambda] \\ & + b_h[\lambda] \cdot x[\theta_s \times \theta_v, U_{H_2O}, \rho_s, \tau^{a1}] \\ & + c_h[\lambda] \cdot x[\theta_s \times \theta_v, U_{H_2O}, \rho_s, \tau^{a1}]^2 \\ & + d_h[\lambda] \cdot x[\theta_s \times \theta_v, U_{H_2O}, \rho_s, \tau^{a1}]^3 \end{aligned}$$

### Scientific content:

These sets of polynomial coefficients are useful to compute the residual H<sub>2</sub>O absorptions within the 10 selected MERIS band (510, 560, 620, 665, 681.25, 708.75, 753.75, 778.75, 865, and 885 nm) whatever the illumination ( $\theta_s$ ) and viewing ( $\theta_v$ ) configuration, whatever the absorber amount, whatever the surface reflectance ( $\rho_s$ ), and whatever the aerosol optical thickness ( $\tau^{a1}$ ), by using the corresponding H<sub>2</sub>O transmittance in the MERIS band #15 (900 nm). For the other MERIS bands (412.5, 442.5, 490, 761.875, 900 nm)  $a_h[\lambda]$  are set to 1 and  $b_h[\lambda]$ ,  $c_h[\lambda]$ ,  $d_h[\lambda]$  are set to 0.

Note that here, all the computations are completed for a MLS profile with several water vapor amounts ( $u_{H_2O}$ ), using a continental aerosol model with several aerosol optical thicknesses ( $\tau^{a1}$ ), and over a black surface ( $\rho_s=0$ ) for reducing the computation times.

### Resources:

Estimated CPU time: 39767 sec  
Output disk space: 15 × 4 × 4 bytes/fl = 240 bytes

### Acceptance:

These polynomial coefficients can be tested by applying them to the ratio  $x[\theta_s \times \theta_v, U_{H_2O}, \rho_s, \tau^{a1}]$  computed with another RTC, and by comparing the H<sub>2</sub>O transmittances (within each of these 10 selected MERIS bands) derived from these polynomial fits with those generated using the same other RTC.

## 6.11.7 GADS Rayleigh Scattering Function

### 6.11.7.1 Fourier series terms of polynomial coefficients for multiplicative Rayleigh scattering function retrieval

Reference: Rayscatt\_coef\_LUT, LUT101

[AD-8] Section 6.11.7, GADS field 1, 2 & 3.

Dependencies:

LUT075, LUT080, LUT081

Tools:

RTC/UPRAD (SO)  
Polynomial fit

Procedure:

Inputs:  $\tau^R$  Rayleigh optical thickness [dl], see Section 6.11.4.2, (LUT075)  
 $\theta$  Gaussian angle [deg], see Section 6.11.4.7, (LUT080)  
 $\theta_s \times \theta_v$  Stored indices for angular combinations [dl] (78 values), see Section 6.11.4.8, (LUT081)  
 $s$  Fourier series term [dl],  $s = [0;2]$   
 $k$  Polynomial coefficient order [dl],  $k = [0;3]$

Output: *Rayscatt\_coef\_LUT*[ $s, \theta_s \times \theta_v, k$ ]  
 Fourier series terms of multiplicative Rayleigh scattering function polynomial coefficients as function of the acceptable combinations (sun/view zenith angles)

units: [dl]

**Warning:** One temporary file is created during the procedure: *RayFactor.LUT101*. If we want fully restart the generation procedure, then the temporary binary file should be first deleted before relaunching the process.

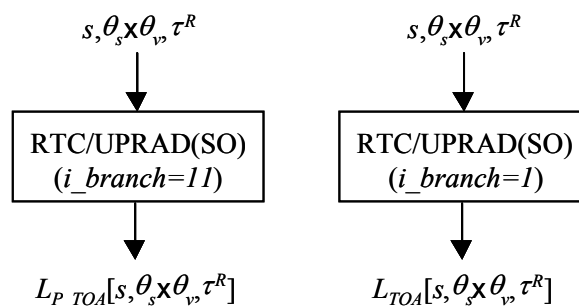
Step-1: Compute the normalized TOA radiances  $L_{TOA}[s, \theta_s \times \theta_v, \tau^R]$  and the primary scattering radiance  $L_{P\_TOA}[s, \theta_s \times \theta_v, \tau^R]$  for the first 3 Fourier series terms ( $s$  varying between 0 and  $I_s=2$ ) and the last Fourier series term ( $I_s=79$ ), computed with the RTC/UPRAD (SO) for a pure Rayleigh atmosphere over a black surface.

**RTC/UPRAD (SO) Inputs (LAND)**

| Variable          | Value               | Comments                                  |
|-------------------|---------------------|---|
| <i>out_file</i>   | "/OUTPUT/uprad_out" |   |
| <i>i_branch</i>   | 1 and 11            | 1 for $L_{TOA}$ , and 11 for $L_{P\_TOA}$ |
| $n(\lambda)$      | 1                   | 412.5 nm                                  |
| $U_{H2O}$         | 0                   |   |
| $U_{O2}$          | 0                   |   |
| <i>ESFT</i>       |                     | N/A                                       |
| $P_s$             | 1013.25             |   |
| $\tau^R(\lambda)$ | tauR                | see Section 6.11.4.2                      |
| <i>aerosoll</i>   | -                   |   |
| $\tau^{a1}(550)$  | 0                   |   |



| Variable                   | Value                 | Comments   |
|----------------------------|-----------------------|--|
| <i>aerosol2</i>            | -                     |  |
| $\tau^{a^2}(550)$          | 0                     |  |
| <i>aerosol3</i>            | -                     |  |
| $\tau^{a^3}(550)$          | 0                     |  |
| <i>cloud1</i>              | -                     | N/A  |
| <i>cloud2</i>              | -                     | N/A  |
| <i>cloud3</i>              | -                     | N/A  |
| <i>phyto</i>               | -                     | N/A  |
| $\sigma_{e,\lambda}^p$     | -                     | N/A  |
| $\omega_{o,\lambda}^p$     | -                     | N/A  |
| <i>spm</i>                 | -                     | N/A  |
| $\sigma_{e,\lambda}^{spm}$ | -                     | N/A  |
| $\omega_{o,\lambda}^{spm}$ | -                     | N/A  |
| $\sigma_{e,\lambda}^{ys}$  | -                     | N/A  |
| <i>vertical</i>            | "/INPUT/vertical_out" | Not used, vertical distribution determined in RTC/SO ( $H_R=8$ km)                                 |
| $I_s$                      | 0, 1, 2<br>79         | For <i>i_branch</i> = 11<br>For <i>i_branch</i> = 1  |
| $\rho_s$                   | 0                     |  |
| $E_o$                      | 1                     |  |
| $\sigma_{e,\lambda}^w$     | -                     | N/A  |
| $\omega_{o,\lambda}^w$     | -                     | N/A  |
| $w_s$                      | 0                     |  |
| $n_s, n_v, n_{\Delta\phi}$ | 12, 12, 1             | Use a loop for 78 $\theta_s \times \theta_v$ combinations only for minimizing the computation time |
| $\theta_s$                 | see inputs            | see <a href="#">Section 6.11.4.7</a> and <a href="#">Section 6.11.4.8</a>                          |
| $\theta_v$                 | see inputs            | see <a href="#">Section 6.11.4.7</a> and <a href="#">Section 6.11.4.8</a>                          |
| $\Delta\phi$               | 0                     |  |
| <i>pol</i>                 | 1                     |  |



Step-2: Compute the multiplicative *Rayleigh* scattering function  $f_R[s, \theta_s \times \theta_v, \tau^R]$ , as follows,

$$f_R[s, \theta_s \times \theta_v, \tau^R] = L_{TOA}[s, \theta_s \times \theta_v, \tau^R] / L_{P\_TOA}[s, \theta_s \times \theta_v, \tau^R]$$

Step-3: Apply a polynomial fit on the multiplicative *Rayleigh* scattering function  $f_R[s, \theta_s \times \theta_v, \tau^R]$  as function of the *Rayleigh* optical thickness ( $\tau^R$ ) for retrieving polynomial coefficients  $Rayscatt\_coef\_LUT[s, \theta_s \times \theta_v, k]$ ,

$$\begin{aligned} f_R[s, \theta_s \times \theta_v, \tau^R] = & Rayscatt\_coef\_LUT[s, \theta_s \times \theta_v, 0] \\ & + Rayscatt\_coef\_LUT[s, \theta_s \times \theta_v, 1] \cdot (\tau^R) \\ & + Rayscatt\_coef\_LUT[s, \theta_s \times \theta_v, 2] \cdot (\tau^R)^2 \\ & + Rayscatt\_coef\_LUT[s, \theta_s \times \theta_v, 3] \cdot (\tau^R)^3 \end{aligned}$$

### Scientific content:

These sets of polynomial coefficients are useful to compute the multiplicative *Rayleigh* scattering function whatever the illumination ( $\theta_s$ ) and viewing ( $\theta_v$ ) configuration, whatever the *Rayleigh* optical thickness ( $\tau^R$ ), and for each *Fourier* series ( $s$ ) term used in the *Fourier* series expansion of the TOA normalized radiance. This multiplicative *Rayleigh* scattering function is then used to correct the *Rayleigh* primary TOA radiance for the multiple scattering.

#### Note:

To reduce the size of the LUT related to the *Rayleigh* reflectance ( $\rho_R$ ) computations, the latter is expanded into a *Fourier* series to cancel the azimuthal dependence,

$$\rho_R(\vartheta_s, \vartheta_v, \Delta\phi) = \sum_{s=0}^2 (2 - \delta_{0,s}) \cdot \rho_R^{(s)}(\vartheta_s, \vartheta_v) \cdot \cos(s \cdot \Delta\phi)$$

with  $\delta_{0,s}$  the *Dirac's* function, and the scattering phenomenon for each *Fourier* series term  $s$  is treated as a primary scattering term  $\rho_{R,P}^{(s)}$  corrected by a multiplicative function  $f_R^{(s)}$  which accounts for the multiple scattering. Thus the *Rayleigh* reflectance  $\rho_R^{(s)}$  for each *Fourier* series term  $s$  is written as:

$$\rho_R^{(s)}(\vartheta_s, \vartheta_v, \tau^R) = \rho_{R,P}^{(s)}(\vartheta_s, \vartheta_v, \tau^R) \cdot f_R^{(s)}(\vartheta_s, \vartheta_v, \tau^R)$$

where  $\rho_{R,P}^{(s)}$ , the primary scattering reflectance for *Rayleigh*, is determined in the atmospheric correction algorithm over land. Note that the *Rayleigh* scattering functions ( $f_R^{(s)}$ ) are pre-computed as function of *Rayleigh* optical thickness ( $\tau^R$ ) instead of the MERIS wavelength ( $\lambda$ ) because of the barometric pressure variation with the terrain elevation.

The multiplicative *Rayleigh* scattering function ( $f_R^{(s)}$ ) for each of the first 3 *Fourier* series terms ( $s$ ) is then deduced by simulating  $\rho_R^{(s)}$  with the RTC/UPRAD(SO) and computing  $\rho_{R,P}^{(s)}$  as:

$$\rho_{R,P}^{(s)}(\vartheta_s, \vartheta_v, \tau^R) = P_R^{(s)}(\vartheta_s, \vartheta_v) \cdot \frac{(1 - e^{-M \cdot \tau^R})}{4 \cdot (\cos \vartheta_s + \cos \vartheta_v)}$$

with  $M$  the airmass and  $P_R^{(s)}$  the *Rayleigh* phase function for each *Fourier* series term  $s$  expressed as:

$$\left\{ \begin{array}{l} P_R^{(0)}(\vartheta_s, \vartheta_v) = \frac{3A}{4} \cdot \left( 1 + \cos^2 \vartheta_s \cdot \cos^2 \vartheta_v + \frac{\sin^2 \vartheta_s \cdot \sin^2 \vartheta_v}{2} \right) + B \\ P_R^{(1)}(\vartheta_s, \vartheta_v) = -\frac{3A}{8} \cdot \cos \vartheta_s \cdot \cos \vartheta_v \cdot \sin \vartheta_s \cdot \sin \vartheta_v \\ P_R^{(2)}(\vartheta_s, \vartheta_v) = \frac{3A}{16} \cdot \sin^2 \vartheta_s \cdot \sin^2 \vartheta_v \end{array} \right.$$

$A$  and  $B$  are the 2 coefficients which account for the molecular asymmetry,  $A = 0.9587256$ ,  $B = 1 - A$  (see [Section 6.11.4.9](#) and [\[RD-5\]](#)).

A third order polynomial fit ( $k = [0;3]$ ) as function of  $\tau^R$  has then been applied on the set of multiplicative *Rayleigh* scattering functions ( $f_R^{(s)}$ ) determined for each of the first 3 *Fourier* series terms ( $s = [0;2]$ ):

$$f_R^{(s)}(\vartheta_s, \vartheta_v, \tau^R) = \sum_{k=0}^3 C_k^{(s)}(\vartheta_s, \vartheta_v) \cdot (\tau^R)^k$$

with  $C_k^{(s)}$  the polynomial coefficients for the *Fourier* series term  $s$ .

Moreover, the multiplicative *Rayleigh* scattering function ( $f_R$ ) will be computed by recombining the first 3 *Fourier* series terms as follows:

$$f_R(\vartheta_s, \vartheta_v, \Delta\phi, \tau^R) = \sum_{s=0}^2 (2 - \delta_{0,s}) \cdot f_R^{(s)}(\vartheta_s, \vartheta_v, \tau^R) \cdot \cos(s \cdot \Delta\phi)$$

#### Resources:

Estimated CPU time: 691 sec

Output disk space:  $3 \times 78 \times 4 \times 4$  bytes/fl = 3744 bytes

#### Acceptance:

These polynomial coefficients can be tested by comparing the derived multiplicative *Rayleigh* scattering functions to those generated with another RTC based on the *Fourier* series expansion of the radiative transfer equation.

### 6.11.8 GADS Rayleigh Spherical Albedo

#### 6.11.8.1 Rayleigh spherical albedo, $S_R(\tau^R)$

Reference: Rayalb\_LUT,

LUT102

[AD-8] Section 6.11.8, GADS field 1.

Dependencies:

LUT075

Tools:

RTC/UPRAD (SO)  
RTC/GAUSS  
Polynomial fit

Procedure:

Input:  $\tau^R$  *Rayleigh* optical thickness, see [Section 6.11.4.2](#) (LUT075)

Output: *Rayalb\_LUT* [ $\tau^R$ ]  
*Rayleigh* spherical albedo (17 values)

units: [dl]

Step-1: Compute *Gaussian* angles ( $n=24$ ) and associated weights  $w[\mu]$  with the RTC/GAUSS.

Step-2: Calculate the *Rayleigh* transmittance  $T_R[\tau^R, \mu_s]$  corresponding to the first order of *Legendre* decomposition ( $I_s=0$ ) of phase function with the RTC/UPRAD (SO). For extracting the total atmospheric transmittance, we need to set  $I_s=0$  and  $\theta_v=-I$ .  $\mu_s$  is defined as  $\cos(\theta_s)$ .

***RTC/UPRAD (SO) Inputs (LAND)***

| <b>Variable</b>         | <b>Value</b>        | <b>Comments</b>                      |
|-------------------------|---------------------|--------------------------------------|
| <i>out_file</i>         | "/OUTPUT/uprad_out" |                                      |
| <i>i_branch</i>         | 1                   |                                      |
| <i>n</i> ( $\lambda$ )  | 1                   | 412.5 nm                             |
| <i>U</i> <sub>H2O</sub> | 0                   |                                      |
| <i>U</i> <sub>O2</sub>  | 0                   |                                      |
| <i>ESFT</i>             |                     | N/A                                  |
| <i>P<sub>s</sub></i>    | 1013.25             |                                      |
| $\tau^R$ ( $\lambda$ )  | tauR                | see <a href="#">Section 6.11.4.2</a> |
| <i>aerosol1</i>         | -                   |                                      |
| $\tau^{a1}$ (550)       | 0                   |                                      |
| <i>aerosol2</i>         | -                   |                                      |
| $\tau^{a2}$ (550)       | 0                   |                                      |
| <i>aerosol3</i>         | -                   |                                      |
| $\tau^{a3}$ (550)       | 0                   |                                      |
| <i>cloud1</i>           | -                   | N/A                                  |
| <i>cloud2</i>           | -                   | N/A                                  |

| Variable                   | Value                 | Comments   |
|----------------------------|-----------------------|--|
| <i>cloud3</i>              | -                     | N/A  |
| <i>phyto</i>               | -                     | N/A  |
| $\sigma_{e,\lambda}^p$     | -                     | N/A  |
| $\omega_{o,\lambda}^p$     | -                     | N/A  |
| <i>spm</i>                 | -                     | N/A  |
| $\sigma_{e,\lambda}^{spm}$ | -                     | N/A  |
| $\omega_{o,\lambda}^{spm}$ | -                     | N/A  |
| $\sigma_{e,\lambda}^{ys}$  | -                     | N/A  |
| <i>vertical</i>            | "/INPUT/vertical_out" | Not used, vertical distribution determined in RTC/SO ( $H_R=8$ km) |
| $I_s$                      | 0                     |  |
| $\rho_s$                   | 0                     |  |
| $E_o$                      | 1                     |  |
| $\sigma_{e,\lambda}^w$     | -                     | N/A  |
| $\omega_{o,\lambda}^w$     | -                     | N/A  |
| $w_s$                      | 0                     |  |
| $n_s, n_v, n_{\Delta\phi}$ | 24, 1, 1              | Use a loop for 24 $\theta_s$ .                                     |
| $\theta_s$                 | Gaussian angles       | Computed with RTC/GAUSS  |
| $\theta_v$                 | -1                    | To get the total atmospheric transmittance                         |
| $\Delta\phi$               | 0                     |  |
| <i>pol</i>                 | 1                     |  |

Step-3: Compute the *Rayleigh* spherical albedo  $Rayalb\_LUT[\tau^R]$  as follows, knowing that  $\mu=\cos(\theta_s)$ ,

$$Rayalb\_LUT[\tau^R] = 1 - 2 \cdot \int_0^1 T_R[\tau^R, \mu] \cdot w[\mu] \cdot \mu \cdot d\mu$$

Scientific content:

The *Rayleigh* spherical albedo  $Rayalb\_LUT$  is used in the atmospheric correction algorithm over land, and is precomputed with a RTC for a set of *Rayleigh* optical thicknesses.

Resources:

Estimated CPU time: 17 sec  
Output disk space: 17 × 4 bytes/fl = 68 bytes

Acceptance:

Comparison of these *Rayleigh* spherical albedos with those computed with another RTC.

## 6.11.9 ADS O2 Transmission around 778.75 nm

### 6.11.9.1 O2 transmittances around 778.75 nm (21 shifted filters)

Reference: TO2[ $\lambda'$ ,  $L_{779}$ ,  $\theta_s$ ,  $\theta_v$ ,  $\Delta\phi$ ], LUT099

[AD-8] Section 6.11.6, GADS field 1.

FUB/ACRI provided

#### Dependencies:

LUT085, LUT086, LUT087, LUT088, LUT095

#### Tool:

Neural Network

#### Procedure:

Inputs:  $\lambda'$  21 reference wavelengths [nm] corresponding to the 21 spectral shifts ( $\Delta\lambda$ ) of  $\pm 0.1$  nm applied on the MERIS O<sub>2</sub> filter centred at 778.5 nm, see [Section 6.11.4.11](#), (LUT095)  
 $L_{779}$  25 normalized radiances at 778.75 nm [ $sr^{-1}$ ], see [Section 6.11.4.12](#), (LUT085)  
 $\theta_s$  Solar zenith angle [deg], see [Section 6.11.4.13](#), (LUT086)  
 $\theta_v$  Viewing zenith angle [deg], see [Section 6.11.4.14](#), (LUT087)  
 $\Delta\phi$  Relative azimuth angle [deg], see [Section 6.11.4.15](#), (LUT088)

Output: TO2[ $\lambda'$ ,  $L_{779}$ ,  $\theta_s$ ,  $\theta_v$ ,  $\Delta\phi$ ]  
O<sub>2</sub> transmittances around 778.75 nm

units: [dl]

Step: User specified.

LUT processed at the FUB institute with a NN tool and delivered to ACRI.

#### Scientific content:

TO2[ $\lambda'$ ,  $L_{779}$ ,  $\theta_s$ ,  $\theta_v$ ,  $\Delta\phi$ ] correspond to the residual O<sub>2</sub> absorption within the MERIS band #12 (778.75 nm), accounting for the smile effect (21 shifted filters ( $\lambda'$ )), the normalized radiance at 778.75 nm (25 values of  $L_{779}$ ) and whatever the illumination and viewing geometry ( $\theta_s$ ,  $\theta_v$ ,  $\Delta\phi$ ). Note that the set of 25 values of  $L_{779}$  have been pre-computed with RTC/MOMO for a set of surface reflectances ( $\rho_s$ ), a set of surface pressures ( $P_s$ ), and a set of aerosol optical thicknesses ( $\tau^{a1}$ ).

#### Resources:

Estimated CPU time: -

Output disk space:  $21 \times 25 \times 15 \times 10 \times 19 \times 4$  bytes/fl = 5985000 bytes

Acceptance:

Corresponds to the latest definition.

### 6.11.10 ADS Apparent Pressure Parameters

#### 6.11.10.1 O<sub>2</sub> Rayleigh transmittances around 778.75 nm (21 shifted filters)

Reference: TO2\_ray[ $\lambda'$ ,  $\theta_s$ ,  $\theta_v$ ], LUT103

[AD-8] Section 6.11.10, GADS field 1.

FUB/ACRI provided

Dependencies:

LUT471, LUT472

Tool:

Neural Network

Procedure:

Inputs:  $\lambda'$  21 reference wavelengths [nm] corresponding to the 21 spectral shifts ( $\Delta\lambda$ ) of  $\pm 0.1$  nm applied on the MERIS O<sub>2</sub> filter centred around 761.7 nm, see Section 6.11.4.26, (LUT471)  
 $\theta_s$  Solar zenith angle [deg], see Section 6.11.4.29, (LUT472)  
 $\theta_v$  Viewing zenith angle [deg], see Section 6.11.4.29, (LUT472)

Output: TO2\_ray[ $\lambda'$ ,  $\theta_s$ ,  $\theta_v$ ]  
O<sub>2</sub> Rayleigh transmittances around 778.75 nm

units: [dl]

Step: User specified.

LUT processed at the FUB institute with a NN tool and delivered to ACRI.

Scientific content:

TO2\_ray[ $\lambda'$ ,  $\theta_s$ ,  $\theta_v$ ] corresponds to the residual O<sub>2</sub> absorption within the MERIS band #12 (778.75 nm) over a flat black surface, including the molecular scattering effects and accounting for the smile effect (21 shifted filters ( $\lambda'$ )) whatever the illumination and viewing geometry ( $\theta_s$ ,  $\theta_v$ ).

Resources:

Estimated CPU time: -  
Output disk space:  $21 \times 24 \times 24 \times 4$  bytes/fl = 48384 bytes

Acceptance:

Corresponds to the latest definition.

6.11.10.2 O<sub>2</sub> aerosol transmittances around 778.75 nm (21 shifted filters; H<sub>a</sub>=2 km)

Reference: TO2\_aer[ $\lambda'$ ,  $\theta_s$ ,  $\theta_v$ ], LUT104

[AD-8] Section 6.11.10, GADS field 2.

FUB/ACRI provided

Dependencies:

LUT471, LUT472

Tool:

Neural Network

Procedure:

Inputs:  $\lambda'$  21 reference wavelengths [nm] corresponding to the 21 spectral shifts ( $\Delta\lambda$ ) of  $\pm 0.1$  nm applied on the MERIS O<sub>2</sub> filter centred around 761.7 nm, see Section 6.11.4.26, (LUT471)  
 $\theta_s$  Solar zenith angle [deg], see Section 6.11.4.29, (LUT472)  
 $\theta_v$  Viewing zenith angle [deg], see Section 6.11.4.29, (LUT472)

Output: TO2\_aer[ $\lambda'$ ,  $\theta_s$ ,  $\theta_v$ ]  
O<sub>2</sub> aerosol transmittances around 778.75 nm

units: [dl]

Step: User specified.  
LUT processed at the FUB institute with a NN tool and delivered to ACRI.

Scientific content:

TO2\_aer[ $\lambda'$ ,  $\theta_s$ ,  $\theta_v$ ] correspond to the residual O<sub>2</sub> absorption within the MERIS band #12 (778.75 nm) over a flat black surface, including the aerosol scattering effects and accounting for the smile effect (21 shifted filters ( $\lambda'$ )) whatever the illumination and viewing geometry ( $\theta_s$ ,  $\theta_v$ ). An aerosol scale height ( $H_a$ ) of 2 km has been selected to generate these transmittances.



Resources:

Estimated CPU time: -  
Output disk space:  $21 \times 24 \times 24 \times 4$  bytes/fl = 48384 bytes

Acceptance:

Corresponds to the latest definition.

6.11.10.3 O<sub>2</sub> aerosol Fresnel transmittances around 778.75 nm (21 shifted filters; Ha=2 km)

Reference: TO2\_aer\_Fresnel[ $\lambda'$ ,  $\theta_s$ ,  $\theta_v$ ], LUT105

[AD-8] Section 6.11.10, GADS field 3.

FUB/ACRI provided

Dependencies:

LUT471, LUT472

Tool:

Neural Network

Procedure:

Inputs:  $\lambda'$  21 reference wavelengths [nm] corresponding to the 21 spectral shifts ( $\Delta\lambda$ ) of  $\pm 0.1$  nm applied on the MERIS O<sub>2</sub> filter centred around 761.7 nm, see Section 6.11.4.26, (LUT471)  
 $\theta_s$  Solar zenith angle [deg], see Section 6.11.4.29, (LUT472)  
 $\theta_v$  Viewing zenith angle [deg], see Section 6.11.4.29, (LUT472)

Output: TO2\_aer\_Fresnel[ $\lambda'$ ,  $\theta_s$ ,  $\theta_v$ ]  
O<sub>2</sub> aerosol Fresnel transmittances around 778.75 nm

units: [dl]

Step: User specified.  
LUT processed at the FUB institute with a NN tool and delivered to ACRI.

Scientific content:

TO2\_aer\_Fresnel[ $\lambda'$ ,  $\theta_s$ ,  $\theta_v$ ] correspond to the residual O<sub>2</sub> absorption within the MERIS band #12 (778.75 nm) of the Fresnel reflection contribution over a flat black surface, including the aerosol scattering effects and accounting for the smile effect (21 shifted filters ( $\lambda'$ )) whatever the illumination

and viewing geometry ( $\theta_s, \theta_v$ ). An aerosol scale height ( $H_a$ ) of  $2\text{ km}$  has been selected to generate these transmittances.

Resources:

Estimated CPU time: -  
Output disk space:  $21 \times 24 \times 24 \times 4 \text{ bytes/fl} = 48384 \text{ bytes}$

Acceptance:

Corresponds to the latest definition.

6.11.10.4 O<sub>2</sub> atmospheric transmittances around 778.75 nm (21 shifted filters; 21 layers;  $H_a=2 \text{ km}$ )

Reference: TO2\_atm[ $\lambda', P_k, \theta_s, \theta_v$ ], LUT107

[AD-8] Section 6.11.10, GADS field 4.

FUB/ACRI provided

Dependencies:

LUT471, LUT472, LUT473

Tool:

Neural Network

Procedure:

Inputs:  $\lambda'$  21 reference wavelengths [nm] corresponding to the 21 spectral shifts ( $\Delta\lambda$ ) of  $\pm 0.1 \text{ nm}$  applied on the MERIS O<sub>2</sub> filter centred around  $761.7 \text{ nm}$ , see Section 6.11.4.26, (LUT471)  
 $P_k$  21 reference pressure levels [hPa], see Section 6.11.4.30, (LUT473)  
 $\theta_s$  Solar zenith angle [deg], see Section 6.11.4.29, (LUT472)  
 $\theta_v$  Viewing zenith angle [deg], see Section 6.11.4.29, (LUT472)

Output: TO2\_atm[ $\lambda', P_k, \theta_s, \theta_v$ ]  
O<sub>2</sub> atmospheric transmittances around  $778.75 \text{ nm}$

units: [dl]

Step: User specified.

LUT processed at the FUB institute with a NN tool and delivered to ACRI.

Scientific content:

$TO2_{atm}[\lambda', P_k, \theta_s, \theta_v]$  correspond to the residual  $O_2$  absorption within the MERIS band #12 (778.75nm) over a flat black surface, including the aerosol and *Rayleigh* scattering effects and accounting for the smile effect (21 shifted filters ( $\lambda'$ )) whatever the illumination and viewing geometry ( $\theta_s, \theta_v$ ) and the pressure level (21 values of  $P_k$ ). An aerosol scale height ( $H_a$ ) of 2km has been selected to generate these transmittances.

Resources:

Estimated CPU time: -  
Output disk space: 21 × 21 × 24 × 24 × 4 bytes/fl = 1016064 bytes

Acceptance:

Corresponds to the latest definition.

**6.11.11 (Spare)**

Reference:

[AD-8] Section 6.11.11

**6.11.12 ADS Rayleigh Reflectance Over Ocean**

This LUT can be generated with both the 2 RTCs (FUB & UdL). Consequently, two recipes are proposed hereafter to generate this LUT either with the RTC/FUB (without polarization) or with the RTC/UdL(SO) including the polarization processes (used for the current MERIS reprocessing).

6.11.12.1 *Rayleigh reflectance over ocean*

6.11.12.1.1 FUB Recipe

Reference:  $\rho_R[\lambda, w_s, \theta_s, \theta_v, \Delta\phi]$ , LUT110

[AD-8] Section 6.11.12, GADS fields 1, 2 & 3

Dependencies:

LUT076, LUT077, LUT078, LUT079, LUT92, LUT93, LUT410

Tools:

RTC/MOMO (FUB)  
Multi-linear interpolation

Procedure:

Inputs:  $\lambda$  MERIS wavelength [nm], see Section 6.11.4.3, (LUT076)

|              |  |
|--------------|--|
| $w_s$        | Wind-speed [ $m.s^{-1}$ ] above sea level, <i>see</i> <a href="#">Section 6.11.4.20</a> , (LUT093) |
| $\theta_s$   | Solar zenith angle [ $deg$ ], <i>see</i> <a href="#">Section 6.11.4.4</a> , (LUT077).              |
| $\theta_v$   | Viewing zenith angle [ $deg$ ], <i>see</i> <a href="#">Section 6.11.4.5</a> , (LUT078).            |
| $\Delta\phi$ | Relative azimuth angle [ $deg$ ], <i>see</i> <a href="#">Section 6.11.4.6</a> , (LUT079).          |
| $P_s$        | Surface pressure [ $hPa$ ], <i>see</i> <a href="#">Section 6.11.4.19</a> , (LUT092).               |
| $t^R$        | Rayleigh optical thickness [ $dI$ ], <i>see</i> <a href="#">Section 6.11.1.1</a> , (LUT410)        |

Output:  $\rho_R[\lambda, w_s, \theta_s, \theta_v, \Delta\phi]$   
Rayleigh reflectance over ocean as function of the MERIS wavelength ( $\lambda$ ), the wind-speed above sea level ( $w_s$ ), and the illumination and viewing configuration ( $\theta_s, \theta_v, \Delta\phi$ )

units: [ $dI$ ]

Step-1: Generate TOA normalized Rayleigh radiance  $L_R[\lambda, w_s, \theta_s, \theta_v, \Delta\phi]$  for a pure Rayleigh atmosphere over 3 wind-roughened black sea surfaces ( $w_s=1.5, 5.0$  and  $10 m.s^{-1}$ ) with the RTC/MOMO.

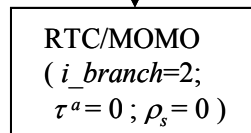
Note: The sun glint (*i.e.*, direct to direct contribution) is accounted for in  $L_R[\lambda, w_s, \theta_s, \theta_v, \Delta\phi]$ .

**RTC/MOMO Inputs (OCEAN)**

| Variable        | Value  | Comments   |
|-----------------|--|--|
| <i>out_file</i> | "/up_out/uprad_out"                                  |  |
| <i>i_branch</i> | 2  |  |
| $n(\lambda)$    | 1, 2, 3, 4, 5, 6, 7, 8, 9, 10, 11, 12, 13, 14 and 15 | All MERIS bands, <i>see</i> <a href="#">Section 6.11.4.3</a> |
| $U_{H2O}$       | 0  |  |
| $ESFT_{H2O}$    | -  | N/A  |
| $U_{O2}$        | 0  |  |
| $ESFT_{O2}$     | -  | N/A  |
| $U_{O3}$        | 0  |  |
| $ESFT_{O3}$     | -  | N/A  |
| $P_s$           | 1013.25  | <i>see</i> <a href="#">Section 6.11.4.19</a>                 |
| $t^R(\lambda)$  | tauR   | <i>see</i> <a href="#">Section 6.11.1.1</a>                  |
| <i>aerosol1</i> | -  |  |
| $t^{a1}(550)$   | 0  |  |
| <i>aerosol2</i> | -  |  |
| $t^{a2}(550)$   | 0  |  |
| <i>aerosol3</i> | -  |  |
| $t^{a3}(550)$   | 0  |  |
| <i>cloud1</i>   | -  | N/A  |
| $t^{c1}(550)$   | 0  |  |
| <i>cloud2</i>   | -  | N/A  |
| $t^{c2}(550)$   | 0  |  |
| <i>cloud3</i>   | -  | N/A  |

| Variable                   | Value                   | Comments                                    |
|----------------------------|-------------------------|---|
| $\tau^3(550)$              | 0                       |   |
| <i>phyto</i>               | -                       | N/A   |
| $\sigma_{e,\lambda}^p$     | -                       | N/A   |
| $\omega_{o,\lambda}^p$     | -                       | N/A   |
| <i>spm</i>                 | -                       | N/A   |
| $\sigma_{e,\lambda}^{spm}$ | -                       | N/A   |
| $\omega_{o,\lambda}^{spm}$ | -                       | N/A   |
| $\sigma_{a,\lambda}^{ys}$  | -                       | N/A   |
| <i>vertical</i>            | "/sca_vert/vtp1_lut110" | Vertical profile with 12 atmospheric layers |
| $I_s$                      | 70                      |   |
| $\rho_s$                   | 0                       |   |
| $E_o$                      | 1                       |   |
| $\sigma_{a,\lambda}^w$     | 99                      |   |
| $w_s$                      | 1.5, 5.0 and 10         | see Section 6.11.4.20                       |
| $n_s, n_v, n_{\Delta\phi}$ | 16, 10, 25              |   |
| $\theta_s'$                | Gaussian angles         | From Gauss-Lobatto quadrature (in RTC/FUB)  |
| $\theta_v'$                | Gaussian angles         | From Gauss-Lobatto quadrature (in RTC/FUB)  |
| $\Delta\phi$               | see inputs              | see Section 6.11.4.6                        |

$$n(\lambda), w_s, \theta_s', \theta_v', \Delta\phi$$



$$L_R(\lambda, w_s, \theta_s', \theta_v', \Delta\phi)$$

Step-2: Compute the *Rayleigh* reflectance  $\rho_R[\lambda, w_s, \theta_s', \theta_v', \Delta\phi]$  as follows,

$$\rho_R[\lambda, w_s, \theta_s', \theta_v', \Delta\phi] = \pi \cdot \frac{L_R[\lambda, w_s, \theta_s', \theta_v', \Delta\phi]}{\cos(\theta_s')}$$

Step-3: Remove the sun glint reflectance at TOA ( $\rho_{G\_TOA}$ ) from the *Rayleigh* reflectance (only for the case where  $w_s \neq 0$ ). This is achieved by following this procedure:

In the *Cox and Munk* surface representation (see [RD-7] for more details), the probability density function of facet slopes  $p(\theta'_s, \theta'_v, \Delta\phi)$  for the illumination and viewing configurations  $(\theta'_s, \theta'_v, \Delta\phi)$  is expressed as:

$$p(\theta'_s, \theta'_v, \Delta\phi) = \frac{1}{\pi \sigma^2} \cdot \exp\left(\frac{-\tan^2 \beta}{\sigma^2}\right)$$

where  $\beta$ , the angle between the local normal and the normal to the facet, is defined as,

$$\cos \beta = \frac{\cos \theta'_s + \cos \theta'_v}{2 \cos \omega}$$

with  $\cos 2\omega = \cos \theta'_s \cdot \cos \theta'_v - \sin \theta'_s \cdot \sin \theta'_v \cdot \cos \Delta\phi$

and  $\sigma$  the root mean square of facet slopes (which are generated by the wind-speed  $w_s$  just above sea surface) is written as,

$$\sigma^2 = 0.003 + 5.12 \cdot 10^{-3} \cdot w_s$$

The sunglint  $\rho_G$  (i.e., the specular reflection of the sunlight over the ocean waves) just above sea level is then computed as:

$$\rho_G(w_s, \theta'_s, \theta'_v, \Delta\phi) = \rho_F(\omega) \cdot \frac{\pi \cdot p(\theta'_s, \theta'_v, \Delta\phi)}{4 \cdot \cos \theta'_s \cos \theta'_v \cos^4 \beta}$$

where  $\rho_F(\omega)$  is the *Fresnel* reflectance at the *air-sea* interface for an angle  $\omega$  given by

$$\left\{ \begin{array}{l} \rho_F(\omega) = \frac{1}{2} \cdot \left[ \left( \frac{\sin(\omega - \mathcal{G}_t)}{\sin(\omega + \mathcal{G}_t)} \right)^2 + \left( \frac{\tan(\omega - \mathcal{G}_t)}{\tan(\omega + \mathcal{G}_t)} \right)^2 \right] \text{ for } \omega \neq \mathcal{G}_t \\ \rho_F(\omega) = \left( \frac{n_w - 1}{n_w + 1} \right)^2 \text{ for } \omega = \mathcal{G}_t \end{array} \right.$$

with  $\mathcal{G}_t = \arcsin(\sin \omega / n_w)$ , and  $n_w$  the water refractive index ( $n_w=1.34$ ).

Finally, the sun glint reflectance at TOA ( $\rho_{G\_TOA}$ ) is expressed as:

$$\rho_{G\_TOA}(w_s, \theta'_s, \theta'_v, \Delta\phi) = \rho_G(w_s, \theta'_s, \theta'_v, \Delta\phi) \cdot T(\theta'_s) \cdot T(\theta'_v)$$

where  $T(\theta)$  is the direct atmospheric transmittance for the zenith angle  $\theta$  defined as,

$$T(\theta) = e^{-\tau / \cos(\theta)}$$

with  $\tau$  the total optical thickness (*Rayleigh* + aerosols +  $O_3$  + etc.).

Step-4: Apply a multi-linear interpolation to output the *Rayleigh* reflectance  $\rho_R[\lambda, w_s, \theta_s', \theta_v', \Delta\phi]$  into the input angular grid in  $(\theta_s, \theta_v)$ :

$$\rho_R[\lambda, w_s, \theta_s, \theta_v, \Delta\phi] = \text{interpolation}(\rho_R[\lambda, w_s, \theta_s', \theta_v', \Delta\phi])$$

and build the *Rayleigh* reflectance  $\rho_R[\lambda, w_s, \theta_s, \theta_v, \Delta\phi]$  for all parameters.

Scientific content:

$\rho_R[\lambda, w_s, \theta_s, \theta_v, \Delta\phi]$  describes the *Rayleigh* reflectances simulated at each of the 15 MERIS wavelengths over 3 wind-roughened black sea surfaces ( $w_s = 1.5, 5.0$  and  $10 \text{ m.s}^{-1}$ ), for various illumination and viewing conditions, and a standard atmospheric pressure ( $1013.25 \text{ hPa}$ ). The boundary condition is a black (*Fresnel* reflecting) ocean. Note that the sun glint component at TOA has been removed from these *Rayleigh* reflectances.

Resources:

Estimated CPU time: 1024 sec  
Output disk space:  $23 \times 3 \times 15 \times 13 \times 25 \times 4 \text{ bytes/fl} = 1345500 \text{ bytes}$

Note that the storage of this table is completed using different records for each  $\theta_s$  tabulated value (see [\[AD-8\]](#) for exact structure).

Acceptance:

Comparison with another RTC that does not account for the polarization processes.

6.11.12.1.2 UdL Recipe

Reference:  $\rho_R[\lambda, w_s, \theta_s, \theta_v, \Delta\phi]$ , LUT110

[\[AD-8\]](#) Section 6.11.12, GADS fields 1, 2 & 3

Dependencies:

LUT076, LUT077, LUT078, LUT079, LUT92, LUT93, LUT410

Tool:

RTC/UPRAD (SO)

Procedure:

Inputs:  $\lambda$  MERIS wavelength [*nm*], see [Section 6.11.4.3](#), (LUT076)  
 $w_s$  Wind-speed [ $\text{m.s}^{-1}$ ] above sea level, see [Section 6.11.4.20](#), (LUT093)  
 $\theta_s$  Solar zenith angle [*deg*], see [Section 6.11.4.4](#), (LUT077).

$\theta_v$  Viewing zenith angle [*deg*], *see* [Section 6.11.4.5](#), (LUT078).  
 $\Delta\phi$  Relative azimuth angle [*deg*], *see* [Section 6.11.4.6](#), (LUT079).  
 $P_s$  Surface pressure [*hPa*], *see* [Section 6.11.4.19](#), (LUT092).  
 $\tau^R$  *Rayleigh* optical thickness [*dl*], *see* [Section 6.11.1.1](#), (LUT410)

Output:  $\rho_R[\lambda, w_s, \theta_s, \theta_v, \Delta\phi]$   
*Rayleigh* reflectance over ocean as function of the MERIS wavelength ( $\lambda$ ), the wind-speed above sea level ( $w_s$ ), and the illumination and viewing configuration ( $\theta_s, \theta_v, \Delta\phi$ )

units: [*dl*]

Step-1: Generate TOA normalized *Rayleigh* radiance  $L_R[\lambda, w_s, \theta_s, \theta_v, \Delta\phi]$  for a pure *Rayleigh* atmosphere over 3 wind-roughened black sea surfaces ( $w_s=1.5, 5.0$  and  $10m.s^{-1}$ ) with the RTC/UPRAD (SO). The sun glint (*i.e.*, the direct to direct contribution) is not accounted for in  $L_R[\lambda, w_s, \theta_s, \theta_v, \Delta\phi]$ .

Note: An internal sun glint flag has been deactivated in the RTC/SO for excluding the direct to direct contribution in the computation of TOA normalized radiance.

**RTC/UPRAD (SO) Inputs (OCEAN)**

| Variable               | Value  | Comments   |
|------------------------|--|--|
| <i>out_file</i>        | "/OUTPUT/uprad_out"                                  |  |
| <i>i_branch</i>        | 2  |  |
| $n(\lambda)$           | 1, 2, 3, 4, 5, 6, 7, 8, 9, 10, 11, 12, 13, 14 and 15 | All MERIS bands, <i>see</i> <a href="#">Section 6.11.4.3</a> |
| $U_{H2O}$              | 0  |  |
| $U_{O2}$               | 0  |  |
| <i>ESFT</i>            | -  |  |
| $P_s$                  | 1013.25  | <i>see</i> <a href="#">Section 6.11.4.19</a>                 |
| $\tau^R(\lambda)$      | tauR   | <i>see</i> <a href="#">Section 6.11.1.1</a>                  |
| <i>aerosol1</i>        | -  |  |
| $\tau^{a1}(550)$       | 0  |  |
| <i>aerosol2</i>        | -  |  |
| $\tau^{a2}(550)$       | 0  |  |
| <i>aerosol3</i>        | -  |  |
| $\tau^{a3}(550)$       | 0  |  |
| <i>cloud1</i>          | -  | N/A  |
| <i>cloud2</i>          | -  | N/A  |
| <i>cloud3</i>          | -  | N/A  |
| <i>phyto</i>           | -  | N/A  |
| $\sigma_{e,\lambda}^p$ | -  | N/A  |
| $\omega_{o,\lambda}^p$ | -  | N/A  |



| Variable                   | Value                 | Comments  |
|----------------------------|-----------------------|---|
| $spm$                      | -                     | N/A   |
| $\sigma_{e,\lambda}^{spm}$ | -                     | N/A   |
| $\omega_{o,\lambda}^{spm}$ | -                     | N/A   |
| $\sigma_{e,\lambda}^{ys}$  | -                     | N/A   |
| $vertical$                 | "/INPUT/vertical_out" | Not used, vertical distribution determined in RTC/SO ( $H_R=8 km$ ) |
| $I_s$                      | 79                    |   |
| $\rho_s$                   | 0                     |   |
| $E_o$                      | 1                     |   |
| $\sigma_{e,\lambda}^w$     | -                     | N/A   |
| $\omega_{o,\lambda}^w$     | -                     | N/A   |
| $w_s$                      | 1.5, 5.0 and 10       | see Section 6.11.4.20   |
| $n_s, n_v, n_{\Delta\phi}$ | 16, 10, 25            |   |
| $\theta_s$                 | Gaussian angles       | Selected from a Gauss quadrature;<br>see Section 6.11.4.4           |
| $\theta_v$                 | Gaussian angles       | Selected from a Gauss quadrature;<br>see Section 6.11.4.5           |
| $\Delta\phi$               | see inputs            | see Section 6.11.4.6  |
| $pol$                      | 1                     |   |

$$n(\lambda, w_s, \theta_s, \theta_v, \Delta\phi)$$

RTC/UPRAD(SO)  
( $i\_branch=2$ ;  
 $\tau^a=0$ ;  $\rho_s=0$ )

$$L_R[\lambda, w_s, \theta_s, \theta_v, \Delta\phi]$$

Step-2: Compute the *Rayleigh* reflectance  $\rho_R[\lambda, w_s, \theta_s, \theta_v, \Delta\phi]$  as follows,

$$\rho_R[\lambda, w_s, \theta_s, \theta_v, \Delta\phi] = \pi \cdot \frac{L_R[\lambda, w_s, \theta_s, \theta_v, \Delta\phi]}{\cos(\theta_s)}$$

#### Scientific content:

$\rho_R[\lambda, w_s, \theta_s, \theta_v, \Delta\phi]$  describes the *Rayleigh* reflectances simulated at each of the 15 MERIS wavelengths over 3 wind-roughened black sea surfaces ( $w_s = 1.5, 5.0$  and  $10 m \cdot s^{-1}$ ), for various illumination and viewing conditions, and a standard atmospheric pressure ( $1013.25 hPa$ ). The boundary condition is a black (*Fresnel* reflecting) ocean. Note that the sun glint component at TOA has been removed from these *Rayleigh* reflectances.

Resources:

Estimated CPU time: 259 sec  
Output disk space:  $23 \times 3 \times 15 \times 13 \times 25 \times 4$  bytes/fl = 1345500 bytes  
Note that the storage of this table is completed using different records for each  $\theta_s$  tabulated value (see [AD-8] for exact structure).

Acceptance:

Comparison with another RTC that does account for the polarization processes.

**6.11.13 ADS Photosynthetically Active Radiation**

6.11.13.1 Photosynthetically active radiation,  $PAR(\alpha, U_{H2O}, U_{O3}, \tau^a)$

Reference: PAR[ $\alpha, u_{O3}, \tau^a, u_{H2O}$ ], LUT111

[AD-8] Section 6.11.13, GADS field 1.

ACRI provided

Dependencies:

LUT94, LUT305, LUT306, LUT307

Tool:

None

Procedure:

Input:  $\alpha$  Angstroem exponent, see Section 6.11.4.22 (LUT305)  
 $u_{H2O}$  water vapor amount [ $g.cm^{-2}$ ], see Section 6.11.4.25, (LUT094)  
 $u_{O3}$  ozone amount [DU], see Section 6.11.4.23, (LUT306)  
 $\tau^a$  aerosol optical thickness at 865 nm [dl], see Section 6.11.4.24, (LUT307)

Output: PAR[ $\alpha, u_{O3}, \tau^a, u_{H2O}$ ]  
Photosynthetically available radiation as function of the Angström exponent, the ozone amount, the aerosol optical thickness, and the water vapor content.

units: [ $\mu Einstein/m^2/s$ ]

Step: User specified.

Resources:

Estimated CPU time: -  
Output disk space:  $20 \times 20 \times 20 \times 20 \times 4$  bytes/fl = 640000 bytes

Acceptance:

Corresponds to the latest definition.

## 6.12 WATER-VAPOUR PARAMETERS

### 6.12.1 C.P.

None

### 6.12.2 MPH

Not covered in this document (*see* [AD-8] for a detailed description)

### 6.12.3 SPH

Not covered in this document (*see* [AD-8] for a detailed description)

### 6.12.4 GADS General

#### 6.12.4.1 Solar zenith angles

Reference: SZA, LUT112

[AD-8] Section 6.12.4, GADS field 1

ACRI provided

Dependencies:

None

Tool:

None

Procedure:

Input: none

Output: SZA Solar zenith angle (27 values of  $\theta_s$ )

units: [ $10^{-6}$  deg]

Step: User specified.

Scientific content:

Set of 27 solar zenith angles ( $\theta_s$ ) regularly spaced

Current baseline: 27  $\theta$ , values within [15;80] *deg.*, with a step of 2.5 *deg.*

Resources:

Estimated CPU time: -  
Output disk space: 27  $\times$  4 bytes/ul = 108 bytes

Acceptance:

Corresponds to the latest definitions

6.12.4.2 *View zenith angles*

Reference: VZA, LUT113

[AD-8] Section 6.12.4, GADS field 2

ACRI provided

Dependencies:

None

Tool:

None

Procedure:

Input: none  
Output: VZA View zenith angle (18 values of  $\theta$ ,)  
units: [10<sup>-6</sup> *deg*]  
Step: User specified.

Scientific content:

Set of 18 view zenith angles ( $\theta$ ,) regularly spaced

Current baseline: 18  $\theta$ , values within [0;42.5] *deg.*, with a step of 2.5 *deg.*

Resources:

Estimated CPU time: -  
Output disk space: 18  $\times$  4 bytes/ul = 72 bytes

Acceptance:

Corresponds to the latest definitions

6.12.4.3 *Relative azimuth angles*

Reference: RAA, LUT114

[AD-8] Section 6.12.4, GADS field 3

ACRI provided

Dependencies:

None

Tool:

None

Procedure:

Input: none

Output: RAA Relative azimuth angle (25 values of  $\Delta\phi$ )

units:  $[10^{-6} \text{ deg}]$

Step: User specified.

Scientific content:

Set of 25 relative azimuth angle ( $\Delta\phi$ ) regularly spaced

Current baseline: 25  $\Delta\phi$  values within  $[0;180] \text{ deg.}$ , with a step of  $7.5 \text{ deg.}$

Resources:

Estimated CPU time: -

Output disk space:  $25 \times 4 \text{ bytes/ul} = 100 \text{ bytes}$

Acceptance:

Corresponds to the latest definitions

6.12.4.4 *Threshold value on radiance at 885 nm for marking pixel as invalid for water vapour processing*

Reference: inv\_WV, LUT115

[AD-8] Section 6.12.4, GADS field 4

ACRI provided

Dependencies:

None

Tool:

None

Procedure:

Input: none

Output: *inv\_WV* Threshold value on the radiance at 885 nm ( $L_{\text{Thresh}}^{885}$ ) from which the water vapor content cannot be retrieved.

units: [ $W \cdot m^{-2} \cdot \mu m^{-1} \cdot sr^{-1}$ ]

Step: User specified.

Scientific content:

*inv\_WV* represents the threshold value on the radiance at 885 nm ( $L_{\text{Thresh}}^{885}$ ) from which the water vapor content cannot be retrieved. In the water vapor retrieval algorithm, all the pixels, for which the radiance at 885 nm is lower than this threshold value, will be systematically discarded from the water vapor retrieval processing.

Current baseline: 310 [ $W \cdot m^{-2} \cdot \mu m^{-1} \cdot sr^{-1}$ ]

Resources:

Estimated CPU time: -

Output disk space:  $1 \times 4$  bytes/fl = 4 bytes

Acceptance:

According to the MERIS sensor specifications.

6.12.4.5 *Minimum threshold for out of range output value of water vapour content*

Reference: out\_Min, LUT116

[AD-8] Section 6.12.4, GADS field 5

ACRI provided

Dependencies:

None

Tool:

None

Procedure:

Input: none

Output: out\_Min Acceptable minimum value of water vapor content ( $u_{H_2O}^{\min}$ ) retrieved from the algorithm

units: [g.cm<sup>-2</sup>]

Step: User specified.

Scientific content:

out\_Min corresponds to the lowest acceptable value of water vapor content ( $u_{H_2O}^{\min}$ ) retrieved from the algorithm. Pixels for which the retrieved water vapor content is lower than this threshold, are set to out\_Min.

Current baseline: 0.1 g.cm<sup>-2</sup>

Resources:

Estimated CPU time: -

Output disk space: 1 × 4 bytes/fl = 4 bytes

Acceptance:

Corresponds to the latest definition.

6.12.4.6 *Maximum threshold for out of range output value of water vapour content*

Reference: out\_Max, LUT117

[AD-8] Section 6.12.4, GADS field 6

ACRI provided

Dependencies:

None

Tool:

None

Procedure:

Input: none

Output: *out\_max* Acceptable maximum value of water vapor content ( $u_{H_2O}^{\max}$ ) retrieved from the algorithm

units:  $[g.cm^{-2}]$

Step: User specified.

Scientific content:

*out\_Max* corresponds to the highest acceptable value of water vapor content ( $u_{H_2O}^{\max}$ ) retrieved from the algorithm. Pixels for which the retrieved water vapor content is larger than this threshold, are set to *out\_Min*.

Current baseline:  $7 g.cm^{-2}$

Resources:

Estimated CPU time: -

Output disk space:  $1 \times 4 \text{ bytes/fl} = 4 \text{ bytes}$

Acceptance:

Corresponds to the latest definition.

6.12.4.7 Sun irradiances at 778.75 nm, 865 nm, 885nm and 900 nm (consistent with cloud LUTs)

Reference: Eo\_779, Eo\_865, LUT118  
Eo\_885, Eo\_900

[AD-8] Section 6.12.4, GADS field 7

ACRI provided



Dependencies:

None

Tool:

None

Procedure:

Input: none

Outputs:  $E_o^{779}$ ,  $E_o^{865}$ ,  $E_o^{885}$ ,  $E_o^{900}$

Extraterrestrial solar irradiances respectively at 778.75nm (band#12), 865.00nm (band#13), 885.00nm (band#14) and 900.00nm (band#15), not corrected for Sun-Earth distance ( $d$ ).

units:  $[W.m^{-2}.\mu m^{-1}]$

Step: User specified.

Scientific content:

Set of 4 extraterrestrial solar irradiances ( $E_o^{779}$ ,  $E_o^{865}$ ,  $E_o^{885}$ ,  $E_o^{900}$ ) in MERIS band#12 (778.755nm), #13 (865.00nm), #14 (885.00nm) and 15 (900.00nm) respectively, are used in the water vapour retrieval algorithm to convert radiances into reflectances. Note that these solar irradiances are not corrected for the Sun-Earth distance ( $d$ ).

Current baseline: {1193.696, 967.772, 926.348, 894.569}  $W.m^{-2}.\mu m^{-1}$

Resources:

Estimated CPU time: -

Output disk space:  $4 \times 4$  bytes/fl = 16 bytes

Acceptance:

Corresponds to the latest definition.

6.12.4.8 Aerosol optical thicknesses at 885 nm

Reference: AOT885, LUT119

[AD-8] Section 6.12.4, GADS field 8

ACRI provided

Dependencies:

None

Tool:

None

Procedure:

Input: none

Output:  $\tau_0^a$  Aerosol optical thickness at 885nm (20 values)

units: [dl]

Step: User specified.

Scientific content:

Set of 20 pre-selected aerosol optical thicknesses at 885nm ( $\tau_0^a$ ) used in the water vapour retrieval algorithm

Current baseline: [0.03;0.60] by step of 0.03

Resources:

Estimated CPU time: -

Output disk space:  $20 \times 4$  bytes/fl = 80 bytes

Acceptance:

Corresponds to the latest definition.

**6.12.4.9 Surface albedos**

Reference: Salb, LUT120

[AD-8] Section 6.12.4, GADS field 9

ACRI provided

Dependencies:

None

Tool:

None

Procedure:

Input: none

Output:  $S_{alb}^o$  Surface albedo (10 values)

units: [dl]

Step: User specified.

Scientific content:

Set of 10 pre-selected surface albedo ( $S_{alb}^o$ ) used in the water vapour retrieval algorithm

Current baseline: [0;0.9] by step of 0.1

Resources:

Estimated CPU time: -

Output disk space:  $10 \times 4$  bytes/fl = 40 bytes

Acceptance:

Corresponds to the latest definition.

**6.12.4.10 Cloud optical thicknesses at 550nm**

Reference: COT550, LUT308

[AD-8] Section 6.12.4, GADS field 10

ACRI provided

Dependencies:

None

Tool:

None

Procedure:

Input: none

Output:  $\tau_o^c$  Cloud optical thickness at 550nm (20 values)

units: [dl]

Step: User specified.

Scientific content:

Set of 20 pre-selected cloud optical thicknesses at 550nm ( $\tau_o^c$ ) used in the water vapour retrieval algorithm

Current baseline: [5;100] by step of 5

Resources:

Estimated CPU time: -

Output disk space:  $20 \times 4$  bytes/fl = 80 bytes

Acceptance:

Corresponds to the latest definition.

*6.12.4.11 Wind-speeds for GADS polynomial coefficients for water vapour retrieval over ocean*

Reference: ws, LUT433

[AD-8] Section 6.12.4, GADS field 11

ACRI provided

Dependencies:

None

Tool:

None

Procedure:

Input: none

Output: ws Wind-speed just above sea level (5 values of  $w_s$ )

units: [ $m.s^{-1}$ ]

Step: User specified.

Scientific content:

Set of 5 pre-selected wind-speeds ( $w_s$ ) used to account for the sea surface roughness in the water vapour retrieval algorithm

Current baseline: {2; 4; 6; 8; 10}  $m.s^{-1}$

Resources:

Estimated CPU time: -

Output disk space:  $5 \times 4$  bytes/fl = 20 bytes

Acceptance:

Corresponds to the latest definition.

**6.12.4.12 Latitudes for ADS surface albedo slope between 900 nm & 885 nm and ADS surface albedo at 885 nm**

Reference: lat, LUT476

[AD-8] Section 6.12.4, GADS field 12

ACRI provided

Dependencies:

None

Tool:

None

Procedure:

Input: none

Output: *lat* Latitudes (3600 values)

units:  $[10^{-6} deg.]$

Step: User specified.

Scientific content:

Set of 3600 latitudes (*lat*) used as the geographic grid for the albedo map used in the water vapour retrieval algorithm

Current baseline: [-89.975;89.975] *deg.* by step of 0.05 *deg.*

Resources:

Estimated CPU time: -  
Output disk space: 3600 × 4 bytes/sl = 14400 bytes

Acceptance:

Corresponds to the latest definition.

6.12.4.13 *Longitudes for ADS surface albedo slope between 900 nm & 885 nm and ADS surface albedo at 885 nm*

Reference: long, LUT477

[AD-8] Section 6.12.4, GADS field 13

ACRI provided

Dependencies:

None

Tool:

None

Procedure:

Input: none  
Output: *long* Longitudes (7200 values)  
units: [10<sup>-6</sup> *deg.*]  
Step: User specified.

Scientific content:

The albedo map used in the water vapour retrieval algorithm is defined on a grid of 7200 longitudes.

Current baseline: [-179.975 ; 179.975] *deg.* by step of 0.05 *deg.*

Resources:

Estimated CPU time: -  
Output disk space: 7200 × 4 bytes/sl = 28800 bytes

Acceptance:

Corresponds to the latest definition.

6.12.4.14 *Offset and scaling factor for surface albedo ratio between 900 nm & 885 nm*

Reference: SalbRat\_offset, SalbRat\_scale, LUT478

[AD-8] Section 6.12.4, GADS field 14

ACRI provided

Dependencies:

None

Tool:

None

Procedure:

Input: none

Output: *SalbRat\_offset, SalbRat\_scale*  
Offset and scaling factor for surface albedo ratio between 900 & 885 nm  
(2 values)

units: [dl]

Step: User specified.

Scientific content:

Current baseline: {0.9, 7.8740175 10<sup>-4</sup>}

Resources:

Estimated CPU time: -

Output disk space: 2 × 4 bytes/sl = 8 bytes

Acceptance:

Corresponds to the latest definition.

6.12.4.15 *Scaling factor for surface albedo at 885 nm*

Reference: Salb885\_scale, LUT479

[AD-8] Section 6.12.4, GADS field 15

ACRI provided

Dependencies:

None

Tool:

None

Procedure:

Input: none

Output: *Salb885\_scale*

Scaling factor for surface albedo at 885 nm

units: [dl]

Step: User specified.

Scientific content:

Current baseline: 0.0039215689

Resources:

Estimated CPU time: -

Output disk space: 1 × 4 bytes/sl = 4 bytes

Acceptance:

Corresponds to the latest definition.

6.12.4.16 *Bad data value for surface albedo ratio between 900 nm & 885 nm*

Reference: SalbRat\_flag, LUT480

[AD-8] Section 6.12.4, GADS field 16

ACRI provided

Dependencies:

None



Tool:

None

Procedure:

Input: none

Output: *SalbRat\_flag*

Flag to detect bad value of surface albedo ratio between 900 & 885 nm

units: [dl]

Step: User specified.

Scientific content:

Current baseline: 255

Resources:

Estimated CPU time: -

Output disk space: 1 × 1 byte/uc = 1 byte

Acceptance:

Corresponds to the latest definition.

6.12.4.17 *Minimum valid values for neural network inputs*

Reference: MinDataIn\_NN, LUT481

[AD-8] Section 6.12.4, GADS field 17

ACRI provided

Dependencies:

None

Tool:

None

Procedure:

Input: none

Output: *MinDataIn\_NN*

Minimum valid values for NN inputs

units: [dl]

Step: User specified.

Scientific content:

Current baseline: {0.342, 0.680, -0.733, 0.0041, 0.899, -0.863, 0.0054, -1.670, 759.0, 648.0}

Resources:

Estimated CPU time: -  
Output disk space:  $10 \times 4$  bytes/fl = 40 bytes

Acceptance:

Corresponds to the latest definition.

6.12.4.18 Maximum valid values for neural network inputs

Reference: MaxDataIn\_NN, LUT482

[AD-8] Section 6.12.4, GADS field 18

ACRI provided

Dependencies:

None

Tool:

None

Procedure:

Input: none  
Output: *MaxDataIn\_NN*  
Maximum valid values for NN inputs

units: [dl]

Step: User specified.

Scientific content:

Current baseline: {0.948, 1.000, 0.733, 0.198, 1.070, 0.0356, 0.197, 9.070, 765.00, 1020.00}

Resources:

Estimated CPU time: -  
Output disk space: 10 × 4 bytes/fl = 40 bytes

Acceptance:

Corresponds to the latest definition.

6.12.4.19 Minimum valid value for neural network output

Reference: MinDataOut\_NN, LUT483

[AD-8] Section 6.12.4, GADS field 19

ACRI provided

Dependencies:

None

Tool:

None

Procedure:

Input: none  
Output: *MinDataOut\_NN*  
Minimum valid value for NN output  
units: [g.cm<sup>-2</sup>]  
Step: User specified.

Scientific content:

Current baseline: 0.13 g.cm<sup>-2</sup>

Resources:

Estimated CPU time: -  
Output disk space: 1 × 4 bytes/fl = 4 bytes

Acceptance:

Corresponds to the latest definition.

#### 6.12.4.20 Maximum valid value for neural network output

Reference: MaxDataOut\_NN, LUT484

[AD-8] Section 6.12.4, GADS field 20

ACRI provided

#### Dependencies:

None

#### Tool:

None

#### Procedure:

Input: none

Output: *MaxDataOut\_NN*  
Maximum valid value for NN output

units:  $[g.cm^{-2}]$

Step: User specified.

#### Scientific content:

Current baseline:  $5.63 g.cm^{-2}$

#### Resources:

Estimated CPU time: -

Output disk space:  $1 \times 4 \text{ bytes/fl} = 4 \text{ bytes}$

#### Acceptance:

Corresponds to the latest definition.

### 6.12.5 GADS Neural Network for Water-Vapour Retrieval over Land

#### 6.12.5.1 Neural network (NN) parameters for water vapour retrieval over land

Reference: WV\_Land, LUT121

[AD-8] Section 6.12.5, GADS field 1

FUB/ACRI provided

Dependencies:

None

Tool:

Neural Network

Procedure:

Input: none

Output: *WV\_Land* NN parameters for water vapour retrieved over land  
units: [dl]

Step: User specified.

LUT processed at the FUB institute with a NN tool and delivered to ACRI.

Scientific content:

*WV\_Land* provides the water vapor content (*WV*) retrieved over land with a NN tool and an huge amount of RTC/MOMO simulations in MERIS band#14 (885 nm) and #15 (900 nm). RTC computations were completed over various reflective land surfaces ( $S_{alb}$ ), for various atmospheric profiles (VTP files) with different surface pressures ( $P_s$ ), and for various illumination and viewing geometries ( $\theta_s, \theta_v, \Delta\phi$ ). Simulations were corrected for the slope effect of the surface albedo between 900 and 885 nm.

Current baseline: 262144 values

Resources:

Estimated CPU time: -

Output disk space:  $262144 \times 1 \text{ byte/uc} = 262144 \text{ bytes}$

The storage of this table is completed with only one record (see [AD-8], Annex-6) for the full description of the output structure).

Acceptance:

Corresponds to the latest definition (or last delivery by the FUB institute).

## 6.12.6 ADS Polynomial Coefficients for Water-Vapour Retrieval over Ocean (without Sun Glint)

### 6.12.6.1 Polynomial coefficients for water vapour retrieval over ocean (no glint)

Reference: WV\_Ocean\_NoGlint, LUT122

[AD-8] Section 6.12.6, GADS fields 1, 2 & 3

FUB/ACRI provided

#### Dependencies:

LUT112, LUT113, LUT114, LUT119, LUT433

#### Tool:

Neural Network

#### Procedure:

Inputs:  $\theta_s$  Solar zenith angle [deg], see Section 6.12.4.1, (LUT112)  
 $\theta_v$  View zenith angle [deg], see Section 6.12.4.2, (LUT113)  
 $\Delta\phi$  Relative azimuth angle [deg], see Section 6.12.4.3, (LUT114)  
 $\tau_0^a$  AOT885 [dl] (20 values), see Section 6.12.4.8 (LUT119)  
 $w_s$  Wind-speeds ASL [ $m.s^{-1}$ ] (5 values), see Section 6.12.4.11 (LUT433)  
 $k$  Polynomial coefficient orders [dl],  $k = [0;2]$

Output:  $WV\_Ocean\_NoGlint[\theta_s, k, \theta_v, \Delta\phi, \tau_0^a, w_s]$   
 Polynomial coefficients for water vapour retrieval over ocean (no glint)

units: [ $g.cm^{-2}$ ]

Step: User specified.

LUT processed at the FUB institute with a NN tool and delivered to ACRI.

#### Scientific content:

$WV\_Ocean\_NoGlint[\theta_s, k, \theta_v, \Delta\phi, \tau_0^a, w_s]$  describes the coefficients of the polynomial fit expressing the water vapor content (WV) over ocean (without sun glint) as function of the ratio of TOA normalized radiances at 900 and 885 nm ( $R_{TOA\_15/14}[\tau_0^a, w_s, \theta_s, \theta_v, \Delta\phi]$ ) computed with RTC/MOMO, for each of 5 wind-speeds ( $w_s$ ; LUT433), for each of 20 AOT885 ( $\tau_0^a$ ; LUT119), for each illumination and viewing geometry ( $\theta_s, \theta_v, \Delta\phi$ ) and for many different vertical atmos-pheric profiles (VTP files). As previously (see Section 6.12.5.1), a NN tool is then used to determine these polynomial fits for retrieving the WV over ocean:

$$\begin{aligned}
 WV = & \quad WV\_Ocean\_NoGlint[\theta_s, 0, \theta_v, \Delta\phi, \tau_o^a, w_s] \\
 & + WV\_Ocean\_NoGlint[\theta_s, 1, \theta_v, \Delta\phi, \tau_o^a, w_s] \cdot \log(R_{TOA\_15/14}[\tau_o^a, w_s, \theta_s, \theta_v, \Delta\phi]) \\
 & + WV\_Ocean\_NoGlint[\theta_s, 2, \theta_v, \Delta\phi, \tau_o^a, w_s] \cdot \log^2(R_{TOA\_15/14}[\tau_o^a, w_s, \theta_s, \theta_v, \Delta\phi])
 \end{aligned}$$

Resources:

Estimated CPU time: -

Output disk space:  $27 \times 3 \times 18 \times 25 \times 20 \times 5 \times 4$  bytes/float = 14580000 bytes

The storage of this table is completed with different records for each  $\theta_s$  tabulated value (see [AD-8] for the full description of the output structure).

Acceptance:

Corresponds to the latest definition (or last delivery by the FUB institute).

**6.12.7 (Deleted)**

Reference:

[AD-8] Section 6.12.7

**6.12.8 ADS Polynomial Coefficients for Water-Vapour Retrieval over Clouds**

*6.12.8.1 Polynomial coefficients for water vapour retrieval over clouds*

Reference: WV\_Cloud, LUT123

[AD-8] Section 6.12.8, GADS fields 1, 2 & 3

FUB/ACRI provided

Dependencies:

LUT112, LUT113, LUT114, LUT120, LUT308

Tool:

Neural Network

Procedure:

Inputs:  $\theta_s$  Solar zenith angle [deg], see Section 6.12.4.1, (LUT112)  
 $\theta_v$  View zenith angle [deg], see Section 6.12.4.2, (LUT113)  
 $\Delta\phi$  Relative azimuth angle [deg], see Section 6.12.4.3, (LUT114)

$S_{alb}^o$  Surface albedo [ $dI$ ] (10 values), *see* [Section 6.12.4.9](#) (LUT120)  
 $\tau_o^c$  Cloud optical thickness at 550nm [ $dI$ ] (20 values), *see* [Section 6.12.4.10](#),  
(LUT308)  
 $k$  Polynomial coefficient orders [ $dI$ ],  $k = [0;2]$

Output:  $WV\_Cloud[\theta_s, k, \theta_v, \Delta\phi, S_{alb}^o, \tau_o^c]$   
Polynomial coefficients for water vapour retrieval over clouds  
units:  $[g.cm^{-2}]$

Step: User specified.  
LUT processed at the FUB institute with a NN tool and delivered to ACRI.

Scientific content:

$WV\_Cloud[\theta_s, k, \theta_v, \Delta\phi, S_{alb}^o, \tau_o^c]$  describes the coefficients of the polynomial fit expressing the water vapor content ( $WV$ ) over clouds as function of the ratio of TOA normalized radiances at 900 and 885 nm ( $R_{TOA\_15/14}[\tau_o^c, S_{alb}^o, \theta_s, \theta_v, \Delta\phi]$ ) computed with RTC/MOMO, for each of 20 COT550 ( $\tau_o^c$ ; LUT308), for each of 10 surface albedo ( $S_{alb}^o$ ; LUT120), for each illumination and viewing geometry ( $\theta_s, \theta_v, \Delta\phi$ ) and for many different vertical atmospheric profiles (VTP files). As previously (*see* [Section 6.12.5.1](#)), a NN tool is then used to determine the polynomial fit to retrieve the  $WV$  over clouds:

$$WV = WV\_Cloud[\theta_s, 0, \theta_v, \Delta\phi, S_{alb}^o, \tau_o^c] + WV\_Cloud[\theta_s, 1, \theta_v, \Delta\phi, S_{alb}^o, \tau_o^c] \cdot \log(R_{TOA\_15/14}[\tau_o^c, S_{alb}^o, \theta_s, \theta_v, \Delta\phi]) + WV\_Cloud[\theta_s, 2, \theta_v, \Delta\phi, S_{alb}^o, \tau_o^c] \cdot \log^2(R_{TOA\_15/14}[\tau_o^c, S_{alb}^o, \theta_s, \theta_v, \Delta\phi])$$

Resources:

Estimated CPU time: -  
Output disk space:  $27 \times 3 \times 18 \times 25 \times 10 \times 20 \times 4$  bytes/float = 29160000 bytes

The storage of this table is completed with different records for each  $\theta_s$  tabulated value (*see* [\[AD-8\]](#) for the full description of the output structure). Moreover, within each  $\theta_s$  block the records corresponding to the second  $S_{alb}^o$  are duplicated in each of the last 8  $S_{alb}^o$  values.

Acceptance:

Corresponds to the latest definition (or last delivery by the FUB institute).



## 6.12.9 ADS Surface Albedo Slope between 900 nm and 885 nm

### 6.12.9.1 Surface albedo slope between 900 nm and 885 nm

Reference: Salb\_slope, LUT124

[AD-8] Section 6.12.9, GADS field 1

FUB/ACRI provided

Dependencies:

LUT476, LUT477

Tool:

None

Procedure:

Inputs:     *month*           Month (12 values) [*dl*]  
                  *lat*                Latitude (180 values) [*deg.*], see [Section 6.12.4.12](#), (LUT476)  
                  *long*             Longitude (360 values) [*deg.*], see [Section 6.12.4.13](#), (LUT477)

Output:     *Salb\_slope* [*month, lat, long*]  
                                  Monthly map of surface albedo slope between 900 and 885 nm

units:        [*dl*]

Step:         User specified.

Scientific content:

*Salb\_slope*[*month, lat, long*] describes the monthly surface albedo slope between 900 nm (band#15) and 885 nm (band#14), for an angular grid of 0.05 *deg.* in latitude (*lat*) and in longitude (*long*).

These monthly maps are employed in the water vapour content retrieval algorithm in order to correct the ratio of TOA normalized between MERIS band#15 and #14 for the surface albedo slope effect.

Resources:

Estimated CPU time:    -  
Output disk space:     12 × 3600 × 7200 × 1 byte/uc = 311040000 bytes

Acceptance:

Corresponds to the latest definition (or last delivery by the FUB institute).

## 6.12.10 ADS Aerosol Corrections

### 6.12.10.1 Polynomial coefficients for aerosol corrections at 885 nm

Reference: Aerosol\_wv\_corr, LUT125

[AD-8] Section 6.12.10, GADS fields 1, 2 & 3

FUB/ACRI provided

Dependencies:

LUT112, LUT113, LUT114

Tool:

Neural Network

Procedure:

Inputs:  $\theta_s$  Solar zenith angle [deg], see Section 6.12.4.1, (LUT112)  
 $\theta_v$  View zenith angle [deg], see Section 6.12.4.2, (LUT113)  
 $\Delta\phi$  Relative azimuth angle [deg], see Section 6.12.4.3, (LUT114)  
 $k$  Polynomial coefficient orders [dl],  $k = [0;2]$

Output: *Aerosol\_wv\_corr* [ $\theta_s, \theta_v, \Delta\phi, k$ ]  
 Polynomial coefficients for aerosol corrections at 885 nm

units: [dl]

Step: User specified.  
 LUT processed at the FUB institute with a NN tool and delivered to ACRI.

Scientific content:

*Aerosol\_wv\_corr* [ $\theta_s, \theta_v, \Delta\phi, k$ ] describes the coefficients of the polynomial fit expressing the corrected aerosol optical thicknesses ( $\tau^a$ ) at 885nm (MERIS band #14) as function of the TOA normalized radiances  $L_{TOA\_12}[\theta_s, \theta_v, \Delta\phi]$  and  $L_{TOA\_13}[\theta_s, \theta_v, \Delta\phi]$  computed with the MERIS bands #12 and 13, respectively. These regression coefficients ( $k=[0;2]$ ) depends on the illumination and viewing geometries ( $\theta_s, \theta_v, \Delta\phi$ ). The latters are useful for the aerosol corrections of the retrieved aerosol optical thicknesses ( $\tau^a$ ) at 885nm.

Note: Due to the fact that the MERIS bands #12 and 13 are the nearest ones of the water vapor absorption bands, the total aerosol optical thicknesses ( $\tau^a$ ) at 885nm will can be retrieved from the polynomial fit with an absolute accuracy of 0.03.

As previously (see Section 6.12.5.1), a NN tool is then used to determine the polynomial fit to to retrieve the corrected aerosol optical thicknesses ( $\tau^a$ ) at 885nm:

$$\tau^a = \text{Aerosol\_wv\_LUT}[\theta_s, \theta_v, \Delta\phi, 0] \\ + \text{Aerosol\_wv\_LUT}[\theta_s, \theta_v, \Delta\phi, 1] \cdot L_{TOA\_12}^*[\theta_s, \theta_v, \Delta\phi] \\ + \text{Aerosol\_wv\_LUT}[\theta_s, \theta_v, \Delta\phi, 2] \cdot L_{TOA\_13}^*[\theta_s, \theta_v, \Delta\phi]$$

where  $L_{TOA\_12}[P_s, \theta_s, \theta_v, \Delta\phi]$ ,  $L_{TOA\_13}[P_s, \theta_s, \theta_v, \Delta\phi]$  and  $L_{TOA\_14}[P_s, \theta_s, \theta_v, \Delta\phi]$  are respectively the TOA normalized radiances within the MERIS bands #12, 13 and 14.

Resources:

Estimated CPU time: -  
Output disk space:  $27 \times 3 \times 18 \times 25 \times 4$  bytes/fl = 145800 bytes

The storage of this table is completed with different records for each  $\theta_s$  tabulated value (see [AD-8] for the full description of the output structure).

Acceptance:

Corresponds to the latest definition (or last delivery by the FUB institute).

**6.12.11 ADS Surface Albedo at 885 nm**

6.12.11.1 Surface albedo map at 885 nm

Reference: Salb885, LUT126

[AD-8] Section 6.12.11, GADS field 1

FUB/ACRI provided

Dependencies:

LUT476, LUT477

Tool:

None

Procedure:

Inputs: *month* Month (12 values) [*dl*]  
*lat* Latitude (180 values) [*deg.*], see Section 6.12.4.12, (LUT476)  
*long* Longitude (360 values) [*deg.*], see Section 6.12.4.13, (LUT477)

Output: *Salb885*[*month, lat, long*]  
Monthly map of surface albedo at 885 nm

units: [*dl*]

Scientific content:

*Salb885*[*month, lat, long*] describes the monthly surface albedo at 885 nm (band#14), for an angular grid of 0.05 deg. in latitude (*lat*) and in longitude (*long*).

These monthly maps are employed in the water vapour content retrieval algorithm.

Resources:

Estimated CPU time: -

Output disk space:  $12 \times 3600 \times 7200 \times 1 \text{ byte/uc} = 311040000 \text{ bytes}$

Acceptance:

Corresponds to the latest definition (or last delivery by the FUB institute).

## 6.13 OCEAN-AEROSOL PARAMETERS

All the LUTs from this MERIS ADF can be generated with both the tools from FUB & UdL. Consequently, two different recipes are systematically proposed to generate all these LUTs either with the tools from FUB or with the tools from UdL.

### 6.13.1 C.P.

#### 6.13.1.1 C.P. AOT at 550 nm (boundary layer) for all ocean-aerosol assemblages, $\tau_a^{550}(iaer, itau)$

Reference: tauA1 LUT136

PARBLEU provided

Dependencies:

None

Tool:

None

Procedure:

Input: none

Output: tauA1 Aerosol optical thickness at 550nm for boundary aerosol layer (7 values)  
units: [dl]

Step: User specified.

Scientific content:

Set of 7 AOT550 (tauA1) used in the boundary layer of the 34 aerosol assemblages. Note that the first null tauA1 value is not employed in the LUTs computations but defined to make easy the use of output LUTs in the MERIS processor (IPF).

Current baseline: 34 x 7 values (see table in [Section 6.13.5.1](#))

Resources:

Estimated CPU time: -  
Output disk space: 34 x 7 x 4 bytes/fl = 952 bytes

Acceptance:

Corresponds to the latest definition.

6.13.1.2 C.P. AOT at 550 nm (dust layer) for all ocean-aerosol assemblages,  $\tau_a^{a2}(iaer, itau)$

Reference: tauA2 LUT137

PARBLEU provided

Dependencies:

None

Tool:

None

Procedure:

Input: none

Output: tauA2 Aerosol optical thickness at 550nm for dust aerosol layer (7 values)

units: [dl]

Step: User specified.

Scientific content:

Set of 7 AOT550 (tauA2), the first null value being 0, used in the dust layer of the 34 aerosol assemblages. Note that the first null tauA2 value is not employed in the LUTs computations but defined to make easy the use of output LUTs in the MERIS processor (IPF).

Current baseline: 34 x 7 values (see table in [Section 6.13.5.1](#))

Resources:

Estimated CPU time: -

Output disk space: 34 x 7 x 4 bytes/fl = 952 bytes

Acceptance:

Corresponds to the latest definition.

6.13.1.3 C.P. AOT at 550 nm (troposphere layer) for all ocean-aerosol assemblages,  $\tau_a^{a3}(iaer, itau)$

Reference: tauA3 LUT409

PARBLEU provided

Dependencies:

None

Tool:

None

Procedure:

Input: none

Output: *tauA3* Aerosol optical thickness at 550nm for tropospheric layer (7 values)  
units: [dl]

Step: User specified.

Scientific content:

Set of 7 AOT550 (*tauA3*), the first null value being 0, used in the tropospheric layer of the 34 aerosol assemblages. Note that the first null *tauA3* value is not employed in the LUTs computations but defined to make easy the use of output LUTs in the MERIS processor (IPF).

Current baseline: 34 x 7 values (*see* table in [Section 6.13.5.1](#))

Resources:

Estimated CPU time: -

Output disk space:  $34 \times 7 \times 4$  bytes/fl = 952 bytes

Acceptance:

Corresponds to the latest definition.

6.13.1.4 C.P. FUB-scattering phase matrices and IOPs for all the aerosol models

Reference:  $Q_{sca}$ ,  $Q_{ext}$  &  $SSA[model, \lambda]$  LUT399

Dependencies:

LUT130

Tool:

OTC/MIE (FUB)

Procedure:

Inputs: *model* Aerosol model# [*dl*] (selected among a set of 23 models)  
*λ* MERIS wavelength [*nm*], see Section 6.13.4.1 (LUT130)

Output:  $Q_{sca}[model, \lambda]$ ,  $Q_{ext}[model, \lambda]$  &  $SSA[model, \lambda]$   
Scattering ( $Q_{sca}$ ) and extinction ( $Q_{ext}$ ) coefficients, and single scattering albedo ( $SSA$ ) (referred also as to  $\sigma_s$ ,  $\sigma_e$ ,  $\omega_0$ ) for each of the 23 aerosol models (*model*) used in the 34 assemblages and each of the 15 MERIS spectral bands ( $\lambda$ ).

units:  $[\mu m^{-1}, \mu m^{-1}, dl]$

Step-1: For each of the 23 aerosol model (*model*) used in the ocean-aerosol assemblages, launch the *Mie*'s computations at each of the 15 MERIS wavelengths ( $\lambda$ ) with the OTC/MIE (FUB) and the associated input *Mie* card:

*/FUB/sca\_in/sc\_marxx\_byy, sc\_coaxx\_byy, sc\_rurxx\_byy, sc\_dbdsz\_byy, sc\_dbdwz\_byy,*  
*sc\_IOPww\_byy, sc\_conti\_byy, sc\_H2SO4\_byy*

with  $\mathbf{xx} = \{50, 70, 90, 99\}$  (i.e., relative humidity),  $\mathbf{yy} = \{01, \dots, 15\}$  (i.e., MERIS bands #),  
 $\mathbf{z} = \{1, 2, 3\}$  (i.e., 3 scale heights),  $\mathbf{ww} = \{01, 02, 03\}$  (i.e., 3 Log-normal distributions)

Note: These output *Mie* files will be used as inputs for generating the LUT138 & LUT139, and the LUT142 & LUT143 with the RTC/FUB (MOMO).

Step-2: For each of the 23 aerosol model (*model*) and for each wavelength ( $\lambda$ ), extract from the output *Mie*'s file the IOPs, i.e., the normalized extinction coefficient,  $Q_{ext, norm}(model, \lambda)$  (labelled as "*ex\_norm*"), the single scattering albedo,  $SSA$  or  $\omega_0(model, \lambda)$  (labelled as "*w\_o*") and the extinction coefficient  $Q_{ext, 550}(model)$  at the 550nm reference wavelength (labelled as "*ex\_ref*"), and compute the extinction coefficient  $Q_{ext}(model, \lambda)$  and the scattering coefficient  $Q_{sca}(model, \lambda)$  as follows:

$$Q_{ext}[model, \lambda] = Q_{ext, 550}[model] \cdot Q_{ext, norm}[model, \lambda]$$

$$Q_{sca}[model, \lambda] = \omega_0[model, \lambda] \cdot Q_{ext}[model, \lambda]$$

Step-3: Build the output LUT399 with  $Q_{sca}(model, \lambda)$ ,  $Q_{ext}(model, \lambda)$  and  $\omega_0(model, \lambda)$  respectively for each of the 23 aerosol models (*model*) and each of the 15 MERIS bands ( $\lambda$ ).

Scientific content:

Scattering phase function and IOPs (scattering coefficient, extinction coefficient and single scattering albedo) of the 23 models used in the 34 ocean-aerosol assemblages.

Current baseline: 23 x 15 x 3 values

Resources:



Estimated CPU time:  $23 \times 15 \times (\sim 52 \text{ sec}) = 18197 \text{ sec}$   
Output disk space:  $23 \times 15 \times 3 \times 4 \text{ bytes/fl} = 4140 \text{ bytes}$

Acceptance:

Corresponds to the latest definition.

6.13.1.5 C.P. UdL-scattering phase matrices and IOPs for all the aerosol models

Reference:  $Q_{sca}$ ,  $Q_{ext}$  &  $SSA[model, \lambda]$  LUT419

Dependencies:

LUT130

Tool:

OTC/SCAMAT (UdL)

Procedure:

Inputs:  $model$  Aerosol model# [*dl*] (selected among a set of 23 models)  
 $\lambda$  MERIS wavelength [*nm*], see [Section 6.13.4.1](#) (LUT130)

Output:  $Q_{sca}[model, \lambda]$ ,  $Q_{ext}[model, \lambda]$  &  $SSA[model, \lambda]$   
Scattering ( $Q_{sca}$ ) and extinction ( $Q_{ext}$ ) coefficients, and single scattering albedo ( $SSA$ ) for each of the 17 aerosol models ( $model$ ) used in the 16 SAMs and each of the 15 MERIS spectral bands ( $\lambda$ ).

units:  $[\mu m^{-1}, \mu m^{-1}, dl]$

Step-1: For each of the 17 aerosol model ( $model$ ) used in the 16 SAMs, launch the *Mie*'s computations at each of the 15 MERIS wavelengths ( $\lambda$ ) with the OTC/SCAMAT (UdL) and the associated input *Scamat* card:

*/UdL/INPUT/sca\_in/sc\_marxx\_byy, sc\_coaxx\_byy, sc\_rurxx\_byy, sc\_IOPww\_byy,*  
*sc\_conti\_byy, sc\_H2SO4\_byy*

*with xx = {50, 70, 90, 99} (i.e., relative humidity), yy = {01,...,15} (i.e., MERIS bands #),*  
*ww = {01, 02, 03} (i.e., 3 Log-normal distributions)*

Note: These output *Scamat* files will be used as inputs for generating the LUT138 & LUT139, and the LUT143 with the RTC/UdL (SO).

Step-2: For each of the 17 aerosol model ( $model$ ) and for each wavelength ( $\lambda$ ), extract from the output *Mie*'s file the IOPs, i.e., the normalized extinction coefficient,  $Q_{ext, norm}(model, \lambda)$  (labelled as " $Q_{ext}(\lambda)/Q_{ext}(\lambda_{ref})$ "), the single scattering albedo,  $SSA$  or  $\omega_0(model, \lambda)$  (labelled as " $wo(\lambda)$ ") and the extinction coefficient  $Q_{ext, 550}(model)$  at the reference

wavelength (550nm) (labelled as  $Q_{ext}(\lambda_{ref})$ ), and compute the extinction coefficient  $Q_{ext}(model, \lambda)$  and the scattering coefficient  $Q_{sca}(model, \lambda)$  as follows:

$$Q_{ext}[model, \lambda] = Q_{ext,550}[model] \cdot Q_{ext,norm}[model, \lambda]$$

$$Q_{sca}[model, \lambda] = \omega_o[model, \lambda] \cdot Q_{ext}[model, \lambda]$$

Step-3: Build the output LUT419 with  $Q_{sca}(model, \lambda)$ ,  $Q_{ext}(model, \lambda)$  and  $\omega_o(model, \lambda)$  respectively for each of the 17 aerosol models ( $model$ ) and each of the 15 MERIS bands ( $\lambda$ ).

### Scientific content:

Scattering phase function and IOPs (scattering coefficient, extinction coefficient and single scattering albedo) of the 17 models used in the 16 SAMs (MAR, COA, RUR, BLU-IOP).

Current baseline: 17 x 15 x 3 values

### Resources:

Estimated CPU time: 17 x 15 x (~52 sec) = 13260 sec

Output disk space: 17 x 15 x 3 x 4 bytes/fl = 3060 bytes

#### 6.13.1.6 C.P. TOA normalized radiances, $L_{TOA}(\lambda, \theta_s, \theta_v, \Delta\phi)$

Reference: (no variable used) LUT401

Intermediate results stored in LUTs.

LUT dimension:  $N_{SZA} \times N_{VZA} \times N_{RAA} = 23 \times 13 \times 25$ .

Number of intermediate LUTs:

- with RTC/FUB:  $N_{wvl} \times N_{model} \times N_{aot550} \times N_{ws} = 15 \times 34 \times 6 \times 3$
- with RTC/UdL:  $N_{wvl} \times N_{model} \times N_{aot550} \times N_{ws} = 15 \times 16 \times 6 \times 3$

### Resources:

Estimated CPU time: -

Output disk space:

- with RTC/FUB: 15 x 23 x 13 x 25 x 34 x 6 x 3 x 4 bytes/fl = 274482000 bytes
- with RTC/UdL: 15 x 23 x 13 x 25 x 16 x 6 x 3 x 4 bytes/fl = 129168000 bytes

#### 6.13.1.7 C.P. FUB total and Rayleigh optical thicknesses, $\tau(iaer, type, itau, iband)$

Reference: (no variable used) LUT405

Intermediate results stored in a LUT

LUT dimension:  $N_{model} \times N_{type} \times N_{aot550} \times N_{wvl} = 34 \times 2 \times 6 \times 15$ .

with type being the index used to refer to the total and the *Rayleigh* optical thickness.

Resources:

Estimated CPU time: -

Output disk space:  $34 \times 2 \times 6 \times 15 \times 4$  bytes/fl = 24480 bytes

**6.13.1.8 C.P. Spectral dependence of the AOT (without normalization at reference wavelength),  $f(iaer, \lambda, itau)$**

Reference: (no variable used) LUT408

Intermediate results stored in a LUT:  $\tau_{a\_bl865}$  (LUT139)  $\times$  *specdep* (LUT138)

LUT dimension:  $N_{model} \times N_{wvl} \times N_{aot550} = 34 \times 15 \times 7$ .

Resources:

Estimated CPU time: -

Output disk space:  $34 \times 15 \times 7 \times 4$  bytes/fl = 14280 bytes

**6.13.2 MPH**

Not covered in this document (see [AD-8] for a detailed description)

**6.13.3 SPH**

Not covered in this document (see [AD-8] for a detailed description)

**6.13.4 GADS General**

**6.13.4.1 Nominal wavelengths of the 15 MERIS spectral bands**

Reference: Wvl, LUT130

[AD-8] Section 6.13.4, GADS field 1

ACRI provided

Dependencies:

None

Tool:

None

Procedure:

Input: none

Output: *Wvl* Nominal wavelengths of MERIS spectral bands (15 values)  
units: [nm]

Step: User specified.

Scientific content:

Nominal wavelengths of the 15 MERIS spectral bands

Current baseline: {412.5, 442.5, 490.0, 510.0, 560.0, 620.0, 665.0, 681.25, 708.75, 753.75, 761.875, 778.75, 865.0, 885.0, 900.0} nm

Resources:

Estimated CPU time: -

Output disk space: 15 × 4 bytes/fl = 60 bytes

Acceptance:

Corresponds to the latest definition.

6.13.4.2 (*Spare*)

Reference:

[AD-8] Section 6.13.4, GADS field 2

6.13.4.3 *Solar zenith angles*

Reference: SZA, LUT132

[AD-8] Section 6.13.4, GADS field 3

ACRI provided

Dependencies:

None

Tool:

None

Procedure:

Input: none

Output: *SZA* Solar zenith angle (23 values)

units:  $[10^{-6} \text{ deg}]$

Step: User specified.

Scientific content:

The set of solar zenith angles (SZA) derives from the *Gauss* quadrature used in the RTC/SO (UdL) [RD-1] *Fell, F., and J. Fischer, 2001*. "Numerical simulation of the light field in the atmosphere-ocean system using the matrix-operator method", *Journal of Quantitative Spectroscopy & Radiative Transfer: 69* (3), 351-388.

[RD-2]. The values are listed hereafter:

Current baseline: 23 SZA values ( $\theta_s$ ) selected as the first 23 angles from the *Gauss* quadrature (24 discrete directions including the zenith direction).

| $\theta_s$ [deg.] | $\theta_s$ [deg.] | $\theta_s$ [deg.] | $\theta_s$ [deg.] |
|-------------------|-------------------|-------------------|-------------------|
| 0.000000          | 21.347983         | 43.611442         | 65.877652         |
| 2.840906          | 25.058051         | 47.322394         | 69.588762         |
| 6.521063          | 28.768427         | 51.033390         | 73.299882         |
| 10.222955         | 32.479006         | 54.744420         | 77.011011         |
| 13.929756         | 36.189726         | 58.455477         | 80.722147         |
| 17.638419         | 39.900547         | 62.166556         |                   |

Resources:

Estimated CPU time: -

Output disk space:  $23 \times 4 \text{ bytes/ul} = 92 \text{ bytes}$

Acceptance:

Corresponds to the latest definition.

6.13.4.4 View zenith angles

Reference: VZA, LUT133

[AD-8] Section 6.13.4, GADS field 4

ACRI provided

Dependencies:

None

Tool:

None

Procedure:

Input: none

Output: *VZA* View zenith angle (13 values)  
units:  $[10^{-6} \text{ deg}]$

Step: User specified.

Scientific content:

The set of view zenith angles (VZA) derives from the *Gauss* quadrature used in the RTC/SO (UdL) [RD-1] *Fell, F., and J. Fischer, 2001*. "Numerical simulation of the light field in the atmosphere-ocean system using the matrix-operator method", *Journal of Quantitative Spectroscopy & Radiative Transfer: 69* (3), 351-388.  
[RD-2]. The values are listed hereafter:

Current baseline: 13 VZA values ( $\theta_v$ ) selected as the first 13 angles from the *Gauss* quadrature (24 discrete directions including the zenith direction).

| $\theta_v$ [deg.] | $\theta_v$ [deg.] |
|-------------------|-------------------|
| 0.000000          | 25.058051         |
| 2.840906          | 28.768427         |
| 6.521063          | 32.479006         |
| 10.222955         | 36.189726         |
| 13.929756         | 39.900547         |
| 17.638419         | 43.611442         |
| 21.347983         |                   |

Resources:

Estimated CPU time: -  
Output disk space:  $13 \times 4 \text{ bytes/ul} = 52 \text{ bytes}$

Acceptance:

Corresponds to the latest definition.

#### 6.13.4.5 Relative azimuth angles

Reference: RAA, LUT134

[AD-8] Section 6.13.4, GADS field 5

ACRI provided

Dependencies:

None

Tool:

None

Procedure:

Input: none

Output: RAA Relative azimuth angle (25 values)

units:  $[10^{-6} \text{ deg}]$

Step: User specified.

Scientific content:

The set of the relative azimuth angles ( $\Delta\phi$ ) between illumination and viewing directions is regularly spaced and listed hereafter:

Current baseline: 25 RAA values ( $\Delta\phi$ ) within  $[0;180]$  deg., with a step of 7.5 deg.

|                           |                           |                           |                           |                           |
|---------------------------|---------------------------|---------------------------|---------------------------|---------------------------|
| $\Delta\phi[\text{deg.}]$ | $\Delta\phi[\text{deg.}]$ | $\Delta\phi[\text{deg.}]$ | $\Delta\phi[\text{deg.}]$ | $\Delta\phi[\text{deg.}]$ |
| 0.00                      | 37.50                     | 75.00                     | 112.50                    | 150.00                    |
| 7.50                      | 45.00                     | 82.50                     | 120.00                    | 157.50                    |
| 15.00                     | 52.50                     | 90.00                     | 127.50                    | 165.00                    |
| 22.50                     | 60.00                     | 97.50                     | 135.00                    | 172.50                    |
| 30.00                     | 67.50                     | 105.00                    | 142.50                    | 180.00                    |

Resources:

Estimated CPU time: -

Output disk space:  $25 \times 4 \text{ bytes/ul} = 100 \text{ bytes}$

Acceptance:

Corresponds to the latest definition.

6.13.4.6 *Wind-speeds*

Reference: ws, LUT135

[AD-8] Section 6.13.4, GADS field 6

ACRI provided

Dependencies:

None

Tool:

None.

Procedure:

Input: none

Output: ws Wind-speed just above sea level (3 values)

units:  $[m.s^{-1}]$

Step: User specified.

Scientific content:

Above water surfaces, the wind-speed ( $w_s$ ) is responsible for the surface roughness. The effect of the *air-sea* interface shape on the *Fresnel* reflection and refraction is then modelled according to the statistical description of the wave facet distribution derived by *Cox and Munk* [RD-7]. This surface model assumes an isotropic distribution of the facet slopes independently of the wind orientation, and the surface reflectance only depends on the wind-speed (shadowing effects are not accounted for in the total upwelling radiances). Thus, within the sun glint area this reflectance will be much higher than the one originated from the water body itself.

Since the sun glint area depends on the wave slope distribution, 3 wind-speeds ( $w_s$ ) have been then selected in the algorithm for generating LUT143

Current baseline:  $\{1.5, 5.0, 10\} m.s^{-1}$

Resources:

Estimated CPU time: -



Output disk space: 3 x 4 bytes/fl = 12 bytes

Acceptance:

Corresponds to the latest definition.

6.13.4.7 *Vicarious adjustment gains*

Reference: Vic\_Gain[b], LUT131

[AD-8] Section 6.13.4, GADS field 7

ACRI provided

Dependencies:

None

Tool:

None.

Procedure:

Input: *b* MERIS spectral band# (15 values) *see* [Section 6.13.4.1](#),(LUT130)

Output: *Vic\_Gain[b]* Vicarious adjustment gain (15 values)  
units: [*dl*]

Step: User specified.

Scientific content:

15 vicarious gain values given for the 15 MERIS spectral bands

Current baseline: {0.9868575931, 0.9924236536, 0.9990998507, 1.0003386736, 1.0045168400,  
1.0082343817, 1.0074515343, 1.0063384771, 1.0000000000, 1.0033472776,  
1.0000000000, 1.0000000000, 0.9864488244, 0.9829149246, 1.0000000000}

Resources:

Estimated CPU time: -  
Output disk space: 15 x 4 bytes/fl = 60 bytes

Acceptance:

Corresponds to the latest definition.

#### 6.13.4.8 (spare)

Reference:

[AD-8] Section 6.13.4, GADS field 8

### 6.13.5 GADS Spectral Optical Thickness

#### 6.13.5.1 Spectral dependence factor of the total AOT (with normalization at reference wavelength)

##### 6.13.5.1.1 FUB Recipe

Reference: specdep, LUT138

[AD-8] Section 6.13.5, GADS field 1

Dependencies:

LUT130, LUT136, LUT137, LUT409

Tool:

OTC/MIE

Note: The optical properties (*i.e.*, phase function, extinction and scattering coefficients, and single scattering albedo) for the aerosol models have to be computed with the *Mie's* theory (see [AD-7] for more details).

Procedure:

Inputs:

|             |  |
|-------------|--|
| <i>iaer</i> | Aerosol model # [ <i>dl</i> ] (among the 34 aerosol assemblages)   |
| $\lambda$   | MERIS wavelength [ <i>nm</i> ] (15 values), see Section 6.13.4.1, (LUT130)   |
| $\tau^a$    | Total aerosol optical thickness at 550 <i>nm</i> [ <i>dl</i> ] (7 values, but only the last 6 ones have to be considered), see table below, Section 6.13.1.1 (LUT136), Section 6.13.1.2 (LUT137) and Section 6.13.1.3 (LUT409) |

Output: *Specdep*[*iaer*, $\lambda$ , $\tau^a$ ], referred also as *f*[*iaer*, $\lambda$ , $\tau^a$ ]  
 Spectral dependence of the aerosol optical thickness for each of the 34 aerosol assemblages (*iaer*), for each of the 15 MERIS wavelengths, and for each of the 7 total aerosol optical thicknesses ( $\tau^a$ ) at 550*nm*.

units: [*dl*]

Note: The *Mie's* computations for the different aerosol models have to be performed with the input cards placed in */FUB/sca\_in*. All the input parameters for these calculations are described and defined in [AD-6] and [AD-7], respectively.

Here is an example of an input card for the *Mie's* computations with OTC/MIE (FUB)

|  |      |  |
|--|------|--|
| 'sca out:                                  | '    | sc conti b01.s                               |
| 'wavelength:                               | '    | 412.50                                       |
| 'ref. wavelength:                          | '    | 550.00                                       |
| 'number of angles (n2):                    | '    | 171  |
| 'number of size distributions (N):         | '    | 3  |
| 'real, imag. refrac. index (m i,k i) #1:'  | #1:' | 1.530 0.5000000E-02                          |
| 'ref. refractive index (m r i,k r i) #1:'  | #1:' | 1.530 0.6000000E-02                          |
| 'min_max_step of particles (r0,rf,dr) #1:' | #1:' | 4.7173841954562E-06 0.48141415860349 0.0001  |
| 'size distrib. parameters (ind,a,b) #1:'   | #1:' | 2 0.0050 2.99                                |
| 'volume percentage (n i/n) #1:'            | #1:' | 0.93876773E+00                               |
| 'real, imag. refrac. index (m i,k i) #2:'  | #2:' | 1.530 0.8000000E-02                          |
| 'ref. refractive index (m r i,k r i) #2:'  | #2:' | 1.530 0.8000000E-02                          |
| 'min_max_step of particles (r0,rf,dr) #2:' | #2:' | 4.7173841954562E-04 48.14141586034900 0.0100 |
| 'size distrib. parameters (ind,a,b) #2:'   | #2:' | 2 0.5000 2.99                                |
| 'volume percentage (n i/n) #2:'            | #2:' | 0.00000227E+00                               |
| 'real, imag. refrac. index (m i,k i) #3:'  | #3:' | 1.750 0.4586364E+00                          |
| 'ref. refractive index (m r i,k r i) #3:'  | #3:' | 1.750 0.4387952E+00                          |
| 'min_max_step of particles (r0,rf,dr) #3:' | #3:' | 1.8955848629255E-04 0.28027805069842 0.0001  |
| 'size distrib. parameters (ind,a,b) #3:'   | #3:' | 2 0.0118 2.00                                |
| 'volume percentage (n i/n) #3:'            | #3:' | 0.06123000E+00                               |
| 'volume (1) and particle (2) ratio :       | '    | 2  |

31 aerosol assemblages have been defined and given in the table hereafter. The latter result from different mixtures in aerosol components (*i.e.*, desert dust particles, dust-like particles, oceanic particles, rural aerosol mixtures, soot-like particles, water soluble particles, and H<sub>2</sub>SO<sub>4</sub>) for each of the 3 aerosol layers (boundary, troposphere and stratosphere), which yield to 6 different kinds of aerosol assemblages (*i.e.*, maritime, coastal, rural, dust-BDS, dust-BDW).

3 blue aerosols have been determined with an approach combining the micro-physical properties of these small particles with their inherent optical properties (IOP's) derived from CIMEL measurements acquired over ocean sites [RD-15].

| Aerosols Assemblage |            |       | Boundary Layer | Tropospheric Layer |             |             | Stratosph. Layer               |
|---------------------|------------|-------|----------------|--------------------|-------------|-------------|--------------------------------|
| iaer                | Assemblage | RH(%) | [0-2km]        | [2-5km]            | [5-7km]     | [7-12km]    | [12-50km]                      |
| 0                   | MAR-99     | 99    | Maritime       | -                  | -           | -           | -                              |
| 1                   | MAR-50     | 50    | Maritime       | Continental        | Continental | Continental | H <sub>2</sub> SO <sub>4</sub> |
| 2                   | MAR-70     | 70    | Maritime       | Continental        | Continental | Continental | H <sub>2</sub> SO <sub>4</sub> |
| 3                   | MAR-90     | 90    | Maritime       | Continental        | Continental | Continental | H <sub>2</sub> SO <sub>4</sub> |
| 4                   | MAR-99     | 99    | Maritime       | Continental        | Continental | Continental | H <sub>2</sub> SO <sub>4</sub> |
| 5                   | COA-50     | 50    | Coastal        | Continental        | Continental | Continental | H <sub>2</sub> SO <sub>4</sub> |
| 6                   | COA-70     | 70    | Coastal        | Continental        | Continental | Continental | H <sub>2</sub> SO <sub>4</sub> |
| 7                   | COA-90     | 90    | Coastal        | Continental        | Continental | Continental | H <sub>2</sub> SO <sub>4</sub> |
| 8                   | COA-99     | 99    | Coastal        | Continental        | Continental | Continental | H <sub>2</sub> SO <sub>4</sub> |
| 9                   | RUR-50     | 50    | Rural          | Continental        | Continental | Continental | H <sub>2</sub> SO <sub>4</sub> |
| 10                  | RUR-70     | 70    | Rural          | Continental        | Continental | Continental | H <sub>2</sub> SO <sub>4</sub> |
| 11                  | RUR-90     | 90    | Rural          | Continental        | Continental | Continental | H <sub>2</sub> SO <sub>4</sub> |
| 12                  | RUR-99     | 99    | Rural          | Continental        | Continental | Continental | H <sub>2</sub> SO <sub>4</sub> |

| iaer | Aerosols Assemblage |       | Boundary Layer          | Tropospheric Layer         |                            |                  | Stratosph. Layer |
|------|---------------------|-------|-------------------------|----------------------------|----------------------------|------------------|------------------|
|      | Assemblage          | RH(%) | [0-2km]                 | [2-5km]                    | [5-7km]                    | [7-12km]         | [12-50km]        |
| 13   | MAR-BDS1-1          | 90    | Maritime<br>Dust - BDS1 | Continental<br>-           | Continental<br>-           | Continental<br>- | H2SO4            |
| 14   | MAR-BDS1-2          | 90    | Maritime<br>Dust - BDS1 | Continental<br>Dust - BDS1 | Continental<br>-           | Continental<br>- | H2SO4            |
| 15   | MAR-BDS1-3          | 90    | Maritime<br>Dust - BDS1 | Continental<br>Dust - BDS1 | Continental<br>Dust - BDS1 | Continental<br>- | H2SO4            |
| 16   | MAR-BDS2-1          | 90    | Maritime<br>Dust - BDS2 | Continental<br>-           | Continental<br>-           | Continental<br>- | H2SO4            |
| 17   | MAR-BDS2-2          | 90    | Maritime<br>Dust - BDS2 | Continental<br>Dust - BDS2 | Continental<br>-           | Continental<br>- | H2SO4            |
| 18   | MAR-BDS2-3          | 90    | Maritime<br>Dust - BDS2 | Continental<br>Dust - BDS2 | Continental<br>Dust - BDS2 | Continental<br>- | H2SO4            |
| 19   | MAR-BDS3-1          | 90    | Maritime<br>Dust - BDS3 | Continental<br>-           | Continental<br>-           | Continental<br>- | H2SO4            |
| 20   | MAR-BDS3-2          | 90    | Maritime<br>Dust - BDS3 | Continental<br>Dust - BDS3 | Continental<br>-           | Continental<br>- | H2SO4            |
| 21   | MAR-BDS3-3          | 90    | Maritime<br>Dust - BDS3 | Continental<br>Dust - BDS3 | Continental<br>Dust - BDS3 | Continental<br>- | H2SO4            |
| 22   | MAR-BDW1-1          | 90    | Maritime<br>Dust - BDW1 | Continental<br>-           | Continental<br>-           | Continental<br>- | H2SO4            |
| 23   | MAR-BDW1-2          | 90    | Maritime<br>Dust - BDW1 | Continental<br>Dust - BDW1 | Continental<br>-           | Continental<br>- | H2SO4            |
| 24   | MAR-BDW1-3          | 90    | Maritime<br>Dust - BDW1 | Continental<br>Dust - BDW1 | Continental<br>Dust - BDW1 | Continental<br>- | H2SO4            |
| 25   | MAR-BDW2-1          | 90    | Maritime<br>Dust - BDW2 | Continental<br>-           | Continental<br>-           | Continental<br>- | H2SO4            |
| 26   | MAR-BDW2-2          | 90    | Maritime<br>Dust - BDW2 | Continental<br>Dust - BDW2 | Continental<br>-           | Continental<br>- | H2SO4            |
| 27   | MAR-BDW2-3          | 90    | Maritime<br>Dust - BDW2 | Continental<br>Dust - BDW2 | Continental<br>Dust - BDW2 | Continental<br>- | H2SO4            |
| 28   | MAR-BDW3-1          | 90    | Maritime<br>Dust - BDW3 | Continental<br>-           | Continental<br>-           | Continental<br>- | H2SO4            |
| 29   | MAR-BDW3-2          | 90    | Maritime<br>Dust - BDW3 | Continental<br>Dust - BDW3 | Continental<br>-           | Continental<br>- | H2SO4            |
| 30   | MAR-BDW3-3          | 90    | Maritime<br>Dust - BDW3 | Continental<br>Dust - BDW3 | Continental<br>Dust - BDW3 | Continental<br>- | H2SO4            |
| 31   | BLU-IOP01           | -     | Blue IOP01              | Blue IOP01                 | Blue IOP01                 | Blue IOP01       | Blue IOP01       |
| 32   | BLU-IOP02           | -     | Blue IOP02              | Blue IOP02                 | Blue IOP02                 | Blue IOP02       | Blue IOP02       |
| 33   | BLU-IOP03           | -     | Blue IOP03              | Blue IOP03                 | Blue IOP03                 | Blue IOP03       | Blue IOP03       |

Description of the 34 aerosol assemblages (iaer): 4 maritime aerosol assemblages, 4 coastal aerosol assemblages, and 4 rural aerosol assemblages with 4 relative humidity (RH) values, and 18 dust aerosol assemblages with 3 scale heights, and 3 blue IOP aerosol assemblages.

All *Mie*'s input parameters (spectral refractive indices, particle size distribution, minimum/maximum radii and size increment, mixing ratio) for each aerosol component used in the aerosol models for the 34 assemblages, are fully described in the reference model document [AD-6].

Optical properties (aerosol optical thickness at 550nm) of each aerosol layers (boundary, dust, troposphere, and stratosphere) are summarized in the table below:

| Aerosols Assemblage |            |       | Boundary Layer                 | Dust Layer                   | Tropospheric Layer    | Stratospheric Layer    |
|---------------------|------------|-------|--------------------------------|------------------------------|-----------------------|------------------------|
| <i>iaer</i>         | Assemblage | RH(%) | $\tau_{550, bound}^a$          | $\tau_{550, dust}^a$         | $\tau_{550, tropo}^a$ | $\tau_{550, strato}^a$ |
| 0                   | MAR-99     | 99    | 0.01, 0.03, 0.1, 0.3, 0.5, 0.8 | 0                            | 0                     | 0                      |
| 1                   | MAR-50     | 50    | 0.01, 0.03, 0.1, 0.3, 0.5, 0.8 | 0                            | 0.025                 | 0.005                  |
| 2                   | MAR-70     | 70    | 0.01, 0.03, 0.1, 0.3, 0.5, 0.8 | 0                            | 0.025                 | 0.005                  |
| 3                   | MAR-90     | 90    | 0.01, 0.03, 0.1, 0.3, 0.5, 0.8 | 0                            | 0.025                 | 0.005                  |
| 4                   | MAR-99     | 99    | 0.01, 0.03, 0.1, 0.3, 0.5, 0.8 | 0                            | 0.025                 | 0.005                  |
| 5                   | COA-50     | 50    | 0.01, 0.03, 0.1, 0.3, 0.5, 0.8 | 0                            | 0.025                 | 0.005                  |
| 6                   | COA-70     | 70    | 0.01, 0.03, 0.1, 0.3, 0.5, 0.8 | 0                            | 0.025                 | 0.005                  |
| 7                   | COA-90     | 90    | 0.01, 0.03, 0.1, 0.3, 0.5, 0.8 | 0                            | 0.025                 | 0.005                  |
| 8                   | COA-99     | 99    | 0.01, 0.03, 0.1, 0.3, 0.5, 0.8 | 0                            | 0.025                 | 0.005                  |
| 9                   | RUR-50     | 50    | 0.01, 0.03, 0.1, 0.3, 0.5, 0.8 | 0                            | 0.025                 | 0.005                  |
| 10                  | RUR-70     | 70    | 0.01, 0.03, 0.1, 0.3, 0.5, 0.8 | 0                            | 0.025                 | 0.005                  |
| 11                  | RUR-90     | 90    | 0.01, 0.03, 0.1, 0.3, 0.5, 0.8 | 0                            | 0.025                 | 0.005                  |
| 12                  | RUR-99     | 99    | 0.01, 0.03, 0.1, 0.3, 0.5, 0.8 | 0                            | 0.025                 | 0.005                  |
| 13                  | MAR-BDS1-1 | 90    | 0.05;0.05;0.05;0.05;0.05;0.05  | 0.01; 0.05; 0.2; 0.5; 0.8; 2 | 0.025                 | 0.005                  |
| 14                  | MAR-BDS1-2 | 90    | 0.05;0.05;0.05;0.05;0.05;0.05  | 0.01; 0.05; 0.2; 0.5; 0.8; 2 | 0.025                 | 0.005                  |
| 15                  | MAR-BDS1-3 | 90    | 0.05;0.05;0.05;0.05;0.05;0.05  | 0.01; 0.05; 0.2; 0.5; 0.8; 2 | 0.025                 | 0.005                  |
| 16                  | MAR-BDS2-1 | 90    | 0.05;0.05;0.05;0.05;0.05;0.05  | 0.01; 0.05; 0.2; 0.5; 0.8; 2 | 0.025                 | 0.005                  |
| 17                  | MAR-BDS2-2 | 90    | 0.05;0.05;0.05;0.05;0.05;0.05  | 0.01; 0.05; 0.2; 0.5; 0.8; 2 | 0.025                 | 0.005                  |
| 18                  | MAR-BDS2-3 | 90    | 0.05;0.05;0.05;0.05;0.05;0.05  | 0.01; 0.05; 0.2; 0.5; 0.8; 2 | 0.025                 | 0.005                  |
| 19                  | MAR-BDS3-1 | 90    | 0.05;0.05;0.05;0.05;0.05;0.05  | 0.01; 0.05; 0.2; 0.5; 0.8; 2 | 0.025                 | 0.005                  |
| 20                  | MAR-BDS3-2 | 90    | 0.05;0.05;0.05;0.05;0.05;0.05  | 0.01; 0.05; 0.2; 0.5; 0.8; 2 | 0.025                 | 0.005                  |
| 21                  | MAR-BDS3-3 | 90    | 0.05;0.05;0.05;0.05;0.05;0.05  | 0.01; 0.05; 0.2; 0.5; 0.8; 2 | 0.025                 | 0.005                  |
| 22                  | MAR-BDW1-1 | 90    | 0.05;0.05;0.05;0.05;0.05;0.05  | 0.01; 0.05; 0.2; 0.5; 0.8; 2 | 0.025                 | 0.005                  |
| 23                  | MAR-BDW1-2 | 90    | 0.05;0.05;0.05;0.05;0.05;0.05  | 0.01; 0.05; 0.2; 0.5; 0.8; 2 | 0.025                 | 0.005                  |
| 24                  | MAR-BDW1-3 | 90    | 0.05;0.05;0.05;0.05;0.05;0.05  | 0.01; 0.05; 0.2; 0.5; 0.8; 2 | 0.025                 | 0.005                  |
| 25                  | MAR-BDW2-1 | 90    | 0.05;0.05;0.05;0.05;0.05;0.05  | 0.01; 0.05; 0.2; 0.5; 0.8; 2 | 0.025                 | 0.005                  |
| 26                  | MAR-BDW2-2 | 90    | 0.05;0.05;0.05;0.05;0.05;0.05  | 0.01; 0.05; 0.2; 0.5; 0.8; 2 | 0.025                 | 0.005                  |
| 27                  | MAR-BDW2-3 | 90    | 0.05;0.05;0.05;0.05;0.05;0.05  | 0.01; 0.05; 0.2; 0.5; 0.8; 2 | 0.025                 | 0.005                  |
| 28                  | MAR-BDW3-1 | 90    | 0.05;0.05;0.05;0.05;0.05;0.05  | 0.01; 0.05; 0.2; 0.5; 0.8; 2 | 0.025                 | 0.005                  |
| 29                  | MAR-BDW3-2 | 90    | 0.05;0.05;0.05;0.05;0.05;0.05  | 0.01; 0.05; 0.2; 0.5; 0.8; 2 | 0.025                 | 0.005                  |
| 30                  | MAR-BDW3-3 | 90    | 0.05;0.05;0.05;0.05;0.05;0.05  | 0.01; 0.05; 0.2; 0.5; 0.8; 2 | 0.025                 | 0.005                  |
| 31                  | BLU-IOP01  | -     | 0.01, 0.03, 0.1, 0.3, 0.5, 0.8 | 0                            | 0.025                 | 0.005                  |
| 32                  | BLU-IOP02  | -     | 0.01, 0.03, 0.1, 0.3, 0.5, 0.8 | 0                            | 0.025                 | 0.005                  |
| 33                  | BLU-IOP03  | -     | 0.01, 0.03, 0.1, 0.3, 0.5, 0.8 | 0                            | 0.025                 | 0.005                  |

Aerosol optical thickness at 550 nm for each of the 4 aerosol layers (i.e., boundary, dust, troposphere, and stratosphere) and for each of the 34 aerosol assemblages (iaer). Note that the first null value of AOT-550 for boundary layer is not reported in this table.

Using the spectral dependence in the Mie's inputs (i.e., spectral characteristics of the aerosols) and the aerosol optical thicknesses at 550nm,  $f[iaer, \lambda, \tau^a]$  is then estimated with the following steps:

Step-1: Select each aerosol model among the 23 models used in the 34 ocean-aerosol assemblages, and compute the scattering phase matrix and the IOPs (extinction & scattering coefficients, and single scattering albedo) at each of the 15 MERIS wavelengths ( $\lambda$ ) with the OTC/MIE (FUB) and the associated input Mie card:

*/FUB/sca\_in/sc\_marxx\_byy, sc\_coaxx\_byy, sc\_rurxx\_byy, sc\_dbdsz\_byy, sc\_dbdwz\_byy, sc\_IOPww\_byy, sc\_conti\_byy, sc\_H2SO4\_byy*

with  $\mathbf{xx} = \{50, 70, 90, 99\}$  (i.e., relative humidity),  $\mathbf{yy} = \{01, \dots, 15\}$  (i.e., MERIS bands #),  $\mathbf{z} = \{1, 2, 3\}$  (i.e., 3 scale heights),  $\mathbf{ww} = \{01, 02, 03\}$  (i.e., 3 Log-normal distributions)

Step-2: Determine the extinction coefficient at 865 nm ( $\sigma_{e,865}^{layer}$ ) from OTC/MIE for each of the 4 aerosol layers (layer= boundary, dust, troposphere, or stratosphere).

Step-3: Extract the extinction coefficients  $\sigma_{e,\lambda}^{layer}$  for each of the 4 aerosol layers (layer) and for each of the 15 MERIS wavelengths ( $\lambda$ ).

Step-4: Compute the spectral dependence factor of the total aerosol optical thickness  $\tau^a, f[iaer, \lambda, \tau^a]$ , as follows,

$$f[iaer, \lambda, \tau^a] = \frac{\sum_{layer=1}^4 \tau_{550,layer}^a [iaer, \tau^a] \cdot \frac{\sigma_{e,\lambda}^{layer}}{\sigma_{e,550}^{layer}}}{\sum_{layer=1}^4 \tau_{550,layer}^a [iaer, \tau^a] \cdot \frac{\sigma_{e,865}^{layer}}{\sigma_{e,550}^{layer}}}, \quad \text{with} \quad \tau^a = \sum_{layer=1}^4 \tau_{550,layer}^a$$

$\tau_{550,layer}^a$  is the aerosol optical thickness at 550nm for the aerosol layer layer, and  $\sigma_e^{layer}$  its associated extinction coefficient at the wavelength  $\lambda$  or 550nm or 865nm. Note that the layer values of 1, 2, 3 and 4 correspond respectively to the boundary layer (layer #1 referred also as 'bound'), the dust aerosol layer (layer #2 referred also as 'dust'), the tropospheric aerosol layer (layer #3 referred also as 'tropo') and the stratospheric aerosol layer (layer #4 referred also as 'strato').

**Warning:** Only the last 6  $\tau_{550,layer}^a$  values from LUT136 (Section 6.13.1.1), from LUT137 (Section 6.13.1.2) and from LUT409 (Section 6.13.1.3) are considered for the  $f$  table computation. The fields corresponding to the first AOT value (i.e.,  $\tau_{550,layer}^a = 0$ ) in the  $f$  table are filled with 0 values.

The extinction coefficients for the 4 aerosol layers ('bound', 'dust', 'tropo' and 'strato') are computed with the OTC/MIE and are already normalized at a reference wavelength (here, 550nm), thus  $\sigma_{e,550}^{layer} = 1$ .

Scientific content:

$f[iaer, \lambda, \tau^a]$  describes the spectral dependence of the total aerosol optical thickness, for each of the 34 aerosol assemblages (*iaer*), for each of the 15 MERIS wavelengths ( $\lambda$ ), and for each of the 6 (non-null) pre-selected total aerosol optical thicknesses ( $\tau^a$ ) at 550nm. Values of  $f[iaer, \lambda, \tau^a]$  are normalized to the reference wavelength at 865nm.

The aerosol assemblages are defined as homogeneous mixtures of basic constituents which are assumed to be spherical particles characterized by their complex refractive index at all the wavelengths and their particle size distribution with the microphysical characteristics (see [AD-6] for more details). The extinction (absorption + scattering) coefficients are then computed via the *Mie's* theory, as a function of the aerosol size distribution and the complex refractive index.

The choice of a set of 6 (non-null) pre-selected nominal  $\tau^a$  values at 550nm relies on a better comparison between the aerosol models which also differ with respect to their spectral characteristics. The spectral change in optical thickness of a given assemblage is therefore dependent on the optical thickness specified at 550nm.

Resources:

Estimated CPU time: 3 sec (if LUT399 already generated, otherwise 18200 sec)  
Output disk space:  $34 \times 15 \times 7 \times 4$  bytes/fl = 14280 bytes

Acceptance:

Comparison with another OTC from the LOV institute.

6.13.5.1.2 UdL Recipe

Reference: specdep, LUT138

[AD-8] Section 6.13.5, GADS field 1

Dependencies:

LUT130, LUT136, LUT409

Tool:

OTC/SCAMAT

Note: The optical properties (*i.e.*, phase function, extinction and scattering coefficients, and single scattering albedo) for the aerosol models have to be computed with the *Mie's* theory (see [AD-7] for more details).

Procedure:

Inputs: *iaer* Aerosol model # [*dl*] (16 SAMs [*iaer*#0 + MAR+ COA + RUR + BLU-IOP])  
 $\lambda$  MERIS wavelength [*nm*] (15 values), see Section 6.13.4.1, (LUT130)  
 $\tau^a$  Total aerosol optical thickness at 550*nm* [*dl*] (7 values, but only the last 6 ones has to be considered), see table below, Section 6.13.1.1 (LUT136) and Section 6.13.1.3 (LUT409)

Output: *Specdep*[*iaer*, $\lambda$ , $\tau^a$ ], referred also as *f*[*iaer*, $\lambda$ , $\tau^a$ ]  
Spectral dependence of the aerosol optical thickness for each of the 16 SAMs (*iaer*), for each of the 15 MERIS wavelengths, and for each of the 7 total aerosol optical thicknesses ( $\tau^a$ ) at 550*nm*.

units: [*dl*]

Note: The *Mie*'s computations for the different aerosol models have to be performed with the input cards placed in */UdL/INPUT/sca\_in*. All the input parameters for these calculations are described and defined in [AD-6] and [AD-7], respectively.

Here is an example of an input card for the *Mie*'s computations with OTC/SCAMAT (UdL)

| sc_conti_b01.s                               | Output filename  |
|--|--|
| 412.50                                       | Nominal wavelength (nm)  |
| 550.00                                       | Reference wavelength (nm)  |
| 83   | Number of scattering angles (fixed to 83)  |
| 3  | Number of size distribution (3 max.)   |
| 1.530 0.5000000E-02                          | Refractive index (Re,Im) at nominal wavelength for particle size distribution #1                     |
| 1.530 0.6000000E-02                          | Refractive index (Re,Im) at reference wavelength for particle size distribution #1                   |
| 4.7173841954562E-06 0.48141415860349 0.0001  | Minimum, maximum radii and size increment ( $\mu\text{m}$ ) for particle size distribution #1        |
| 2 0.0050 2.99                                | Index of selected particle size distribution and its 2 parameters, for particle size distribution #1 |
| 0.93876773E+00                               | Component mixing ratio for particle size distribution #1   |
| 1.530 0.8000000E-02                          | Refractive index (Re,Im) at nominal wavelength for particle size distribution #2                     |
| 1.530 0.8000000E-02                          | Refractive index (Re,Im) at reference wavelength for particle size distribution #2                   |
| 4.7173841954562E-04 48.14141586034900 0.0100 | Minimum, maximum radii and size increment ( $\mu\text{m}$ ) for particle size distribution #2        |
| 2 0.5000 2.99                                | Index of selected particle size distribution and its 2 parameters, for particle size distribution #2 |
| 0.00000227E+00                               | Component mixing ratio for particle size distribution #2   |
| 1.750 0.4586364E+00                          | Refractive index (Re,Im) at nominal wavelength for particle size distribution #3                     |
| 1.750 0.4387952E+00                          | Refractive index (Re,Im) at reference wavelength for particle size distribution #3                   |
| 1.8955848629255E-04 0.28027805069842 0.0001  | Minimum, maximum radii and size increment ( $\mu\text{m}$ ) for particle size distribution #3        |
| 2 0.0118 2.00                                | Index of selected particle size distribution and its 2 parameters, for particle size distribution #3 |
| 0.06123000E+00                               | Component mixing ratio for particle size distribution #3   |



The 16 SAMs consist in the maritime (MAR), coastal (COA), rural (RUR) and blue-IOP (BLU) assemblages given in [Section 6.13.5.1.1](#). The latter are referred by *iaer* from #0 to #12 and #31, #32 and #33.

Using the spectral dependence in the *Mie*'s inputs (*i.e.*, spectral characteristics of the aerosols) and the aerosol optical thicknesses at 550nm tabulated in the previous section,  $f[iaer, \lambda, \tau^a]$  is then estimated with the following steps:

Step-1: Select each aerosol model among the 17 models used in the 16 SAMs, and compute the scattering phase matrix and the IOPs (extinction & scattering coefficients, and single scattering albedo) at each of the 15 MERIS wavelengths ( $\lambda$ ) with the OTC/SCAMAT (UdL) and the associated input *Scamat* card:

*/UdL/INPUT/sca\_in/sc\_marxx\_byy, sc\_coaxx\_byy, sc\_rurxx\_byy, sc\_IOPww\_byy,  
sc\_conti\_byy, sc\_H2SO4\_byy*

with  $\mathbf{xx} = \{50, 70, 90, 99\}$  (*i.e.*, relative humidity),  $\mathbf{yy} = \{01, \dots, 15\}$  (*i.e.*, MERIS bands #),  
 $\mathbf{ww} = \{01, 02, 03\}$  (*i.e.*, 3 Log-normal distributions)

Step-2: Determine the extinction coefficient at 865nm ( $\sigma_{e,865}^{layer}$ ) from OTC/SCAMAT for each of the 3 aerosol layers (*layer*= boundary, troposphere, or stratosphere).

Step-3: Extract the extinction coefficients  $\sigma_{e,\lambda}^{layer}$  for each of the 3 aerosol layers (*layer*) and for each of the 15 MERIS wavelengths ( $\lambda$ ).

Step-4: Compute the spectral dependence factor of the total aerosol optical thickness  $\tau^a, f[iaer, \lambda, \tau^a]$ , as follows,

$$f[iaer, \lambda, \tau^a] = \frac{\sum_{layer=1}^3 \tau_{550,layer}^a [iaer, \tau^a] \cdot \frac{\sigma_{e,\lambda}^{layer}}{\sigma_{e,550}^{layer}}}{\sum_{layer=1}^3 \tau_{550,layer}^a [iaer, \tau^a] \cdot \frac{\sigma_{e,865}^{layer}}{\sigma_{e,550}^{layer}}}, \quad \text{with } \tau^a = \sum_{layer=1}^3 \tau_{550,layer}^a$$

$\tau_{550,layer}^a$  is the aerosol optical thickness at 550nm for the aerosol layer *layer*, and  $\sigma_e^{layer}$  its associated extinction coefficient at the wavelength  $\lambda$  or 550nm or 865nm. Note that the *layer* values of 1, 2 and 3 correspond respectively to the boundary layer (*layer* #1 referred also as '*bound*'), the tropospheric aerosol layer (*layer* #2 referred also as '*tropo*') and the stratospheric aerosol layer (*layer* #3 referred also as '*strato*').

**Warning:** Only the last 6  $\tau_{550,layer}^a$  values from LUT136 ([Section 6.13.1.1](#)) and from LUT409 ([Section 6.13.1.3](#)) are considered for the *f* table computation. The fields corresponding to the first AOT value (*i.e.*,  $\tau_{550,layer}^a = 0$ ) in the *f* table are filled with 0 values.

The extinction coefficients for the 3 aerosol layers ('*bound*', '*tropo*' and '*strato*') are computed with the OTC/SCAMAT and are already normalized at a reference wavelength (here, 550nm), thus  $\sigma_{e,550}^{layer} = 1$ .

Note: In order to keep the size of the output LUT as defined in the previous FUB recipe above, the  $f[iaer, \lambda, \tau^a]$  LUT is completed with null values for  $iaer$  from #13 to #30.

Scientific content:

$f[iaer, \lambda, \tau^a]$  describes the spectral dependence of the total aerosol optical thickness, for each of the 16 SAMs ( $iaer$ ), for each of the 15 MERIS wavelengths ( $\lambda$ ), and for each of the 6 (non-null) pre-selected total aerosol optical thicknesses ( $\tau^a$ ) at 550nm. Values of  $f[iaer, \lambda, \tau^a]$  are normalized to the reference wavelength at 865nm.

Resources:

Estimated CPU time: 3 sec (if LUT419 already generated, otherwise 13263 sec)  
Output disk space:  $34 \times 15 \times 7 \times 4$  bytes/fl = 14280 bytes

Acceptance:

Comparison with another OTC from the LOV institute.

### 6.13.6 GADS Aerosol Optical Thickness at 865 nm

#### 6.13.6.1 Aerosol optical thickness at 865 nm, $\tau^a_{865}(iaer, \tau^a)$

##### 6.13.6.1.1 FUB Recipe

Reference:  $\tau_a\_bl865$ , LUT139

[AD-8] Section 6.13.6, GADS field 1

Dependencies:

LUT136, LUT137, LUT409

Tool:

OTC/MIE

Note: The optical properties (*i.e.*, phase function, extinction and scattering coefficients, and single scattering albedo) for the aerosol models have to be computed with the *Mie's* theory (see [AD-7] for more details).

Procedure:

Inputs:  $iaer$  Aerosol assemblage # [ $dI$ ] (among the 34 aerosol assemblages)  
 $\tau^a$  Aerosol optical thickness at 550nm [ $dI$ ] for the boundary layer (aerosol layer #1), see Section 6.13.1.1 (LUT136)

|             |  |
|-------------|--|
| $\tau^{a2}$ | Aerosol optical thickness at 550nm [dl] for the dust layer (aerosol layer #2), see Section 6.13.1.2 (LUT137)   |
| $\tau^{a3}$ | Aerosol optical thickness at 550nm [dl] for the tropospheric layer (aerosol layer #3), see Section 6.13.1.3 (LUT409)   |
| $\tau^{a4}$ | Aerosol optical thickness at 550nm [dl] for the stratospheric layer (aerosol layer #4) fixed to 0.005 whatever the wavelength and the assemblage except for the first one (iaer#0, $\tau^{a4} = 0$ ) |

Output:  $\tau_{a\_bl865}[iaer, \tau^a]$ , referred also as  $\tau_{865}^a [iaer, \tau^a]$   
Aerosol optical thickness at 865nm for each of the 34 aerosol assemblages (iaer) and for each aerosol optical thickness ( $\tau^a$ ) at 550nm.

units: [dl]

$\tau_{865}^a [iaer, \tau^a]$  is computed as the sum of the products between the aerosol optical thickness  $\tau_{550, layer}^a [iaer, \tau^a]$  at 550nm and the extinction coefficients ratio ( $\sigma_{e,865}^{layer} / \sigma_{e,550}^{layer}$ ), describing the spectral dependence of the aerosol model, for each of the 4 aerosol layers (layer) (i.e., boundary, dust, troposphere and stratosphere). This calculation is achieved with the following steps:

Step-1: Select each aerosol model among the 23 models used in the 34 ocean-aerosol assemblages, and compute the scattering phase matrix and the IOPs (extinction & scattering coefficients, and single scattering albedo) at each of the 15 MERIS wavelengths ( $\lambda$ ) with the OTC/MIE (FUB) and the associated input Mie card:

*/FUB/sca\_in/sc\_marxx\_byy, sc\_coaxx\_byy, sc\_rurxx\_byy, sc\_dbdsz\_byy, sc\_dbdwz\_byy,  
sc\_IOPww\_byy, sc\_conti\_byy, sc\_H2SO4\_byy*

with  $\mathbf{xx} = \{50, 70, 90, 99\}$  (i.e., relative humidity),  $\mathbf{yy} = \{01, \dots, 15\}$  (i.e., MERIS bands #),  
 $\mathbf{z} = \{1, 2, 3\}$  (i.e., 3 scale heights),  $\mathbf{ww} = \{01, 02, 03\}$  (i.e., 3 Log-normal distributions)

Step-2: Extract the extinction coefficients at 865nm ( $\sigma_{e,865}^{model}$ ) and 550nm ( $\sigma_{e,550}^{model}$ ) from the 4 aerosol models, and compute  $\tau_{865}^a [iaer, \tau^a]$ , the total optical thickness at 865nm, as follows,

$$\tau_{865}^a [iaer, \tau^a] = \sum_{layer=1}^4 \tau_{550, layer}^a [iaer, \tau_{550}^a] \cdot \frac{\sigma_{e,865}^{layer}}{\sigma_{e,550}^{layer}}$$

$$\text{with } \tau^a = \sum_{layer=1}^4 \tau_{550, layer}^a = \tau_{550, bound}^a + \tau_{550, dust}^a + \tau_{550, tropo}^a + \tau_{550, strato}^a$$

where  $\tau_{550, bound}^a, \tau_{550, dust}^a, \tau_{550, tropo}^a, \tau_{550, strato}^a$  correspond to  $\tau^{a1}, \tau^{a2}, \tau^{a3}, \tau^{a4}$ , respectively.

**Warning:** Only the last 6  $\tau_{550, layer}^a$  values from LUT136 (Section 6.13.1.1), from LUT137 (Section 6.13.1.2) and from LUT409 (Section 6.13.1.3) are considered for the  $\tau_{865}^a$  table computation. The fields corresponding to the first AOT value (i.e.,  $\tau_{550, layer}^a = 0$ ) in the  $\tau_{865}^a$  table are filled with 0 values.

Scientific content:

$\tau_{865}^a$  [*iaer*,  $\tau^a$ ] describes the aerosol optical thickness at 865nm for the whole atmosphere (0–50km), for each of the 34 aerosol assemblages (*iaer*) and for each of the 6 (non null) total aerosol optical thicknesses ( $\tau^a$ ) at 550nm, from which depends the aerosol *mixing ratio*. This reference table is required due to the fact that the AOTs are normalized to the 865nm wavelength.

Resources:

Estimated CPU time: 1 sec (if LUT399 already generated, otherwise 18198 sec)  
Output disk space:  $34 \times 7 \times 4$  bytes/fl = 952 bytes

Acceptance:

Comparison with another OTC from the LOV institute.

6.13.6.1.2 UdL Recipe

Reference:  $\tau_{a\_bl865}$ , LUT139

[AD-8] Section 6.13.6, GADS field 1

Dependencies:

LUT136, LUT409

Tool:

OTC/SCAMAT

Note: The optical properties (*i.e.*, phase function, extinction and scattering coefficients, and single scattering albedo) for the aerosol models have to be computed with the *Mie's* theory (*see* [AD-7] for more details).

Procedure:

Inputs: *iaer* Aerosol assemblage # [*dl*] (16 SAMs [*iaer*#0+MAR+COA+RUR+BLU-IOP])  
 $\tau^{a1}$  Aerosol optical thickness at 550nm [*dl*] for the boundary layer (aerosol layer #1), *see* Section 6.13.1.1 (LUT136)  
 $\tau^{a2}$  Aerosol optical thickness at 550nm [*dl*] for the tropospheric layer (aerosol layer #3), *see* Section 6.13.1.3 (LUT409)  
 $\tau^{a3}$  Aerosol optical thickness at 550nm [*dl*] for the stratospheric layer (aerosol layer #4) fixed to 0.005 whatever the wavelength and the assemblage except for the first one (*iaer*#0,  $\tau^{a4} = 0$ )

Output:  $\tau_{a\_bl865}[iaer, \tau^a]$ , referred also as  $\tau_{865}^a [iaer, \tau^a]$   
Aerosol optical thickness at 865 nm for each of the 16 SAMs (*iaer*) and for each aerosol optical thickness ( $\tau^a$ ) at 550 nm.

units: [dl]

$\tau_{865}^a [iaer, \tau^a]$  is computed as the sum of the products between the aerosol optical thickness  $\tau_{550, layer}^a [iaer, \tau^a]$  at 550 nm and the extinction coefficients ratio ( $\sigma_{e,865}^{layer} / \sigma_{e,550}^{layer}$ ), describing the spectral dependence of the aerosol model, for each of the 3 aerosol layers (*layer*) (i.e., boundary, troposphere and stratosphere). This calculation is achieved with the following steps:

Step-1: Select each aerosol model among the 17 models used in the 16 SAMs, and compute the scattering phase matrix and the IOPs (extinction & scattering coefficients, and single scattering albedo) at each of the 15 MERIS wavelengths ( $\lambda$ ) with the OTC/SCAMAT (UdL) and the associated input *Scamat* card:

*/UdL/INPUT/sca\_in/sc\_marxx\_byy, sc\_coaxx\_byy, sc\_rurxx\_byy, sc\_IOPww\_byy, sc\_conti\_byy, sc\_H2SO4\_byy*

with  $\mathbf{xx} = \{50, 70, 90, 99\}$  (i.e., relative humidity),  $\mathbf{yy} = \{01, \dots, 15\}$  (i.e., MERIS bands #),  $\mathbf{ww} = \{01, 02, 03\}$  (i.e., 3 Log-normal distributions)

Step-2: Extract the extinction coefficients at 865 nm ( $\sigma_{e,865}^{model}$ ) and 550 nm ( $\sigma_{e,550}^{model}$ ) for each of the 3 aerosol layers (*layer*), and compute  $\tau_{865}^a [iaer, \tau^a]$ , the total optical thickness at 865 nm, as follows,

$$\tau_{865}^a [iaer, \tau^a] = \sum_{layer=1}^3 \tau_{550, layer}^a [iaer, \tau_{550}^a] \cdot \frac{\sigma_{e,865}^{layer}}{\sigma_{e,550}^{layer}}$$

$$\text{with } \tau^a = \sum_{layer=1}^3 \tau_{550, layer}^a = \tau_{550, bound}^a + \tau_{550, tropo}^a + \tau_{550, strato}^a$$

where  $\tau_{550, bound}^a, \tau_{550, tropo}^a, \tau_{550, strato}^a$  correspond to  $\tau^{a1}, \tau^{a2}, \tau^{a3}$ , respectively.

**Warning:** Only the last 6  $\tau_{550, layer}^a$  values from LUT136 (Section 6.13.1.1) and from LUT409 (Section 6.13.1.3) are considered for the  $\tau_{865}^a$  table computation. The fields corresponding to the first AOT value (i.e.,  $\tau_{550, layer}^a = 0$ ) in the  $\tau_{865}^a$  table are filled with 0 values.

**Note:** In order to keep the size of the output LUT as defined in the previous FUB recipe above, the  $\tau_{865}^a [iaer, \tau^a]$  LUT is completed with null values for *iaer* from #13 to #30.

### Scientific content:

$\tau_{865}^a [iaer, \tau^a]$  describes the aerosol optical thickness at 865 nm for the whole atmosphere (0 - 50 km), for each of the 16 SAMs (*iaer*) and for each of the 6 (non null) total aerosol optical thicknesses ( $\tau^a$ ) at

550nm, from which depends the aerosol *mixing ratio*. This reference table is required due to the fact that the aerosol optical properties are normalized to the 865nm wavelength.

Resources:

Estimated CPU time: 1 sec (if LUT419 already generated, otherwise 13261 sec)  
Output disk space: 34 × 7 × 4 bytes/fl = 952 bytes

Acceptance:

Comparison with another OTC from the LOV institute.

### 6.13.7 GADS Aerosol Single Scattering Albedo

#### 6.13.7.1 Aerosol single scattering albedo, $\omega_o^a(iaer, \lambda)$

##### 6.13.7.1.1 FUB Recipe

Reference:  $\omega_a$ tab\_LUT, LUT140

[AD-8] Section 6.13.7, GADS field 1

Dependencies:

LUT130

Tool:

OTC/MIE

Note: The optical properties (*i.e.*, phase function, extinction and scattering coefficients, and single scattering albedo) for the aerosol models have to be computed with the *Mie's* theory (*see* [AD-7] for more details).

Procedure:

Inputs:  $iaer$  Aerosol model # [dl] (among the 34 aerosol assemblages)  
 $\lambda$  MERIS wavelength [nm] (15 values), *see* Section 6.13.4.1, (LUT130)

Output:  $\omega_a$ tab\_LUT[ $iaer, \lambda$ ], referred also as  $\omega_o^a[iaer, \lambda]$   
Aerosol single scattering albedo for each of the 34 aerosol assemblages ( $iaer$ ) and for each of the 15 MERIS wavelengths ( $\lambda$ ).

units: [dl]

Note: The *Mie*'s computations for the different aerosol models have to be performed with the input cards placed in */FUB/sca\_in*. All the input parameters for these calculations are described and defined in [AD-6] and [AD-7], respectively.

Step-1: Select each aerosol model among the 23 models used in the 34 ocean-aerosol assemblages, and compute the scattering phase matrix and the IOPs (extinction & scattering coefficients, and single scattering albedo) at each of the 15 MERIS wavelengths ( $\lambda$ ) with the OTC/MIE (FUB) and the associated input *Mie* card:

*/FUB/sca\_in/sc\_marxx\_byy, sc\_coaxx\_byy, sc\_rurxx\_byy, sc\_dbdsz\_byy, sc\_dbdwz\_byy,*  
*sc\_IOPww\_byy, sc\_conti\_byy, sc\_H2SO4\_byy*

with  $\mathbf{xx} = \{50, 70, 90, 99\}$  (i.e., relative humidity),  $\mathbf{yy} = \{01, \dots, 15\}$  (i.e., MERIS bands #),  
 $\mathbf{z} = \{1, 2, 3\}$  (i.e., 3 scale heights),  $\mathbf{ww} = \{01, 02, 03\}$  (i.e., 3 Log-normal distributions)

Step-2: Determine the single scattering albedo  $\omega_0^a[iaer, \lambda]$  for each of the 34 aerosol assemblages (*iaer*) and for each of the 15 MERIS wavelengths ( $\lambda$ ), by combining the different aerosol components in each of the 4 aerosol layers (as defined according to WCRP or *Shettle and Fenn (1979)* [RD-8], see also [AD-6] for more details) and their optical properties (i.e., extinction / scattering coefficients and single scattering albedo) for the boundary, dust, tropospheric and stratospheric layers.

The single scattering albedo ( $\omega_0$ ) is defined as the ratio between the scattering (*b*) and the extinction (*c*) coefficient.  $\omega_0^a[iaer, \lambda]$  will then be computed as the ratio of a weighted average on the scattering to a weighted average on the extinction. The weighting factor is defined by the optical thickness. As an example, for an aerosol assemblage composed with the aerosol models  $a_1$  (boundary layer),  $a_2$  (dust layer),  $a_3$  (troposphere) and  $a_4$  (stratosphere) for which the optical thicknesses are respectively  $\tau^{a1}$ ,  $\tau^{a2}$ ,  $\tau^{a3}$  and  $\tau^{a4}$  the scattering coefficients  $b_1$ ,  $b_2$ ,  $b_3$  and  $b_4$  and the extinction coefficients  $c_1$ ,  $c_2$ ,  $c_3$  and  $c_4$ , the resulting single scattering albedo  $\omega_0$  will be:

$$\omega_0 = \frac{\sum_{k=1}^4 b_k \cdot \tau^{a_k}}{\sum_{k=1}^4 c_k \cdot \tau^{a_k}}$$

For the computation,  $\tau^{a1}$  and  $\tau^{a2}$  will be selected as the 5<sup>th</sup> value in the set of 7 AOT550 respectively for the boundary and the dust layer (LUT136 & LUT137).

Note that the  $\omega_0$  values have to be positive and lower or equal to 1.

### Scientific content:

$\omega_0^a[iaer, \lambda]$  describes the aerosol single scattering albedo for the whole atmosphere (0 - 50km), for each of the 34 aerosol assemblages (*iaer*) and for each of the 15 MERIS wavelengths ( $\lambda$ ). This table is required for the atmospheric correction algorithm over ocean.

Resources:

Estimated CPU time: 1 *sec* (if LUT399 already generated, otherwise 18198 *sec*)  
Output disk space: 34 × 15 × 4 bytes/fl = 2040 bytes

Acceptance:

Comparison with another OTC from the LOV institute.

6.13.7.1.2 UdL Recipe

Reference:  $\omega_a$ tab\_LUT, LUT140

[AD-8] Section 6.13.7, GADS field 1

Dependencies:

LUT130

Tool:

OTC/SCAMAT

Note: The optical properties (*i.e.*, phase function, extinction and scattering coefficients, and single scattering albedo) for the aerosol models have to be computed with the *Mie's* theory (*see* [AD-7] for more details).

Procedure:

Inputs: *iaer* Aerosol model # [*dl*] (16 SAMs [*iaer*#0 + MAR+ COA + RUR + BLU-IOP])  
 $\lambda$  MERIS wavelength [*nm*] (15 values), *see* Section 6.13.4.1, (LUT130)

Output:  $\omega_a$ tab\_LUT[*iaer*, $\lambda$ ], referred also as  $\omega_o^a$ [*iaer*, $\lambda$ ]  
Aerosol single scattering albedo for each of the 16 SAMs (*iaer*) and for each of the 15 MERIS wavelengths ( $\lambda$ ).

units: [*dl*]

Step-1: Select each aerosol model among the 17 models used in the 16 SAMs, and compute the scattering phase matrix and the IOPs (extinction & scattering coefficients, and single scattering albedo) at each of the 15 MERIS wavelengths ( $\lambda$ ) with the OTC/SCAMAT (UdL) and the associated input *Scamat* card:

*/UdL/INPUT/sca\_in/sc\_marxx\_byy, sc\_coaxx\_byy, sc\_rurxx\_byy, sc\_IOPww\_byy,  
sc\_conti\_byy, sc\_H2SO4\_byy*

*with xx = {50, 70, 90, 99} (i.e., relative humidity), yy = {01,...,15} (i.e., MERIS bands #),  
ww = {01, 02, 03} (i.e., 3 Log-normal distributions)*



Step-2: Determine the single scattering albedo  $\omega_0^a[iaer, \lambda]$  for each of the 16 SAMs (*iaer*) and for each of the 15 MERIS wavelengths ( $\lambda$ ), by combining the different aerosol components in each of the 3 aerosol layers and their optical properties (*i.e.*, extinction / scattering coefficients and single scattering albedo) for the boundary, dust, tropospheric and stratospheric layers.

$\omega_0^a[iaer, \lambda]$  is then computed as the ratio of a weighted average on the scattering to a weighted average on the extinction. For an aerosol assemblage composed with the aerosol models  $a_1$  (boundary layer),  $a_2$  (troposphere) and  $a_3$  (stratosphere) for which the optical thicknesses are respectively  $\tau^{a1}$ ,  $\tau^{a2}$  and  $\tau^{a3}$ , the scattering coefficients  $b_1$ ,  $b_2$  and  $b_3$  and the extinction coefficients  $c_1$ ,  $c_2$  and  $c_3$ , the resulting single scattering albedo  $\omega_0$  is computed as:

$$\omega_0 = \frac{\sum_{k=1}^3 b_k \cdot \tau^{a_k}}{\sum_{k=1}^3 c_k \cdot \tau^{a_k}}$$

For the computation,  $\tau^{a1}$  will be selected as the 5<sup>th</sup> value in the set of 7 AOT550 for the boundary layer (LUT136).

Note that the  $\omega_0$  values have to be positive and lower or equal to 1.

Note: In order to keep the size of the output LUT as defined in the previous FUB recipe above, the  $\omega_0^a [iaer, \lambda]$  LUT is completed with null values for *iaer* from #13 to #30.

### Scientific content:

$\omega_0^a[iaer, \lambda]$  describes the aerosol single scattering albedo for the whole atmosphere (0 - 50km), for each of the 16 SAMs (*iaer*) and for each of the 15 MERIS wavelengths ( $\lambda$ ). This table is required for the atmospheric correction algorithm over ocean.

### Resources:

Estimated CPU time: 1 sec (if LUT419 already generated, otherwise 13261 sec)  
Output disk space:  $34 \times 15 \times 4$  bytes/fl = 2040 bytes

### Acceptance:

Comparison with another OTC from the LOV institute.

## 6.13.8 GADS Aerosol Forward Scattering Proportion

### 6.13.8.1 Aerosol forward scattering proportion, $fp^a(iaer, \lambda)$

#### 6.13.8.1.1 FUB Recipe

Reference:  $f_{atab\_LUT}$ , LUT141

[AD-8] Section 6.13.8, GADS field 1

#### Dependencies:

LUT130

#### Tools:

OTC/MIE  
OTC/SCFP\_2

Note: The optical properties (*i.e.*, phase function, extinction and scattering coefficients, and single scattering albedo) for the aerosol models have to be computed with the *Mie's* theory (*see* [AD-7] for more details).

The OTC/SCFP\_2 allows one to compute the aerosol forward scattering proportion using aerosol optical properties generated with the OTC/MIE.

#### Procedure:

Inputs:  $iaer$  Aerosol model # [ $dl$ ](among the 34 aerosol assemblages)  
 $\lambda$  MERIS wavelength [ $nm$ ] (15 values), *see* Section 6.13.4.1, (LUT130)

Output:  $f_{atab\_LUT}[iaer, \lambda]$ , referred also as  $f_a[iaer, \lambda]$   
aerosol forward scattering proportion for each of the 34 aerosol assemblages ( $iaer$ ) and for each of the 15 MERIS wavelengths ( $\lambda$ ).

units: [ $dl$ ]

Note: The *Mie's* computations for the different aerosol models have to be performed with the input cards placed in **/FUB/sca\_in**. All the input parameters for these calculations are described and defined in [AD-6] and [AD-7], respectively.

Step-1: Select each aerosol model among the 23 models used in the 34 ocean-aerosol assemblages, and compute the scattering phase matrix and the IOPs (extinction & scattering coefficients, and single scattering albedo) at each of the 15 MERIS wavelengths ( $\lambda$ ) with the OTC/MIE (FUB) and the associated input *Mie* card:

**/FUB/sca\_in/sc\_marxx\_byy, sc\_coaxx\_byy, sc\_rurxx\_byy, sc\_dbdsz\_byy, sc\_dbdwz\_byy,  
sc\_IOPww\_byy, sc\_conti\_byy, sc\_H2SO4\_byy**

with  $xx = \{50, 70, 90, 99\}$  (*i.e.*, relative humidity),  $yy = \{01, \dots, 15\}$  (*i.e.*, MERIS bands #),  
 $z = \{1, 2, 3\}$  (*i.e.*, 3 scale heights),  $ww = \{01, 02, 03\}$  (*i.e.*, 3 Log-normal distributions)

Step-2: Build the '*scpf.ein*' file with the list of aerosol models, launch the computations of the aerosol forward scattering proportion for each aerosol models with the OTC/SCFP\_2, and save results in an output file namely '*ae\_fp.d*'.

Step-3: Determine the forward scattering proportion  $f_a[iaer, \lambda]$  for each of the 34 aerosol assemblages (*iaer*) and for each of the 15 MERIS wavelengths ( $\lambda$ ), by combining the different aerosol components in each of the 4 aerosol layers (as defined according to WCRP or *Shettle and Fenn (1979)* [RD-8], see also [AD-6] for more details).

The forward scattering proportion ( $f_a$ ) is defined as the sum of the individual forward scattering probabilities of the aerosol models in the 4 aerosol layers weighted by their associated optical thicknesses. As an example, for an aerosol assemblage composed with the aerosol models  $a_1$  (boundary layer),  $a_2$  (dust layer),  $a_3$  (troposphere) and  $a_4$  (stratosphere) for which the optical thicknesses are respectively  $\tau^{a1}$ ,  $\tau^{a2}$ ,  $\tau^{a3}$  &  $\tau^{a4}$  and the forward scattering probabilities  $f_{a_1}$ ,  $f_{a_2}$ ,  $f_{a_3}$  &  $f_{a_4}$ , the resulting forward scattering proportion  $f_a$  will be:

$$f_a = \frac{\sum_{k=1}^4 f_{a_k} \cdot \tau^{a_k}}{\sum_{k=1}^4 \tau^{a_k}}$$

For the computation,  $\tau^{a1}$  and  $\tau^{a2}$  will be selected as the 5<sup>th</sup> value in the set of 7 AOT550 respectively for the boundary and the dust layer (LUT136 & LUT137).

Note that the  $f_a$  values have to be positive and lower or equal to 1.

### Scientific content:

$f_a[iaer, \lambda]$  describes the aerosol forward scattering proportion for the whole atmosphere (0 - 50km), for each of the 34 aerosol assemblages (*iaer*) and for each of the 15 MERIS wavelengths ( $\lambda$ ). This table is required for the atmospheric correction algorithm over ocean.

### Resources:

Estimated CPU time: 2 sec (if LUT399 already generated, otherwise 64808 sec)  
Output disk space:  $34 \times 15 \times 4$  bytes/fl = 2040 bytes

### Acceptance:

Comparison with another computations should have be done.

#### 6.13.8.1.2 UdL Recipe

Reference:  $f_a$ tab\_LUT, LUT141

[AD-8] Section 6.13.8, GADS field 1

Dependencies:

LUT130

Tools:

OTC/SCAMAT  
OTC/COMPUTE\_FSP

Note: The optical properties (*i.e.*, phase function, extinction and scattering coefficients, and single scattering albedo) for the aerosol models have to be computed with the *Mie's* theory (*see* [AD-7] for more details).

The OTC/COMPUTE\_FSP allows one to compute the aerosol forward scattering proportion using aerosol optical properties generated with the OTC/SCAMAT.

Procedure:

Inputs: *iaer* Aerosol model # [*dl*] (16 SAMs [*iaer*#0 + MAR+ COA + RUR + BLU-IOP])  
*λ* MERIS wavelength [*nm*] (15 values), *see* Section 6.13.4.1, (LUT130)

Output: *f<sub>a</sub>tab\_LUT[iaer,λ]*, referred also as *f<sub>a</sub>[iaer,λ]*  
Aerosol forward scattering proportion for each of the 16 SAMs (*iaer*) and for each of the 15 MERIS wavelengths (*λ*).

units: [*dl*]

Step-1: Select each aerosol model among the 17 models used in the 16 SAMs, and compute the scattering phase matrix and the IOPs (extinction & scattering coefficients, and single scattering albedo) at each of the 15 MERIS wavelengths (*λ*) with the OTC/SCAMAT (UdL) and the associated input *Scamat* card:

*/UdL/INPUT/sca\_in/sc\_marxx\_byy, sc\_coaxx\_byy, sc\_rurxx\_byy, sc\_IOPww\_byy, sc\_conti\_byy, sc\_H2SO4\_byy*

with *xx* = {50, 70, 90, 99} (*i.e.*, relative humidity), *yy* = {01,...,15} (*i.e.*, MERIS bands #), *ww* = {01, 02, 03} (*i.e.*, 3 Log-normal distributions)

Step-2: Compute the aerosol forward scattering proportion for each of all the aerosol models with OTC/COMPUTE\_FSP by using as input the *Scamat* output files from step-1.

Step-3: For each of the 16 SAMs (*iaer*) and each of the 15 MERIS wavelengths (*λ*), extract from the output files generated with OTC/COMPUTE\_FSP the aerosol forward scattering proportion *f<sub>a</sub>[k,λ]* (value at *θ*=0 *deg.*) for each of the 3 models (*k*) used in the boundary, tropospheric and stratospheric layers, then compute the forward scattering proportion *f<sub>a</sub>[iaer,λ]* as:

$$f_a = \frac{\sum_{k=1}^3 f_{a_k} \cdot \tau^{a_k}}{\sum_{k=1}^3 \tau^{a_k}}$$

where  $\tau^{a_k}$  is the associated optical thicknesses with the aerosol model ( $k$ ).

$$f_a = \frac{\sum_{k=1}^3 f_{a_k} \cdot \tau^{a_k}}{\sum_{k=1}^3 \tau^{a_k}}$$

For the computation,  $\tau^{a_l}$  will be selected as the 5<sup>th</sup> value in the set of 7 AOT550 for the boundary layer (LUT136).

Note that the  $f_a$  values have to be positive and lower or equal to 1.

Note: In order to keep the size of the output LUT as defined in the previous FUB recipe above, the  $f_a \text{tab\_LUT}[iaer, \lambda]$  LUT is completed with null values for  $iaer$  from #13 to #30.

#### Scientific content:

$f_a[iaer, \lambda]$  describes the aerosol forward scattering proportion for the whole atmosphere (0–50 km), for each of the 16 SAMs ( $iaer$ ) and for each of the 15 MERIS wavelengths ( $\lambda$ ). This table is required for the atmospheric correction algorithm over ocean.

#### Resources:

Estimated CPU time: 2 sec (if LUT419 already generated, otherwise 45902 sec)  
Output disk space:  $34 \times 15 \times 4$  bytes/fl = 2040 bytes

#### Acceptance:

Comparison with another computations should have be done.

### **6.13.9 GADS Blue TOA Reflectance Threshold - ROGC**

#### *6.13.9.1 Threshold on the glint corrected blue TOA reflectance $\rho_{GC}(412.5)$*

Reference:  $\rho_{GC\text{thresh\_LUT}}$ , LUT142

[AD-8] Section 6.13.9, ADSR field 1

#### Dependencies:

LUT130, LUT132, LUT133, LUT134, LUT136, LUT137, LUT409, LUT410

Tools:

RTC/UPRAD (MOMO)  
Multi-linear interpolation

Procedure:

Inputs:  $iaer$  Aerosol assemblage #27 ('MAR-BDW2-3')  
 $\lambda$  MERIS band #1 (412.5 nm), see Section 6.13.4.1, (LUT130)  
 $\theta_s$  Solar zenith angle [deg], see Section 6.13.4.3, (LUT132)  
 $\theta_v$  View zenith angle [deg], see Section 6.13.4.4, (LUT133)  
 $\Delta\phi$  Relative azimuth angle [deg], see Section 6.13.4.5, (LUT134)  
 $k$  Polynomial coefficient order [dl],  $k = [0;2]$   
 $\tau^{a1}$  Aerosol optical thickness at 550nm [dl] for the boundary layer (aerosol layer #1), see Section 6.13.1.1 (LUT136)  
 $\tau^{a2}$  Aerosol optical thickness at 550nm [dl] for the dust layer (aerosol layer #2), see Section 6.13.1.2 (LUT137)  
 $\tau^{a3}$  Aerosol optical thickness at 550nm [dl] for the troposphere layer (aerosol layer #3), see Section 6.13.1.3 (LUT409)  
 $\tau^{a4}$  Aerosol optical thickness at 550nm [dl] for the stratospheric layer, fixed to 0.005 whatever wavelength and assemblage except for the first one ( $iaer\#0$ ,  $\tau^{a4} = 0$ ).  
 $\tau^R$  Rayleigh optical thickness [dl] (15 values), see Section 6.11.1.1, (LUT410)

Output:  $\rho_{GCthresh\_LUT}[\theta_s, \theta_v, \Delta\phi]$   
 TOA reflectance thresholds at 412.5 nm as function of the illumination and viewing configuration ( $\theta_s, \theta_v, \Delta\phi$ )

units: [dl]

Step-0: Select each aerosol model used in the ocean-aerosol assemblage #27 ('MAR-BDW2-3'), and compute the scattering phase matrix and the IOPs (extinction & scattering coefficients, and single scattering albedo) at the 412.5 nm MERIS wavelength ( $\lambda$ ) with the OTC/MIE (FUB) and the associated input Mie card:

*/FUB/sca\_in/sc\_mar90\_b01, sc\_dbdw2\_b01, sc\_conti\_b01, sc\_H2SO4\_b01*

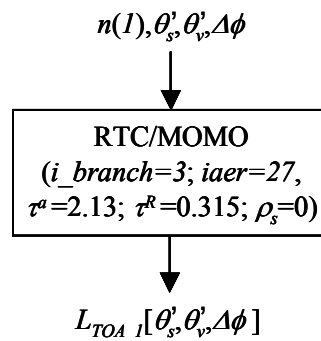
Step-1: Generate TOA normalized radiance  $L_{TOA\_1}[\theta_s', \theta_v', \Delta\phi]$  at 412.5 nm (MERIS band #1) for a maritime atmosphere (using aerosol assemblage #27, 'MAR-BDW2-3') over a flat black sea surface, for all illumination and viewing configurations ( $\theta_s', \theta_v', \Delta\phi$ ), with the RTC/MOMO (FUB). Note that the first cloud layer is used as an aerosol layer for stratosphere.

**RTC/MOMO Inputs (OCEAN)**

| Variable | Value | Comments |
|----------|-------|----------|
|----------|-------|----------|

| Variable                   | Value                         | Comments   |
|----------------------------|-------------------------------|--|
| <i>out_file</i>            | "/up_out/uprad_out"           |  |
| <i>i_branch</i>            | 3                             | For including the 4 aerosol layers in the radiative transfer computation   |
| $n(\lambda)$               | 1                             | Selected from Section 6.13.4.1 (412.5 nm)  |
| $U_{H2O}$                  | 0                             |  |
| $ESFT_{H2O}$               | -                             | N/A  |
| $U_{O2}$                   | 0                             |  |
| $ESFT_{O2}$                | -                             | N/A  |
| $U_{O3}$                   | 0                             |  |
| $ESFT_{O3}$                | -                             | N/A  |
| $P_s$                      | 1013.25                       |  |
| $\tau^R(\lambda)$          | tauR                          | Selected from Section 6.11.1.1   |
| <i>aerosol1</i>            | "/sca_out/sc_mar90_b01.s"     | Boundary layer (assemblage #27)  |
| $\tau^{a1}(550)$           | 0.05                          | Selected from Section 6.13.1.1   |
| <i>aerosol2</i>            | "/sca_out/sc_dbdw2_b01.s"     | Dust layer [0-7 km] (assemblage#27)  |
| $\tau^{a2}(550)$           | 2.0                           | Selected from Section 6.13.1.2   |
| <i>aerosol3</i>            | "/sca_out/sc_conti_b01.s"     | Troposphere layer (assemblage #27)   |
| $\tau^{a3}(550)$           | 0.025                         | Selected from Section 6.13.1.3   |
| <i>cloud1</i>              | "/sca_out/sc_H2SO4_b01.s"     | Stratosphere layer (assemblage #27)  |
| $\tau^{c1}(550)$           | 0.005                         |  |
| <i>cloud2</i>              | -                             | N/A  |
| $\tau^{c2}(550)$           | 0                             |  |
| <i>cloud3</i>              | -                             | N/A  |
| $\tau^{c3}(550)$           | 0                             |  |
| <i>phyto</i>               | -                             | N/A  |
| $\sigma_{e,\lambda}^p$     | -                             | N/A  |
| $\omega_{o,\lambda}^p$     | -                             | N/A  |
| <i>spm</i>                 | -                             | N/A  |
| $\sigma_{e,\lambda}^{spm}$ | -                             | N/A  |
| $\omega_{o,\lambda}^{spm}$ | -                             | N/A  |
| $\sigma_{a,\lambda}^{ys}$  | -                             | N/A  |
| <i>vertical</i>            | "/sca_vert/vtp1_lut143_0_7km" | Vertical profile with 12 atmospheric layers: boundary layer [0;2 km]; dust layer [0;7 km]; troposphere [2;12 km]; stratosphere [ >12 km] |
| $I_s$                      | 70                            |  |
| $\rho_s$                   | 0                             |  |
| $E_o$                      | 1                             |  |
| $\sigma_{a,\lambda}^w$     | 99                            |  |
| $w_s$                      | 0                             |  |
| $n_s, n_v, n_{\Delta\phi}$ | 16, 10, 25                    |  |

| Variable     | Value           | Comments                                   |
|--------------|-----------------|--|
| $\theta_s'$  | Gaussian angles | From Gauss-Lobatto quadrature (in RTC/FUB) |
| $\theta_v'$  | Gaussian angles | From Gauss-Lobatto quadrature (in RTC/FUB) |
| $\Delta\phi$ | see inputs      | See Section 6.13.4.5                       |



Step-2: Apply a multi-linear interpolation to output the TOA normalized *Rayleigh* radiance  $L_{TOA\_I}[\theta_s', \theta_v', \Delta\phi]$  into the input angular grid in  $(\theta_s, \theta_v)$ :

$$L_{TOA\_I}[\theta_s, \theta_v, \Delta\phi] = interpolation(L_{TOA\_I}[\theta_s', \theta_v', \Delta\phi])$$

Step-3: Compute blue TOA reflectance thresholds at 412.5 nm ( $\rho_{GCthresh\_LUT}[\theta_s, \theta_v, \Delta\phi]$ ) as,

$$\rho_{GCthresh\_LUT}[\theta_s, \theta_v, \Delta\phi] = \pi \cdot \frac{L_{TOA\_I}[\theta_s, \theta_v, \Delta\phi]}{\cos(\theta_s)}$$

#### Scientific content:

These blue TOA reflectance thresholds define the maximum reflectance as observed at 412.5 nm over flat sea surfaces (*i.e.*, oceanic surfaces corrected for the sun glint).

#### Resources:

Estimated CPU time: 31 sec  
Output disk space:  $23 \times 13 \times 25 \times 4$  bytes/fl = 29900 bytes

#### Acceptance:

Comparison with another RTC.



### 6.13.10 ADS Coefficients of $\rho_T/\rho_R$ to $\tau_a$ Relation

#### 6.13.10.1 Polynomial coefficients for $(\rho_T/\rho_R)$ to total AOT relationship

##### 6.13.10.1.1 FUB Recipe

Reference: XCTab\_LUT, LUT143

[AD-8] Section 6.13.10, ADSR field 1, 2 & 3

#### Dependencies:

LUT130, LUT132, LUT133, LUT134, LUT135, LUT136, LUT137, LUT409, LUT410

#### Tools:

RTC/MOMO (FUB)  
Multi-linear interpolation  
Polynomial fit

#### Procedure:

Inputs:  $iaer$  Aerosol assemblage # [dl] (among the 34 aerosol assemblages)  
 $\lambda$  MERIS wavelength [nm] (15 values), see Section 6.13.4.1, (LUT130)  
 $w_s$  Wind-speed [ $m.s^{-1}$ ] (3 values), see Section 6.13.4.6, (LUT135)  
 $\theta_s$  Solar zenith angle [deg], see Section 6.13.4.3, (LUT132)  
 $\theta_v$  View zenith angle [deg], see Section 6.13.4.4, (LUT133)  
 $\Delta\phi$  Relative azimuth angle [deg], see Section 6.13.4.5, (LUT134)  
 $k$  Polynomial coefficient order [dl],  $k = [0;2]$   
 $\tau^{a1}$  Aerosol optical thickness at 550nm [dl] for the boundary layer (aerosol layer #1), see Section 6.13.1.1 (LUT136)  
 $\tau^{a2}$  Aerosol optical thickness at 550nm [dl] for the dust layer (aerosol layer #2), see Section 6.13.1.2 (LUT137)  
 $\tau^{a3}$  Aerosol optical thickness at 550nm [dl] for the troposphere layer (aerosol layer #3), see Section 6.13.1.3 (LUT409)  
 $\tau^{a4}$  Aerosol optical thickness at 550nm [dl] for the stratospheric layer, fixed to 0.005 whatever wavelength and assemblage except for the first one ( $iaer\#0, \tau^{a4}=0$ ).  
 $\tau^R$  Rayleigh optical thickness [dl] (15 values), see Section 6.11.1.1, (LUT410)

Output:  $XCTab\_LUT[iaer, \lambda, w_s, \theta_s, \theta_v, \Delta\phi, k]$   
 polynomial coefficients for the relation between the normalized radiance ratio ( $\rho_T/\rho_R$ ) to the total aerosol optical thickness ( $\tau^a$ ) at 550nm, as function of the aerosol assemblage ( $iaer$ ), the MERIS wavelength ( $\lambda$ ), the wind-speed above sea level ( $w_s$ ), and the illumination and viewing configuration ( $\theta_s, \theta_v, \Delta\phi$ )

units: [dl]

**Note:** The total aerosol optical thicknesses ( $\tau^a$ ) at 550nm is the sum of the 4 aerosol optical thicknesses (*resp.*,  $\tau^{a1}$ ,  $\tau^{a2}$ ,  $\tau^{a3}$  and  $\tau^{a4}$ ) at 550nm for the 4 aerosol layers (*resp.*, boundary, dust, troposphere, and stratosphere), *see* table from [Section 6.13.5.1](#).

**Warning:** The process for generating this *XCTab\_LUT* table is very time-consuming. To avoid losing data in case of a power failure during the processing, temporary binary files are created after *Step3* and *Step7* described below: *Rayleigh\_Wy.LUT401* and *Mxx\_Wy\_Tz.LUT401* (*where xx stands for the identification of the aerosol assemblage [00 .. 33], y for the identification of the wind-speed [0,1], and z for the identification of the total aerosol optical thickness at 550nm*). This allows one to resume the processing after a power failure. If we want fully restart the generation procedure, then the temporary binary files should be first deleted before relaunching the process.

*See* [Section 6.13.1.7](#) (LUT401) for the description of these intermediate tables.

Moreover the total aerosol thickness ( $\tau_\lambda^a$ ) for each RTC/MOMO run is saved in the intermediate binary file (LUT405), *see* [Section 6.13.1.7](#).

**Step-1:** Generate TOA normalized *Rayleigh* radiance  $L_R[\lambda, w_s, \theta_s, \theta_v, \Delta\phi]$  for a pure *Rayleigh* atmosphere over 3 wind-roughened black sea surfaces ( $w_s=1.5, 5.0$  and  $10m.s^{-1}$ ), for each MERIS wavelength ( $\lambda$ ), and for all illumination and viewing configurations ( $\theta_s, \theta_v, \Delta\phi$ ), with the RTC/MOMO (FUB). Note that the first cloud layer is used as an aerosol layer for stratosphere.

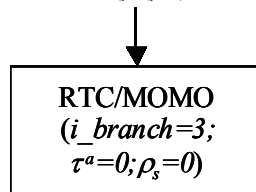
**Note:** The sun glint (*i.e.*, the direct to direct contribution) is accounted for in  $L_R[\lambda, w_s, \theta_s, \theta_v, \Delta\phi]$ .

***RTC/MOMO Inputs (OCEAN)***

| <b>Variable</b>                    | <b>Value</b>   | <b>Comments</b>  |
|------------------------------------|--|--|
| <i>out_file</i>                    | "/up_out/uprad_out"                                  |  |
| <i>i_branch</i>                    | 3  | For using 4 aerosol layers in RTC                            |
| <i>n</i> ( $\lambda$ )             | 1, 2, 3, 4, 5, 6, 7, 8, 9, 10, 11, 12, 13, 14 and 15 | All MERIS bands, <i>see</i> <a href="#">Section 6.13.4.1</a> |
| <i>U<sub>H2O</sub></i>             | 0  |  |
| <i>ESFT<sub>H2O</sub></i>          | -  | N/A  |
| <i>U<sub>O2</sub></i>              | 0  |  |
| <i>ESFT<sub>O2</sub></i>           | -  | N/A  |
| <i>U<sub>O3</sub></i>              | 0  |  |
| <i>ESFT<sub>O3</sub></i>           | -  | N/A  |
| <i>P<sub>s</sub></i>               | 1013.25  |  |
| <i>t<sup>R</sup></i> ( $\lambda$ ) | tauR   | <i>See</i> <a href="#">Section 6.11.1.1</a>                  |
| <i>aerosol1</i>                    | -  |  |
| <i>t<sup>a1</sup></i> (550)        | 0  |  |
| <i>aerosol2</i>                    | -  |  |
| <i>t<sup>a2</sup></i> (550)        | 0  |  |
| <i>aerosol3</i>                    | -  |  |
| <i>t<sup>a3</sup></i> (550)        | 0  |  |

| Variable                   | Value                         | Comments                                    |
|----------------------------|-------------------------------|---|
| cloud1                     | -                             | N/A   |
| $\tau^1(550)$              | 0                             |   |
| cloud2                     | -                             | N/A   |
| $\tau^2(550)$              | 0                             |   |
| cloud3                     | -                             | N/A   |
| $\tau^3(550)$              | 0                             |   |
| phyto                      | -                             | N/A   |
| $\sigma_{e,\lambda}^p$     | -                             | N/A   |
| $\omega_{o,\lambda}^p$     | -                             | N/A   |
| spm                        | -                             | N/A   |
| $\sigma_{e,\lambda}^{spm}$ | -                             | N/A   |
| $\omega_{o,\lambda}^{spm}$ | -                             | N/A   |
| $\sigma_{a,\lambda}^{ys}$  | -                             | N/A   |
| vertical                   | "/sca_vert/vtp1_lut143_0_2km" | Vertical profile with 12 atmospheric layers |
| $I_s$                      | 70                            |   |
| $\rho_s$                   | 0                             |   |
| $E_o$                      | 1                             |   |
| $\sigma_{a,\lambda}^w$     | 99                            |   |
| $w_s$                      | 1.5, 5.0 and 10               | See Section 6.13.4.6                        |
| $n_s, n_v, n_{\Delta\phi}$ | 16, 10, 25                    |   |
| $\theta_s'$                | Gaussian angles               | From Gauss-Lobatto quadrature (in RTC/FUB)  |
| $\theta_v'$                | Gaussian angles               | From Gauss-Lobatto quadrature (in RTC/FUB)  |
| $\Delta\phi$               | see inputs                    | See Section 6.13.4.5                        |

$n(\lambda, w_s, \theta_s', \theta_v', \Delta\phi$



$L_R[\lambda, w_s, \theta_s', \theta_v', \Delta\phi]$

Step-2: Compute the Rayleigh reflectance  $\rho_R[\lambda, w_s, \theta_s', \theta_v', \Delta\phi]$  as follows,

$$\rho_R[\lambda, w_s, \theta_s', \theta_v', \Delta\phi] = \pi \cdot \frac{L_R[\lambda, w_s, \theta_s', \theta_v', \Delta\phi]}{\cos(\theta_s')}$$

Remove the sun glint reflectance at TOA ( $\rho_{G\_TOA}$ ) from the *Rayleigh* reflectance (only for the case where  $w_s \neq 0$ ). This is achieved with the procedure described in [Section 6.11.12.1](#).

Step-3: Apply a multi-linear interpolation to output the *Rayleigh* reflectance  $\rho_R[\lambda, w_s, \theta_s', \theta_v', \Delta\phi]$  into the input angular grid in  $(\theta_s, \theta_v)$ :

$$\rho_R[\lambda, w_s, \theta_s, \theta_v, \Delta\phi] = interpolation(\rho_R[\lambda, w_s, \theta_s', \theta_v', \Delta\phi])$$

Step-4: Select each aerosol model among the 23 models used in the 34 ocean-aerosol assemblages, and compute the scattering phase matrix and the IOPs (extinction & scattering coefficients, and single scattering albedo) at each of the 15 MERIS wavelengths ( $\lambda$ ) with the OTC/MIE (FUB) and the associated input *Mie* card:

*/FUB/sca\_in/sc\_marxx\_byy, sc\_coaxx\_byy, sc\_rurxx\_byy, sc\_dbdsz\_byy, sc\_dbdwz\_byy, sc\_IOPww\_byy, sc\_conti\_byy, sc\_H2SO4\_byy*

with  $xx = \{50, 70, 90, 99\}$  (i.e., relative humidity),  $yy = \{01, \dots, 15\}$  (i.e., MERIS bands #),  $z = \{1, 2, 3\}$  (i.e., 3 scale heights),  $ww = \{01, 02, 03\}$  (i.e., 3 Log-normal distributions)

Step-5: Generate TOA normalized radiances  $L_T[\lambda, w_s, \theta_s', \theta_v', \Delta\phi, \tau^a, iaer]$  for a maritime atmosphere (*Rayleigh* + aerosols) over 3 wind-roughened black sea surfaces ( $w_s = 1.5, 5.0$  and  $10 m.s^{-1}$ ), for each selected aerosol assemblage ( $\tau^a, iaer$ ), for each MERIS wavelength ( $\lambda$ ), and for all illumination and viewing configurations  $(\theta_s, \theta_v, \Delta\phi)$ , with the RTC/MOMO (FUB). Note that the first cloud layer is used as an aerosol layer for stratosphere.

Note: The sun glint (i.e., the direct to direct contribution) is accounted for in  $L_T[\lambda, w_s, \theta_s', \theta_v', \Delta\phi, \tau^a, iaer]$ .

**RTC/MOMO Inputs (OCEAN)**

| Variable                           | Value  | Comments  |
|------------------------------------|--|---|
| <i>out_file</i>                    | "/up_out/uprad_out"  |   |
| <i>i_branch</i>                    | 3  | For using 4 aerosol layers in RTC   |
| <i>n</i> ( $\lambda$ )             | 1, 2, 3, 4, 5, 6, 7, 8, 9, 10, 11, 12, 13, 14 and 15   | All MERIS bands, see <a href="#">Section 6.13.4.1</a>   |
| <i>U<sub>H2O</sub></i>             | 0  |   |
| <i>ESFT<sub>H2O</sub></i>          | -  | N/A   |
| <i>U<sub>O2</sub></i>              | 0  |   |
| <i>ESFT<sub>O2</sub></i>           | -  | N/A   |
| <i>U<sub>O3</sub></i>              | 0  |   |
| <i>ESFT<sub>O3</sub></i>           | -  | N/A   |
| <i>P<sub>s</sub></i>               | 1013.25  |   |
| <i>t<sup>a</sup></i> ( $\lambda$ ) |  | See <a href="#">Section 6.11.1.1</a>  |
| <i>aerosol</i>                     | "/sca_out/sc_marxx_byy.s"<br>"/sca_out/sc_coaxx_byy.s"<br>"/sca_out/sc_rurxx_byy.s"<br>"/sca_out/sc_bluew_byy.s" | For maritime, coastal and rural aerosols, xx depends on RH and yy on <i>n</i> ( $\lambda$ ).<br>For blue aerosols, w depends on the <i>Ang-ström</i> exponent and yy on <i>n</i> ( $\lambda$ ). |

| Variable                   | Value   | Comments  |
|----------------------------|---|---|
| $t^{a1}(550)$              | tauA1   | See Section 6.13.1.1 (last 6 values only) or table in Section 6.13.5.1  |
| aerosol2                   | "/sca_out/sc_dbdsz_byy.s"<br>"/sca_out/sc_dbdwz_byy.s"  | yy depends on $n(\lambda)$ and z on the height of the top of aerosol layer  |
| $t^{a2}(550)$              | tauA2   | See Section 6.13.1.2 (last 6 values only) or table in Section 6.13.5.1  |
| aerosol3                   | "/sca_out/sc_conti_byy.s"   | yy depends on $n(\lambda)$  |
| $t^{a3}(550)$              | tauA3   | See Section 6.13.1.3 (last 6 values only) or table in Section 6.13.5.1  |
| cloud1                     | "/sca_out/sc_H2SO4_byy.s"   | yy depends on $n(\lambda)$  |
| $t^l(550)$                 | 0<br>0.005  | For the first assemblage ( <i>iaer</i> #0)<br>For the other assemblages ( <i>iaer</i> )   |
| cloud2                     | -   | N/A   |
| $t^2(550)$                 | 0   |   |
| cloud3                     | -   | N/A   |
| $t^3(550)$                 | 0   |   |
| phyto                      | -   | N/A   |
| $\sigma_{e,\lambda}^p$     | -   | N/A   |
| $\omega_{o,\lambda}^p$     | -   | N/A   |
| spm                        | -   | N/A   |
| $\sigma_{e,\lambda}^{spm}$ | -   | N/A   |
| $\omega_{o,\lambda}^{spm}$ | -   | N/A   |
| $\sigma_{a,\lambda}^{ys}$  | -   | N/A   |
| vertical                   | "/sca_vert/vtp1_lut143_0_7km"<br>"/sca_vert/vtp1_lut143_0_5km"<br>"/sca_vert/vtp1_lut143_0_2km" | For assemblages: <i>iaer</i> #15, 18, 21, 24, 27, 30<br>For assemblages: <i>iaer</i> #14, 17, 20, 23, 26, 29<br>For the other assemblages |
| $I_s$                      | 70  |   |
| $\rho_s$                   | 0   |   |
| $E_o$                      | 1   |   |
| $\sigma_{a,\lambda}^w$     | 99  |   |
| $w_s$                      | 1.5, 5.0 and 10   | See Section 6.13.4.6  |
| $n_s, n_v, n_{\Delta\phi}$ | 16, 10, 25  |   |
| $\theta_s^r$               | Gaussian angles   | From Gauss-Lobatto quadrature (in RTC/FUB)  |
| $\theta_v^r$               | Gaussian angles   | From Gauss-Lobatto quadrature (in RTC/FUB)  |
| $\Delta\phi$               | see inputs  | See Section 6.13.4.5  |

$n(\lambda, w_s, \theta_s, \theta_v, \Delta\phi, \tau^a, iaer)$

RTC/MOMO  
( $i\_branch=3$ ;  
 $\rho_s=0$ )

$L_T[\lambda, w_s, \theta_s, \theta_v, \Delta\phi, \tau^a, iaer]$

Step-6: Compute the total TOA reflectance (*Rayleigh* + aerosols)  $\rho_T[\lambda, w_s, \theta_s, \theta_v, \Delta\phi, \tau^a, iaer]$  as follows,

$$\rho_T[\lambda, w_s, \theta_s, \theta_v, \Delta\phi, \tau^a, iaer] = \pi \cdot \frac{L_T[\lambda, w_s, \theta_s, \theta_v, \Delta\phi, \tau^a, iaer]}{\cos(\theta_s')}$$

Remove the sun glint reflectance at TOA ( $\rho_{G\_TOA}$ ) from the *Rayleigh* reflectance (only for the case where  $w_s \neq 0$ ). This is achieved with the procedure described in [Section 6.11.12.1](#).

Note: For each RTC/MOMO run, the total aerosol optical thickness ( $\tau_\lambda^a$ ) is extracted from the output MOMO file (in the '/FUB/mom\_out/' directory) and saved in an intermediate binary file (LUT405), see [Section 6.13.1.7](#).

Step-7: Apply a multi-linear interpolation to output the total TOA reflectance  $\rho_T[\lambda, w_s, \theta_s, \theta_v, \Delta\phi, \tau^a, iaer]$  into the input angular grid in  $(\theta_s, \theta_v)$ :

$$\rho_T[\lambda, w_s, \theta_s, \theta_v, \Delta\phi, \tau^a, iaer] = interpolation(\rho_T[\lambda, w_s, \theta_s, \theta_v, \Delta\phi, \tau^a, iaer])$$

Step-8: Compute the TOA reflectance ratio  $\rho_T/\rho_R[\lambda, w_s, \theta_s, \theta_v, \Delta\phi, \tau^a, iaer]$ ,

$$\rho_T / \rho_R[\lambda, w_s, \theta_s, \theta_v, \Delta\phi, \tau^a, iaer] = \frac{\rho_T[\lambda, w_s, \theta_s, \theta_v, \Delta\phi, \tau^a, iaer]}{\rho_R[\lambda, w_s, \theta_s, \theta_v, \Delta\phi]}$$

Step-9: Apply a 2<sup>nd</sup> order polynomial fit on the TOA reflectance ratio  $\rho_T/\rho_R[\lambda, w_s, \theta_s, \theta_v, \Delta\phi, \tau^a, iaer]$  as function of the total aerosol optical thickness  $\tau_\lambda^a$ , for retrieving polynomial coefficients  $XCTab\_LUT[iaer, \lambda, w_s, \theta_s, \theta_v, \Delta\phi, k]$ ,

$$\begin{aligned} \rho_T/\rho_R[\lambda, w_s, \theta_s, \theta_v, \Delta\phi, \tau^a, iaer] = & \quad XCTab\_LUT[iaer, \lambda, w_s, \theta_s, \theta_v, \Delta\phi, 0] \\ & + XCTab\_LUT[iaer, \lambda, w_s, \theta_s, \theta_v, \Delta\phi, 1] \cdot \tau_\lambda^a \\ & + XCTab\_LUT[iaer, \lambda, w_s, \theta_s, \theta_v, \Delta\phi, 2] \cdot [\tau_\lambda^a]^2 \end{aligned}$$

Note that these coefficients will be determined by fitting 7 points to a 2<sup>nd</sup> order polynomial for which 6 of these points derive from the MOMO simulations (*i.e.*, 6 total AOTs ( $\tau^a$ )), and the 7<sup>th</sup> one is simply (0,1) corresponding to a TOA reflectance ratio of 1 for an aerosol-free

atmosphere. More a quality test is applied to the 2<sup>nd</sup> order polynomial fits in order to check the unique solution in the total AOT ( $\tau_\lambda^a$ ) retrieval (*i.e.*, to avoid the  $\tau_\lambda^a$  value corresponding to the extremum of the 2<sup>nd</sup> order polynomial fit within the range of AOTs used as input for this fitting). The approach consists to establish the fit by decreasing the number of points (while keeping an acceptable range in  $\tau^a$  defined by the first 2 non-null input  $\tau^a$  values) as long as the quality test is not valid.

Step-10: Build the  $XCTab\_LUT[iaer, \lambda, w_s, \theta_s, \theta_v, \Delta\phi, k]$  table.

### Scientific content:

$XCTab\_LUT[iaer, \lambda, w_s, \theta_s, \theta_v, \Delta\phi, k]$  describes the coefficients of a polynomial fit which expresses the TOA reflectance ratio  $\rho_T/\rho_R[iaer, \lambda, w_s, \theta_s, \theta_v, \Delta\phi]$  (in other words, the relative increase in the path reflectance from an aerosol-free atmosphere to an atmosphere with an aerosol loading) as function of the total aerosol optical thickness  $\tau_\lambda^a$ . These regression coefficients ( $k = [0;2]$ ) depends on the aerosol assemblage (*iaer*), the MERIS wavelength ( $\lambda$ ), the wind-speed above sea level ( $w_s$ ), and the illumination and viewing geometries ( $\theta_s, \theta_v, \Delta\phi$ ).

This table is useful for the aerosol correction algorithm over wind-roughened oceanic surface, and allows one to compute the total path to *Rayleigh* reflectances ratio ( $\rho_T/\rho_R[iaer, \lambda, w_s, \theta_s, \theta_v, \Delta\phi, \tau^a]$ ) knowing the total aerosol optical thickness  $\tau_\lambda^a$  at wavelength  $\lambda$ .

Note that the values of these coefficients will be extracted from this table by using multiple linear interpolations.

The current baseline is:

- $N_{w_s}$  which corresponds to 3 predefined wind-speeds of 1.5, 5.0 and  $10 m.s^{-1}$
- $N_{\theta_s}$  which corresponds to 23 predefined values (*see* [Section 6.13.4.3](#))
- $N_{\theta_v}$  which corresponds to 13 predefined values (*see* [Section 6.13.4.4](#))
- $N_{\Delta\phi}$  which corresponds to 25 preselected values (*see* [Section 6.13.4.5](#))

### Resources:

Estimated CPU time: 101663 *sec* (if LUT399 already generated, otherwise 166469 *sec*)  
Output disk space:  $34 \times 15 \times 3 \times 23 \times 13 \times 25 \times 3 \times 4$  bytes/fl = 137241000 bytes

### Acceptance:

Some comparisons with another RTC, such as the RTC/UPRAD (SO) from UdL have been done, as well as a quality check with tables generated by the LOV institute.

#### 6.13.10.1.2 UdL Recipe

Reference:  $XCTab\_LUT$ , LUT143

[AD-8] Section 6.13.10, ADSR field 1, 2 & 3

Dependencies:

LUT130, LUT132, LUT133, LUT134, LUT135, LUT136, LUT409, LUT410

Tools:

RTC/UPRAD (SO)  
Polynomial fit

Procedure:

Inputs: *iaer* Aerosol assemblage # [*dI*] (16 SAMs [*iaer*#0+MAR+COA+RUR+BLU-IOP])  
 $\lambda$  MERIS wavelength [*nm*] (15 values), see Section 6.13.4.1, (LUT130)  
 $w_s$  Wind-speed [*m.s<sup>-1</sup>*] (3 values), see Section 6.13.4.6, (LUT135)  
 $\theta_s$  Solar zenith angle [*deg*], see Section 6.13.4.3, (LUT132)  
 $\theta_v$  View zenith angle [*deg*], see Section 6.13.4.4, (LUT133)  
 $\Delta\phi$  Relative azimuth angle [*deg*], see Section 6.13.4.5, (LUT134)  
 $k$  Polynomial coefficient order [*dI*],  $k = [0;2]$   
 $\tau^{a1}$  Aerosol optical thickness at 550*nm* [*dI*] for the boundary layer (aerosol layer #1), see Section 6.13.1.1 (LUT136)  
 $\tau^{a2}$  Aerosol optical thickness at 550*nm* [*dI*] for the tropospheric layer (aerosol layer #3), see Section 6.13.1.3 (LUT409)  
 $\tau^{a3}$  Aerosol optical thickness at 550*nm* [*dI*] for the stratospheric layer (aerosol layer #4) fixed to 0.005 whatever the wavelength and the assemblage except for the first one (*iaer*#0,  $\tau^{a4} = 0$ )  
 $\tau^R$  Rayleigh optical thickness [*dI*] (15 values), see Section 6.11.1.1, (LUT410)

Output:  $XCTab\_LUT[iaer, \lambda, w_s, \theta_s, \theta_v, \Delta\phi, k]$   
 Polynomial coefficients for the relation between the normalized radiance ratio ( $\rho_T/\rho_R$ ) to the total aerosol optical thickness ( $\tau^a$ ) at 550*nm*, as function of the aerosol assemblage (*iaer*), the MERIS wavelength ( $\lambda$ ), the wind-speed above sea level ( $w_s$ ), and the illumination and viewing configuration ( $\theta_s, \theta_v, \Delta\phi$ )

units: [*dI*]

Note: Because the RTC/SO (UdL) composes with 3 aerosol layers only, then the 18 dust assemblages are discarded. The total aerosol optical thicknesses ( $\tau^a$ ) at 550*nm* is then the sum of the 3 aerosol optical thicknesses (*resp.*,  $\tau^{a1}, \tau^{a2}$  and  $\tau^{a3}$ ) at 550*nm* for the 3 aerosol layers (*resp.*, boundary, troposphere and stratosphere), see table from Section 6.13.5.1.

**Warning:** The process for generating this  $XCTab\_LUT$  table is very time-consuming. To avoid losing data in case of a power failure during the processing, temporary binary files are created after *Step2* and *Step5* described below: *Rayleigh\_Wy.LUT401* and *Mxx\_Wy\_Tz.LUT401* (where *xx*



stands for the identification of the aerosol assemblage [00 .. 16],  $y$  for the identification of the wind-speed [0,1,2], and  $z$  for the identification of the total aerosol optical thickness at 550 nm). This allows one to resume the processing after a power failure. If we want fully restart the generation procedure, then the temporary binary files should be first deleted before relaunching the process.

See [Section 6.13.1.7](#) (LUT401) for the description of these intermediate tables.

Moreover the total aerosol thickness ( $\tau_{\lambda}^a$ ) for each RTC/SO run is saved in the intermediate binary file (LUT405), see [Section 6.13.1.7](#). Because the size of this LUT remains unchanged then it will be completed with null values.

Step-1: Generate TOA normalized *Rayleigh* radiance  $L_R[\lambda, w_s, \theta_s, \theta_v, \Delta\phi]$  for a pure *Rayleigh* atmosphere over 3 wind-roughened black sea surfaces ( $w_s=1.5, 5.0$  and  $10m.s^{-1}$ ), for each MERIS wavelength ( $\lambda$ ), and for all illumination and viewing configurations ( $\theta_s, \theta_v, \Delta\phi$ ), with the RTC/UPRAD (SO). The sun glint (*i.e.*, the direct to direct contribution) is not accounted for in  $L_R[\lambda, w_s, \theta_s, \theta_v, \Delta\phi]$ .

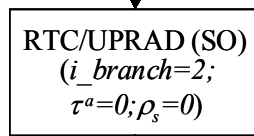
Note: An internal sun glint flag has been deactivated in the RTC/SO for excluding the direct to direct contribution in the computation of TOA normalized radiance.

**RTC/UPRAD (SO) Inputs (OCEAN)**

| Variable               | Value  | Comments  |
|------------------------|--|---|
| <i>out_file</i>        | "/OUTPUT/uprad_out"                                  |   |
| <i>i_branch</i>        | 2  |   |
| $n(\lambda)$           | 1, 2, 3, 4, 5, 6, 7, 8, 9, 10, 11, 12, 13, 14 and 15 | All MERIS bands, see <a href="#">Section 6.13.4.1</a> |
| $U_{H2O}$              | 0  |   |
| $U_{O2}$               | 0  |   |
| <i>ESFT</i>            | -  | N/A   |
| $P_s$                  | 1013.25  |   |
| $\tau^R(\lambda)$      | tauR   | See <a href="#">Section 6.11.1.1</a>                  |
| <i>aerosol1</i>        | -  |   |
| $\tau^{a1}(550)$       | 0  |   |
| <i>aerosol2</i>        | -  |   |
| $\tau^{a2}(550)$       | 0  |   |
| <i>aerosol3</i>        | -  |   |
| $\tau^{a3}(550)$       | 0  |   |
| <i>cloud1</i>          | -  | N/A   |
| <i>cloud2</i>          | -  | N/A   |
| <i>cloud3</i>          | -  | N/A   |
| <i>phyto</i>           | -  | N/A   |
| $\sigma_{e,\lambda}^p$ | -  | N/A   |

| Variable                   | Value                 | Comments  |
|----------------------------|-----------------------|---|
| $\omega_{o,\lambda}^p$     | -                     | N/A   |
| $spm$                      | -                     | N/A   |
| $\sigma_{e,\lambda}^{spm}$ | -                     | N/A   |
| $\omega_{o,\lambda}^{spm}$ | -                     | N/A   |
| $\sigma_{a,\lambda}^{ys}$  | -                     | N/A   |
| <i>vertical</i>            | "/INPUT/vertical_out" | Not used, vertical distribution determined in RTC/SO ( $H_R=8$ km)          |
| $I_s$                      | 79                    |   |
| $\rho_s$                   | 0                     |   |
| $E_o$                      | 1                     |   |
| $\sigma_{e,\lambda}^w$     | -                     | N/A   |
| $\omega_{o,\lambda}^w$     | -                     | N/A   |
| $w_s$                      | 1.5, 5.0 and 10       | See Section 6.13.4.6  |
| $n_s, n_v, n_{\Delta\phi}$ | 23, 13, 25            |   |
| $\theta_s$                 | Gaussian angles       | First 23 angles selected from <i>Gauss</i> quadrature; See Section 6.13.4.3 |
| $\theta_v$                 | Gaussian angles       | First 13 angles selected from <i>Gauss</i> quadrature; See Section 6.13.4.4 |
| $\Delta\phi$               | see inputs            | See Section 6.13.4.5  |
| <i>pol</i>                 | 1                     |   |

$$n(\lambda, w_s, \theta_s, \theta_v, \Delta\phi)$$



$$L_R[\lambda, w_s, \theta_s, \theta_v, \Delta\phi]$$

Step-2: Compute the *Rayleigh* reflectance  $\rho_R[\lambda, w_s, \theta_s, \theta_v, \Delta\phi]$  as follows,

$$\rho_R[\lambda, w_s, \theta_s, \theta_v, \Delta\phi] = \pi \cdot \frac{L_R[\lambda, w_s, \theta_s, \theta_v, \Delta\phi]}{\cos(\theta_s)}$$

Step-3: Select each aerosol model among the 17 models used in the 16 SAMs, and compute the scattering phase matrix and the IOPs (extinction & scattering coefficients, and single scattering albedo) at each of the 15 MERIS wavelengths ( $\lambda$ ) with the RTC/SCAMAT (UdL) and the associated input *Scamat* card:

*/UdL/INPUT/sca\_in/sc\_marxx\_byy, sc\_coaxx\_byy, sc\_rurxx\_byy, sc\_IOPww\_byy, sc\_conti\_byy, sc\_H2SO4\_byy*  
with  $\mathbf{xx} = \{50, 70, 90, 99\}$  (i.e., relative humidity),  $\mathbf{yy} = \{01, \dots, 15\}$  (i.e., MERIS bands #),  $\mathbf{ww} = \{01, 02, 03\}$  (i.e., 3 Log-normal distributions)

Step-4: Generate TOA normalized radiances  $L_T[\lambda, w_s, \theta_s, \theta_v, \Delta\phi, \tau^a, iaer]$  for a maritime atmosphere (Rayleigh + aerosols) over 3 wind-roughened black sea surfaces ( $w_s = 1.5, 5.0$  and  $10 m.s^{-1}$ ), for each selected aerosol assemblage ( $\tau^a, iaer$ ), for each MERIS wavelength ( $\lambda$ ), and for all illumination and viewing configurations ( $\theta_s, \theta_v, \Delta\phi$ ), with the RTC/UPRAD (SO).

Note: An internal sun glint flag has been deactivated in the RTC/SO for excluding the direct to direct contribution in the computation of TOA normalized radiance.

**RTC/UPRAD (SO) Inputs (OCEAN)**

| Variable               | Value  | Comments  |
|------------------------|--|---|
| <i>out_file</i>        | "/OUTPUT/uprad_out"  |   |
| <i>i_branch</i>        | 2  |   |
| $n(\lambda)$           | 1, 2, 3, 4, 5, 6, 7, 8, 9, 10, 11, 12, 13, 14 and 15   | All MERIS bands, see <a href="#">Section 6.13.4.1</a>   |
| $U_{H2O}$              | 0  |   |
| $U_{O2}$               | 0  |   |
| <i>ESFT</i>            | -  | N/A   |
| $P_s$                  | 1013.25  |   |
| $\tau^R(\lambda)$      | tauR   | See <a href="#">Section 6.11.1.1</a>  |
| <i>aerosol1</i>        | "/INPUT/sca_out/sc_marxx_byy"<br>"/INPUT/sca_out/sc_coaxx_byy"<br>"/INPUT/sca_out/sc_rurxx_byy"<br>"/INPUT/sca_out/sc_bluew_byy" | For maritime, coastal and rural aerosols, <i>xx</i> depends on RH and <i>yy</i> on $n(\lambda)$ .<br>For blue aerosols, <i>w</i> depends on the <i>Ang-ström</i> exponent and <i>yy</i> on $n(\lambda)$ . |
| $\tau^{a1}(550)$       | tauA1  | See <a href="#">Section 6.13.1.1</a> (last 6 values only) or table in <a href="#">Section 6.13.5.1</a>  |
| <i>aerosol2</i>        | "/INPUT/sca_out/sc_conti_byy"  | <i>yy</i> depends on $n(\lambda)$   |
| $\tau^{a2}(550)$       | tauA2  | See <a href="#">Section 6.13.1.3</a> (last 6 values only) or table in <a href="#">Section 6.13.5.1</a>  |
| <i>aerosol3</i>        | "/INPUT/sca_out/sc_H2SO4_byy"  | <i>yy</i> depends on $n(\lambda)$   |
| $\tau^{a3}(550)$       | 0<br>0.005   | For the first assemblage ( <i>iaer</i> #0)<br>For the other assemblages ( <i>iaer</i> )   |
| <i>cloud1</i>          | -  | N/A   |
| <i>cloud2</i>          | -  | N/A   |
| <i>cloud3</i>          | -  | N/A   |
| <i>phyto</i>           | -  | N/A   |
| $\sigma_{e,\lambda}^p$ | -  | N/A   |
| $\omega_{o,\lambda}^p$ | -  | N/A   |

|                            |                       |   |
|----------------------------|-----------------------|---|
| $spm$                      | -                     | N/A   |
| $\sigma_{e,\lambda}^{spm}$ | -                     | N/A   |
| $\omega_{o,\lambda}^{spm}$ | -                     | N/A   |
| $\sigma_{a,\lambda}^{ys}$  | -                     | N/A   |
| $vertical$                 | "/INPUT/vertical_out" | Not used, vertical distribution determined in RTC/SO (optically homogeneous layers) |
| $I_s$                      | 79                    |   |
| $\rho_s$                   | 0                     |   |
| $E_o$                      | 1                     |   |
| $\sigma_{e,\lambda}^w$     | -                     | N/A   |
| $\omega_{o,\lambda}^w$     | -                     | N/A   |
| $w_s$                      | 1.5, 5.0 and 10       | See Section 6.13.4.6  |
| $n_s, n_v, n_{\Delta\phi}$ | 23, 13, 25            |   |
| $\theta_s$                 | Gaussian angles       | First 23 angles selected from Gauss quadrature; See Section 6.13.4.3                |
| $\theta_v$                 | Gaussian angles       | First 23 angles selected from Gauss quadrature; See Section 6.13.4.4                |
| $\Delta\phi$               | see inputs            | See Section 6.13.4.5  |
| $pol$                      | 1                     |   |

$n(\lambda), w_s, \theta_s, \theta_v, \Delta\phi, \tau^a, iaer$

RTC/UPRAD (SO)  
( $i\_branch=2$ ;  
 $\rho_s=0$ )

$L_T[\lambda, w_s, \theta_s, \theta_v, \Delta\phi, \tau^a, iaer]$

Step-5: Compute the total TOA reflectance (Rayleigh + aerosols)  $\rho_T[\lambda, w_s, \theta_s, \theta_v, \Delta\phi, \tau^a, iaer]$  as follows,

$$\rho_T[\lambda, w_s, \theta_s, \theta_v, \Delta\phi, \tau^a, iaer] = \pi \cdot \frac{L_T[\lambda, w_s, \theta_s, \theta_v, \Delta\phi, \tau^a, iaer]}{\cos(\theta_s)}$$

Note: For each RTC/UPRAD (SO) run, the total aerosol optical thickness ( $\tau_\lambda^a$ ) is extracted from the output file ('/OUTPUT/uprad\_out') and saved in an intermediate binary file (LUT405), see Section 6.13.1.7.

Step-6: Compute the TOA reflectance ratio  $\rho_T/\rho_R[\lambda, w_s, \theta_s, \theta_v, \Delta\phi, \tau^a, iaer]$ ,

$$\rho_T / \rho_R[\lambda, w_s, \theta_s, \theta_v, \Delta\phi, \tau^a, iaer] = \frac{\rho_T[\lambda, w_s, \theta_s, \theta_v, \Delta\phi, \tau^a, iaer]}{\rho_R[\lambda, w_s, \theta_s, \theta_v, \Delta\phi]}$$

Step-7: Apply a 2<sup>nd</sup> order polynomial fit on the TOA reflectance ratio  $\rho_T/\rho_R[\lambda, w_s, \theta_s, \theta_v, \Delta\phi, \tau^a, iaer]$  as function of the total aerosol optical thickness  $\tau_\lambda^a$ , for retrieving polynomial coefficients  $XCTab\_LUT[iaer, \lambda, w_s, \theta_s, \theta_v, \Delta\phi, k]$ ,

$$\begin{aligned} \rho_T/\rho_R[\lambda, w_s, \theta_s, \theta_v, \Delta\phi, \tau^a, iaer] = & \quad XCTab\_LUT[iaer, \lambda, w_s, \theta_s, \theta_v, \Delta\phi, 0] \\ & + XCTab\_LUT[iaer, \lambda, w_s, \theta_s, \theta_v, \Delta\phi, 1] \cdot \tau_\lambda^a \\ & + XCTab\_LUT[iaer, \lambda, w_s, \theta_s, \theta_v, \Delta\phi, 2] \cdot [\tau_\lambda^a]^2 \end{aligned}$$

Note that these coefficients will be determined by fitting 7 points to a 2<sup>nd</sup> order polynomial for which 6 of these points derive from the MOMO simulations (*i.e.*, 6 total AOTs ( $\tau^a$ )), and the 7<sup>th</sup> one is simply (0,1) corresponding to a TOA reflectance ratio of 1 for an aerosol-free atmosphere. More a quality test is applied to the 2<sup>nd</sup> order polynomial fits in order to check the unique solution in the total AOT ( $\tau_\lambda^a$ ) retrieval (*i.e.*, to avoid the  $\tau_\lambda^a$  value corresponding to the extremum of the 2<sup>nd</sup> order polynomial fit within the range of AOTs used as input for this fitting). The approach consists to establish the fit by decreasing the number of points (while keeping an acceptable range in  $\tau^a$  defined by the first 2 non-null input  $\tau^a$  values) as long as the quality test is not valid.

Step-8: Build the  $XCTab\_LUT[iaer, \lambda, w_s, \theta_s, \theta_v, \Delta\phi, k]$  table for the 16 SAMs (iaer#0, 4 MAR, 4 COA, 4 RUR, 3 BLU-IOP).

Note: In order to keep the same LUT size as the one defined in the previous FUB recipe above then this  $XCTab\_LUT[iaer, \lambda, w_s, \theta_s, \theta_v, \Delta\phi, k]$  LUT will be completed with null values for *iaer* from #13 to #30.

### Scientific content:

$XCTab\_LUT[iaer, \lambda, w_s, \theta_s, \theta_v, \Delta\phi, k]$  describes the coefficients of a polynomial fit which expresses the TOA reflectance ratio  $\rho_T/\rho_R[iaer, \lambda, w_s, \theta_s, \theta_v, \Delta\phi]$  (in other words, the relative increase in the path reflectance from an aerosol-free atmosphere to an atmosphere with an aerosol loading) as function of the total aerosol optical thickness  $\tau_\lambda^a$ . These regression coefficients ( $k = [0;2]$ ) depends on the aerosol assemblage (*iaer*), the MERIS wavelength ( $\lambda$ ), the wind-speed above sea level ( $w_s$ ), and the illumination and viewing geometries ( $\theta_s, \theta_v, \Delta\phi$ ).

This table is useful for the aerosol correction algorithm over wind-roughened oceanic surface, and allows one to compute the total path to *Rayleigh* reflectances ratio ( $\rho_T/\rho_R[iaer, \lambda, w_s, \theta_s, \theta_v, \Delta\phi, \tau^a]$ ) knowing the total aerosol optical thickness  $\tau_\lambda^a$  at wavelength  $\lambda$ .

Note that the values of these coefficients will be extracted from this table by using multiple linear interpolations.

The current baseline is:

$N_{w_s}$  which corresponds to 3 predefined wind-speeds of 1.5, 5.0 and  $10 m.s^{-1}$   
 $N_{\theta_s}$  which corresponds to 23 predefined values (see Section 6.13.4.3)  
 $N_{\theta_v}$  which corresponds to 13 predefined values (see Section 6.13.4.4)  
 $N_{\Delta\phi}$  which corresponds to 25 preselected values (see Section 6.13.4.5)

Resources:

Estimated CPU time: 47841 sec (if LUT419 already generated, otherwise 93741 sec)  
 Output disk space:  $34 \times 15 \times 3 \times 23 \times 13 \times 25 \times 3 \times 4$  bytes/fl = 137241000 bytes

Acceptance:

Some comparisons with another RTC, such as the RTC/MOMO from FUB have been done, as well as a quality check with tables generated by the LOV institute.

**6.13.11 ADS Transmittances**

6.13.11.1 Total downward transmittance (direct+diffuse)

**NOTE:** The recipe of this LUT is presently not included in the MERISAT tool. This LUT is currently generated with an input user specified file.

Reference: Tdown\_LUT, LUT485

[AD-8] Section 6.13.11, ADSR field 1, 2 & 3

Dependencies:

LUT130, LUT132, LUT135, LUT136, LUT409, LUT410

Tools:

RTC/UPRAD (SO)

Procedure:

Inputs:  $iaer$  Aerosol assemblage # [dl] (16 SAMs [iaer#0+MAR+COA+RUR+BLU-IOP])  
 $\lambda$  MERIS wavelength [nm] (15 values), see Section 6.13.4.1, (LUT130)  
 $w_s$  Wnd-speed [ $m.s^{-1}$ ] (3 values), see Section 6.13.4.6, (LUT135)  
 $\theta_s$  Solar zenith angle [deg], see Section 6.13.4.3, (LUT132)  
 $\tau^{a1}$  Aerosol optical thickness at 550nm [dl] for the boundary layer (aerosol layer #1), see Section 6.13.1.1 (LUT136)  
 $\tau^{a2}$  Aerosol optical thickness at 550nm [dl] for the tropospheric layer (aerosol layer #3), see Section 6.13.1.3 (LUT409)

$\tau^{a^3}$  Aerosol optical thickness at 550nm [dl] for the stratospheric layer (aerosol layer #4) fixed to 0.005 whatever the wavelength and the assemblage except for the first one ( $iaer\#0$ ,  $\tau^{a^4} = 0$ )

$\tau^R$  Rayleigh optical thickness [dl] (15 values), see Section 6.11.1.1, (LUT410)

**Output:**  $T_{down\_LUT}[iaer, w_s, \lambda, \theta_s, \tau^a]$   
Total downward (diffuse+direct) transmittance, as function of the aerosol assemblage ( $iaer$ ), the wind-speed above sea level ( $w_s$ ), the MERIS wavelength ( $\lambda$ ), the solar zenith angle ( $\theta_s$ ), and the total AOT550 ( $\tau^a$ )

**units:** [dl]

**Note:** Because the RTC/SO (UdL) composes with 3 aerosol layers only, then the 18 dust assemblages are discarded. The total aerosol optical thicknesses ( $\tau^a$ ) at 550nm is then the sum of the 3 aerosol optical thicknesses (*resp.*,  $\tau^{a^1}$ ,  $\tau^{a^2}$  and  $\tau^{a^3}$ ) at 550nm for the 3 aerosol layers (*resp.*, boundary, troposphere and stratosphere), see table from Section 6.13.5.1.

**Step-1:** Select each aerosol model among the 17 models used in the 16 SAMs, and compute the scattering phase matrix and the IOPs (extinction & scattering coefficients, and single scattering albedo) at each of the 15 MERIS wavelengths ( $\lambda$ ) with the OTC/SCAMAT (UdL) and the associated input Scamat card:

*/UdL/INPUT/sca\_in/sc\_marxx\_byy, sc\_coaxx\_byy, sc\_rurxx\_byy, sc\_IOPww\_byy, sc\_conti\_byy, sc\_H2SO4\_byy*  
with  $\mathbf{xx} = \{50, 70, 90, 99\}$  (*i.e.*, relative humidity),  $\mathbf{yy} = \{01, \dots, 15\}$  (*i.e.*, MERIS bands #),  $\mathbf{ww} = \{01, 02, 03\}$  (*i.e.*, 3 Log-normal distributions)

**Step-2:** Generate total downwelling atmospheric transmittance  $T_{down}[iaer, w_s, \lambda, \theta_s, \tau^a]$  for a pure Rayleigh atmosphere and a maritime atmosphere (Rayleigh + aerosols) over 3 wind-roughened black sea surfaces ( $w_s=1.5, 5.0$  and  $10m.s^{-1}$ ), for each selected aerosol assemblage ( $\tau^a$ ,  $iaer$ ), for each MERIS wavelength ( $\lambda$ ), and for all illumination configurations ( $\theta_s$ ), with the RTC/UPRAD (SO).

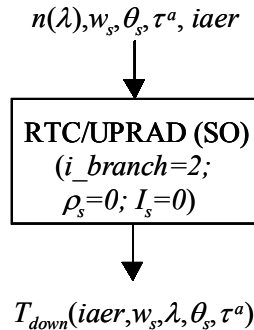
**Note:** An internal sun glint flag has been deactivated in the RTC/SO for excluding the direct to direct contribution in the computation of total downwelling atmospheric transmittance.

**RTC/UPRAD (SO) Inputs (OCEAN)**

| Variable       | Value  | Comments                              |
|----------------|--|---------------------------------------|
| out_file       | "/OUTPUT/uprad_out"                                  |                                       |
| i_branch       | 2  |                                       |
| n( $\lambda$ ) | 1, 2, 3, 4, 5, 6, 7, 8, 9, 10, 11, 12, 13, 14 and 15 | All MERIS bands, see Section 6.13.4.1 |
| $U_{H2O}$      | 0  |                                       |
| $U_{O2}$       | 0  |                                       |
| ESFT           | -  | N/A                                   |

|                            |  |   |
|----------------------------|--|---|
| $P_s$                      | 1013.25  |   |
| $t^R(\lambda)$             | tauR   | See Section 6.11.1.1  |
| <i>aerosol1</i>            | "/INPUT/sca_out/sc_marxx_byy"<br>"/INPUT/sca_out/sc_coaxx_byy"<br>"/INPUT/sca_out/sc_rurxx_byy"<br>"/INPUT/sca_out/sc_bluew_byy" | For maritime, coastal and rural aerosols, <i>xx</i> depends on RH and <i>yy</i> on $n(\lambda)$ .<br>For blue aerosols, <i>w</i> depends on the <i>Ang-ström</i> exponent and <i>yy</i> on $n(\lambda)$ . |
| $t^{a1}(550)$              | tauA1  | See Section 6.13.1.1 (7 values)   |
| <i>aerosol2</i>            | "/INPUT/sca_out/sc_conti_byy"  | <i>yy</i> depends on $n(\lambda)$   |
| $t^{a2}(550)$              | tauA2  | See Section 6.13.1.3 (7 values)   |
| <i>aerosol3</i>            | "/INPUT/sca_out/sc_H2SO4_byy"  | <i>yy</i> depends on $n(\lambda)$   |
| $t^{a3}(550)$              | 0<br>0.005   | For the first assemblage ( <i>iaer#0</i> )<br>For the other assemblages ( <i>iaer</i> )   |
| <i>cloud1</i>              | -  | N/A   |
| <i>cloud2</i>              | -  | N/A   |
| <i>cloud3</i>              | -  | N/A   |
| <i>phyto</i>               | -  | N/A   |
| $\sigma_{e,\lambda}^p$     | -  | N/A   |
| $\omega_{o,\lambda}^p$     | -  | N/A   |
| <i>spm</i>                 | -  | N/A   |
| $\sigma_{e,\lambda}^{spm}$ | -  | N/A   |
| $\omega_{o,\lambda}^{spm}$ | -  | N/A   |
| $\sigma_{a,\lambda}^{ys}$  | -  | N/A   |
| <i>vertical</i>            | "/INPUT/vertical_out"  | Not used, vertical distribution determined in RTC/SO (optically homogeneous layers)   |
| $I_s$                      | 0  | First <i>Fourier</i> term only  |
| $\rho_s$                   | 0  |   |
| $E_o$                      | 1  |   |
| $\sigma_{e,\lambda}^w$     | -  | N/A   |
| $\omega_{o,\lambda}^w$     | -  | N/A   |
| $w_s$                      | 1.5, 5.0 and 10  | See Section 6.13.4.6  |
| $n_s, n_v, n_{\Delta\phi}$ | 23, 13, 25   |   |
| $\theta_s$                 | <i>Gaussian</i> angles   | First 23 angles selected from <i>Gauss</i> quadrature;<br>See Section 6.13.4.3  |
| $\theta_v$                 | <i>Gaussian</i> angles   | First 13 angles selected from <i>Gauss</i> quadrature;<br>See Section 6.13.4.4  |
| $\Delta\phi$               | see inputs   | See Section 6.13.4.5  |
| <i>pol</i>                 | 1  |   |





Step-3: For each RTC/UPRAD (SO) run, extract the total downwelling transmittance in the output file ('./OUTPUT/uprad\_out') and build the  $T_{down\_LUT}[iaer, w_s, \lambda, \theta_s, \tau^a]$  table for the 16 SAMs (iaer#0, 4 MAR, 4 COA, 4 RUR, 3 BLU-IOP).

Note: This  $T_{down\_LUT}[iaer, w_s, \lambda, \theta_s, \tau^a]$  LUT will be completed with null values for *iaer* from #13 to #30.

#### Scientific content:

$T_{down\_LUT}[iaer, w_s, \lambda, \theta_s, \tau^a]$  describes the total downwelling atmospheric transmittance.

This table is useful for the aerosol correction algorithm over wind-roughened oceanic surface.

Note that the values of these coefficients will be extracted from this table by using multiple linear interpolations.

The current baseline is:

- $N_{w_s}$  which corresponds to 3 predefined wind-speeds of 1.5, 5.0 and  $10 m.s^{-1}$
- $N_{\theta_s}$  which corresponds to 23 predefined values (see [Section 6.13.4.3](#))
- $N_{\tau^a}$  which corresponds to 7 predefined values (including the pure *Rayleigh* case)

#### Resources:

Estimated CPU time: 21600 *sec* (if LUT419 already generated, otherwise 34860 *sec*)  
Output disk space:  $34 \times 15 \times 3 \times 23 \times 7 \times 4$  bytes/fl = 985320 bytes

#### Acceptance:

Some comparisons with *Gordon and Wrang* (1994) approximation and with another RTC, such as the RTC/MOMO from FUB have been done, as well as a quality check with tables generated by the LOV institute.

### 6.13.11.2 Total upward transmittance (direct+diffuse)

**NOTE:** The recipe of this LUT is presently not included in the MERISAT tool. This LUT is currently generated with an input user specified file.

Reference: Tup\_LUT, LUT486

[AD-8] Section 6.13.12, ADSR field 1

#### Dependencies:

LUT130, LUT133, LUT136, LUT409, LUT410

#### Tools:

RTC/UPRAD (SO)

#### Procedure:

Inputs:  $iaer$  Aerosol assemblage # [ $dI$ ] (16 SAMs [ $iaer\#0 + MAR + COA + RUR + BLU-IOP$ ])  
 $\lambda$  MERIS wavelength [ $nm$ ] (15 values), see Section 6.13.4.1, (LUT130)  
 $w_s$  Wind-speed [ $m.s^{-1}$ ] (3 values), see Section 6.13.4.6, (LUT135)  
 $\theta_v$  View zenith angle [ $deg$ ], see Section 6.13.4.4, (LUT133)  
 $\tau^{a1}$  Aerosol optical thickness at 550nm [ $dI$ ] for the boundary layer (aerosol layer #1), see Section 6.13.1.1 (LUT136)  
 $\tau^{a2}$  Aerosol optical thickness at 550nm [ $dI$ ] for the tropospheric layer (aerosol layer #3), see Section 6.13.1.3 (LUT409)  
 $\tau^{a3}$  Aerosol optical thickness at 550nm [ $dI$ ] for the stratospheric layer (aerosol layer #4) fixed to 0.005 whatever the wavelength and the assemblage except for the first one ( $iaer\#0$ ,  $\tau^{a4} = 0$ )  
 $\tau^R$  Rayleigh optical thickness [ $dI$ ] (15 values), see Section 6.11.1.1, (LUT410)

Output:  $Tup\_LUT[iaer, \lambda, \theta_v, \tau^a]$   
 Total downward (diffuse+direct) transmittance, as function of the aerosol assemblage ( $iaer$ ), the MERIS wavelength ( $\lambda$ ), the view zenith angle ( $\theta_v$ ), and the total AOT550 ( $\tau^a$ )

units: [ $dI$ ]

Notes: Because the RTC/SO (UdL) composes with 3 aerosol layers only, then the 18 dust assemblages are discarded. The total aerosol optical thicknesses ( $\tau^a$ ) at 550nm is then the sum of the 3 aerosol optical thicknesses (*resp.*,  $\tau^{a1}$ ,  $\tau^{a2}$  and  $\tau^{a3}$ ) at 550nm for the 3 aerosol layers (*resp.*, boundary, troposphere and stratosphere), see table from Section 6.13.5.1.

Using the principle of reciprocity, the upwelling atmospheric transmittance over a wind-roughened black sea surface corresponds to the downwelling atmospheric transmittance over a black land surface.

Step-1: Select each aerosol model among the 17 models used in the 16 SAMs, and compute the scattering phase matrix and the IOPs (extinction & scattering coefficients, and single scattering albedo) at each of the 15 MERIS wavelengths ( $\lambda$ ) with the OTC/SCAMAT (UdL) and the associated input *Scamat* card:

*/UdL/INPUT/sca\_in/sc\_marxx\_byy, sc\_coaxx\_byy, sc\_rurxx\_byy, sc\_IOPww\_byy, sc\_conti\_byy, sc\_H2SO4\_byy*

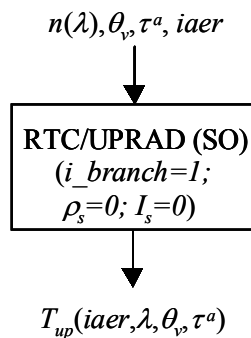
with  $\mathbf{xx} = \{50, 70, 90, 99\}$  (i.e., relative humidity),  $\mathbf{yy} = \{01, \dots, 15\}$  (i.e., MERIS bands #),  $\mathbf{ww} = \{01, 02, 03\}$  (i.e., 3 Log-normal distributions)

Step-2: Generate total upwelling atmospheric transmittance  $T_{up}[iaer, \lambda, \theta, \tau^a]$  for a pure *Rayleigh* atmosphere and a maritime atmosphere (*Rayleigh* + aerosols) over a black land, for each selected aerosol assemblage ( $\tau^a$ , *iaer*), for each MERIS wavelength ( $\lambda$ ), and for all illumination configurations ( $\theta$ ), with the RTC/UPRAD (SO).

**RTC/UPRAD (SO) Inputs (OCEAN)**

| Variable               | Value  | Comments  |
|------------------------|--|---|
| <i>out_file</i>        | "/OUTPUT/uprad_out"  |   |
| <i>i_branch</i>        | 1  |   |
| $n(\lambda)$           | 1, 2, 3, 4, 5, 6, 7, 8, 9, 10, 11, 12, 13, 14 and 15   | All MERIS bands, see <a href="#">Section 6.13.4.1</a>   |
| $U_{H2O}$              | 0  |   |
| $U_{O2}$               | 0  |   |
| <i>ESFT</i>            | -  | N/A   |
| $P_s$                  | 1013.25  |   |
| $\tau^R(\lambda)$      | tauR   | See <a href="#">Section 6.11.1.1</a>  |
| <i>aerosol1</i>        | "/INPUT/sca_out/sc_marxx_byy"<br>"/INPUT/sca_out/sc_coaxx_byy"<br>"/INPUT/sca_out/sc_rurxx_byy"<br>"/INPUT/sca_out/sc_bluew_byy" | For maritime, coastal and rural aerosols, <i>xx</i> depends on RH and <i>yy</i> on $n(\lambda)$ .<br>For blue aerosols, <i>w</i> depends on the <i>Ang-ström</i> exponent and <i>yy</i> on $n(\lambda)$ . |
| $\tau^a(550)$          | tauA1  | See <a href="#">Section 6.13.1.1</a> (7 values)   |
| <i>aerosol2</i>        | "/INPUT/sca_out/sc_conti_byy"  | <i>yy</i> depends on $n(\lambda)$   |
| $\tau^a(550)$          | tauA2  | See <a href="#">Section 6.13.1.3</a> (7 values)   |
| <i>aerosol3</i>        | "/INPUT/sca_out/sc_H2SO4_byy"  | <i>yy</i> depends on $n(\lambda)$   |
| $\tau^a(550)$          | 0<br>0.005   | For the first assemblage ( <i>iaer</i> #0)<br>For the other assemblages ( <i>iaer</i> )   |
| <i>cloud1</i>          | -  | N/A   |
| <i>cloud2</i>          | -  | N/A   |
| <i>cloud3</i>          | -  | N/A   |
| <i>phyto</i>           | -  | N/A   |
| $\sigma_{e,\lambda}^p$ | -  | N/A   |
| $\omega_{o,\lambda}^p$ | -  | N/A   |

|                            |                        |  |
|----------------------------|------------------------|--|
| $spm$                      | -                      | N/A  |
| $\sigma_{e,\lambda}^{spm}$ | -                      | N/A  |
| $\omega_{o,\lambda}^{spm}$ | -                      | N/A  |
| $\sigma_{a,\lambda}^{ys}$  | -                      | N/A  |
| <i>vertical</i>            | "/INPUT/vertical_out"  | Not used, vertical distribution determined in RTC/SO (optically homogeneous layers)            |
| $I_s$                      | 0                      | First <i>Fourier</i> term only   |
| $\rho_s$                   | 0                      |  |
| $E_o$                      | 1                      |  |
| $\sigma_{e,\lambda}^w$     | -                      | N/A  |
| $\omega_{o,\lambda}^w$     | -                      | N/A  |
| $w_s$                      | 0                      |  |
| $n_s, n_v, n_{\Delta\phi}$ | 23, 13, 25             |  |
| $\theta_s$                 | <i>Gaussian</i> angles | First 23 angles selected from <i>Gauss</i> quadrature;<br>See <a href="#">Section 6.13.4.3</a> |
| $\theta_v$                 | <i>Gaussian</i> angles | First 13 angles selected from <i>Gauss</i> quadrature;<br>See <a href="#">Section 6.13.4.4</a> |
| $\Delta\phi$               | see inputs             | See <a href="#">Section 6.13.4.5</a>   |
| <i>pol</i>                 | 1                      |  |



Step-3: For each RTC/UPRAD (SO) run, extract from the total downwelling transmittance in the output file ('/OUTPUT/uprad\_out') and build the  $T_{up\_LUT}[iaer, \lambda, \theta_v, \tau^a]$  table for the 16 SAMs (*iaer*#0, 4 MAR, 4 COA, 4 RUR, 3 BLU-IOP).

Note: This  $T_{up\_LUT}[iaer, \lambda, \theta_v, \tau^a]$  LUT will be completed with null values for *iaer* from #13 to #30.

**Scientific content:**

$T_{up\_LUT}[iaer, \lambda, \theta_v, \tau^a]$  describes the total upwelling atmospheric transmittance.

This table is useful for the aerosol correction algorithm over wind-roughened oceanic surface.

Note that the values of these coefficients will be extracted from this table by using multiple linear interpolations.

The current baseline is:

$N_{\theta_v}$  which corresponds to 13 predefined values (see [Section 6.13.4.4](#))  
 $N_{\tau^a}$  which corresponds to 7 predefined values (including the pure *Rayleigh* case)

Resources:

Estimated CPU time: 7200 *sec* (if LUT419 already generated, otherwise 20460 *sec*)  
Output disk space:  $34 \times 15 \times 13 \times 7 \times 4$  bytes/fl = 185640 bytes

Acceptance:

Some comparisons with *Gordon and Wrang* (1994) approximation and with another RTC, such as the RTC/MOMO from FUB have been done, as well as a quality check with tables generated by the LOV institute.

## 6.14 LAND-AEROSOL PARAMETERS

### 6.14.1 C.P.

#### 6.14.1.1 C.P. Imaginary parts of refractive indices for land-aerosol models

Reference: ni, LUT144

[AD-6]

PARBLEU provided

Dependencies:

None

Tool:

None

Procedure:

Input: none

Output: *ni* Imaginary parts of refractive indices for land-aerosol models (78 values)  
units: [*dl*]

Step: User specified.

Scientific content:

Set of 78  $n_i$  values corresponding to the imaginary parts of refractive indices of particles included in the 78 land-aerosol models

Current baseline: vector with 78 null values [*dl*]

Resources:

Estimated CPU time: -

Output disk space:  $78 \times 4$  bytes/fl = 312 bytes

Acceptance:

Corresponds to the latest definition.

### 6.14.2 MPH

Not covered in this document (see [\[AD-8\]](#) for a detailed description)

### 6.14.3 SPH

Not covered in this document (see [\[AD-8\]](#) for a detailed description)

### 6.14.4 GADS General

#### 6.14.4.1 Zenith angles

Reference: ZA, LUT147

[\[AD-8\]](#) Section 6.14.4, GADS field 1.

ACRI provided

#### Dependencies:

None

#### Tool:

None

#### Procedure:

Input: none

Output: ZA Zenith angles (12 values)

units:  $[10^{-6} \text{ deg}]$

Step: User specified.

#### Scientific content:

Set of 12 zenith angles ( $\theta$ ) selected from the *Gauss* quadrature generated for 24 discrete directions with the RTC/Gauss tool (UdL)

Current baseline: 12 *Gaussian* angles (see [Section 6.2.13.1](#))

#### Resources:

Estimated CPU time: -

Output disk space:  $15 \times 4 \text{ bytes/ul} = 60 \text{ bytes}$

Acceptance:

Corresponds to the latest definition.

6.14.4.2 Stored indices for  $(\theta_s, \times \theta_v)$  combinations

Reference: SVZA\_index, LUT148

[AD-8] Section 6.14.4, GADS field 2.

ACRI provided

Dependencies:

None

Tool:

None

Procedure:

Input: none

Output: SVZA\_index Stored indices for  $(\theta_s, \times \theta_v)$  combinations (78 values)

units: [dl]

Step: User specified.

Scientific content:

Current baseline: 78 angular combinations (SZA x VZA) (see [Section 6.10.7.14](#))

Note: Due to the fact that the matrix is symmetrical in the  $(\theta_s \times \theta_v)$  directions, we can then store only a half triangular matrix, *i.e.*,  $N(N+1)/2$  instead of  $N^2$  elements (78 instead of 144).

Resources:

Estimated CPU time: -

Output disk space:  $78 \times 2 \times 1$  byte/uc = 156 bytes

Acceptance:

Corresponds to the latest definition.



#### 6.14.4.3 Relative azimuth angles

Reference: RAA, LUT149

[AD-8] Section 6.14.4, GADS field 3.

ACRI provided

Dependencies:

None

Tool:

None

Procedure:

Input: none

Output: RAA Relative azimuth angle (18 values)

units:  $[10^{-6} \text{ deg}]$

Step: User specified.

Scientific content:

The set of the relative azimuth angles ( $\Delta\phi$ ) between illumination and viewing directions is regularly spaced and listed hereafter:

Current baseline: 18 RAA values ( $\Delta\phi$ ) within  $[0;180]$  deg., with a step of 10 deg.

Resources:

Estimated CPU time: -

Output disk space:  $19 \times 4 \text{ bytes/ul} = 76 \text{ bytes}$

Acceptance:

Corresponds to the latest definitions

#### 6.14.4.4 Cosine of scattering angles

Reference: Cos\_Theta\_Sca, LUT150

[AD-8] Section 6.14.4, GADS field 4.

ACRI provided

Dependencies:

None

Tool:

None

Procedure:

Input: none

Output: *Cos\_Theta\_Sca*  
Cosine of scattering angle

units: [dl]

Step: User specified.

Scientific content:

Set of 83 scattering angles ( $\Theta$ ) computed with angles deriving from the *Gauss* quadrature for 40 discrete directions (+ nadir/zenith) with the RTC/Gauss tool (UdL)

Current baseline: 83 values of  $\cos(\Theta)$

| <i>i</i> | $\cos(\Theta_i)$ | <i>i</i> | $\cos(\Theta_i)$ | <i>i</i> | $\cos(\Theta_i)$ | <i>i</i> | $\cos(\Theta_i)$ |
|----------|------------------|----------|------------------|----------|------------------|----------|------------------|
| 1        | -1.000000000     | 22       | -0.6896376010    | 43       | 0.0195113830     | 64       | 0.7440002561     |
| 2        | -0.9995538000    | 23       | -0.6608598830    | 44       | 0.0585044362     | 65       | 0.7695024014     |
| 3        | -0.9976498480    | 24       | -0.6310757400    | 45       | 0.0974083543     | 66       | 0.7938326597     |
| 4        | -0.9942275290    | 25       | -0.6003305910    | 46       | 0.1361640096     | 67       | 0.8169541359     |
| 5        | -0.9892912510    | 26       | -0.5686712270    | 47       | 0.1747122407     | 68       | 0.8388314247     |
| 6        | -0.9828485250    | 27       | -0.5361458660    | 48       | 0.2129944563     | 69       | 0.8594313860     |
| 7        | -0.9749091270    | 28       | -0.5028041010    | 49       | 0.2509523034     | 70       | 0.8787225485     |
| 8        | -0.9654850360    | 29       | -0.4686965940    | 50       | 0.2885280252     | 71       | 0.8966755271     |
| 9        | -0.9545907380    | 30       | -0.4338753220    | 51       | 0.3256643414     | 72       | 0.9132630825     |
| 10       | -0.9422427420    | 31       | -0.3983933930    | 52       | 0.3623047471     | 73       | 0.9284598231     |
| 11       | -0.9284598230    | 32       | -0.3623047470    | 53       | 0.3983933926     | 74       | 0.9422427416     |
| 12       | -0.9132630830    | 33       | -0.3256643410    | 54       | 0.4338753223     | 75       | 0.9545907378     |
| 13       | -0.8966755270    | 34       | -0.2885280250    | 55       | 0.4686965942     | 76       | 0.9654850364     |
| 14       | -0.8787225480    | 35       | -0.2509523030    | 56       | 0.5028041005     | 77       | 0.9749091268     |
| 15       | -0.8594313860    | 36       | -0.2129944560    | 57       | 0.5361458659     | 78       | 0.9828485250     |
| 16       | -0.8388314250    | 37       | -0.1747122410    | 58       | 0.5686712265     | 79       | 0.9892912507     |
| 17       | -0.8169541360    | 38       | -0.1361640100    | 59       | 0.6003305912     | 80       | 0.9942275286     |
| 18       | -0.7938326600    | 39       | -0.0974083540    | 60       | 0.6310757399     | 81       | 0.9976498485     |

| <i>i</i> | cos( $\Theta_i$ ) | <i>i</i> | cos( $\Theta_i$ ) | <i>i</i> | cos( $\Theta_i$ ) | <i>i</i> | cos( $\Theta_i$ ) |
|----------|-------------------|----------|-------------------|----------|-------------------|----------|-------------------|
| 19       | -0.7695024010     | 40       | -0.0585044360     | 61       | 0.6608598828      | 82       | 0.9995537996      |
| 20       | -0.7440002560     | 41       | -0.0195113830     | 62       | 0.6896376014      | 83       | 1.0000000000      |
| 21       | -0.7173651460     | 42       | 0.0000000000      | 63       | 0.7173651457      |          |                   |

Resources:

Estimated CPU time: -  
Output disk space: 83 × 4 bytes/fl = 332 bytes

Acceptance:

Corresponds to the latest definitions

6.14.4.5 *Indices of band numbers (starting from 1) for in-land waters and islands screening*

Reference: (No variable used), LUT151

[AD-8] Section 6.14.4, GADS field 5

ACRI provided

Dependencies:

None

Tool:

None

Procedure:

Input: none

Output: (no variable) Indices of band numbers for in-land waters and islands screening (2 values)

units: [dl]

Step: User specified.

Scientific content:

2 MERIS bands selected for in-land waters and islands screening

Current baseline: {7, 13}

Resources:

Estimated CPU time: -  
Output disk space: 1 × 2 bytes/us = 2 bytes

Acceptance:

Corresponds to the latest definitions

**6.14.4.6 Threshold for in-land waters screening spectral slope test**

Reference: (No variable used), LUT152

[AD-8] Section 6.14.4, GADS field 6

ACRI provided

Dependencies:

None

Tool:

None

Procedure:

Input: none

Output: (no variable) Threshold for in-land waters screening spectral slope test  
units: [dl]

Step: User specified.

Scientific content:

Threshold used for in-land waters screening spectral slope test

Current baseline: 1

Resources:

Estimated CPU time: -  
Output disk space: 1 × 4 bytes/fl = 4 bytes

Acceptance:

Corresponds to the latest definitions

6.14.4.7 *Threshold for islands screening spectral slope test*

Reference: (No variable used), LUT153

[AD-8] Section 6.14.4, GADS field 7

ACRI provided

Dependencies:

None

Tool:

None

Procedure:

Input: none

Output: *(no variable)* Threshold for islands screening spectral slope test

units: [dl]

Step: User specified.

Scientific content:

Threshold used for islands screening spectral slope test

Current baseline: 1

Resources:

Estimated CPU time: -

Output disk space: 1 × 4 bytes/fl = 4 bytes

Acceptance:

Corresponds to the latest definitions

6.14.4.8 *Aerosol optical properties (real part of refractive index, Angstrom exponent) for land-aerosol models*

Reference: Aerosol\_angstrom, LUT154  
& Aerosol\_refindex

[AD-8] Section 6.14.4, GADS field 8.

ACRI provided

Dependencies:

None

Tool:

None

Procedure:

Inputs: *iaer* Aerosol model # [*dl*] (among the 78 aerosol models)  
*k* Output index [*dl*] (for selecting the aerosol property)

Outputs: *Aerosol\_refindex[iaer]* *k=1* refractive index (real part)  
*Aerosol\_angstrom[iaer]* *k=2* Angström coefficient ( $\alpha$ )

units: [*dl*]

Step: User specified.

Scientific content:

The first parameter is the *Angström* exponent ( $\alpha$ ) which describes the wavelength dependence of the aerosol optical thickness  $\tau^a(\lambda)$ ,

$$\frac{\tau^a(\lambda)}{\tau^a(\lambda')} = \left( \frac{\lambda}{\lambda'} \right)^\alpha$$

The latter is employed in the definition of the *Junge* size distribution  $n(r)$  which is a power-law well known as the simplest but realistic description.

$$n(r) \approx r^{\alpha-3}$$

The second parameter is the real part of the refractive index  $m$  (referred as  $Re(m)$ ) which is related to the aerosol optical characteristic. The aerosol absorption is accounted for with the imaginary part of the refractive index ( $Im(m)$ ).

78 aerosol models have been defined to be used in the atmospheric correction algorithm over land. The latter results from different values for the *Angström* exponent ( $\alpha$ ) and the refractive index ( $m$ ) which is considered as independent on the wavelength.

Current baseline: 78 x 2 values

| <i>iaer</i> | <i>Re(m)</i><br>[k=1] | $\alpha$<br>[k=2] | <i>Im(m)</i> |
|-------------|-----------------------|-------------------|--------------|
| 1           | 1.33                  | 0.0               | 0            |
| 2           | 1.33                  | 0.1               | 0            |
| 3           | 1.33                  | 0.2               | 0            |
| 4           | 1.33                  | 0.3               | 0            |
| 5           | 1.33                  | 0.4               | 0            |
| 6           | 1.33                  | 0.5               | 0            |
| 7           | 1.33                  | 0.6               | 0            |
| 8           | 1.33                  | 0.7               | 0            |
| 9           | 1.33                  | 0.8               | 0            |
| 10          | 1.33                  | 0.9               | 0            |
| 11          | 1.33                  | 1.0               | 0            |
| 12          | 1.33                  | 1.1               | 0            |
| 13          | 1.33                  | 1.2               | 0            |
| 14          | 1.33                  | 1.3               | 0            |
| 15          | 1.33                  | 1.4               | 0            |
| 16          | 1.33                  | 1.5               | 0            |
| 17          | 1.33                  | 1.6               | 0            |
| 18          | 1.33                  | 1.7               | 0            |
| 19          | 1.33                  | 1.8               | 0            |
| 20          | 1.33                  | 1.9               | 0            |
| 21          | 1.33                  | 2.0               | 0            |
| 22          | 1.33                  | 2.1               | 0            |
| 23          | 1.33                  | 2.2               | 0            |
| 24          | 1.33                  | 2.3               | 0            |
| 25          | 1.33                  | 2.4               | 0            |
| 26          | 1.33                  | 2.5               | 0            |

| <i>iaer</i> | <i>Re(m)</i><br>[k=1] | $\alpha$<br>[k=2] | <i>Im(m)</i> |
|-------------|-----------------------|-------------------|--------------|
| 27          | 1.44                  | 0.0               | 0            |
| 28          | 1.44                  | 0.1               | 0            |
| 29          | 1.44                  | 0.2               | 0            |
| 30          | 1.44                  | 0.3               | 0            |
| 31          | 1.44                  | 0.4               | 0            |
| 32          | 1.44                  | 0.5               | 0            |
| 33          | 1.44                  | 0.6               | 0            |
| 34          | 1.44                  | 0.7               | 0            |
| 35          | 1.44                  | 0.8               | 0            |
| 36          | 1.44                  | 0.9               | 0            |
| 37          | 1.44                  | 1.0               | 0            |
| 38          | 1.44                  | 1.1               | 0            |
| 39          | 1.44                  | 1.2               | 0            |
| 40          | 1.44                  | 1.3               | 0            |
| 41          | 1.44                  | 1.4               | 0            |
| 42          | 1.44                  | 1.5               | 0            |
| 43          | 1.44                  | 1.6               | 0            |
| 44          | 1.44                  | 1.7               | 0            |
| 45          | 1.44                  | 1.8               | 0            |
| 46          | 1.44                  | 1.9               | 0            |
| 47          | 1.44                  | 2.0               | 0            |
| 48          | 1.44                  | 2.1               | 0            |
| 49          | 1.44                  | 2.2               | 0            |
| 50          | 1.44                  | 2.3               | 0            |
| 51          | 1.44                  | 2.4               | 0            |
| 52          | 1.44                  | 2.5               | 0            |

| <i>iaer</i> | <i>Re(m)</i><br>[k=1] | $\alpha$<br>[k=2] | <i>Im(m)</i> |
|-------------|-----------------------|-------------------|--------------|
| 53          | 1.55                  | 0.0               | 0            |
| 54          | 1.55                  | 0.1               | 0            |
| 55          | 1.55                  | 0.2               | 0            |
| 56          | 1.55                  | 0.3               | 0            |
| 57          | 1.55                  | 0.4               | 0            |
| 58          | 1.55                  | 0.5               | 0            |
| 59          | 1.55                  | 0.6               | 0            |
| 60          | 1.55                  | 0.7               | 0            |
| 61          | 1.55                  | 0.8               | 0            |
| 62          | 1.55                  | 0.9               | 0            |
| 63          | 1.55                  | 1.0               | 0            |
| 64          | 1.55                  | 1.1               | 0            |
| 65          | 1.55                  | 1.2               | 0            |
| 66          | 1.55                  | 1.3               | 0            |
| 67          | 1.55                  | 1.4               | 0            |
| 68          | 1.55                  | 1.5               | 0            |
| 69          | 1.55                  | 1.6               | 0            |
| 70          | 1.55                  | 1.7               | 0            |
| 71          | 1.55                  | 1.8               | 0            |
| 72          | 1.55                  | 1.9               | 0            |
| 73          | 1.55                  | 2.0               | 0            |
| 74          | 1.55                  | 2.1               | 0            |
| 75          | 1.55                  | 2.2               | 0            |
| 76          | 1.55                  | 2.3               | 0            |
| 77          | 1.55                  | 2.4               | 0            |
| 78          | 1.55                  | 2.5               | 0            |

*Angström* exponent ( $\alpha$ ) and real and imaginary part of refractive index (*m*) for each of the 78 aerosol models used in the atmospheric correction algorithm.

Resources:

Estimated CPU time: -  
Output disk space: 78 × 2 × 4 bytes/fl = 624 bytes

Acceptance:

Corresponds to the latest definitions

6.14.4.9 Aerosol optical thicknesses at 550 nm

Reference: AOT550, LUT155

[AD-8] Section 6.14.4, GADS field 9.

ACRI provided

Dependencies:

None

Tool:

None

Procedure:

Inputs: none

Outputs: *tauA* Aerosol optical thickness (16 values of  $\tau_a$ )  
units: [*dI*]

Step: User specified.

Scientific content:

Set of 16 aerosol optical thicknesses at 550nm ( $\tau_a$ ) used for the aerosol climatology over land

Current baseline: 16  $\tau_a$  values from 0 to 1.5 by step of 0.1.

Resources:

Estimated CPU time: -

Output disk space:  $16 \times 4 \text{ bytes/fl} = 64 \text{ bytes}$

Acceptance:

Corresponds to the latest definitions.

6.14.4.10 Gamma coefficient for ARVI computation

Reference: Gamma, LUT156

[AD-8] Section 6.14.4, ADSR field 10

ACRI provided

Dependencies:



None

Tool:

None

Procedure:

Inputs: none

Outputs: *Gamma* Gamma coefficient for ARVI computation ( $\gamma$ )  
units: [dl]

Step: User specified.

Scientific content:

This  $\gamma$  coefficient is required for the ARVI (Atmospherically Resistant Vegetation Index) computation. The latter has been introduced by *Kauffman and Tanré (1992)* [RD-9] to decrease the atmospheric effects by adding a blue band to the NDVI (Normalized Difference Vegetation Index). Using the MERIS bands, ARVI is expressed as:

$$ARVI = \frac{\rho_{aG}(865) - \rho_{RB}}{\rho_{aG}(865) + \rho_{RB}}$$

where  $\rho_{aG}(865)$  is the *Rayleigh*-corrected TOA reflectance at the 865 nm MERIS wavelength and  $\rho_{RB}$  is a linear combinaison of *Rayleigh*-corrected TOA reflectances in the blue and red bands. For the MERIS wavelengths, the latter is defined as:

$$\rho_{RB} = \rho_{aG}(665) - \gamma \cdot [\rho_{aG}(442.5) - \rho_{aG}(665)]$$

From a practical point of view, an optimal value for the  $\gamma$  coefficient could be derived from RTC simulations for a selected DDV (Dense Dark Vegetation) model, several aerosol models and different illumination and viewing geometries. This sensitivity study on the simulated ARVI versus the  $\gamma$  value should allow then to deduce the optimized  $\gamma$  value of DDV remote sensing for which the ARVI is less sensitive to the aerosol loading and models.

*Kauffman and Tanré (1992)* stressed that this optimal  $\gamma$  value may be set up to 1.3 for DDVs over forest covers [RD-9].

Current baseline: 1.3

Resources:

Estimated CPU time: -  
Output disk space: 1 × 4 bytes/fl = 4 bytes

Acceptance:

Numerous studies have already stressed that the  $\gamma$  optimal value for DDV was equal to 1.3.

**6.14.4.11 Aerosol optical thickness increment for iterative procedure**

Reference: dtauA, LUT157

[AD-8] Section 6.14.4, ADSR field 11

ACRI provided

Dependencies:

None

Tool:

None

Procedure:

Inputs: none

Outputs: dtauA Aerosol optical thickness increment ( $\Delta\tau_a$ )  
units: [dl]

Step: User specified.

Scientific content:

This increment in aerosol optical thickness ( $\Delta\tau_a$ ) is used in the iterative procedure.

Current baseline: 0.1

Resources:

Estimated CPU time: -

Output disk space: 1 × 4 bytes/fl = 4 bytes

Acceptance:

Corresponds to the latest definition.

**6.14.4.12 Dense dark vegetation, DDV(biome,month)**

Reference: DDV, LUT309

[AD-8] Section 6.14.4, ADSR field 12

ACRI provided

Dependencies:

None

Tool:

None

Procedure:

Inputs: *Bi* Biome # [*dl*], type of vegetation (11 values)  
*month* Period [*month*] (12 values)

Outputs: *DDV* Dense dark vegetation  
units: [*dl*]

Step: User specified.

Scientific content:

This increment in aerosol optical thickness ( $\Delta\tau_a$ ) is used in the iterative procedure.

Current baseline: 11 x 12 values

| <i>Jan</i> | <i>Feb</i> | <i>Mar</i> | <i>Apr</i> | <i>May</i> | <i>June</i> | <i>July</i> | <i>Aug</i> | <i>Sept</i> | <i>Oct</i> | <i>Nov</i> | <i>Dec</i> |
|------------|------------|------------|------------|------------|-------------|-------------|------------|-------------|------------|------------|------------|
| 9          | 9          | 9          | 9          | 9          | 9           | 9           | 9          | 9           | 9          | 9          | 9          |
| 10         | 10         | 10         | 10         | 10         | 10          | 10          | 10         | 10          | 10         | 10         | 10         |
| 0          | 0          | 11         | 11         | 11         | 11          | 11          | 11         | 0           | 0          | 0          | 0          |
| 1          | 1          | 12         | 12         | 12         | 12          | 12          | 12         | 12          | 12         | 1          | 1          |
| 2          | 2          | 13         | 13         | 13         | 13          | 13          | 13         | 2           | 2          | 2          | 2          |
| 3          | 3          | 14         | 14         | 14         | 14          | 14          | 14         | 3           | 3          | 3          | 3          |
| 4          | 4          | 15         | 15         | 15         | 15          | 15          | 15         | 4           | 4          | 4          | 4          |
| 5          | 5          | 16         | 16         | 16         | 16          | 16          | 16         | 5           | 5          | 5          | 5          |
| 6          | 6          | 17         | 17         | 17         | 17          | 17          | 17         | 6           | 6          | 6          | 6          |
| 7          | 7          | 18         | 18         | 18         | 18          | 18          | 18         | 7           | 7          | 7          | 7          |
| 8          | 8          | 19         | 19         | 19         | 19          | 19          | 19         | 8           | 8          | 8          | 8          |

Resources:

Estimated CPU time: -  
Output disk space: 11 x 12 x 1 byte/uc = 132 bytes

Acceptance:

Corresponds to the latest definition.

#### 6.14.4.13 Latitudes for DDV climatology

Reference: lat, LUT310

[AD-8] Section 6.14.4, ADSR field 13

ACRI provided

#### Dependencies:

None

#### Tool:

None

#### Procedure:

Inputs: none

Outputs: lat Latitude (180 values)

units:  $[10^{-6} \text{ deg}]$

Step: User specified.

#### Scientific content:

Set of 180 latitudes (*lat*) used as the geographic grid for the DDV climatology

Current baseline:  $[-89.5;89.5] \text{ deg.}$  by step of 1 *deg.*

#### Resources:

Estimated CPU time: -

Output disk space:  $180 \times 4 \text{ bytes/sl} = 720 \text{ bytes}$

#### Acceptance:

Corresponds to the latest definition.

#### 6.14.4.14 Longitudes for DDV climatology

Reference: Long, LUT311

[AD-8] Section 6.14.4, ADSR field 14

ACRI provided

Dependencies:

None

Tool:

None

Procedure:

Inputs: none

Outputs: *long* Longitude (360 values)  
units:  $[10^{-6} \text{ deg}]$

Step: User specified.

Scientific content:

Set of 360 longitudes (*long*) used as the geographic grid for the DDV climatology

Current baseline:  $[-179.5; 179.5] \text{ deg.}$  by step of 1 *deg.*

Resources:

Estimated CPU time: -

Output disk space:  $360 \times 4 \text{ bytes/sl} = 1440 \text{ bytes}$

Acceptance:

Corresponds to the latest definition.

6.14.4.15 *Effective radius values*

Reference: Strato\_rad, LUT312

[AD-8] Section 6.14.4, ADSR field 15

ACRI provided

Dependencies:

None

Tool:

None

Procedure:

Inputs: none

Outputs: *Strato\_rad* Effective radius for stratospheric aerosols (18 values)

units: [dl]

Step: User specified.

Scientific content:

Set of 18 effective radii for the 18 stratospheric aerosol models

Current baseline: {0, 1, 2, 0, 1, 2, 0, 1, 2, 0, 1, 2, 0, 1, 2, 0, 1, 2}

Resources:

Estimated CPU time: -

Output disk space:  $18 \times 1 \text{ byte/uc} = 18 \text{ bytes}$

Acceptance:

Corresponds to the latest definition.

**6.14.4.16 Record numbers of GADS multiplicative function to account for volcanic aerosol multiple scattering effects**

Reference: Strato\_multi, LUT313

[AD-8] Section 6.14.4, ADSR field 16

ACRI provided

Dependencies:

None

Tool:

None

Procedure:

Inputs: none

Outputs: *Strato\_multi* Record numbers of GADS multiplicative function to account for volcanic aerosol multiple scattering effects (18 values)

units: [dl]

Step: User specified.

Scientific content:

Set of 18 record numbers for the 18 stratospheric aerosol models

Current baseline: {12, 13, 14, 12, 13, 14, 12, 13, 14, 12, 13, 14, 12, 13, 14, 12, 13, 14}

Resources:

Estimated CPU time: -

Output disk space:  $18 \times 1 \text{ byte/uc} = 18 \text{ bytes}$

Acceptance:

Corresponds to the latest definition.

**6.14.4.17 Volcanic aerosol optical thicknesses,  $\tau^{va}(iaer)$**

Reference: Strato\_tau, LUT314

[AD-8] Section 6.14.4, ADSR field 17

ACRI provided

Dependencies:

None

Tool:

None

Procedure:

Inputs: none

Outputs: *Strato\_tau* Volcanic aerosol optical thickness (18 values)

units: [dl]

Step: User specified.

Scientific content:

Set of 18 volcanic aerosol optical thicknesses ( $\tau^{va}$ ) for the 18 stratospheric aerosol models

Current baseline: {0.1, 0.1, 0.1, 0.1, 0.1, 0.1, 0.1, 0.1, 0.1, 0.1, 0.1, 0.1, 0.1, 0.1, 0.1, 0.1, 0.1}

Resources:

Estimated CPU time: -

Output disk space:  $18 \times 4 \text{ bytes/fl} = 72 \text{ bytes}$

Acceptance:

Corresponds to the latest definition.

*6.14.4.18 Reflectance threshold at 865 nm for DDV screening*

Reference: (No variable used), LUT439

[AD-8] Section 6.14.4, ADSR field 18

ACRI provided

Dependencies:

None

Tool:

None

Procedure:

Inputs: none

Outputs: (no variable) Reflectance threshold at 865nm for DDV screening

units: [dl]

Step: User specified.

Scientific content:

Threshold on reflectance at 865nm for screening the DDV pixels

Current baseline: 0.2



Resources:

Estimated CPU time: -  
Output disk space: 1 × 4 bytes/fl = 4 bytes

Acceptance:

Corresponds to the latest definition.

6.14.4.19 Ground reflectance threshold at 665 nm for iterative aerosol identification

Reference: (No variable used), LUT487

[AD-8] Section 6.14.4, ADSR field 19

ACRI provided

Dependencies:

None

Tool:

None

Procedure:

Inputs: none

Outputs: (no variable) Ground reflectance threshold at 665 nm for iterative aerosol identification  
units: [dl]

Step: User specified.

Scientific content:

Threshold on ground reflectance at 665 nm for iterative aerosol identification

Current baseline: 0.2

Resources:

Estimated CPU time: -  
Output disk space: 1 × 4 bytes/fl = 4 bytes

Acceptance:

Corresponds to the latest definition.

6.14.4.20 *List of band indices (starting from 1) to be used for land aerosols remote sensing*

Reference: (No variable used), LUT488

[AD-8] Section 6.14.4, ADSR field 20

ACRI provided

Dependencies:

None

Tool:

None

Procedure:

Inputs: none

Outputs: *(no variable)* List of band indices (starting from 1) to be used for land aerosols remote sensing (3 values)

units: [dl]

Step: User specified.

Scientific content:

4 MERIS bands are available for the land-aerosol remote sensing algorithm (band#1 [412.5nm], band#2 [442.5nm], band#3 [490nm], band#7 [665nm]). 2 or 3 bands can be then selected. If only 2 bands are used then the last index will be set to 1.

For the current MERIS processing, only 2 bands are used for the land-aerosols remote sensing algorithm (band#2 and #7)).

Current baseline: {2, 7, -1}

Resources:

Estimated CPU time: -

Output disk space: 3 × 2 bytes/us = 6 bytes

Acceptance:

Corresponds to the latest definition.

## 6.14.5 GADS Reflectance Thresholds for Inland Waters and Islands Screening

### 6.14.5.1 $\alpha$ - Constant applied to threshold for inland waters screening

Reference:  $\alpha_{7\text{thresh}}$ , LUT158

[AD-8] Section 6.14.5, ADSR field 1

ACRI provided

#### Dependencies:

None

#### Tool:

None

#### Procedure:

Inputs: none

Outputs:  $\alpha_{7\text{thresh}}$   $\alpha$  - constant applied to threshold for inland waters screening  
units: [dl]

Step: User specified.

#### Scientific content:

This multiplicative factor ( $\alpha_{7\text{thresh}}$ ) is applied to the TOA reflectance thresholds at 665nm for inland waters screening processing identification to take the environment and the bathymetric effects into account.

Current baseline: 1

#### Resources:

Estimated CPU time: -

Output disk space: 1 × 4 bytes/fl = 4 bytes

#### Acceptance:

Corresponds to the latest definition.

### 6.14.5.2 TOA reflectance thresholds at 665 nm for inland waters screening, $\rho_{T,665}(\theta_s \times \theta_v, \Delta\phi)$

Reference:  $\rho_{7\text{thresh\_LUT}}$ , LUT159

[AD-8] Section 6.14.5, ADSR field 2

Dependencies:

LUT144, LUT147, LUT148, LUT149, LUT154

Tools:

OTC/SCAMAT  
OTC/RAYLEIGH  
RTC/UPRAD (SO)

Procedure:

Inputs: *iaer* Aerosol model # [dl] (among the 78 Junge's models) characterized by an Angström exponent ( $\alpha$ ) and a refractive index, see Section 6.14.4.4 (LUT144) and Section 6.14.1.1 (LUT154).  
 $\theta$  Zenith angle [deg]; tabulated values used for ( $\theta_s \times \theta_v$ ) combinations, see Section 6.14.4.1, (LUT147)  
 $\theta_s \times \theta_v$  Stored indices for angular combinations [dl] (78 values), see Section 6.14.4.2, (LUT148)  
 $\Delta\phi$  Relative azimuth angle [deg], see Section 6.14.4.3, (LUT149)

Output:  $\rho_{7thresh\_LUT}[\theta_s \times \theta_v, \Delta\phi]$   
TOA reflectance thresholds at 665nm as function of the illumination and viewing configuration ( $\theta_s, \theta_v, \Delta\phi$ )  
units: [dl]

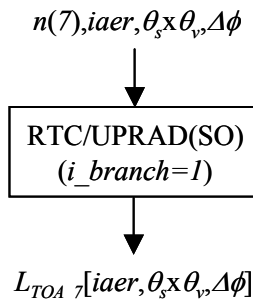
Step-0: Compute the IOPs (aerosol phase function, single scattering albedo, extinction coefficient) for all the 78 aerosol models. Eihier generate the LUT170 (see Section 6.14.11) or launch the Mie's computations with OTC/SCAMAT using as inputs the Angström exponent and refractive index (real and imaginary parts).

Step-1: Generate TOA normalized radiance  $L_{TOA, \gamma}[iaer, \theta_s \times \theta_v, \Delta\phi]$  at 665nm (MERIS band #7) for a continental atmosphere over a land reflective surface, for each of the 78 land aerosol models (*iaer*) and all illumination and viewing configurations ( $\theta_s, \theta_v, \Delta\phi$ ), with the RTC/UPRAD (SO).

**RTC/UPRAD (SO) Inputs (LAND)**

| Variable        | Value               | Comments |
|-----------------|---------------------|----------|
| <i>out_file</i> | "/OUTPUT/uprad_out" |          |
| <i>i_branch</i> | 1                   |          |
| $n(\lambda)$    | 7                   | 665nm    |
| $U_{H2O}$       | 0                   |          |
| $U_{O2}$        | 0                   |          |

| Variable                   | Value                          | Comments   |
|----------------------------|--------------------------------|--|
| <i>ESFT</i>                | -                              | N/A  |
| $P_s$                      | 1013.25                        |  |
| $\tau^R(\lambda)$          | tauR                           | Computed with OTC/RAYLEIGH   |
| <i>aerosol1</i>            | "/INPUT/sca_out/sc_landyy_b05" | yy depends on the selected <i>Junge's</i> model ( <i>iaer</i> =1 to 78)        |
| $\tau^{a1}(550)$           | 1.5                            |  |
| <i>aerosol2</i>            | -                              |  |
| $\tau^{a2}(550)$           | 0                              |  |
| <i>aerosol3</i>            | -                              |  |
| $\tau^{a3}(550)$           | 0                              |  |
| <i>cloud1</i>              | -                              | N/A  |
| <i>cloud2</i>              | -                              | N/A  |
| <i>cloud3</i>              | -                              | N/A  |
| <i>phyto</i>               | -                              | N/A  |
| $\sigma_{e,\lambda}^p$     | -                              | N/A  |
| $\omega_{o,\lambda}^p$     | -                              | N/A  |
| <i>spm</i>                 | -                              | N/A  |
| $\sigma_{e,\lambda}^{spm}$ | -                              | N/A  |
| $\omega_{o,\lambda}^{spm}$ | -                              | N/A  |
| $\sigma_{e,\lambda}^{ys}$  | -                              | N/A  |
| <i>vertical</i>            | "/INPUT/vertical_out"          | Not used, vertical distribution determined in RTC/SO ( $H_a=2$ km; $H_R=8$ km) |
| $I_s$                      | 79                             |  |
| $\rho_s$                   | 0.02                           |  |
| $E_o$                      | 1                              |  |
| $\sigma_{e,\lambda}^w$     | -                              | N/A  |
| $\omega_{o,\lambda}^w$     | -                              | N/A  |
| $w_s$                      | 0                              |  |
| $n_s, n_v, n_{\Delta\phi}$ | 12, 12, 19                     | Use a loop for 78 $\theta_s \times \theta_v$ combinations.                     |
| $\theta_s$                 | see inputs                     | See <a href="#">Section 6.14.4.1</a> and <a href="#">Section 6.14.4.2</a>      |
| $\theta_v$                 | see inputs                     | See <a href="#">Section 6.14.4.1</a> and <a href="#">Section 6.14.4.2</a>      |
| $\Delta\phi$               | see inputs                     | See <a href="#">Section 6.14.4.3</a>   |
| <i>pol</i>                 | 1                              |  |



Step-2: Select among all the aerosol models the one which yields to the highest number of maximum values of  $L_{TOA\_7}$  for all  $\theta_s \times \theta_v$  and  $\Delta\phi$  combinations, and use this  $L_{TOA\_7}$  value to compute the TOA reflectance threshold at 665nm ( $\rho_{7thresh\_LUT}[\theta_s \times \theta_v, \Delta\phi]$ ) as,

$$\rho_{7thresh\_LUT}[\theta_s \times \theta_v, \Delta\phi] = \pi \cdot \frac{L_{TOA\_7}[\theta_s \times \theta_v, \Delta\phi]}{\cos(\theta_s)}$$

Scientific content:

These TOA reflectance thresholds define the maximum reflectances as observed at 665nm over water surfaces. The latter are useful for the inland waters discrimination in the pixels classification algorithm.

Resources:

Estimated CPU time: 7078 sec  
Output disk space:  $78 \times 19 \times 4$  bytes/fl = 5928 bytes

Acceptance:

Comparison with another RTC.

**6.14.5.3  $\alpha$  - Constant applied to threshold for islands screening**

Reference:  $\alpha_{13thresh}$ , LUT437

[AD-8] Section 6.14.5, ADSR field 8

ACRI provided

Dependencies:

None

Tool:

None

Procedure:

Inputs: none

Outputs:  $\alpha_{13thresh}$   $\alpha$  - constant applied to threshold for islands screening  
units: [dl]

Step: User specified.

Scientific content:

This multiplicative factor ( $\alpha_{13thresh}$ ) is applied to the TOA reflectance thresholds at 865nm for islands screening processing identification.

Current baseline: 0.375

Resources:

Estimated CPU time: -  
Output disk space:  $1 \times 4$  bytes/fl = 4 bytes

Acceptance:

Corresponds to the latest definition.

6.14.5.4 TOA reflectance thresholds at 865 nm for islands screening,  $\rho_{T,865}(\theta_s \times \theta_v, \Delta\phi)$

Reference:  $\rho_{13thresh\_LUT}$ , LUT438

[AD-8] Section 6.14.5, ADSR field 4

Dependencies:

LUT144, LUT147, LUT148, LUT149, LUT154

Tools:

OTC/SCAMAT  
OTC/RAYLEIGH  
RTC/UPRAD (SO)

Procedure:

Inputs: *iaer* Aerosol model # [dl] (among the 78 Junge's models) characterized by an Angström exponent ( $\alpha$ ) and a refractive index, see Section 6.14.4.4 (LUT144) and Section 6.14.1.1 (LUT154).

$\theta$  Zenith angle [deg]; tabulated values used for  $(\theta_s \times \theta_v)$  combinations, see Section 6.14.4.1, (LUT147)  
 $\theta_s \times \theta_v$  Stored indices for angular combinations [dl] (78 values), see Section 6.14.4.2, (LUT148)  
 $\Delta\phi$  Relative azimuth angle [deg], see Section 6.14.4.3, (LUT149)

Output:  $\rho_{13\text{thresh\_LUT}}[\theta_s \times \theta_v, \Delta\phi]$   
 TOA reflectance thresholds at 865 nm as function of the illumination and viewing configuration  $(\theta_s, \theta_v, \Delta\phi)$   
 units: [dl]

Step-0: Compute the IOPs (aerosol phase function, single scattering albedo, extinction coefficient) for all the 78 aerosol models. Either generate the LUT170 (see Section 6.14.11) or launch the Mie's computations with OTC/SCAMAT using as inputs the Angström exponent and refractive index (real and imaginary parts).

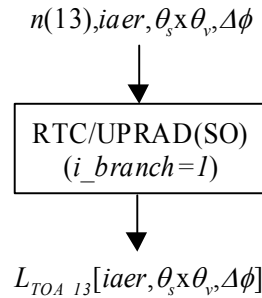
Step-1: Generate TOA normalized radiance  $L_{TOA\_13}[iaer, \theta_s \times \theta_v, \Delta\phi]$  at 865 nm (MERIS band #13) for a continental atmosphere over a land reflective surface, for each of the 78 continental aerosol models (*iaer*) and all illumination and viewing configurations  $(\theta_s, \theta_v, \Delta\phi)$ , with the RTC/UPRAD (SO).

**RTC/UPRAD (SO) Inputs (LAND)**

| Variable                           | Value                          | Comments  |
|------------------------------------|--------------------------------|---|
| <i>out_file</i>                    | "/OUTPUT/uprad_out"            |   |
| <i>i_branch</i>                    | 1                              |   |
| <i>n</i> ( $\lambda$ )             | 13                             | 865 nm  |
| <i>U<sub>H2O</sub></i>             | 0                              |   |
| <i>U<sub>O2</sub></i>              | 0                              |   |
| <i>ESFT</i>                        | -                              | N/A   |
| <i>P<sub>s</sub></i>               | 1013.25                        |   |
| <i>t<sup>r</sup></i> ( $\lambda$ ) | tauR                           | Computed with OTC/RAYLEIGH                              |
| <i>aerosol1</i>                    | "/INPUT/sca_out/sc_landyy_b05" | yy depends on the Junge's model ( <i>iaer</i> =1 to 78) |
| <i>t<sup>1</sup></i> (550)         | 1.5                            |   |
| <i>aerosol2</i>                    | -                              |   |
| <i>t<sup>2</sup></i> (550)         | 0                              |   |
| <i>aerosol3</i>                    | -                              |   |
| <i>t<sup>3</sup></i> (550)         | 0                              |   |
| <i>cloud1</i>                      | -                              | N/A   |
| <i>cloud2</i>                      | -                              | N/A   |
| <i>cloud3</i>                      | -                              | N/A   |
| <i>phyto</i>                       | -                              | N/A   |
| $\sigma_{e,\lambda}^p$             | -                              | N/A   |
| $\omega_{o,\lambda}^p$             | -                              | N/A   |



| Variable                   | Value                 | Comments   |
|----------------------------|-----------------------|--|
| $spm$                      | -                     | N/A  |
| $\sigma_{e,\lambda}^{spm}$ | -                     | N/A  |
| $\omega_{o,\lambda}^{spm}$ | -                     | N/A  |
| $\sigma_{e,\lambda}^{ys}$  | -                     | N/A  |
| $vertical$                 | "/INPUT/vertical_out" | Not used, vertical distribution determined in RTC/SO ( $H_a=2\text{ km}$ ; $H_R=8\text{ km}$ ) |
| $I_s$                      | 79                    |  |
| $\rho_s$                   | 0.02                  |  |
| $E_o$                      | 1                     |  |
| $\sigma_{e,\lambda}^w$     | -                     | N/A  |
| $\omega_{o,\lambda}^w$     | -                     | N/A  |
| $w_s$                      | 0                     |  |
| $n_s, n_v, n_{\Delta\phi}$ | 12, 12, 19            | Use a loop for 78 $\theta_s \times \theta_v$ combinations.                                     |
| $\theta_s$                 | see inputs            | See Section 6.14.4.1 and Section 6.14.4.2  |
| $\theta_v$                 | see inputs            | See Section 6.14.4.1 and Section 6.14.4.2  |
| $\Delta\phi$               | see inputs            | See Section 6.14.4.3   |
| $pol$                      | 1                     |  |



Step-2: Select among all the aerosol models the one which yields to the highest number of maximum values of  $L_{TOA\_13}$  for all  $\theta_s \times \theta_v$  and  $\Delta\phi$  combinations, and use this  $L_{TOA\_13}$  value to compute the TOA reflectance threshold at 865 nm ( $\rho_{13thresh\_LUT}[\theta_s \times \theta_v, \Delta\phi]$ ) as,

$$\rho_{13thresh\_LUT}[\theta_s \times \theta_v, \Delta\phi] = \pi \cdot \frac{L_{TOA\_13}[\theta_s \times \theta_v, \Delta\phi]}{\cos(\theta_s)}$$

**Scientific content:**

These TOA reflectance thresholds define the maximum reflectances as observed at 865 nm over water surfaces. The latter are useful for the islands discrimination in the pixels classification algorithm.

Resources:

Estimated CPU time: 7078 *sec*  
Output disk space:  $78 \times 19 \times 4$  bytes/fl = 5928 bytes

Acceptance:

Comparison with another RTC.

6.14.5.5 *Altitude threshold above which in-land waters screening is disabled*

Reference: Alt\_thresh, LUT489

[AD-8] Section 6.14.5, ADSR field 5

ACRI provided

Dependencies:

None

Tool:

None

Procedure:

Inputs: none

Outputs: *Alt\_thresh* Altitude threshold above which in-land waters screening is disabled  
units: [*m*]

Step: User specified.

Scientific content:

Altitude threshold above which in-land waters screening is disabled.

Current baseline: 0 *m*

Resources:

Estimated CPU time: -  
Output disk space:  $1 \times 4$  bytes/fl = 4 bytes

Acceptance:

Corresponds to the latest definition.

## 6.14.6 ADS ARVI Thresholds for DDV models

### 6.14.6.1 ARVI thresholds used for DDV models, $ARVI\_thresh(iddv, \theta_s \times \theta_v, \Delta\phi)$

Reference: ARVI\_thresh, LUT160

[AD-8] Section 6.14.6, ADSR field 1

Dependencies:

LUT147, LUT148, LUT149, LUT156

Tool:

RTC/UPRAD (SO)

**Warning:** Take care with the azimuth angle ( $\phi$ ) convention. The CESBIO files and the MERIS sensor used the same azimuth (relative azimuth angle) convention ( $\Delta\phi$ ) while the RTCs works in the opposite convention ( $\pi - \Delta\phi$ ).

Procedure:

Inputs:

|                            |  |
|----------------------------|--|
| $\theta$                   | Zenith angle [ <i>deg</i> ], tabulated values used for ( $\theta_s \times \theta_v$ ) combinations, see <a href="#">Section 6.14.4.1</a> , (LUT147)  |
| $\theta_s \times \theta_v$ | Stored indices for angular combinations [ <i>dl</i> ] (78 values), see <a href="#">Section 6.14.4.2</a> , (LUT148)   |
| $\Delta\phi$               | Relative azimuth angle [ <i>deg</i> ], see <a href="#">Section 6.14.4.3</a> , (LUT149)   |
| $\gamma$                   | gamma coefficient for ARVI computation [ <i>dl</i> ], see <a href="#">Section 6.14.4.10</a> , (LUT156)   |
| <i>iddv</i>                | DDV model # [ <i>dl</i> ] (among the 20 DDV models, [0..19])<br>CESBIO DDV reflectances files (i.e., 'lut12-xx' with xx in [1-20]),<br>$\rho_{DDV}(\lambda, \theta_v, \Delta\phi, \theta_s, \rho_o)$ |

Output:  $DDV\_ARVI\_LUT[iddv, \theta_s \times \theta_v, \Delta\phi]$   
ARVI threshold as function of the DDV model (*iddv*) and the illumination and viewing configuration ( $\theta_s, \theta_v, \Delta\phi$ )

units: [*dl*]

**Warning:** The process for generating this table is time-consuming. To avoid losing data in case of a power failure, several temporary binary files are created after few hours of processing: LTOA443\_xx.LUT160, LTOA665\_xx.LUT160, LTOA865\_xx.LUT160 (xx stands for the 20 DDV models [00..19]). This allows one to resume the processing after a power failure. If we want fully restart the generation procedure, then the temporary binary files should be first deleted before relaunching the process.

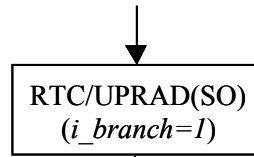
Step-1: Generate TOA normalized radiance  $L_{TOA\_aer}[iddv, iaer, \tau^a(\lambda), \theta_s \times \theta_v, \Delta\phi]$  for 442.5 nm, 665 nm and 865 nm (MERIS band #2, 7 and 13 used for ARVI) for a pure aerosol atmosphere over each of the 20 DDV models (*iddv*), for 1 aerosol model (*iaer*=37) and all illumination and viewing configurations ( $\theta_s, \theta_v, \Delta\phi$ ), with the RTC/UPRAD (SO).

**RTC/UPRAD (SO) Inputs (LAND)**

| Variable                   | Value  | Comments  |
|----------------------------|--|---|
| <i>out_file</i>            | "/OUTPUT/uprad_out"                                    |   |
| <i>i_branch</i>            | 1  |   |
| <i>n</i> ( $\lambda$ )     | 2, 7 and 13  | 442.5, 665 & 865 nm   |
| $U_{H2O}$                  | 0  |   |
| $U_{O2}$                   | 0  |   |
| <i>ESFT</i>                | -  | N/A   |
| $P_s$                      | 1013.25  |   |
| $\tau^R(\lambda)$          | 0  |   |
| <i>aerosol1</i>            | "/INPUT/sc_land37_b05"                                 | Junge's model #37 ( $m=1.44, \alpha=-1$ )                           |
| $\tau^{a1}(550)$           | 0.310 (442.5 nm), 0.207 (665 nm)<br>and 0.159 (865 nm) |   |
| <i>aerosol2</i>            | -  |   |
| $\tau^{a2}(550)$           | 0  |   |
| <i>aerosol3</i>            | -  |   |
| $\tau^{a3}(550)$           | 0  |   |
| <i>cloud1</i>              | -  | N/A   |
| <i>cloud2</i>              | -  | N/A   |
| <i>cloud3</i>              | -  | N/A   |
| <i>phyto</i>               | -  | N/A   |
| $\sigma_{e,\lambda}^p$     | -  | N/A   |
| $\omega_{o,\lambda}^p$     | -  | N/A   |
| <i>spm</i>                 | -  | N/A   |
| $\sigma_{e,\lambda}^{spm}$ | -  | N/A   |
| $\omega_{o,\lambda}^{spm}$ | -  | N/A   |
| $\sigma_{e,\lambda}^{ys}$  | -  | N/A   |
| <i>vertical</i>            | "/INPUT/vertical_out"                                  | Not used, vertical distribution determined in RTC/SO ( $H_a=2 km$ ) |
| $I_s$                      | 79   |   |
| $\rho_s$                   | "/INPUT/lut12_yy"                                      | yy depends on the DDV model #                                       |
| $E_o$                      | 1  |   |
| $\sigma_{e,\lambda}^w$     | -  | N/A   |
| $\omega_{o,\lambda}^w$     | -  | N/A   |

| Variable                   | Value      | Comments   |
|----------------------------|------------|--|
| $w_s$                      | 0          |  |
| $n_s, n_v, n_{\Delta\phi}$ | 12, 12, 19 | Use a loop for 78 $\theta_s \times \theta_v$ combinations. |
| $\theta_s$                 | see inputs | See Section 6.14.4.1 and Section 6.14.4.2                  |
| $\theta_v$                 | see inputs | See Section 6.14.4.1 and Section 6.14.4.2                  |
| $\Delta\phi$               | see inputs | See Section 6.14.4.3                                       |
| $pol$                      | 1          |  |

$iddv \ iqer=37, \tau^a(\lambda), \theta_s \times \theta_v, \Delta\phi$



$L_{TOA\_aer}[iddv,37,\tau^a(\lambda),\theta_s \times \theta_v,\Delta\phi]$

Step-2: Determine the ARVI threshold ( $DDV\_ARVI\_LUT[iddv, \theta_s \times \theta_v, \Delta\phi]$ ) using the 3 TOA normalized radiances  $L_{TOA\_aer}[iddv,37,\tau^a(\lambda),\theta_s \times \theta_v,\Delta\phi]$  at 442.5nm, 665nm and 865nm for each of the 20 DDV models ( $iddv$ ) as follows,

$$DDV\_ARVI\_LUT[iddv, \theta_s \times \theta_v, \Delta\phi] = \frac{L_{865}[iddv, \theta_s \times \theta_v, \Delta\phi] - L_{RB}[iddv, \theta_s \times \theta_v, \Delta\phi]}{L_{865}[iddv, \theta_s \times \theta_v, \Delta\phi] + L_{RB}[iddv, \theta_s \times \theta_v, \Delta\phi]}$$

$$\text{with } L_{RB} = L_{665} - \gamma \cdot [L_{443} - L_{665}]$$

where,

$$L_{443}[iddv, \theta_s \times \theta_v, \Delta\phi] = L_{TOA\_aer}[iddv, 37, \tau^a(442.5), \theta_s \times \theta_v, \Delta\phi]$$

$$L_{665}[iddv, \theta_s \times \theta_v, \Delta\phi] = L_{TOA\_aer}[iddv, 37, \tau^a(665), \theta_s \times \theta_v, \Delta\phi]$$

$$L_{865}[iddv, \theta_s \times \theta_v, \Delta\phi] = L_{TOA\_aer}[iddv, 37, \tau^a(865), \theta_s \times \theta_v, \Delta\phi]$$

and,  $\gamma=1.3$  (optimal value found for dense dark forests)

### Scientific content:

$DDV\_ARVI\_LUT[iddv, \theta_s \times \theta_v, \Delta\phi]$  defines the TOA ARVI threshold simulated as function of each DDV model ( $iddv$ ) and each illumination and viewing configuration ( $\theta_s, \theta_v, \Delta\phi$ ). In the DDV detection algorithm the ARVI is computed for each pixel ( $iddv, \theta_s, \theta_v, \Delta\phi$ ) within the MERIS scene, and this value is compared with the corresponding tabulated ARVI threshold simulated with the RTC/SO at TOA. If the latter is greater than the tabulated ARVI threshold, then the pixel will be identified as a DDV pixel.

### Resources:

Estimated CPU time: 94428 sec

Output disk space:  $20 \times 78 \times 19 \times 4$  bytes/fl = 118560 bytes

Acceptance:

Comparison with another RTC.

**6.14.7 ADS Standard Surface Reflectance Ranges for DDV Models**

*6.14.7.1 Mean DDV reflectances for 412.5 nm, 442.5 nm, 490 nm and 665 nm,  $\rho_{DDV\_mean}(iaer, \lambda)$*

Reference: DDV\_THR\_LUT, LUT161

[AD-8] Section 6.14.7, ADSR field 1, 2, 3 and 4

ACRI provided

Dependencies:

LUT147, LUT148, LUT149

Tool:

None

Procedure:

Inputs:

|                            |  |
|----------------------------|--|
| $\lambda$                  | 4 MERIS wavelengths [ <i>nm</i> ] (412.5, 442.5, 490 and 665 <i>nm</i> )   |
| $\theta$                   | Zenith angle [ <i>deg</i> ], tabulated values used for ( $\theta_s \times \theta_v$ ) combinations, see Section 6.14.4.1, (LUT147) |
| $\theta_s \times \theta_v$ | Stored indices for angular combinations [ <i>dl</i> ] (78 values), see Section 6.14.4.2, (LUT148)                                  |
| $\Delta\phi$               | Relative azimuth angle [ <i>deg</i> ], see Section 6.14.4.3, (LUT149)  |
| <i>iddv</i>                | DDV model # [ <i>dl</i> ] (among the 20 DDV models, [0..19])   |
| <i>lut12-xx</i>            | CESBIO DDV reflectances files, $\rho_{DDV}(\lambda, \theta_v, \Delta\phi, \theta_s, \rho_o)$ (with <i>xx</i> in [1-20])            |

Output: DDV\_THR\_LUT[*iddv*,  $\lambda$ ,  $\theta_s \times \theta_v$ ,  $\Delta\phi$ ]  
Mean DDV reflectances at 4 wavelengths ( $\lambda$ ), as function of the DDV model (*iddv*) and the illumination and viewing configuration ( $\theta_s, \theta_v, \Delta\phi$ )

units: [*dl*]

Step: User specified

Scientific content:

DDV\_THR\_LUT[*iddv*,  $\lambda$ ,  $\theta_s \times \theta_v$ ,  $\Delta\phi$ ] defines the mean DDV reflectances at 412.5, 442.5, 490 and 665 *nm* for each of the 20 DDV models and for a set of illumination and viewing geometries ( $\theta_s, \theta_v, \Delta\phi$ ). These table is useful for retrieving aerosol optical characteristics over DDV pixels.

Current baseline: (20 × 4 × 78 × 19) values

Resources:

Estimated CPU time: -  
Output disk space: 20 × 4 × 78 × 19 × 4 bytes/fl = 474240 bytes

Acceptance:

Corresponds to the latest definitions

**6.14.8 ADS Aerosol Spherical Albedo**

6.14.8.1 Aerosol spherical albedo,  $S_a(iaer, \tau^a)$

Reference: SA\_LUT, LUT167

[AD-8] Section 6.14.8, ADSR field 1

Dependencies:

LUT144, LUT154, LUT155

Tools:

OTC/SCAMAT  
RTC/GAUSS  
RTC/UPRAD (SO)  
Numerical integration

Procedure:

Inputs:  $iaer$  Aerosol model # [dl] (among the 78 *Junge's* models) characterized by an *Angström* exponent ( $\alpha$ ) and a refractive index, see Section 6.14.4.4 (LUT144) and Section 6.14.1.1 (LUT154).  
 $\tau^a$  Aerosol optical thickness at 550 nm [dl] (16 values), see Section 6.14.4.9, (LUT155)  
 $\theta_s$  Solar zenith angle[deg], *Gaussian* angles computed with RTC/GAUSS

Output: SA\_LUT[ $iaer, \tau^a$ ]  
Aerosol spherical albedo for each *Junge's* model ( $iaer$ ) and each aerosol optical thickness at 550 nm ( $\tau^a$ )

units: [dl]

Step-0: Compute the IOPs (aerosol phase function, single scattering albedo, extinction coefficient) for all the 78 aerosol models. Eihier generate the LUT170 (see Section 6.14.11) or launch the *Mie's*

computations with OTC/SCAMAT using as inputs the *Angström* exponent and refractive index (real and imaginary parts).

Step-1: Compute *Gaussian* angles  $\mu$  ( $=\cos\theta_s$ ) and their corresponding weighting factors  $w(\mu)$  with the RTC/GAUSS ( $n_s=12$ ).

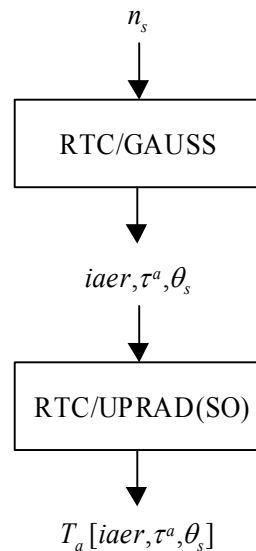
Step-2: Compute the aerosol transmittance  $T_a[iaer, \tau^a, \theta_s]$  corresponding to the first order of *Legendre* decomposition ( $I_s=0$ ) of phase function with the RTC/UPRAD (SO). For extracting the total atmospheric transmittance, we need to set  $I_s=0$  and  $\theta_v=-1$ .

**RTC/UPRAD (SO) Inputs (LAND)**

| Variable                   | Value                          | Comments  |
|----------------------------|--------------------------------|---|
| <i>out_file</i>            | "/OUTPUT/uprad_out"            |   |
| <i>i_branch</i>            | 1                              |   |
| $n(\lambda)$               | 1                              | Not used. Aerosol transmittance is computed as function of $\tau^a$ (tabulated values). |
| $U_{H2O}$                  | 0                              |   |
| $U_{O2}$                   | 0                              |   |
| <i>ESFT</i>                | -                              | N/A   |
| $P_s$                      | 1013.25                        |   |
| $t^R(\lambda)$             | 0                              |   |
| <i>aerosol1</i>            | "/INPUT/sca_out/sc_landyy_b05" | yy depends on the <i>Junge</i> 's model ( <i>iaer</i> =1 to 78)                         |
| $\tau^a(550)$              | tauA1                          | See Section 6.14.4.9, if $\tau^a(550)=0$ then $T_a=1.0$                                 |
| <i>aerosol2</i>            | -                              |   |
| $\tau^a(550)$              | 0                              |   |
| <i>aerosol3</i>            | -                              |   |
| $\tau^a(550)$              | 0                              |   |
| <i>cloud1</i>              | -                              | N/A   |
| <i>cloud2</i>              | -                              | N/A   |
| <i>cloud3</i>              | -                              | N/A   |
| <i>phyto</i>               | -                              | N/A   |
| $\sigma_{e,\lambda}^p$     | -                              | N/A   |
| $\omega_{o,\lambda}^p$     | -                              | N/A   |
| <i>spm</i>                 | -                              | N/A   |
| $\sigma_{e,\lambda}^{spm}$ | -                              | N/A   |
| $\omega_{o,\lambda}^{spm}$ | -                              | N/A   |
| $\sigma_{e,\lambda}^{ys}$  | -                              | N/A   |
| <i>vertical</i>            | "/INPUT/vertical_out"          | Not used, vertical distribution determined in RTC/SO ( $H_a=2$ km)                      |
| $I_s$                      | 0                              |   |
| $\rho_s$                   | "/INPUT/lut12_yy"              | yy depends on the DDV model #   |



| Variable                   | Value           | Comments                                   |
|----------------------------|-----------------|--|
| $E_0$                      | 1               |  |
| $\sigma_{e,\lambda}^w$     | -               | N/A  |
| $\omega_{o,\lambda}^w$     | -               | N/A  |
| $w_s$                      | 0               |  |
| $n_s, n_v, n_{\Delta\phi}$ | 24, 1, 1        | Use a loop for 24 $\theta_s$               |
| $\theta_s$                 | Gaussian angles | Computed with RTC/GAUSS                    |
| $\theta_v$                 | -1              | To get the total atmospheric transmittance |
| $\Delta\phi$               | 0               |  |
| $pol$                      | 1               |  |



Step-3: Compute the aerosol spherical albedo  $SA\_LUT[iaer, \tau^a]$  by the following angular numerical integration,

$$SA\_LUT[iaer, \tau^a] = 1 - 2 \cdot \int_0^1 T_a[iaer, \tau^a, \mu] \cdot w(\mu) \cdot \mu \cdot d\mu$$

with  $\mu$  the Gaussian angle ( $\mu = \cos(\theta_s)$ ) and  $w(\mu)$  its associated weighting factor.

$$T_a [iaer, \tau^a, \theta_s], w(\mu)$$



Numerical Integration

$$1 - 2 \cdot \Sigma T_a [iaer, \tau^a, \theta_s] \cdot w(\mu) \cdot \mu \cdot \delta\mu$$



$$SA\_LUT[iaer, \tau^a]$$

Scientific content:

$SA\_LUT[iaer, \tau^a]$  defines the aerosol spherical albedo for each of the 78 continental aerosol models (*iaer*) and each of 16 aerosol optical thicknesses at 550nm ( $\tau^a$ ). This table is useful to account for the multiple coupling between the ground surface and the aerosol layers in the TOA aerosol correction algorithm over land.

Resources:

Estimated CPU time: 2044 sec  
Output disk space: 78 × 16 × 4 bytes/fl = 4992 bytes

Acceptance:

Comparison with another RTC.

**6.14.9 ADS Aerosol Transmittance**

6.14.9.1 Aerosol transmittance,  $T_a(iaer, \theta_s, \tau^a)$

Reference: TA\_LUT, LUT168

[AD-8] Section 6.14.9, ADSR field 1

Dependencies:

LUT144, LUT147, LUT154, LUT155

Tool:

OTC/SCAMAT  
RTC/UPRAD (SO)

Procedure:

Inputs:  $iaer$  Aerosol model # [ $dI$ ] (among the 78 *Junge*'s models) characterized by an *Angström* exponent ( $\alpha$ ) and a refractive index, see Section 6.14.4.4 (LUT144) and Section 6.14.1.1 (LUT154).  
 $\theta_s$  Solar zenith angle [ $deg$ ], see Section 6.14.4.1, (LUT147)  
 $\tau^a$  Aerosol optical thickness at 550 nm (16 values), see Section 6.14.4.9, (LUT155)

Output:  $TA\_LUT[iaer, \tau^a, \theta_s]$  (also referred as  $T_a[iaer, \tau^a, \theta_s]$ )  
Aerosol transmittance for each aerosol model ( $iaer$ ), for each aerosol optical thickness at 550 nm ( $\tau^a$ ) and for each illumination direction ( $\theta_s$ )

units: [ $dI$ ]

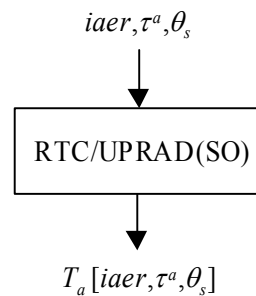
Step-0: Compute the IOPs (aerosol phase function, single scattering albedo, extinction coefficient) for all the 78 aerosol models. Either generate the LUT170 (see Section 6.14.11) or launch the *Mie*'s computations with OTC/SCAMAT using as inputs the *Angström* exponent and refractive index (real and imaginary parts).

Step-1: Compute the aerosol transmittance  $T_a[iaer, \tau^a, \theta_s]$  with the RTC/UPRAD (SO). For extracting the total atmospheric transmittance, we need to set  $I_s=0$  and  $\theta_v=-1$ .

**RTC/UPRAD (SO) Inputs (LAND)**

| Variable               | Value                          | Comments   |
|------------------------|--------------------------------|--|
| $out\_file$            | "/OUTPUT/uprad_out"            |  |
| $i\_branch$            | 1                              |  |
| $n(\lambda)$           | 1                              | Not used. Aerosol transmittance is computed as function of $\tau^{a1}$ (tabulated values). |
| $U_{H2O}$              | 0                              |  |
| $U_{O2}$               | 0                              |  |
| $ESFT$                 | -                              | N/A  |
| $P_s$                  | 1013.25                        |  |
| $\tau^R(\lambda)$      | 0                              |  |
| $aerosol1$             | "/INPUT/sca_out/sc_landyy_b05" | $yy$ depends on the <i>Junge</i> 's model ( $iaer=1$ to 78)                                |
| $\tau^{a1}(550)$       | tauA1                          | See Section 6.14.4.9, if $\tau^{a1}(550)=0$ then $T_a=1.0$                                 |
| $aerosol2$             | -                              |  |
| $\tau^{a2}(550)$       | 0                              |  |
| $aerosol3$             | -                              |  |
| $\tau^{a3}(550)$       | 0                              |  |
| $cloud1$               | -                              | N/A  |
| $cloud2$               | -                              | N/A  |
| $cloud3$               | -                              | N/A  |
| $phyto$                | -                              | N/A  |
| $\sigma_{e,\lambda}^P$ | -                              | N/A  |

| Variable                   | Value                 | Comments   |
|----------------------------|-----------------------|--|
| $\omega_{o,\lambda}^p$     | -                     | N/A  |
| $spm$                      | -                     | N/A  |
| $\sigma_{e,\lambda}^{spm}$ | -                     | N/A  |
| $\omega_{o,\lambda}^{spm}$ | -                     | N/A  |
| $\sigma_{e,\lambda}^{ys}$  | -                     | N/A  |
| $vertical$                 | "/INPUT/vertical_out" | Not used, vertical distribution determined in RTC/SO ( $H_a=2\text{ km}$ ) |
| $I_s$                      | 0                     |  |
| $\rho_s$                   | "/INPUT/lut12_yy"     | yy depends on the DDV model #  |
| $E_o$                      | 1                     |  |
| $\sigma_{e,\lambda}^w$     | -                     | N/A  |
| $\omega_{o,\lambda}^w$     | -                     | N/A  |
| $w_s$                      | 0                     |  |
| $n_s, n_v, n_{\Delta\phi}$ | 12, 1, 1              | Use a loop for 12 $\theta_s$   |
| $\theta_s$                 | Gaussian angles       | See Section 6.14.4.1   |
| $\theta_v$                 | -1                    | To get the total atmospheric transmittance                                 |
| $\Delta\phi$               | 0                     |  |
| $pol$                      | 1                     |  |



Scientific content:

$TA\_LUT[iaer, \tau^a, \theta_s]$  defines the aerosol transmittance for each of the 78 continental aerosol models ( $iaer$ ), for each of 16 aerosol optical thicknesses at  $550\text{nm}$  ( $\tau^a$ ), and for each of the 12 solar zenith angles (*Gaussian angles*). This table is useful for the TOA aerosol correction algorithm over land.

Resources:

Estimated CPU time: 1022 sec  
Output disk space:  $78 \times 12 \times 16 \times 4 \text{ bytes/fl} = 59904 \text{ bytes}$

Acceptance:

Comparison with another RTC.

**6.14.10 ADS Multiplicative Function to account for Aerosol Multiple Scattering Effects**

*6.14.10.1 Fourier series terms of polynomial coefficients for multiplicative aerosol scattering function retrieval*

Reference: Aermult\_LUT, LUT169

[AD-8] Section 6.14.10, ADSR field 1

Dependencies:

LUT144, LUT147, LUT148, LUT149, LUT154, LUT155

Tools:

OTC/SCAMAT  
RTC/UPRAD (SO)  
Fourier series expansion (FTS)  
Polynomial fit

Procedure:

Inputs: *iaer* Aerosol model # [*dl*] (among the 78 Junge's models + 3 stratospheric models) characterized by an *Angström* exponent ( $\alpha$ ) and a refractive index, see Section 6.14.4.4 (LUT144) and Section 6.14.1.1 (LUT154).  
 *$\theta$*  Zenith angle [*deg*]; tabulated values used for ( $\theta_s \times \theta_v$ ) combinations, see Section 6.14.4.1, (LUT147)  
 *$\theta_s \times \theta_v$*  Stored indices for angular combinations [*dl*] (78 values), see Section 6.14.4.2, (LUT148)  
 *$\Delta\phi$*  Relative azimuth angle [*deg*], see Section 6.14.4.3, (LUT149)  
 *$\tau^a$*  Aerosol optical thickness at 550 nm [*dl*] (16 values), see Section 6.14.4.9, (LUT155)  
*s* Fourier series term [*dl*],  $s = [0;5]$   
*k* Polynomial coefficient orders [*dl*],  $k = [0;3]$

Output: *Aermult\_LUT* [*iaer,  $\theta_s \times \theta_v, s, k$* ]  
*Fourier* series terms of multiplicative aerosol scattering function polynomial coefficients for each continental aerosol model, as function of the acceptable combinations (sun/view zenith angles)

units: [*dl*]

**Warning:** The process for generating this *Aermult\_LUT* table is very time-consuming. To avoid losing data in case of a power failure during the processing, temporary binary files are created after

*Step1* and *Step2* described below:  $L_{TOA\_xx.LUT169}$ ,  $LP\_TOA\_xx.LUT169$  (where  $xx$  stands for the identification of the aerosol model [00 .. 80]) and  $MultiFactor.LUT169$ , respectively. This allows one to resume the processing after a power failure. If we want fully restart the generation procedure, then the temporary binary files should be first deleted before relaunching the process.

Step-0: Compute the IOPs (aerosol phase function, single scattering albedo, extinction coefficient) for all the 78 aerosol models. Either generate the LUT170 (see Section 6.14.11) or launch the *Mie*'s computations with OTC/SCAMAT using as inputs the *Angström* exponent and refractive index (real and imaginary parts).

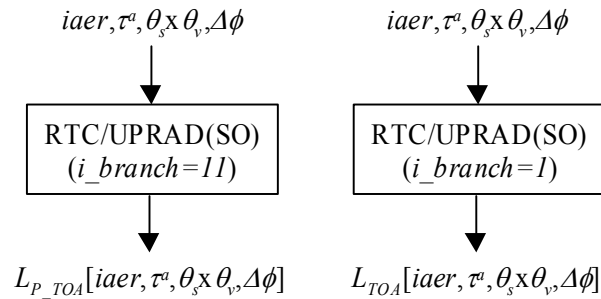
Step-1: Generate TOA normalized radiances  $L_{TOA}[iaer, \tau^a, \theta_s \times \theta_v, \Delta\phi]$  and the TOA normalized primary radiances  $L_{P\_TOA}[iaer, \tau^a, \theta_s \times \theta_v, \Delta\phi]$ , with the RTC/UPRAD (SO) for a pure aerosol atmosphere over a black land surface.

Note that for a first LUT generation, the computations have been completed with the same 'scamat' inputs ('sc\_land27\_b05') both for the 3 stratospheric aerosol models. This LUT will be reprocessed as soon as the definitions of these stratospheric aerosol models will be available.

**RTC/UPRAD (SO) Inputs (LAND)**

| Variable               | Value                          | Comments  |
|------------------------|--------------------------------|---|
| <i>out_file</i>        | "/OUTPUT/uprad_out"            |   |
| <i>i_branch</i>        | 1 and 11                       | 1 for $L_{TOA}$ , and 11 for $L_{P\_TOA}$   |
| $n(\lambda)$           | 1                              |   |
| $U_{H2O}$              | 0                              |   |
| $U_{O2}$               | 0                              |   |
| <i>ESFT</i>            | -                              | N/A   |
| $P_s$                  | 1013.25                        |   |
| $\tau^R(\lambda)$      | 0                              |   |
| <i>aerosol1</i>        | "/INPUT/sca_out/sc_landyy_b05" | yy depends on the set of 78 <i>Junge</i> 's models + 3 stratospheric models ( $iaer=1$ to 81) |
| $\tau^{a1}(550)$       | tauA1                          | See Section 6.14.4.9  |
| <i>aerosol2</i>        | -                              |   |
| $\tau^{a2}(550)$       | 0                              |   |
| <i>aerosol3</i>        | -                              |   |
| $\tau^{a3}(550)$       | 0                              |   |
| <i>cloud1</i>          | -                              | N/A   |
| <i>cloud2</i>          | -                              | N/A   |
| <i>cloud3</i>          | -                              | N/A   |
| <i>phyto</i>           | -                              | N/A   |
| $\sigma_{e,\lambda}^p$ | -                              | N/A   |
| $\omega_{o,\lambda}^p$ | -                              | N/A   |
| <i>spm</i>             | -                              | N/A   |

| Variable                   | Value                 | Comments   |
|----------------------------|-----------------------|--|
| $\sigma_{e,\lambda}^{spm}$ | -                     | N/A  |
| $\omega_{o,\lambda}^{spm}$ | -                     | N/A  |
| $\sigma_{e,\lambda}^{ys}$  | -                     | N/A  |
| vertical                   | "/INPUT/vertical_out" | Not used, vertical distribution determined in RTC/SO ( $H_a=2$ km) |
| $I_s$                      | 79                    |  |
| $\rho_s$                   | 0                     |  |
| $E_o$                      | 1                     |  |
| $\sigma_{e,\lambda}^w$     | -                     | N/A  |
| $\omega_{o,\lambda}^w$     | -                     | N/A  |
| $w_s$                      | 0                     |  |
| $n_s, n_v, n_{\Delta\phi}$ | 12, 12, 19            | Use a loop for 78 $\theta_s \times \theta_v$ combinations.         |
| $\theta_s$                 | Gaussian angles       | See Section 6.14.4.1 and Section 6.14.4.2                          |
| $\theta_v$                 | Gaussian angles       | See Section 6.14.4.1 and Section 6.14.4.2                          |
| $\Delta\phi$               | see inputs            | See Section 6.14.4.3   |
| pol                        | 1                     |  |



Step-2: Compute the multiplicative aerosol scattering function  $f_a[iaer, \tau^a, \theta_s \times \theta_v, \Delta\phi]$  as follows,

$$f_a[iaer, \tau^a, \theta_s \times \theta_v, \Delta\phi] = L_{TOA}[iaer, \tau^a, \theta_s \times \theta_v, \Delta\phi] / L_{P\_TOA}[iaer, \tau^a, \theta_s \times \theta_v, \Delta\phi]$$

Step-3: Expand  $f_a[iaer, \tau^a, \theta_s \times \theta_v, \Delta\phi]$  into a *Fourier* series of 6 terms with the FTS tool (which expands a function into *Fourier* series terms),

$$f_a[iaer, \tau^a, \theta_s \times \theta_v, s] = FTS(f_a[iaer, \tau^a, \theta_s \times \theta_v, \Delta\phi])$$

Step-4: Apply a 3<sup>rd</sup> order polynomial fit on each of the 6 *Fourier* terms of the multiplicative aerosol scattering function (i.e., on each term  $f_a[iaer, \tau^a, \theta_s \times \theta_v, \Delta\phi, s]$ ) as function of the aerosol optical thickness ( $\tau^a$ ) for retrieving polynomial coefficients  $Aermult\_LUT[iaer, \theta_s \times \theta_v, s, k]$ ,

$$f_a[iaer, \tau^a, \theta_s \times \theta_v, s] = Aermult\_LUT[iaer, \theta_s \times \theta_v, s, 0] + Aermult\_LUT[iaer, \theta_s \times \theta_v, s, 1] \cdot (\tau^a) + Aermult\_LUT[iaer, \theta_s \times \theta_v, s, 2] \cdot (\tau^a)^2$$

$$+ Aermult\_LUT [iaer, \theta_s \times \theta_v, s, 3] \cdot (\tau^a)^3$$

Scientific content:

These sets of polynomial coefficients are useful to compute the multiplicative aerosol scattering function whatever the illumination ( $\theta_i$ ) and viewing ( $\theta_v$ ) configuration, whatever the aerosol model (*iaer*) and aerosol optical thickness at 550nm ( $\tau^a$ ), and for each *Fourier* series (*s*) term used in the *Fourier* series expansion of these polynomial coefficients. This multiplicative aerosol scattering function is then used to correct the aerosol primary TOA radiance for the multiple scattering.

Note:

The computation of the aerosol reflectance is based on the same approximations as for the *Rayleigh* reflectance (*i.e.*, by decoupling the primary and the multiple scattering and using the *Fourier* series expansion to remove the azimuthal dependence).

Thus for a selected aerosol model (*iaer*), the aerosol reflectance ( $\rho_a$ ) is written as,

$$\rho_a(iaer, \vartheta_s, \vartheta_v, \Delta\phi, \tau^a) = \rho_{a,p}(iaer, \vartheta_s, \vartheta_v, \Delta\phi, \tau^a) \cdot f_a(iaer, \vartheta_s, \vartheta_v, \Delta\phi, \tau^a)$$

with  $\rho_{a,p}$  the primary scattering reflectance for the aerosols computed in the atmospheric correction algorithm over land, and  $f_a$  the multiplicative aerosol function which depends on the aerosol optical thickness ( $\tau^a$ ) at 550nm and accounts for the multiple scattering.

The multiplicative aerosol scattering function ( $f_a$ ) is then deduced from this formulation by simulating  $\rho_a$  and  $\rho_{a,p}$  with the RTC/UPRAD (SO). The *Fourier* series expansion is then applied on  $f_a$  instead of  $\rho_a$  due to the fact that  $f_a$  is less sensitive to the azimuthal angle than  $\rho_a$ , which permits to reduce the order of the series (*i.e.*, to the first 6 *Fourier* series terms).

For each *Fourier* series term *s*, a third order polynomial fit as function of  $\tau^a$  has been determined using the set of multiplicative aerosol scattering functions ( $f_a^{(s)}$ ):

$$f_a^{(s)}(iaer, \vartheta_s, \vartheta_v, \tau^a) = \sum_{i=0}^3 k_i^{(s)}(iaer, \vartheta_s, \vartheta_v) \cdot (\tau^a)^i$$

with  $k_i^{(s)}$  the polynomial coefficient for the *Fourier* series terms *s*.

The aerosol scattering function ( $f_a$ ) is then computed by recombining the first 6 *Fourier* series terms:

$$f_a(iaer, \vartheta_s, \vartheta_v, \Delta\phi, \tau^a) = \sum_{s=0}^5 (2 - \delta_{0,s}) \cdot f_a^{(s)}(iaer, \vartheta_s, \vartheta_v, \tau^a) \cdot \cos(s \cdot \Delta\phi) \quad (1)$$

Resources:

Estimated CPU time: 177329 sec  
Output disk space: 81 × 78 × 6 × 4 × 4 bytes/fl = 606528 bytes

Acceptance:



Comparison with another RTC.

### 6.14.11 ADS Aerosol Phase Function times Single Scattering Albedo

#### 6.14.11.1 Aerosol phase function times single scattering albedo, $\omega_o^a(iaer).P_a(iaer, \cos \Theta)$

Reference: Aerpha\_LUT, LUT170

[AD-8] Section 6.14.11, ADSR field 1

Dependencies:

LUT144, LUT150, LUT154

Tool:

OTC/SCAMAT

Note: The imaginary part of the refractive index is stored in a C.P. file, see Section 6.14.1.1. (LUT144).

Procedure:

Inputs: *iaer* Aerosol model # [*dl*] (among the 78 Junge's models)  
*Sca\_cos* Cosine of scattering angle [*dl*], see Section 6.14.4.4, (LUT150)  
*k* Output index (for selecting the aerosol property)  
*Aerosol\_refindex[iaer]* *k*=1 refractive index (real part) [*dl*],  
*Aerosol\_angstrom[iaer]* *k*=2 Angström coefficient ( $\alpha$ ) [*dl*],  
see Section 6.14.4.8, (LUT154)  
*n<sub>i</sub>* Imaginary part of refractive index [*dl*], see Section 6.14.1.1., (LUT144)

Output: *Aerpha\_LUT[iaer,Sca\_cos]* Aerosol phase function times single scattering albedo for each aerosol model (*iaer*)

units: [*dl*]

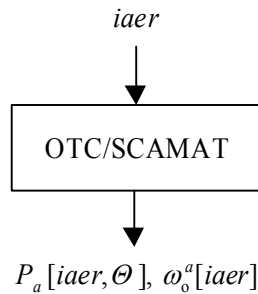
Step-1: Compute the aerosol scattering phase matrix  $P_a[iaer, \Theta]$  (with  $\Theta$  the scattering angle derived from the OTC/SCAMAT) and the single scattering albedo ( $\omega_o^a[iaer]$ ) with the OTC/SCAMAT, for each of the 78 aerosol models.

**SCAMAT Inputs**

| Variable | Value | Comments |
|----------|-------|----------|
|----------|-------|----------|

| Variable                                     | Value                           | Comments   |
|--|---------------------------------|--|
| <i>scamat_out</i>                            | "/INPUT/sca_out/sc_landyy_b05"  | <i>yy</i> depends on the continental aerosol model ( <i>iaer</i> =1 to 78) |
| $\lambda$                                    | 550                             | Wavelength   |
| $\lambda_{ref}$                              | 550                             | Reference wavelength   |
| $n_2$  | 83                              | Number of scattering angles  |
| $N$  | 1                               | Number of size distribution  |
| $m_\lambda(1), k_\lambda(1)$                 | see inputs                      | See Section 6.14.4.8 and Section 6.14.1.1                                  |
| $m_{\lambda_{ref}}(1), k_{\lambda_{ref}}(1)$ | see inputs                      | See Section 6.14.4.8 and Section 6.14.1.1                                  |
| $r_{min}(1), r_{max}(1), dr(1)$              | 0.001, 20, 0.001                | Minimum, maximum radii and size increment                                  |
| $ind(1), a(1), b(1)$                         | 1<br>0.01, $m_\lambda(i+1) + 3$ | Junge size distribution<br>See Section 6.14.4.8 for $m_\lambda(i)$         |
| $n(1)/n$                                     | 1                               | Component mixing ratio   |

Note: Refractive index are independent on the wavelength for the continental aerosol models.



Step-2: Determine  $Aerpha\_LUT[iaer, \Theta]$  for each of the 78 continental aerosol models (*iaer*) as follows,

$$Aerpha\_LUT[iaer, \Theta] = \omega_o^a [iaer] \times P_a[iaer, \Theta].$$

Step-3: Interpolate values from  $Aerpha\_LUT[iaer, \Theta]$  to the input scattering angles (*Sca\_cos*) to obtain  $Aerpha\_LUT[iaer, Sca\_cos]$  with the interpolation tool.

$$Aerpha\_LUT[iaer, Sca\_cos] = Interpolation(Aerpha\_LUT[iaer, \Theta])$$

### Scientific content:

$Aerpha\_LUT[iaer, Sca\_cos]$  determines the aerosol phase function times the single scattering albedo for each of the 78 continental aerosol models. The latter which describes the aerosol reflectances for each aerosol model (*iaer*), is useful for the aerosol correction algorithm over land.

### Resources:

Estimated CPU time: 2458 sec  
Output disk space:  $78 \times 83 \times 4$  bytes/fl = 25896 bytes

Acceptance:

Comparison with another OTC, such as the OTC/MIE from the FUB institute.

**6.14.12 ADS Volcanic Aerosol Spherical Albedo**

6.14.12.1 Volcanic aerosol spherical albedo,  $S_{va}(iaer, \lambda)$

Reference: Strato\_sphalb, LUT315

[AD-8] Section 6.14.12, ADSR field 1

Dependencies:

None

Tools:

RTC/GAUSS  
RTC/UPRAD (SO)  
Numerical integration

Procedure:

Inputs:  $iaer$  Aerosol model # [*dl*] (among the 18 volcanic aerosol models)  
 $\theta_s$  Solar zenith angle [*deg*], *Gaussian* angles computed with RTC/GAUSS  
 $\lambda$  MERIS wavelength [*nm*], (15 values)

Output:  $Strato\_sphalb[iaer, \lambda]$   
Volcanic aerosol spherical albedo for each aerosol model (*iaer*) and each  
MERIS wavelength ( $\lambda$ )

units: [*dl*]

Step-1: Compute *Gaussian* angles  $\mu (= \cos \theta_s)$  and their corresponding weighting factors  $w(\mu)$  with the RTC/GAUSS ( $n_s=12$ ).

Step-2: Compute the volcanic aerosol transmittance  $T_{va}[iaer, \theta_s, \lambda]$  with the RTC/UPRAD (SO). For extracting the total atmospheric transmittance, we need to set  $I_s=0$  and  $\theta_v=-I$ .

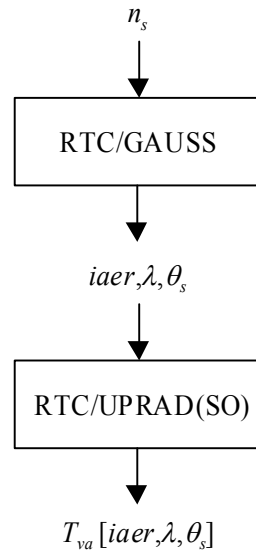
Note that for a first LUT generation, the computations have been completed with the same 'scamat' inputs ('*sc\_land27\_b05'*) both for all the 18 volcanic aerosol models whatever the wavelength. This LUT will be reprocessed as soon as the definitions of these volcanic aerosol models will be available.

**RTC/UPRAD (SO) Inputs (LAND)**

| Variable | Value | Comments |
|----------|-------|----------|
|----------|-------|----------|

| Variable                   | Value  | Comments  |
|----------------------------|--|---|
| <i>out_file</i>            | "/OUTPUT/uprad_out"                                  |   |
| <i>i_branch</i>            | 1  |   |
| <i>n</i> ( $\lambda$ )     | 1, 2, 3, 4, 5, 6, 7, 8, 9, 10, 11, 12, 13, 14 and 15 | All MERIS bands, but only one band is implemented in the MERISAT tool.  |
| $U_{H_2O}$                 | 0  |   |
| $U_{O_2}$                  | 0  |   |
| <i>ESFT</i>                | -  | N/A   |
| $P_s$                      | 1013.25  |   |
| $t^R(\lambda)$             | 0  |   |
| <i>aerosol1</i>            | "/INPUT/sc_landyy_b05"                               | yy depends on the volcanic aerosol model # ( <i>iaer</i> =1 to 18). However these models are not available, and only 1 aerosol model (' <i>sc_land27_b05</i> ') is implemented in the MERISAT tool. |
| $t^{a1}(550)$              | 0.1  |   |
| <i>aerosol2</i>            | -  |   |
| $t^{a2}(550)$              | 0  |   |
| <i>aerosol3</i>            | -  |   |
| $t^{a3}(550)$              | 0  |   |
| <i>cloud1</i>              | -  | N/A   |
| <i>cloud2</i>              | -  | N/A   |
| <i>cloud3</i>              | -  | N/A   |
| <i>phyto</i>               | -  | N/A   |
| $\sigma_{e,\lambda}^p$     | -  | N/A   |
| $\omega_{o,\lambda}^p$     | -  | N/A   |
| <i>spm</i>                 | -  | N/A   |
| $\sigma_{e,\lambda}^{spm}$ | -  | N/A   |
| $\omega_{o,\lambda}^{spm}$ | -  | N/A   |
| $\sigma_{e,\lambda}^{ys}$  | -  | N/A   |
| <i>vertical</i>            | "/INPUT/vertical_out"                                | Not used, vertical distribution determined in RTC/SO ( $H_a=2$ km)  |
| $I_s$                      | 0  |   |
| $\rho_s$                   | 0  |   |
| $E_o$                      | 1  |   |
| $\sigma_{e,\lambda}^w$     | -  | N/A   |
| $\omega_{o,\lambda}^w$     | -  | N/A   |
| $w_s$                      | 0  |   |
| $n_s, n_v, n_{\Delta\phi}$ | 24, 1, 1   | Use a loop for 24 $\theta_s$  |
| $\theta_s$                 | Gaussian angles                                      | Computed with RTC/GAUSS   |
| $\theta_v$                 | -1   | To get the total atmospheric transmittance  |

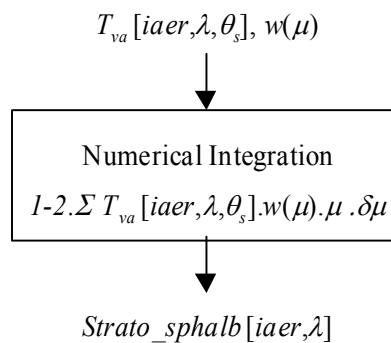
| Variable     | Value | Comments |
|--------------|-------|----------|
| $\Delta\phi$ | 0     |          |
| pol          | 1     |          |



Step-2: Compute the volcanic aerosol spherical albedo  $Strato\_sphalb[iaer, \lambda]$  by the following angular numerical integration,

$$Strato\_sphalb[iaer, \lambda] = 1 - 2 \cdot \int_0^1 T_{va}[iaer, \lambda, \mu] \cdot w(\mu) \cdot \mu \cdot d\mu$$

with  $\mu$  the Gaussian angle ( $\mu = \cos(\theta_s)$ ) and  $w(\mu)$  its associated weighting factor.



Scientific content:

$Strato\_sphalb[iaer, \lambda]$  defines the volcanic aerosol spherical albedo for each of the 18 volcanic aerosol models ( $iaer$ ) and each of 15 MERIS wavelengths ( $\lambda$ ). This table is useful for the stratospheric aerosol correction algorithm over land.

Resources:

Estimated CPU time: 363 sec  
Output disk space: 18 × 15 × 4 bytes/fl = 1080 bytes

Acceptance:

Comparison with another RTC.

**6.14.13 ADS Volcanic Aerosol Transmittance**

6.14.13.1 Volcanic aerosol transmittance,  $T_{va}(iaer, \lambda, \theta_s)$

Reference: TA\_strato\_LUT, LUT316

[AD-8] Section 6.14.13, ADSR field 1

Dependencies:

LUT147

Tool:

RTC/UPRAD (SO)

Procedure:

Inputs: *iaer* Aerosol model # [*dl*] (among the 18 volcanic aerosol models)  
*θ<sub>s</sub>* Solar zenith angle [*deg*], see Section 6.14.4.1, (LUT147)  
*λ* MERIS wavelength [*nm*], (15 values)

Output: TA\_strato\_LUT[*iaer, λ, θ<sub>s</sub>*] (also referred as  $T_{va}[iaer, \lambda, \theta_s]$ )  
Volcanic aerosol transmittance for each aerosol model (*iaer*), for each  
MERIS wavelength (*λ*), and for each illumination direction (*θ<sub>s</sub>*)

units: [*dl*]

Step: Compute the volcanic aerosol transmittance  $T_{va}[iaer, \lambda, \theta_s]$  with the RTC/UPRAD (SO). For extracting the total atmospheric transmittance, we need to set  $I_s=0$  and  $\theta_v=-I$ .

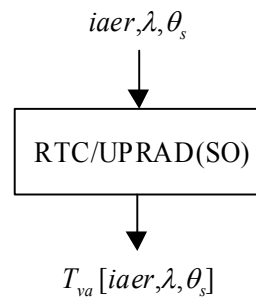
Note that for a first LUT generation, the computations have been completed with the same 'scamat' inputs ('sc\_land27\_b05') both for all the 18 volcanic aerosol models whatever the wavelength. This LUT will be reprocessed as soon as the definitions of these volcanic aerosol models will be available.

**RTC/UPRAD (SO) Inputs (LAND)**

| Variable | Value | Comments |
|----------|-------|----------|
|----------|-------|----------|

| Variable                   | Value  | Comments  |
|----------------------------|--|---|
| <i>out_file</i>            | "/OUTPUT/uprad_out"                                  |   |
| <i>i_branch</i>            | 1  |   |
| <i>n</i> ( $\lambda$ )     | 1, 2, 3, 4, 5, 6, 7, 8, 9, 10, 11, 12, 13, 14 and 15 | All MERIS bands, but only 1 band is implemented in the MERISAT tool.  |
| $U_{H_2O}$                 | 0  |   |
| $U_{O_2}$                  | 0  |   |
| <i>ESFT</i>                | -  | N/A   |
| $P_s$                      | 1013.25  |   |
| $t^R(\lambda)$             | 0  |   |
| <i>aerosol1</i>            | "/INPUT/sc_landyy_b05"                               | yy depends on the volcanic aerosol model # ( <i>iaer</i> =1 to 18). However these models are not available, and only 1 aerosol model (' <i>sc_land27_b05</i> ') is implemented in the MERISAT tool. |
| $t^{a1}(550)$              | 0.1  |   |
| <i>aerosol2</i>            | -  |   |
| $t^{a2}(550)$              | 0  |   |
| <i>aerosol3</i>            | -  |   |
| $t^{a3}(550)$              | 0  |   |
| <i>cloud1</i>              | -  | N/A   |
| <i>cloud2</i>              | -  | N/A   |
| <i>cloud3</i>              | -  | N/A   |
| <i>phyto</i>               | -  | N/A   |
| $\sigma_{e,\lambda}^p$     | -  | N/A   |
| $\omega_{o,\lambda}^p$     | -  | N/A   |
| <i>spm</i>                 | -  | N/A   |
| $\sigma_{e,\lambda}^{spm}$ | -  | N/A   |
| $\omega_{o,\lambda}^{spm}$ | -  | N/A   |
| $\sigma_{e,\lambda}^{ys}$  | -  | N/A   |
| <i>vertical</i>            | "/INPUT/vertical_out"                                | Not used, vertical distribution determined in RTC/SO ( $H_a=2\text{ km}$ )  |
| $I_s$                      | 0  |   |
| $\rho_s$                   | 0  |   |
| $E_o$                      | 1  |   |
| $\sigma_{e,\lambda}^w$     | -  | N/A   |
| $\omega_{o,\lambda}^w$     | -  | N/A   |
| $w_s$                      | 0  |   |
| $n_s, n_v, n_{\Delta\phi}$ | 12, 1, 1   | Use a loop for 12 $\theta_s$  |
| $\theta_s$                 | Gaussian angles                                      | See Section 6.14.4.1  |
| $\theta_v$                 | -1   | To get the total atmospheric transmittance  |

| <i>Variable</i> | <i>Value</i> | <i>Comments</i> |
|-----------------|--------------|-----------------|
| $\Delta\phi$    | 0            |                 |
| <i>pol</i>      | 1            |                 |



Scientific content:

$TA\_strato\_LUT[iaer, \lambda, \theta_s]$  defines the volcanic aerosol transmittance for each of the 18 volcanic aerosol models (*iaer*), for each of 15 MERIS wavelengths ( $\lambda$ ), and for each of the 12 solar zenith angles (*Gaussian* angles). This table is useful for the volcanic aerosol correction algorithm over land.

Resources:

Estimated CPU time: 183 sec  
Output disk space:  $18 \times 15 \times 12 \times 4$  bytes/fl = 12960 bytes

Acceptance:

Comparison with another RTC.

**6.14.14 ADS Volcanic Aerosol Reflectance**

*6.14.14.1 Volcanic aerosol phase function times single scattering albedo,  $\omega_o^{va}(iaer, \lambda).P_{va}(iaer, \lambda, \cos \Theta)$*

Reference: Strato\_aerpha\_LUT, LUT317

[AD-8] Section 6.14.14, ADSR field 1

Dependencies:

LUT150, LUT154

Tools:

OTC/SCAMAT  
Interpolation



Procedure:

Inputs: *iaer* Aerosol model # [*dl*] (among the 3 stratospheric models distinguished by the effective volcanic aerosol radius)

*Sca\_cos* Cosine of scattering angle [*dl*], see Section 6.14.4.4, (LUT150)

*k* Output index (for selecting the aerosol property)

*Aerosol\_refindex*[*iaer*] *k*=1 refractive index (real part) [*dl*],

*Aerosol\_angstrom*[*iaer*] *k*=2 Angström coefficient ( $\alpha$ ) [*dl*], see Section 6.14.4.8, (LUT154)

Output: *Strato\_aerpha\_LUT*[*iaer*, $\lambda$ ,*Sca\_cos*] Aerosol phase function times single scattering albedo for each aerosol model (*iaer*)

units: [*dl*]

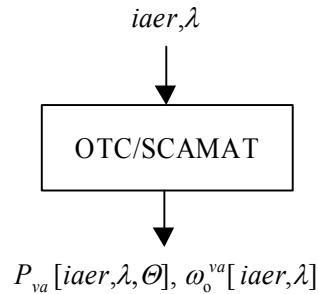
Step-1: Compute the aerosol scattering phase matrix  $P_{va}[iaer, \lambda, \Theta]$  (with  $\Theta$  the scattering angle derived from the OTC/SCAMAT) and the single scattering albedo ( $\omega_o^{va}[iaer, \lambda]$ ) with the OTC/SCAMAT, for each of the 3 stratospheric aerosol models.

Note that for a first LUT generation, the computations have been completed with the same 'scamat' inputs ('sc\_land27\_b05') both for all the 3 stratospheric aerosol models whatever the wavelength. This LUT will be reprocessed as soon as the definitions of these volcanic aerosol models will be available.

**SCAMAT Inputs**

| Variable                                      | Value                            | Comments  |
|---|----------------------------------|---|
| <i>Scamat_out</i>                             | "/INPUT/sca_out/sc_stratoyy_b05" | <i>yy</i> depends on the stratospheric aerosol model ( <i>iaer</i> =1 to 3). However these models are not available, and only 1 aerosol model ('sc_strato_b05') is implemented in the MERISAT tool. |
| $\lambda$                                     | 550                              | Wavelength  |
| $\lambda_{ref}$                               | 550                              | Reference wavelength  |
| $n_2$   | 83                               | Number of scattering angles   |
| $N$   | 1                                | Number of size distribution   |
| $m_\lambda(1), k_\lambda(1)$                  | see inputs                       | See Section 6.14.4.8 and Section 6.14.1.1   |
| $m_{\lambda_{ref}}(1), k_{\lambda_{ref}}(1)$  | see inputs                       | See Section 6.14.4.8 and Section 6.14.1.1   |
| $r_{min}(1), r_{max}(1), dr(1)$               | 0.001, 20, 0.001                 | Minimum, maximum radii and size increment   |
| <i>ind</i> (1),<br><i>a</i> (1), <i>b</i> (1) | 1<br>0.01, $m_\lambda(i+1) + 3$  | Junge size distribution<br>See Section 6.14.4.8 for $m_\lambda(i)$  |
| <i>n</i> (1)/ <i>n</i>                        | 1                                | Component mixing ratio  |

Note: These scamat inputs are the same as for the continental aerosol models du to the fact that the definitions of the 3 stratospheric aerosol models are not available.



Step-2: Determine  $Strato\_aerpha\_LUT[iaer,\lambda,\Theta]$  for each of the 3 stratospheric aerosol models ( $iaer$ ) as follows,

$$Strato\_aerpha\_LUT[iaer,\lambda,\Theta] = \omega_o^{va}[iaer,\lambda] \times P_{va}[iaer,\lambda,\Theta]$$

Step-3: Interpolate values from  $Strato\_aerpha\_LUT[iaer,\lambda,\Theta]$  to the input scattering angles ( $Sca\_cos$ ) to obtain  $Strato\_aerpha\_LUT[iaer,\lambda,Sca\_cos]$  with the interpolation tool.

$$Strato\_aerpha\_LUT[iaer,\lambda,Sca\_cos] = Interpolation(Strato\_aerpha\_LUT[iaer,\lambda,\Theta])$$

Scientific content:

$Strato\_aerpha\_LUT[iaer,\lambda,Sca\_cos]$  defines the stratospheric aerosol phase function times the single scattering albedo for each of the 3 volcanic aerosol models, and each of the 15 MERIS wavelengths. The latter, which describes the volcanic aerosol spectral reflectances for each model ( $iaer$ ), is useful for the volcanic aerosol correction algorithm over land.

Resources:

Estimated CPU time: 40 sec  
Output disk space:  $3 \times 15 \times 83 \times 4$  bytes/fl = 14940 bytes

Acceptance:

Comparison with another OTC, such as the OTC/MIE from the FUB institute.

6.14.14.2 Spectral dependence of the volcanic aerosol optical thickness (with normalization at reference wavelength)

Reference: Strato\_spectr, LUT318

[AD-8] Section 6.14.14, ADSR field 2

ACRI provided

Dependencies:

None

Tool:

None

Procedure:

Inputs: *iaer* Volcanic aerosol model # (among 3 models)  
*b* MERIS band # (15 bands)

Outputs: *Strato\_spectr[iaer,b]*  
Spectral dependence ( $f_{strato}[iaer,\lambda]$ ) of the volcanic aerosol optical thickness (with normalization at reference wavelength)

units: [*dI*]

Step: User specified.

Scientific content:

$f_{strato}[iaer,\lambda]$  describes the spectral dependence of the volcanic aerosol optical thickness (stratosphere), for each of the 3 aerosol models (*iaer*) and for each of the 15 MERIS wavelengths ( $\lambda$ ). These values are normalized to the reference wavelength at 865 nm.

Current baseline: (3 x 15) values set to 1

Resources:

Estimated CPU time: -  
Output disk space: 3 x 15 x 4 bytes/fl = 180 bytes

Acceptance:

Corresponds to the latest definition.

## 6.14.15 GADS Dense Dark Vegetation Climatology

### 6.14.15.1 Biome index, *DDV\_clim(lat,long)*

Reference: *DDV\_clim*, LUT319

[AD-8] Section 6.14.15, ADSR field 1

ACRI provided

Dependencies:

LUT310, LUT311

Tool:

None

Procedure:

Inputs: *lat* Latitude [*deg*] (180 values), see [Section 6.14.4.13](#) (LUT310)  
*long* Longitude [*deg*] (360 values), see [Section 6.14.4.14](#) (LUT311)

Outputs: *DDV\_clim[lat,long]*  
Spectral dependence ( $f_{strato}[iaer,\lambda]$ ) of the volcanic aerosol optical thickness (with normalization at reference wavelength)

units: [*dI*]

Step: User specified.

Scientific content:

DDV climatology given on a geographic map with a 1 *deg* cell resolution in (*lat*, *long*)

Current baseline: (180 x 360) values.

Resources:

Estimated CPU time: -

Output disk space: 180 x 360 x 1 byte/uc = 64800 bytes

Acceptance:

Corresponds to the latest definition.

**6.14.16 ADS DDV Parameters for Bidirectionality Correction**

*6.14.16.1 Rayleigh-ground DDV coupling bidirectionality term,  $\bar{\rho}_{RG}(iddv,\lambda,\theta_v)$*

Reference: robar\_Rg\_LUT, LUT320

[AD-8] Section 6.14.16, ADSR field 1

Dependencies:

LUT147

Tools:

RTC/MOS (lut\_rhob\_Rgddv)  
Interpolation  
Numerical integration (*Gauss* quadrature)  
Numerical integration (*Newton-Cotes* method)

Note: Both the interpolation and numerical integrations tools are included in the RTC/MOS (lut\_rhob\_Rgddv). The latter has been developed for the sun/view geometries in the MOS ground-segment.

Procedure:

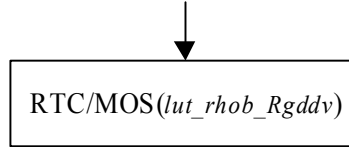
Inputs:  $\lambda$  4 MERIS wavelengths [*nm*] (412.5, 442.5, 490 and 665 *nm*)  
 $\theta$  Zenith angle [*deg*]; tabulated values used for  $(\theta_s \times \theta_v)$  combinations, *see* Section 6.14.4.1, (LUT147)  
 $\Delta\phi$  Relative azimuth angle [*deg*]; 72 values derived from a parabolic distribution centred at 0 *deg*.  
*iddv* DDV model # [*dl*] (among the 20 DDV models, [0..19])  
*param\_Hapke* CESBIO input file containing 4 *Hapke's* parameters ( $\omega, g, S$  and  $h$ ) for each of the 20 DDV models, each of the 4 wavelengths (*i.e.*, 412.5, 442.5, 490 and 665 *nm*) and for all illumination and viewing configurations (*see* [AD-7] for more details).  
 $\omega$  : single scattering albedo  
 $g$  : assymetry factor  
 $S$  : amplitude of the hot-spot  
 $h$  : width of the hot-spot

Output:  $robar\_Rg\_LUT[iddv, \lambda, \theta_v]$ , referred also as  $\bar{\rho}_{RG}[iddv, \lambda, \theta_v]$   
*Rayleigh-ground* DDV coupling bidirectionality term as function of the DDV model (*iddv*), the wavelength ( $\lambda$ ), and the viewing zenith angle ( $\theta_v$ )  
 units: [*dl*]

The steps, described hereafter, are implemented in the RTC/MOS (lut\_rhob\_Rgddv).

Step-1: Generate the DDV BRDF  $R_{DDV}[iddv, \lambda, \mathcal{G}', \mathcal{G}_v, \Delta\phi']$  with the RTC/MOS (lut\_rhob\_Rgddv) using the *Hapke's* parameters ( $\omega, g, S, h$ ) file, for each DDV model, each wavelength, and each illumination and viewing configuration  $\mathcal{G}', \mathcal{G}_v$  and  $\Delta\phi'$  ( $N_{\mathcal{G}'} = 24$ ;  $N_{\mathcal{G}_v} = 12$ ;  $N_{\Delta\phi'} = 72$ ). The zenith angles ( $\mathcal{G}', \mathcal{G}_v$ ) (within  $[0^\circ; 90^\circ]$ ) derive from the *Gauss* quadratures and the relative azimuth angles ( $\Delta\phi'$ ) (within  $[-180^\circ; 180^\circ]$ ) follow a parabolic distribution centred at  $0^\circ$ .

$\lambda, \theta_v, iddv(\omega, g, S, h)$



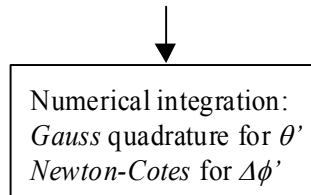
$R_{DDV}[iddv, \lambda, \theta', \theta_v, \Delta\phi']$

Step-2: Compute the *Rayleigh*-ground DDV coupling bidirectionality term *robar\_Rg\_LUT*[*iddv*,  $\lambda$ ,  $\theta_v$ ] for each DDV model, each wavelength  $\lambda$ , and each viewing angle  $\theta_v$ , using the numerical angular integration of  $R_{DDV}[iddv, \lambda, \theta', \theta_v, \Delta\phi']$  on  $\mu'$  and  $\Delta\phi'$ :

$$robar\_Rg\_LUT[iddv, \lambda, \theta_v] = \frac{1}{2\pi} \cdot \int_0^{2\pi} \int_0^{\pi} R_{DDV}[iddv, \lambda, \theta', \theta_v, \Delta\phi'] \cdot d\mu' \cdot d\Delta\phi'$$

This angular integration on  $\mu'$  is performed using a *Gauss* quadrature whereas the azimuthal integration on  $\Delta\phi'$  is completed with the *Newton-Cotes* method.

$R_{DDV}[iddv, \lambda, \theta', \theta_v, \Delta\phi']$



*robar\_Rg\_LUT*[*iddv*,  $\lambda$ ,  $\theta_v$ ]

Scientific content:

*robar\_Rg\_LUT*[*iddv*,  $\lambda$ ,  $\theta_v$ ] defines the *Rayleigh*-ground DDV coupling bidirectionality term as function of the DDV model (*iddv*), the wavelength ( $\lambda$ ), and the viewing zenith angle ( $\theta_v$ ). The latter which accounts for the multiple scatterings between the ground DDV interface and the *Rayleigh* atmosphere, is useful for the atmospheric correction algorithm over land.

Resources:

Estimated CPU time: 5 sec (If ASCII LUT exists)  
 Output disk space:  $20 \times 4 \times 12 \times 4$  bytes/fl = 3840 bytes

Acceptance:

Comparison with another code.

6.14.16.2 Aerosol-ground DDV coupling bidirectionality term,  $\bar{\rho}_{aG}(iddv, \lambda, iaer, \theta_s, \theta_v, s)$

Reference: robar\_ag\_LUT, LUT321

[AD-8] Section 6.14.16, ADSR field 2

Dependencies:

LUT144, LUT147, LUT148, LUT150, LUT154

Tools:

OTC/SCAMAT  
RTC/MOS (lut\_rhob\_agddv)  
Fourier series expansion (FTS)  
Interpolation  
Numerical integration (*Gauss* quadrature)  
Numerical integration (*Newton-Cotes* method)

Note: Both the FTS, interpolation and numerical integrations tools are included in the RTC/MOS (lut\_rhob\_agddv). The latter has been developed for the sun/view geometries in the MOS ground-segment.

Procedure:

|         |                            |   |
|---------|----------------------------|---|
| Inputs: | $\lambda$                  | 4 MERIS wavelengths [ <i>nm</i> ] (412.5, 442.5, 490 and 665 <i>nm</i> )  |
|         | $\theta$                   | Zenith angle [ <i>deg</i> ]; tabulated values used for $(\theta_s \times \theta_v)$ combinations, see <a href="#">Section 6.14.4.1</a> , (LUT147)   |
|         | $\theta_s \times \theta_v$ | Stored indices for angular combinations [ <i>dl</i> ] (78 values), see <a href="#">Section 6.14.4.2</a> , (LUT148)  |
|         | $\Delta\phi$               | Relative azimuth angle [ <i>deg</i> ]; 72 values derived from a parabolic distribution centred at 0 <i>deg</i> .  |
|         | <i>iaer</i>                | Aerosol model # [ <i>dl</i> ] (among the 78 <i>Junge</i> 's models) characterized by an <i>Angström</i> exponent ( $\alpha$ ) and a refractive index, see <a href="#">Section 6.14.4.4</a> (LUT144) and <a href="#">Section 6.14.1.1</a> (LUT154).  |
|         | <i>Sca_cos</i>             | Cosine of scattering angle [ <i>dl</i> ], see <a href="#">Section 6.14.4.4</a> , (LUT150)   |
|         | <i>iddv</i>                | DDV model # [ <i>dl</i> ] (among the 20 DDV models, [0..19])  |
|         | <i>param_Hapke</i>         | CESBIO input file containing 4 <i>Hapke</i> 's parameters ( $\omega$ , $g$ , $S$ and $h$ ) for each of the 20 DDV models, each of the 4 wavelengths ( <i>i.e.</i> , 412.5, 442.5, 490 and 665 <i>nm</i> ) and for all illumination and viewing configurations (see <a href="#">[AD-7]</a> for more details).<br>$\omega$ : single scattering albedo<br>$g$ : asymmetry factor<br>$S$ : amplitude of the hot-spot<br>$h$ : width of the hot-spot |
|         | <i>phase_aer78</i>         | Input file containing scattering phase functions for 78 aerosol models (see <a href="#">[AD-7]</a> for more details).   |

Output:  $robar\_ag\_LUT[iddv, \lambda, iaer, \theta_s \times \theta_v, s]$ , referred also as  $\bar{\rho}_{ag}[iddv, \lambda, iaer, \theta_s \times \theta_v, s]$   
Aerosol-ground DDV coupling bidirectionality term as function of the DDV model ( $iddv$ ), the wavelength ( $\lambda$ ), the aerosol model ( $iaer$ ), the illumination and viewing geometry ( $\theta_s, \theta_v$ ), and the *Fourier* term ( $s$ ) used to remove the azimuthal dependence

units:  $[dl]$

Step-0: Compute the IOPs (aerosol phase function, single scattering albedo, extinction coefficient) for all the 78 aerosol models. Either generate the LUT170 (see Section 6.14.11) or launch the *Mie*'s computations with OTC/SCAMAT using as inputs the *Angström* exponent and refractive index (real and imaginary parts).

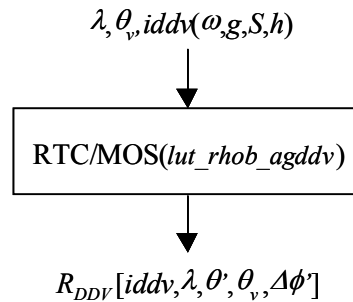
Step-1: For each of the 78 aerosol models ( $iaer$ ), interpolate the scattering phase function  $P_{scat}[iaer, \Theta]$  to the input scattering angles ( $Sca\_cos$ ) to get  $P_{scat}[iaer, Sca\_cos]$  with the interpolation tool,

$$P_{scat}[iaer, Sca\_cos] = Interpolation(P_{scat}[iaer, \Theta]),$$

and generate the input file,  $phase\_aer78$ , with the 78 interpolated scattering phase functions.

The steps, described hereafter, are implemented in the RTC/MOS ( $lut\_rhob\_agddv$ ).

Step-2: Generate the DDV BRDF  $R_{DDV}[iddv, \lambda, \mathcal{G}', \mathcal{G}_v, \Delta\phi']$  with the RTC/MOS ( $lut\_rhob\_agddv$ ) using the *Hapke's* parameters ( $\omega, g, S, h$ ) file, for each DDV model, each wavelength, and each illumination and viewing configuration  $\mathcal{G}', \mathcal{G}_v$  and  $\Delta\phi'$  ( $N_{\mathcal{G}'} = 24$ ;  $N_{\mathcal{G}_v} = 12$ ;  $N_{\Delta\phi'} = 72$ ). The zenith angles ( $\mathcal{G}', \mathcal{G}_v$ ) (within  $[0^\circ; 90^\circ]$ ) derive from the *Gauss* quadratures and the relative azimuth angles ( $\Delta\phi'$ ) (within  $[-180^\circ; 180^\circ]$ ) follow a parabolic distribution centred at  $0^\circ$ .



Step-3: Set a table with pre-computed values of downward normalized aerosol phase function with  $N_{\mathcal{G}_s} = 12$ ,  $N_{\mathcal{G}'} = 24$ ,  $N_{\Delta\phi'} = 30$ ,  $N_{\Delta\phi} = 72$  for all the aerosol models ( $N_{aer} = 78$ ) and all the scattering geometries ( $N_{\theta} = 83$ ).

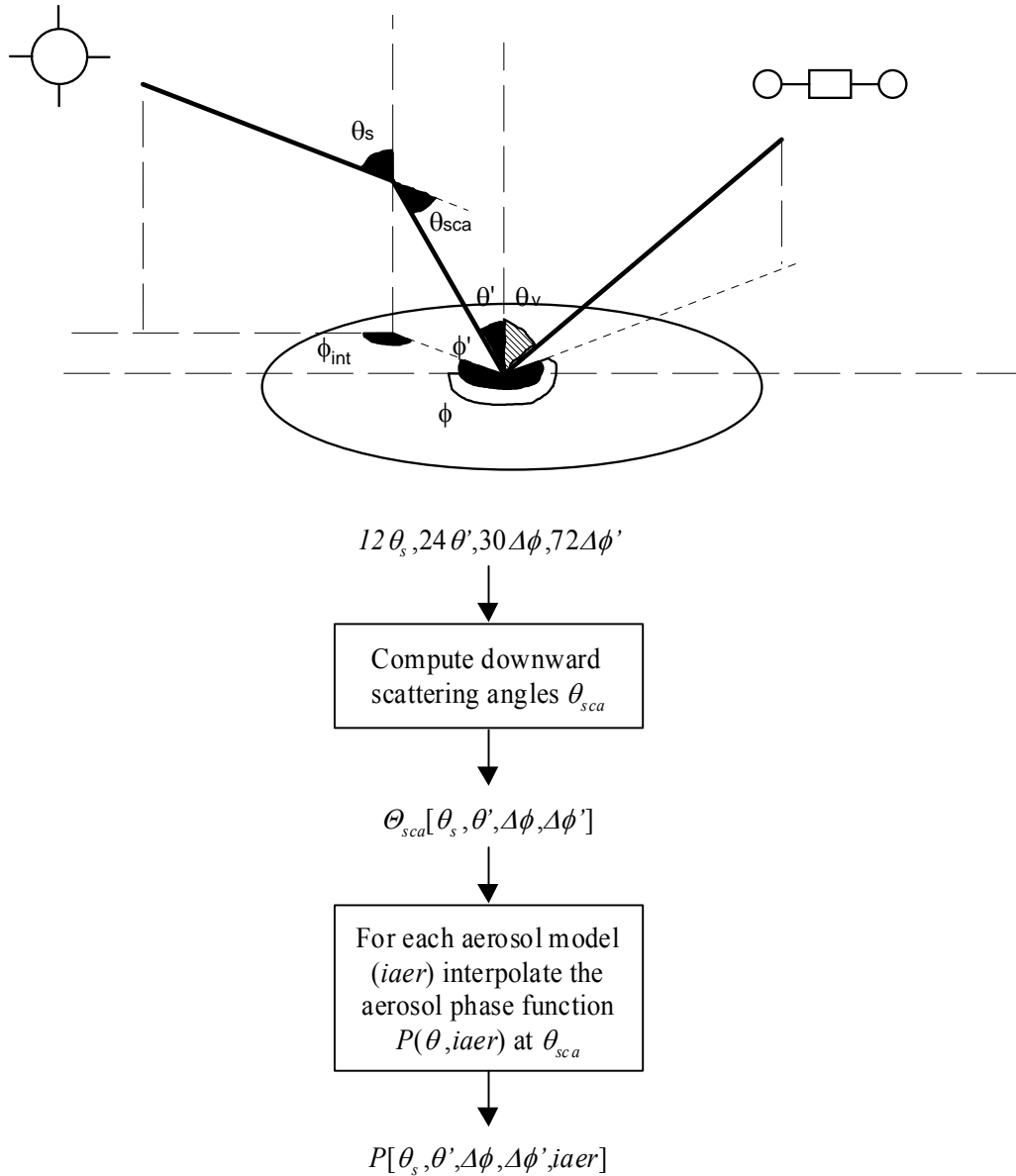
For each combination ( $\mathcal{G}_s, \mathcal{G}', \Delta\phi, \Delta\phi'$ ), we compute:

(a) the scattering angle  $\theta_{sca}$  as follows:

$$\cos(\theta_{sca}) = \cos(\mathcal{G}_s) \cos(\mathcal{G}') + \sin(\mathcal{G}_s) \cdot \sin(\mathcal{G}') \cdot \cos(\Delta\phi' - \Delta\phi)$$



(b) the aerosol phase function  $P(\theta_{sca}, iaer)$  for each aerosol model ( $iaer$ ) by interpolation from tabulated values of  $P(\theta, N_{aer})$ .



Step-4: Compute the aerosol-ground DDV coupling bidirectionality term  $\bar{\rho}_{aG}[iddv, \lambda, iaer, \vartheta_s, \vartheta_v, \Delta\phi]$  for each DDV, each wavelength  $\lambda$ , each aerosol model  $iaer$  and each illumination and viewing configuration  $(\vartheta_s, \vartheta_v, \Delta\phi)$  (with  $N_{\vartheta_s} = 12, N_{\vartheta_v} = 12, N_{\Delta\phi} = 30$ ):

$$\bar{\rho}_{aG}[iddv, \lambda, iaer, \theta_s, \theta_v, \Delta\phi] = \frac{\int_0^{2\pi} \int_0^{2\pi} R_{DDV}[iddv, \lambda, \theta_s', \theta_v', \Delta\phi'] \cdot P[\theta_s, \theta_s', \Delta\phi, \Delta\phi', iaer] \cdot d\mu' \cdot d\Delta\phi'}{\int_0^{2\pi} \int_0^{2\pi} P[\theta_s, \theta_s', \Delta\phi, \Delta\phi', iaer] \cdot d\mu' \cdot d\Delta\phi'}$$

This angular integration is numerically performed using a *Gauss* quadrature for  $\mu'$  and the *Newton-Cotes* method for  $\Delta\phi'$ .

For each  $iddv, \lambda, iaer, \theta_s, \theta_v, \Delta\phi$ :  
call  $P[\theta_s, \theta_s', \Delta\phi, \Delta\phi', iaer]$   
call  $R_{DDV}[iddv, \lambda, \theta_s', \theta_v', \Delta\phi']$

Numerical integration:  
*Gauss* quadrature for  $\theta'$   
*Newton-Cotes* for  $\Delta\phi'$

$$\bar{\rho}_{aG}[iddv, \lambda, iaer, \theta_s, \theta_v, \Delta\phi]$$

Step-5: Remove the azimuthal dependence  $\Delta\phi$  by expanding  $\bar{\rho}_{aG}[iddv, \lambda, iaer, \theta_s, \theta_v, \Delta\phi]$  into *Fourier* series at the 4<sup>th</sup> order:

$$\bar{\rho}_{aG}[iddv, \lambda, iaer, \theta_s, \theta_v, \Delta\phi]$$

FTS (*Fourier* series expansion)

$$robar\_ag\_LUT[iddv, \lambda, iaer, \theta_s \times \theta_v, s]$$

### Scientific content:

$robar\_ag\_LUT[iddv, \lambda, iaer, \theta_s \times \theta_v, s]$  defines the aerosol-ground DDV coupling bidirectionality term as function of the DDV model ( $iddv$ ), the wavelength ( $\lambda$ ), the aerosol model ( $iaer$ ), the illumination and viewing geometry ( $\theta_s, \theta_v$ ), and the *Fourier* term ( $s$ ) used to remove the azimuthal dependence. The latter which accounts for the multiple scatterings between the ground DDV interface and the aerosol atmosphere, is useful for the atmospheric correction algorithm over land.

### Resources:

Estimated CPU time: 6 sec (If ASCII LUT exists)  
Output disk space:  $20 \times 5 \times 4 \times 78 \times 78 \times 4$  bytes/fl = 9734400 bytes

Acceptance:

Comparison with another code.

6.14.16.3 Ground DDV albedo,  $\rho_{DDV}(iddv, \lambda)$

Reference: albedo\_g, LUT322

[AD-8] Section 6.14.16, ADSR field 3

Dependencies:

None

Tool:

RTC/MOS (lut\_alb\_gddv)

Procedure:

Inputs:  $\lambda$  4 MERIS wavelengths [*nm*] (412.5, 442.5, 490 and 665 *nm*)  
 $iddv$  DDV model # [*dl*] (among the 20 DDV models, [0..19])  
 $param\_Hapke$  CESBIO input file containing 4 *Hapke's* parameters ( $\omega$ ,  $g$ ,  $S$  and  $h$ ) for each of the 20 DDV models, each of the 4 wavelengths (*i.e.*, 412.5, 442.5, 490 and 665 *nm*) and for all illumination and viewing configurations (*see* [AD-7] for more details).  
 $\omega$  : single scattering albedo  
 $g$  : assymetry factor  
 $S$  : amplitude of the hot-spot  
 $h$  : width of the hot-spot

Output:  $albedo\_g[iddv, \lambda]$ , referred also as  $\rho_{DDV}[iddv, \lambda]$   
 Ground albedo for each DDV model (*iddv*) and each wavelength ( $\lambda$ )

units: [*dl*]

Step : Generate the ground DDV albedo  $albedo\_g[iddv, \lambda]$  for each DDV model and each wavelength, with the RTC/MOS (*lut\_alb\_gddv*).

$\lambda, iddv(\omega, g, S, h)$

RTC/MOS(*lut\_alb\_gddv*)

*albedo\_g* [*iddv*,  $\lambda$ ]

Scientific content:

*albedo\_g* [*iddv*,  $\lambda$ ] defines the ground DDV albedo as function of the DDV model (*iddv*) and the wavelength ( $\lambda$ ). The latter is useful for the atmospheric correction algorithm over land.

Resources:

Estimated CPU time: 7 sec (If ASCII LUT exists)  
Output disk space:  $20 \times 4 \times 4$  bytes/fl = 320 bytes

Acceptance:

Comparison with another code.

**6.14.17 ADS Aerosol Parameters for Bi-Directionality Correction**

6.14.17.1 Polynomial coefficients for aerosol-molecule coupling bidirectionality term retrieval

Reference: robar\_aR\_LUT, LUT324

[AD-8] Section 6.14.17, ADSR field 1

Dependencies:

LUT144, LUT147, LUT150, LUT154, LUT169

Tool:

OTC/SCAMAT  
RTC/MOS (*lut\_rhob\_aR*)  
Numerical integration (*Gauss* quadrature)  
Polynomial fit

Note: Both the numerical integration and polynomial fit tools are included in the RTC/MOS (*lut\_rhob\_aR*). The latter has been developed for the sun/view geometries in the MOS ground-segment.

Procedure:

|         |                    |   |
|---------|--------------------|---|
| Inputs: | $\theta$           | Zenith angle [ <i>deg</i> ]; tabulated values used for $(\theta_s \times \theta_v)$ combinations, <i>see Section 6.14.4.1</i> , (LUT147)  |
|         | $\tau^a$           | Aerosol optical thickness at 550nm [ <i>dl</i> ] (15 values in [0.1;1.5] by step of 0.1)  |
|         | <i>iaer</i>        | Aerosol model # [ <i>dl</i> ] (among the 78 <i>Junge's</i> models) characterized by an <i>Angström</i> exponent ( $\alpha$ ) and a refractive index, <i>see Section 6.14.4.4</i> (LUT144) and <i>Section 6.14.1.1</i> (LUT154). |
|         | <i>Sca_cos</i>     | Cosine of scattering angle [ <i>dl</i> ], <i>see Section 6.14.4.4</i> , (LUT150)  |
|         | <i>phase_aer78</i> | Input file containing scattering phase functions for 78 continental aerosol models ( <i>see [AD-7]</i> for more details).   |
|         | <i>k</i>           | Polynomial coefficient orders [ <i>dl</i> ], $k = [0;3]$  |

Output: *robar\_aR\_LUT[iaer,θ,k]*  
Polynomial coefficients for the aerosol-molecule coupling bidirectionality term retrieval as function of the aerosol model (*iaer*), and the solar zenith angle  $\theta$

units: [*dl*]

Step-0: Compute the IOPs (aerosol phase function, single scattering albedo, extinction coefficient) for all the 78 aerosol models. Either generate the LUT170 (*see Section 6.14.1.1*) or launch the *Mie's* computations with OTC/SCAMAT using as inputs the *Angström* exponent and refractive index (real and imaginary parts).

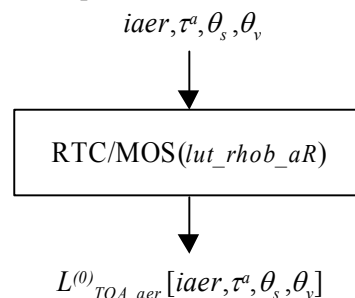
Step-1: For each of the 78 aerosol models (*iaer*), interpolate the scattering phase function  $P_{scat}[iaer, \Theta]$  to the input scattering angles (*Sca\_cos*) to get  $P_{scat}[iaer, Sca\_cos]$  with the interpolation tool,

$$P_{scat}[iaer, Sca\_cos] = Interpolation(P_{scat}[iaer, \Theta]),$$

and generate the input file, *phase\_aer78*, with the 78 interpolated scattering phase functions.

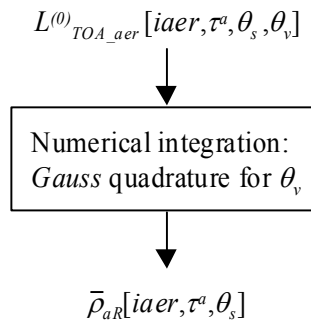
The steps, described hereafter, are implemented in the RTC/MOS (*lut\_rhob\_agddv*).

Step-2: Generate the top of aerosol normalized radiance  $L^{(0)}_{TOA\_aer}[iaer, \tau^a, \theta_s, \theta_v]$  corresponding to the first order of *Legendre* decomposition ( $I_s=0$ ) of phase function, over a black land surface with the RTC/MOS (*lut\_rhob\_aR*). Computations have to be completed for each of the 78 continental aerosol models (*iaer*), each of the 15 aerosol optical thickness ( $\tau^a$ ) at 550nm (*i.e.*, [0.1;1.5] by step of 0.1), and the pre-selected illumination and viewing configurations ( $\theta_s, \theta_v$ ).



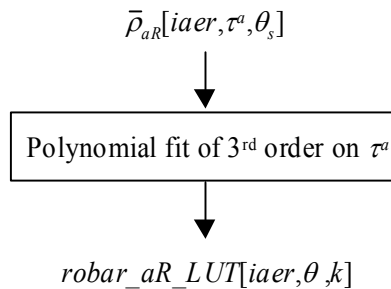
Step-3: Determine the aerosol-molecule coupling bidirectionality term retrieval  $\bar{\rho}_{aR}(iaer, \tau^a, \vartheta_s)$  for each aerosol model (*iaer*) and each aerosol optical thickness ( $\tau^a$ ) at 550nm by performing the numerical angular integration of the top of aerosol normalized radiance  $L^{(0)}_{TOA\_aer}[iaer, \tau^a, \theta_s, \theta_v]$  over the hemispherical sphere (*i.e.*, over the 24 *Gaussian* angles,  $\mu_v = \cos\theta_v$ ) as follows,

$$\bar{\rho}_{aR}(iaer, \tau^a, \vartheta_s) = \int_0^1 L^{(0)}(iaer, \tau^a, \vartheta_s, \vartheta_v) \cdot d\mu_v$$



Step-4: Apply a 3<sup>rd</sup> order polynomial fit on the  $\bar{\rho}^{aR}(iaer, \tau^a, \vartheta_s)$  as function of the aerosol optical thickness ( $\tau^a$ ) at 550nm, for retrieving the polynomial coefficients *robar\_aR\_LUT*[*iaer*,  $\theta$ , *k*],

$$\begin{aligned} \bar{\rho}_{aR}(iaer, \tau^a, \vartheta_s) = & \text{robar\_aR\_LUT}[iaer, \theta, 0] \\ & + \text{robar\_aR\_LUT}[iaer, \theta, 1] \cdot (\tau^a) \\ & + \text{robar\_aR\_LUT}[iaer, \theta, 2] \cdot (\tau^a)^2 \\ & + \text{robar\_aR\_LUT}[iaer, \theta, 3] \cdot (\tau^a)^3 \end{aligned}$$



Scientific content:

*robar\_aR\_LUT*[*iaer*,  $\theta$ , *k*] defines the polynomial coefficients for the aerosol-molecule coupling bidirectionality term retrieval as function of the aerosol model (*iaer*), and the solar zenith angle  $\theta$ . The latter which accounts for the coupling between the aerosol and the molecule scatterings, is useful for the atmospheric correction algorithm over land.

Resources:

Estimated CPU time: 54 sec  
Output disk space: 78 × 12 × 4 × 4 bytes/fl = 14976 bytes

Acceptance:

Comparison with another RTC.

6.14.17.2 (Spare)

Reference:

[AD-8] Section 6.14.17, ADSR field 2

**6.14.18 ADS DDV Reflectance Correction Parameters**

6.14.18.1 Monthly adjustment for bands at 412.5 nm, 442.5 nm, 490 nm & 665 nm, C(month, lat, long, band)

Reference: C, LUT434

[AD-8] Section 6.14.18, ADSR field 1

ACRI provided

Dependencies:

LUT310, LUT311

Tool:

None

Procedure:

Inputs: *month* Month [*dl*] (12 values)  
*lat* Latitude [*deg.*] (180 values)  
*long* Longitude [*deg.*] (360 values)  
*iband* DDV band # [*dl*] (among 4 MERIS bands: 412.5, 442.5, 490 & 665 nm)

Output: C[*month, lat, long, iband*]  
Monthly adjustment as function of geographic location (*lat, long*) and for each of the 4 MERIS DDV bands

units: [*dl*]

Step: User specified.

Scientific content:

Monthly adjustment coefficients applied on the DDV reflectances at 412.5, 442.5, 490 and 665 nm.

Current baseline: (12 x 180 x 360 x 4) values

Resources:

Estimated CPU time: -

Output disk space: 12 x 180 x 360 x 4 x 4 bytes/fl = 12441600 bytes

Acceptance:

Corresponds to the latest definition.

6.14.18.2 *Linear corrections for bands at 412.5 nm, 442.5 nm, 490 nm & 665 nm, LC(month, lat, long, band)*

Reference: LC, LUT435

[AD-8] Section 6.14.18, ADSR field 2

ACRI provided

Dependencies:

None

Tool:

None

Procedure:

Inputs:     *month*           Month [*dl*] (12 values)  
                  *lat*                Latitude [*deg.*] (180 values)  
                  *long*           Longitude [*deg.*] (360 values)  
                  *iband*           DDV band # [*dl*] (among 4 MERIS bands: 412.5, 442.5, 490 & 665 nm)

Output:     *LC[month, lat, long, iband]*  
                  Monthly linear correction as function of geographic location (*lat, long*)  
                  and for each of the 4 MERIS DDV bands

units:            [*dl*]

Step:            User specified.

Scientific content:



Monthly linear corrections applied on the DDV reflectances at 412.5, 442.5, 490 and 665 *nm*.

Resources:

Estimated CPU time: -  
Output disk space:  $12 \times 180 \times 360 \times 4 \times 4$  bytes/fl = 12441600 bytes

Acceptance:

Corresponds to the latest definition.

**6.14.18.3 Minimum and maximum seasonal variation of ARVI, [ $\Delta ARVI_{min}$ ,  $\Delta ARVI_{max}$ ](month, DDV model)**

Reference:  $\Delta ARVI_{min}$ ,  $\Delta ARVI_{max}$ , LUT436

[AD-8] Section 6.14.18, ADSR field 3

ACRI provided

Dependencies:

None

Tool:

None

Procedure:

Inputs: *month* Month [*dl*] (12 values)  
*lat* Latitude [*deg.*] (180 values)  
*long* Longitude [*deg.*] (360 values)

Outputs:  $\Delta ARVI_{min}[month, lat, long]$ ,  $\Delta ARVI_{max}[month, lat, long]$   
Monthly minimum and maximum seasonal variation of the ARVI  
units: [*dl*]


Step: User specified.

Scientific content:

Monthly minimum and maximum seasonal variation of ARVI.

Resources:

Estimated CPU time: -  
Output disk space:  $12 \times 180 \times 360 \times 2 \times 4$  bytes/fl = 6220800 bytes

|   |   |   |
|---|---|---|
|  | <b>MERIS / ENVISAT-1</b><br>MEdium Resolution Imaging<br>Spectrometer | <u>Ref.:</u> PO-RS-PAR-GS-0002<br><u>Issue:</u> 3 <u>Rev.:</u> C<br><u>Date:</u> 27-Feb-11 <u>Page:</u> 393 |
|---|---|---|

Acceptance:

Corresponds to the latest definition.

## 6.15 OCEAN CASE-I PARAMETERS

### 6.15.1 C.P.

#### 6.15.1.1 C.P. Extinction coefficient and single scattering albedo for chlorophyll

Reference:  $Q_{ext}[chl,\lambda]$ ,  $\omega_o[chl,\lambda]$  LUT418

Configuration file

PARBLEU provided

Dependencies:

None

Tool:

None

Procedure:

Input:  $\lambda$  MERIS wavelength [*nm*] (412.5, 442.5, 490, 510, 560, 620, 665, 681.25 and 708.75 *nm*)

$chl$  Chlorophyll content [ $mg.m^{-3}$ ] (0.03, 0.1, 0.3, 1.0, 3.0 and 10  $mg.m^{-3}$ )

Output:  $Q_{ext}[chl,\lambda]$ ,  $\omega_o[chl,\lambda]$   
Extinction coefficient and single scattering albedo for chlorophyll, for 6  $chl$ -contents and 9 wavelengths (6 x 9 x 2 values)

units: [ $\mu m^{-1}$ , *dl*]

Step: User specified.

Scientific content:

The approach used to compute the inherent optical properties (IOPs) of chlorophyll (*i.e.*, the extinction coefficient  $\sigma_{e,\lambda}^p$  and the single scattering albedo  $\omega_{s,\lambda}^p$  of phytoplankton) are detailed in [AD-6]. These IOPs are tabulated as function of 9 MERIS wavelengths and 6 chlorophyll contents:

Current baseline: (6 x 9 x 2) values

| $\lambda$<br>[chl] mg/m <sup>3</sup> | $\sigma_{e,\lambda}^p$ [chl, $\lambda$ ]<br>0.03 | $\omega_{o,\lambda}^p$ [chl, $\lambda$ ]<br>0.03 | $\sigma_{e,\lambda}^p$ [chl, $\lambda$ ]<br>0.1 | $\omega_{o,\lambda}^p$ [chl, $\lambda$ ]<br>0.1 | $\sigma_{e,\lambda}^p$ [chl, $\lambda$ ]<br>0.3 | $\omega_{o,\lambda}^p$ [chl, $\lambda$ ]<br>0.3 |
|--------------------------------------|--|--|---|---|---|---|
| 412.50                               | 0.04697350                                       | 0.78449339                                       | 0.10981160                                      | 0.78280801                                      | 0.23639670                                      | 0.78764635                                      |
| 442.50                               | 0.04276818                                       | 0.80822474                                       | 0.10192190                                      | 0.80578268                                      | 0.22355400                                      | 0.80918258                                      |
| 490.00                               | 0.03609181                                       | 0.87273818                                       | 0.08890710                                      | 0.86450017                                      | 0.20056330                                      | 0.86488408                                      |
| 510.00                               | 0.03307195                                       | 0.91832507                                       | 0.08366360                                      | 0.89510131                                      | 0.19162710                                      | 0.89043772                                      |
| 560.00                               | 0.02792019                                       | 0.99888992                                       | 0.07462377                                      | 0.94434255                                      | 0.17617400                                      | 0.93198204                                      |
| 620.00                               | 0.02541830                                       | 1.00000000                                       | 0.06595910                                      | 1.00000000                                      | 0.15759933                                      | 0.99909687                                      |
| 665.00                               | 0.02384580                                       | 1.00000000                                       | 0.06302240                                      | 1.00000000                                      | 0.15298200                                      | 1.00000000                                      |
| 681.25                               | 0.02332680                                       | 1.00000000                                       | 0.06204120                                      | 1.00000000                                      | 0.15147001                                      | 1.00000000                                      |
| 708.75                               | 0.02250040                                       | 1.00000000                                       | 0.06046560                                      | 1.00000000                                      | 0.14902399                                      | 1.00000000                                      |
| [chl] mg/m <sup>3</sup>              | 1.00   | 1.00   | 3.00  | 3.00  | 10  | 10  |
| 412.50                               | 0.54620302                                       | 0.79520619                                       | 1.19614506                                      | 0.80683446                                      | 2.93732905                                      | 0.82630515                                      |
| 442.50                               | 0.52726638                                       | 0.81513631                                       | 1.17101502                                      | 0.82414913                                      | 2.89315701                                      | 0.83892095                                      |
| 490.00                               | 0.48726630                                       | 0.86866462                                       | 1.10366905                                      | 0.87443882                                      | 2.74862409                                      | 0.88303459                                      |
| 510.00                               | 0.47157121                                       | 0.89220464                                       | 1.07605398                                      | 0.89687973                                      | 2.68517804                                      | 0.90389913                                      |
| 560.00                               | 0.44491819                                       | 0.93247926                                       | 1.02966285                                      | 0.93728840                                      | 2.57210302                                      | 0.94363642                                      |
| 620.00                               | 0.42658740                                       | 0.95781308                                       | 1.01728654                                      | 0.94869143                                      | 2.55924201                                      | 0.94837844                                      |
| 665.00                               | 0.42385781                                       | 0.95390248                                       | 1.03372216                                      | 0.93360770                                      | 2.61654711                                      | 0.92760801                                      |
| 681.25                               | 0.42002830                                       | 0.95912111                                       | 1.03110266                                      | 0.93597960                                      | 2.61319804                                      | 0.92879683                                      |
| 708.75                               | 0.40047300                                       | 1.00000000                                       | 0.96509099                                      | 1.00000000                                      | 2.42712998                                      | 1.00000000                                      |

Resources:

Estimated CPU time: -  
Output disk space:  $6 \times 9 \times 2 \times 4$  bytes/fl = 216 bytes

Acceptance:

Corresponds to the latest definition.

**6.15.2 MPH**

Not covered in this document (see [AD-8] for a detailed description)

**6.15.3 SPH**

Not covered in this document (see [AD-8] for a detailed description)

**6.15.4 GADS General**

*6.15.4.1 Wind-speeds for GADS geometrical factor  $R_{goth}$*

Reference: Ws\_Rg, LUT171

[AD-8] Section 6.15.4, GADS field 1

ACRI provided

Dependencies:

None

Tool:

None

Procedure:

Input: none

Output:  $Ws\_Rg$  Wind-speed ( $w_s$ ) just above sea level for GADS geometrical  $\mathcal{R}(w_s)$  factor  
(4 values)

units:  $[m.s^{-1}]$

Step: User specified.

Scientific content:

Set of 4 wind-speeds ( $w_s$ ) just above sea level used for GADS geometrical  $\mathcal{R}(w_s)$  factor

Current baseline:  $\{0, 4, 10, 16\} m.s^{-1}$

Resources:

Estimated CPU time: -

Output disk space:  $4 \times 1 \text{ byte/uc} = 4 \text{ bytes}$

Acceptance:

Corresponds to the latest definition.

6.15.4.2 Wavelengths for ADS  $f_1/Q$

Reference:  $Wvl\_fQ$ , LUT172

[AD-8] Section 6.15.4, GADS field 2

ACRI provided

Dependencies:

None

Tool:

None

Procedure:

Input: none

Output:  $Wvl\_fQ$  MERIS nominal wavelength for ADS  $f_i/Q$  (9 values)  
units: [nm]

Step: User specified.

Scientific content:

Current baseline: {412.5, 442.5, 490.0, 510.0, 560.0, 620.0, 665.0, 681.25, 708.75} nm

Resources:

Estimated CPU time: -  
Output disk space:  $9 \times 4$  bytes/fl = 36 bytes

Acceptance:

Corresponds to the latest definition.

**6.15.4.3 Solar zenith angles for ADS  $f_i/Q$**

Reference: SZA\_fQ, LUT173

[AD-8] Section 6.15.4, GADS field 3

ACRI provided

Dependencies:

None

Tool:

None

Procedure:

Input: none

Output: *SZA\_fQ* Solar zenith angle for ADS  $f_i/Q$  (6 values)  
units:  $[10^{-6}deg.]$   
Step: User specified.

Scientific content:

Set of 6 solar zenith angles ( $\theta_i$ ) regularly spaced  
Current baseline:  $\{0, 15, 30, 45, 60, 75\} deg$

Resources:

Estimated CPU time: -  
Output disk space:  $6 \times 4 \text{ bytes/ul} = 24 \text{ bytes}$

Acceptance:

Corresponds to the latest definition.

**6.15.4.4 Solar zenith angles for GADS thresholds and ADS glint reflectance**

Reference: SZA, LUT174

[AD-8] Section 6.15.4, GADS field 4

ACRI provided

Dependencies:

None

Tool:

None

Procedure:

Input: none  
Output: *SZA* Solar zenith angle for GADS thresholds and ADS glint reflectance (27 values)  
units:  $[10^{-6}deg.]$   
Step: User specified.

Scientific content:

Set of 27 solar zenith angles ( $\theta_s$ ) regularly spaced

Current baseline: 27 angles in [15 ; 80] *deg.* by step of 2.5 *deg.*

Resources:

Estimated CPU time: -

Output disk space: 27 × 4 bytes/ul = 108 bytes

Acceptance:

Corresponds to the latest definition.

6.15.4.5 Zenith angles in water for ADS  $f_i/Q$

Reference: theta\_fQ, LUT175

[AD-8] Section 6.15.4, GADS field 5

ACRI provided

Dependencies:

None

Tool:

None

Procedure:

Input: none

Output: theta\_fQ Zenith angle in water for ADS  $f_i/Q$  (14 values)

units: [10<sup>-6</sup>*deg.*]

Step: User specified.

Scientific content:

Set of 14 zenith angles in water ( $\theta_w$ )

Current baseline: {1.078, 3.411, 6.289, 9.278, 12.30, 15.33, 18.37, 21.41, 24.45, 27.50, 30.54, 33.59, 36.64, 39.69} *deg.*



Resources:

Estimated CPU time: -  
Output disk space:  $14 \times 4 \text{ bytes/ul} = 56 \text{ bytes}$

Acceptance:

Corresponds to the latest definition.

6.15.4.6 Zenith angles in water for GADS geometrical factor  $R_{goth}$

Reference: theta\_Rg, LUT176

[AD-8] Section 6.15.4, GADS field 6

ACRI provided

Dependencies:

None

Tool:

None

Procedure:

Input: none  
Output: *theta\_Rg* Zenith angle in water for GADS geometrical  $\mathcal{R}(w_s)$  factor (19 values)  
units:  $[10^{-6} \text{deg.}]$   
Step: User specified.

Scientific content:

Set of 19 zenith angles in water ( $\theta_w$ ) used for GADS geometrical  $\mathcal{R}(w_s)$  factor  
Current baseline:  $\{0, 5, 10, 15, 20, 25, 30, 35, 40, 45, 50, 55, 60, 60, 60, 60, 60, 60, 60\} \text{ deg.}$

Resources:

Estimated CPU time: -  
Output disk space:  $19 \times 4 \text{ bytes/ul} = 76 \text{ bytes}$

Acceptance:

Corresponds to the latest definition.

#### 6.15.4.7 View zenith angles for GADS thresholds and ADS glint reflectance

Reference: VZA, LUT177

[AD-8] Section 6.15.4, GADS field 7

ACRI provided

#### Dependencies:

None

#### Tool:

None

#### Procedure:

Input: none

Output: *VZA* View zenith angle for GADS thresholds and ADS glint reflectance (19 values)

units:  $[10^{-6}deg.]$

Step: User specified.

#### Scientific content:

Set of 19 view zenith angles ( $\theta_v$ ) regularly spaced

Current baseline: 19 angles in  $[0 ; 45] deg.$  by step of 2.5 *deg.*

#### Resources:

Estimated CPU time: -

Output disk space:  $19 \times 4 \text{ bytes/ul} = 76 \text{ bytes}$

#### Acceptance:

Corresponds to the latest definition.

#### 6.15.4.8 Relative azimuth angles for ADS $f_r/Q$

Reference: RAA\_fQ, LUT178

[AD-8] Section 6.15.4, GADS field 8

ACRI provided

Dependencies:

None

Tool:

None

Procedure:

Input: none

Output: *RAA\_fQ* Relative azimuth angle for ADS  $f_i/Q$  (13 values)  
units:  $[10^{-6}deg.]$

Step: User specified.

Scientific content:

Set of 13 relative azimuth angles ( $\Delta\phi$ ) regularly spaced

Current baseline: 13 values in  $[0 ; 180] deg.$  by step of  $15 deg.$

Resources:

Estimated CPU time: -

Output disk space:  $13 \times 4 \text{ bytes/ul} = 52 \text{ bytes}$

Acceptance:

Corresponds to the latest definition.

**6.15.4.9 Relative azimuth angles for GADS thresholds and ADS glint reflectance**

Reference: RAA, LUT179

[AD-8] Section 6.15.4, GADS field 9

ACRI provided

Dependencies:

None

Tool:

None

Procedure:

Input: none

Output: *RAA* Relative azimuth angle for GADS thresholds and ADS glint reflectance  
(25 values)

units:  $[10^{-6}deg.]$

Step: User specified.

Scientific content:

Set of 25 relative azimuth angles ( $\Delta\phi$ ) regularly spaced

Current baseline: 25 values in  $[0 ; 180]$  deg. by step of 7.5 deg.

Resources:

Estimated CPU time: -

Output disk space:  $25 \times 4$  bytes/ul = 100 bytes

Acceptance:

Corresponds to the latest definition.

**6.15.4.10 Chlorophyll contents for ADS  $f_1/Q$**

Reference: Ch11, LUT180

[AD-8] Section 6.15.4, GADS field 10

ACRI provided

Dependencies:

None

Tool:

None

Procedure:

Input: none  
Output: *Chl1* Chlorophyll content for ADS  $f_i/Q$  (5 values)  
units:  $[10^{-3} \text{ mg.m}^{-3}]$   
Step: User specified.

Scientific content:

Set of 5 chlorophyll contents  
Current baseline:  $\{0.03, 0.10, 0.30, 1.0, 3.0\} \text{ mg.m}^{-3}$ .

Resources:

Estimated CPU time: -  
Output disk space:  $5 \times 4 \text{ bytes/fl} = 20 \text{ bytes}$

Acceptance:

Corresponds to the latest definition.

6.15.4.11 Aerosol optical thicknesses for ADS  $f_i/Q$

Reference: tauA, LUT181

[AD-8] Section 6.15.4, GADS field 11

ACRI provided

Dependencies:

None

Tool:

None

Procedure:

Input: none  
Output: *tauA* Aerosol optical thickness for ADS  $f_i/Q$  (2 values)  
units:  $[dl]$   
Step: User specified.

Scientific content:

Set of 5 chlorophyll contents

Current baseline: {0.2, 0.6}

Resources:

Estimated CPU time: -

Output disk space:  $2 \times 4$  bytes/fl = 8 bytes

Acceptance:

Corresponds to the latest definition.

6.15.4.12 *Wind-speeds for ADS  $f_1/Q$*

Reference:  $Ws\_fQ$ , LUT182

[AD-8] Section 6.15.4, GADS field 12

ACRI provided

Dependencies:

None

Tool:

None

Procedure:

Input: none

Output:  $Ws\_fQ$  Wind-speed just above sea level for ADS  $f_1/Q$  (2 values)

units:  $[m.s^{-1}]$

Step: User specified.

Scientific content:

Set of 2 wind-speeds ( $w_s$ ) just above sea level

Current baseline: {0, 7.2}  $m.s^{-1}$

Resources:

Estimated CPU time: -  
Output disk space:  $2 \times 4$  bytes/fl = 8 bytes

Acceptance:

Corresponds to the latest definition.

6.15.4.13 Initial algal pigment index value for ADS  $f_i/Q$

Reference: Chl1\_fQ, LUT183

[AD-8] Section 6.15.4, GADS field 13

ACRI provided

Dependencies:

None

Tool:

None

Procedure:

Input: none  
Output: *Chl1\_fQ* Chlorophyll content for ADS  $f_i/Q$  (2 values)  
units:  $[mg \cdot m^{-3}]$   
Step: User specified.

Scientific content:

This initial algal pigment index value is required by the *Chl1\_fQ* algorithm. The latter is computed from chlorophyll tabulated values  $f_i/Q$  used for correction of viewing angle.

Typical values range between  $0.03 < Chl1\_fQ < Chl1\_fQ_{thresrangeout}$

Current baseline:  $0.3 mg \cdot m^{-3}$

Resources:

Estimated CPU time: -  
Output disk space:  $1 \times 4$  bytes/fl = 8 bytes

Acceptance:

Corresponds to the latest definition.

6.15.4.14  $C_i$  constants for downward atmospheric transmittance

Reference:  $C_i$ , LUT184

[AD-8] Section 6.15.4, GADS field 14

ACRI provided

Dependencies:

None

Tool:

None

Procedure:

Input: none

Output:  $C_i$  Constants for downward atmospheric transmittance (6 values)  
units: [dl]

Step: User specified.

Scientific content:

These constants are used for computing the downward atmospheric transmittance.

Current baseline: {0.15; 93.885; 1.253; 1.0035; 0.007; 0.95}

Resources:

Estimated CPU time: -

Output disk space:  $6 \times 4$  bytes/fl = 24 bytes

Acceptance:

Corresponds to the latest definition.



6.15.4.15  $C_7$  constant for scattering detection

Reference:  $C_7$ , LUT185

[AD-8] Section 6.15.4, GADS field 15

ACRI provided

Dependencies:

None

Tool:

None

Procedure:

Input: none

Output:  $C_7$  Constant for scattering detection

units: [dl]

Step: User specified.

Scientific content:

This constant is used for scattering detection.

Current baseline: 1.7

Resources:

Estimated CPU time: -

Output disk space:  $1 \times 4$  bytes/fl = 4 bytes

Acceptance:

Corresponds to the latest definition.

6.15.4.16 Factor relating  $b_p/a$  to reflectance just below water surface for a sun at zenith

Reference: (No variable used), LUT186

[AD-8] Section 6.15.4, GADS field 16

ACRI provided

Dependencies:

None

Tool:

None

Procedure:

Input: none

Output: (no variable) Factor relating  $b_b/a$  to reflectance just below water surface for a sun at zenith

units: [dl]

Step: User specified.

Scientific content:

$f_0(\lambda, Chl1)$  defines the factor which relates the reflectance just below the surface ( $R$ ) to the IOP of the water ( $b_b/a$ ) for a sun at zenith ( $\theta_s = 0$ ) as follows:

$$R(\lambda, Chl1) = f_0(\lambda, Chl1) \cdot \frac{b_b(\lambda)}{a(\lambda)}$$

with  $b_b$  the backscattering coefficient directly related to the selected scattering phase function, and  $a$  the absorption coefficient.  $R$  is defined as the ratio of the upward ( $E_{u,(0-)}$ ) to downward ( $E_{d,(0-)}$ ) irradiances just beneath the water surface.

Current baseline: 0.33

Resources:

Estimated CPU time: -

Output disk space:  $1 \times 4$  bytes/fl = 4 bytes

Acceptance:

Corresponds to the latest definition.

6.15.4.17 Wind-speeds for GADS glint reflectance

Reference: Ws\_rhoG, LUT187

[AD-8] Section 6.15.4, GADS field 17

ACRI provided

Dependencies:

None

Tool:

None

Procedure:

Input: none

Output:  $Ws\_Rg$  Wind-speed ( $w_s$ ) just above sea level for GADS glint reflectance (4 values)

units:  $[m.s^{-1}]$

Step: User specified.

Scientific content:

Set of 5 wind-speeds ( $w_s$ ) just above sea level used for GADS glint reflectance

Current baseline:  $\{3.0, 5.0, 7.0, 10., 14.\} m.s^{-1}$

Resources:

Estimated CPU time: -

Output disk space:  $5 \times 4$  bytes/fl = 20 bytes

Acceptance:

Corresponds to the latest definition.

6.15.4.18 *Wind azimuth orientations for GADS glint reflectance*

Reference: Xhi, LUT188

[AD-8] Section 6.15.4, GADS field 18

ACRI provided

Dependencies:

None

Tool:

None

Procedure:

Input: none

Output: *Xhi* Wind azimuth orientations for GADS glint reflectance (7 values)  
units:  $[10^{-6}deg]$

Step: User specified.

Scientific content:

Set of 7 wind azimuth orientations ( $\chi$ ) regularly spaced for GADS glint reflectance

Current baseline: 7 values in  $[0 ; 180]$  *deg.* by step of 30 *deg.*

Resources:

Estimated CPU time: -

Output disk space:  $7 \times 4$  bytes/fl = 28 bytes

Acceptance:

Corresponds to the latest definition.

6.15.4.19 (*Spare*)

Reference:

[AD-8] Section 6.15.4, GADS field 19

6.15.4.20 *Value of f/Q factor for a nadir viewing angle at 510nm*

Reference: fQ510\_nadir, LUT326

[AD-8] Section 6.15.4, GADS field 20

ACRI provided

Dependencies:

None

Tool:

None

Procedure:

Input: none

Output:  $fQ510\_nadir$  Value of  $f_i/Q$  factor for a nadir viewing angle at 510nm

units: [dl]

Step: User specified.

Scientific content:

Value of  $f_i/Q$  factor for a nadir viewing angle at 510nm

Current baseline: 0.095624961

Resources:

Estimated CPU time: -

Output disk space:  $1 \times 4$  bytes/fl = 4 bytes

Acceptance:

Corresponds to the latest definition.

*6.15.4.21 Mean value of chlorophyll content*

Reference: Chl\_mean, LUT327

[AD-8] Section 6.15.4, GADS field 21

ACRI provided

Dependencies:

None

Tool:

None

Procedure:

Input: none

Output: *Chl\_mean* Chlorophyll content in mean value  
units: [ $mg.m^{-3}$ ]  
Step: User specified.

Scientific content:

Chlorophyll content in mean value  
Current baseline:  $0.1 mg.m^{-3}$

Resources:

Estimated CPU time: -  
Output disk space:  $1 \times 4 \text{ bytes/fl} = 4 \text{ bytes}$

Acceptance:

Corresponds to the latest definition.

6.15.4.22 *Water refractive index*

Reference: *Nw*, LUT328

[AD-8] Section 6.15.4, GADS field 22

ACRI provided

Dependencies:

None

Tool:

None

Procedure:

Input: none  
Output: *Nw* Water refractive index  
units: [ $dI$ ]  
Step: User specified.

Scientific content:

Refractive index of sea water (assumed to be constant whatever the temperature and salinity)

Current baseline: 1.34

Resources:

Estimated CPU time: -  
Output disk space: 1 × 4 bytes/fl = 4 bytes

Acceptance:

Corresponds to the latest definition.

**6.15.4.23 Value of  $\Delta\rho_{510}$  to set the annotation flag**

Reference: DRO510\_LIM, LUT329

[AD-8] Section 6.15.4, GADS field 23

ACRI provided

Dependencies:

None

Tool:

None

Procedure:

Input: none  
Output: *DRO510\_LIM* Value of  $\Delta\rho_{510}$  to set the annotation flag  
units: [dl]  
Step: User specified.

Scientific content:

$\Delta\rho_{510}$  to set the annotation flag

Current baseline: 0.005

Resources:

Estimated CPU time: -  
Output disk space: 1 × 4 bytes/fl = 4 bytes

Acceptance:

Corresponds to the latest definition.

6.15.4.24 Value of the scattering angle  $\Theta_p$  for a nadir viewing

Reference: ThetaP\_Zenith, LUT330

[AD-8] Section 6.15.4, GADS field 24

ACRI provided

Dependencies:

None

Tool:

None

Procedure:

Input: none

Output: *ThetaP\_Zenith*  
Value of the scattering angle ( $\Theta_p$ ) for a nadir viewing

units:  $[10^{-6}deg]$

Step: User specified.

Scientific content:

Scattering angle ( $\Theta_p$ ) for a nadir viewing

Current baseline: 0 deg.

Resources:

Estimated CPU time: -  
Output disk space: 1 × 4 bytes/ul = 4 bytes

Acceptance:

Corresponds to the latest definition.



6.15.4.25 *Scaling factor for decoding mean value of water-leaving reflectance at 510 nm*

Reference: rhow510mean\_scale, LUT440

[AD-8] Section 6.15.4, GADS field 25

ACRI provided

Dependencies:

None

Tool:

None

Procedure:

Input: none

Output: *rhow510mean\_scale*  
Scaling factor for decoding mean value of water-leaving reflectance at  
510nm

units: [dl]

Step: User specified.

Scientific content:

Scaling factor for decoding mean value of water-leaving reflectance at 510nm

Current baseline:  $6.25 \cdot 10^{-5}$

Resources:

Estimated CPU time: -

Output disk space:  $1 \times 4$  bytes/fl = 4 bytes

Acceptance:

Corresponds to the latest definition.

6.15.4.26 *Offset for decoding mean value of water-leaving reflectance at 510nm*

Reference: rhow510mean\_offset, LUT441

[AD-8] Section 6.15.4, GADS field 25

ACRI provided

Dependencies:

None

Tool:

None

Procedure:

Input: none

Output: *rhow510mean\_offset*  
Offset factor for decoding mean value of water-leaving reflectance at  
510nm

units: [dl]

Step: User specified.

Scientific content:

Offset factor for decoding mean value of water-leaving reflectance at 510nm

Current baseline: 0

Resources:

Estimated CPU time: -

Output disk space: 1 × 4 bytes/fl = 4 bytes

Acceptance:

Corresponds to the latest definition.

6.15.4.27 *Scaling factor for decoding variability value of water-leaving reflectance at 510nm*

Reference: rhow510var\_scale, LUT442

[AD-8] Section 6.15.4, GADS field 27

ACRI provided

Dependencies:

None

Tool:

None

Procedure:

Input: none

Output: *rhow510var\_scale*

Scaling factor for decoding variability value of water-leaving reflectance at 510nm

units: [dl]

Step: User specified.

Scientific content:

Scaling factor for decoding variability value of water-leaving reflectance at 510nm

Current baseline:  $1.953125 \cdot 10^{-5}$

Resources:

Estimated CPU time: -

Output disk space:  $1 \times 4 \text{ bytes/fl} = 4 \text{ bytes}$

Acceptance:

Corresponds to the latest definition.

**6.15.4.28 Offset for decoding variability value of water-leaving reflectance at 510nm**

Reference: rhow510var\_offset, LUT443

[AD-8] Section 6.15.4, GADS field 28

ACRI provided

Dependencies:

None

Tool:

None

Procedure:

Input: none

Output: *rhov510var\_offset*

Offset factor for decoding variability value of water-leaving reflectance at 510nm

units: [dl]

Step: User specified.

Scientific content:

Offset factor for decoding variability value of water-leaving reflectance at 510nm

Current baseline: 0

Resources:

Estimated CPU time: -

Output disk space: 1 × 4 bytes/fl = 4 bytes

Acceptance:

Corresponds to the latest definition.

**6.15.4.29 Latitudes for mean values of water-leaving reflectance at 510nm**

Reference: Latitude[lat], LUT444

[AD-8] Section 6.15.4, GADS field 29

ACRI provided

Dependencies:

None

Tool:

None

Procedure:

Input: none

Output: *Latitude[lat]*

Latitude for mean values of water-leaving reflectance at 510nm (1024 values)

units:  $[10^{-6}deg.]$

Step: User specified.

Scientific content:

Latitudes used for geographic map of mean values of water-leaving reflectance at 510nm

Current baseline: 1024 latitude values in [89.912109 ; -89.912109] deg. by step of -0.175781 deg.

Resources:

Estimated CPU time: -

Output disk space:  $1024 \times 4 \text{ bytes/sl} = 4096 \text{ bytes}$

Acceptance:

Corresponds to the latest definition.

*6.15.4.30 Longitudes for water-leaving reflectance mean values at 510nm (tabulated values)*

Reference: Longitude[long], LUT445

[AD-8] Section 6.15.4, GADS field 30

ACRI provided

Dependencies:

None

Tool:

None

Procedure:

Input: none

Output: *Longitude[long]*

Longitude for mean values of water-leaving reflectance at 510nm (2048 values)

units:  $[10^{-6}deg.]$

Step: User specified.

Scientific content:

Longitudes used for geographic map of mean values of water-leaving reflectance at 510nm

Current baseline: 2048 longitude values in [-179.912109 ; -179.912109] deg. by step of 0.175781 deg.

Resources:

Estimated CPU time: -

Output disk space: 2048 × 4 bytes/sl = 8192 bytes

Acceptance:

Corresponds to the latest definition.

6.15.4.31 Chlorophyll contents for ADS  $f_o$  factor

Reference: Chl\_fo, LUT490

[AD-8] Section 6.15.4, GADS field 31

ACRI provided

Dependencies:

None

Tool:

None

Procedure:

Input: none

Output: Chl\_fo Chlorophyll contents for ADS  $f_o$  factor (6 values)

units:  $[10^{-3} \text{ mg.m}^{-3}]$

Step: User specified.

Scientific content:

Chlorophyll contents for ADS  $f_o$  factor

Current baseline: {0.03, 0.1, 0.3, 1, 3, 10}  $mg.m^{-3}$

Resources:

Estimated CPU time: -  
Output disk space:  $6 \times 4$  bytes/fl = 24 bytes

Acceptance:

Corresponds to the latest definition.

**6.15.5 GADS Geometrical factor  $R_{goth}$**

6.15.5.1 Geometrical factor  $R_{goth}(\theta', w_s)$

Reference:  $R_{ghot}[\theta', w_s]$ , LUT189

[AD-8] Section 6.15.5, GADS field 1

ACRI provided

Dependencies:

LUT171, LUT176, LUT328

Tool:

None

Procedure:

Input:  $\theta'$  Zenith angle in water (19 values), *see* Section 6.15.4.6 (LUT176)  
 $w_s$  Wind-speed ( $w_s$ ) just above sea level [ $m.s^{-1}$ ] (4 values), *see* Section 6.15.4.1 (LUT170)  
 $n_w$  Water refractive index [ $dI$ ], *see* Section 6.15.4.22 (LUT328)

Output:  $R_{ghot}[\theta', w_s]$  Geometrical factor  $\mathcal{R}(\theta', w_s)$   
units: [ $dI$ ]

Step: User specified.

Scientific content:

$R_{ghot}[\theta', w_s]$  defines the geometrical factor, accounting for all refraction and reflection effects at the *air-sea* interface, as function of the solar zenith angle ( $\theta_s$ ) and the wind-speed ( $w_s$ ) just above sea level. The latter is expressed with the *Morel and Gentili* (1996) [RD-10] formula as follows:

$$R_{ghot}[\theta', w_s] = \frac{(1 - \bar{\rho}) \cdot (1 - \rho_F(\theta'))}{n_w^2 \cdot (1 - \bar{r} \cdot R)}$$

- with  $n_w$  : the refractive index of water ( $n_w = 1.34$ )  
 $\rho_F(\theta')$  : the *Fresnel* reflection coefficient for incident angle  $\theta'$   
 $\bar{\rho}$  : the mean reflection coefficient for the downwelling irradiance at the sea surface  
 $\bar{r}$  : the average reflection for upwelling irradiance at the *water-air* interface  
 $R$  : the irradiance reflectance just below the surface (or the diffuse reflectance at null depth) defined as the ratio of the upward ( $E_u$ ) to downward ( $E_d$ ) irradiance.

Note that  $\theta'$  is expressed as:

$$\theta' = \sin^{-1} \left( \frac{\sin(\theta_v)}{n_w} \right)$$

Current baseline: (19 x 4) values

| $\theta'$<br>[ $w_s$ ] $m.s^{-1}$ | $\Re[\theta', w_s]$<br>0 | $\Re[\theta', w_s]$<br>4 | $\Re[\theta', w_s]$<br>10 | $\Re[\theta', w_s]$<br>16 |
|-----------------------------------|--------------------------|--------------------------|---------------------------|---------------------------|
| 0                                 | 0.5287                   | 0.5287                   | 0.5287                    | 0.5287                    |
| 5                                 | 0.5287                   | 0.5287                   | 0.5287                    | 0.5287                    |
| 10                                | 0.5287                   | 0.5287                   | 0.5287                    | 0.5287                    |
| 15                                | 0.5287                   | 0.5287                   | 0.5286                    | 0.5286                    |
| 20                                | 0.5286                   | 0.5286                   | 0.5285                    | 0.5284                    |
| 25                                | 0.5284                   | 0.5283                   | 0.5283                    | 0.5282                    |
| 30                                | 0.5280                   | 0.5279                   | 0.5278                    | 0.5276                    |
| 35                                | 0.5274                   | 0.5272                   | 0.5270                    | 0.5268                    |
| 40                                | 0.5262                   | 0.5260                   | 0.5257                    | 0.5253                    |
| 45                                | 0.5242                   | 0.5239                   | 0.5234                    | 0.5229                    |
| 50                                | 0.5209                   | 0.5204                   | 0.5197                    | 0.5191                    |
| 55                                | 0.5153                   | 0.5147                   | 0.5138                    | 0.5129                    |
| 60                                | 0.5061                   | 0.5053                   | 0.5042                    | 0.5034                    |

Resources:

- Estimated CPU time: -  
Output disk space:  $19 \times 4 \times 4$  bytes/fl = 304 bytes

Acceptance:

Corresponds to the latest definition.



## 6.15.6 GADS Thresholds

### 6.15.6.1 Threshold on water reflectance at 560nm for input validity

Reference: rhow560\_thresh, LUT190

[AD-8] Section 6.15.6, GADS field 1

ACRI provided

Dependencies:

None

Tool:

None

Procedure:

Input: none

Output: *rhow560\_thresh* Threshold on water reflectance at 560nm ( $\rho_{w\_thresh}(560)$ )

units: [dl]

Step: User specified.

Scientific content:

This reflectance threshold defines the maximum reflectance value at 560nm for which the *Chl1* algorithm can be applied.

Current baseline: 0.3

Resources:

Estimated CPU time: -

Output disk space: 1 × 4 bytes/fl = 4 bytes

Acceptance:

Corresponds to the latest definition.

### 6.15.6.2 Chlorophyll content range (thresholds) for output validity

Reference: Chl1\_thresh, LUT191

[AD-8] Section 6.15.6, GADS field 2

ACRI provided

Dependencies:

None

Tool:

None

Procedure:

Input: none

Output:  $ChlI_{thresh}$  Range of chlorophyll content (*min*, *max* values)  
units:  $[10^{-3} \text{ mg.m}^{-3}]$

Step: User specified.

Scientific content:

This range of chlorophyll content defines the validity domain of retrieved chlorophyll content with the *ChlI* algorithm.

Current baseline:  $\{0.01, 30\} \text{ mg.m}^{-3}$

Resources:

Estimated CPU time: -

Output disk space:  $2 \times 4 \text{ bytes/fl} = 8 \text{ bytes}$

Acceptance:

Corresponds to the latest definition.

6.15.6.3 (*Spare*)

Reference:

[AD-8] Section 6.15.6, GADS field 3

6.15.6.4 (*Spare*)

Reference:

[AD-8] Section 6.15.6, GADS field 4

#### 6.15.6.5 Low glint threshold

Reference: lowG\_thresh, LUT194

[AD-8] Section 6.15.6, GADS field 5

ACRI provided

#### Dependencies:

None

#### Tool:

None

#### Procedure:

Input: none

Output: *lowG\_thresh* Threshold on the low glint reflectance  
units: [dl]

Step: User specified.

#### Scientific content:

Threshold on the low glint reflectance

Current baseline:  $5 \cdot 10^{-4}$

#### Resources:

Estimated CPU time: -

Output disk space:  $1 \times 4$  bytes/fl = 4 bytes

#### Acceptance:

Corresponds to the latest definition.

#### 6.15.6.6 Medium glint threshold

Reference: medG\_thresh, LUT195

[AD-8] Section 6.15.6, GADS field 6

ACRI provided

Dependencies:

None

Tool:

None

Procedure:

Input: none

Output: *medG\_thresh* Threshold on the medium glint reflectance  
units: [dl]

Step: User specified.

Scientific content:

Threshold on the medium glint reflectance

Current baseline: 0.2

Resources:

Estimated CPU time: -

Output disk space: 1 × 4 bytes/fl = 4 bytes

Acceptance:

Corresponds to the latest definition.

6.15.6.7 *Wind-speed threshold for whitecaps flagging*

Reference: *Ws\_thresh*, LUT196

[AD-8] Section 6.15.6, GADS field 7

ACRI provided

Dependencies:

None

Tool:

None

Procedure:

Input: none

Output: *Ws\_thresh* Threshold on the wind-speed to flag whitecaps  
units: [ $m.s^{-1}$ ]

Step: User specified.

Scientific content:

Threshold on the wind-speed to flag whitecaps

Current baseline:  $10 m.s^{-1}$

Resources:

Estimated CPU time: -

Output disk space:  $1 \times 4 \text{ bytes/fl} = 4 \text{ bytes}$

Acceptance:

Corresponds to the latest definition.

**6.15.6.8 Reflectance thresholds at 708.75nm for turbid water identification**

Reference: ROW9\_LUT, LUT197

[AD-8] Section 6.15.6, GADS field 8

Dependencies:

LUT174, LUT177, LUT179, LUT328, LUT417

Tools:

OTC/RAYLEIGH (or used LUT417)

RTC/FUB (MOMO)

Note: '*Mom\_in/mom\_def*' input file have to be correctly set for computing the water-leaving radiance just below the *water-air* interface. The following parameter have to be set into:

' CtrlString (30) - ESA\_L\_0- ' 1

Procedure:

Inputs:  $n(\lambda)$  MERIS band #9 ( $\lambda=708.75\text{ nm}$ )  
 $\theta_s$  Solar zenith angles [deg], see Section 6.15.4.4, (LUT174)  
 $\theta_v$  View zenith angles [deg], see Section 6.15.4.7, (LUT177)  
 $\Delta\phi$  Relative azimuth angles [deg], see Section 6.15.4.9, (LUT179)  
 $n_w$  Refractive index of water [dl], see Section 6.15.4.22 (LUT328)  
 $\rho_F$  Fresnel reflectance coefficients as function of wind-speed ( $w_s$ ) and incident angle ( $\theta$ ), see Section 3.2, (LUT417)

Output:  $ROW9\_LUT[\theta_s, \theta_v, \Delta\phi]$   
radiometric thresholds on atmospherically corrected TOA water reflectance at 708.75 nm as a function of the solar zenith angle ( $\theta_s$ ), view zenith angle ( $\theta_v$ ) and relative azimuth angle ( $\Delta\phi$ ) between sun and viewing directions.

units: [dl]

Note: The radiometric thresholds on the water reflectance at the 708.75 nm (MERIS band #9) will be based on the computation of the water-leaving radiances just below the *water-air* interface  $L_{w(0-)_9}[\theta_s, \theta_v, \Delta\phi]$  rather than the water-leaving radiances just above the *water-air* interface  $L_{w(0+)_9}[\theta_s, \theta_v, \Delta\phi]$ . In fact, the reflected atmospheric radiances  $L_{w(0+)}$  contain both the sun glint and the reflection of diffuse sky light (sometimes referred as the sky glitter). For the sun glint, only one direction is affected when the sea surface is perfectly flat, while all the directions can be concerned as soon as the sea surface becomes rough. For the sky glitter, all directions are virtually concerned. There exist a simple way to cope with the sun glint (by computing it separately) while the sky glitter cannot be easily removed. Consequently a simple and valid solution will consist in taking the upward radiances just below the sea surface and to apply the *Snellius-Fresnel* law.

Step-1: Generate the water-leaving radiances  $L_{w(0-)_9}[\theta_s, \theta_v, \Delta\phi]$  just below the *water-air* interface from a turbid water ( $SPM=1g.m^{-3}$ ) at the 708.75 nm wavelength (MERIS band #9) and for all geometries ( $\theta_s, \theta_v, \Delta\phi$ ), with the RTC/MOMO. For that, simulations have to be completed over a wind-roughened oceanic surface with purely SPM waters under a maritime atmosphere. The aerosol assemblage #0 with one aerosol optical thickness is selected (see table in Section 6.13.5.1).

**RTC/MOMO Inputs (OCEAN)**

| Variable        | Value               | Comments  |
|-----------------|---------------------|-----------|
| <i>out_file</i> | "/up_out/uprad_out" |           |
| <i>i_branch</i> | 2                   |           |
| $n(\lambda)$    | 9                   | 708.75 nm |
| $U_{H2O}$       | 0                   |           |
| $ESFT_{H2O}$    | -                   | N/A       |
| $U_{O2}$        | 0                   |           |
| $ESFT_{O2}$     | -                   | N/A       |

| Variable                   | Value                        | Comments   |
|----------------------------|------------------------------|--|
| $U_{O_3}$                  | 0                            |  |
| $ESFT_{O_3}$               | -                            | N/A  |
| $P_s$                      | 1013.25                      |  |
| $t^R(\lambda)$             | tauR                         | Computed with OTC/RAYLEIGH   |
| $aerosol1$                 | "/sca_out/sc_mar99_bxx.s"    | xx depends on $n(\lambda)$   |
| $t^{a1}(550)$              | 0.2                          |  |
| $aerosol2$                 | "/sca_out/sc_conti_bxx.s"    | xx depends on $n(\lambda)$   |
| $t^{a2}(550)$              | 0                            |  |
| $aerosol3$                 | "/sca_out/sc_H2SO4_bxx.s"    | xx depends on $n(\lambda)$   |
| $t^{a3}(550)$              | 0                            |  |
| $cloud1$                   | -                            | N/A  |
| $t^{c1}(550)$              | 0                            |  |
| $cloud2$                   | -                            | N/A  |
| $t^{c2}(550)$              | 0                            |  |
| $cloud3$                   | -                            | N/A  |
| $t^{c3}(550)$              | 0                            |  |
| $phyto$                    | -                            | N/A  |
| $\sigma_{e,\lambda}^p$     | 0                            | $Chl=0.0\text{mg}\cdot\text{m}^{-3}$   |
| $\omega_{o,\lambda}^p$     | 0                            | $Chl=0.0\text{mg}\cdot\text{m}^{-3}$   |
| $spm$                      | "/sca_out/sc_spm_1_0.s"      | $SPM=1.0\text{g}\cdot\text{m}^{-3}$  |
| $\sigma_{e,\lambda}^{spm}$ | 0.4810840                    | $SPM=1.0\text{g}\cdot\text{m}^{-3}$  |
| $\omega_{o,\lambda}^{spm}$ | 0.9933980                    | $SPM=1.0\text{g}\cdot\text{m}^{-3}$  |
| $\sigma_{a,\lambda}^{ys}$  | 0                            |  |
| $vertical$                 | "/sca_vert/oc/vtp1_12_ocean" | Vertical profile with 12 atmospheric layers and 2 oceanic layers (levels at -1 m and -500 m); boundary layer [0;2 km]; troposphere [2;12 km]; stratosphere [ $>12\text{ km}$ ] |
| $I_s$                      | 70                           |  |
| $\rho_s$                   | 0                            |  |
| $E_o$                      | 1                            |  |
| $\sigma_{a,\lambda}^w$     | 0.79150                      | Database: Pope and Fry (1997) [RD-13]  |
| $w_s$                      | 3.0                          |  |
| $n_s, n_v, n_{\Delta\phi}$ | 27, 19, 25                   |  |
| $\theta_s$                 | Gaussian angles              | See Section 6.15.4.4   |
| $\theta_v$                 | Gaussian angles              | See Section 6.15.4.7   |
| $\Delta\phi$               | see inputs                   | See Section 6.15.4.9   |

Step-2: Extract the downwelling spectral irradiance just above the *water-air* interface  $E_{d(0^+)_9}[\theta_s]$  from 'FUB/mom\_out/flux\_0001' file. The latter is the sum of the 'DOWNWARD DIFFUSE VECTOR IRRAD.' and the 'DOWNWARD DIRECT VECTOR IRRAD.' at the height = 0.

Step-3: Determine the water-leaving radiance just above the *water-air* interface  $L_{w(0+)_9}[\theta_s, \theta_v, \Delta\phi]$ , by applying the *Snellius-Fresnel* law on the upward radiances just below the sea surface  $L_{w(0-)_9}[\theta_s, \theta_v, \Delta\phi]$  as follows,

$$L_{w(0+)_9}[\theta_s, \theta_v, \Delta\phi] = L_{w(0-)_9}[\theta_s, \theta_v, \Delta\phi] \cdot \left( \frac{1 - \rho_F}{n_w^2} \right)$$

with  $\rho_F$  the relevant *Fresnel* reflection coefficient and  $n_w$  the water refractive index ( $n_w=1.34$ ).

Step-4: Compute the radiometric thresholds on the water reflectance just above the *water-air* interface from a wind-roughened turbid water, as follows,

$$ROW9\_LUT[\theta_s, \theta_v, \Delta\phi] = \pi \cdot \frac{L_{w(0+)_9}[\theta_s, \theta_v, \Delta\phi]}{E_{d(0+)_9}[\theta_s]}$$

#### Scientific content:

In the turbid water identification algorithm, the single scattering corrected water reflectance at  $708.75nm$  is compared to the corresponding radiometric threshold interpolated from the  $ROW9\_LUT[\theta_s, \theta_v, \Delta\phi]$  table. If this corrected water reflectance is greater than the threshold value then the pixel will be considered as a turbid water, otherwise it will not be it.

#### Resources:

Estimated CPU time: 24 sec  
Output disk space:  $27 \times 19 \times 25 \times 4$  bytes/fl = 51300 bytes

#### Acceptance:

Comparisons with another RTC should have to be done.

#### 6.15.6.9 Water vapour high glint threshold

Reference: (No variable used), LUT205

[AD-8] Section 6.15.6, GADS field 9

ACRI provided

#### Dependencies:

None

#### Tool:

None



Procedure:

Input: none  
Output: (no variable) Water vapour high glint threshold  
units: [dl]  
Step: User specified.

Scientific content:

Water vapour high glint threshold  
Current baseline: 0.6

Resources:

Estimated CPU time: -  
Output disk space: 1 × 4 bytes/fl = 4 bytes

Acceptance:

Corresponds to the latest definition.

*6.15.6.10 Shallow water depth threshold*

Reference: (No variable used), LUT206

[AD-8] Section 6.15.6, GADS field 10

ACRI provided

Dependencies:

None

Tool:

None

Procedure:

Input: none  
Output: (no variable) Threshold on shallow water depth  
units: [m]

Step: User specified.

Scientific content:

Threshold on shallow water depth

Current baseline: 1000 m

Resources:

Estimated CPU time: -

Output disk space: 1 × 4 bytes/fl = 4 bytes

Acceptance:

Corresponds to the latest definition.

### 6.15.7 GADS Log10 polynomial coefficients

#### 6.15.7.1 Log10 polynomial coefficients for 443, 490 and 510 nm

Reference: log10coeff, LUT198

[AD-8] Section 6.15.7, GADS field 1

ACRI provided

Dependencies:

None

Tool:

None

Procedure:

Input: none

Output: *log10coeff* Log10 polynomial coefficients (6 values)

units: [dl]

Step: User specified.

Scientific content:

Ratios of  $(b_b/a)$  at 443, 490 and 510nm upon  $(b_b/a)$  at 560nm are computed for several chlorophyll contents (*Chl*) using the models from [RD-11] and from [RD-12]. For each of the 3 wavelengths ( $\lambda=443, 490$  and  $510nm$ ), the corresponding set of  $[b_b(\lambda)/a(\lambda)]/[b_b(560)/a(560)]$  values are then fitted to a 5<sup>th</sup> order polynomial in  $\log_{10}(Chl)$ .

This table contains 3 sets of 6 polynomial coefficients (*i.e.*, for each of the 3 wavelengths  $\lambda$ ), which allows one to determine the pigment index from the ratio  $[b_b(\lambda)/a(\lambda)]/[b_b(560)/a(560)]$  either at  $\lambda = 443, 490$ , or  $510 nm$ .

These coefficients are here empirically estimated from *Morel's* measurements [RD-12], and they are used in the Case 1 waters algorithm for deriving the chlorophyll content.

Current baseline: {0.4389, -3.3626, 3.9348, -3.0787, 0.6298, 0.}

Resources:

Estimated CPU time: -  
Output disk space:  $6 \times 4$  bytes/fl = 24 bytes

Acceptance:

Corresponds to the latest computations completed at ACRI.

6.15.7.2 *Convergence criterium for iterative chlorophyll retrieval*

Reference: (No variable used), LUT199

[AD-8] Section 6.15.7, GADS field 2

ACRI provided

Dependencies:

None

Tool:

None

Procedure:

Input: none  
Output: (no variable) Convergence criterium for iterative chlorophyll retrieval  
units: [dl]  
Step: User specified.

Scientific content:

Convergence criterium for iterative *Chl1* retrieval algorithm

Current baseline: 0.01

Resources:

Estimated CPU time: -

Output disk space: 1 × 4 bytes/fl = 4 bytes

Acceptance:

Corresponds to the latest definition.

6.15.7.3 Irradiance reflectance ratio validity range for *algal1* computation using log10 polynomials

Reference: (No variable used), LUT491

[AD-8] Section 6.15.7, GADS field 3

ACRI provided

Dependencies:

None

Tool:

None

Procedure:

Input: none

Output: (*no variable*) Irradiance reflectance ratio validity range for *algal1* computation using log10 polynomials (*min, max* values)

units: [*dl*]

Step: User specified.

Scientific content:

Validity range of irradiance reflectance ratio for *algal1* computation with the log10 polynomials

Current baseline: {0.5, 20}

Resources:

Estimated CPU time: -  
Output disk space:  $2 \times 4$  bytes/fl = 8 bytes

Acceptance:

Corresponds to the latest definition.

*6.15.7.4 Highest order of log10 polynomial coefficients used in the Case-1 waters algorithm*

Reference:  $N_{A1}$ , LUT201

[AD-8] Section 6.15.7, GADS field 4

ACRI provided

Dependencies:

None

Tool:

None

Procedure:

Input: none

Output:  $N_{A1}$  Highest order of log10 polynomial coefficients used in the Case-1 waters algorithm

units: [dl]

Step: User specified.

Scientific content:

Highest order of log10 polynomials used in the Case-1 waters algorithm

Current baseline: 5

Resources:

Estimated CPU time: -  
Output disk space:  $1 \times 1$  byte/uc = 1 byte

Acceptance:

Corresponds to the latest definition.

6.15.7.5 Bands selected for computation of chlorophyll content (*Chl1*) (band number starting at 1)

Reference: (No variable used), LUT202

[AD-8] Section 6.15.7, GADS field 5

ACRI provided

Dependencies:

None

Tool:

None

Procedure:

Input: none

Output: (no variable) MERIS bands selected for *Chl1* computation (3 bands)

units: [dl]

Step: User specified.

Scientific content:

Selected bands used for algal pigment index retrieval (see Section 6.15.7.1). Note that the  $\log_{10}$  coefficients change from band to band, and depend on the chlorophyll content thresholds.

3 MERIS bands are currently selected for *Chl1* computation: band#2 (442.5nm), band#3 (490nm) and band#4 (510nm)

Current baseline: {2, 3, 4}

Resources:

Estimated CPU time: -

Output disk space:  $3 \times 1$  byte/uc = 3 bytes

Acceptance:

Corresponds to the latest definition.

## 6.15.8 ADS f/Q Factor

### 6.15.8.1 f/Q factor

Reference: f\_over\_Q1\_LUT, LUT203

[AD-8] Section 6.15.8, GADS field 1, 2, 3 & 4

Dependencies:

LUT172, LUT173, LUT175, LUT178, LUT180, LUT181, LUT182, LUT418

Tools:

OTC/RAYLEIGH (or used LUT417)  
RTC/FUB (MOMO)

Note: 'Mom\_in/mom\_def' input file have to be correctly set for computing the water-leaving radiance just below the *water-air* interface. The following parameter have to be set into:

' CtrlString (30) - ESA\_L\_0- ' 1

Procedure:

Inputs:  $\lambda$  MERIS wavelength [nm] (9 values), see Section 6.15.4.2, (LUT172)  
 $\theta_s$  Solar zenith angle [deg], see Section 6.15.4.3, (LUT173)  
 $\theta'$  View zenith angle [deg], see Section 6.15.4.5, (LUT175)  
 $\Delta\phi$  Relative azimuth angle [deg], see Section 6.15.4.8, (LUT178)  
 $w_s$  Wind-speed [ $m.s^{-1}$ ] (2 values), see Section 6.15.4.12, (LUT182)  
 $\tau^a$  Aerosol optical thickness at 550nm (2 values), see Section 6.15.4.11, (LUT181)  
 $Chl$  Chlorophyll content [ $mg.m^{-3}$ ] (5 values), see Section 6.15.4.10, (LUT180)  
 $\sigma_{e,\lambda}^p, \omega_{o,\lambda}^p$  Extinction coefficient and single scattering albedo for chlorophyll, see Section 6.15.1.1, (LUT418)

Output:  $f\_over\_Q\_LUT[\lambda, w_s, \tau^a, Chl, \theta_s, \theta', \Delta\phi]$   
 $f/Q$  factor characterizing the bidirectionality for oceanic diffuse reflectance as a function of the MERIS wavelength ( $\lambda$ ), the wind-speed ( $w_s$ ), the chlorophyll content ( $Chl$ ), the aerosol optical thickness at 550nm ( $\tau^a$ ), the solar zenith angle ( $\theta_s$ ), view zenith angle ( $\theta'$ ) and relative azimuth angle ( $\Delta\phi$ ) between sun and viewing directions.

units: [dl]

Step-1: Extract according to the chlorophyll content ( $Chl$ ) the absorption  $a$  and backscattering coefficients  $b_b$  from a table provided by ACRI (see Section 6.15.1.1).

Step-2: Calculate  $\theta_v = \text{asin}(n_w \cdot \sin\theta)$  with  $n_w$  the water refractive index ( $n_w=1.34$ ). Note that this step is automatically taken care by the RTC/MOMO because there exist two sets of *Gauss-Lobatto* quadrature angles, one in the atmosphere and another in the water.

Step-3: Generate the water-leaving radiances  $L_{w(0-)}[\lambda, w_s, \tau^a, Chl, \theta_s, \theta_v, \Delta\phi]$  just below the *water-air* interface from a turbid water (with chlorophyll only) at 9 MERIS wavelengths ( $\lambda$ ), for 2 wind-speeds ( $w_s$ ), 2 aerosol optical thicknesses ( $\tau^a$ ), 5 chlorophyll contents (*Chl*), and for all geometries ( $\theta_s, \theta_v, \Delta\phi$ ), with the RTC/MOMO. For that, simulations have to be completed over purely chlorophyll waters under a maritime atmosphere. The aerosol assemblage #0 is selected (see table in Section 6.13.5.1).

**RTC/MOMO Inputs (OCEAN)**

| Variable               | Value                        | Comments  |
|------------------------|------------------------------|---|
| <i>out_file</i>        | "/up_out/uprad_out"          |   |
| <i>i_branch</i>        | 2                            |   |
| $n(\lambda)$           | 1, 2, 3, 4, 5, 6, 7, 8 and 9 | See Section 6.15.4.2  |
| $U_{H2O}$              | 0                            |   |
| $ESFT_{H2O}$           | -                            | N/A   |
| $U_{O2}$               | 0                            |   |
| $ESFT_{O2}$            | -                            | N/A   |
| $U_{O3}$               | 0                            |   |
| $ESFT_{O3}$            | -                            | N/A   |
| $P_s$                  | 1013.25                      |   |
| $\tau^R(\lambda)$      | tauR                         | Computed with OTC/Rayleigh  |
| <i>aerosol1</i>        | "/sca_out/sc_mar99_bxx.s"    | xx depends on $n(\lambda)$  |
| $\tau^{a1}(550)$       | 0.2 and 0.6                  | See Section 6.15.4.11   |
| <i>aerosol2</i>        | "/sca_out/sc_conti_bxx.s"    | xx depends on $n(\lambda)$  |
| $\tau^{a2}(550)$       | 0                            |   |
| <i>aerosol3</i>        | "/sca_out/sc_H2SO4_bxx.s"    | xx depends on $n(\lambda)$  |
| $\tau^{a3}(550)$       | 0                            |   |
| <i>cloud1</i>          | -                            | N/A   |
| $\tau^{c1}(550)$       | 0                            |   |
| <i>cloud2</i>          | -                            | N/A   |
| $\tau^{c2}(550)$       | 0                            |   |
| <i>cloud3</i>          | -                            | N/A   |
| $\tau^{c3}(550)$       | 0                            |   |
| <i>phyto</i>           | "/sca_out/sc_chl_y_y.s"      | <i>y_y</i> depends on the <i>Chl</i> concentration.<br><i>Chl</i> =0.03, 0.1, 0.3, 1.0 and 3.0 $mg \cdot m^{-3}$        |
| $\sigma_{e,\lambda}^p$ | ChlExt                       | Values extracted from CP-LUT"Extinction coefficient and single scattering albedo for chlorophyll". See Section 6.15.1.1 |
| $\omega_{o,\lambda}^p$ | ChlAlb                       | Values extracted from CP-LUT"Extinction coefficient and single scattering albedo for chlorophyll". See Section 6.15.1.1 |



| Variable                   | Value                         | Comments   |
|----------------------------|-------------------------------|--|
| $spm$                      | -                             | N/A  |
| $\sigma_{e,\lambda}^{spm}$ | 0                             | $SPM=0.0g.m^{-3}$  |
| $\omega_{o,\lambda}^{spm}$ | 0                             | $SPM=0.0g.m^{-3}$  |
| $\sigma_{a,\lambda}^{ys}$  | 0                             |  |
| <i>vertical</i>            | "/sca_vert/oce/vtp1_12_ocean" | Vertical profile with 12 atmospheric layers and 2 oceanic layers (levels at -1 m and -500 m): boundary layer [0;2 km]; troposphere [2;12 km]; stratosphere [ >12 km] |
| $I_s$                      | 70                            |  |
| $\rho_s$                   | 0                             |  |
| $E_o$                      | 1                             |  |
| $\sigma_{a,\lambda}^w$     | Water_Abs                     | Database: Pope and Fry (1997) [RD-13]  |
| $w_s$                      | 0 and 7.2                     | See Section 6.15.4.12  |
| $n_s, n_v, n_{\Delta\phi}$ | 6, 14, 13                     |  |
| $\theta_s$                 | see inputs                    | See Section 6.15.4.3   |
| $\theta_v$                 | see inputs                    | See Section 6.15.4.5   |
| $\Delta\phi$               | see inputs                    | See Section 6.15.4.8   |

Step-4: Extract the downwelling spectral irradiance just below the *water-air* interface  $E_{d(0-)}[\lambda, w_s, \tau^a, Chl, \theta_s]$  from 'FUB/mom\_out/flux\_0001' file. The latter is the sum of the 'DOWNWARD DIFFUSE VECTOR IRRAD.' and the 'DOWNWARD DIRECT VECTOR IRRAD.' at the height = 0.01

Step-5: Interpolate  $L_{w(0-)}[\lambda, w_s, \tau^a, Chl, \theta_s, \theta_v, \Delta\phi]$  and  $E_{d(0-)}[\lambda, w_s, \tau^a, Chl, \theta_s]$  to the desired geometry

Step-6: Determine the  $f\_over\_Q\_LUT[\lambda, w_s, \tau^a, Chl, \theta_s, \theta', \Delta\phi]$  ratio as follows,

$$f\_over\_Q\_LUT[\lambda, w_s, \tau^a, Chl, \theta_s, \theta', \Delta\phi] = \frac{L_{w(0-)}[\lambda, w_s, \tau^a, Chl, \theta_s, \theta', \Delta\phi]}{E_{d(0-)}[\lambda, w_s, \tau^a, Chl, \theta_s]} \cdot \frac{a[\lambda, Chl]}{b_b[\lambda, Chl]}$$

### Scientific content:

$f\_over\_Q\_LUT[\lambda, w_s, \tau^a, Chl, \theta_s, \theta', \Delta\phi]$  characterizes the bidirectionality for oceanic diffuse reflectance and the sun zenith dependence of the relationship between this reflectance and the inherent optical properties of the Case 1 waters. This LUT, which is function of the MERIS wavelength ( $\lambda$ ), the wind-speed ( $w_s$ ), the chlorophyll content ( $Chl$ ), the aerosol optical thickness at 550nm ( $\tau^a$ ), the solar zenith angle ( $\theta_s$ ), view zenith angle ( $\theta'$ ) and relative azimuth angle ( $\Delta\phi$ ) between sun and viewing directions, is used for the computation of the pigment index and the normalized water-leaving radiances from the water-leaving radiances (which are output of the atmospheric corrections).

The MERIS band #9 (708.75 nm) is not used in the chlorophyll content retrieval algorithm.

Current baseline:

- $\lambda$  corresponds to the 9 following MERIS wavelengths: 412.5, 442.5, 490, 510, 560, 620, 665, 681.25, and 708.75 nm
- $w_s$  corresponds to the 2 following wind-speeds: 0 and 7.2 m.s<sup>-1</sup>
- $\tau^a$  corresponds to the 2 following optical thicknesses: 0.2 and 0.6
- $chl$  corresponds to the 5 following values: 0.03, 0.1, 0.3, 1.0, 3.0 mg.m<sup>-3</sup>
- $\theta_s$  corresponds to the 6 following solar zenith angles: from 0° to 75° with a step of 15°
- $\theta'$  corresponds to the 14 following view zenith angles from the *Gauss-Lobatto* quadrature (i.e., ranging from 1.078° to 39.69°)
- $\Delta\phi$  corresponds to the 13 following relative azimuth angles: from 0° to 180° with a step of 15°

Resources:

Estimated CPU time: 4356 sec

Output disk space: 6 × 2 × 2 × 9 × 14 × 13 × 5 × 4 bytes/fl = 786240 bytes

The storage of this table is achieved by records for different combinations of  $\tau^a$  and  $w_s$  (see [AD-8] for exact structure).

Acceptance:

The range checking as well as the examination of trends will be performed (i.e., change as a function of wavelength or of viewing angle).

## 6.15.9 ADS Glint reflectance

### 6.15.9.1 Glint reflectance

Reference: rhoG[ $\theta_s, w_s, \chi, \theta_v, \Delta\phi$ ], LUT207

[AD-8] Section 6.15.9, ADS field 1, 2, 3, 4, 5

ACRI provided

Dependencies:

LUT174, LUT177, LUT179, LUT187; LUT188

Tool:

None

Procedure:

Input:  $\theta_s$  Solar zenith angle [deg] (27 values), see Section 6.15.4.4, (LUT174)  
 $\theta_v$  View zenith angle [deg] (19 values), see Section 6.15.4.7, (LUT177)  
 $\Delta\phi$  Relative azimuth angle [deg] (25 values), see Section 6.15.4.9, (LUT179)

$w_s$  Wind-speed [ $m.s^{-1}$ ] (5 values), see [Section 6.15.4.17](#), (LUT187)  
 $\chi$  Wind azimuth orientations [ $deg.$ ] (7 values), see [Section 6.15.4.18](#), (LUT188)

Output:  $\rho G[\theta_s, w_s, \chi, \theta_v, \Delta\phi]$   
Glint reflectance (27 x 19 x 25 x 5 x 7 values)

units: [dl]

Step: User specified.

Scientific content:

This LUT contains specular reflectance as a function of geometry, wind-speed and wind direction.

Current baseline:

$w_s$  corresponds to 5 values = 3, 5, 7, 10, 14  $m.s^{-1}$   
 $\chi_w$  corresponds to 7 values varying from 0° to 180° with increment 30°  
 $\theta_s$  corresponds to 27 values varying from 15° to 80° with increment 2.5°  
 $\theta_v$  corresponds to 19 values varying from 0° to 45° with increment 2.5°  
 $\Delta\phi$  corresponds to 25 values varying from 0° to 180° with increment 7.5°

Resources:

Estimated CPU time: -  
Output disk space: 27 x 5 x 7 x 19 x 25 x 4 bytes/fl = 1795500 bytes

Acceptance:

Corresponds to the latest definition.

**6.15.10 ADS Mean water-leaving reflectance at 510nm**

*6.15.10.1 Mean value of water-leaving reflectance at 510 nm,  $\rho_{w510\_mean}(month, lat, long)$*

Reference:  $\rho_{w510\_mean}[month, lat, long]$ , LUT446

[AD-8] Section 6.15.10, GADS field 1

ACRI provided

Tool:

None

Procedure:

Inputs: *month* Month (12 values)

*lat* Latitude [*deg*] (1024 values), see [Section 6.15.4.29](#), (LUT444)  
*long* Longitude [*deg*] (2048 values), see [Section 6.15.4.30](#), (LUT445)

Output: *rhow510\_mean*[*month, lat, long*]  
Mean value of water-leaving reflectance at 510nm as a function of the period (*month*) and the geographic location (*lat, long*).

units: [*dl*]

Step: User specified.

Scientific content:

This LUT contains the mean value of water-leaving reflectance at 510nm as function of the geographic location (*lat, long*) and the period (*month*).

Current baseline:

*lat* corresponds to 1024 values varying from -90° to 90° with increment 0.176°  
*long* corresponds to 2048 values varying from -180° to 180° with increment 0.176°

Resources:

Estimated CPU time: -  
Output disk space:  $12 \times 1024 \times 2048 \times 1 \text{ byte/uc} = 25165824 \text{ bytes}$

Acceptance:

Corresponds to the latest definition.

6.15.10.2 Variability of water-leaving reflectance at 510 nm, *rhow510\_var*(*month,lat,long*)

Reference: *rhow510\_var*[*month,lat,long*], LUT447

[AD-8] Section 6.15.10, GADS field 2

ACRI provided

Tool:

None

Procedure:

Inputs: *month* Month (12 values)  
*lat* Latitude [*deg*] (1024 values), see [Section 6.15.4.29](#), (LUT444)  
*long* Longitude [*deg*] (2048 values), see [Section 6.15.4.30](#), (LUT445)

Output: *rhow510\_var*[*month, lat, long*]

Variability of water-leaving reflectance at 510nm as a function of the period (*month*) and the geographic location (*lat, long*).

units: [dl]

Step: User specified.

Scientific content:

This LUT contains the variability of water-leaving reflectance at 510nm as function of the geographic location (*lat, long*) and the period (*month*).

Current baseline:

*lat* corresponds to 1024 values varying from -90° to 90° with increment 0.176°

*long* corresponds to 2048 values varying from -180° to 180° with increment 0.176°

Resources:

Estimated CPU time: -

Output disk space:  $12 \times 1024 \times 2048 \times 1 \text{ byte/uc} = 25165824 \text{ bytes}$

Acceptance:

Corresponds to the latest definition.

**6.15.11 GADS  $f_o$  factor**

6.15.11.1 Factor  $f_o$

Reference:  $f_o[\text{iband}, \text{Chl}]$ , LUT492

[AD-8] Section 6.15.11, GADS field 1

ACRI provided

Tool:

None

Procedure:

Inputs: *iband* Index of MERIS band (4 bands) (starting from 0)  
*Chl* Chlorophyll content [ $\text{mg.m}^{-3}$ ] (6 values), see Section 6.15.4.31, (LUT490)

Output:  $f_o[\text{iband}, \text{Chl}]$   $f_o$  factor as a function of the MERIS wavelength (*iband*) and the chlorophyll content (*Chl*).

units: [dl]

Step: User specified.

Scientific content:

The  $f_o[\lambda, Chl]$  factor relates the ratio of 2 water IOPs ( $b_b/a$ ) to the irradiance reflectance just beneath the surface when the Sun is at the zenith.  $b_b$  and  $a$  are respectively the backscattering and absorption coefficients of sea water.

This LUT contains  $f_o[\lambda, Chl]$  as function of the MERIS wavelength and the chlorophyll content ( $Chl$ ).

Current baseline:

$\lambda$  corresponds to the MERIS band#2 (442.5 nm), band#3 (490 nm), band#4 (510 nm) and band#5 (560 nm)

$Chl$  corresponds to 6 values of chlorophyll contents: {0.03, 0.1, 0.3, 1, 3, 10}  $mg.m^{-3}$

| $\lambda$<br>[chl] $mg/m^3$ | $f_o[\lambda,chl]$<br>0.03 | $f_o[\lambda,chl]$<br>0.10 | $f_o[\lambda,chl]$<br>0.30 | $f_o[\lambda,chl]$<br>1.0 | $f_o[\lambda,chl]$<br>3.0 | $f_o[\lambda,chl]$<br>10 |
|-----------------------------|----------------------------|----------------------------|----------------------------|---------------------------|---------------------------|--------------------------|
| 442.50                      | 0.311601                   | 0.328292                   | 0.341049                   | 0.352109                  | 0.360004                  | 0.370684                 |
| 490.00                      | 0.347460                   | 0.345364                   | 0.350692                   | 0.362050                  | 0.374337                  | 0.389326                 |
| 510.00                      | 0.360108                   | 0.350301                   | 0.349293                   | 0.359842                  | 0.376623                  | 0.398074                 |
| 560.00                      | 0.375790                   | 0.358839                   | 0.349959                   | 0.357937                  | 0.383813                  | 0.424393                 |

Resources:

Estimated CPU time: -

Output disk space:  $4 \times 6 \times 4$  bytes/fl = 96 bytes

Acceptance:

Corresponds to the latest definition.

## 6.16 OCEAN CASE-II PARAMETERS

### 6.16.1 C.P.

Not covered in this document (*see* [AD-8] for a detailed description)

### 6.16.2 MPH

Not covered in this document (*see* [AD-8] for a detailed description)

### 6.16.3 SPH

Not covered in this document (*see* [AD-8] for a detailed description)

### 6.16.4 GADS General

#### 6.16.4.1 Wavelengths (tabulated values)

Reference: Wvl, LUT332

[AD-8] Section 6.16.4, GADS field 1

ACRI provided

Dependencies:

None

Tool:

None

Procedure:

Input: none

Output: Wvl MERIS wavelength (10 values)

units: [nm]

Step: User specified.

Scientific content:

Set of 15 nominal wavelengths ( $\lambda$ ) of the 15 MERIS spectral bands

Current baseline: {412.50, 442.50, 490.00, 510.00, 560.00, 620.00, 665.00, 681.25, 708.75, 753.75, 761.875, 778.75, 865.00, 885.00, 900.00} *nm*

Resources:

Estimated CPU time: -  
Output disk space: 15 × 4 bytes/fl = 60 bytes

Acceptance:

Corresponds to the latest definition.

6.16.4.2 *Number of polynomial coefficients in  $F_p$  computation*

Reference: Ncoef, LUT333

[AD-8] Section 6.16.4, GADS field 2

ACRI provided

Dependencies:

None

Tool:

None

Procedure:

Input: none

Output: *Ncoef* Number of polynomial coefficients in  $F_p$  computation  
units: [*dI*]

Step: User specified.

Scientific content:

Number of polynomial coefficients in  $F_p$  computation

Current baseline: 8

Resources:

Estimated CPU time: -



Output disk space:  $1 \times 4 \text{ bytes/ul} = 4 \text{ bytes}$

Acceptance:

Corresponds to the latest definition.

6.16.4.3 Wind-speeds for ADS  $F_p$  factor

Reference:  $W_s$ , LUT334

[AD-8] Section 6.16.4, GADS field 3

ACRI provided

Dependencies:

None

Tool:

None

Procedure:

Input: none

Output:  $W_s$  Wind-speed ( $w_s$ ) just above sea level (4 values) for ADS  $F_p$  factor  
units:  $[m.s^{-1}]$

Step: User specified.

Scientific content:

Set of 4 wind-speeds ( $w_s$ )

Current baseline:  $\{0.25, 1.0, 2.75, 5.0\} m.s^{-1}$

Resources:

Estimated CPU time: -

Output disk space:  $4 \times 4 \text{ bytes/fl} = 16 \text{ bytes}$

Acceptance:

Corresponds to the latest definition.

#### 6.16.4.4 View zenith angles for ADS $F_p$ factor

Reference: VZA, LUT335

[AD-8] Section 6.16.4, GADS field 4

ACRI provided

Dependencies:

None

Tool:

None

Procedure:

Input: none

Output: VZA View zenith angle ( $\theta_v$ ) for ADS  $F_p$  factor (5 values)

units: [ $10^{-6}deg.$ ]

Step: User specified.

Scientific content:

Set of 5 view zenith angles ( $\theta_v$ ) regularly spaced

Current baseline: 5 values of  $\theta_v$  within  $[0;60]deg.$  with a step of  $15deg.$

Resources:

Estimated CPU time: -

Output disk space:  $5 \times 4$  bytes/ul = 20 bytes

Acceptance:

Corresponds to the latest definition.

#### 6.16.4.5 Solar zenith angles for ADS $F_p$ factor

Reference: SZA, LUT336

[AD-8] Section 6.16.4, GADS field 5

ACRI provided

Dependencies:

None

Tool:

None

Procedure:

Input: none

Output: *SZA* Solar zenith angle ( $\theta_s$ ) for ADS  $F_p$  factor (5 values)  
units: [ $10^{-6}deg.$ ]

Step: User specified.

Scientific content:

Set of 5 solar zenith angles ( $\theta_s$ ) regularly spaced

Current baseline: 5 values of  $\theta_s$  within [ $15;75$ ] *deg.* with a step of  $15deg.$

Resources:

Estimated CPU time: -

Output disk space:  $5 \times 4$  bytes/ul = 20 bytes

Acceptance:

Corresponds to the latest definition.

**6.16.4.6 Relative azimuth angles for ADS  $F_p$  factor**

Reference: RAA, LUT337

[AD-8] Section 6.16.4, GADS field 6

ACRI provided

Dependencies:

None

Tool:

None

Procedure:

Input: none

Output: *RAA* Relative azimuth angle ( $\Delta\phi$ ) for ADS  $F_p$  factor (13 values)  
units: [ $10^{-6}deg.$ ]

Step: User specified.

Scientific content:

Set of 13 relative azimuth angles ( $\Delta\phi$ ) regularly spaced

Current baseline: 13 values of  $\Delta\phi$  within  $[0;180]deg.$  with a step of  $15deg.$

Resources:

Estimated CPU time: -

Output disk space:  $13 \times 4$  bytes/ul = 52 bytes

Acceptance:

Corresponds to the latest definition.

**6.16.4.7 View zenith angles for GADS anomalous scattering detection**

Reference: VZA\_asd, LUT338

[AD-8] Section 6.16.4, GADS field 7

ACRI provided

Dependencies:

None

Tool:

None

Procedure:

Input: none

Output: *VZA\_asd* View zenith angle ( $\theta_v$ ) for GADS anomalous scattering detection (10 values)  
units:  $[10^{-6}deg.]$   
Step: User specified.

Scientific content:

Set of 10 view zenith angles ( $\theta_v$ ) regularly spaced

Current baseline: 10 values of  $\theta_v$  within  $[0;45]deg.$  with a step of  $5deg.$

Resources:

Estimated CPU time: -  
Output disk space:  $10 \times 4$  bytes/ul = 40 bytes

Acceptance:

Corresponds to the latest definition.

*6.16.4.8 Solar zenith angles for GADS anomalous scattering detection*

Reference: *SZA\_asd*, LUT339

[\[AD-8\]](#) Section 6.16.4, GADS field 8

ACRI provided

Dependencies:

None

Tool:

None

Procedure:

Input: none  
Output: *SZA\_asd* Solar zenith angle ( $\theta_s$ ) for GADS anomalous scattering detection (10 values)  
units:  $[10^{-6}deg.]$   
Step: User specified.

Scientific content:

Set of 10 solar zenith angles ( $\theta$ ) regularly spaced

Current baseline: {0, 8.33, 16.66, 25.00, 33.33, 41.66, 50.00, 58.33, 66.66, 75} deg

Resources:

Estimated CPU time: -

Output disk space: 10 × 4 bytes/ul = 40 bytes

Acceptance:

Corresponds to the latest definition.

6.16.4.9 *Relative azimuth angles for GADS anomalous scattering detection*

Reference: RAA\_asd, LUT340

[AD-8] Section 6.16.4, GADS field 9

ACRI provided

Dependencies:

None

Tool:

None

Procedure:

Input: none

Output: RAA\_asd Relative azimuth angle ( $\Delta\phi$ ) for GADS anomalous scattering detection  
(19 values)

units: [10<sup>-6</sup>deg.]

Step: User specified.

Scientific content:

Set of 19 relative azimuth angles ( $\Delta\phi$ ) regularly spaced

Current baseline: 19 values in [0;180]deg. with a setp of 10deg.

Resources:

Estimated CPU time: -  
Output disk space:  $19 \times 4$  bytes/ul = 76 bytes

Acceptance:

Corresponds to the latest definition.

6.16.4.10 Conversion factors for *Chl2*

Reference: (No variable used), LUT431

[AD-8] Section 6.16.4, GADS field 10

ACRI provided

Dependencies:

None

Tool:

None

Procedure:

Input: none  
Output: (no variable) Conversion factors for chlorophyll content (*Chl2*) (4 values)  
units:  $[mg.m^{-3}, dl, dl, dl]$   
Step: User specified.

Scientific content:

Set of 4 conversion factors for chlorophyll content in Case-2 waters (*Chl2*)

Current baseline:  $\{21, 0, 0, 1.04\} mg.m^{-3}, dl, dl, dl$

Resources:

Estimated CPU time: -  
Output disk space:  $4 \times 4$  bytes/fl = 16 bytes

Acceptance:

Corresponds to the latest definition.

#### 6.16.4.11 Conversion factors for SPM

Reference: (No variable used), LUT432

[AD-8] Section 6.16.4, GADS field 11

ACRI provided

#### Dependencies:

None

#### Tool:

None

#### Procedure:

Input: none

Output: (no variable) Conversion factors for SPM content  
units:  $[g.m^{-3}]$

Step: User specified.

#### Scientific content:

Conversion factor for SPM content in Case-2 waters (SPM)

Current baseline:  $1.73 g.m^{-3}$

#### Resources:

Estimated CPU time: -

Output disk space:  $1 \times 4 \text{ bytes/fl} = 4 \text{ bytes}$

#### Acceptance:

Corresponds to the latest definition.

#### 6.16.4.12 Absorption coefficients of pure water

Reference:  $a_w[\text{iband}]$ , LUT448

[AD-8] Section 6.16.4, GADS field 12



ACRI provided

Dependencies:

None

Tool:

None

Procedure:

Input: *iband* Index of MERIS band (15 bands) (starting from 0)

Output:  $a_w[iband]$  Absorption coefficient ( $a_w(\lambda)$ ) of pure water in the 15 MERIS spectral bands (15 values)

units:  $[m^{-1}]$

Step: User specified.

Scientific content:

Set of 15 absorption coefficients of pure water ( $a_w(\lambda)$ ) given at the 15 MERIS wavelengths

Current baseline: 15 values

| $\lambda$ [nm] | $a_w(\lambda)$ [ $m^{-1}$ ] |
|----------------|-----------------------------|
| 412.500        | 0.00460                     |
| 442.500        | 0.00688                     |
| 490.000        | 0.01518                     |
| 510.000        | 0.03185                     |
| 560.000        | 0.06202                     |
| 620.000        | 0.27554                     |
| 665.000        | 0.42828                     |
| 681.250        | 0.47929                     |
| 708.750        | 0.81911                     |
| 753.750        | 2.86712                     |
| 761.875        | 2.86710                     |
| 778.750        | 2.69492                     |
| 865.000        | 4.61577                     |
| 885.000        | 5.55930                     |
| 900.000        | 6.40580                     |

Resources:

Estimated CPU time: -

Output disk space: 15 × 4 bytes/fl = 60 bytes

Acceptance:

Corresponds to the latest definition.

6.16.4.13 Backscattering coefficients of pure water

Reference:  $b_w[\text{iband}]$ , LUT449

[AD-8] Section 6.16.4, GADS field 13

ACRI provided

Dependencies:

None

Tool:

None

Procedure:

Input:  $\text{iband}$  Index of MERIS band (15 bands) (starting from 0)

Output:  $b_w[\text{iband}]$  Backscattering coefficient ( $b_w(\lambda)$ ) of pure water in the 15 MERIS spectral bands (15 values)

units:  $[m^{-1}]$

Step: User specified.

Scientific content:

Set of 15 backscattering coefficients of pure water ( $b_w(\lambda)$ ) given at the 15 MERIS wavelengths

Current baseline: 15 values

| $\lambda [nm]$ | $b_w(\lambda) [m^{-1}]$ |
|----------------|-------------------------|
| 412.500        | 0.00330584              |
| 442.500        | 0.00244100              |
| 490.000        | 0.00157132              |
| 510.000        | 0.00132193              |
| 560.000        | 0.00088255              |
| 620.000        | 0.00056857              |
| 665.000        | 0.00042007              |
| 681.250        | 0.00037847              |
| 708.750        | 0.00031899              |
| 753.750        | 0.00024451              |

| $\lambda$ [nm] | $b_w(\lambda)$ [ $m^{-1}$ ] |
|----------------|-----------------------------|
| 761.875        | 0.00023510                  |
| 778.750        | 0.00021236                  |
| 865.000        | 0.00013490                  |
| 885.000        | 0.00012221                  |
| 900.000        | 0.00011365                  |

Resources:

Estimated CPU time: -  
Output disk space:  $15 \times 4$  bytes/fl = 60 bytes

Acceptance:

Corresponds to the latest definition.

**6.16.4.14 Specific backscattering coefficients of coccoliths**

Reference:  $b_{sc}[iband]$ , LUT450

[AD-8] Section 6.16.4, GADS field 14

ACRI provided

Dependencies:

None

Tool:

None

Procedure:

Input:  $iband$  Index of MERIS band (15 bands) (starting from 0)  
Output:  $b_{sc}[iband]$  Specific backscattering coefficient ( $b_{sc}(\lambda)$ ) of coccoliths in the 15 MERIS spectral bands (15 values)  
units: [ $m^2 \cdot g^{-1}$ ]  
Step: User specified.

Scientific content:

Set of 15 specific backscattering coefficients of coccoliths ( $b_{sc}(\lambda)$ ) given at the 15 MERIS wavelengths

Current baseline: 15 values

| $\lambda$ [nm] | $b_{sc}(\lambda)$ [ $m^2 \cdot g^{-1}$ ] |
|----------------|--|
| 412.500        | 0.01186331                               |
| 442.500        | 0.01153480                               |
| 490.000        | 0.01107381                               |
| 510.000        | 0.01089801                               |
| 560.000        | 0.01049784                               |
| 620.000        | 0.01007903                               |
| 665.000        | 0.00980046                               |
| 681.250        | 0.00970628                               |
| 708.750        | 0.00955384                               |
| 753.750        | 0.00932147                               |
| 761.875        | 0.00928768                               |
| 778.750        | 0.00920060                               |
| 865.000        | 0.00882204                               |
| 885.000        | 0.00874174                               |
| 900.000        | 0.00868317                               |

Resources:

Estimated CPU time: -  
Output disk space:  $15 \times 4$  bytes/fl = 60 bytes

Acceptance:

Corresponds to the latest definition.

6.16.4.15 Specific backscattering coefficients of SPM

Reference:  $b_{spm}$ [iband], LUT451

[AD-8] Section 6.16.4, GADS field 15

ACRI provided

Dependencies:

None

Tool:

None

Procedure:

Input: *iband* Index of MERIS band (15 bands) (starting from 0)

Output:  $b_{spm}[iband]$  Specific backscattering coefficient ( $b_{spm}(\lambda)$ ) of SPM in the 15 MERIS spectral bands (15 values)

units:  $[m^2.g^{-1}]$

Step: User specified.

Scientific content:

Set of 15 specific backscattering coefficients of SPM ( $b_{spm}(\lambda)$ ) given at the 15 MERIS wavelengths

Current baseline: 15 values

| $\lambda [nm]$ | $b_{spm}(\lambda) [m^2.g^{-1}]$ |
|----------------|---------------------------------|
| 412.500        | 0.01186331                      |
| 442.500        | 0.01153480                      |
| 490.000        | 0.01107381                      |
| 510.000        | 0.01089801                      |
| 560.000        | 0.01049784                      |
| 620.000        | 0.01007903                      |
| 665.000        | 0.00980046                      |
| 681.250        | 0.00970628                      |
| 708.750        | 0.00955384                      |
| 753.750        | 0.00932147                      |
| 761.875        | 0.00928768                      |
| 778.750        | 0.00920060                      |
| 865.000        | 0.00882204                      |
| 885.000        | 0.00874174                      |
| 900.000        | 0.00868317                      |

Resources:

Estimated CPU time: -

Output disk space:  $15 \times 4 \text{ bytes/fl} = 60 \text{ bytes}$

Acceptance:

Corresponds to the latest definition.

**6.16.4.16 Number of iterations in brigh pixel atmospheric correction for band set LOW and band set HIGH**

Reference: (No variable used), LUT452

[AD-8] Section 6.16.4, GADS field 16

ACRI provided

Dependencies:

None

Tool:

None

Procedure:

Input: none

Output: *(no variable)* Number of iterations in bright pixel atmospheric correction for band set LOW and band set HIGH (2 values)

units: [dl]

Step: User specified.

Scientific content:

Number of iterations to be used in BPAC for band set LOW and band set HIGH

Current baseline: {30, 60}

Resources:

Estimated CPU time: -

Output disk space: 2 × 2 bytes/us = 4 bytes

Acceptance:

Corresponds to the latest definition.

*6.16.4.17 Threshold value on total suspended particulate matters to raise CASE2\_S flag*

Reference: (No variable used), LUT453

[AD-8] Section 6.16.4, GADS field 17

ACRI provided

Dependencies:

None

Tool:

None

Procedure:

Input: none  
Output: *(no variable)* Threshold on total SPM to raise CASE2\_S flag  
units:  $[g.m^{-3}]$   
Step: User specified.

Scientific content:

Threshold on total SPM to raise CASE2\_S flag  
Current baseline:  $0.75 g.m^{-3}$

Resources:

Estimated CPU time: -  
Output disk space:  $1 \times 4 \text{ bytes/fl} = 4 \text{ bytes}$

Acceptance:

Corresponds to the latest definition.

6.16.4.18 *Convergence criteria on bbp in the BPAC iterations*

Reference: (No variable used), LUT342

[\[AD-8\]](#) Section 6.16.4, GADS field 18

ACRI provided

Dependencies:

None

Tool:

None

Procedure:

Input: none  
Output: *(no variable)* Convergence criteria on *bbp* in the BPAC iterations  
units:  $[dl]$

Step: User specified.

Scientific content:

Convergence criteria on *bbp* in the BPAC iterations

Current baseline: 0.001

Resources:

Estimated CPU time: -

Output disk space: 1 × 4 bytes/fl = 4 bytes

Acceptance:

Corresponds to the latest definition.

6.16.4.19 Convergence criteria on *bb* in the *rhow\_to\_bb* routine

Reference: (No variable used), LUT343

[AD-8] Section 6.16.4, GADS field 19

ACRI provided

Dependencies:

None

Tool:

None

Procedure:

Input: none

Output: (*no variable*) Convergence criteria on *bb* in the *rhow\_to\_bb* routine

units: [*dl*]

Step: User specified.

Scientific content:

Convergence criteria on *bb* in the *rhow\_to\_bb* routine

Current baseline: 0.0001



Resources:

Estimated CPU time: -  
Output disk space: 1 × 4 bytes/fl = 4 bytes

Acceptance:

Corresponds to the latest definition.

6.16.4.20 Number of iterations in the *rhow\_to\_bb* routine

Reference: (No variable used), LUT344

[AD-8] Section 6.16.4, GADS field 20

ACRI provided

Dependencies:

None

Tool:

None

Procedure:

Input: none  
Output: (*no variable*) Number of iterations in the *rhow\_to\_bb* routine  
units: [dl]  
Step: User specified.

Scientific content:

Number of iterations in the *rhow\_to\_bb* routine  
Current baseline: 70

Resources:

Estimated CPU time: -  
Output disk space: 1 × 2 bytes/us = 2 bytes

Acceptance:

Corresponds to the latest definition.

6.16.4.21 *Specific absorption coefficients of coccoliths*

Reference:  $a_c[iband]$ , LUT345

[AD-8] Section 6.16.4, GADS field 21

ACRI provided

Dependencies:

None

Tool:

None

Procedure:

Input:  $iband$  Index of MERIS band (15 bands) (starting from 0)

Output:  $a_c[iband]$  Specific absorption coefficient ( $a_c(\lambda)$ ) of coccoliths in the 15 MERIS spectral bands (15 values)

units:  $[m^2.g^{-1}]$

Step: User specified.

Scientific content:

Set of 15 specific absorption coefficients of coccoliths ( $a_c(\lambda)$ ) given at the 15 MERIS wavelengths

Current baseline: 15 values

| $\lambda [nm]$ | $a_c(\lambda) [m^2.g^{-1}]$ |
|----------------|-----------------------------|
| 412.500        | 0                           |
| 442.500        | 0                           |
| 490.000        | 0                           |
| 510.000        | 0                           |
| 560.000        | 0                           |
| 620.000        | 0                           |
| 665.000        | 0                           |
| 681.250        | 0                           |
| 708.750        | 0.98298699                  |
| 753.750        | 0.88159001                  |
| 761.875        | 0                           |
| 778.750        | 0.82985902                  |

| $\lambda$ [nm] | $a_c(\lambda)$ [ $m^2 \cdot g^{-1}$ ] |
|----------------|---------------------------------------|
| 865.000        | 0.67356098                            |
| 885.000        | 0.64175397                            |
| 900.000        | 0                                     |

Resources:

Estimated CPU time: -  
Output disk space:  $15 \times 4$  bytes/fl = 60 bytes

Acceptance:

Corresponds to the latest definition.

6.16.4.22 *Specific absorption coefficients of SPM*

Reference:  $a_{spm}[iband]$ , LUT346

[AD-8] Section 6.16.4, GADS field 22

ACRI provided

Dependencies:

None

Tool:

None

Procedure:

Input:  $iband$  Index of MERIS band (15 bands) (starting from 0)  
Output:  $a_{spm}[iband]$  Specific absorption coefficient ( $a_c(\lambda)$ ) of SPM in the 15 MERIS spectral bands (15 values)  
units: [ $m^2 \cdot g^{-1}$ ]  
Step: User specified.

Scientific content:

Set of 15 specific absorption coefficients of SPM ( $a_{spm}(\lambda)$ ) given at the 15 MERIS wavelengths

Current baseline: 15 values

| $\lambda$ [nm] | $a_c(\lambda)$ [ $m^2 \cdot g^{-1}$ ] |
|----------------|---------------------------------------|
| 412.500        | 0                                     |
| 442.500        | 0                                     |
| 490.000        | 0                                     |
| 510.000        | 0                                     |
| 560.000        | 0                                     |
| 620.000        | 0                                     |
| 665.000        | 0                                     |
| 681.250        | 0                                     |
| 708.750        | 0.98298699                            |
| 753.750        | 0.88159001                            |
| 761.875        | 0                                     |
| 778.750        | 0.82985902                            |
| 865.000        | 0.67356098                            |
| 885.000        | 0.64175397                            |
| 900.000        | 0                                     |

Resources:

Estimated CPU time: -  
Output disk space:  $15 \times 4$  bytes/fl = 60 bytes

Acceptance:

Corresponds to the latest definition.

*6.16.4.23 Initial estimate of backscatters at 778.75 nm for the LOW and HIGH band estimates*

Reference: (No variable used), LUT347

[AD-8] Section 6.16.4, GADS field 23

ACRI provided

Dependencies:

None

Tool:

None

Procedure:

Input: none

Output: (no variable) Initial estimate of backscatters at 778.75 nm for the LOW and HIGH band estimates (2 values)

units: [ $m^{-1}$ ]

Step: User specified.

Scientific content:

Initial estimate of backscatters at 778.75 nm for the LOW and HIGH band estimates

Current baseline: {0.001, 0.5}  $m^{-1}$

Resources:

Estimated CPU time: -

Output disk space:  $2 \times 4$  bytes/fl = 8 bytes

Acceptance:

Corresponds to the latest definition.

6.16.4.24 Initial estimate of the Angstroem exponent

Reference: (No variable used), LUT348

[AD-8] Section 6.16.4, GADS field 24

ACRI provided

Dependencies:

None

Tool:

None

Procedure:

Input: none

Output: (no variable) Initial estimate of the Angstroem exponent

units: [ $dI$ ]

Step: User specified.

Scientific content:

Initial estimate of the *Angstroem* exponent

Current baseline: -0.4

Resources:

Estimated CPU time: -

Output disk space: 1 × 4 bytes/fl = 4 bytes

Acceptance:

Corresponds to the latest definition.

6.16.4.25 *Threshold on water-leaving reflectance at 778.75 nm to activate the HIGH band set*

Reference: (No variable used), LUT349

[AD-8] Section 6.16.4, GADS field 25

ACRI provided

Dependencies:

None

Tool:

None

Procedure:

Input: none

Output: (*no variable*) Threshold on water-leaving reflectance at 778.75nm to activate the HIGH band set

units: [dl]

Step: User specified.

Scientific content:

Threshold on water-leaving reflectance at 778.75nm to activate the HIGH band set

Current baseline: 0.015

Resources:

Estimated CPU time: -  
Output disk space: 1 × 4 bytes/fl = 4 bytes

Acceptance:

Corresponds to the latest definition.

*6.16.4.26 Threshold on water-leaving reflectance at 778.75 nm to deactivate the LOW band set*

Reference: (No variable used), LUT350

[AD-8] Section 6.16.4, GADS field 26

ACRI provided

Dependencies:

None

Tool:

None

Procedure:

Input: none

Output: *(no variable)* Threshold on water-leaving reflectance at 778.75nm to deactivate the LOW band set

units: [dl]

Step: User specified.

Scientific content:

Threshold on water-leaving reflectance at 778.75nm to deactivate the LOW band set

Current baseline: 0.02

Resources:

Estimated CPU time: -  
Output disk space: 1 × 4 bytes/fl = 4 bytes

Acceptance:

Corresponds to the latest definition.

6.16.4.27 *Minimum TOA normalized radiance measurable at 708.75 nm*

Reference: (No variable used), LUT351

[AD-8] Section 6.16.4, GADS field 27

ACRI provided

Dependencies:

None

Tool:

None

Procedure:

Input: none

Output: *(no variable)* Minimum TOA normalized radiance measurable at 708.75 nm  
units: [sr<sup>-1</sup>]

Step: User specified.

Scientific content:

Minimum TOA normalized radiance measurable at 708.75 nm

Current baseline: 0

Resources:

Estimated CPU time: -

Output disk space: 1 × 4 bytes/fl = 4 bytes

Acceptance:

Corresponds to the latest definition.

6.16.4.28 *bbp value to initialize the rhow\_to\_bb routine*

Reference: (No variable used), LUT352

[AD-8] Section 6.16.4, GADS field 28

ACRI provided



Dependencies:

None

Tool:

None

Procedure:

Input: none

Output: (no variable) *bbp* value to initialize the *rhow\_to\_bb* routine  
units:  $[m^{-1}]$

Step: User specified.

Scientific content:

*bbp* value to initialize the *rhow\_to\_bb* routine

Current baseline:  $10^{-5} m^{-1}$

Resources:

Estimated CPU time: -

Output disk space:  $1 \times 4$  bytes/fl = 4 bytes

Acceptance:

Corresponds to the latest definition.

**6.16.4.29 Threshold for flagging yellow substance dominated waters**

Reference: YS\_thresh, LUT353

[AD-8] Section 6.16.4, GADS field 29

ACRI provided

Dependencies:

None

Tool:

None

Procedure:

Input: none  
Output: *YS\_thresh* Threshold for flagging yellow substance dominated waters  
units: [dl]  
Step: User specified.

Scientific content:

Threshold for flagging yellow substance dominated waters  
Current baseline: 5

Resources:

Estimated CPU time: -  
Output disk space: 1 × 4 bytes/fl = 4 bytes

Acceptance:

Corresponds to the latest definition.

**6.16.4.30 Chl values for GADS anomalous scattering detection**

Reference: Chl\_asd, LUT454

[AD-8] Section 6.16.4, GADS field 30

ACRI provided

Dependencies:

None

Tool:

None

Procedure:

Input: none  
Output: *Chl\_asd* Chlorophyll contents for GADS anomalous scattering detection (26 values)

units:  $[mg.m^{-3}]$

Step: User specified.

Scientific content:

Set of 26 chlorophyll contents (*Chl*) for GADS anomalous scattering detection

Current baseline: {0.03162, 0.03981, 0.05012, 0.063096, 0.07943, 0.10000, 0.12589, 0.15849,  
0.19953, 0.25119, 0.31623, 0.39811, 0.50119, 0.63096, 0.79433, 1.00000,  
1.25893, 1.58489, 1.99526, 2.51189, 3.16228, 3.98107, 5.01187, 6.30957,  
7.94328, 10.00000}  $mg.m^{-3}$

Resources:

Estimated CPU time: -  
Output disk space:  $26 \times 4 \text{ bytes/fl} = 104 \text{ bytes}$

Acceptance:

Corresponds to the latest definition.

6.16.4.31 *Floor values for NN inputs [reflectance threshold, floor NN input]*

Reference: (No variable used), LUT455

[AD-8] Section 6.16.4, GADS field 31

ACRI provided

Dependencies:

None

Tool:

None

Procedure:

Input: none

Output: (*no variable*) Floor values for NN inputs [reflectance threshold, floor NN input] (2 values)

units:  $[dl]$

Step: User specified.

Scientific content:

Floor values for NN inputs: reflectance threshold, floor NN input

Current baseline: {3 10<sup>-4</sup>, -9. 6458282}

Resources:

Estimated CPU time: -

Output disk space: 2 × 4 bytes/fl = 8 bytes

Acceptance:

Corresponds to the latest definition.

6.16.4.32 *Threshold for white scatterers detection*

Reference: (No variable used), LUT456

[AD-8] Section 6.16.4, GADS field 32

ACRI provided

Dependencies:

None

Tool:

None

Procedure:

Input: none

Output: *(no variable)* Threshold for white scatterers detection

units: [dl]

Step: User specified.

Scientific content:

Threshold for white scatterers detection

Current baseline: 4.8

Resources:

Estimated CPU time: -  
Output disk space:  $1 \times 4 \text{ bytes/fl} = 4 \text{ bytes}$

Acceptance:

Corresponds to the latest definition.

## 6.16.5 GADS Case II Yellow Substance Detection Coefficients

### 6.16.5.1 $B_i$ constants

Reference:  $B_i$ , LUT354

[AD-8] Section 6.16.5, GADS field 1

ACRI provided

Dependencies:

None

Tool:

None

Procedure:

Input: none

Output:  $B_i$  Constant values (2 values)

units:  $[dl]$

Step: User specified.

Scientific content:

2 constant values

Current baseline:  $\{2, 2\}$

Resources:

Estimated CPU time: -  
Output disk space:  $2 \times 4 \text{ bytes/fl} = 8 \text{ bytes}$

Acceptance:

Corresponds to the latest definition.

#### 6.16.5.2 $A_i$ constants for $H(443\text{ nm}, 560\text{ nm})$ estimation

Reference: A\_b2\_b5, LUT355

[AD-8] Section 6.16.5, GADS field 2

ACRI provided

#### Dependencies:

None

#### Tool:

None

#### Procedure:

Input: none

Output: A\_b2\_b5 Constants for  $H(443,560)$  estimation (3 values)

units: [dl]

Step: User specified.

#### Scientific content:

3 constant values for  $H(443,560)$  estimation

Current baseline: {20, -20, -1}

#### Resources:

Estimated CPU time: -

Output disk space:  $3 \times 4$  bytes/fl = 12 bytes

#### Acceptance:

Corresponds to the latest definition.

#### 6.16.5.3 $A_i$ constants for $H(490\text{ nm}, 560\text{ nm})$ estimation

Reference: A\_b3\_b5, LUT356

[AD-8] Section 6.16.5, GADS field 3

ACRI provided

Dependencies:

None

Tool:

None

Procedure:

Input: none

Output: *A\_b3\_b5* Constants for  $H(490,560)$  estimation (3 values)  
units: [dl]

Step: User specified.

Scientific content:

3 constant values for  $H(490,560)$  estimation

Current baseline: {20, -20, -1}

Resources:

Estimated CPU time: -

Output disk space:  $3 \times 4$  bytes/fl = 12 bytes

Acceptance:

Corresponds to the latest definition.

**6.16.5.4 A; constants for  $H(510\text{ nm}, 560\text{ nm})$  estimation**

Reference: *A\_b4\_b5*, LUT357

[AD-8] Section 6.16.5, GADS field 4

ACRI provided

Dependencies:

None

Tool:

None

Procedure:

Input: none

Output: *A\_b4\_b5* Constants for *H*(510,560) estimation (3 values)  
units: [*dl*]

Step: User specified.

Scientific content:

3 constant values for *H*(510,560) estimation

Current baseline: {20, -20, -1}

Resources:

Estimated CPU time: -

Output disk space: 3 × 4 bytes/fl = 12 bytes

Acceptance:

Corresponds to the latest definition.

6.16.5.5 *Ni* exponents

Reference: Ni, LUT358

[AD-8] Section 6.16.5, GADS field 5

ACRI provided

Dependencies:

None

Tool:

None

Procedure:

Input: none



Output:  $N_1, N_2, N_3$  Exponents (3 values)  
units: [dl]

Step: User specified.

Scientific content:

3 exponent values ( $N_1, N_2, N_3$ )

Current baseline: {0, 0, 0}

Resources:

Estimated CPU time: -  
Output disk space:  $3 \times 4$  bytes/fl = 12 bytes

Acceptance:

Corresponds to the latest definition.

## 6.16.6 GADS Anomalous Scattering Detection

### 6.16.6.1 Threshold on reflectance at 560nm

Reference: rhow560\_thresh[ $\theta_s, \theta_v, \Delta\phi, Chl2$ ] LUT457

[AD-8] Section 6.16.6, GADS field 1

ACRI provided

Dependencies:

LUT338, LUT339, LUT340, LUT454

Tool:

None

Procedure:

Input:  $\theta_s$  Solar zenith angle (10 values) [dl], (see Section 6.16.4.8), LUT339  
 $\theta_v$  View zenith angle (10 values) [deg.], (see Section 6.16.4.7), LUT338  
 $\Delta\phi$  Relative azimuth angle (19 values)[deg.], (see Section 6.16.4.9), LUT340  
 $Chl2$  Chlorophyll content (26 values) [ $mg/m^3$ ], (see Section 6.16.4.30), LUT454

**Output:** rhow560\_thresh[ $\theta_s, \theta_v, \Delta\phi, Chl2$ ]  
Threshold on reflectance at 560nm as function of illumination and viewing geometries ( $\theta_s, \theta_v, \Delta\phi$ ) and chlorophyll content ( $Chl2$ )

**Units:** [dl]

**Step:** User Specified

Scientific content:

This LUT contains the thresholds on reflectance at 560nm as function of sun/view geometries ( $\theta_s, \theta_v, \Delta\phi$ ) and several chlorophyll contents ( $Chl2$ ).

Current baseline: (10 × 10 × 19 × 26) values

Resources:

Estimated CPU time: -  
Output disk space: 10 × 10 × 19 × 26 × 4 bytes/fl = 197600 bytes

Acceptance:

Corresponds to the latest definition.

**6.16.7 GADS Coefficient of F' Factor to IOPs Relation**

*6.16.7.1 Coefficients of  $F_p$  factor to IOPs relation for 4 wind-speeds*

Reference: Coef[ $\theta_s, w_s, k, \lambda, \theta_v, \Delta\phi$ ], LUT371

[AD-8] Section 6.16.7, GADS field 1

ACRI provided

Dependencies:


LUT332, LUT333, LUT334, LUT335, LUT336, LUT337

Tool:

None

Procedure:

**Input:**  $\lambda$  MERIS wavelength (15 values) [dl], (see Section 6.16.4.1), LUT332  
 $\theta_s$  Solar zenith angle (5 values) [dl], (see Section 6.16.4.5), LUT336  
 $\theta_v$  View zenith angle (5 values) [deg.], (see Section 6.16.4.4), LUT335  
 $\Delta\phi$  Relative azimuth angle (13 values)[deg.], (see Section 6.16.4.6), LUT337

|   |  |   |
|---|--|---|
|  | <b>MERIS / ENVISAT-1</b><br>Medium Resolution Imaging Spectrometer | <u>Ref.:</u> PO-RS-PAR-GS-0002<br><u>Issue:</u> 3 <u>Rev.:</u> C<br><u>Date:</u> 27-Feb-11 <u>Page:</u> 482 |
|---|--|---|

$w_s$                       Wind-speed just above sea level (4 values) [ $m.s^{-1}$ ], (see Section 6.16.4.3), LUT334  
 $k$                               Polynomial coefficient order (8 values) [ $dI$ ], (see Section 6.16.4.2), LUT333

**Output:**      Coef[ $\theta_s, w_s, k, \lambda, \theta_v, \Delta\phi$ ]  
Coefficients of  $F'$  factor to IOPs relation as function of wavelength ( $\lambda$ ), illumination and viewing geometries ( $\theta_s, \theta_v, \Delta\phi$ ), and wind-speed just above sea level ( $w_s$ )  
**Units:**                      [ $dI$ ]  
**Step:**                      User Specified

Scientific content:

This LUT contains the 7<sup>th</sup> order polynomial coefficients of  $F'$  factor to IOPs relation (*Coef*) as function of wavelength ( $\lambda$ ), illumination and viewing geometries ( $\theta_s, \theta_v, \Delta\phi$ ), and wind-speed just above sea level ( $w_s$ ).

Current baseline:      ( $5 \times 4 \times 8 \times 15 \times 5 \times 13$ ) values

Resources:

Estimated CPU time:      -  
Output disk space:       $5 \times 4 \times 8 \times 15 \times 5 \times 13 \times 4$  bytes/fl = 624000 bytes

Acceptance:

Corresponds to the latest definition.

**6.16.8 GADS CASE-II Water Neural Network Parameters**

*6.16.8.1 Case-2 waters neural network parameters*

Reference:      (No variable used),                      LUT372

[AD-8]      Section 6.16.10, GADS field 1

ACRI provided

Dependencies:

None

Tool:

None

Procedure:

Input: none  
Output: *(no variable)* Case-2 waters NN Parameters  
units: [dl]  
Step: User specified.

Scientific content:

This LUT contains the case-2 waters NN parameters.

Current baseline: 262144 values

Resources:

Estimated CPU time: -  
Output disk space:  $262144 \times 1 \text{ byte/uc} = 262144 \text{ bytes}$

Acceptance:

Corresponds to the latest definition.

6.16.8.2 *Switch for reflectance log-scaling*

Reference: (No variable used), LUT458

[AD-8] Section 6.16.10, GADS field 2

ACRI provided

Dependencies:

None

Tool:

None

Procedure:

Input: none  
Output: *(no variable)* Switch for reflectance log-scaling  
units: [dl]

Step: User specified.

Scientific content:

Switch for reflectance log-scaling

Current baseline: 1

Resources:

Estimated CPU time: -

Output disk space:  $1 \times 1 \text{ byte/uc} = 1 \text{ byte}$

Acceptance:

Corresponds to the latest definition.

## 6.17 CLOUD PARAMETERS

### 6.17.1 C.P.

#### 6.17.1.1 C.P. Normalized TOA radiances, $L_{TOA}(\lambda, \theta_s, \theta_v, \Delta\phi)$

Reference: (no variable used) LUT402

Intermediate results stored in LUTs.

LUT dimension:  $N_{SZA} \times N_{VZA} \times N_{RAA} = 27 \times 18 \times 25$ .

Number of intermediate LUTs:

- with RTC/FUB: 1754 output simulation files

Resources:

Estimated CPU time: -

Output disk space:  $1754 \times 27 \times 18 \times 25 \times 4$  bytes/fl = 85244400 bytes

#### 6.17.1.2 C.P. Cloud spherical albedos, $Calb(\theta_s)$

Reference:  $Calb[\theta_s]$ , LUT404

Intermediate results stored in LUTs.

LUT dimension:  $N_{SZA} = 27$ .

Number of intermediate LUTs:

- with RTC/FUB: 1754 output simulation files

Resources:

Estimated CPU time: -

Output disk space:  $1754 \times 27 \times 4$  bytes/fl = 189432 bytes

### 6.17.2 MPH

Not covered in this document (see [\[AD-8\]](#) for a detailed description)

### 6.17.3 SPH

Not covered in this document (see [\[AD-8\]](#) for a detailed description)

## 6.17.4 GADS General

### 6.17.4.1 Latitudes for ADS surface albedo at 761.875 nm

Reference: lat, LUT212

[AD-8] Section 6.17.4, ADSR field 1

ACRI provided

#### Dependencies:

None

#### Tool:

None

#### Procedure:

Inputs: none

Outputs: *lat* Latitude (3600 values)

units:  $[10^{-6} \text{ deg}]$

Step: User specified.

#### Scientific content:

Set of 3600 latitudes (*lat*) used as the geographic grid for the surface albedo map at 761.875 nm

Current baseline:  $[89.975; -89.975] \text{ deg.}$  by step of  $-0.05 \text{ deg.}$

#### Resources:

Estimated CPU time: -

Output disk space:  $3600 \times 4 \text{ bytes/sl} = 14400 \text{ bytes}$

#### Acceptance:

Corresponds to the latest definition.

### 6.17.4.2 Longitudes for ADS surface albedo at 761.875 nm

Reference: long, LUT213

[AD-8] Section 6.17.4, GADS field 2

ACRI provided

Dependencies:

None

Tool:

None

Procedure:

Input: none

Output: *long* Longitudes (7200 values)  
units:  $[10^{-6} \text{ deg.}]$

Step: User specified.

Scientific content:

Set of 7200 longitudes (*long*) used as the geographic grid for the surface albedo map at 761.875 nm

Current baseline:  $[-179.975; 179.975]$  deg. by step of 0.05 deg.

Resources:

Estimated CPU time: -

Output disk space:  $7200 \times 4 \text{ bytes/sl} = 28800 \text{ bytes}$

Acceptance:

Corresponds to the latest definition.

6.17.4.3 *Solar zenith angles for ADS polynomial coefficients for cloud albedo retrieval & for ADS polynomial coefficients for cloud optical thickness retrieval*

Reference: SZA, LUTT214

[AD-8] Section 6.17.4, GADS field 3

ACRI provided

Dependencies:

None



Tool:

None

Procedure:

Input: none

Output: *SZA* Solar zenith angle ( $\theta_s$ ) for ADS polynomial coefficients for CALB & COT retrievals (27 values)

units:  $[10^{-6}deg.]$

Step: User specified.

Scientific content:

Set of 27 solar zenith angles ( $\theta_s$ ) regularly spaced

Current baseline: 27 values in  $[15;80]deg.$  by step of  $2.5deg$

Resources:

Estimated CPU time: -

Output disk space:  $27 \times 4$  bytes/ul = 108 bytes

Acceptance:

Corresponds to the latest definition.

*6.17.4.4 View zenith angles for ADS polynomial coefficients for cloud albedo retrieval & for ADS polynomial coefficients for cloud optical thickness retrieval*

Reference: VZA, LUTT215

[AD-8] Section 6.17.4, GADS field 4

ACRI provided

Dependencies:

None

Tool:

None

Procedure:

Input: none

Output: *SZA* View zenith angle ( $\theta_v$ ) for ADS polynomial coefficients for CALB & COT retrievals (18 values)

units:  $[10^{-6}deg.]$

Step: User specified.

Scientific content:

Set of 18 view zenith angles ( $\theta_v$ ) regularly spaced

Current baseline: 18 values in  $[0;42.5]deg.$  by step of  $2.5deg$

Resources:

Estimated CPU time: -

Output disk space:  $18 \times 4$  bytes/ul = 72 bytes

Acceptance:

Corresponds to the latest definition.

**6.17.4.5 Relative azimuth angles for ADS polynomial coefficients for cloud albedo retrieval & for ADS polynomial coefficients for cloud optical thickness retrieval**

Reference: RAA, LUT216

[AD-8] Section 6.17.4, GADS field 5

ACRI provided

Dependencies:

None

Tool:

None

Procedure:

Input: none

Output: *RAA* Relative azimuth angle for ADS polynomial coefficients for CALB & COT retrievals (25 values)  
units:  $[10^{-6} \text{ deg}]$   
Step: User specified.

Scientific content:

Set of 25 relative azimuth angle ( $\Delta\phi$ ) regularly spaced  
Current baseline: 25 values within  $[180;0] \text{ deg.}$ , with a step of  $-7.5 \text{ deg.}$

Resources:

Estimated CPU time: -  
Output disk space:  $25 \times 4 \text{ bytes/ul} = 100 \text{ bytes}$

Acceptance:

Corresponds to the latest definition

*6.17.4.6 Surface albedos for ADS polynomial coefficients for cloud albedo retrieval & for ADS polynomial coefficients for cloud optical thickness retrieval*

Reference: *Salb*, LUT217

[AD-8] Section 6.17.4, GADS field 6

ACRI provided

Dependencies:

None

Tool:

None

Procedure:

Input: none  
Output: *Salb* Surface albedo for ADS polynomial coefficients for CALB & COT retrievals (9 values)  
units:  $[dl]$   
Step: User specified.

Scientific content:

Set of 9 surface albedo ( $S_{alb}$ )

Current baseline: {0., 0.1, 0.2, 0.3, 0.4, 0.5, 0.6, 0.7, 0.8}.

Resources:

Estimated CPU time: -

Output disk space:  $9 \times 4$  bytes/fl = 36 bytes

Acceptance:

Corresponds to the latest definition

6.17.4.7 *Surface albedo scaling factor*

Reference: Salb\_scale, LUT218

[AD-8] Section 6.17.4, GADS field 7

ACRI provided

Dependencies:

None

Tool:

None

Procedure:

Input: none

Output: *Scale\_Salb* Scaling factor for surface albedo  
units: [*dl*]

Step: User specified.

Scientific content:

Scale factor for surface albedo

Current baseline: 0.0039215686

Resources:

Estimated CPU time: -  
Output disk space: 1 × 8 bytes/db = 8 bytes

Acceptance:

Corresponds to the latest definition

**6.17.4.8 Cloud top pressure neural network solar flux at 753.75 nm & for the 761.875 nm / 753.75 nm ratio**

Reference: Eo\_754, Eo\_ratio LUT416

[AD-8] Section 6.17.4, GADS field 8

ACRI provided

Dependencies:

None

Tool:

None

Procedure:

Input: none

Output: Eo\_754, Eo\_ratio  
Solar flux at 753.75nm and solar fluxes ratio between 761.875nm and 753.75nm MERIS bands

units: [W.m<sup>2</sup>.μm<sup>-1</sup>, dl]

Step: User specified.

Scientific content:

Both the solar flux at 753.75nm and the solar fluxes ratio between 761.875nm and 753.75nm are used in the cloud top pressure NN. These fluxes (*i.e.*, extraterrestrial solar irradiances) are not corrected for the Sun-Earth distance.

Current baseline: {1261.5169678, 1.0184140205} W.m<sup>2</sup>.μm<sup>-1</sup> and dl, respectively.

Resources:

Estimated CPU time: -  
Output disk space: 2 × 4 bytes/fl = 8 bytes

Acceptance:

Corresponds to the latest definitions

6.17.4.9 Minimum acceptable radiance value for TOA reflectance at 753.75 nm

Reference: min\_TOARb753, LUT373

[AD-8] Section 6.17.4, GADS field 9

ACRI provided

Dependencies:

None

Tool:

None

Procedure:

Input: none

Output: min\_TOARb753 Minimum acceptable radiance value for TOA reflectance at 753.75 nm  
units: [ $W.m^{-2}.\mu m^{-1}.sr^{-1}$ ]

Step: User specified.

Scientific content:

Minimum radiance value which can be accepted for TOA reflectance at 753.75 nm

Current baseline:  $0 W.m^{-2}.\mu m^{-1}.sr^{-1}$

Resources:

Estimated CPU time: -

Output disk space:  $1 \times 4$  bytes/fl = 4 bytes

Acceptance:

Corresponds to the latest definition

6.17.4.10 Maximum acceptable radiance value for TOA reflectance at 753.75 nm

Reference: max\_TOARb753, LUT374

[AD-8] Section 6.17.4, GADS field 10

ACRI provided

Dependencies:

None

Tool:

None

Procedure:

Input: none

Output: *max\_TOARb753* Maximum acceptable radiance value for TOA reflectance at 753.75 nm  
units:  $[W.m^{-2}.\mu m^{-1}.sr^{-1}]$

Step: User specified.

Scientific content:

Maximum radiance value which can be accepted for TOA reflectance at 753.75 nm

Current baseline:  $700 W.m^{-2}.\mu m^{-1}.sr^{-1}$

Resources:

Estimated CPU time: -

Output disk space:  $1 \times 4$  bytes/fl = 4 bytes

Acceptance:

Corresponds to the latest definition

6.17.4.11 Minimum acceptable radiance value for TOA reflectance at 761.875 nm

Reference: min\_TOARb762, LUT375

[AD-8] Section 6.17.4, GADS field 11

ACRI provided

Dependencies:

None

Tool:

None

Procedure:

Input: none

Output: *min\_TOARb762* Minimum acceptable radiance value for TOA reflectance at 761.875 nm  
units:  $[W.m^{-2}.\mu m^{-1}.sr^{-1}]$

Step: User specified.

Scientific content:

Minimum radiance value which can be accepted for TOA reflectance at 761.875 nm

Current baseline:  $0 W.m^{-2}.\mu m^{-1}.sr^{-1}$

Resources:

Estimated CPU time: -

Output disk space:  $1 \times 4$  bytes/fl = 4 bytes

Acceptance:

Corresponds to the latest definition

**6.17.4.12 Maximum acceptable radiance value for TOA reflectance at 761.875 nm**

Reference: max\_TOARb762, LUT376

[AD-8] Section 6.17.4, GADS field 12

ACRI provided

Dependencies:

None

Tool:

None



Procedure:

Input: none

Output: *max\_TOARb762*

Maximum acceptable radiance value for TOA reflectance at 761.875 nm

units: [ $W.m^{-2}.\mu m^{-1}.sr^{-1}$ ]

Step: User specified.

Scientific content:

Maximum radiance value which can be accepted for TOA reflectance at 761.875 nm

Current baseline: 400  $W.m^{-2}.\mu m^{-1}.sr^{-1}$

Resources:

Estimated CPU time: -

Output disk space: 1 × 4 bytes/fl = 4 bytes

Acceptance:

Corresponds to the latest definition

**6.17.4.13 Switch to use spectral shift index**

Reference: NN\_Use\_Shift, LUT415

[AD-8] Section 6.17.4, GADS field 13

ACRI provided

Dependencies:

None

Tool:

None

Procedure:

Input: none

Output: *NN\_Use\_shift* Shift used for spectral shift index

units: [dl]

Step: User specified.

Scientific content:

Shift used for the spectral shift index

Current baseline: 1

Resources:

Estimated CPU time: -

Output disk space: 1 × 4 bytes/ul = 4 bytes

Acceptance:

Corresponds to the latest definition

*6.17.4.14 FR-band#11 wavelengths for surface pressure neural network*

Reference: NN\_FR\_b11, LUT493

[AD-8] Section 6.17.4, GADS field 14

ACRI provided

Dependencies:

None

Tool:

None

Procedure:

Input: none

Output: NN\_FR\_b11 FR-band#11wavelengths for surface pressure NN (3700 values)

units: [nm]

Step: User specified.

Scientific content:

Set of 3700 wavelengths for MERIS band#11 to be used in the surface pressure NN in the full resolution mode

Current baseline: 3700 values

Resources:

Estimated CPU time: -  
Output disk space:  $3700 \times 4 \text{ bytes/fl} = 14800 \text{ bytes}$

Acceptance:

Corresponds to the latest definition

*6.17.4.15 RR-band#11 wavelengths for surface pressure neural network*

Reference: NN\_RR\_b11, LUT494

[AD-8] Section 6.17.4, GADS field 15

ACRI provided

Dependencies:

None

Tool:

None

Procedure:

Input: none  
Output: *NN\_RR\_b11* RR- band#11wavelengths for surface pressure NN (925 values)  
units: [nm]  
Step: User specified.

Scientific content:

Set of 925 wavelengths for MERIS band#11 to be used in the surface pressure NN in the reduced resolution mode

Current baseline: 925 values

Resources:

Estimated CPU time: -  
Output disk space:  $925 \times 4 \text{ bytes/fl} = 3700 \text{ bytes}$

Acceptance:

Corresponds to the latest definition

6.17.4.16 *FR residual stray-light correction factor*

Reference: FR\_SL\_corr, LUT495

[AD-8] Section 6.17.4, GADS field 16

ACRI provided

Dependencies:

None

Tool:

None

Procedure:

Input: none

Output: *FR\_SL\_corr* FR residual stray-light correction factor (3700 values)

units: [dl]

Step: User specified.

Scientific content:

Set of 3700 corrective factors for the residual effect of the stray-light in the full resolution mode

Current baseline: 3700 values

Resources:

Estimated CPU time: -

Output disk space:  $3700 \times 4 \text{ bytes/fl} = 14800 \text{ bytes}$

Acceptance:

Corresponds to the latest definition

#### 6.17.4.17 RR residual stray-light correction factor

Reference: RR\_SL\_corr, LUT496

[AD-8] Section 6.17.4, GADS field 17

ACRI provided

#### Dependencies:

None

#### Tool:

None

#### Procedure:

Input: none

Output: *RR\_SL\_corr* RR residual stray-light correction factor (925 values)  
units: [dl]

Step: User specified.

#### Scientific content:

Set of 925 corrective factors for the residual effect of the stray-light in the reduced resolution mode

Current baseline: 925 values

#### Resources:

Estimated CPU time: -

Output disk space:  $925 \times 4 \text{ bytes/fl} = 3700 \text{ bytes}$

#### Acceptance:

Corresponds to the latest definition

#### 6.17.4.18 Minimum acceptable value for surface albedo

Reference: Min\_Salb, LUT377

[AD-8] Section 6.17.4, GADS field 18

ACRI provided

Dependencies:

None

Tool:

None

Procedure:

Input: none

Output: *min\_Salb* Minimum acceptable value for surface albedo  
units: [dl]

Step: User specified.

Scientific content:

Minimum value which can be accepted for surface albedo

Current baseline: 0

Resources:

Estimated CPU time: -

Output disk space: 1 × 4 bytes/fl = 4 bytes

Acceptance:

Corresponds to the latest definition

*6.17.4.19 Maximum acceptable value for surface albedo*

Reference: Max\_Salb, LUT378

[AD-8] Section 6.17.4, GADS field 19

ACRI provided

Dependencies:

None

Tool:

None

Procedure:

Input: none  
Output: *max\_Salb* Maximum acceptable value for surface albedo  
units: [dl]  
Step: User specified.

Scientific content:

Minimum value which can be accepted for surface albedo  
Current baseline: 1.

Resources:

Estimated CPU time: -  
Output disk space: 1 × 4 bytes/fl = 4 bytes

Acceptance:

Corresponds to the latest definition

6.17.4.20 Cloud top pressures (CTP) for ADS cloud type index

Reference: Ctype\_P\_range, LUT379

[AD-8] Section 6.17.4, GADS field 20

ACRI provided

Dependencies:

None

Tool:

None

Procedure:

Input: none  
Output: *Ctype\_P\_range* Cloud top pressure for ADS cloud type index (10 values)  
units: [hPa]

Step: User specified.

Scientific content:

Set of 10 cloud top pressures used for ADS cloud type index

Current baseline: {50., 440., 680., 1000., 1000., 1000., 1000., 1000., 1000., 1000.} *hPa*

Resources:

Estimated CPU time: -

Output disk space: 10 × 4 bytes/fl = 40 bytes

Acceptance:

Corresponds to the latest definition

**6.17.4.21 Cloud optical thicknesses (CTP) for ADS cloud type index**

Reference: Ctype\_OT\_range, LUT380

[AD-8] Section 6.17.4, GADS field 21

ACRI provided

Dependencies:

None

Tool:

None

Procedure:

Input: none

Output: *Ctype\_OT\_range*  
Cloud optical thickness for ADS cloud type index (10 values)

units: [*dl*]

Step: User specified.

Scientific content:

Set of 10 cloud optical thicknesses used for ADS cloud type index



Current baseline: {0., 3.6, 23., 379., 379., 379., 379., 379., 379., 379.}

Resources:

Estimated CPU time: -  
Output disk space: 10 × 4 bytes/fl = 40 bytes

Acceptance:

Corresponds to the latest definition

6.17.4.22 *Number of cloud top pressures*

Reference: Ctype\_n\_P, LUT381

[AD-8] Section 6.17.4, GADS field 22

ACRI provided

Dependencies:

None

Tool:

None

Procedure:

Input: none  
Output: Ctype\_n\_P Number of cloud top pressures  
units: [dl]  
Step: User specified.

Scientific content:

Number of cloud top pressures used for ADS cloud type index

Current baseline: 4

Resources:

Estimated CPU time: -  
Output disk space: 1 × 1 byte/uc = 1 byte

Acceptance:

Corresponds to the latest definition

#### 6.17.4.23 Number of cloud optical thicknesses

Reference: Ctype\_n\_OT, LUT382

[AD-8] Section 6.17.4, GADS field 23

ACRI provided

#### Dependencies:

None

#### Tool:

None

#### Procedure:

Input: none

Output: Ctype\_n\_OT Number of cloud optical thicknesses  
units: [dl]

Step: User specified.

#### Scientific content:

Number of cloud optical thicknesses for ADS cloud type index

Current baseline: 4

#### Resources:

Estimated CPU time: -

Output disk space: 1 × 1 byte/uc = 1 byte

#### Acceptance:

Corresponds to the latest definition

#### 6.17.4.24 Solar flux at 753.75 nm for cloud LUTs

Reference: Eo\_754, LUT383

[AD-8] Section 6.17.4, GADS field 24

ACRI provided

Dependencies:

None

Tool:

None

Procedure:

Input: none

Output:  $Eo_{754}$  Solar flux at 753.75 nm

units:  $[W.m^2.\mu m^{-1}, dl]$

Step: User specified.

Scientific content:

Solar flux at 753.75 nm used for the cloud LUTs. This flux (*i.e.*, extraterrestrial solar irradiances) is not corrected for the *Sun-Earth* distance.

Current baseline: 1261.5169678  $W.m^2.\mu m^{-1}$

Resources:

Estimated CPU time: -

Output disk space: 1 × 4 bytes/fl = 4 bytes

Acceptance:

Corresponds to the latest definition

6.17.4.25 *Minimum valid values for surface pressure neural network inputs*

Reference: (no variable used), LUT497

[AD-8] Section 6.17.4, GADS field 25

ACRI provided

Dependencies:

None

Tool:

None

Procedure:

Input: none

Output: *(no variable)* Minimum valid values for surface pressure NN inputs (7 values)

units: [dl]

Step: User specified.

Scientific content:

Minimum valid values for the surface pressure NN input parameters

Current baseline: {0.0129, 0.181, 0.149, 0.342, 0.680, -0.733, 760.00}

Resources:

Estimated CPU time: -

Output disk space:  $7 \times 4$  bytes/fl = 28 bytes

Acceptance:

Corresponds to the latest definition

6.17.4.26 *Maximum valid values for surface pressure neural network inputs*

Reference: (no variable used), LUT498

[AD-8] Section 6.17.4, GADS field 26

ACRI provided

Dependencies:

None

Tool:

None

Procedure:

Input: none  
Output: *(no variable)* Maximum valid values for surface pressure NN inputs (7 values)  
units: [dl]  
Step: User specified.

Scientific content:

Maximum valid values for the surface pressure NN input parameters  
Current baseline: {0.307, 0.771, 0.151, 0.975, 1.000, 0.733, 763.00}

Resources:

Estimated CPU time: -  
Output disk space:  $7 \times 4 \text{ bytes/fl} = 28 \text{ bytes}$

Acceptance:

Corresponds to the latest definition

*6.17.4.27 Minimum valid value for surface pressure neural network output*

Reference: (no variable used), LUT499

[AD-8] Section 6.17.4, GADS field 27  
ACRI provided

Dependencies:

None

Tool:

None

Procedure:

Input: none  
Output: *(no variable)* Minimum valid value for surface pressure NN output  
units: [hPa]  
Step: User specified.

Scientific content:

Minimum valid values for the surface pressure NN output

Current baseline: 300 *hPa*

Resources:

Estimated CPU time: -  
Output disk space: 1 × 4 bytes/fl = 4 bytes

Acceptance:

Corresponds to the latest definition

**6.17.4.28 Maximum valid value for surface pressure neural network output**

Reference: (no variable used), LUT500

[AD-8] Section 6.17.4, GADS field 28

ACRI provided

Dependencies:

None

Tool:

None

Procedure:

Input: none  
Output: (no variable) Maximum valid value for surface pressure NN output  
units: [*hPa*]  
Step: User specified.

Scientific content:

Maximum valid values for the surface pressure NN output

Current baseline: 1050 *hPa*

Resources:

Estimated CPU time: -

Output disk space: 1 × 4 bytes/fl = 4 bytes

Acceptance:

Corresponds to the latest definition

6.17.4.29 Default AOT value for surface pressure neural network

Reference: (no variable used), LUT501

[AD-8] Section 6.17.4, GADS field 29

ACRI provided

Dependencies:

None

Tool:

None

Procedure:

Input: none

Output: (no variable) Default AOT value for surface pressure NN  
units: [dl]

Step: User specified.

Scientific content:

Default AOT value for surface pressure NN

Current baseline: 0.15

Resources:

Estimated CPU time: -

Output disk space: 1 × 4 bytes/fl = 4 bytes

Acceptance:

Corresponds to the latest definition

#### 6.17.4.30 Maximum allowed surface pressure difference

Reference: (no variable used), LUT502

[AD-8] Section 6.17.4, GADS field 30

ACRI provided

#### Dependencies:

None

#### Tool:

None

#### Procedure:

Input: none

Output: (no variable) Maximum allowed surface pressure difference  
units: [hPa]

Step: User specified.

#### Scientific content:

Maximum allowed surface pressure difference

Current baseline: 60

#### Resources:

Estimated CPU time: -

Output disk space:  $1 \times 4$  bytes/fl = 4 bytes

#### Acceptance:

Corresponds to the latest definition

### 6.17.5 GADS Surface Albedo

#### 6.17.5.1 Surface albedo at 761.875 nm, $S_{alb}(month,latitude,longitude)$

Reference: Salb, LUT219

[AD-8] Section 6.17.5, GADS field 1



ACRI provided

Dependencies:

LUT212, LUT213

Tool:

None

Procedure:

Inputs:     *month*            Month [*dl*] (12 values)  
              *lat*                Latitude [*deg*] (3600 values), *see* [Section 6.17.4.1](#) (LUT212)  
              *long*             Longitude [*deg*] (7200 values), *see* [Section 6.17.4.2](#) (LUT213)

Outputs:     *Salb[month, lat, long]*  
                                  Monthly value of surface albedo at 761.875nm as function of geographic location (*lat, long*)

units:        [*dl*]

Step:         User specified.

Scientific content:

*Salb[month, lat, long]* describes the monthly surface albedo at 761.875nm (band#11), for an angular grid of 0.05 *deg.* in latitude (*lat*) and in longitude (*long*).

Current baseline: Set of 311040000 values given for 12 months and for an accurate angular *lat-long* grid (3600 x 7200).

Resources:

Estimated CPU time:    -

Output disk space:     12 × 3600 × 7200 × 1 byte/uc = 311040000 bytes

Acceptance:

Corresponds to the latest definition.

**6.17.6 ADS Polynomial Coefficients for Cloud Albedo Retrieval**

*6.17.6.1 Polynomial coefficients for cloud albedo retrieval*

Reference:    Calb,                                    LUT220

[AD-8] Section 6.17.6, GADS field 1, 2 & 3

ACRI provided

Dependencies:

LUT214, LUT215, LUT216, LUT217

Tool:

OTC/RAYLEIGH  
RTC/FUB (MOMO)  
Polynomial fit

Procedure:

Inputs:  $\theta_s$  Solar zenith angle [*deg*], see Section 6.17.4.3, (LUT214)  
 $\theta_v$  View zenith angle [*deg*], see Section 6.17.4.4, (LUT215)  
 $\Delta\phi$  Relative azimuth angle [*deg*], see Section 6.17.4.5, (LUT216)  
 $S_{alb}$  Surface albedo [*dl*], see Section 6.17.4.6, (LUT217) or the input database from the 'FUB/input.cloud' file (9 values)  
 $k$  Polynomial coefficient orders [*dl*],  $k = [0;2]$

Output:  $Calb[S_{alb}, \theta_s, \theta_v, \Delta\phi, k]$   
 Polynomial coefficients for cloud albedo retrieval

units: [*dl*]

Step-1: Build input cards for the RTC/MOMO using the input database from the 'FUB/input.cloud' file. The latter is formatted in 6 columns and comprises,  
 (a) the identification number of the simulation case (*xxxx*)  
 (b) the cloud optical thickness ( $\tau^c$ ) at 550nm  
 (c) the cloud top height ( $z_c$ ) [*m*]  
 (d) the effective radius of cloud droplets ( $r_e$ ) [ $\mu m$ ]  
 (e) the index (*itau*) to select the aerosol type (*i.e.*, for selecting the aerosol layer, #1 or #2)  
 (f) the surface albedo x 100 ( $S_{alb}$ )

A LUT file with TOA normalized radiances will be generated for each case (*i.e.*, for each input data line from the 'FUB/input.cloud' file) at 753.75nm (MERIS band #10) and for all illumination/viewing geometries ( $\theta_s, \theta_v, \Delta\phi$ ).

Step-2: Generate TOA normalized radiances  $L_{TOA\_10}[S_{alb}, \theta_s, \theta_v, \Delta\phi]$  for each case (*i.e.*, for each input data line from the 'FUB/input.cloud' file), for all illumination/viewing geometries ( $\theta_s, \theta_v, \Delta\phi$ ) over a black/reflective surface ( $S_{alb}$ ), with the RTC/MOMO.

**Warning:** The process for generating this table is very time-consuming. To avoid loosing data in case of a power failure, temporary binary files are created after few hours of processing: *CLOUD\_xxx.LUT404* (*xxx stands for the simulation identification*). This allows one to resume

the processing after a power failure. If we want fully restart the generation procedure, then the temporary binary files should be first deleted before relaunching the process.

**RTC/MOMO Inputs (CLOUD)**

| Variable                   | Value   | Comments  |
|----------------------------|---|---|
| <i>out_file</i>            | "/up_out/uprad_out"                                     |   |
| <i>i_branch</i>            | 3   |   |
| $n(\lambda)$               | 10  | 753.75 nm   |
| $U_{H2O}$                  | 0   |   |
| $ESFT_{H2O}$               | -   | N/A   |
| $U_{O2}$                   | 0   |   |
| $ESFT_{O2}$                | -   | N/A   |
| $U_{O3}$                   | 0   |   |
| $ESFT_{O3}$                | -   | N/A   |
| $P_s$                      | 1013.25   |   |
| $\tau^R(\lambda)$          | tauR  | Computed with OTC/RAYLEIGH  |
| <i>aerosol1</i>            | "/sca_out/sc_marcl90_bxx.s"                             | xx depends on $n(\lambda)$  |
| $\tau^{a1}(550)$           | 0.15  | Only if <i>aerotype</i> = 0 otherwise $\tau^{a1}(550) = 0$<br>Value of <i>aerotype</i> is taken from the<br>'FUB/input.wv.cloud' definition table |
| <i>aerosol2</i>            | "/sca_out/sc_conticld_bxx.s"                            | xx depends on $n(\lambda)$  |
| $\tau^{a2}(550)$           | 0.3   | Only if <i>aerotype</i> = 1 otherwise $\tau^{a2}(550) = 0$<br>Value of <i>aerotype</i> is taken from the<br>'FUB/input.wv.cloud' definition table |
| <i>aerosol3</i>            | -   |   |
| $\tau^{a3}(550)$           | 0   |   |
| <i>cloud1</i>              | "/sca_out/sc_cldyy_bxx.s"                               | xx depends on $n(\lambda)$ and yy on the effective<br>cloud droplets radius. yy is taken from the<br>'FUB/input.cloud' definition table.          |
| $\tau^{c1}(550)$           | tauC/2 (if <i>cloudtype</i> =10)<br>or tauC (otherwise) | Values of <i>cloudtype</i> and <i>tauC</i> are taken from<br>the 'FUB/input.cloud' definition table   |
| <i>cloud2</i>              | "/sca_out/sc_cld17_bxx.s"                               | xx depends on $n(\lambda)$  |
| $\tau^{c2}(550)$           | tauC/2 (if <i>cloudtype</i> =10)<br>or 0 (otherwise)    | Values of <i>cloudtype</i> and <i>tauC</i> are taken from<br>the 'FUB/input.cloud' definition table   |
| <i>cloud3</i>              | -   |   |
| $\tau^{c3}(550)$           | 0   |   |
| <i>phyto</i>               | -   | N/A   |
| $\sigma_{e,\lambda}^p$     | -   | N/A   |
| $\omega_{o,\lambda}^p$     | -   | N/A   |
| <i>spm</i>                 | -   | N/A   |
| $\sigma_{e,\lambda}^{spm}$ | -   | N/A   |

| Variable                   | Value                     | Comments  |
|----------------------------|---------------------------|---|
| $\omega_{o,\lambda}^{spm}$ | -                         | N/A   |
| $\sigma_{a,\lambda}^{ys}$  | -                         | N/A   |
| <i>vertical</i>            | "/sca_vert/cld/vtp1_####" | #### depends on the cloud top altitude (2500, 5000, 7500 and 10000m). The latter is taken from the 'FUB/input.cloud' definition table |
| $I_s$                      | 70                        |   |
| $\rho_s$                   | Salb                      | Surface albedo taken from the 'FUB/input.cloud' definition table (see <a href="#">Section 6.17.4.7</a> )                              |
| $E_o$                      | 1                         |   |
| $\sigma_{a,\lambda}^w$     | -                         | N/A   |
| $w_s$                      | 0                         |   |
| $n_s, n_v, n_{\Delta\phi}$ | 27, 18, 25                |   |
| $\theta_s$                 | Gaussian angles           | See <a href="#">Section 6.17.4.3</a>  |
| $\theta_v$                 | Gaussian angles           | See <a href="#">Section 6.17.4.4</a>  |
| $\Delta\phi$               | see inputs                | See <a href="#">Section 6.17.4.5</a>  |

Extract after each simulation the cloud albedo ( $S_{cld}[S_{alb}, \theta_s, \theta_v, \Delta\phi]$ ) from the 'FUB/mom\_out/flux\_0001' file. The latter is referred as the 'HEMISPHERICAL REFLECTANCE' label at the TOA and the corresponding value is saved in the MERISAT internal tables: *CLOUD\_xxx.LUT404*.

Step-3: Apply a 2<sup>nd</sup> order polynomial fit on the cloud albedos  $S_{cld}[S_{alb}, \theta_s, \theta_v, \Delta\phi]$  (extracted from *CLOUD\_xxx.LUT404* files) as function of the TOA normalized radiances  $L_{TOA\_10}[S_{alb}, \theta_s, \theta_v, \Delta\phi]$ , for retrieving polynomial coefficients  $Calb\_LUT[S_{alb}, \theta_s, \theta_v, \Delta\phi, k]$ .

$$S_{cld}[S_{alb}, \theta_s, \theta_v, \Delta\phi] = \begin{aligned} & Calb\_LUT[S_{alb}, \theta_s, \theta_v, \Delta\phi, 0] \\ & + Calb\_LUT[S_{alb}, \theta_s, \theta_v, \Delta\phi, 1] \cdot L_{TOA\_10}[S_{alb}, \theta_s, \theta_v, \Delta\phi] \\ & + Calb\_LUT[S_{alb}, \theta_s, \theta_v, \Delta\phi, 2] \cdot (L_{TOA\_10}[S_{alb}, \theta_s, \theta_v, \Delta\phi])^2 \end{aligned}$$

### Scientific content:

$Calb\_LUT[S_{alb}, \theta_s, \theta_v, \Delta\phi, k]$  describes the coefficients of the polynomial fit applied on the cloud albedos  $S_{cld}[S_{alb}, \theta_s, \theta_v, \Delta\phi]$ , as function of the TOA normalized radiances  $L_{TOA\_10}[S_{alb}, \theta_s, \theta_v, \Delta\phi]$ , computed in the MERIS band #10. These regression coefficients ( $k=[0;2]$ ) depends on the illumination and viewing geometries ( $\theta_s, \theta_v, \Delta\phi$ ) and on the surface albedo ( $S_{alb}$ ) at 753.75 nm.

Note that the radiance computations with the RTC/MOMO are completed with an angular grid ( $\theta_s, \theta_v, \Delta\phi$ ) which differs from the one defined as input. In fact, the radiance propagation directions (zenith angles) within the RTC/MOMO are determined with the *Gauss-Lobatto* quadrature. Consequently, an interpolation scheme will be applied to superimpose the output radiance matrices derived from the RTC/MOMO computations with the requested angular grid (specified as input).

Current baseline:

$\theta_s$  corresponds to 27 solar zenith angles from 15° to 80° with a step of 2.5°  
 $\theta_v$  corresponds to 18 view zenith angles from 0° to 42.5° with a step of 2.5°  
 $\Delta\phi$  corresponds to 25 relative azimuth angles from 0° to 180° with a step of 7.5°  
 $S_{alb}$  corresponds to 9 surface albedos from 0 to 0.8 with a step of 0.1

Resources:

Estimated CPU time: 19129 *sec*  
 Output disk space:  $27 \times 3 \times 18 \times 25 \times 9 \times 4$  bytes/fl = 1312200 bytes

The storage of this table is completed with several records for the different indices of polynomial coefficients (*see* [AD-8] for the exact structure).

Acceptance:

The quality check of the polynomial fits can be tested by applying them on the input dataset.

### 6.17.7 ADS Polynomial Coefficients for Cloud Optical Thickness Retrieval

#### 6.17.7.1 Polynomial coefficients for cloud optical thickness retrieval

Reference: Cthick\_LUT, LUT223

[AD-8] Section 6.17.7, GADS field 1, 2, 3 & 4

ACRI provided

Dependencies:

LUT214, LUT215, LUT216, LUT217

Tool:

OTC/RAYLEIGH  
 RTC/FUB (MOMO)  
 Polynomial fit

Procedure:

Inputs:  $\theta_s$  Solar zenith angle [*deg*], *see* Section 6.17.4.3, (LUT214)  
 $\theta_v$  View zenith angle [*deg*], *see* Section 6.17.4.4, (LUT215)  
 $\Delta\phi$  Relative azimuth angle [*deg*], *see* Section 6.17.4.5, (LUT216)  
 $S_{alb}$  Surface albedo [*dl*], *see* Section 6.17.4.6, (LUT217) or the input database from the '*FUB/input.cloud*' file (9 values)  
 $k$  Polynomial coefficient orders [*dl*],  $k = [0;3]$

Output:  $COT[S_{alb}, \theta_s, \theta_v, \Delta\phi, k]$

Polynomial coefficients for cloud optical thickness retrieval

units: [dl]

Step-1: Build input cards for the RTC/MOMO using the input database from the 'FUB/input.cloud' file.

The latter is formatted in 6 columns and comprises,

- (a) the identification number of the simulation case (xxxx)
- (b) the cloud optical thickness ( $\tau^c$ ) at 550nm
- (c) the cloud top height ( $z_c$ ) [m]
- (d) the effective radius of cloud droplets ( $r_e$ ) [ $\mu\text{m}$ ]
- (e) the index (*itau*) to select the aerosol type (*i.e.*, for selecting the aerosol layer, #1 or #2)
- (f) the surface albedo x 100 ( $S_{alb}$ )

A LUT file with TOA normalized radiances will be generated for each case (*i.e.*, for each input data line from the 'FUB/input.cloud' file) at 753.75nm (MERIS band #10) and for all illumination/viewing geometries ( $\theta_s, \theta_v, \Delta\phi$ ).

Step-2: Generate TOA normalized radiances  $L_{TOA\_10}[S_{alb}, \theta_s, \theta_v, \Delta\phi]$  for each case (*i.e.*, for each input data line from the 'FUB/input.cloud' file), for all illumination/viewing geometries ( $\theta_s, \theta_v, \Delta\phi$ ) over a black/reflective surface ( $S_{alb}$ ), with the RTC/MOMO.

**Warning:** The process for generating this table is very time-consuming. To avoid loosing data in case of a power failure, temporary binary files are created after few hours of processing: *CLOUD\_xxx.LUT402* (*xxx stands for the simulation identification*). This allows one to resume the processing after a power failure. If we want fully restart the generation procedure, then the temporary binary files should be first deleted before relaunching the process. Note that the output radiances will be the same as those computed for LUT220 (*see Section 6.17.6.1*).

**RTC/MOMO Inputs (CLOUD)**

| Variable        | Value                        | Comments  |
|-----------------|------------------------------|---|
| <i>out_file</i> | "/up_out/uprad_out"          |   |
| <i>i_branch</i> | 3                            |   |
| $n(\lambda)$    | 10                           | 753.75 nm   |
| $U_{H2O}$       | 0                            |   |
| $ESFT_{H2O}$    | -                            | N/A   |
| $U_{O2}$        | 0                            |   |
| $ESFT_{O2}$     | -                            | N/A   |
| $U_{O3}$        | 0                            |   |
| $ESFT_{O3}$     | -                            | N/A   |
| $P_s$           | 1013.25                      |   |
| $t^R(\lambda)$  | tauR                         | Computed with OTC/RAYLEIGH  |
| <i>aerosol1</i> | "/sca_out/sc_marcl90_bxx.s"  | xx depends on $n(\lambda)$  |
| $t^{a1}(550)$   | 0.15                         | Only if <i>aerotype</i> = 0 otherwise $t^{a1}(550) = 0$<br>Value of <i>aerotype</i> is taken from the 'FUB/input.wv.cloud' definition table |
| <i>aerosol2</i> | "/sca_out/sc_conticld_bxx.s" | xx depends on $n(\lambda)$  |

| Variable                   | Value   | Comments  |
|----------------------------|---|---|
| $\tau^{a2}(550)$           | 0.3   | Only if <i>aerotype</i> = 1 otherwise $\tau^{a2}(550) = 0$<br>Value of <i>aerotype</i> is taken from the 'FUB/input.wv.cloud' definition table          |
| <i>aerosol3</i>            | -   |   |
| $\tau^{a3}(550)$           | 0   |   |
| <i>cloud1</i>              | "/sca_out/sc_cldyy_bxx.s"                               | <i>xx</i> depends on $n(\lambda)$ and <i>yy</i> on the effective cloud droplets radius. <i>yy</i> is taken from the 'FUB/input.cloud' definition table. |
| $\tau^1(550)$              | tauC/2 (if <i>cloudtype</i> =10)<br>or tauC (otherwise) | Values of <i>cloudtype</i> and <i>tauC</i> are taken from the 'FUB/input.cloud' definition table  |
| <i>cloud2</i>              | "/sca_out/sc_cld17_bxx.s"                               | <i>xx</i> depends on $n(\lambda)$   |
| $\tau^2(550)$              | tauC/2 (if <i>cloudtype</i> =10)<br>or 0 (otherwise)    | Values of <i>cloudtype</i> and <i>tauC</i> are taken from the 'FUB/input.cloud' definition table  |
| <i>cloud3</i>              | -   |   |
| $\tau^3(550)$              | 0   |   |
| <i>phyto</i>               | -   | N/A   |
| $\sigma_{e,\lambda}^p$     | -   | N/A   |
| $\omega_{o,\lambda}^p$     | -   | N/A   |
| <i>spm</i>                 | -   | N/A   |
| $\sigma_{e,\lambda}^{spm}$ | -   | N/A   |
| $\omega_{o,\lambda}^{spm}$ | -   | N/A   |
| $\sigma_{a,\lambda}^{ys}$  | -   | N/A   |
| <i>vertical</i>            | "/sca_vert/cld/vtp1_ffff"                               | <i>ffff</i> depends on the cloud top altitude (2500, 5000, 7500 and 10000m). The latter is taken from the 'FUB/input.cloud' definition table            |
| $I_s$                      | 70  |   |
| $\rho_s$                   | Salb  | Surface albedo taken from the 'FUB/input.cloud' definition table (see <a href="#">Section 6.17.4.7</a> )  |
| $E_o$                      | 1   |   |
| $\sigma_{a,\lambda}^w$     | -   | N/A   |
| $w_s$                      | 0   |   |
| $n_s, n_v, n_{\Delta\phi}$ | 27, 18, 25  |   |
| $\theta_s$                 | Gaussian angles   | See <a href="#">Section 6.17.4.3</a>  |
| $\theta_v$                 | Gaussian angles   | See <a href="#">Section 6.17.4.4</a>  |
| $\Delta\phi$               | see inputs  | See <a href="#">Section 6.17.4.5</a>  |

Step-2: Extract the cloud optical thicknesses ( $\tau^c$ ) for all the simulation cases from the input database 'FUB/input.cloud'.

Step-3: Apply a 3<sup>rd</sup> order polynomial fit on the cloud optical thicknesses ( $\tau^c$ ) as function of the TOA normalized radiances  $L_{TOA\_10}[S_{alb}, \theta_s, \theta_v, \Delta\phi]$ , for retrieving the polynomial coefficients  $COT[S_{alb}, \theta_s, \theta_v, \Delta\phi, k]$ .

$$\tau^c = \text{Exp} \{ COT[S_{alb}, \theta_s, \theta_v, \Delta\phi, 0] + COT[S_{alb}, \theta_s, \theta_v, \Delta\phi, 1] \cdot L_{TOA\_10}[S_{alb}, \theta_s, \theta_v, \Delta\phi] + COT[S_{alb}, \theta_s, \theta_v, \Delta\phi, 2] \cdot (L_{TOA\_10}[S_{alb}, \theta_s, \theta_v, \Delta\phi])^2 + COT[S_{alb}, \theta_s, \theta_v, \Delta\phi, 3] \cdot (L_{TOA\_10}[S_{alb}, \theta_s, \theta_v, \Delta\phi])^3 \}$$

### Scientific content:

$Cthick\_LUT[S_{alb}, \theta_s, \theta_v, \Delta\phi, k]$  describes the coefficients of the polynomial fit applied on the cloud optical thicknesses  $\tau^c$ , as function of the TOA radiances  $L_{TOA\_10}[S_{alb}, \theta_s, \theta_v, \Delta\phi]$ , computed in the MERIS band #10. These regression coefficients ( $k=[0;3]$ ) depends on the illumination and viewing geometries ( $\theta_s, \theta_v, \Delta\phi$ ) and on the surface albedo ( $S_{alb}$ ) at 753.75 nm.

Note that the radiance computations with the RTC/MOMO are completed with an angular grid ( $\theta_s, \theta_v, \Delta\phi$ ) which differs from the one defined as input. In fact, the radiance propagation directions (zenith angles) within the RTC/MOMO are determined with the *Gauss-Lobatto* quadrature. Consequently, an interpolation scheme will be applied to superimpose the output radiance matrices derived from the RTC/MOMO computations with the requested angular grid (specified as input).

Current baseline:

- $\theta_s$  corresponds to the 27 following solar zenith angles: from 15° to 80° with a step of 2.5°
- $\theta_v$  corresponds to the 18 following view zenith angles: from 0° to 42.5° with a step of 2.5°
- $\Delta\phi$  corresponds to the 25 following relative azimuth angles: from 0° to 180° with a step of 7.5°
- $S_{alb}$  corresponds to the 9 following surface albedos: from 0 to 0.8 with a step of 0.1

### Resources:

Estimated CPU time: 19016 sec  
Output disk space:  $27 \times 4 \times 18 \times 25 \times 9 \times 4$  bytes/fl = 1749600 bytes

### Acceptance:

The quality check of the polynomial fits can be tested by applying them on the input dataset.

## **6.17.8 GADS Cloud Top Pressure Neural Network for not null Surface Albedo**

### *6.17.8.1 Cloud top pressure neural network for not null surface albedo*

Reference: (No variable used), LUT384

[AD-8] Section 6.17.8, GADS field 1

ACRI provided

### Dependencies:



None

Tool:

None

Procedure:

Input: none

Output: *(no variable)* Cloud top pressure NN parameters for not null surface albedo  
units: [dl]

Step: User specified.

LUT processed at the FUB institute with a NN tool and delivered to ACRI.

Scientific content:

Cloud top pressure NN parameters for not null surface albedo

Current baseline: 262144 values

Resources:

Estimated CPU time: -

Output disk space:  $262144 \times 1 \text{ byte/uc} = 262144 \text{ bytes}$

Acceptance:

Corresponds to the latest definition

### 6.17.9 GADS Cloud Top Pressure Neural Network for null Surface Albedo

#### 6.17.9.1 Cloud top pressure neural network for null surface albedo

Reference: (No variable used), LUT385

[AD-8] Section 6.17.9, GADS field 1

ACRI provided

Dependencies:

None

Tool:

None

Procedure:

Input: none

Output: *(no variable)* Cloud top pressure NN parameters for null surface albedo  
units: [dl]

Step: User specified.  
LUT processed at the FUB institute with a NN tool and delivered to ACRI.

Scientific content:

Cloud top pressure NN parameters for null surface albedo

Current baseline: 262144 values

Resources:

Estimated CPU time: -

Output disk space:  $262144 \times 1 \text{ byte/uc} = 262144 \text{ bytes}$

Acceptance:

Corresponds to the latest definition

## 6.17.10 GADS Cloud type index

### 6.17.10.1 Cloud type index

Reference: Ctype[ctp,cot], LUT386

[AD-8] Section 6.17.10, GADS field 1

ACRI provided

Dependencies:

LUT379, LUT380

Tool:

None

Procedure:

Input: *ctp* Cloud top pressure [hPa] (10 values), see Section 6.17.4.20, LUT379  
*cot* Cloud top pressure [dl] (10 values), see Section 6.17.4.21, LUT380

Output: *Ctype[ctp,cot]* Cloud type index as function of the cloud top pressure (*ctp*) and of the cloud optical thickness (*cot*).

units: [dl]

Step: User specified.

Scientific content:

Cloud type index (*Ctype[ctp,cot]*) depending on the cloud top pressure (*ctp*) and the cloud optical thickness (*cot*)

Current baseline: (10 × 10) values

Resources:

Estimated CPU time: -  
 Output disk space: 10 × 10 × 1 byte/uc = 100 bytes

| COT   | Cloud Top Pressure [hPa] |     |     |      |      |      |      |      |      |      |
|-------|--------------------------|-----|-----|------|------|------|------|------|------|------|
|       | 50                       | 440 | 680 | 1000 | 1000 | 1000 | 1000 | 1000 | 1000 | 1000 |
| 0.0   | 135                      | 136 | 137 | 128  | 128  | 128  | 128  | 128  | 128  | 128  |
| 3.6   | 132                      | 133 | 134 | 128  | 128  | 128  | 128  | 128  | 128  | 128  |
| 23.0  | 129                      | 130 | 131 | 128  | 128  | 128  | 128  | 128  | 128  | 128  |
| 379.0 | 128                      | 128 | 128 | 128  | 128  | 128  | 128  | 128  | 128  | 128  |
| 379.0 | 128                      | 128 | 128 | 128  | 128  | 128  | 128  | 128  | 128  | 128  |
| 379.0 | 128                      | 128 | 128 | 128  | 128  | 128  | 128  | 128  | 128  | 128  |
| 379.0 | 128                      | 128 | 128 | 128  | 128  | 128  | 128  | 128  | 128  | 128  |
| 379.0 | 128                      | 128 | 128 | 128  | 128  | 128  | 128  | 128  | 128  | 128  |
| 379.0 | 128                      | 128 | 128 | 128  | 128  | 128  | 128  | 128  | 128  | 128  |

Acceptance:

Corresponds to the latest definition

**6.17.11 GADS Surface Pressure Neural Network Parameters**

6.17.11.1 Surface pressure neural network

Reference: (No variable used), LUT503

[AD-8] Section 6.17.10, GADS field 1

ACRI provided

Dependencies:

None

Tool:

None

Procedure:

Input: None

Output: *(No variable)* Surface pressure NN parameters.

units: [dl]

Step: User specified.

Scientific content:

Surface pressure NN parameters

Current baseline: 262144 values

Resources:

Estimated CPU time: -

Output disk space:  $262144 \times 1 \text{ byte/uc} = 262144 \text{ bytes}$

Acceptance:

Corresponds to the latest definition

## 6.18 LAND VEGETATION INDEX PARAMETERS

### 6.18.1 C.P.

None

### 6.18.2 MPH

Not covered in this document (*see* [AD-8] for a detailed description)

### 6.18.3 SPH

Not covered in this document (*see* [AD-8] for a detailed description)

### 6.18.4 GADS General

#### 6.18.4.1 Blue wavelength band number for TOA-VI computation

Reference: Blue\_band\_N, LUT387

[AD-8] Section 6.18.4, GADS field 1

ACRI provided

#### Dependencies:

None

#### Tool:

None

#### Procedure:

Input: none

Output: *Blue\_band\_N* Blue band # for TOA-vegetation index computation  
units: [dl]

Step: User specified.

#### Scientific content:

MERIS band in the blue region used for computation of TOA vegetation index

Current baseline: 2

Resources:

Estimated CPU time: -  
Output disk space: 1 × 1 byte/uc = 1 byte

Acceptance:

Corresponds to the latest definition.

6.18.4.2 Red wavelength band number for TOA-VI computation

Reference: Red\_band\_N, LUT388

[AD-8] Section 6.18.4, GADS field 2

ACRI provided

Dependencies:

None

Tool:

None

Procedure:

Input: none  
Output: Red\_band\_N Red band # for TOA-vegetation index computation  
units: [dl]  
Step: User specified.


Scientific content:

MERIS band in the red region used for computation of TOA vegetation index

Current baseline: 8

Resources:

Estimated CPU time: -  
Output disk space: 1 × 1 byte/uc = 1 byte

|   |  |   |
|---|--|---|
|  | <b>MERIS / ENVISAT-1</b><br>Medium Resolution Imaging Spectrometer | <u>Ref.:</u> PO-RS-PAR-GS-0002<br><u>Issue:</u> 3 <u>Rev.:</u> C<br><u>Date:</u> 27-Feb-11 <u>Page:</u> 526 |
|---|--|---|

Acceptance:

Corresponds to the latest definition.

6.18.4.3 *Near-infrared wavelength band number for TOA-VI computation*

Reference:    NIR\_band\_N,                    LUT389

[AD-8]    Section 6.18.4, GADS field 3

ACRI provided

Dependencies:

None

Tool:

None

Procedure:

Input:            none

Output:        *NIR\_band\_N*    NIR band # for TOA-vegetation index computation

units:            [dl]

Step:            User specified.

Scientific content:

MERIS band in the NIR region used for computation of TOA vegetation index

Current baseline: 13

Resources:

Estimated CPU time: -

Output disk space:    1 × 1 byte/uc = 1 byte

Acceptance:

Corresponds to the latest definition.

6.18.4.4 *K<sub>i</sub> normalization parameters for blue, red & NIR bands and for vegetated & bright soils*

Reference:    K<sub>i</sub>,    LUT390

[AD-8] Section 6.18.4, GADS field 4

ACRI provided

Dependencies:

None

Tool:

None

Procedure:

Input: none

Output:  $K_i$   $k_i$  normalization parameters for blue, red & NIR bands and for vegetated & bright soils (2 x 3 values)

units: [dl]

Step: User specified.

Scientific content:

$K_i$  normalization parameters in blue, red and NIR MERIS bands for vegetated and bright soils

Current baseline: 2 sets of 3 coefficients  $k(\lambda)$  in 3 spectral bands (blue, red, NIR) for vegetated and bright soils

|                    | $k(blue)$ | $k(red)$ | $k(NIR)$ |
|--------------------|-----------|----------|----------|
| <i>Vegetated</i>   | 0.56192   | 0.70879  | 0.86523  |
| <i>Bright soil</i> | 0.68545   | 0.87412  | 0.89788  |

Resources:

Estimated CPU time: -

Output disk space:  $2 \times 3 \times 4$  bytes/fl = 24 bytes

Acceptance:

Corresponds to the latest definition.

6.18.4.5  $\Theta_i$  normalization parameters for blue, red & NIR bands and for vegetated & bright soils

Reference:  $\Theta_i$ , LUT391



[AD-8] Section 6.18.4, GADS field 5

ACRI provided

Dependencies:

None

Tool:

None

Procedure:

Input: none

Output:  $\theta_i$   $\theta_i$  normalization parameters for blue, red & NIR bands and for vegetated & bright soils (2 x 3 values)

units: [dl]

Step: User specified.

Scientific content:

$\theta_i$  normalization parameters in blue, red and NIR MERIS bands for vegetated area and bright soils

Current baseline: 2 sets of 3 coefficients  $\theta(\lambda)$  in 3 spectral bands (blue, red, NIR) for vegetated and bright soils

|                    | $\theta(\text{blue})$ | $\theta(\text{red})$ | $\theta(\text{NIR})$ |
|--------------------|-----------------------|----------------------|----------------------|
| <i>Vegetated</i>   | -0.04203              | 0.03700              | -0.00123             |
| <i>Bright soil</i> | -0.02263              | -0.00357             | -0.01377             |

Resources:

Estimated CPU time: -

Output disk space:  $2 \times 3 \times 4$  bytes/fl = 24 bytes

Acceptance:

Corresponds to the latest definition.

**6.18.4.6  $\rho_i$  normalization parameters for blue, red & NIR bands and for vegetated & bright soils**

Reference:  $\rho_i$ , LUT392

[AD-8] Section 6.18.4, GADS field 6

ACRI provided

Dependencies:

None

Tool:

None

Procedure:

Input: none

Output:  $Rho_i$   $\rho_i$  normalization parameters for blue, red & NIR bands and for vegetated & bright soils (2 x 3 values)

units: [dl]

Step: User specified.

Scientific content:

$Rho_i$  normalization parameters in blue, red and NIR MERIS bands for vegetated area and bright soils

Current baseline: 2 sets of 3 coefficients  $\rho(\lambda)$  in 3 spectral bands (blue, red, NIR) for vegetated and bright soils

|                    | $\rho(blue)$ | $\rho(red)$ | $\rho(NIR)$ |
|--------------------|--------------|-------------|-------------|
| <i>Vegetated</i>   | 0.24012      | -0.46273    | 0.63841     |
| <i>Bright soil</i> | 0.42640      | 0.55649     | 0.65740     |

Resources:

Estimated CPU time: -

Output disk space:  $2 \times 3 \times 4$  bytes/fl = 24 bytes

Acceptance:

Corresponds to the latest definition.

**6.18.4.7 Maximum reflectances for blue, red and NIR bands used in TOA-VI computation**

Reference: Rho\_max, LUT393

[AD-8] Section 6.18.4, GADS field 7

ACRI provided

Dependencies:

None

Tool:

None

Procedure:

Input: none

Output: *Rho\_max* Maximum reflectances for blue, red and NIR bands used in TOA  
vegetation index computation (3 values)

units: [dl]

Step: User specified.

Scientific content:

Maximum reflectances for blue, red and NIR bands used in TOA-VI computation

Current baseline: {0.3, 0.5, 0.7}

Resources:

Estimated CPU time: -

Output disk space: 3 × 4 bytes/fl = 12 bytes

Acceptance:

Corresponds to the latest definition.

**6.18.4.8 Polynomial coefficients for blue, red and NIR bands for TOA-VI computation**

Reference: L, LUT394

[AD-8] Section 6.18.4, GADS field 8

ACRI provided

Dependencies:

None

Tool:

None

Procedure:

Input: none

Output: *L* Polynomial coefficients for blue, red and 3 NIR bands used in TOA vegetation index computation (12 x 5 values)

units: [*dl*]

Step: User specified.

Scientific content:

Polynomial coefficients for blue, red and NIR bands used in TOA-VI computation

Current baseline: Set of 12 coefficients  $L(\lambda)$  for 5 spectral bands (blue, red, NIR#1, NIR#2, NIR#3)

| Coefficient        | <i>L</i> <sub>1</sub> | 2        | 3        | 4        | 5        | 6        |
|--------------------|-----------------------|----------|----------|----------|----------|----------|
| <i>Blue band</i>   | 0.00000               | 0.00000  | 0.00000  | -0.30600 | 0.25500  | 0.00450  |
| <i>Red band</i>    | -9.26150              | 3.25450  | 9.82680  | 0.53737  | 0.36349  | 0.00235  |
| <i>NIR band #1</i> | -0.47131              | -0.04516 | -0.80707 | 0.19812  | -0.00691 | -0.02108 |
| <i>NIR band #2</i> | 0.79999               | -0.24396 | -1.73300 | 0.40182  | -0.30209 | -0.04305 |
| <i>NIR band #3</i> | -0.10065              | 0.12671  | -0.39783 | 0.08429  | -0.07737 | -0.00584 |

| Coefficient        | 7        | 8        | 9        | 10      | 11       | 12       |
|--------------------|----------|----------|----------|---------|----------|----------|
| <i>Blue band</i>   | 1.00000  | 1.00000  | 0.00000  | 0.64000 | -0.64000 | 0.19980  |
| <i>Red band</i>    | 0.00000  | 0.00000  | 0.00000  | 0.00000 | 0.00000  | 1.00000  |
| <i>NIR band #1</i> | -0.04836 | -0.54507 | -1.10270 | 0.12063 | 0.51893  | -0.19873 |
| <i>NIR band #2</i> | 6.30930  | -0.10645 | -9.12470 | 2.03210 | 0.60438  | -0.69423 |
| <i>NIR band #3</i> | 0.56605  | -0.11131 | -0.87161 | 0.05628 | 0.23144  | -0.11890 |

Resources:

Estimated CPU time: -

Output disk space: 5 x 12 x 4 bytes/fl = 240 bytes

Acceptance:

Corresponds to the latest definition.

6.18.4.9 Infrared to NIR reflectance ratio threshold for TOA-VI computation

Reference: IR-NIR\_rho\_ratio\_thresh, LUT395

[AD-8] Section 6.18.4, GADS field 9

ACRI provided

Dependencies:

None

Tool:

None

Procedure:

Input: none

Output: *IR-NIR\_rho\_ratio\_thresh*  
Threshold on reflectance ratio between infrared and NIR for TOA  
vegetation index computation

units: [dl]

Step: User specified.

Scientific content:

Threshold on infrared to NIR reflectance ratio for TOA-VI computation

Current baseline: 1.3

Resources:

Estimated CPU time: -

Output disk space: 1 × 4 bytes/fl = 4 bytes

Acceptance:

Corresponds to the latest definition.

6.18.4.10 Red wavelength band number for BOA-VI computation

Reference: BOAVI\_Red\_band\_N, LUT396

[AD-8] Section 6.18.4, GADS field 10

ACRI provided

Dependencies:

None

Tool:

None

Procedure:

Input: none

Output: *BOAVI\_Red\_band\_N*  
Red band # used in BOA vegetation index computation

units: [dl]

Step: User specified.

Scientific content:

MERIS band in the red region used for computation of BOA vegetation index

Current baseline: 8

Resources:

Estimated CPU time: -

Output disk space: 1 × 1 byte/uc = 1 byte

Acceptance:

Corresponds to the latest definition.

*6.18.4.11 Near-infrared wavelength band #1 for BOA-VI computation*

Reference: BOAVI\_NIR\_band1\_N, LUT397

[AD-8] Section 6.18.4, GADS field 11

ACRI provided

Dependencies:

None

Tool:

None

Procedure:

Input: none  
Output: *BOAVI\_NIR\_band1\_N*  
NIR band #1 used in BOA vegetation index computation  
units: [dl]  
Step: User specified.

Scientific content:

MERIS band#1 in the NIR region used for computation of BOA vegetation index  
Current baseline: 9

Resources:

Estimated CPU time: -  
Output disk space: 1 × 1 byte/uc = 1 byte

*6.18.4.12 Near-infrared wavelength band #2 for BOA-VI computation*

Reference: BOAVI\_NIR\_band2\_N, LUT459

[AD-8] Section 6.18.4, GADS field 12

ACRI provided

Dependencies:

None

Tool:

None

Procedure:

Input: none  
Output: *BOAVI\_NIR\_band2\_N*  
NIR band #2 used in BOA vegetation index computation  
units: [dl]  
Step: User specified.

Scientific content:

MERIS band#2 in the NIR region used for computation of BOA vegetation index

Current baseline: 10

Resources:

Estimated CPU time: -

Output disk space: 1 × 1 byte/uc = 1 byte

*6.18.4.13 Near-infrared wavelength band #3 for BOA-VI computation*

Reference: BOAVI\_NIR\_band3\_N, LUT460

[AD-8] Section 6.18.4, GADS field 13

ACRI provided

Dependencies:

None

Tool:

None

Procedure:

Input: none

Output: *BOAVI\_NIR\_band3\_N*  
NIR band #3 used in BOA vegetation index computation

units: [dl]

Step: User specified.

Scientific content:

MERIS band#3 in the NIR region used for computation of BOA vegetation index

Current baseline: 13

Resources:

Estimated CPU time: -

Output disk space: 1 × 1 byte/uc = 1 byte



6.18.4.14 BOA-VI acceptable range

Reference: BOAVI\_min, BOAVI\_max, LUT398

[AD-8] Section 6.18.4, GADS field 14

ACRI provided

Dependencies:

None

Tool:

None

Procedure:

Input: none

Output: *BOAVI\_min, BOAVI\_max*  
Acceptable range for BOA vegetation index (*min & max* values)

units: [*dl*]

Step: User specified.

Scientific content:

Acceptable range for BOA vegetation index

Current baseline: {0., 5.5}

Resources:

Estimated CPU time: -

Output disk space: 2 × 4 bytes/fl = 8 bytes

6.18.4.15 Maximum value of top of aerosol reflectance in red band to allow the MTCI computation

Reference: rhoaer\_red\_max, LUT461

[AD-8] Section 6.18.4, GADS field 14

ACRI provided

Dependencies:

None

Tool:

None

Procedure:

Input: none

Output: *rhoer\_red\_max*  
Maximum top of aerosol reflectance in red band

units: [dl]

Step: User specified.

Scientific content:

Maximum value of top of aerosol reflectance in the red band to allow the computation of the MERIS terrestrial chlorophyll index

Current baseline: 0.3

Resources:

Estimated CPU time: -

Output disk space: 1 × 4 bytes/fl = 4 bytes

**6.18.4.16 Minimum value of top of aerosol reflectance in NIR band#2 for MTCI**

Reference: rhoer\_NIR\_b2\_min, LUT462

[AD-8] Section 6.18.4, GADS field 14

ACRI provided

Dependencies:

None

Tool:

None

Procedure:

Input: none

Output: *rhoer\_NIR\_b2\_min*  
Minimum top of aerosol reflectance in NIR band#2  
units: [dl]  
Step: User specified.

Scientific content:

Minimum value of top of aerosol reflectance in the red band to allow the computation of the MERIS terrestrial chlorophyll index

Current baseline: 0.1

Resources:

Estimated CPU time: -  
Output disk space: 1 × 4 bytes/fl = 4 bytes

*6.18.4.17 Minimum value of top of aerosol reflectance difference between NIR#1 and red bands to allow the MTCI computation*

Reference: rhoer\_NIR1\_red\_min, LUT463

[AD-8] Section 6.18.4, GADS field 14

ACRI provided

Dependencies:

None

Tool:

None

Procedure:

Input: none  
Output: *rhoer\_NIR1\_red\_min*  
Minimum of top of aerosol reflectance difference between NIR#1 and red bands  
units: [dl]  
Step: User specified.

Scientific content:

Minimum value of top of aerosol reflectance difference between NIR #1 and red bands to allow the computation of the MERIS terrestrial chlorophyll index

Current baseline:  $10^{-6}$

Resources:

Estimated CPU time: -

Output disk space:  $1 \times 4 \text{ bytes/fl} = 4 \text{ bytes}$

*6.18.4.18 Minimum value of top of aerosol reflectance difference between NIR#3 and red bands to allow the MTCL computation*

Reference: rhoer\_NIR3\_red\_min, LUT464

[AD-8] Section 6.18.4, GADS field 14

ACRI provided

Dependencies:

None

Tool:

None

Procedure:

Input: none

Output: *rhoer\_NIR3\_red\_min*  
Minimum of top of aerosol reflectance difference between NIR#3 and red bands

units: [dl]

Step: User specified.

Scientific content:

Minimum value of top of aerosol reflectance difference between NIR #3 and red bands to allow the computation of the MERIS terrestrial chlorophyll index

Current baseline: 0.05

Resources:

Estimated CPU time: -  
Output disk space: 1 × 4 bytes/fl = 4 bytes

**- END OF DOCUMENT -**